



HAL
open science

Décryptage des interactions bactériennes entre *Pseudomonas aeruginosa* et *Staphylococcus aureus* dans un contexte d'infection pulmonaire

Laura Camus

► **To cite this version:**

Laura Camus. Décryptage des interactions bactériennes entre *Pseudomonas aeruginosa* et *Staphylococcus aureus* dans un contexte d'infection pulmonaire. Maladies infectieuses. Université de Lyon, 2020. Français. NNT : 2020LYSE1319 . tel-03365152

HAL Id: tel-03365152

<https://theses.hal.science/tel-03365152v1>

Submitted on 5 Oct 2021

HAL is a multi-disciplinary open access archive for the deposit and dissemination of scientific research documents, whether they are published or not. The documents may come from teaching and research institutions in France or abroad, or from public or private research centers.

L'archive ouverte pluridisciplinaire **HAL**, est destinée au dépôt et à la diffusion de documents scientifiques de niveau recherche, publiés ou non, émanant des établissements d'enseignement et de recherche français ou étrangers, des laboratoires publics ou privés.

N°d'ordre NNT : 2020LYSE1319



THESE de DOCTORAT DE L'UNIVERSITE DE LYON

Opérée au sein de
L'Université Claude Bernard Lyon 1

Ecole Doctorale N° 341
Evolution, Ecosystèmes, Microbiologie, Modélisation (E2M2)

Spécialité de doctorat : Microbiologie

Soutenue publiquement le 18/12/2020, par :

Laura Camus

Décryptage des interactions bactériennes entre *Pseudomonas aeruginosa* et *Staphylococcus aureus* dans un contexte d'infection pulmonaire

Facteurs génétiques, transcriptomiques et métaboliques
de *P. aeruginosa* impliqués dans l'état de coexistence

Devant le jury composé de :

ELSEN Sylvie, MCU-PH, Université de Grenoble

Examinatrice

FILLOUX Alain, PU-PH, London Imperial College

Examineur

MARCHANDIN Hélène, PU-PH, Université de Montpellier

Rapporteuse

MOREAU Karen, PU, Université Lyon 1

Co-directrice de thèse

TOUSSAINT Bertrand, PU-PH, Université de Grenoble

Rapporteur

VANDENESCH François, PU-PH, Université Lyon 1

Directeur de thèse

VIANNEY Anne, MCU, Université Lyon 1

Examinatrice

Remerciements

Mes premiers remerciements s'adressent aux chercheurs qui ont accepté d'évaluer cette thèse : **Mme Marchandin** et **M. Toussaint** pour le temps passé à corriger mon manuscrit, ainsi que **Mme Elsen**, **Mme Vianney** et **M. Filloux** pour leur participation en tant que jury.

Karen, je ne saurais assez te remercier pour cette thèse. Tu as su me passionner par cette thématique de recherche, me booster quand les manips ne marchaient pas, me guider quand j'étais bloquée. Et ce toujours en me laissant une liberté et une autonomie qui m'ont permis d'évoluer. Merci également pour ton soutien et ta patience dans mes déboires avec les démons de l'administration, mes lubies de concours, et toutes les répétitions d'oraux que tu as dû endurer. Comme Paul l'avait si bien dit, je te considère comme ma « maman scientifique », et je ne pouvais pas rêver d'une meilleure encadrante que toi. Mille merci pour tout ça !



François, un énorme merci également pour votre soutien tout au long de cette thèse, votre aide, vos conseils toujours avisés. Travailler dans votre équipe et sous votre direction fut une superbe expérience.

Je tiens ensuite à remercier tous les membres (ou ex-membres) de cette équipe de recherche, qui ont rendu toutes ces heures passées au laboratoire plus chaleureuses et agréables :



Polo (désolée mais je n'arrive plus à t'appeler autrement haha), quelle tristesse de finir ma thèse sans mon acolyte de co-cultures et de soirées jusqu'au bout de la night ! Je te remercie d'avoir été un super encadrant de stage, puis un super collègue (et ami !) de thèse. J'espère qu'on aura à nouveau l'occasion de travailler ensemble un jour !

Remerciements

Sylvère, Princesse Sysy, Pimprenelle, merci pour le gigantesque travail que tu as effectué sur TOUS les projets de ma thèse. Sans toi, ce manuscrit n'aurait clairement pas la même tête : j'hésite entre te mettre co-auteur ou te payer 1000 (!) bières pour te remercier :P Merci également pour toutes les embuscades alcoolisées auxquelles je n'ai pas su dire non, mais qui ont toujours été géniales ! Je te souhaite un bon courage pour cette thèse que tu espérais tant.



Florence, ma collègue de bureau et ma seconde maman du labo ! Merci pour ton aide et ta bienveillance au labo comme à l'extérieur, les fous-rire à la pause repas ou en P2, et toutes les discussions que nous avons pu avoir dans le bureau ! ☺

Katia, merci d'avoir égayé mes matinées au laboratoire en me faisant des peurs pas possibles par le fenêtre du P2 ! :P Ton rire qui résonne dans le couloir, tes blagues et les instants « commérages-laverie » vont trop me manquer !



Cédric, le Chouchou du labo ! Merci pour ta bonne humeur et ton aide tous les jours au laboratoire. Heureusement que tu as été là pour m'apprendre mes premiers Gram et galeries API (entre autres !), même si certaines étaient un peu bizarres, hein... :P

Remerciements

Mariane, petite dernière (et pas des moindres) de la triplée de thésards du 6^{ème} ! Merci pour tous les bons moments que nous avons partagé au labo ou à l'extérieur. Merci d'avoir vivement contribué au mur de post-it, notamment grâce aux sessions mots-fléchés ! Tu réussiras sans nul doute à percer les secrets de ce satané opéron, courage ! :P



Jess, je regrette ta gaité et l'ambiance que tu as su mettre au laboratoire ! Merci pour ces bons moments, les pauses thés, ainsi que ton aide et tes conseils avisés au laboratoire. J'espère que tu te plais dans ta « nouvelle » équipe avec ce poste plus que mérité.

Sabine, Floriane et Maëlle, merci à vous aussi pour votre bonne humeur et ces moments partagés dans le P2 ou le bureau !

A toutes les personnes que j'ai pu croiser au cours de ma thèse et qui m'ont soutenue :

Fanny, mon chaton, merci pour tous nos fous-rires et discussions pendant notre M2 et une partie de ma thèse ! **Louis**, merci pour toutes tes blagues qui ont mis une sacrée ambiance au laboratoire (et les castors que l'on continue à retrouver !).

Jérôme, merci pour toutes ces discussions et conseils au détour d'un couloir, d'un repas ou d'une bière ! Tu vas sans nul doute continuer ton ascension dans le domaine du Staph :P Merci également à toutes les personnes du 5^{ème} ou de Croix-Rousse pour votre bonne humeur, les repas ou les sessions foot : **Andréa, Anaïs, Alexia, Camille, Marie, Aubin, Alan, Jason, Yousef, Lélia, Frédéric...** Merci !!! Un énorme merci également à **Patricia** et **Christophe** pour votre aide et conseils pour les séquençages et les autres expériences, ainsi que pour votre soutien.

Marie, Alice, Marion, Aurélia, Amélie (très digne héritière !), vous avez été de supers stagiaires et je vous remercie pour votre aide, votre bonne humeur et de m'avoir appris à être pédagogue :P

Enfin, merci à toutes les personnes du CIRI avec qui j'ai eu l'opportunité d'échanger au cours de réunions ou de la fameuse Retraite : **Corentin, Anne-Sophie, Elisabeth, Nathalie A., Sandrine A., Floriane F**, et bien-sûr **M. Cosset** pour votre soutien.

Remerciements

Je tiens également à remercier les chercheurs avec lesquels j'ai pu collaborer, sans qui plusieurs projets n'auraient pas pu aboutir : **Anne**, merci pour tout le travail que tu effectues à l'hôpital avec les souches cliniques, ton implication dans nos projets de recherche et ta bienveillance à toute épreuve. **Sylvie**, merci pour ton aide précieuse pour la construction des mutants chez *P. aeruginosa*, et ta patience face à tous mes mails de détresse ! **Erwan**, merci de m'avoir formée et accueillie pour mettre au point le Tn-seq, qui a d'ailleurs donné de supers résultats. **M. Filloux**, merci pour l'envoi du nécessaire de mutagenèse et votre soutien pour mes candidatures. Merci également au **Centre d'Etude des Substances Naturelles** de m'avoir accueillie pour la mise au point certains dosages.

Mais que serait ma thèse sans ma famille et mes amis ? Pas grand-chose !

Je ne remercierai jamais assez **toute ma famille** pour votre soutien sans faille, pour avoir toujours essayé de comprendre ce que je bidouillais au labo (de la tambouille, dirait Thomas), et pour avoir supporté mes moments de doute et de fatigue. Mention spéciale à **Aline** et **Bernard** d'avoir fait le déplacement de Grenoble pour assister à une présentation, c'était adorable !

Merci à **Benjamin**, mon Ours, pour son soutien durant ces dernières années : heureusement que tu étais là pour essayer de me faire déstresser, me dissuader de passer au laboratoire le week-end, me reconforter par les meilleurs repas après les longues journées. Si seulement tu m'avais remerciée à ta thèse, ça aurait été parfait... :P ♥



Les Petrouchka, Béa et Clem, merci pour votre soutien et votre amitié, ainsi que pour toutes nos escapades qui nous ont permis de boire la pression plutôt que de la subir... Bientôt nous serons enfin toutes les trois libérées et nous irons fêter ça dignement, j'ai hâte ! Merci également à **Elodie** pour nos petites promenades et goûters, ainsi que **Solene** et **Laura** pour nos soirées girls !

Merci également aux **Bobbies**, **Nicolas**, **Clémence G.**, **Michel** et **Huguette**, **Emma**, **Colin**, **Florian**, l'association **DocE2M2** pour votre soutien et votre amitié. **Et à tous ceux que j'aurais pu oublier, pardon et merci !!!**

Résumé

Les patients atteints de mucoviscidose souffrent d'infections pulmonaires polymicrobiennes dont les principaux agents d'intérêt clinique sont *Staphylococcus aureus* et *Pseudomonas aeruginosa*. Ces deux bactéries co-infectent jusqu'à 40% des patients et sont capables, dans ces conditions, d'interagir de deux façons différentes. Les souches d'infection précoce de *P. aeruginosa* sont dans un état de compétition avec *S. aureus*, alors que les souches d'infection chronique sont capables de coexister. Ce dernier état reste peu décrit mais pourrait favoriser la persistance des deux pathogènes dans les poumons des patients. Nous cherchons donc à comprendre les mécanismes de cet état de coexistence par l'étude de souches cliniques.

Nous avons tout d'abord étudié l'impact de la coexistence sur la physiologie bactérienne de *P. aeruginosa* par une approche transcriptomique, et avons mis en évidence une coopération trophique entre les deux espèces. La production d'acétoïne par *S. aureus* et le catabolisme de cette molécule par *P. aeruginosa* favorisent ainsi la survie des deux pathogènes.

Parallèlement à cela, nous avons étudié les facteurs génétiques de *P. aeruginosa* impliqués dans l'établissement et le maintien de la coexistence avec *S. aureus*. Différentes approches ont été utilisées : (i) le séquençage de souches isolées de patients présentant différents états d'interaction ; (ii) l'établissement d'un protocole d'évolution expérimentale *in vitro* et (iii) le criblage d'une banque de mutants par Transposon-sequencing. Ces approches ont permis l'identification de deux facteurs impliqués dans l'établissement de l'état de coexistence : le gène codant pour le régulateur du quorum-sensing *lasR*, et l'opéron *yecS-fliY*, impliqué dans le transport de la cystéine. Le maintien *P. aeruginosa* dans cet état de coexistence avec *S. aureus* semble quant à lui faire intervenir le métabolisme de différents acides aminés et du glucose de *P. aeruginosa*.

Ces travaux ont donc démontré l'importance du métabolisme carboné de *P. aeruginosa* dans l'interaction de coexistence avec *S. aureus*, et ont permis de mieux comprendre les causes et impacts de cet état encore peu décrit. Ces résultats ouvrent également de nombreuses perspectives pour l'étude des interactions entre *P. aeruginosa* et *S. aureus*.

Mots clés : *P. aeruginosa*, *S. aureus*, mucoviscidose, interaction, coexistence.

Abstract

Cystic fibrosis patients suffer from polymicrobial lung infections. The main agents of clinical interest are *Staphylococcus aureus* and *Pseudomonas aeruginosa*. These two bacteria co-infect up to 40% of patients and are able, under these conditions, to interact in two different ways. *P. aeruginosa* strains of early infection are in competition with *S. aureus*, while strains of chronic infection can coexist. The latter state remains little described but could favour the persistence of the two pathogens in the lungs of the patients. We therefore seek to understand the mechanism of this coexistence state by studying clinical strains.

We first studied the impact of coexistence on *P. aeruginosa* physiology using a transcriptomic approach and highlighted a trophic cooperation between the two species. Acetoin production by *S. aureus* and catabolism by *P. aeruginosa* thus promote the survival of both pathogens.

Meanwhile, we studied the genetic factors of *P. aeruginosa* involved in establishing and maintaining coexistence with *S. aureus*. Different approaches have been used: (i) sequencing of strains isolated from patients with different interaction states; (ii) the implementation of an experimental *in vitro* evolution protocol and (iii) the screening of a Transposon-sequencing bank of mutants. These approaches allowed the identification of two factors involved in the establishment of coexistence: the gene encoding the quorum sensing regulator *lasR*, and the operon *yecS-fliY* responsible for cysteine transport. The survival of *P. aeruginosa* during coexistence with *S. aureus* seems to involve the metabolism of different amino acids and glucose of *P. aeruginosa*.

Altogether, these results demonstrated the importance of *P. aeruginosa* carbon metabolism for the coexisting interaction with *S. aureus* and allowed a better understanding of the causes and impacts of coexistence. This work also opens numerous perspectives in the study of the relationship between *P. aeruginosa* and *S. aureus*.

Key words: *P. aeruginosa*, *S. aureus*, cystic fibrosis, interaction, coexistence.

Laboratoire de rattachement

Ce doctorat a été préparé au sein du laboratoire

INSERM U1111 – Centre International de Recherche en Infectiologie, équipe Pathogénie des staphylocoques.

Adresse postale du laboratoire

CIRI-INSERMU1111 Faculté de Médecine Lyon-Est,
7 rue Guillaume Paradin
69008 LYON CEDEX 8 – France

Financement

Ce doctorat a été financé par la Fondation pour la Recherche Médicale. **This work is supported by the Fondation pour la Recherche Médicale (FRM grant number ECO20170637499 to LC).**



Abréviations

1-OH-PHZ	1-hydroxyphénazine	COG	Clusters of Orthologous Groups
ABC	ATP-Binding Cassette	CRCM	Centre de Ressources et de Compétences en Mucoviscidose
aco	Acetoin Catabolism Operon	cre	Catabolite Responsive Element
ADN (DNA)	Acide Deoxyribonucléique	DAP	Acide Diaminopimélique
ADNg	Acide Deoxyribonucléique Génomique	DO (OD)	Densité optique
AHL	N-Acyl-Homoserine Lactone	EDDHA	Ethylènediamine-N, N'-bis
AHMP	4-amino-5-hydroxymethyl-2-methylpyrimidine	EDTA	Éthylènediaminetétraacétique
ANOVA	Analysis of Variance	EPS	Exopolysaccharide
AQP	Aquaporine	FAMD	Factor Analysis of Mixed Data
ARN (RNA)	Acide Ribonucléique	FAMD	Factor Analysis of Mixed Data
ARNm	Acide Ribonucléique Messenger	FC	Facteur d'expression différentielle (Fold Change)
BET	Bromure d'Ethidium	FEV1	Force Expiratoire Maximale par seconde
BHI	Brain Heart Infusion	GC-MS	Gas Chromatography-Mass Spectrometry
BSM	Bifidus Selective Medium	GlcNac	N-acetyl Glucosamine
CcpA	Carbon Catabolite Protein A	Gm	Gentamycine
CF	Mucoviscidose (Cystic Fibrosis)	GSH	Glutathion
CFRD	Diabète Lié à la Mucoviscidose	HCL	Hospices Civils de Lyon
CFTR	Cystic Fibrosis Transmembrane Regulator	HHQ	2-heptyl-4-quinolone
CMI (MIC)	Concentration Minimale Inhibitrice	HMM	Hidden Markov Model
CMTE	2-(2-carboxy-4-methyl-thiazol-5-yl) éthyl phosphate	HQNO	2-heptyl-4-hydroxyquinoline n-oxide

Liste des abréviations

HSL	Homosérine Lactone	RBS	Site de fixation du Ribosome
IAI	Institut des Agents Infectieux	REG	Reticulum Endoplasmique Rugueux
IMC	Indice de Masse Corporelle	Res.	Resampling
IR	Séquence Répétée Inversée	RNAseq	Séquençage des ARN
KEGG	Kyoto Encyclopedia of Genes and Genomes	ROS	Espèces Réactives de l'Oxygène
LB	Lysogeny Broth	rpm	Rotation Par Minute
LPS	Lipopolysaccharide	SA	<i>Staphylococcus aureus</i> , <i>S. aureus</i>
MCAB	5- methylphénazine-1-carboxylic acide bétaine	SARM	<i>S. aureus</i> Résistant à la Méthicilline
MSA	Mannitol Salt Agar	SCFM	Synthetic CF Sputum Medium
ND	Non Déterminé	SCN	Thiocyanate
NGS	Next Generation Sequencing	SCV	Small Colony Variant
NS	Non Significatif	SED	Standard Error of the Difference
P, P_{adj}	P-valeur, P-valeur ajustée	SEM	Standard Error of the Mean
PA	<i>Pseudomonas aeruginosa</i> , <i>P. aeruginosa</i>	SST_n	Système de Sécrétion de Type n
PCA	Phénazine2-carboxylique	TD	Thymidine
PCN	Phénazine-1-carboxamide	Tn-seq	Transposon-sequencing
PQS	<i>Pseudomonas</i> Quinolone Signal	TPP	Thiamine Pyrophosphate
PSI	Polysaccharide Synthesis Locus	TSA	Tryptic Soy Agar
PSM	Poste de Sécurité Microbiologique	UFC	Unité Formant Colonie (CFU)
RT-qPCR	Rétrotranscription et PCR quantitative	UV	Ultra-Violet
QS	Quorum sensing	WT	Sauvage (Wild-type)

Table des matières

16	Liste des tableaux et des figures
19	INTRODUCTION
21	1. Les interactions microbiennes
21	1.1. Importance de l'étude des interactions microbiennes
23	1.2. Les différents types d'interactions microbiennes
23	1.2.1. Interactions positives
26	1.2.2. Interactions négatives
29	1.3. Impact des interactions microbiennes sur l'hôte
31	1.4. Modèles d'étude des interactions microbiennes
33	2. La mucoviscidose comme contexte d'étude des interactions microbiennes
33	2.1. Physiopathologie de la mucoviscidose
33	2.1.1. Généralités
33	2.1.2. Origine génétique de la maladie
33	a. Mutations du gène <i>cftr</i>
35	b. Fonctionnement normal du canal CFTR
36	c. Conséquences des mutations du gène <i>cftr</i>
39	2.2. Infections pulmonaires polymicrobiennes
39	2.2.1. Caractérisation du microbiome pulmonaire
40	2.2.2. Evolution du microbiome pulmonaire pendant l'infection
42	2.2.3. Principaux pathogènes pulmonaires
44	2.3. <i>S. aureus</i> et <i>P. aeruginosa</i> dans la mucoviscidose
44	2.3.1. <i>S. aureus</i>
45	2.3.2. <i>P. aeruginosa</i>
45	a. Colonisation des poumons
47	b. Etablissement des infections chroniques
48	Publication From genotype to phenotype: adaptations of <i>Pseudomonas aeruginosa</i> to the Cystic Fibrosis environment (MGen, 2021)
69	3. Etude de cas : les interactions entre <i>P. aeruginosa</i> et <i>S. aureus</i> chez les patients atteints de mucoviscidose
69	3.1. L'état de compétition
71	3.2. Evolution des interactions entre <i>P. aeruginosa</i> et <i>S. aureus</i>
72	Publication How bacterial adaptation to Cystic Fibrosis environment shapes interactions between <i>Pseudomonas aeruginosa</i> and <i>Staphylococcus aureus</i> (Front. Microbiol., 2021)
89	4. Objectifs de la thèse

91	TRAVAUX DE RECHERCHE
93	1. AXE 1 : Impact de la coexistence sur le transcriptome et le métabolisme de <i>P. aeruginosa</i>
93	1.1. Introduction
95	1.2. Publication Trophic cooperation promotes bacterial survival of <i>Staphylococcus aureus</i> and <i>Pseudomonas aeruginosa</i> (ISME, 2020)
130	1.3. Résultats complémentaires et perspectives
130	1.3.1. Facteurs influençant le métabolisme de l'acétoïne
130	a. Induction du système aco par l'acétoïne
131	b. Autres régulateurs du système aco
136	c. Rôle des conditions acido-basiques
138	1.3.2. Restauration chromosomique du système aco chez PA2600
143	2. AXE 2 : Facteurs génétiques de <i>P. aeruginosa</i> impliqués dans l'établissement de l'état de coexistence
143	2.1. Introduction
145	2.2. Publication <i>Pseudomonas aeruginosa</i> genetic factors involved in establishment of coexistence interaction state with <i>Staphylococcus aureus</i> (en préparation)
165	2.3. Résultats complémentaires et perspectives
165	2.3.1. Diversification au sein de la population bactérienne
167	2.3.2. Pigmentation et coexistence
171	3. AXE 3 : Facteurs génétiques de <i>P. aeruginosa</i> essentiels à son maintien lors de l'interaction de coexistence
171	3.1. Introduction
174	3.2. Matériels et méthodes
174	3.2.1. Souches bactériennes et plasmides
175	3.2.2. Conjugaison et mutation de <i>P. aeruginosa</i> par transposition
175	a. Détermination de l'efficacité de conjugaison
176	b. Construction de la banque de mutants chez PA235A
177	3.2.3. Culture de la banque
178	3.2.4. Préparation des bibliothèques de séquençage
178	a. Extraction des ADNg
178	b. Digestion de l'ADNg par Mmel et purifications
178	c. Création des adaptateurs double-brin
180	d. Ligature des échantillons aux adaptateurs double-brin
180	e. Amplification et purification des produits de ligature

181	3.2.5. Séquençage et analyse bio-informatique
181	a. Séquençage et annotations
183	b. Détermination des gènes essentiels, favorables et défavorables
183	3.3. Résultats
183	3.3.1. Choix des souches
184	3.3.2. Production de la banque chez PA235A
186	3.3.3. Identification des gènes favorables et défavorables à la coexistence
194	3.4. Discussion et perspectives
194	3.4.1. Production de la banque
196	3.4.2. Gènes favorables
198	3.4.3. Gènes défavorables
201	3.4.4. Perspectives et conclusions
203	4. Autres travaux
203	4.1. Impact de la coexistence sur le transcriptome et la résistance antibiotique de <i>S. aureus</i>
204	Publication Coexistence with <i>Pseudomonas aeruginosa</i> alters <i>Staphylococcus aureus</i> transcriptome, antibiotic resistance and internalization into epithelial cells (Sci. Rep., 2019)
219	4.2. Impact de la coexistence sur l'état de santé des patients co-infectés par <i>P. aeruginosa</i> et <i>S. aureus</i>
220	Publication Impact of Coexistence Phenotype Between <i>Staphylococcus aureus</i> and <i>Pseudomonas aeruginosa</i> Isolates on Clinical Outcomes Among Cystic Fibrosis Patients (Front. Cell. Infect. Microbiol., 2020)
231	CONCLUSION GENERALE
235	COMMUNICATIONS
237	1. Communication scientifique
237	1.1. Présentations orales
238	1.2. Présentations affichées
242	2. Médiation et vulgarisation scientifique
243	REFERENCES

Liste des tableaux et des figures

TABLEAUX

		Introduction
24	Tableau 1	Classification des interactions microbiennes selon leur effet positif, négatif ou neutre sur les microorganismes impliqués.
34	Tableau 2	Classes de mutations du gène <i>cftr</i> .
		Axe 1
134	Tableau I-1	Abondance des transcrits des gènes du système <i>aco</i> chez un mutant Hfq et un mutant Crc, en comparaison à la souche PAO1 sauvage.
		Axe 2
166	Tableau II-1	Résultats des tests de compétition réalisés pour 12 colonies de la souche PA190B ²⁵ .
168	Tableau II-2	Tableau récapitulatif des caractéristiques des isolats évolués expérimentalement.
		Axe 3
174	Tableau III-1	Souches bactériennes et plasmides utilisés dans cette étude.
177	Tableau III-2	Adaptateurs, codes-barres et échantillons correspondants utilisés dans cette étude.
181	Tableau III-3	Amorces utilisées lors de la construction des bibliothèques de séquençage.
184	Tableau III-4	Nombre de lectures de séquençage et densité d'insertion du transposon dans la banque pure de PA235A, la monoculture et la co-culture de la banque.
188	Tableau III-5A	Gènes favorables au maintien de <i>P. aeruginosa</i> PA235A en coexistence avec <i>S. aureus</i> SA235.
189	Tableau III-5B	Gènes défavorables au maintien de <i>P. aeruginosa</i> PA235A en coexistence avec <i>S. aureus</i> SA235.

FIGURES

		Introduction
24	Figure 1	Exemples d'interactions microbiennes positives et négatives entre deux microorganismes.
27	Figure 2	Conditions écologiques favorisant les comportements compétitifs entre microorganismes.
35	Figure 3	Classes de mutations du gène <i>cftr</i> .
38	Figure 4	Conséquences physiologiques du fonctionnement normal ou du dysfonctionnement du canal CFTR au niveau des cellules épithéliales pulmonaires.
40	Figure 5	Prévalence et abondance relative des genres bactériens identifiés dans le microbiome pulmonaire des patients atteints de mucoviscidose.
41	Figure 6	Modèle Climax-Attack des exacerbations chez les patients atteints de mucoviscidose proposé par Quinn <i>et al.</i>
43	Figure 7	Prévalence des principales espèces pathogènes colonisant les poumons des patients atteints de mucoviscidose selon leur classe d'âge.
46	Figure 8	Représentation schématique de l'évolution des infections à <i>P. aeruginosa</i> .
71	Figure 9	Modélisation de la relation existant entre la cinétique d'infection par <i>S. aureus</i> et <i>P. aeruginosa</i> , leur état d'interaction et l'adaptation de <i>P. aeruginosa</i> au milieu pulmonaire.
		Axe 1
130	Figure I-1	Facteurs d'expression différentielle des gènes <i>acoR</i> et <i>PA4148</i> chez <i>P. aeruginosa</i> en co-culture avec <i>S. aureus</i> , par rapport à la monoculture et dosages de l'acétoïne en monoculture et co-cultures de <i>S. aureus</i> , <i>B. subtilis</i> et <i>E. coli</i> .

131	Figure I-2	Facteurs d'expression différentielle des gènes <i>acoR</i> et <i>PA4148</i> chez <i>P. aeruginosa</i> en co-culture avec <i>S. aureus</i> , en fonction de la concentration en acétoïne produite par <i>S. aureus</i> .
133	Figure I-3	Mécanismes hypothétiques de répression et d'activation du système <i>aco</i> chez <i>P. aeruginosa</i> .
135	Figure I-4	Expression du système <i>aco</i> et catabolisme de l'acétoïne chez <i>P. aeruginosa</i> PA14 sauvage et Δ <i>lasR</i> cultivées dans du surnageant de <i>S. aureus</i> ou dans du milieu riche.
136	Figure I-5	Régulation simplifiée de la synthèse d'acétate et d'acétoïne chez <i>S. aureus</i> .
137	Figure I-6	Suivi du pH et de la concentration en acétoïne dans la culture de <i>S. aureus</i> en absence ou en présence d'acide, de base, de <i>P. aeruginosa</i> Δ <i>aco</i> ou de <i>E. coli</i> .
138	Figure I-7	Suivi du pH dans des monocultures et co-cultures de <i>S. aureus</i> , <i>P. aeruginosa</i> sauvage, Δ <i>acoR</i> et Δ <i>aco</i> pendant 5 jours.
139	Figure I-8	Cinétiques de la concentration en acétoïne et de la croissance de <i>P. aeruginosa</i> dans du milieu minimum supplémenté en acétoïne.
140	Figure I-9	Cinétiques de survie de <i>S. aureus</i> , <i>P. aeruginosa</i> et de la concentration en acétoïne durant les co-cultures prolongées.
141	Figure I-10	Dénombrements bactériens de <i>P. aeruginosa</i> après 5 jours de monoculture ou de co-culture avec <i>S. aureus</i> .
Axe 2		
144	Figure II-1	Schéma de la méthodologie employée.
166	Figure II-2	Evolution hypothétique des populations de <i>P. aeruginosa</i> initialement coexistante ou compétitrice.
169	Figure II-3	Suivi de l'état d'interaction de <i>P. aeruginosa</i> au cours du protocole d'évolution expérimentale.
170	Figure II-4	Pigmentation et fluorescence des isolats évolués M1 à M5 en présence ou en conditions de privation en fer.
170	Figure II-5	Voie de synthèse des principales phénazines chez <i>P. aeruginosa</i> .
Axe 3		
173	Figure III-1	Principe du Transposon-sequencing.
175	Figure III-2	Carte du plasmide pSAM_DGm
179	Figure III-3	Préparation des bibliothèques de séquençage de la région ADN-transposon.
183	Figure III-4	Nombre de clones obtenus par expérience de conjugaison chez deux souches contrôles et dix souches cliniques de <i>P. aeruginosa</i> .
184	Figure III-5	Géloses étalées pour la construction de la banque chez PA235A.
185	Figure III-6	Gènes essentiels de <i>P. aeruginosa</i> PA235A identifiés par séquençage de la banque pure.
186	Figure III-7	Cinétique de croissance bactérienne de la banque de mutants de <i>P. aeruginosa</i> PA235A et de <i>S. aureus</i> SA235 en monoculture et co-culture.
187	Figure III-8	Nombre de gènes favorables et défavorables de <i>P. aeruginosa</i> PA235A identifiés en co-culture par rapport à la monoculture et en monoculture par rapport à la banque pure.
191	Figure III-9	Voies métaboliques favorables et défavorables au maintien de <i>P. aeruginosa</i> PA235A en coexistence avec <i>S. aureus</i> SA235.
193	Figure III-10	Comparaison des nombres d'insertions obtenus pour la banque de PA235A pure, cultivée en monoculture ou en co-culture, pour les gènes favorables et défavorables identifiés en Tableau III-5.
195	Figure III-11	Comparaison des gènes favorables et défavorables identifiés dans les études de Tn-seq chez <i>P. aeruginosa</i> .
196	Figure III-12	Cinétique de dosage du glucose en monoculture de <i>S. aureus</i> , <i>P. aeruginosa</i> ou en co-culture.
198	Figure III-13	Concentrations médianes en acides aminés dosées dans les expectorations de 12 patients atteints de mucoviscidose.
200	Figure III-14	Phénotypes associés aux gènes favorables et défavorables au maintien de <i>P. aeruginosa</i> PA235A en coexistence avec <i>S. aureus</i> SA235.



INTRODUCTION

1 Les interactions microbiennes

1.1. Importance de l'étude des interactions microbiennes

Depuis les premières découvertes dans le domaine de la microbiologie, l'étude des microorganismes repose sur l'isolement d'une espèce de son environnement et sa caractérisation dans des conditions contrôlées. Si cette approche permet d'identifier les caractères génétiques et phénotypiques intrinsèques au microorganisme, elle est bien souvent insuffisante pour décrypter son comportement et son rôle dans son habitat naturel. En effet, les conditions générées en laboratoire ne retranscrivent que très partiellement la complexité physico-chimique et biotique des écosystèmes, qui joue pourtant un rôle majeur sur la physiologie microbienne. Une attention croissante est ainsi portée à la mise au point de dispositifs expérimentaux reproduisant les conditions environnementales dans lesquelles les microorganismes évoluent. La composition des milieux de cultures peut alors être ajustée pour mimer les caractéristiques physico-chimiques d'un environnement ; la viscosité et la forte composition en acides aminés des expectorations des patients atteints de mucoviscidose a ainsi été reproduite dans le milieu SCFM (*Synthetic Cystic Fibrosis sputum Medium*) (1). Dans le cas des écosystèmes faisant intervenir un organisme hôte (qu'il soit microbien, animal ou végétal), ce dernier peut être pris en compte *via* l'utilisation de modèles d'infection cellulaire ou d'organoïdes (2).

Ces dispositifs *in vitro* sont cependant limités par l'absence des autres microorganismes de l'écosystème. En effet, que ce soit dans le sol, l'eau ou les organismes vivants, les microorganismes n'évoluent jamais seuls mais au sein de communautés microbiennes complexes (3–7). Ces communautés sont composées du microbiote propre à l'écosystème d'intérêt mais peuvent être perturbées par d'autres microorganismes colonisateurs ; ceci est particulièrement vrai dans le cas d'infection d'organismes vivants par des espèces pathogènes. Le rôle du microbiote dans ces infections est de plus en plus considéré et étudié *via* l'utilisation de modèles d'expérimentation *in vivo*. L'étude des communautés microbiennes et de leur impact reste cependant limitée par deux aspects : d'une part, bien que présent dans l'organisme modèle, le rôle exact du microbiote pendant l'infection demeure difficile à estimer du fait de sa richesse et sa diversité. La difficulté d'isolement et de culture de nombreuses espèces du microbiote constitue un autre frein à son étude (3–7). D'autre part, les infections expérimentales *in vivo* sont le plus souvent réalisées à l'aide d'un

seul pathogène d'intérêt. Si cette approche est adaptée pour l'étude de pathologies mono-microbiennes répondant aux postulats de Koch comme la tuberculose ou le cholera (8), elle ne permet pas de prendre en compte le caractère polymicrobien de nombreuses infections. L'association de plusieurs microorganismes est en effet impliquée dans les pneumonies, les infections des plaies, du péritoine, du vagin ou encore du tractus urinaire, et contribue à la sévérité de ces pathologies (9–11). Il a été prouvé que cette synergie polymicrobienne résultait d'interactions entre les microorganismes colonisateurs.

Au sein d'un écosystème, qu'il soit infectieux ou non, les microorganismes sont en effet capables d'interagir entre eux *via* de nombreux mécanismes. Ces mécanismes sont très souvent régulés par les systèmes de communication microbienne appelés quorum-sensing (QS), dont la versatilité permet des interactions entre individus d'une même espèce ou d'espèces différentes (12). Les cellules peuvent ainsi interagir directement par le biais d'éléments membranaires tels que le système de sécrétion de type 6 (SST6), les pilis ou les structures hyphales (13, 14). Les interactions indirectes, plus fréquentes et diverses, reposent quant à elles sur la modification des propriétés physico-chimiques du milieu, notamment *via* la sécrétion et la consommation de molécules. En résultante, les interactions entre microorganismes affectent à la fois leur environnement et leur physiologie, deux éléments particulièrement importants dans un contexte infectieux. Ces interactions, depuis leurs mécanismes jusqu'à leurs conséquences, sont toutefois très variées et parfois difficiles à caractériser. Il est néanmoins possible de catégoriser les interactions selon leurs impacts positifs ou négatifs sur la physiologie microbienne (15, 16).

1.2. Les différents types d'interactions microbiennes

1.2.1. *Interactions positives*

Les interactions dites positives sont caractérisées par un effet bénéfique sur au moins un des deux partenaires de l'interaction, sans effet négatif sur le second microorganisme. Elles regroupent les interactions de type commensales et mutualistes (**Tableau 1**) (**Fig. 1**). Ce dernier type d'interaction est ainsi bénéfique pour les deux microorganismes impliqués, et peut avoir un caractère obligatoire et/ou permanent (symbiose), ou facultatif (coopération).

L'établissement de la **symbiose** requiert une proximité physique très importante et de longue durée entre deux espèces différentes, qui co-évoluent vers une interdépendance bénéfique dans un environnement donné (17).

La **coopération**, affectant également la physiologie des deux partenaires microbiens, n'induit en revanche pas d'interdépendance puisque les microorganismes peuvent se développer indépendamment au sein du même environnement. Elle est également beaucoup moins spécifique, nécessite une proximité physique moindre et peut s'établir sur des périodes plus courtes que la symbiose (18). Les coopérations entre microorganismes sont ainsi plus fréquemment décrites que les interactions symbiotiques. De nombreux comportements coopératifs sont d'ailleurs observés au sein d'une même espèce microbienne pour maximiser la valeur sélective de la population dans un environnement donné. Les systèmes de QS sont particulièrement importants pour ces coopérations intra-spécifiques mais favorisent l'émergence de tricheurs dans la population (12, 13). Chez *P. aeruginosa* par exemple, la production d'exoprotéases est coûteuse pour un individu mais bénéficie à toute la population. Suite à des altérations génétiques, une baisse de production de ces protéines peut alors s'observer chez certains individus, qui vont néanmoins continuer à profiter des exoprotéases produites par le reste de la population (12, 19).

Enfin, le **commensalisme** ne bénéficie qu'à un seul partenaire de l'interaction, le second n'étant pas affecté. Les conditions de son établissement sont similaires à celles de la coopération (**Tableau 1**) (**Fig. 1**).

	Interaction	Impacts sur les micro-organismes A et B		Caractère obligatoire	Contact rapproché nécessaire	Durée d'interaction
		A	B			
Positive	Symbiose	+	+	Oui	Oui	Longue
	Coopération	+	+	Non	Non	Courte
	Commensalisme	+	0	Non	Non	Courte
Négatives	Parasitisme	+	-	Parfois	Oui	Longue
	Prédation	+	-	Non	Oui	Courte
	Amensalisme	0	-	Non	Non	Courte
	Compétition	-	-	Non	Non	Courte

Tableau 1 : Classification des interactions microbiennes selon leur effet positif (+), négatif (-) ou neutre (0) sur les microorganismes impliqués.

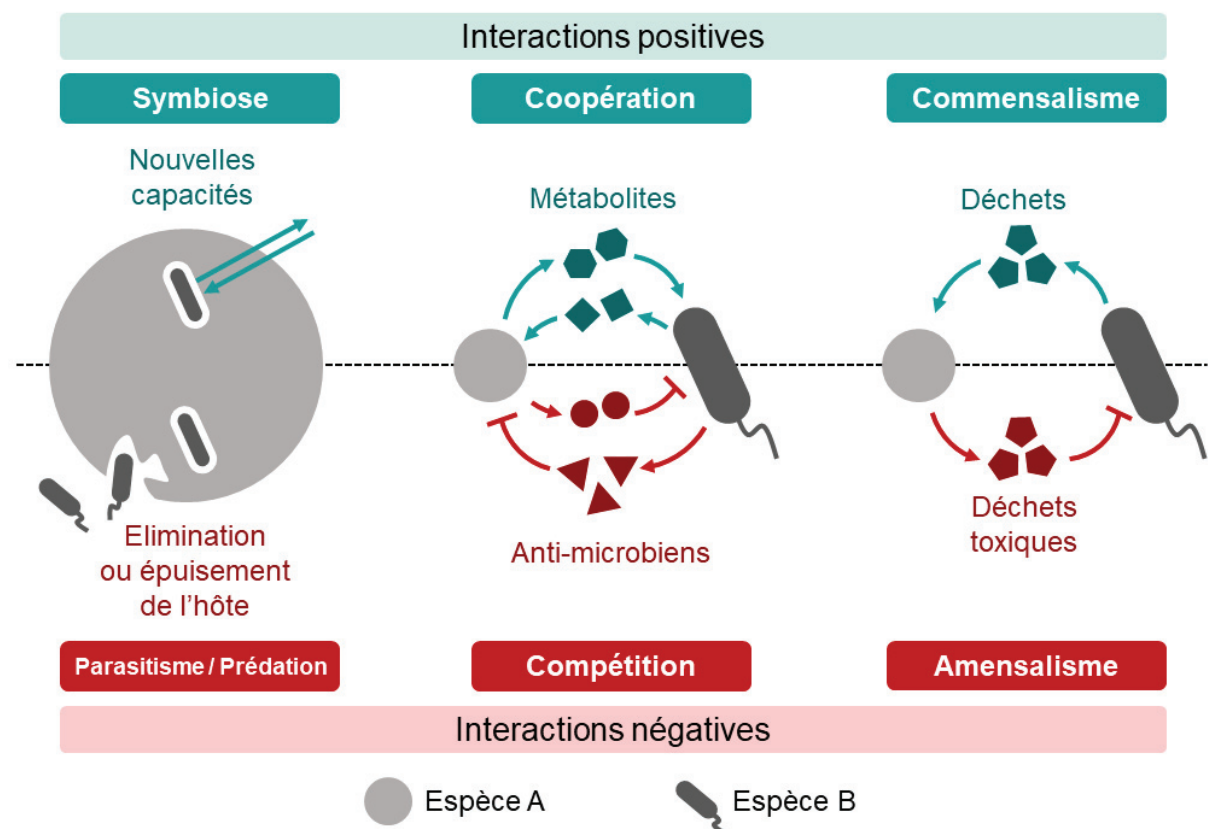


Figure 1 : Exemples d'interactions microbiennes positives et négatives entre deux microorganismes. Symbiose : Les espèces bénéficient toutes deux de nouvelles capacités métaboliques. Coopération : Les deux espèces se fournissent mutuellement des ressources. Commensalisme : L'espèce A est commensale de l'espèce B en bénéficiant des déchets rejetés par l'espèce B. Parasitisme : L'espèce B est parasite de l'espèce A, épuisant ses ressources potentiellement jusqu'à la lyse. Compétition : Les espèces inhibent leur croissance mutuelle à l'aide d'antimicrobiens. Amensalisme : L'espèce B est amensale de l'espèce A en étant négativement affectée par les déchets rejetés par l'espèce A.

Les interactions positives favorisent ainsi la valeur sélective d'au moins un des deux partenaires dans un environnement donné. De nombreux exemples de tels comportements sont décrits dans la littérature. Il a par exemple été montré que deux souches de *Escherichia coli* ne pouvaient survivre en présence d'ampicilline et de chloramphénicol qu'en conditions de co-culture, grâce à une protection croisée contre ces deux antibiotiques (20). Dans l'intestin des termites, la croissance du spirochète *Treponema primitia* est permise via l'acquisition de folate produit par d'autres microorganismes de l'écosystème tels que *Lactococcus lactis* et *Serratia grimesii* (21). Ceci illustre parfaitement la difficulté de catégoriser les interactions microbiennes, puisque les interactions citées dans ces deux exemples présentent un caractère obligatoire pour la croissance dans un écosystème spécifique (ici en présence d'antibiotiques ou dans l'intestin). Ces interactions ne sont cependant pas associées à une symbiose étant donné qu'elles ne nécessitent pas un contact prolongé entre les deux microorganismes pour s'opérer.

En réalité, la plupart des comportements mutualistes décrits chez les microorganismes ne présentent pas un caractère obligatoire, et vont simplement favoriser la valeur sélective des individus dans un environnement particulier. Des coopérations métaboliques sont ainsi fréquemment observées entre les microorganismes colonisateurs de la rhizosphère ou des intestins, favorisant leur développement malgré des conditions nutritives non optimales (13, 22–24) (**Fig. 1**). Au-delà d'une modification du métabolisme énergétique, les comportements coopératifs peuvent fortement impacter les capacités de colonisation des microorganismes. L'invasion du système intestinal par les *E. coli* entéro-hémorragiques est ainsi favorisée par le métabolisme de co-facteurs de type corrinoïdes produits par d'autres microorganismes de l'écosystème (23). D'autres mécanismes impliquent le partage de molécules surfactantes telles que les rhamnolipides (12), ou l'utilisation de structures hyphales ou mycélienne comme vecteurs de déplacement au sein de l'endosphère végétale (13). Enfin, la coexistence de plusieurs espèces microbiennes au sein d'un biofilm mixte peut également constituer une coopération et améliorer la croissance, la résistance antibiotique ou encore le pouvoir pathogène des microorganismes impliqués (25–27). Toutefois, la forte proximité des individus et le partage des ressources au sein du biofilm peuvent également générer des interactions négatives entre les microorganismes (27).

1.2.2. Interactions négatives

Une interaction négative est décrite comme affectant négativement au moins un des deux partenaires microbiens (**Tableau 1**) (**Fig. 1**). Un microorganisme prédateur ou parasite va ainsi bénéficier d'effets positifs aux dépens de la seconde espèce impliquée, et ceci au cours d'une interaction directe. Le **parasitisme** se distingue toutefois de la prédation par la durée prolongée du contact entre les deux microorganismes, à l'image de la symbiose. Il est d'ailleurs documenté que des interactions parasitaires peuvent résulter de l'évolution de relations initialement symbiotiques, et inversement. Dans la plupart des cas, le parasitisme implique également une différence de taille entre les deux microorganismes, permettant au parasite, plus petit, de coloniser son hôte. Les prophages peuvent ainsi être considérés comme des endoparasites obligatoires des bactéries, bénéficiant de la machinerie cellulaire de son hôte en s'intégrant dans son génome. Cette interaction peut d'ailleurs se rapprocher d'une relation symbiotique si la bactérie tire un bénéfice de l'intégration du virus, soulignant le continuum existant entre parasitisme et symbiose (28). Il existe cependant des interactions parasitaires non-obligatoires, comme par exemple entre la bactérie *Bdellovibrio bacteriovorus* et de nombreuses autres bactéries à Gram négatif (29, 30). Selon les études, *B. bacteriovorus* est également classée comme une espèce prédatrice puisque son internalisation et son développement dans le périplasme bactérien induisent rapidement la lyse de son hôte (29, 30). En effet, contrairement au parasitisme, la **prédation** est une interaction de courte durée conduisant à l'élimination de l'individu proie. Ici encore, une notion de différence de taille intervient puisque le prédateur est généralement plus grand que sa cible ; c'est par exemple le cas pour les protozoaires se nourrissant de microorganismes de plus petite taille.

Contrairement au parasitisme et à la prédation, l'**amensalisme** affecte négativement un seul des deux microorganismes, le second n'étant aucunement impacté (**Tableau 1**). Cette interaction est cependant beaucoup moins documentée et serait liée, dans la plupart des cas, à un déchet toxique pour un microorganisme rejeté dans l'environnement par une autre espèce (16, 31).

Enfin, la **compétition** affecte négativement les deux partenaires et est favorisée lorsque les microorganismes utilisent les mêmes ressources et/ou les mêmes niches d'un écosystème (32) (**Tableau 1**) (**Fig. 1**). La probabilité de développer un comportement compétitif est ainsi augmentée entre espèces aux besoins métaboliques proches ou colonisant des milieux peu hétérogènes (**Fig. 2**). La compétition peut alors être indirecte ou

« d'exploitation », si elle repose uniquement sur l'exploitation simultanée des mêmes ressources de l'environnement par les deux agents microbiens. Les microorganismes peuvent également développer des stratégies d'attaques directes envers les espèces concurrentes via une compétition d'interférence, aussi nommée antagonisme. Ce type de compétition fait généralement intervenir la production et la sécrétion de molécules ayant une action antimicrobienne, soit dans le milieu environnant ou directement dans le microorganisme concurrent (12–14, 32).

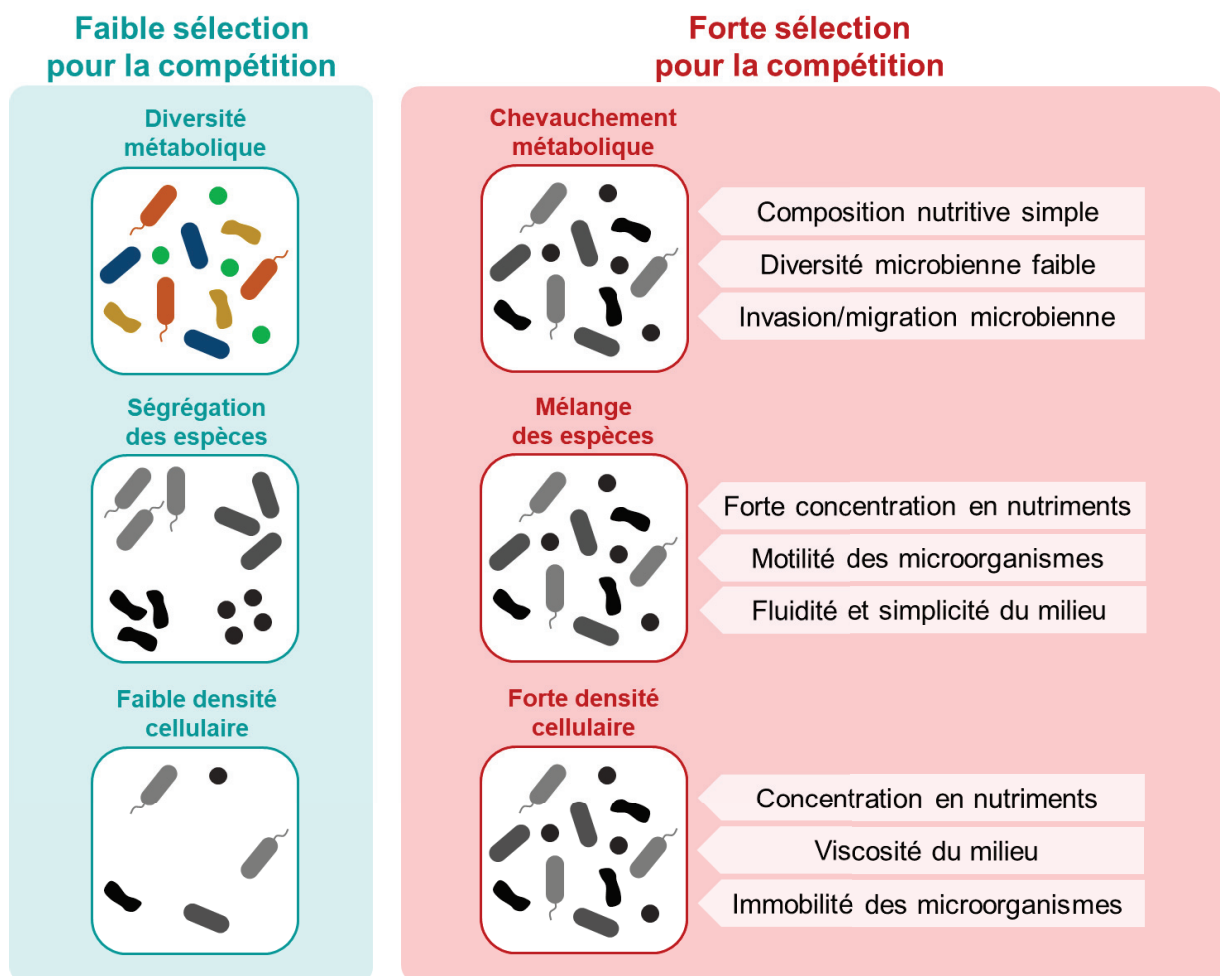


Figure 2 : Conditions écologiques favorisant les comportements compétitifs entre microorganismes. Adapté de Ghoul *et al.* (32).

De nombreux exemples d'interactions négatives sont ainsi décrits dans des environnements variés (32, 33). Elles impliquent fréquemment des membres du microbiote de l'écosystème d'intérêt. Les Lactobacilles du microbiote vaginal présentent par exemple un comportement particulièrement compétitif reposant sur la sécrétion d'acide lactique, de

peroxyde d'hydrogène et de bactériocines (Fig. 1). Les *Lactobacillus* arborent également une compétitivité d'adhésion qui, en parallèle des facteurs sécrétés, empêche la colonisation du tractus urogénital par d'autres microorganismes (34, 35). Dans l'écosystème épidermique, *Staphylococcus epidermidis* produit de nombreuses protéases détruisant le biofilm formé par *S. aureus* (36). De telles compétitions sont aussi observées entre les microorganismes colonisateurs et/ou pathogènes d'un écosystème. Le pathogène opportuniste *P. aeruginosa* inhibe ainsi la croissance de nombreux autres pathogènes comme *S. aureus*, *Candida albicans* ou *Aspergillus fumigatus* lors de la colonisation des poumons des patients atteints de mucoviscidose (37–39). Enfin, une intense compétition est également observée entre les microorganismes associés aux plantes, qui promeuvent leur colonisation en produisant de nombreux métabolites secondaires et volatiles ayant une action antimicrobienne (13). Les interactions négatives affectent ainsi fortement les capacités de colonisation et de persistance des microorganismes dans un écosystème.

1.3. Impact des interactions microbiennes sur l'hôte

En plus d'impacter fortement leur physiologie et leur environnement, les microorganismes et leurs interactions peuvent affecter positivement ou négativement l'hôte qu'ils colonisent. Les interactions négatives impliquant le microbiote et des microorganismes colonisateurs et/ou pathogènes sont généralement bénéfiques pour l'hôte puisqu'elles le protègent de potentielles infections. Ce phénomène a suscité un engouement de la recherche scientifique pour le microbiote depuis ces 10 dernières années, et est maintenant décrit dans de nombreux écosystèmes. Chez les plantes, la sévérité de l'infection racinaire par *Ralstonia solanacearum* est ainsi réduite lorsque le pathogène entre en compétition avec des souches non-pathogènes de la même espèce ou les populations de *Pseudomonas* de la rhizosphère (13). Chez les mammifères, les Lactobacilles vaginaux protègent l'hôte des infections à *S. aureus*, *C. albicans* ou encore *E. coli* en inhibant leur croissance (34, 35), *S. epidermidis* empêche le développement et la formation de biofilm de *S. aureus* sur la peau (36), tandis que le microbiote gastro-intestinal réprime la virulence des pathogènes diarrhéiques du genre *Salmonella* ou *Clostridium* (40). De la même manière, les *Streptococcus* commensaux issus de la cavité orale inhibent la croissance de *P. aeruginosa* dans les poumons, et sont ainsi associés à une stabilisation des fonctions respiratoires des patients atteints de mucoviscidose (41, 42). La colonisation par plusieurs pathogènes peut également bénéficier à l'hôte si cette co-infection est moins sévère qu'une mono-infection. Cependant, ce phénomène repose généralement sur une modification du système immunitaire de l'hôte par un des deux agents, et non sur une interaction directe entre les microorganismes (43–45). Il a toutefois été récemment observé que les produits de sécrétion du pathogène opportuniste *Morganella morganii* avaient une action directe et inhibitrice sur l'activité pathogénique de *Proteus mirabilis*, *E. coli* et *Enterococcus faecalis* au cours des infections du tractus urinaire (46).

Les interactions entre le microbiote et les microorganismes colonisateurs peuvent également avoir un impact négatif sur l'hôte. Ainsi, les infections virales sont favorisées par la richesse du microbiote pulmonaire des patients atteints de mucoviscidose (47). De la même manière, le parasitisme viral des bactéries du tractus intestinal favorise les infections par des virus entériques, dont l'attachement aux cellules hôtes est amélioré par le peptidoglycane bactérien (48). Bien que les streptocoques oraux puissent inhiber la croissance de *P. aeruginosa* dans les poumons des patients atteints de mucoviscidose (41), il a aussi été démontré que leur interaction pouvait stimuler la virulence de *P. aeruginosa* et conduire à une dysbiose de l'écosystème pulmonaire (49, 50). De manière peu surprenante, les interactions

entre les pathogènes co-colonisateurs ont fréquemment un impact négatif sur la santé de l'hôte et participent à la synergie des infections polymicrobiennes (9). Des comportements coopératifs sont par exemple observés entre *S. aureus* et plusieurs pathogènes co-colonisateurs tels que *C. albicans*, *Haemophilus influenzae* ou *E. faecalis*. Le biofilm mixte formé par *C. albicans* et *S. aureus* est ainsi particulièrement stable, améliore la résistance antibiotique de *S. aureus* et augmente la sévérité des infections impliquant ces deux pathogènes (51). Ce phénomène est également observé au sein de l'holobionte végétal, dont certains champignons pathogènes présentent une production de toxine améliorée grâce à leur interaction avec des bactéries endosymbiotiques (13, 52).

1.4. Modèles d'étude des interactions microbiennes

Tous les exemples cités précédemment démontrent l'impact considérable des interactions microbiennes sur la physiologie des microorganismes, leur environnement et l'hôte qu'ils colonisent. La communauté scientifique cherche donc de plus à plus à inclure plusieurs partenaires microbiens dans les dispositifs d'étude afin de mieux évaluer le rôle essentiel de leurs interactions. Cette approche se base sur la création de communautés microbiennes synthétiques composées d'au moins deux espèces, générées *in silico* ou expérimentalement (53, 54). Du fait des contraintes expérimentales, les communautés synthétiques constituées *in vitro* incluent généralement moins de partenaires que celles modélisées informatiquement. De nombreuses études évaluent ainsi les mécanismes de bases des interactions entre deux ou trois microorganismes (55–59), tandis que d'autres cherchent à reproduire des communautés plus complexes de plus de dix partenaires (54, 60). Différents dispositifs expérimentaux peuvent également être employés dans ce contexte. Les modèles de co-culture liquide *in vitro* sont les plus simples à mettre en œuvre mais sont souvent limités par leur manque de réalisme par rapport aux conditions réelles dans lesquelles les microorganismes évoluent. Du fait de la fréquence des biofilms mixtes dans le monde microbien, de nombreuses études évaluent les interactions entre microorganismes au sein de dispositifs statiques ou dynamiques de biofilms multi-espèces (61–64). Enfin, les modèles de co-infection *in vivo* sont sans surprise les plus réalistes puisqu'ils permettent de réunir plusieurs pathogènes et le microbiote hôte au sein de la communauté synthétique (65, 66).

Ces dispositifs expérimentaux ont déjà prouvé leur intérêt dans de nombreux contextes. Par exemple, la compréhension des mécanismes d'antagonisme entre microorganismes permet la découverte de nouvelles stratégies de lutte antimicrobienne (67). Le décryptage de ces interactions permet également d'identifier les facteurs participant au maintien des microorganismes pathogènes dans l'hôte, et ainsi ouvrir de nouvelles perspectives de traitement des infections. La manipulation du microbiote hôte *via* l'utilisation de probiotiques en est un exemple. L'étude des interactions microbiennes apparaît donc essentielle pour améliorer la compréhension et la prise en charge des nombreuses pathologies impliquant plusieurs microorganismes. C'est notamment le cas des infections pulmonaires survenant chez les patients atteints de mucoviscidose, dont le caractère polymicrobien favorise les interactions entre microorganismes et limite l'efficacité des traitements actuels (68, 69).

2 La mucoviscidose comme contexte d'étude des interactions microbiennes

2.1. Physiopathologie de la mucoviscidose

2.1.1. Généralités

La mucoviscidose est une maladie génétique dont les premiers cas furent observés en 1938 (70). On dénombre à ce jour environ 70 000 patients atteints de mucoviscidose dans le monde, avec une incidence très variable entre les pays (71). La maladie est ainsi plus fréquemment retrouvée chez les caucasiens avec une incidence de 1/2500-3000, tandis que seulement un américain d'origine asiatique sur 100 000 est touché par la mucoviscidose (72–75). Cette incidence peut également être très hétérogène au sein d'un même pays : elle est par exemple deux fois plus élevée en Bretagne (1/11 000) que dans le reste de la France (1/23 000) (75, 76). Ces différences d'incidence inter- et intra-pays sont principalement liées à une distribution hétérogène des mutations pouvant causer la maladie, notamment induite par les échanges populationnels ayant eu lieu entre les différentes zones du globe (76).

La population mucoviscidosique est composée d'environ autant d'hommes que de femmes, dont l'espérance de vie est aujourd'hui de plus de 50 ans en Europe et aux Etats-Unis (77–79). Depuis les premières études épidémiologiques en 1983, ceci représente une augmentation de la durée de vie de 26 ans, permise grâce à l'important suivi des patients atteints de mucoviscidose et aux efforts de la recherche scientifique. En effet, la tenue de registres nationaux et internationaux, la constitution des Centres de Ressources et de Compétences en Mucoviscidose (CRCM) ainsi que l'amélioration du diagnostic de la maladie chez les nouveau-nés ont grandement participé à l'amélioration de la prise en charge et ainsi à l'augmentation de l'espérance de vie des patients atteints de mucoviscidose (80).

2.1.2. Origine génétique de la maladie

a. Mutations du gène *cftr*

La mucoviscidose est une maladie monogénique autosomale récessive causée par une altération du gène codant le canal transmembranaire CFTR (*Cystic Fibrosis Transmembrane Regulator*). Ce n'est qu'en 1989 que les premières mutations du gène *cftr* furent mises en évidence et incriminées dans la mucoviscidose, soit 50 ans après les premiers patients identifiés (81). Plus de 2000 mutations différentes du gène *cftr* sont aujourd'hui

recensées et classées selon leur impact sur la fonction du canal CFTR (82, 83) (**Tableau 2**) (**Fig. 3**). Les mutations de type 1 à 3 sont ainsi les plus sévères puisqu'elles engendrent une protéine absente de la membrane et/ou totalement non fonctionnelle, tandis que les mutations de type 4 à 6 permettent à la protéine CFTR de ne remplir que partiellement ses fonctions (82, 84, 85) (**Fig. 3**). Il est important de noter que d'autres systèmes de classification des mutations du gène *cftr* ont été proposés et reposent notamment sur le bilan clinique ou les thérapies possibles (82, 85, 86).

Classe	Défaut	Exemples	Production protéique	Adressage membranaire	Fonction protéique	Sévérité
1	Transcription ou traduction	G542X	X	X	X	Forte
2	Maturation/dégradation de la protéine	F508del	✓	X	X	
3	Régulation du canal CFTR	G551D	✓	✓	X	
4	Conductance	R117H	✓	✓	-	Moyenne
5	Epissage et adressage à la membrane	A455E	-	-	-	
6	Stabilité et recyclage	N287Y	✓	✓	-	

Tableau 2 : Classes de mutations du gène *cftr*. La couleur de la case et le symbole indiquent la fonctionnalité de la synthèse protéique, de l'adressage membranaire ou de la protéine : normale (✓), réduite (-) ou abolie (X).

Sur les 2000 mutations identifiées, seulement 20 sont retrouvées à une fréquence supérieure à 0,1% chez les patients atteints de mucoviscidose à l'échelle mondiale, les autres altérations génétiques restant très rares. Les plus fréquentes sont ainsi les mutations F508del (classe 2), G252X (classe 1) et G551D (classe 3) (82). A l'image des populations mucoviscidosiques, ces mutations présentent une répartition hétérogène et sont davantage retrouvées chez les patients du sud de l'Europe (F508del), du bassin méditerranéen (G252X) ou de République Tchèque (G551D) (83).

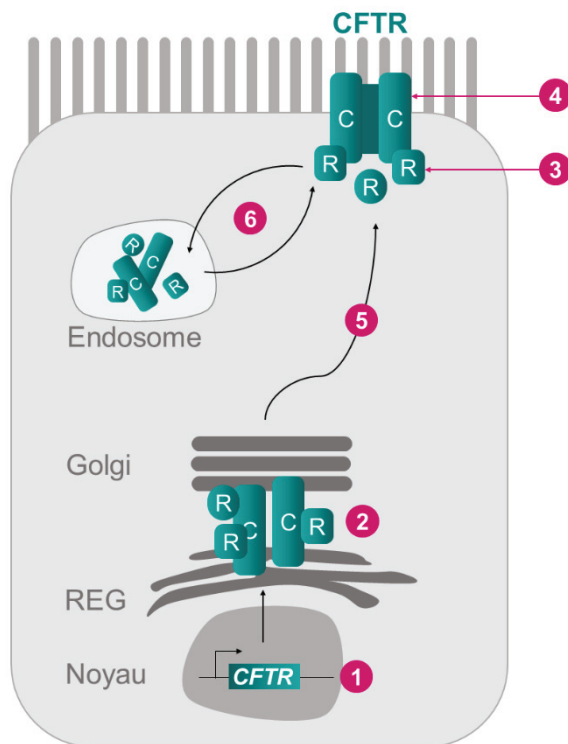


Figure 3 : Classes de mutations du gène *cftr*. Adapté de Fajac *et al.* (82).

Classe 1 : l'ARNm et/ou la protéine ne sont pas synthétisés.

Classe 2 : La protéine n'est pas acheminée correctement à la membrane et dégradée prématurément.

Classe 3 : La protéine est présente à la membrane mais peu ou pas fonctionnelle à cause d'un défaut de régulation.

Classe 4 : La protéine est présente à la membrane mais le canal présente un défaut de conductance.

Classe 5 : La protéine est présente en faible quantité à la membrane suite à un épissage aberrant ou un trafic réduit.

Classe 6 : La protéine est présente en faible quantité à la membrane suite à un recyclage trop important *via* la voie endosomale.

C = sous-unités protéiques formant le canal.

R = sous-unités régulatrices du canal.

REG = réticulum endoplasmique rugueux.

b. Fonctionnement normal du canal CFTR

L'expression du gène *cftr* et la production de la protéine correspondante s'effectuent dans les cellules épithéliales de divers organes comme les poumons, le foie, le pancréas, ainsi que les tractus digestifs et reproducteurs (87, 88). La protéine CFTR est un canal membranaire de type transporteur ABC (*ATP Binding Cassette*), impliqué dans l'import et l'export actifs des ions bromure (Br^-), chlorure (Cl^-), iodure (I^-) et fluorure (F^-). Il peut également prendre en charge les ions bicarbonate (HCO_3^-), le glutathion (GSH) et le thiocyanate (SCN^-) (89, 90). En plus de son rôle de transporteur, le canal CFTR aurait également des fonctions régulatrices sur d'autres transporteurs tels que ENaC (sodium), ORCC (chlorure) ou les aquaporines (91–93). Ce canal intervient ainsi dans l'homéostasie ionique des cellules épithéliales conjointement avec d'autres canaux ioniques et le transport passif de l'eau (**Fig. 4A**) (93). Ainsi, lors de l'excrétion des sels par les cellules épithéliales :

- (1) Le canal CFTR transporte activement les ions chlorure à travers la membrane du pôle apical de la cellule.
- (2) Les anions chlorures s'accumulent et créent une différence de potentiel, favorisant la sortie des cations Na^+ par un transport paracellulaire.

- (3) Les ions sodium et chlorure se condensent alors en NaCl à l'extérieur de la cellule, créant un déséquilibre osmotique par rapport au cytoplasmique.
- (4) Ce déséquilibre est compensé par la sortie passive d'eau des cellules épithéliales via les aquaporines ou le transport paracellulaire.

Les activités de transport de CFTR sont particulièrement importantes au niveau des poumons, du pancréas et de l'intestin. D'une part, l'export passif d'eau induit par l'accumulation des ions Na^+ et Cl^- au pôle apical des cellules permet l'hydratation du mucus des organes. D'autre part, les ions HCO_3^- sécrétés par CFTR sont impliqués dans le contrôle de la réticulation des mucines présentes dans le mucus pulmonaire (90, 93). L'hydratation du mucus et la bonne réticulation des mucines assurent ainsi des bonnes propriétés rhéologiques au mucus, permettant une clairance mucociliaire optimale au niveau des voies respiratoires. Le bicarbonate exporté par CFTR participe également à l'homéostasie acido-basique de ces liquides de surface, essentiel au bon fonctionnement des peptides antimicrobiens et anticorps sécrétés par les cellules. Enfin, le glutathion et le thiocyanate interagissent avec les espèces réactives de l'oxygène (ROS) dans le milieu extracellulaire, avec pour conséquence de contrôler leur concentration et favoriser la production de molécules ayant un effet antimicrobien (89, 94).

c. Conséquences des mutations du gène *cftr*

L'altération du canal CFTR induit une perte partielle ou totale de ses fonctions de transporteur dans les organes impactés (**Fig. 4B**) (**Tableau 2**). En conséquence, les ions chlorures et sodium normalement sécrétés par le canal CFTR ou par export passif se condensent sous forme de sels et s'accumulent dans les cellules épithéliales. Le gradient osmotique généré est alors compensé par une entrée d'eau passive dans le cytoplasme depuis le mucus. En addition, les ions HCO_3^- ne sont plus sécrétés et ne peuvent plus remplir leur rôle régulateur dans la réticulation des mucines et l'homéostasie acido-basique du mucus. Les fluides de surface sont ainsi déshydratés, épaissis et acidifiés, obstruant la lumière des organes impactés et limitant le fonctionnement des protéines sécrétées par les cellules épithéliales. Au niveau des poumons, l'épaississement des liquides de surface respiratoires affecte également fortement l'efficacité de la clairance mucociliaire (90, 93, 95). Enfin, les concentrations en ROS dans le mucus ne sont plus régulées par le glutathion et le thiocyanate, augmentent et endommagent les cellules épithéliales (89, 94) (**Fig. 4B**).

Ces perturbations peuvent avoir de nombreuses conséquences cliniques chez les patients atteints de mucoviscidose : occlusions intestinales et reflux gastriques, malnutrition et diabète, insuffisances et infections pancréatiques, infections pulmonaires et dégradation des fonctions respiratoires (75, 85, 96, 97). D'autres pathologies sont également associées à l'altération du gène *cftr* ou aux traitements de la mucoviscidose telles que des dégénérescences osseuses, la stérilité masculine, la surdité, l'insuffisance rénale ou encore des syndromes dépressifs liés à la prise en charge lourde et difficile de la maladie (75, 98, 99). Les pathologies respiratoires restent cependant les plus graves et constituent la première cause de mortalité chez les patients atteints de mucoviscidose (100). L'efficacité réduite de la clairance mucociliaire et du système immunitaire suite à l'altération du gène *cftr* favorise en effet les infections pulmonaires polymicrobiennes sévères. Ces dernières induisent une inflammation chronique des voies aériennes chez les patients et un déclin progressif de leurs capacités pulmonaires. En addition, des épisodes d'inflammation et de détérioration clinique élevée nommés exacerbations peuvent survenir aléatoirement et accélérer le déclin des fonctions respiratoires des patients (100).

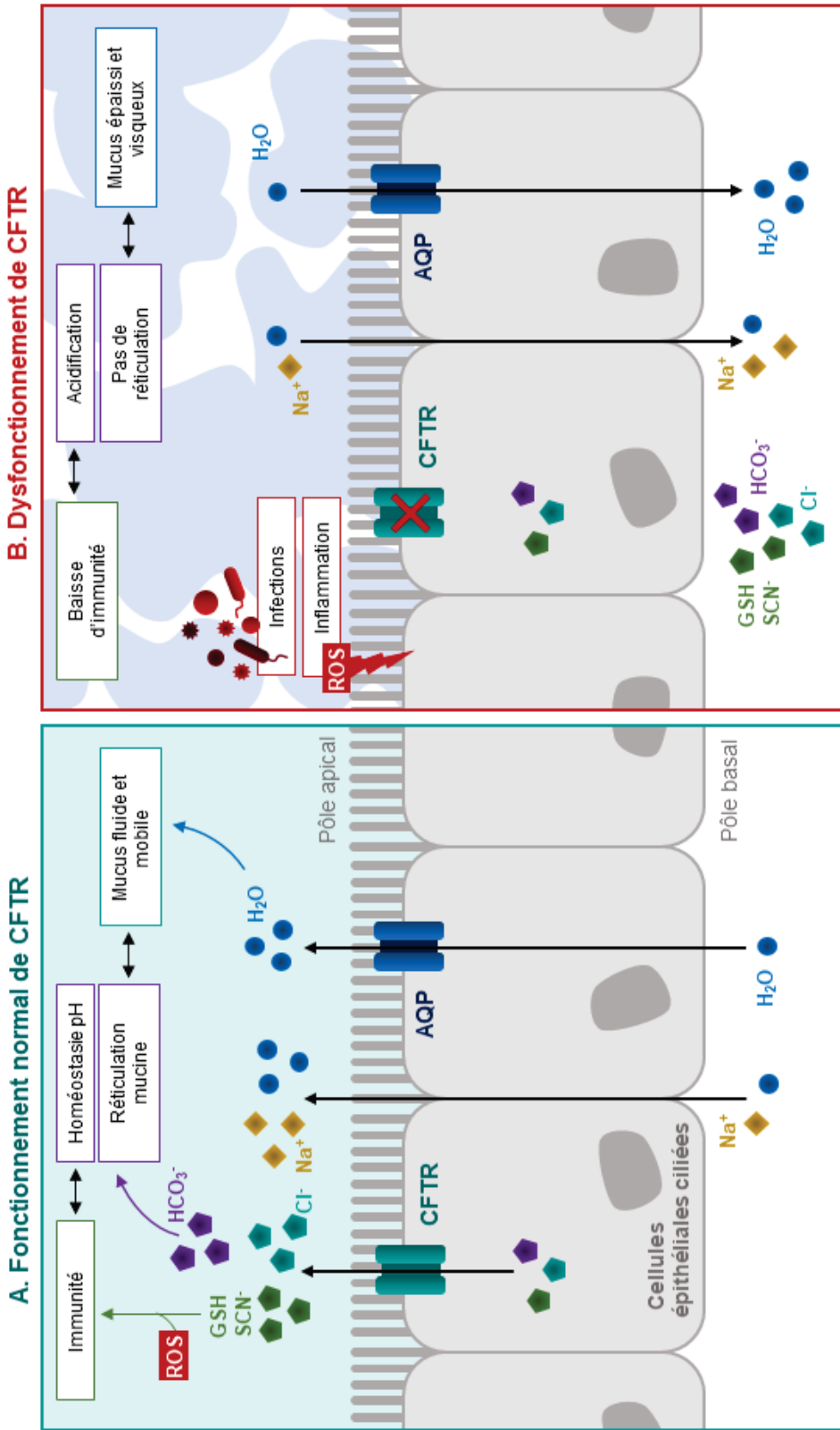


Figure 4 : Conséquences physiologiques du fonctionnement normal (A) ou du dysfonctionnement (B) du canal CFTR au niveau des cellules épithéliales pulmonaires. A. Le canal exporte activement le chlorure (Cl^-), le bicarbonate (HCO_3^-), le glutathion (GSH) et le thiocyanate (SCN^-). Le gradient électrochimique formé favorise le transport passif paracellulaire de sodium (Na^+), puis d'eau par un transport passif paracellulaire ou via les aquaporines (AQP) afin de compenser le choc osmotique induit par l'accumulation extracellulaire de NaCl . Les ions HCO_3^- régulent le pH et la réticulation de la mucine en séquestrant les ions H^+ et Ca^{2+} . Le GSH et le SCN^- interagissent avec les espèces réactives de l'oxygène (ROS). **B.** Le canal CFTR ne remplit plus sa fonction de transport et les molécules Cl^- , HCO_3^- , GSH et SCN^- s'accumulent dans les cellules épithéliales et au pôle basal. La forte concentration en Cl^- favorise l'entrée de Na^+ et d'eau dans la cellule. Les ions HCO_3^- ne régulent plus le pH et la réticulation protéique, induisant une acidification et un épaississement du mucus. Ce mucus et la baisse d'immunité favorisent les infections polymicrobiennes, qui, de concert avec les ROS non séquestrés, induisent une inflammation des cellules épithéliales.

2.2. Infections pulmonaires polymicrobiennes

2.2.1. **Caractérisation du microbiome pulmonaire**

L'environnement pulmonaire a longtemps été considéré comme stérile et exclu des études d'identification du microbiote humain. D'une part, les procédures d'échantillonnages pulmonaires sont généralement difficiles à appliquer du fait de leur caractère invasif et des probabilités de contamination par les microorganismes résidant dans les voies aériennes supérieures (101, 102). D'autre part, les méthodes cultures-dépendantes usuellement réalisées limitent l'identification des espèces plus difficilement cultivables telles que les microorganismes anaérobies. Les approches métagénomiques permettent quant à elles d'étudier le microbiome d'un écosystème : l'ensemble des gènes présents dans le microbiote. Ces approches ont ainsi permis une caractérisation plus exhaustive du microbiome et ainsi du microbiote pulmonaire des individus sains ou atteints de pathologies respiratoires (101–103). Il est toutefois nécessaire de noter que ces méthodes métagénomiques présentent également leurs limites, les résultats de séquençage pouvant être influencés par les protocoles d'extraction ADN effectués ou par l'ADN résiduel de cellules mortes dans l'environnement pulmonaire (102). Les nombreuses études métagénomiques réalisées ont toutefois permis d'identifier que le microbiome pulmonaire des personnes saines était majoritairement constitué de bactéries anaérobies strictes ou facultatives du phylum des *Firmicutes*, *Bacterioidetes*, *Proteobacteria*, *Fusobacteria* et *Actinobacteria*. Les espèces *Prevotella*, *Veillonella* et *Streptococcus* sont prédominantes et acquises dès la naissance via l'environnement ou une transmission par la mère (101, 104, 105). La composition et la diversité du microbiome pulmonaire sont cependant sujettes à d'importantes variations induites par les pathologies respiratoires comme la mucoviscidose (69, 101, 106).

Le microbiome pulmonaire des patients atteints de mucoviscidose est très diversifié entre les sujets et sa signature métagénomique est généralement patient-spécifique, limitant les conclusions des analyses réalisées sur un faible nombre d'échantillons (106–108). En 2016, deux études métagénomiques réalisées sur près de 1000 expectorations de 142 patients ont permis d'observer que les principaux membres du microbiome pulmonaire sain étaient présents chez les patients atteints de mucoviscidose, comme les espèces bactériennes *Streptococcus*, *Prevotella*, *Veillonella* et *Fusobacterium*. Il apparaît cependant que l'abondance de ces microorganismes au sein des poumons des patients atteints de mucoviscidose est plus faible que celle des espèces pathogènes du genre *Pseudomonas*, *Staphylococcus*, *Haemophilus*, *Stenotrophomonas*, *Burkholderia* et *Achromobacter* (103, 106, 109) (Fig. 5).

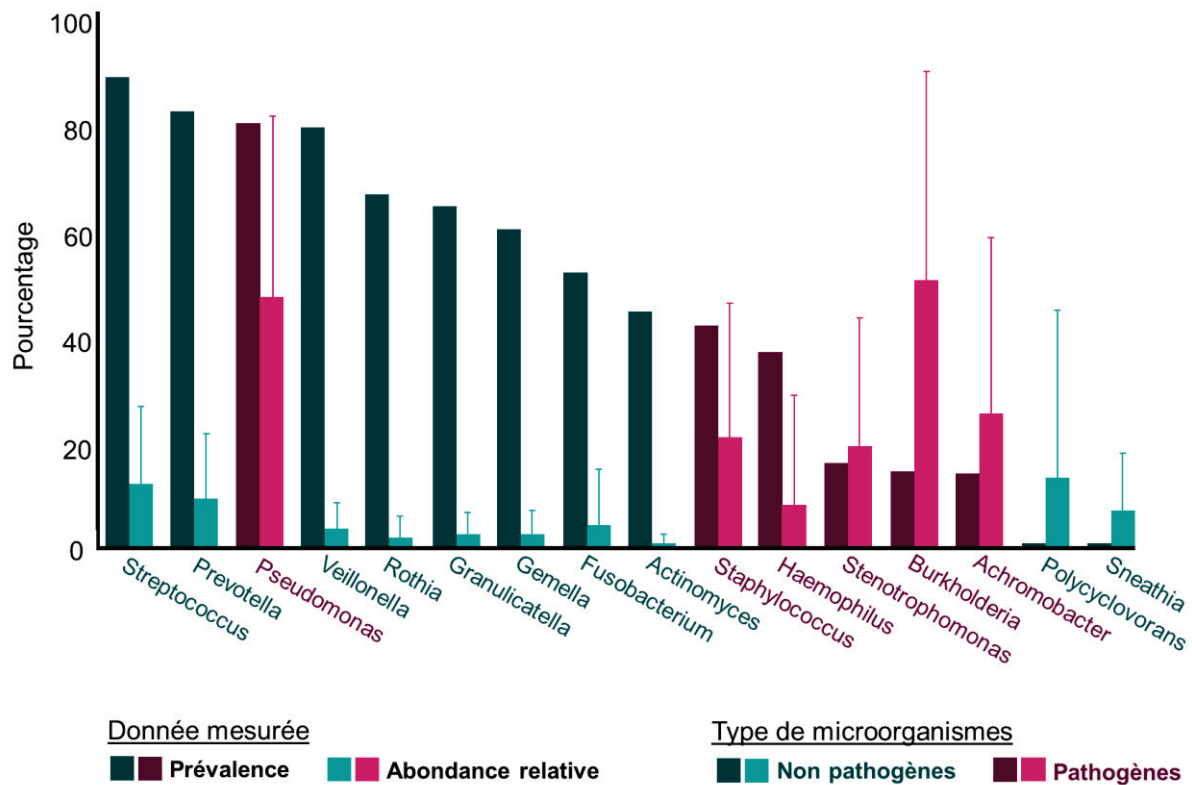


Figure 5 : Prévalence et abondance relative des genres bactériens identifiés dans le microbiome pulmonaire des patients atteints de mucoviscidose. Les barres représentent la prévalence (barres foncées) ou l'abondance relative moyenne + SED (barres claires) des 10 genres microbiens non-pathogènes (barres bleues) ou pathogènes (barres roses) les plus prévalents et /ou abondants détectés dans 945 expectorations de patients. Adapté de Mahboubi *et al.* (103).

2.2.2. Evolution du microbiome pulmonaire pendant l'infection

La composition et la diversité du microbiome pulmonaire des patients atteints de mucoviscidose varient fortement dans le temps. Les sujets pédiatriques présentent ainsi une diversité microbiologique pulmonaire plus élevée que les patients adultes, principalement composée d'espèces du microbiome sain telles que *Streptococcus*, *Prevotella* ou *Veillonella* (110–112). Avec l'avancée de la maladie et le vieillissement des individus, cette diversité tend à diminuer pour favoriser la dominance des microorganismes pathogènes cités précédemment (113–115). Ceci s'effectue au détriment des espèces du microbiome sain, dont l'abondance est négativement corrélée à l'inflammation des voies respiratoires (112, 114). Ces changements de composition du microbiome pulmonaire sont ainsi associés au déclin progressif des fonctions respiratoires des patients : alors que les patients cliniquement stables présentent un microbiome relativement constant dans le temps, une baisse de diversité microbienne associée à une dominance d'espèces pathogènes s'observe chez les patients sévèrement affectés (114, 115).

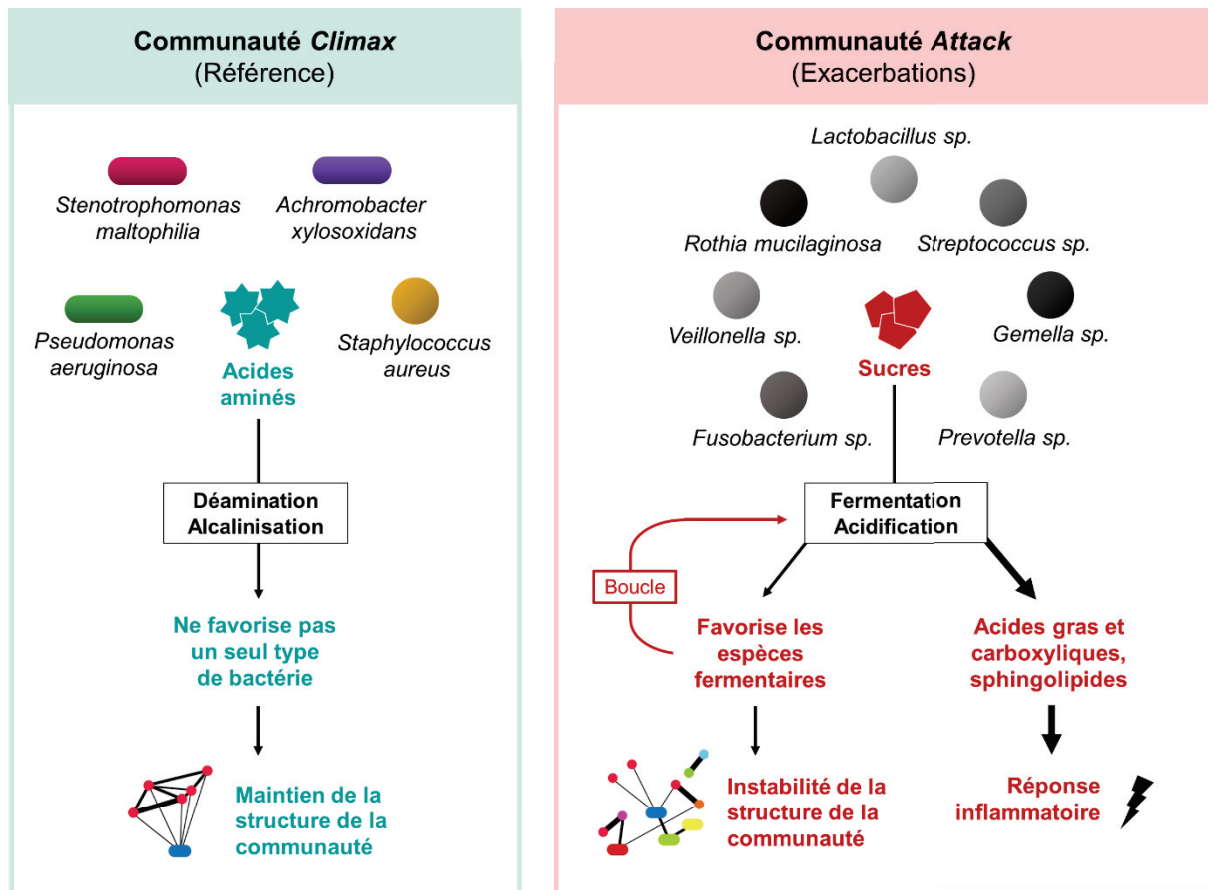


Figure 6 : Modèle Climax-Attack des exacerbations chez les patients atteints de mucoviscidose proposé par Quinn et al.. Les communautés contenant différentes physiologies microbiennes affectent leur environnement différemment, notamment par des changements de pH induits par leurs activités métaboliques. Ceci résulte en une stabilisation de la communauté pendant la croissance de la communauté Climax. Lors des exacerbations, l'acidification et les produits de fermentation générés par la communauté Attack favorisent les espèces fermentaires, destabilisant les communautés et induisant une forte réponse inflammatoire. Adapté de Quinn et al. et Lamoureux et al. (109, 116).

Le développement des exacerbations peut également être partiellement expliqué par des changements dans la composition du microbiome pulmonaire. De façon intéressante, les exacerbations ne sont pas nécessairement liées à une espèce pathogène connue mais résultent fréquemment de la dominance d'espèces anaérobies non pathogènes au sein des poumons. L'abondance des bactéries anaérobies est ainsi augmentée lors de l'exacerbation, puis diminuée par les traitements antibiotiques au profit des pathogènes résistants comme *P. aeruginosa* (117–119). Il a donc été proposé que les exacerbations reposeraient sur le modèle *Climax-Attack* : la communauté microbienne *Climax* serait composée des pathogènes résistants aux antibiotiques et associée à un état basal (c'est-à-dire sans exacerbation), tandis que les anaérobies non-pathogènes constitueraient la communauté *Attack* et domineraient pendant les exacerbations. Lors de leur pic d'abondance, les communautés anaérobies modifieraient les propriétés physico-chimiques de leur écosystème par leur métabolisme de fermentation. L'acidification engendrée limiterait alors la croissance des autres pathogènes

mais favorisait encore davantage celle des bactéries fermentaires, conduisant à un déséquilibre des communautés microbiennes et une forte production de sphingolipides, d'acides gras et carboxyliques par la population anaérobie. Du fait de leur effet sur les réponses inflammatoires et immunitaires des cellules hôtes, ces composés participeraient à la forte inflammation pulmonaire observée lors des exacerbations (Fig. 6). Ces molécules produites par les espèces anaérobies pourraient également augmenter la virulence des espèces pathogènes telles que *P. aeruginosa* (116, 117, 120). Le rôle du microbiote anaérobie dans l'évolution de la maladie demeure donc ambigu et semble dépendre de son abondance : bien qu'une baisse d'abondance soit associée à un déclin des capacités respiratoires, une abondance trop élevée de micro-organismes anaérobies favorise les exacerbations et peut donc aussi avoir un effet négatif sur les fonctions pulmonaires. Les causes de ces variations d'abondance du microbiome anaérobie restent cependant mal comprises (109, 120).

2.2.3. Principaux pathogènes pulmonaires

Les communautés pathogènes du microbiome pulmonaire sont principalement composées de bactéries, dont la prévalence varie selon l'âge des patients. Les bactéries les plus prévalentes sont *S. aureus* et *P. aeruginosa* : alors que la colonisation des poumons par *S. aureus* est très précoce et concerne jusqu'à 80% des patients de 10-14 ans, l'infection par *P. aeruginosa* se développe plus tardivement pour affecter plus de 50% des adultes de 25-29 ans (Fig. 7). Les infections causées par *S. aureus* et *P. aeruginosa* seront davantage détaillées dans le chapitre suivant. En plus de *S. aureus*, les patients pédiatriques présentent fréquemment des infections à *H. influenzae*. La bactérie est ainsi isolée chez 30% des patients de 5 à 9 ans, puis sa prévalence décroît légèrement pour se stabiliser chez les patients plus âgés (10 à 15% des patients). Cette stabilisation est liée à la chronicité de ces infections, favorisée par les capacités élevées de résistance antibiotique et d'adhésion aux cellules hôtes de *H. influenzae* (121). La colonisation des poumons par les bactéries du genre *Burkholderia* est plus rare et touche jusqu'à 5% des patients (Fig. 7). Ces infections sont toutefois sévères et difficiles à traiter du fait de la virulence et de la résistance intrinsèque de la bactérie aux antibiotiques (68). A ces pathogènes parfois considérés « classiques » dans la mucoviscidose s'ajoutent des bactéries pathogènes émergentes tels que *Stenotrophomonas maltophilia*, *Achromobacter xylosoxidans* ou *Mycobacterium abscessus*. La prévalence de leurs infections reste inférieure à 20% mais a augmenté de 1 à 3% en l'espace de 10 ans (75). Leur impact sur la pathologie pulmonaire chez les patients atteints de mucoviscidose est de plus en plus considéré du fait de leur résistance aux antibiotiques, leur capacité à former du biofilm ou encore leur transmissibilité interhumaine (122–124).

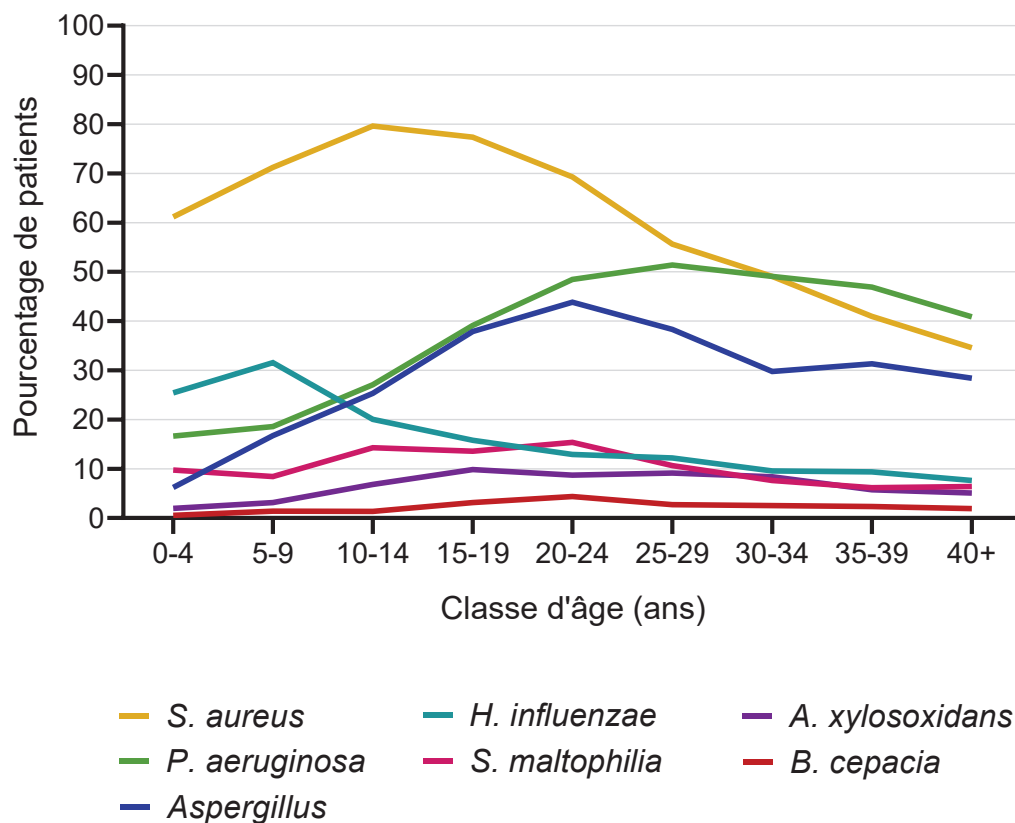


Figure 7 : Prévalence des principales espèces pathogènes colonisant les poumons des patients atteints de mucoviscidose selon leur classe d'âge. Adapté du Registre Français de la Mucoviscidose 2017 (75).

Les patients atteints de mucoviscidose sont également sujets à des infections pulmonaires fongiques. Les champignons du genre *Aspergillus* colonisent environ 30% des patients de façon asymptomatique, mais peuvent être à l'origine d'aspergilloses allergiques induisant un déclin des fonctions respiratoires (125–127). Les espèces du genre *Candida* sont également très fréquemment retrouvées puisqu'elles sont identifiées dans les poumons de 75% des patients atteints de mucoviscidose (126). Leur forte prévalence dans l'écosystème pulmonaire pourrait être liée à leur présence dans les cavités orales, et leur impact sur les fonctions respiratoires reste encore débattu (68, 125, 128). Enfin, bien que leur abondance reste faible, de nombreux virus colonisent le système pulmonaire des patients atteints de mucoviscidose et peuvent augmenter le risque d'exacerbations. Les virus les plus communément retrouvés sont les virus respiratoires syncytial et grippal, ainsi que les rhinovirus (68).

2.3. *S. aureus* et *P. aeruginosa* dans la mucoviscidose

2.3.1. *S. aureus*

La prévalence de *S. aureus* chez les jeunes patients atteints de mucoviscidose est généralement très élevée mais varie fortement selon les pays. Ainsi, si 70 à 80% des patients français et américains présentent une infection précoce par le staphylocoque, elle ne concerne que 30% de la cohorte pédiatrique anglo-saxonne, pour des raisons encore peu claires (75, 129). Dans tous les cas, la colonisation des voies respiratoires par *S. aureus* est associée à une forte inflammation et une diminution des fonctions respiratoires, particulièrement chez les sujets pédiatriques (130–133). Ce phénomène est exacerbé si l'infection à *S. aureus* se produit dans les 2 premières années de vie du patient, et si la souche responsable est résistante à la méthiciline (SARM : *Staphylococcus Aureus Résistant à la Méthiciline*). En comparaison aux souches sensibles à la méthiciline, les infections chroniques par des souches SARM sont associées à une augmentation de l'inflammation, un bilan clinique plus sévère et une mortalité plus élevée (133–136). Cet effet ne peut être que partiellement expliqué par la forte résistance aux antibiotiques des SARM, et reste donc encore mal compris. A l'image des souches de *S. aureus*, la prévalence des SARM varie fortement selon les pays. Bien que relativement faible en France et en Angleterre (2 à 6%), elle est beaucoup plus importante aux Etats-Unis (26%) et serait liée à la plus forte prévalence des SARM dans ce pays et à des facteurs environnementaux (75, 129).

Les procédures de traitement des infections pulmonaires à *S. aureus* sont encore débattues et varient suivant les pays. Du fait de leur impact clinique important, la colonisation des poumons par des SARM est généralement traitée de façon agressive aux antibiotiques, mais ce traitement conduit fréquemment à une récurrence et une persistance de l'infection (129, 135, 136). L'intérêt de l'usage prophylactique des antibiotiques contre la colonisation précoce des poumons à *S. aureus* reste également ambigu, tout comme l'efficacité des traitements contre les infections chroniques au staphylocoque. Effectivement, si certaines études ont montré que la prophylaxie pouvait effectivement retarder l'acquisition de *S. aureus*, d'autres ont observé que ce traitement antibiotique favorisait les infections précoces par *P. aeruginosa*. (129). Pour ces différentes raisons, le traitement des infections pulmonaires par des souches de *S. aureus* sensibles à la méthiciline n'est pas systématique et dépend de l'état de santé du patient.

Enfin, les infections à *S. aureus* sont d'autant plus difficiles à traiter du fait des capacités de persistance élevées de la bactérie. En réponse aux traitements antibiotiques, le staphylocoque est en effet capable de développer le phénotype de SCV (*Small Colony Variants*), identifiés dans les expectorations de 8 à 24% des patients colonisés par *S. aureus* et associés à un déclin des fonctions respiratoires (137–139). Ce phénotype est généralement lié au développement d'une auxotrophie à la thymidine, l'hémine ou le ménadione et induit une croissance ralentie de la bactérie (140). Les SCV sont également caractérisés par une forte résistance aux antimicrobiens, une formation accrue de biofilm et une capacité d'internalisation cellulaire plus importante (137, 138, 140). L'établissement de ce phénotype fait donc partie des adaptations notoires de *S. aureus* au milieu pulmonaire, favorisant sa persistance et la chronicité de ses infections. Ces adaptations seront davantage détaillées dans la revue « *How bacterial adaptation to Cystic Fibrosis environment shapes interactions between Pseudomonas aeruginosa and Staphylococcus aureus* » du chapitre suivant.

2.3.2. *P. aeruginosa*

a. Colonisation des poumons

La colonisation des poumons par *P. aeruginosa* est corrélée à une forte inflammation pulmonaire et au déclin des fonctions respiratoires chez les patients pédiatriques et adultes (130, 133, 141–143). Ces infections sont également associées à une augmentation du risque de mortalité et constituent ainsi un marqueur de sévérité des pathologies pulmonaires chez les patients atteints de mucoviscidose (144).

Pour ces différentes raisons, la présence de *P. aeruginosa* dans les poumons est particulièrement contrôlée lors du suivi des patients, et les premières infections sont systématiquement traitées par antibiothérapie inhalée (145). Ces traitements sont généralement efficaces et conduisent à l'élimination de la souche de *P. aeruginosa* des poumons, mais de nouvelles infections plus ou moins espacées dans le temps surviennent par la suite dans plus de 30% des cas (145). On parle alors d'infections intermittentes, définies par une détection de *P. aeruginosa* dans moins de 50% des cultures sur une période de 12 mois (**Fig. 8**). Ces infections intermittentes peuvent parfois être causées par une rechute d'une infection antérieure, mais elles sont le plus souvent liées à l'acquisition de nouvelles souches de *P. aeruginosa* (146, 147). Ces nouvelles souches sont généralement acquises depuis l'environnement, particulièrement pour les jeunes sujets (148), mais peuvent aussi résulter de transmissions directes entre patients atteints de mucoviscidose (149, 150).

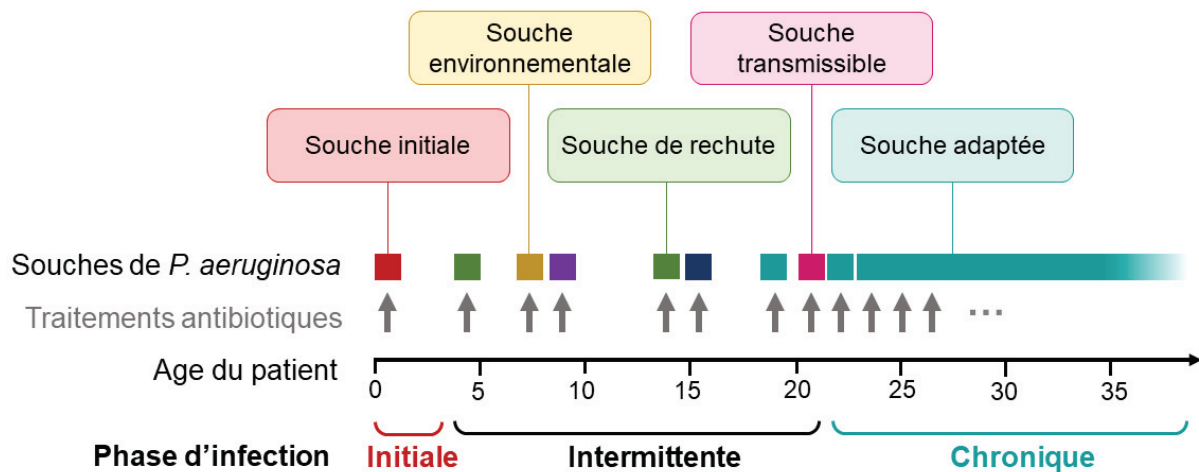


Figure 8 : Représentation schématique de l'évolution des infections à *P. aeruginosa*. Des couleurs différentes représentent des clones de *P. aeruginosa* indépendants. L'infection intermittente peut être éradiquée, permettant au patient de présenter des analyses microbiologiques négatives à *P. aeruginosa* pendant plusieurs années, jusqu'à établissement d'une infection chronique. Adapté de Folkesson *et al.* (147).

La récurrence des infections à *P. aeruginosa* et leur effet négatif sur les fonctions respiratoires des patients sont liés aux fortes capacités de virulence et de colonisation de la bactérie. *P. aeruginosa* est en effet équipée de cinq systèmes de sécrétion différents permettant l'injection de nombreuses protéines dans les cellules eucaryotes, procaryotes ou dans le milieu extracellulaire (151). Les systèmes de type (SST) 1, 2 et 5 sont par exemple impliqués dans la sécrétion des protéases extracellulaires LasA et LasB et d'autres protéines importantes pour la colonisation et l'adhésion de *P. aeruginosa* aux cellules hôtes pulmonaires (151, 152). Les principales protéines sécrétées par le SST3 sont quant à elles des exotoxines (ExoS, ExoT, ExoU, ExoY) directement injectées dans les cellules eucaryotes (153). Enfin, le SST6 vise les autres microorganismes et est donc particulièrement important pour la compétitivité de *P. aeruginosa* dans un écosystème microbien riche (154).

Indépendamment de ces systèmes, la virulence de *P. aeruginosa* repose également sur la sécrétion de molécules pigmentées de la famille des phénazines et des sidérophores. Les phénazines comme la pyocyanine induisent d'importants dommages aux cellules hôtes, inhibent leur respiration et altèrent le fonctionnement du système immunitaire (155). Les sidérophores pyoverdine et pyochéline sont quant à eux impliqués dans l'acquisition du fer chez *P. aeruginosa*, élément essentiel à sa croissance et à sa virulence *in vivo* (156). Les rhamnolipides, des molécules surfactantes également sécrétées, contribuent aux capacités de colonisation de l'écosystème pulmonaire par *P. aeruginosa* en favorisant sa motilité. Cette

motilité repose d'ailleurs sur des structures membranaires très immunogènes, telles que le flagelle et les pilis qui permettent à la bactérie de se déplacer activement vers les cellules hôtes ou procaryotes (157). Les pilis de type IV sont aussi impliqués dans l'agrégation cellulaire, l'adhésion aux cellules hôtes ainsi que la formation de biofilm (158). En plus de cette capacité à former du biofilm, *P. aeruginosa* présente une résistance antibiotique intrinsèque importante et évoluant avec l'infection (159). Cette résistance est d'ailleurs impliquée dans le déclin de l'état de santé des patients colonisés par *P. aeruginosa*, qui subissent des traitements antibiotiques beaucoup plus longs que les patients négatifs à la bactérie (133) (160).

La plupart des fonctions de virulence et de colonisation de *P. aeruginosa* sont régulées par ses trois systèmes de QS, LasRI, RhlRI et PQS (*Pseudomonas Quinolone Signal*) (155, 161). En plus de permettre une coordination de la physiologie bactérienne à l'échelle de la population, ces systèmes sont importants pour les interactions de *P. aeruginosa* avec les autres espèces microbiennes (12). *P. aeruginosa* exhibe alors un comportement particulièrement antagoniste envers de nombreux microorganismes co-colonisateurs tels que *S. aureus*, *A. fumigatus* ou *B. cepacia* (162). Les capacités de virulence, de colonisation et d'interaction microbienne *via* le QS ou le SST6 confèrent ainsi une forte compétitivité à *P. aeruginosa* dans l'écosystème pulmonaire, et sont donc responsables de la récurrence de ses infections durant la phase intermittente (Fig. 8).

b. Etablissement des infections chroniques

Malgré l'efficacité des traitements antibiotiques, les colonisations intermittentes à *P. aeruginosa* finissent par persister et évoluer vers une chronicité dans 20 à 45% des cas (75, 145, 147) (Fig. 8). Cette chronicité est actuellement caractérisée par une détection de *P. aeruginosa* dans plus de 50% des prélèvements effectués sur une période de 12 mois. De façon intéressante, la prévalence des infections chroniques à *P. aeruginosa* a diminué de 6 à 15 points en 10 ans selon l'origine et la tranche d'âge des cohortes, amenant la communauté scientifique à réévaluer la définition de la chronicité et les méthodes d'identification de *P. aeruginosa* dans les échantillons (145). Malgré cette baisse de prévalence, les infections chroniques à *P. aeruginosa* demeurent fréquentes du fait de la difficulté de les prévenir et de les traiter. En effet, l'établissement de cette chronicité repose sur une adaptation spontanée de *P. aeruginosa* au sein du milieu pulmonaire, permettant au pathogène d'ajuster sa virulence, ses capacités de résistance antibiotique et son métabolisme afin de persister durablement dans les poumons. Ces mécanismes d'adaptation sont détaillés dans la revue suivante (MGen, 2021).

From genotype to phenotype: adaptations of *Pseudomonas aeruginosa* to the cystic fibrosis environment

Laura Camus¹, François Vandenesch^{1,2,3} and Karen Moreau^{1,*}

Abstract

Pseudomonas aeruginosa is one of the main microbial species colonizing the lungs of cystic fibrosis patients and is responsible for the decline in respiratory function. Despite the hostile pulmonary environment, *P. aeruginosa* is able to establish chronic infections thanks to its strong adaptive capacity. Various longitudinal studies have attempted to compare the strains of early infection with the adapted strains of chronic infection. Thanks to new '-omics' techniques, convergent genetic mutations, as well as transcriptomic and proteomic dysregulations have been identified. As a consequence of this evolution, the adapted strains of *P. aeruginosa* have particular phenotypes that promote persistent infection.

DATA SUMMARY

Supporting data are available in Table S1, available with the online version of this article.

INTRODUCTION

The ability of *Pseudomonas aeruginosa* to establish a chronic infection in cystic fibrosis (CF) lungs despite a wide range of stress sources highlights its high adaptability. In fact, the high plasticity of the *P. aeruginosa* core and accessory genome allows the bacterium to colonize a wide variety of environments, such as soils, water or abiotic surfaces [1–4]. However, *P. aeruginosa* adaptive processes have been especially described in the context of pulmonary infections. Indeed, the chronicity of *P. aeruginosa* CF lung infections and the difficulty in treating them make it essential to understand the mechanisms of the persistence. Moreover, this chronic infectious disease offers a rare opportunity to study long-term microbial evolution within a human host. The creation of CF centres has facilitated the conservation of the different micro-organisms isolated from CF patient sputa, allowing the constitution of longitudinal isolate banks from numerous subjects. This also contributed to the identification of highly transmissible *P. aeruginosa* strains such as the lineages DK2,

AUST-02, LES (Liverpool epidemic strain) and C that are epidemic in Denmark, Australia and the UK, respectively [5]. Thanks to the development of next-generation sequencing methods, many studies have focused on longitudinal genetic adaptation of *P. aeruginosa* to the CF lung environment (Table 1). In 2006, Smith and colleagues were the first to describe a genetic evolution of a clonal lineage of *P. aeruginosa* *in vivo* by sequencing two *P. aeruginosa* strain isolates collected 7.5 years apart from the same patient [6]. Following studies were performed on a broader range of isolates from unique patients [7–12] or on transmissible lineages such as DK2 or AUST-02 [13–15]. Finally, Marvig *et al.* and Klockgether *et al.* combined both approaches to study the genomics of, respectively, 474 and 262 isolates from more than thirty patients [16–18].

By gathering the results of these different longitudinal studies, we aim to provide an updated description of the main genetic adaptations of *P. aeruginosa* to the CF lung environment. In this review, we will also discuss how these alterations affect transcriptomic and proteomic profiles of *P. aeruginosa* thanks to the latest studies performed on clinical CF isolates. Finally, common phenotypes of CF-adapted *P. aeruginosa* will be described.

Received 30 July 2020; Accepted 21 December 2020; Published 02 February 2021

Author affiliations: ¹CIRI – Centre International de Recherche en Infectiologie, Université de Lyon/Inserm U1111/Université Claude Bernard Lyon 1/ CNRS UMR5308/ENS de Lyon, Lyon, France; ²Centre National de Référence des Staphylocoques, Hospices Civils de Lyon, Lyon, France; ³Institut des Agents Infectieux, Hospices Civils de Lyon, Lyon, France.

*Correspondence: Karen Moreau, karen.moreau@univ-lyon1.fr

Keywords: adaptation; cystic fibrosis; genomic; phenotype; *Pseudomonas aeruginosa*.

Abbreviations: CF, cystic fibrosis; LPS, lipopolysaccharide; PAPI, *Pseudomonas aeruginosa* pathogenic island; QS, quorum sensing; T3SS, type III secretion system; T6SS, type VI secretion system.

Data statement: All supporting data, code and protocols have been provided within the article or through supplementary data files. One supplementary table is available with the online version of this article.

000513 © 2021 The Authors



This is an open-access article distributed under the terms of the Creative Commons Attribution License.

GENOMIC ADAPTATION OF *P. AERUGINOSA*

P. aeruginosa genome accumulates mutations during establishment of chronic colonization

Types and frequency of mutational events

Longitudinal genomic studies highlighted that late isolates of *P. aeruginosa* present numerous genetic modifications in comparison to early isolates. Small mutational events such as SNPs or short insertions and deletions (indels) have been described as the major driver of these modifications. Indeed, the *P. aeruginosa* genome was shown to accumulate a median of 3 SNPs per year, varying between 0.5 and 14 SNPs per year [6–9, 12, 14–18]. Small indels have also been reported at rates ranging from 0.4 to 2.7 indels per year (0.1 to 0.28 indels per SNP) [12, 14, 17]. These modifications could be observed on both core and accessory genomes of clinical isolates, depending on the use of a reference strain for gene annotation. Indeed, while several studies focused on the annotated genes in PAO1 or PA14 [6, 7, 13, 16, 17], others were able to identify SNPs in clone-specific genes using a related ancestral isolate as a reference [8, 9, 12, 14, 17]. The presence of accessory elements such as genomic islands and prophages could also be predicted *in silico* [10, 11].

The role of the accessory genome is in fact increasingly considered for understanding *P. aeruginosa* adaptive processes, due to its plasticity and the richness of its encoded functions [4, 19]. Indeed, the *P. aeruginosa* pathogenic islands (PAPIs) and several LES prophages were shown to affect diversification processes and important pathoadaptive phenotypes of *P. aeruginosa*, including its ability to establish *in vivo* and its antibiotic resistance [20–25]. Such elements can be horizontally transferred between *P. aeruginosa* or even between different microbial species through mechanisms of phage infection or pilus-mediated conjugation of excised and circularized genomic islands [4, 26–30]. However, acquisition of novel DNA through horizontal gene transfer remains rare [31, 32] and the genome of *P. aeruginosa* rather tends to shrink during its adaptation in CF lungs. Rau *et al.* described that the *P. aeruginosa* DK2 lineage underwent a loss of a mean of 4.2 kbp per year [31]. Deletions of more than 1000 bp have been observed in other lineages (in 10 out of 12 lineages in the study of Klockgether and colleagues), with the size of deleted regions reaching 188 kb [6, 7, 11, 17]. Here again, these deletions were shown to affect both core and accessory genomes, as prophages and genomic islands were shown to be partially or totally lost during *P. aeruginosa* adaptation to the CF environment [11, 27, 28, 31, 33–35]. Notably, the genomic islands PAPI-1 and the *P. aeruginosa* genomic island-2 (PAGI-2) were found either excised or impacted by deletions in CF isolates [27, 28]. In contrast, other elements of the accessory genome seem less prone to deletions, as the toxin–antitoxin systems, the clustered regularly interspaced short palindromic repeats (CRISPR) spacers and the genomic island PAGI-1 are well conserved in CF isolates [36–38].

In addition to deletions, the *P. aeruginosa* genome can undergo important chromosomal rearrangements that often involve accessory mobile elements, such as transposons and

Impact Statement

The chronic lung infections caused by *Pseudomonas aeruginosa* are associated with the deterioration of pulmonary functions and general health of cystic fibrosis (CF) patients. The difficulty of efficiently eradicating this pathogen comes from its ability to evolve towards high-persistence phenotypes through genetic adaptation. Understanding the basis and the determinants of this evolution is, thus, essential for the identification of new strategies to limit lung colonization by *P. aeruginosa*. The sequencing studies performed on CF isolates have highlighted numerous different evolutionary paths taken by the bacterium, leading to an intense intrapatient and interpatient diversification of *P. aeruginosa* populations. Fortunately, the identification of convergent patterns of adaptation is now possible thanks to the increasing number of research studies focused on CF isolates worldwide. Previous reviews on the topic often focused on particular aspects of *P. aeruginosa* adaptation, such as the genome dynamic, diversification processes or metabolism. In the present review, all the different aspects, as well as the latest publications on the topic, have been compiled to provide an updated and broader viewpoint of *P. aeruginosa* adaptation to the CF environment. This review also highlights convergent adaptation patterns involving intergenic regions, and transcriptomic and proteomic profiles of *P. aeruginosa*, not fully explored until now.

integrations [4, 19]. The insertion sequence IS6100 was identified as the main perpetrator of the frequent chromosomal inversions observed in the CF strains from clone C [35, 39]. Besides disrupting the reading frame of neighbouring genes [39], such chromosomal rearrangements can have pleiotropic consequences through modifications of regulatory regions or DNA topology [40]. By assessing the phenotype–genotype relationship of 44 isolates from a single patient, Darch *et al.* highlighted that the phenotypic diversity observed between CF isolates was mainly due to homologous recombination mechanisms [41]. However, this result and the high recombination rate obtained were then shown to mainly arise from false-positive events. New bio-informatics analyses of the same sequencing data with correcting filters indeed indicated lower recombination rates [42, 43]. These discrepancies emphasize the importance of bio-informatics tools and settings for the identification of recombination events, and more broadly for all genomic comparisons. In that respect, the detection of genetic alterations can be improved by combining second- and third-generation sequencing methods: while second-generation sequencing such as Illumina provides short reads with low error rates, the longer reads generated by third-generation sequencing allow a better detection of recombination events and large chromosomal rearrangements.

Table 1. Genomic studies performed on longitudinal CF isolates of *P. aeruginosa*

The list of genes or intergenic regions identified in these studies was used to highlight the most mutated regions in Tables 2 and 3. The most representative genomic studies performed on *P. aeruginosa* CF sequential isolates whose isolations were spaced by at least 1 year were selected.

Sequencing type	No. of patients	No. of sequenced isolates	Time span of isolate evolution (years)	No. of studied lineages or clone types	Identification of positively selected genes	Reference
Whole-genome	1	2	7.5	1	No	[6]
Gene-targeted	29	58	5–20	ND	No	
Whole-genome	1	45	20	1 (PA14)	No	[7]
	1	63	23	1 (C)	No	
Whole-genome	6*	12*	35 max.*	1 (DK2)*	No	[13]*
Whole-genome	21*	55*	36*	1 (DK2)*	Yes	[14]*
Whole-genome	1	18	32	1 (DK1)	No	[9]
Whole-genome	1	13	6	1	Yes	[8]
	1	14	20	1		
Whole-genome	34	474	1–8	53 (36 for PE)	Yes	[16]
Whole-genome	4	26	17–19	6	Yes	[18]
Whole-genome	1	2	6.9	1 (OC4A)	No	[10]
Whole-genome	1	2	3	1	No	[12]
Whole-genome	32 (12 for PE)	262	<15–35	12	Yes	[17]
Whole-genome	13 (6 for PE)	63	3–4	1 (AUST-02)	Yes	[15]
Whole-genome	1	40	8	1	Yes	[11]
Reanalysis of whole-genome sequencing	68	534	ND	44	Yes	[81]

ND, Not determined in the study; PE, parallel evolution.

*Isolates sequenced by Yang *et al.* were also used in the study by Marvig *et al.*, making the results of these two studies interconnected [13, 14].

Hypermutability

The rate of spontaneous mutations can be affected by the genetic background of the strain, and even enhanced by previous mutational events. For instance, the high rates of deletion observed by Rau *et al.* can be attributed to stochasticity or to the presence of missense mutations in the coding sequences of the exonucleases *sbcB* and *sbcC* implicated in recombination [31]. In the same way, the well-known hypermutable phenotype of *P. aeruginosa* arises from genetic alterations of DNA repair systems. Indeed, mutations in *mutS/mutL* and *uvrD* genes are commonly observed in CF isolates and induce a significant increase of the mutation rate [44]. Chromosomal inversions were also shown to disrupt the reading frame of *mutS* and induce hypermutability in clinical strains from the C lineage [39]. Hypermutable isolates, thus, accumulate a mean of 16-fold more mutations, with a median of 48 SNPs per year (range of 2 to more than 350 SNPs per year) [7, 8, 15, 17, 45].

Hypermutability increases the genetic diversity of the *P. aeruginosa* population in CF lungs, an advantageous feature for adaptability to stressful conditions [8, 14, 16, 17, 46, 47].

Indeed, it has been shown that antibiotic exposure promotes the emergence of hypermutability in *P. aeruginosa*, then favouring acquisition of antibiotic resistance [45, 48–51]. However, Mehta and colleagues also observed that some hypermutable lineages would spontaneously decline and disappear from the evolving population [49]. This phenomenon could be explained by an accumulation of neutral and/or slightly deleterious mutations whose probability is also increased by hypermutability. Moreover, the fitness benefit of hypermutators seems to be restricted to the conditions in which they evolved, as the accumulated hitchhiking mutations can constitute a burden in non-selective conditions [49, 50]. Hypermutability is, thus, a double-edged sword that does not ensure the success of *P. aeruginosa* adaptation. Indeed, hypermutators rarely dominate the colonizing population and coexist with normo-mutable isolates in CF lungs, potentially through colonization of specific niches [8, 9, 14]. Compensation of the hypermutator phenotype through secondary mutations has also been reported during adaptation to CF environment [8], suggesting an importance of the phenotype at certain stages of evolution. This hypothesis is supported by

the high prevalence of hypermutators in CF cohorts. Since the first estimations by Oliver [44], several studies in European and American cohorts confirmed that a mean of 28% of CF patients were infected by at least one hypermutable isolate of *P. aeruginosa* [44, 52–55]. Finally, despite a high prevalence and an increased ability to develop antibiotic resistance, the impacts of infection by hypermutable *P. aeruginosa* on clinical outcome are unclear. While an association between the presence of hypermutators and the deterioration of lung function was described in English and French cohorts [56, 57], such a result was not confirmed in an Israeli cohort [55]. Moreover, Klockgether and colleagues did not highlight a correlation between annual rate of sequence variation and the severity of the clinical course of German CF patients [17].

Accumulation of mutations relies on selection mechanisms

The accumulation of mutations in the *P. aeruginosa* genome could be the result of genetic drift or neutral selection, during which mutations are stochastically fixed regardless of their impact. However, due to the stressful conditions inherent to the CF lung environment, mutations are actually selected because of their beneficial effect on bacterial fitness. As non-synonymous mutations are more likely to affect protein function and eventually fitness, selective mechanisms can be quantified by the non-synonymous to synonymous mutations ratio (d_N/d_S). This ratio can be calculated over different scales – from all coding regions of the pangenome to specific coding regions. Three type of selective mechanisms, thus, can be observed: (i) a d_N/d_S value over one testifies to positive selection, (ii) a value under one indicates purifying or negative selection, and (iii) a close to one ratio depicts typical genetic drift.

These three selective mechanisms have been observed for the *P. aeruginosa* genome during adaptation to the CF environment. Several studies have highlighted positive selection mechanisms at the genome scale (d_N/d_S of 1.4 and 2) [6, 12], whereas negative selection was observed in others (d_N/d_S between 0.33 and 0.79) [7–9, 14]. In fact, selective mechanisms appear to vary according to the colonization time and clinical status of patients, affecting the accumulation of mutations and the composition of the accessory genome. Klockgether and colleagues observed that the *P. aeruginosa* genome presented d_N/d_S ratios ranging from 0.39 to 1.66 according to the colonization time, mutability of isolates and the severity of infection [17]. A fluctuation of positive, neutral and negative selections with time was depicted for hypermutable strains causing severe and mild infections, and for normo-mutable isolates from mildly affected patients. Interestingly, only genomes of normo-mutable isolates from patients with severe infection presented a signature of positive selection during almost all the course [17]. A relationship between the severity and the accessory genome was also observed as isolates causing severe and mild infections presented divergent repertoires of accessory genes. Similar observations were previously made for persistent and eradicated CF isolates [17, 32]. In addition,

Cramer *et al.* and Markussen *et al.* observed a rapid genetic diversification during the first clades followed by coexistence of more stable sublineages of PA14 and DK1, respectively [7, 9]. Similarly, the DK2 lineage was shown to have accumulated most mutations before 1979 in order to ensure its success in several hosts, after which negative selection was observed [13]. In both studies, late *P. aeruginosa* isolates tended to accumulate fewer mutations than early ones, suggesting modifications of selection mechanisms over the time [7, 9, 11, 13]. Mutations are indeed less likely to improve fitness and, thus, to be fixed once *P. aeruginosa* is adapted to the CF environment. Compensation of the hypermutable phenotype by secondary mutations observed by Feliziani and colleagues [8] supports this notion, as it can rebalance the mutation rate to a regular level after a stage of rapid diversification and adaptation. Finally, several recent research studies on non-CF infections reported that *P. aeruginosa* adaptive mechanisms occur at the very beginning of the colonization, emphasizing the underappreciated role of genetic adaptation in acute infections [51, 58, 59]. Altogether, these results indicate that different modes of selection arise with time, according to infection stage and severity. Thus, we suggest that positive selection first occurs during acute infections, which often severely affect patient clinical status. Thereafter, neutral or negative selection is promoted as *P. aeruginosa* adapts and the infection becomes chronic.

Although general trends of positive or negative selection can be observed for the global genome, it is important to note that selection can vary considerably according to the DNA segment. Thus, genes from the antibiotic resistome can appear positively selected despite negative selection at the genome scale [8, 45]. In contrast, negative selection is particularly depicted in the accessory genome of *P. aeruginosa*, where loss of DNA and accumulation of synonymous SNPs are promoted by mutational hotspots and genomic instability [6, 10, 31, 32, 60, 61]. However, the negative selection in accessory segments compared to the core genome can sometimes be offset by DNA acquisition through horizontal gene transfer, as described in the clones C and PA14 [10, 60]. Finally, the genetic background of *P. aeruginosa* can also influence selection and fixation of mutations in particular genes through epistatic mechanisms. Certain genetic alterations, thus, may be positively selected due to their compensatory effect on former polymorphisms or in a given genetic background, as depicted in several cases. Damkiaer and colleagues observed that a single *rpoD* mutation induced alginate overproduction only in a particular genetic background of the DK2 lineage and, thus, was positively selected [62]. Genic alterations of *mexT* were shown to compensate the effects of *lasR* inactivation, suggesting that positive selection of this mutation may be promoted in *lasR*-negative isolates [63–66]. In the same way, mutations reverting the mutator phenotype might be positively selected only after alteration of the genes from DNA repair systems [8].

Besides colonization time, infection severity and the genetic background of isolates, spatial isolation can affect the dynamics of selection mechanisms. Indeed, it is now well understood that micro-organisms can be subject to highly different selective pressures according to the environment. The heterogeneity of the CF lung ecosystem generates ecological microniches with variable physicochemical and biotic characteristics and, thus, variable selective forces. As a result, a phenomenon of adaptive radiation can be observed during *P. aeruginosa* adaptation to the CF environment. Divergent evolutionary patterns have indeed been depicted between clonally related isolates that have evolved in sinuses or in lungs [9], and even between clones isolated from different lung regions [67]. In both studies, isolates evolved independently within the different regions, as no phenomenon of convergent evolution could be observed. Instead, genotypic and phenotypic diversification was shown to be driven by the spatial isolation of strains [9, 67]. This diversification leads to the coexistence of numerous clonal lineages in the CF airways, as excellently reviewed by Winstanley and colleagues [46].

In addition to this intra-clonal diversification, the heterogeneity of *P. aeruginosa* populations is promoted by the coexistence of several lineages within the lungs of CF patients. Thus, from a single sputum sample, different *P. aeruginosa* lineages are frequently isolated that were independently acquired from the environment or from other CF patients, especially for LES-derived lineages [46, 68, 69]. Williams and colleagues observed that the prevalence of each lineage within a patient was highly dynamic during the course of infection, affecting considerably the diversification processes of *P. aeruginosa* [69]. On the one hand, the lung colonization by divergent lineages was shown to bring more genetic diversity than the *in situ* evolution of *P. aeruginosa*. On the other hand, competition between lineages appeared to select for particular genotypes and, thus, influence the diversification processes of *P. aeruginosa*. In a CF patient, the replacement of a LES lineage by another, thus, could be associated with an increased frequency of pathoadaptive mutations in the *lasR* gene [69]. The other way round, one would also expect that the presence of certain genotypes within lungs can either promote or limit superinfection by other *P. aeruginosa* lineages and, thus, interclonal diversification. This phenomenon can be extended to the colonization by other microbial species, as they have to cope with heterogeneous, adapted and niche-specialized populations of *P. aeruginosa*.

This genetic and phenotypic diversification of *P. aeruginosa* raises important issues concerning the sampling and the study of bacterial colonies from CF expectorations: a single colony is not representative of the infecting *P. aeruginosa* metapopulation [46]. In the case of longitudinal genomic studies, the sequencing of a single strain per time point is an important limitation and provides only a restricted fraction of the different evolutionary paths that the bacterium has taken. This issue obviously feeds through to all genotypic and phenotypic characterizations of CF *P. aeruginosa* strains, but is increasingly taken into account

for sequencing studies and the determination of antibiotic-resistance profiles [34, 45, 68, 69].

CF-adapted *P. aeruginosa* present pathoadaptive mutations

Coding regions

Despite the diversification processes of *P. aeruginosa*, the high number of genomic studies (Table 1) performed on sequential isolates allowed the identification of convergent patterns of adaptation. In addition to the d_N/d_S calculation, genes under positive selection were brought out through different approaches: Marvig and colleagues determined genes that accumulated more mutations than what would be predicted if mutations were randomly distributed across the genome [14, 16, 18]. In other studies, thresholds were set to establish lists of genes that were hit by a minimum quantity of independent mutations and/or in a minimum number of lineages [8, 11, 17].

In order to have a global overview of the mutated genes during *P. aeruginosa* adaptation, the results of 13 longitudinal studies were examined (Table 1). Table 2 provides a list of 48 *P. aeruginosa* coding regions that have been identified as non-synonymously mutated in at least three of these studies. Different types of mutations, thus, were highlighted (missense, frameshift and stop), but their impacts also rely on their position in the gene. Despite the change of a single amino acid, missense mutations can indeed have drastic consequences on translation efficiency or protein function, especially when they affect important functional domains [6, 17, 63]. Missense mutations were notably predicted to drastically affect the protein function of RpoB and GyrB [17], or even induce total loss-of-function of MexS [6] (Fig. 1).

Nonsense mutations and frameshifts induced by insertions and deletions are predicted as high-impact mutations as they induce a disruption and/or an interruption of translation. Most of the genes described in Table 2 have been shown to accumulate high-impact mutations during *P. aeruginosa* adaptation during longitudinal studies (Fig. 1). It is especially the case for numerous global regulators, such as *muca*, *algU*, *rpoN* and *lasR*, but also regulators related to antibiotic resistance (*nfxB*, *mexZ*) or type III secretion (*retS*, *exsA*).

The role of these genes in *P. aeruginosa* adaptation to the CF environment was confirmed in larger cohorts of clinical isolates, but through a wide variety of mutations. In that respect, 173 unique *lasR* variants have been detected by gene-targeted sequencing of 2583 CF isolates, with most of them inducing a loss of function [63]. Mutations in mucoidy related genes have also been researched in *P. aeruginosa* isolates from CF patients [70–73]. A recent study in a Brazilian cohort identified 30 new mutations in the *algUmucABD* operon and confirmed the high frequency of the *mucaA22* mutation, inducing a premature stop codon in the *mucaA* gene [74]. However, it is noteworthy that high-impact mutations do not inevitably induce a complete loss of function. Feltner and colleagues indeed observed a retained LasR activity in 25% of cases despite missense or even nonsense mutations in the *lasR*

Table 2. *P. aeruginosa* genes identified as non-synonymously mutated in at least three independent longitudinal studies

The characteristics of the 13 studies used for the intragenic regions are listed in Table 1.

Gene name	PAO1 locus	Product	Positive selection	Longitudinal studies	
				No.	Reference
<i>gyrB</i>	PA0004	DNA gyrase subunit B	Yes	8	[6, 7, 9, 11, 14–16, 18]
<i>pvdS</i>	PA2426	Sigma factor	No	8	[6, 7, 9, 10, 13, 16–18]
<i>mexA</i>	PA0425	RND multidrug efflux membrane fusion protein MexA precursor	No	6	[6, 7, 15–18]
<i>mexY</i>	PA2018	Multidrug efflux protein	No	6	[6–8, 10, 13, 14, 17]
<i>mexZ</i>	PA2020	Transcriptional regulator of multidrug efflux pump	Yes	6	[6, 9, 13, 16–18]
<i>gyrA</i>	PA3168	DNA gyrase subunit A	No	6	[9, 10, 13, 14, 16–18]
<i>fisI</i>	PA4418	Penicillin-binding protein 3	No	6	[8–10, 13–15, 17]
<i>mexB</i>	PA0426	RND multidrug efflux transporter	No	6	[6, 7, 14, 16–18]
<i>oprD</i>	PA0958	Basic amino acid, basic peptide and imipenem outer-membrane porin	No	6	[9, 10, 14–17]
<i>migA</i>	PA0705	α -1,6-Rhamnosyltransferase	No	5	[7, 9, 12–15]
<i>algU</i>	PA0762	RNA polymerase sigma factor	Yes	5	[9, 13, 14, 16–18]
<i>lasR</i>	PA1430	Transcriptional regulator of QS	Yes	5	[6, 9, 16–18]
<i>pmrB</i>	PA4777	Two-component regulator system signal sensor kinase	No	5	[7, 10, 11, 13–15]
<i>muca</i>	PA0763	Anti-sigma factor	Yes	5	[6, 13, 16–18]
<i>algG</i>	PA3545	Alginate-C5-mannuronan-epimerase	No	5	[7, 9, 12, 13, 17]
<i>mexS</i>	PA2491	Probable oxidoreductase	Yes	4	[6, 15–17]
<i>mexT</i>	PA2492	Transcriptional regulator of multidrug efflux pump	No	4	[6, 10, 12, 15]
<i>rpoB</i>	PA4270	DNA-directed RNA polymerase β chain	No	4	[6, 7, 13, 14, 17]
<i>chpA</i>	PA0413	Component of chemotactic signal transduction system	No	4	[7, 10, 11, 17]
<i>wbpM</i>	PA3141	Nucleotide sugar epimerase/dehydratase	No	4	[9, 10, 16, 17]
<i>fusA1</i>	PA4266	Elongation factor G	Yes	4	[8, 9, 12, 17]
<i>rpoN</i>	PA4462	RNA polymerase C-54 factor	Yes	4	[6, 13, 15, 18]
<i>pagL</i>	PA4661	Lipid A 3-O-deacylase	Yes	4	[9, 12, 13, 17]
<i>retS</i>	PA4856	Regulator of exopolysaccharide and type III secretion	No	4	[7, 10, 16, 18]
<i>rpoC</i>	PA4269	DNA-directed RNA polymerase subunit β	No	3	[7, 13, 14, 17]
<i>exsA</i>	PA1713	Transcriptional regulator of T3SS	No	3	[6, 7, 12]
<i>ampC</i>	PA4110	β -Lactamase/D-alanine carboxypeptidase	Yes	3	[8, 9, 13, 14]
<i>atsA</i>	PA0183	Arylsulfatase	No	3	[7, 10, 13]
<i>pilJ</i>	PA0411	Twitching motility protein	Yes	3	[9, 13, 17]
<i>xdhB</i>	PA1523	Xanthine dehydrogenase	No	3	[7, 8, 10]
<i>dnaX</i>	PA1532	DNA polymerase subunits γ and τ	No	3	[6, 10, 16]
<i>pcoA</i>	PA2065	Copper resistance protein A precursor	No	3	[7, 10, 16]
<i>pvdL</i>	PA2424	Non-ribosomal peptide synthase, pyoverdine biosynthesis	No	3	[9–11]
<i>clpA</i>	PA2620	ATP-binding protease component	Yes	3	[9, 13, 17]
<i>pelA</i>	PA3064	Glycohydrolase involved in Pel biosynthesis	No	3	[10, 14, 16]
<i>hasR</i>	PA3408	Haem uptake outer-membrane receptor precursor	No	3	[7, 10, 17]

Continued

Table 2. Continued

Gene name	PAO1 locus	Product	Positive selection	Longitudinal studies	
				No.	Reference
<i>wspA</i>	PA3708	Chemotaxis transducer	No	3	[10, 16, 17]
<i>PA3728</i>	PA3728	ATPase	Yes	3	[8, 13, 17]
<i>purL</i>	PA3763	Phosphoribosylformylglycinamide synthase	Yes	3	[8, 13, 17]
<i>bfnS</i>	PA4102	Histidine kinase sensor	No	3	[9, 12, 15]
<i>recC</i>	PA4285	Exodeoxyribonuclease V subunit γ	No	3	[7, 8, 10]
<i>ampD</i>	PA4522	<i>N</i> -Acetyl-anhydromuranmyl-L-alanine amidase	No	3	[6, 7, 17]
<i>nfxB</i>	PA4600	Transcriptional regulator	Yes	3	[16–18]
<i>phuR</i>	PA4710	Putative haem/haemoglobin uptake outer-membrane receptor	No	3	[7, 15, 17]
<i>cbrA</i>	PA4725	Two-component sensor CbrA	No	3	[10, 11, 17]
<i>cbrB</i>	PA4726	Two-component response regulator CbrB	No	3	[7, 9, 13]
<i>folP</i>	PA4750	Dihydropteroate synthase	No	3	[7, 10, 15]
<i>spoT</i>	PA5338	Guanosine-3',5'-bis(diphosphate) 3'-pyrophosphohydrolase	Yes	3	[9, 13, 17]

sequence [63]. Similarly, *P. aeruginosa* strains carrying the nonsense *mucA22* mutation were recently shown to respond highly differently than Δ *mucA* mutants to acidified nitrite conditions [75]. These results highlight the complexity of fully evaluating the consequences of mutations on protein features, even for ones predicted to induce a drastic impact or a loss of protein function. It is particularly the case for global transcriptomic regulators as their alteration, however small, can affect the expression and function of numerous other genes.

Synonymous mutations can also have beneficial or detrimental impacts on fitness through alteration of protein folding, translation efficiency and rate [76, 77]. Adaptive synonymous mutations with an associated gain of fitness have been highlighted during experimental evolution of *Pseudomonas fluorescens* [78, 79]. Thus, it would not be surprising that synonymous mutations also contribute to *P. aeruginosa* adaptation in CF lungs, although their impact is still rarely considered.

Intergenic regions

None of the previous studies assessed whether positive selection also occurred in non-coding regions, although intergenic mutations were identified. Recently, an analogous ratio to d_N/d_S was described to assess selective mechanisms occurring in non-coding regions, where d_N is replaced by the number of intergenic SNPs per intergenic site (d_i) [80]. Even though this method has not been used on a *P. aeruginosa* genome yet, the signature of purifying selection was observed for intergenic sites of other species such as *Escherichia coli* or *Staphylococcus aureus* [80, 81]. However, Khademi and colleagues reanalysed the sequencing data of intergenic regions from several longitudinal *P. aeruginosa* genomic studies [6, 14, 16] and were able to establish a list of adaptive non-coding regions mutated in at least 3 of the 44 studied lineages [81] (Table 3).

Interestingly, some of the adaptive intergenic regions identified have been found to be mutated in other longitudinal studies of which the sequencing data were not used in the analysis by Khademi *et al.* [7, 9, 18], supporting their role in *P. aeruginosa* adaptation. Table 3 presents the 15 adaptive intergenic regions most frequently mutated, i.e. regions that accumulated the highest number of mutations, in the most elevated number of lineages and longitudinal studies. The complete table is shown in Table S1. Mutations in the *phuS/phuR* intergenic region were identified in the largest number of studies and at significant rates. Finally, we notice that mutations occurred in the intergenic region between *ampR* and *ampC*, a gene that was also identified as pathoadaptive (Table 2). Genetic modifications of intergenic regions, thus, appear to also play a role in *P. aeruginosa* adaptation to the CF environment, potentially through the transcriptomic dysregulation of surrounding genes [81].

It is noteworthy that the sequencing results of the 13 longitudinal studies analysed in this review could be connected thanks to the genomic annotations from the reference strains PAO1 or PA14. Thus, Tables 2 and 3 are not representative of the numerous mutations occurring within genes or intergenic regions specific to clinical isolates. Moreover, the accessory genome of *P. aeruginosa* presents very divergent profiles according to the isolates, with great variations in its composition and its organization [4, 19]. As a result, accessory elements present a higher sequence diversity [27, 32, 60, 82], limiting the establishment of convergent evolutionary patterns within the accessory genome. Nonetheless, it needs to be kept in mind that some accessory genes can have homologous functions other than those present in the core genome [4, 19] and, thus, sometimes compensate a mutation in a conserved gene.

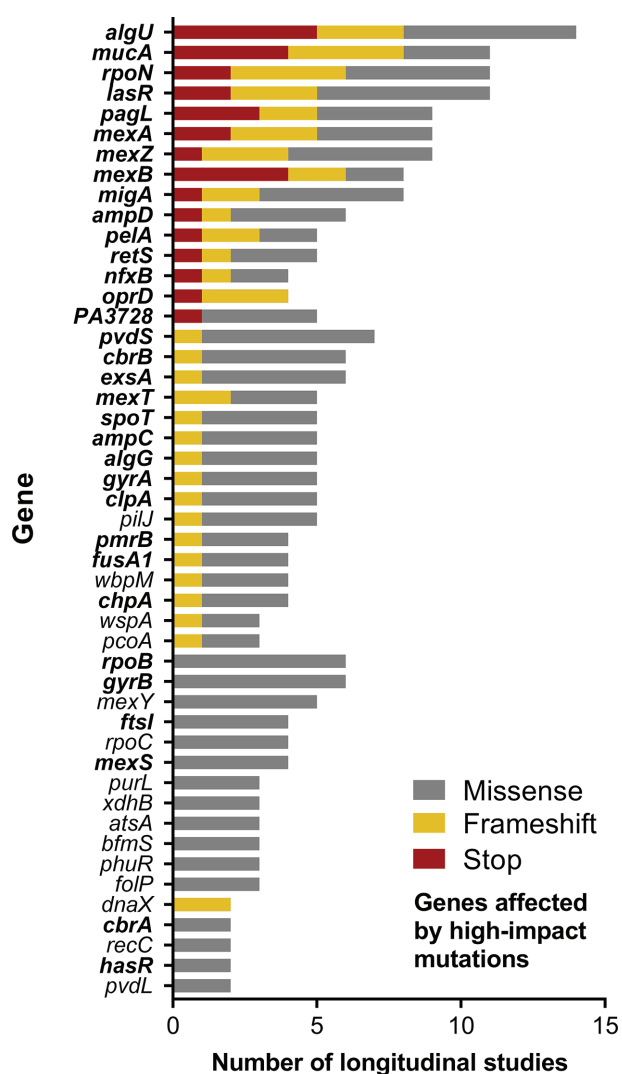


Fig. 1. Number of longitudinal studies identifying stop (red), frameshifts (yellow) or missense (grey) mutations in 48 genes. Non-synonymously mutated genes and corresponding types of mutations were recovered from the longitudinal studies listed in Table 1. Genes in bold were affected by mutations predicted to have a drastic impact on protein function [17] or induce a partial or total loss-of-function [6].

PHENOTYPICAL SIGNATURES OF CF-ADAPTED *P. AERUGINOSA*

P. aeruginosa adapts its expression profiles to the CF environment

Gene expression

The comparison of transcriptomes or proteomes of sequential clinical isolates seems to be the most suitable for assessing impacts of *P. aeruginosa* adaptation on global expression profiles. Several longitudinal studies indeed performed transcriptional profiling and observed differences of global transcript abundance between early and late isolates [9, 13], but also on specific expressed genes [12, 13, 83–85]. Table 4(a) lists 41 *P. aeruginosa* genes differentially expressed between

early and late CF isolates. Convergent patterns of expression could be identified *in vitro* in late isolates in comparison to related early isolates, for instance, a down-regulation of genes involved in secretion (Hcp secretion island I), the pseudomonas quinolone signal (PQS) and phenazine biosynthesis. Interestingly, more than a half of dysregulated genes presented in Table 4 have been shown to be part of RpoN, AlgU or LasR regulons, underscoring their significance in *P. aeruginosa* adaptive mechanisms [86–89].

It is important to remember that gene expression relies highly on growth conditions and that *in vitro* patterns are not necessarily representative of what happens *in vivo*. Thanks to the advance of transcriptomic methods, recent studies evaluated *P. aeruginosa* global gene expression ‘*in vivo*’, i.e. directly on clinical populations within sputum [90–92], ex-planted lungs from CF patients [93], or during non-human infection models [94]. Transcriptomic patterns induced by *in vivo* conditions are presented in Table 4(b). Comparable transcriptomic dysregulations to those observed for *in vitro* transcriptomic analyses were depicted for more than a half of the genes listed in Table 4(a, b), including the down-regulation of genes from the Hcp secretion island. Interestingly, these dysregulations seem to be specific to CF clinical isolates. The PAO1 reference strain, not adapted to the CF-environment, was shown to present a very divergent, if not opposite, transcriptomic pattern during *in vivo* infection. These results were nonetheless obtained using a murine model of acute pneumonia and should be confirmed in a chronic infection context [95] (Table 4c). Altogether, these transcriptomic studies underscored the role of several genes in *P. aeruginosa* adaptation to the CF environment due to: (i) convergent expression in CF-adapted isolates in comparison to non-adapted ones, (ii) convergent expression *in vivo* in comparison to *in vitro* growth, and (iii) specific dysregulations *in vivo* in comparison to PAO1. Genes meeting these three criteria are highlighted in Table 4.

Protein expression

P. aeruginosa protein expression during CF infections was mainly assessed by evaluating proteomic changes between clinical and reference strains or under certain conditions, as reviewed by Hare and Cordwell and by Kamath *et al.* [96, 97]. More recently, this approach was used to evaluate proteome responses of a set of clinical isolates cultivated under different conditions of nutrient and oxygen availability [98–100]. Clinical *P. aeruginosa* isolates presented a distinct proteome profile from PAO1, with convergent expression of many proteins despite a high genomic and phenotypic diversity between isolates. An over-expression of proteins involved in amino acid biosynthesis or drug resistance, with the example of MexY was specifically noted for clinical isolates [98, 99]. Several proteins involved in motility, chemotaxis and adhesion features were also down-regulated, including proteins from the Fli and Pil systems, confirming previous observations [96, 97].

To our knowledge, differences of the global proteome between early and CF-adapted clonal isolates of

Table 3. Selection of *P. aeruginosa* intergenic regions under positive selection

Mutations in intergenic regions were identified as positively selected by Khademi et al. [81] and selected for this table according to their number, the number of affected lineages and the number of longitudinal studies highlighting mutations in the same intergenic region. The complete list is shown in Table S1.

Upstream/ downstream genes	Upstream/ downstream PAO1 locus	Upstream/downstream products	No. of intergenic mutations	No. of lineages	Reference
<u><i>phuS</i></u> // <u><i>phuR</i></u>	<u>PA4709</u> // <u>PA4710</u>	PhuS/haem/haemoglobin uptake outer-membrane receptor	40	4	[7, 9, 18, 81]
<u>PA0428</u> // <u>PA0429</u>	<u>PA0428</u> // PA0429	Probable ATP-dependent RNA helicase/hypothetical protein	34	10	[81]
<u>PA4786</u> // <u>PA4787</u>	PA4786 // PA4787	Probable short-chain dehydrogenase/probable transcriptional regulator	28	12	[81]
<u>PA4690.5</u> // <u>PA4691</u>	<u>PA4690.5</u> // PA4691	16S ribosomal RNA/hypothetical protein	54	6	[81]
<u>PA2535</u> // <u>PA2536</u>	PA2535 // PA2536	Probable oxidoreductase/probable phosphatidate cytidyltransferase	18	6	[7, 81]
<u><i>motY</i></u> // <u><i>pyrC</i></u>	<u>PA3526</u> // <u>PA3527</u>	Probable outer-membrane protein precursor/dihydroorotase	32	6	[81]
<u>PA3230</u> // <u>PA3231</u>	<u>PA3230</u> // PA3231	Conserved hypothetical protein/conserved hypothetical protein	24	7	[81]
<u><i>algL</i></u> // <u><i>algl</i></u>	PA3547 // <u>PA3548</u>	Poly(β -D-mannuronate) lyase precursor/alginate O-acetyltransferase	14	6	[7, 81]
<u>PA0976.1</u> // <u>PA0977</u>	PA0976.1 // PA0977	tRNA-Lys/hypothetical protein	26	6	[81]
<u><i>rplU</i></u> // <u><i>ispB</i></u>	<u>PA4568</u> // <u>PA4569</u>	50S ribosomal protein L21/octaprenyldiphosphate synthase	22	7	[81]
<u><i>phzM</i></u> // <u><i>phzA1</i></u>	<u>PA4209</u> // <u>PA4210</u>	Probable phenazine-specific methyltransferase	12	6	[7, 81]
<u><i>oprO</i></u> // <u>PA3281</u>	<u>PA3280</u> // PA3281	Pyrophosphate-specific outer-membrane porin precursor/hypothetical protein	10	5	[7, 81]
<u><i>ldh</i></u> // <u>PA3419</u>	<u>PA3418</u> // <u>PA3419</u>	Leucine dehydrogenase	10	5	[7, 81]
<u><i>ampR</i></u> // <u><i>ampC</i></u>	<u>PA4109</u> // <u>PA4110</u>	Transcriptional regulator/ β -lactamase precursor	12	4	[9, 81]
<u>PA5160.1</u> // <u><i>rmlB</i></u>	<u>PA5160.1</u> // PA5161	tRNA-Thr/dTDP-D-glucose 4,6- dehydratase	16	6	[81]

Genes of which the promoter is located in the impacted intergenic region are underlined.

P. aeruginosa, however, have not been assessed yet, limiting the establishment of direct relationships between genetic adaptation to the CF environment and protein expression. Nonetheless, a recent study described the *P. aeruginosa* proteome directly from CF sputum. By comparing protein expression in the *P. aeruginosa* population from 35 samples, Wu and colleagues, thus, were able to identify a convergent pattern of protein expression *in vivo* [101] (Table 5a). Some of the proteins identified as more abundantly produced by clinical isolates than by PAO1 were found also to be highly produced *in vitro*, with the example of the chaperone Hfq and the phosphate transporter PtsS (Table 5b) [98, 99, 101–103]. Here again, protein expression pattern appears to largely rely on growth conditions (Table 5b).

Convergent phenotypes are selected by *P. aeruginosa* adaptation

As a result of the diversification of genetic, transcriptomic and proteomic profiles, CF-adapted *P. aeruginosa*

can present various phenotypic signatures (Fig. 2) [46, 47, 104]. Although these are often found to be patient dependent [17, 105], similar phenotypes are frequently observed in adapted *P. aeruginosa* isolates, including alterations of metabolism, antibiotic resistance, biofilm and virulence. These phenotypes are associated with chronic infections as they promote bacterial persistence within lungs and have been extensively described [46, 47, 104, 106–108]. Interestingly, an analogous phenotypic diversification could be recently reproduced *in vitro* by experimental evolution in CF-mimicking conditions. Schick and colleagues observed that the complexity and the viscosity of the synthetic cystic fibrosis sputum medium (SCFM) containing mucin was sufficient to induce several common phenotypes of CF strains, such as antibiotic resistance, biofilm formation, loss of motility and production of virulence factors [109].

Table 4. *P. aeruginosa* transcriptomic alterations during adaptation to the CF lung environment

Square colour indicates gene expression: up-regulation (red), down-regulation (green), undetermined (light grey), divergent according to studies (dark grey). (a) Gene expression in late isolates in comparison to related early isolates of *P. aeruginosa*. The 41 genes with a convergent pattern identified in at least four isolates were selected [12, 13, 83–85]. (b) Gene expression in clinical CF isolates *in vivo* (CF sputum, explanted lungs or zebra fish infection) in comparison to growth *in vitro* [91–94]. (c) Gene expression in PAO1 *in vivo* (murine infection model of acute pneumonia) in comparison to growth *in vitro* [95].

Gene name	PAO1 locus	Product	(a) Expression in late isolates	(b) Expression in CF isolates <i>in vivo</i>	(c) Expression in PAO1 <i>in vivo</i>
PA1323	PA1323 ^f	Hypothetical protein	Up-regulation	Divergent	Down-regulation
PA1324	PA1324 ^f	Hypothetical protein			
PA1471	PA1471	Hypothetical protein			
PA1559	PA1559	Hypothetical protein			
PA1592	PA1592	Hypothetical protein			
<i>mexX</i>	PA2019	RND multidrug efflux membrane fusion protein			
PA2485	PA2485	Hypothetical protein			
PA3691	PA3691 ^g	Hypothetical protein			
<i>lptF</i>	PA3692 ^g	Lipotoxon F			
PA3819	PA3819	Conserved hypothetical protein			
<i>osmE</i>	PA4876	Osmotically inducible lipoprotein			
PA4880	PA4880	Probable bacterioferritin			
PA5212	PA5212	Hypothetical protein			
PA0045	PA0045	Hypothetical protein			
PA0046	PA0046	Hypothetical protein			
PA0047	PA0047	Hypothetical protein			
<i>tagQ1</i>	PA0070 ^a	TagQ1			
<i>pppA</i>	PA0075 ^a	PppA			
<i>tagF1</i>	PA0076 ^a	Hcp secretion island I (HSI-I) T6SS			
<i>icmF1</i>	PA0077 ^a	Hcp secretion island I (HSI-I) T6SS			
<i>tssL1</i>	PA0078 ^b	Hcp secretion island I (HSI-I) T6SS			
<i>tssK1</i>	PA0079 ^b	Hcp secretion island I (HSI-I) T6SS			
<i>tssJ1</i>	PA0080 ^b	Hcp secretion island I (HSI-I) T6SS			
<i>ttsA1</i>	PA0082 ^c	Hcp secretion island I (HSI-I) T6SS			
<i>ttsB1</i>	PA0083 ^c	Hcp secretion island I (HSI-I) T6SS			
<i>ttsC1</i>	PA0084 ^c	Hcp secretion island I (HSI-I) T6SS			
<i>hcp1</i>	PA0085	Hcp secretion island I (HSI-I) T6SS			
<i>tagJ1</i>	PA0086 ^d	Hcp secretion island I (HSI-I) T6SS			
<i>tssE1</i>	PA0087 ^d	Hcp secretion island I (HSI-I) T6SS			
<i>tssG1</i>	PA0089 ^d	Hcp secretion island I (HSI-I) T6SS			
<i>clpV1</i>	PA0090 ^d	ClpV1	Up-regulation	Undetermined	Down-regulation
<i>pqsC</i>	PA0998 ^e	β -Keto-acyl-acyl-carrier protein synthase			

Continued

Table 4. Continued

Gene name	PAO1 locus	Product	(a) Expression in late isolates	(b) Expression in CF isolates <i>in vivo</i>	(c) Expression in PAO1 <i>in vivo</i>
<i>pqsD</i>	PA0999 ^c	Acetyl CoA ACP transacetylase	Green	Grey	Grey
<i>phnA</i>	PA1001	Phenazine biosynthesis protein	Green	Grey	Grey
<i>HsiB2</i>	PA1657	Conserved hypothetical protein	Green	Grey	Green
<i>hcnA</i>	PA2193	Hydrogen cyanide synthase	Green	Green	Green
<i>tse5</i>	PA2684	Cell wall/membrane/envelope biogenesis	Green	Green	Grey
<i>PA3021</i>	PA3021	Hypothetical protein	Green	Grey	Grey
<i>PA3729</i>	PA3729	Conserved hypothetical protein	Green	Green	Red
<i>cytN</i>	PA4133	Cytochrome <i>c</i> oxidase subunit	Green	Green	Green
<i>PA4317</i>	PA4317	Hypothetical protein	Green	Green	Red

Genes annotated with an identical letter belong to the same operon.

Genes in bold respond to the following criteria: (i) convergent expression in CF late isolates in comparison to early ones, (ii) convergent expression *in vivo* in comparison to *in vitro* growth, and (iii) specific dysregulations *in vivo* in comparison to PAO1.

Metabolic alterations

The energetic metabolism of *P. aeruginosa* is largely affected by its adaptation to the CF environment. As a consequence of non-synonymous mutations in numerous metabolism-related genes, adapted *P. aeruginosa* strains present a differential and adjusted assimilation of the nutrients present in the CF lung (Fig. 2a) [17, 67, 105, 107, 110]. Auxotrophy or reduction of catabolic capacities are frequently observed and arise from either low or high molecule availability in the CF environment. Amino acid auxotrophy often arises in CF-adapted *P. aeruginosa* due to the high abundance of these molecules in CF sputum [107, 110–112]; in addition, purine auxotrophy can be established in DNA-rich sputa [113]. Development of new metabolic capacities can nonetheless arise through enrichment of the accessory genome in metabolic functions [17, 28, 60]. This adjusted metabolism increases *P. aeruginosa* fitness in the CF environment, but it often results in a slowed growth in laboratory conditions in comparison to non-adapted isolates [7, 8, 12, 13, 18, 107, 110, 114]. This modification of metabolic activities can limit effective detection and treatment of infecting *P. aeruginosa*, as illustrated by the emergence of highly resistant small colony variants (SCVs) and viable but non-culturable (VBNC) isolates [115–117].

Antimicrobial resistance and biofilm

Another feature limiting treatment of *P. aeruginosa* infection is the development of resistance mechanisms to antimicrobials. In comparison to early strains, late *P. aeruginosa* isolates present a greater antibiotic resistance acquired through different mechanisms: (i) alteration of antibiotic transport, (ii) increase of antibiotic degradation, and (iii) alteration of antibiotic targets [118]. The alteration

of antibiotic transport is characterized by a decrease of antibiotic input through reduction of porin activities, and in an increase of drug output through modification of the efflux pumps activity. Particularly, *oprD* repression and *mexAB* overexpression, induced by mutations in their own coding sequences or in their regulators, are frequently responsible for β -lactam resistance in CF *P. aeruginosa* (Fig. 2b) [10, 118, 119]. Such resistance can also be promoted by the genome enrichment of accessory genes involved in multidrug secretion. The many transporters constituting the accessory genome of the LES epidemic strain, thus, contribute to its high antibiotic resistance and its epidemiological success [23]. The increase in antibiotic degradation is mainly perpetrated by an overproduction of the cephalosporinase AmpC, induced by mutations in the *ampCD* genes but also in the coding sequencing of their regulator AmpR (Fig. 2b) [118]. Finally, the increase of *P. aeruginosa* multidrug resistance can also involve the alteration of several antibiotic targets, such as the DNA gyrase GyrAB, the penicillin-binding protein FtsI or the lipopolysaccharide (LPS) of the bacterial outer membrane [11, 118, 120, 121] (Fig. 2b). The latter undergoes important alterations of its three components during *P. aeruginosa* adaptation to the CF environment. Mutations in *pmrB*, *migA* and *pagL* are associated with structural modifications of the lipid A part of the LPS, inducing resistance to polymyxins [10–12, 120, 122]. The alteration of MigA and LptF can also affect the synthesis of the core oligosaccharide and the transport of the mature LPS, although their impact on antibiotic resistance remains poorly understood [121, 123, 124]. Finally, CF isolates often lack the O-antigen polysaccharide of the LPS due to mutations in *wbp* genes,

Table 5. *P. aeruginosa* proteomic expression *in vivo* in comparison to *in vitro* conditions

Square colour indicates protein expression: up-regulation (red), down-regulation (green), undetermined (light grey). (a) Protein expression in *P. aeruginosa* populations from CF sputa, in comparison to populations grown *in vitro* [101]. The 15 proteins identified with a convergent pattern within the most samples were selected. (b) Protein expression in *P. aeruginosa* CF isolates in comparison to PAO1 determined *in vitro* in minimal medium M9 [99], rich medium LB [98, 102, 103] or in sputum-like media SCFM [99] or ASMDM (artificial sputum medium with high molecular mass DNA and mucin) [103], for the 15 proteins identified as expressed *in vivo*. NA, Not available.

Protein name	PAO1 locus	Product	(a) <i>In vivo</i> vs <i>in vitro</i>			(b) <i>In vitro</i> vs PAO1		
			Expression in CF sputa	No. of samples with convergent pattern	No. of samples with detected protein	Expression in minimal medium	Expression in rich medium	Expression in sputum-like media
OprD	PA0958	Outer-membrane porin precursor	Red	20	25	Red	Green	Green
OprH	PA1178	PhoP/Q and low Mg ²⁺ inducible outer-membrane protein H1 precursor	Red	27	33	Grey	Grey	Grey
PA1288	PA1288	Probable outer-membrane protein precursor	Red	26	33	Grey	Red	Green
OprI	PA2853	Outer-membrane lipoprotein OprI precursor	Red	26	35	Grey	Grey	Grey
AlgE	PA3544	Alginate production outer-membrane protein AlgE precursor	Red	20	21	Red	Green	Grey
FumC1	PA4470	Fumarate hydratase	Red	24	30	Grey	Grey	Grey
PhuR	PA4710	Haem/haemoglobin uptake outer-membrane receptor precursor	Red	22	32	Green	Grey	Red
PA4793	PA4793	Hypothetical protein	Red	23	31	Grey	Red	Grey
PA4837	PA4837	Probable outer-membrane protein precursor	Red	28	31	Green	Grey	Grey
Hfq	PA4944	Hfq	Red	19	29	Grey	Red	Grey
PstS	PA5369	Phosphate ABC transporter, periplasmic phosphate-binding protein	Red	25	26	Grey	Red	Grey
NA	NA	TonB-dependent receptor	Red	24	25	Grey	Grey	Grey
Icd	PA2623	Isocitrate dehydrogenase	Green	21	30	Grey	Grey	Grey
RpsB	PA3656	30S ribosomal protein S2	Red	20	28	Grey	Grey	Grey
RplS	PA3742	50S ribosomal protein L19	Red	23	26	Grey	Red	Grey

resulting in lower virulence and increased tolerance to gentamicin [121, 125].

Besides antibiotics, LPS modifications also affect *P. aeruginosa* resistance to phages and bacteriocins [120]. In CF-adapted *P. aeruginosa*, mutations in LPS biosynthesis genes were shown to decrease phage susceptibility by hampering LPS-mediated recognition [120, 126]. In contrast, chronic CF isolates are often more susceptible to the *P. aeruginosa*-produced bacteriocins, pyocins, due to an improved access to the cell envelope following the structural alterations of the O-antigen [120, 127, 128]. However, pyocin production is also frequently reduced in chronic CF *P. aeruginosa* [126, 127].

Resistance to antimicrobials is also associated with an increased formation of biofilm. The exopolysaccharide matrix, constituted of varying proportions of Pel, Psl or alginate molecules according to the strain, indeed allows the constitution of a physical and chemical barrier against antimicrobials (Fig. 2d) [129–132]. CF-adapted strains

often present an up-regulation of Pel, Psl and/or alginate exopolysaccharides production; hence, increasing biofilm formation, modifying the composition of its matrix and favouring antimicrobial resistance [130]. Pel and Psl overproduction is, thus, responsible for the persistence phenotype of rugose small colony variants (RSCVs) in CF *P. aeruginosa* [133, 134]. Mucoïd isolates, mainly arising from *mucA* alterations inducing alginate overproduction, are also associated with poorer clinical outcome and greater inflammation [135–138]. Interestingly, mucoïd and non-mucoïd isolates are often co-isolated from CF patients, due to diversification or reversion of the phenotype through compensatory mutations, in *algU* for instance (Fig. 2d) [11, 18, 72]. Sessile lifestyle is also promoted by a loss of motility linked to inhibition of pili and flagella synthesis [10, 12, 18]. Alterations of these membrane components, as well as LPS modification and biofilm formation, reduce the induction of the host

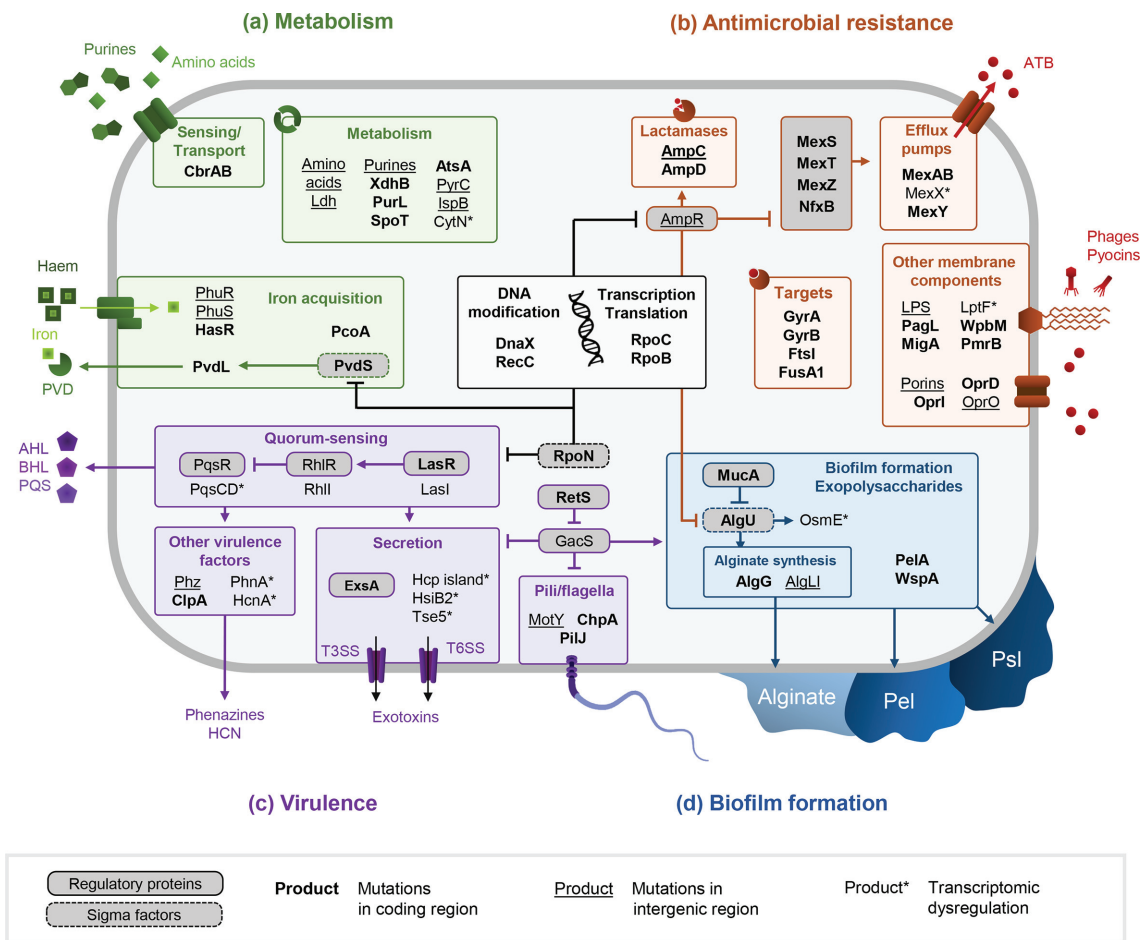


Fig. 2. Pathways related to metabolism (a), antimicrobial resistance (b), virulence (c) and biofilm formation (d) altered during *P. aeruginosa* adaptation to the CF environment. DNA sequences of products in bold have been shown to accumulate non-synonymous mutations. Intergenic regions surrounding products that are underlined are mutated. Late isolates present a convergent transcriptomic dysregulation of the products marked by asterisks in comparison to early isolates.

inflammasome and, thus, efficient bacterial elimination from the lungs [106, 108].

Virulence

In the same way, *P. aeruginosa*-adapted isolates have been shown to secrete fewer virulence factors, which are both immunogenic and costly to produce [10, 18, 108]. Iron plays a pivot role in bacterial virulence and its acquisition is affected during *P. aeruginosa* adaptation to the CF environment. Alteration of pyoverdine siderophore synthesis through mutations in the regulator *pvdS* and the *pvd* genes is often observed, inducing a loss of virulence [125, 139, 140]. In contrast, iron acquisition through haem is promoted in adapted isolates thanks to the up-regulation of Phu and Has systems (Fig. 2a) [139, 141]. Changes in the accessory genome composition also undoubtedly affect *P. aeruginosa* virulence, as chronic or eradicated CF isolates present a different repertoire of accessory functions than virulent ones [17, 32]. Alteration of the genomic islands PAPI-1 and PAPI-2 and the LES phages can greatly lower *P. aeruginosa* virulence [21, 22, 24].

In connection with this, CF isolates from chronic infection strains often lack the PAPI-2 encoded cytotoxin ExoU. They instead harbour the type III secretion system (T3SS) effector ExoS, which is chromosomally encoded and has less virulent properties than ExoU [142–145]. However, mutations in major virulence and quorum-sensing (QS) regulators, such as *retS*, *exsA* or *lasR*, are the main perpetrators of the low-virulence state of chronic *P. aeruginosa* (Fig. 2c).

QS rewiring and modification of microbial interactions

The alterations of QS systems suggest that *P. aeruginosa* adaptation goes along with a reduction of social behaviours. This hypothesis is supported by the high frequency of *lasR* mutations that are also acquired during *in vitro* evolution of *P. aeruginosa* [146, 147]. On the one hand, the emergence of *lasR*-mutant social cheaters within the bacterial population suggest a loss of intra-species cooperative behaviours as these mutants will benefit from extracellular factors produced by other members without paying the energy cost [148–150]. However, this also indicates that QS activities

and social behaviours need to be considered at the whole population scale. On the other hand, several recent studies depicted that *lasR* mutants isolated from CF infections retained an active QS through a *lasR*-independent induction of the Rhl system. This phenomenon was often related to compensatory mutations in the pathoadaptive *mexT* gene [63–66], and not by alteration of *rhl* genes. The latter are indeed rarely mutated during *P. aeruginosa* evolution within CF lungs, underscoring the importance of maintaining a functional Rhl system during chronic infections. Instead of a loss of QS, *P. aeruginosa* adaptation to the CF lung rather induces a rewiring of QS networks for the benefit of a Rhl-mediated social behaviour within the bacterial population. Furthermore, the intra-species interactions of *P. aeruginosa* do not seem to involve pyocins anymore, since both pyocin resistance and production are frequently reduced in chronic isolates [120, 126, 127]. However, pyocins and many of the QS-regulated factors also play a critical role in interspecies interactions, such as the type VI secretion system (T6SS) and pyocyanin (Fig. 2c) [151–155]. And indeed, an increasing number of studies highlight an evolution of *P. aeruginosa* interactions with other co-colonizing microorganisms in the CF environment [155–160].

CONCLUDING REMARKS AND FUTURE PERSPECTIVES

The numerous sequencing studies performed on clinical isolates allowed the description of the main genetic mechanisms of *P. aeruginosa* adaptation to the CF environment. This adaptation mainly relies on the accumulation and the selection of small mutations in pathoadaptive genes. For the first time, this phenomenon was recently shown to occur within intergenic regions as well. As these non-coding elements were rarely taken into account in genomic studies, reanalyses of the vast amount of sequencing data already available should allow a better examination of their role in the *P. aeruginosa* adaptation process. At the same time, the ambiguous impact of recombination and large chromosomal rearrangements on pathoadaptation could be clarified by combining second- and third-generation sequencing methods to assemble complete genomes.

Alteration of pathoadaptive elements allows the establishment of persistence phenotypes in *P. aeruginosa*, such as high antibiotic resistance through an increased efficiency of antimicrobial efflux, an enhanced ability to form biofilm and a slowed metabolism. In addition, the low-virulence state of CF-adapted *P. aeruginosa* limits the proper functioning of the host immune responses. However, the precise relationship between these phenotypes and the *P. aeruginosa* genotype remains difficult to evaluate, especially due to the intense diversification occurring during adaptation and the pleiotropic effects of most mutations. The study of several isolates per time point throughout longitudinal studies would allow a better overview of the different evolutionary paths taken by the bacterium within CF lungs. Assessing the changes in gene and protein expressions during

P. aeruginosa adaptation thanks to -omics methods can also address some of these issues, with particular attention to the expression conditions. Transcriptomic and proteomic studies *in vivo* or in CF-like conditions, thus, appears essential to gain more insight in the physiological adaptation of *P. aeruginosa* to the CF environment.

The description of *P. aeruginosa* adaptive process ensures a better understanding of the selection forces that drive its evolution within the CF lung. While some of them are already known, such as antibiotic and oxidative stresses, other selective pressures remain little explored. Due to the polymicrobial nature of CF infections, the role of other microbial communities in *P. aeruginosa* adaptive mechanisms deserves more consideration. The activities of native or co-colonizing micro-organisms can deeply affect the environment characteristics, such as the distribution and availability of nutrients, iron or antimicrobial molecules. Moreover, a range of microbial interactions can either limit or promote *P. aeruginosa* persistence and, thus, adaptation within CF lung infections [156–158, 160–162]. In line with this, the presence of *Staphylococcus aureus* has been shown to promote *P. aeruginosa* colonization [163], whereas the latter was negatively associated with infection by other pathogens such as *Burkholderia cepacia* and *Stenotrophomonas maltophilia* [164]. Besides pathogens, the role of the normal lung microbiota is increasingly considered since commensal anaerobes have been shown to impact the antibiotic resistance and virulence of *P. aeruginosa* [161, 162]. Thus, the presence of these micro-organisms may influence establishment and adaptation of *P. aeruginosa* in the CF environment. Ultimately, the comprehensive understanding of this adaptation appears pivotal to limit the establishment of chronic *P. aeruginosa* infections.

Funding information

This work was supported by grants from the Fondation pour la Recherche Médicale (grant number EC020170637499 to L. C.), the Finovi foundation (to K. M.), and the associations 'Vaincre la mucoviscidose' and 'Gregory Lemarchal' to (K. M.).

Author contributions

K. M. and L. C. were primarily responsible for writing the original draft. K. M., L. C. and F. V. contributed to the review and editing of the final version.

Conflicts of interest

The authors declare that there are no conflicts of interest.

References

1. Moradali MF, Ghods S, Rehm BHA. *Pseudomonas aeruginosa* lifestyle: a paradigm for adaptation, survival, and persistence. *Front Cell Infect Microbiol* 2017;7:39.
2. Elabed H, González-Tortuero E, Ibacache-Quiroga C, Bakhrouf A, Johnston P et al. Seawater salt-trapped *Pseudomonas aeruginosa* survives for years and gets primed for salinity tolerance. *BMC Microbiol* 2019;19:142.
3. Lewenza S, Abboud J, Poon K, Kobryn M, Humplik I et al. *Pseudomonas aeruginosa* displays a dormancy phenotype during long-term survival in water. *PLoS One* 2018;13:e0198384.
4. Kung VL, Ozer EA, Hauser AR. The accessory genome of *Pseudomonas aeruginosa*. *Microbiol Mol Biol Rev* 2010;74:621–641.

5. Parkins MD, Somayaji R, Waters VJ. Epidemiology, biology, and impact of clonal *Pseudomonas aeruginosa* infections in cystic fibrosis. *Clin Microbiol Rev* 2018;31:e00019-18.
6. Smith EE, Buckley DG, Wu Z, Saenphimmachak C, Hoffman LR et al. Genetic adaptation by *Pseudomonas aeruginosa* to the airways of cystic fibrosis patients. *Proc Natl Acad Sci USA* 2006;103:8487-8492.
7. Cramer N, Klockgether J, Wrasman K, Schmidt M, Davenport CF et al. Microevolution of the major common *Pseudomonas aeruginosa* clones C and PA14 in cystic fibrosis lungs. *Environ Microbiol* 2011;13:1690-1704.
8. Feliziani S, Marvig RL, Luján AM, Moyano AJ, Di Rienzo JA et al. Coexistence and within-host evolution of diversified lineages of hypermutable *Pseudomonas aeruginosa* in long-term cystic fibrosis infections. *PLoS Genet* 2014;10:e1004651.
9. Markussen T, Marvig RL, Gómez-Lozano M, Aanæs K, Burleigh AE et al. Environmental heterogeneity drives within-host diversification and evolution of *Pseudomonas aeruginosa*. *mBio* 2014;5:e01592-14.
10. Bianconi I, Jeukens J, Freschi L, Alcalá-Franco B, Facchini M et al. Comparative genomics and biological characterization of sequential *Pseudomonas aeruginosa* isolates from persistent airways infection. *BMC Genomics* 2015;16:1105.
11. Bianconi I, D'Arcangelo S, Esposito A, Benedet M, Piffer E et al. Persistence and microevolution of *Pseudomonas aeruginosa* in the cystic fibrosis lung: a single-patient longitudinal genomic study. *Front Microbiol* 2018;9:3242.
12. van Mansfeld R, de Been M, Paganelli F, Yang L, Bonten M et al. Within-host evolution of the Dutch high-prevalent *Pseudomonas aeruginosa* clone ST406 during chronic colonization of a patient with cystic fibrosis. *PLoS One* 2016;11:e0158106.
13. Yang L, Jelsbak L, Marvig RL, Damkiaer S, Workman CT et al. Evolutionary dynamics of bacteria in a human host environment. *Proc Natl Acad Sci USA* 2011;108:7481-7486.
14. Marvig RL, Johansen HK, Molin S, Jelsbak L. Genome analysis of a transmissible lineage of *Pseudomonas aeruginosa* reveals pathoadaptive mutations and distinct evolutionary paths of hypermutators. *PLoS Genet* 2013;9:e1003741.
15. Wee BA, Tai AS, Sherrard LJ, Ben Zakour NL, Hanks KR et al. Whole genome sequencing reveals the emergence of a *Pseudomonas aeruginosa* shared strain sub-lineage among patients treated within a single cystic fibrosis centre. *BMC Genomics* 2018;19:644.
16. Marvig RL, Sommer LM, Molin S, Johansen HK. Convergent evolution and adaptation of *Pseudomonas aeruginosa* within patients with cystic fibrosis. *Nat Genet* 2015;47:57-64.
17. Klockgether J, Cramer N, Fischer S, Wiehlmann L, Tümmler B. Long-term microevolution of *Pseudomonas aeruginosa* differs between mildly and severely affected cystic fibrosis lungs. *Am J Respir Cell Mol Biol* 2018;59:246-256.
18. Marvig RL, Dolce D, Sommer LM, Petersen B, Ciofu O et al. Within-host microevolution of *Pseudomonas aeruginosa* in Italian cystic fibrosis patients. *BMC Microbiol* 2015;15:218.
19. Qiu X, Kulasekara BR, Lory S. Role of horizontal gene transfer in the evolution of *Pseudomonas aeruginosa* virulence. *Genome Dyn* 2009;6:126-139.
20. Brockhurst MA, Buckling A, Rainey PB. The effect of a bacteriophage on diversification of the opportunistic bacterial pathogen, *Pseudomonas aeruginosa*. *Proc Biol Sci* 2005;272:1385-1391.
21. Winstanley C, Langille MGI, Fothergill JL, Kukavica-Ibrulj I, Paradis-Bleau C et al. Newly introduced genomic prophage islands are critical determinants of in vivo competitiveness in the Liverpool epidemic strain of *Pseudomonas aeruginosa*. *Genome Res* 2009;19:12-23.
22. Harrison EM, Carter MEK, Luck S, Ou H-Y, He X et al. Pathogenicity islands PAPI-1 and PAPI-2 contribute individually and synergistically to the virulence of *Pseudomonas aeruginosa* strain PA14. *Infect Immun* 2010;78:1437-1446.
23. Dettman JR, Rodrigue N, Aaron SD, Kassen R. Evolutionary genomics of epidemic and nonepidemic strains of *Pseudomonas aeruginosa*. *Proc Natl Acad Sci USA* 2013;110:21065-21070.
24. Lemieux A-A, Jeukens J, Kukavica-Ibrulj I, Fothergill JL, Boyle B et al. Genes required for free phage production are essential for *Pseudomonas aeruginosa* chronic lung infections. *J Infect Dis* 2016;213:395-402.
25. Subedi D, Vijay AK, Kohli GS, Rice SA, Willcox M. Comparative genomics of clinical strains of *Pseudomonas aeruginosa* strains isolated from different geographic sites. *Sci Rep* 2018;8:15668.
26. Qiu X, Gurkar AU, Lory S. Interstrain transfer of the large pathogenicity island (PAPI-1) of *Pseudomonas aeruginosa*. *Proc Natl Acad Sci USA* 2006;103:19830-19835.
27. Klockgether J, Würdemann D, Reva O, Wiehlmann L, Tümmler B. Diversity of the abundant pKLC102/PAGI-2 family of genomic islands in *Pseudomonas aeruginosa*. *J Bacteriol* 2007;189:2443-2459.
28. Mathee K, Narasimhan G, Valdes C, Qiu X, Matewish JM et al. Dynamics of *Pseudomonas aeruginosa* genome evolution. *Proc Natl Acad Sci USA* 2008;105:3100-3105.
29. Carter MQ, Chen J, Lory S. The *Pseudomonas aeruginosa* pathogenicity island PAPI-1 is transferred via a novel type IV pilus. *J Bacteriol* 2010;192:3249-3258.
30. James CE, Fothergill JL, Kalwij H, Hall AJ, Cottell J et al. Differential infection properties of three inducible prophages from an epidemic strain of *Pseudomonas aeruginosa*. *BMC Microbiol* 2012;12:216.
31. Rau MH, Marvig RL, Ehrlich GD, Molin S, Jelsbak L. Deletion and acquisition of genomic content during early stage adaptation of *Pseudomonas aeruginosa* to a human host environment. *Environ Microbiol* 2012;14:2200-2211.
32. Bezuidt OKI, Klockgether J, Elsen S, Attree I, Davenport CF et al. Intraclonal genome diversity of *Pseudomonas aeruginosa* clones CHA and TB. *BMC Genomics* 2013;14:416.
33. Sharma P, Gupta SK, Rolain J-M. Whole genome sequencing of bacteria in cystic fibrosis as a model for bacterial genome adaptation and evolution. *Expert Rev Anti Infect Ther* 2014;12:343-355.
34. Fothergill JL, Mowat E, Ledson MJ, Walshaw MJ, Winstanley C. Fluctuations in phenotypes and genotypes within populations of *Pseudomonas aeruginosa* in the cystic fibrosis lung during pulmonary exacerbations. *J Med Microbiol* 2010;59:472-481.
35. Römling U, Schmidt KD, Tümmler B. Large genome rearrangements discovered by the detailed analysis of 21 *Pseudomonas aeruginosa* clone C isolates found in environment and disease habitats. *J Mol Biol* 1997;271:386-404.
36. Harmer C, Alnassafi K, Hu H, Elkins M, Bye P et al. Modulation of gene expression by *Pseudomonas aeruginosa* during chronic infection in the adult cystic fibrosis lung. *Microbiology* 2013;159:2354-2363.
37. Andersen SB, Ghoult M, Griffin AS, Petersen B, Johansen HK et al. Diversity, prevalence, and longitudinal occurrence of type II toxin-antitoxin systems of *Pseudomonas aeruginosa* infecting cystic fibrosis lungs. *Front Microbiol* 2017;8:1180.
38. England WE, Kim T, Whitaker RJ. Metapopulation structure of CRISPR-Cas immunity in *Pseudomonas aeruginosa* and its viruses. *mSystems* 2018;3:e00075-18.
39. Kresse AU, Dinesh SD, Larbig K, Römling U. Impact of large chromosomal inversions on the adaptation and evolution of *Pseudomonas aeruginosa* chronically colonizing cystic fibrosis lungs. *Mol Microbiol* 2003;47:145-158.
40. Dorman CJ, Bogue MM. The interplay between DNA topology and accessory factors in site-specific recombination in bacteria and their bacteriophages. *Sci Prog* 2016;99:420-437.
41. Darch SE, McNally A, Harrison F, Corander J, Barr HL et al. Recombination is a key driver of genomic and phenotypic diversity in a *Pseudomonas aeruginosa* population during cystic fibrosis infection. *Sci Rep* 2015;5:7649.

42. Williams D, Paterson S, Brockhurst MA, Winstanley C. Refined analyses suggest that recombination is a minor source of genomic diversity in *Pseudomonas aeruginosa* chronic cystic fibrosis infections. *Microb Genom* 2016;2:e000051.
43. Darch SE, McNally A, Corander J, Diggle SP. Response to 'Refined analyses suggest that recombination is a minor source of genomic diversity in *Pseudomonas aeruginosa* chronic cystic fibrosis infections' by Williams et al. (2016). *Microb Genom* 2016;2:e000054.
44. Oliver A. Mutators in cystic fibrosis chronic lung infection: prevalence, mechanisms, and consequences for antimicrobial therapy. *Int J Med Microbiol* 2010;300:563–572.
45. Colque CA, Albarracín Orio AG, Feliziani S, Marvig RL, Tobares AR et al. Hypermutator *Pseudomonas aeruginosa* exploits multiple genetic pathways to develop multidrug resistance during long-term infections in the airways of cystic fibrosis patients. *Antimicrob Agents Chemother* 2020;64:e02142–19.
46. Winstanley C, O'Brien S, Brockhurst MA. *Pseudomonas aeruginosa* evolutionary adaptation and diversification in cystic fibrosis chronic lung infections. *Trends Microbiol* 2016;24:327–337.
47. Clark ST, Guttman DS, Hwang DM. Diversification of *Pseudomonas aeruginosa* within the cystic fibrosis lung and its effects on antibiotic resistance. *FEMS Microbiol Lett* 2018;365:fny026.
48. Davies EV, James CE, Brockhurst MA, Winstanley C. Evolutionary diversification of *Pseudomonas aeruginosa* in an artificial sputum model. *BMC Microbiol* 2017;17:3.
49. Mehta HH, Prater AG, Beabout K, Elworth RAL, Karavis M. The essential role of hypermutation in rapid adaptation to antibiotic stress. *Antimicrob Agents Chemother* 2019;63:e00744–19.
50. Cabot G, Zamorano L, Moyà B, Juan C, Navas A et al. Evolution of *Pseudomonas aeruginosa* antimicrobial resistance and fitness under low and high mutation rates. *Antimicrob Agents Chemother* 2016;60:1767–1778.
51. Khil PP, Dulanto Chiang A, Ho J, Youn J-H, Lemon JK et al. Dynamic emergence of mismatch repair deficiency facilitates rapid evolution of ceftazidime-avibactam resistance in *Pseudomonas aeruginosa* acute infection. *mBio* 2019;10:e01822–19.
52. Hall LMC, Henderson-Begg SK. Hypermutable bacteria isolated from humans – a critical analysis. *Microbiology* 2006;152:2505–2514.
53. Oliver A, Mena A. Bacterial hypermutation in cystic fibrosis, not only for antibiotic resistance. *Clin Microbiol Infect* 2010;16:798–808.
54. Rees VE, Deveson Lucas DS, López-Causapé C, Huang Y, Kotsimbos T. Characterization of hypermutator *Pseudomonas aeruginosa* isolates from patients with cystic osis in Australia. *Antimicrob Agents Chemother* 2019;63:e02538–18.
55. Auerbach A, Kerem E, Assous MV, Picard E, Bar-Meir M. Is infection with hypermutable *Pseudomonas aeruginosa* clinically significant? *J Cyst Fibros* 2015;14:347–352.
56. Waite DJ, Honeybourne D, Smith EG, Whitehouse JL, Dowson CG. Association between hypermutator phenotype, clinical variables, mucoid phenotype, and antimicrobial resistance in *Pseudomonas aeruginosa*. *J Clin Microbiol* 2008;46:3491–3493.
57. Ferroni A, Guillemot D, Moumile K, Bernede C, Le Bourgeois M et al. Effect of mutator *P. aeruginosa* on antibiotic resistance acquisition and respiratory function in cystic fibrosis. *Pediatr Pulmonol* 2009;44:820–825.
58. Wang K, Chen Y-Q, Salido MM, Kohli GS, Kong J-L et al. The rapid *in vivo* evolution of *Pseudomonas aeruginosa* in ventilator-associated pneumonia patients leads to attenuated virulence. *Open Biol* 2017;7:170029.
59. Persyn E, Sassi M, Aubry M, Broly M, Delanou S et al. Rapid genetic and phenotypic changes in *Pseudomonas aeruginosa* clinical strains during ventilator-associated pneumonia. *Sci Rep* 2019;9:4720.
60. Fischer S, Klockgether J, Morán Losada P, Chouvarine P, Cramer N et al. Intraclonal genome diversity of the major *Pseudomonas aeruginosa* clones C and PA14. *Environ Microbiol Rep* 2016;8:227–234.
61. Wiehlmann L, Wagner G, Cramer N, Siebert B, Gudowius P et al. Population structure of *Pseudomonas aeruginosa*. *Proc Natl Acad Sci USA* 2007;104:8101–8106.
62. Damkiaer S, Yang L, Molin S, Jelsbak L. Evolutionary remodeling of global regulatory networks during long-term bacterial adaptation to human hosts. *Proc Natl Acad Sci USA* 2013;110:7766–7771.
63. Feltner JB, Wolter DJ, Pope CE, Groleau M-C, Smalley NE et al. LasR variant cystic fibrosis isolates reveal an adaptable quorum-sensing hierarchy in *Pseudomonas aeruginosa*. *mBio* 2016;7:e01513–16.
64. Chen R, Déziel E, Groleau M-C, Schaefer AL, Greenberg EP. Social cheating in a *Pseudomonas aeruginosa* quorum-sensing variant. *Proc Natl Acad Sci USA* 2019;116:7021–7026.
65. Kostylev M, Kim DY, Smalley NE, Salukhe I, Greenberg EP et al. Evolution of the *Pseudomonas aeruginosa* quorum-sensing hierarchy. *Proc Natl Acad Sci USA* 2019;116:7027–7032.
66. Cruz RL, Asfahl KL, Van den Bossche S, Coenye T, Crabbé A. RhlR-regulated acyl-homoserine lactone quorum sensing in a cystic fibrosis isolate of *Pseudomonas aeruginosa*. *mBio* 2020;11:e00532–20.
67. Jorth P, Staudinger BJ, Wu X, Hisert KB, Hayden H et al. Regional isolation drives bacterial diversification within cystic fibrosis lungs. *Cell Host Microbe* 2015;18:307–319.
68. Williams D, Evans B, Haldenby S, Walshaw MJ, Brockhurst MA et al. Divergent, coexisting *Pseudomonas aeruginosa* lineages in chronic cystic fibrosis lung infections. *Am J Respir Crit Care Med* 2015;191:775–785.
69. Williams D, Fothergill JL, Evans B, Caples J, Haldenby S et al. Transmission and lineage displacement drive rapid population genomic flux in cystic fibrosis airway infections of a *Pseudomonas aeruginosa* epidemic strain. *Microb Genom* 2018;4:000167.
70. Anthony M, Rose B, Pegler MB, Elkins M, Service H et al. Genetic analysis of *Pseudomonas aeruginosa* isolates from the sputa of Australian adult cystic fibrosis patients. *J Clin Microbiol* 2002;40:2772–2778.
71. Bragonzi A, Wiehlmann L, Klockgether J, Cramer N, Worlitzsch D et al. Sequence diversity of the mucABD locus in *Pseudomonas aeruginosa* isolates from patients with cystic fibrosis. *Microbiology* 2006;152:3261–3269.
72. Ciofu O, Lee B, Johannesson M, Hermansen NO, Meyer P et al. Investigation of the algT operon sequence in mucoid and non-mucoid *Pseudomonas aeruginosa* isolates from 115 Scandinavian patients with cystic fibrosis and in 88 *in vitro* non-mucoid revertants. *Microbiology* 2008;154:103–113.
73. Pulcrano G, Iula DV, Raia V, Rossano F, Catania MR. Different mutations in mucA gene of *Pseudomonas aeruginosa* mucoid strains in cystic fibrosis patients and their effect on algU gene expression. *New Microbiol* 2012;35:295–305.
74. Candido Caçador N, Paulino da Costa Capizzani C, Gomes Monteiro Marin Torres LA, Galetti R, Ciofu O et al. Adaptation of *Pseudomonas aeruginosa* to the chronic phenotype by mutations in the algTmucABD operon in isolates from Brazilian cystic fibrosis patients. *PLoS One* 2018;13:e0208013.
75. Panmanee W, Su S, Schurr MJ, Lau GW, Zhu X et al. The anti-sigma factor MucA of *Pseudomonas aeruginosa*: dramatic differences of a mucA22 vs. a ΔmucA mutant in anaerobic acidified nitrite sensitivity of planktonic and biofilm bacteria *in vitro* and during chronic murine lung infection. *PLoS One* 2019;14:e0216401.
76. Brule CE, Grayhack EJ. Synonymous codons: choose wisely for expression. *Trends Genet* 2017;33:283–297.
77. Kristofich J, Morgenthaler AB, Kinney WR, Ebmeier CC, Snyder DJ et al. Synonymous mutations make dramatic contributions to fitness when growth is limited by a weak-link enzyme. *PLoS Genet* 2018;14:e1007615.

78. Bailey SF, Hinz A, Kassen R. Adaptive synonymous mutations in an experimentally evolved *Pseudomonas fluorescens* population. *Nat Commun* 2014;5:4076.
79. Lebeuf-Taylor E, McCloskey N, Bailey SF, Hinz A, Kassen R. The distribution of fitness effects among synonymous mutations in a gene under directional selection. *Elife* 2019;8:e45952.
80. Thorpe HA, Bayliss SC, Hurst LD, Feil EJ. Comparative analyses of selection operating on nontranslated intergenic regions of diverse bacterial species. *Genetics* 2017;206:363–376.
81. Khademi SMH, Sazinas P, Jelsbak L. Within-host adaptation mediated by intergenic evolution in *Pseudomonas aeruginosa*. *Genome Biol Evol* 2019;11:1385–1397.
82. Ernst RK, D'Argenio DA, Ichikawa JK, Bangera MG, Selgrade S et al. Genome mosaicism is conserved but not unique in *Pseudomonas aeruginosa* isolates from the airways of young children with cystic fibrosis. *Environ Microbiol* 2003;5:1341–1349.
83. Huse HK, Kwon T, Zlosnik JEA, Speert DP, Marcotte EM et al. Parallel evolution in *Pseudomonas aeruginosa* over 39,000 generations in vivo. *mBio* 2010;1:e00199-10.
84. Rau MH, Hansen SK, Johansen HK, Thomsen LE, Workman CT et al. Early adaptive developments of *Pseudomonas aeruginosa* after the transition from life in the environment to persistent colonization in the airways of human cystic fibrosis hosts. *Environ Microbiol* 2010;12:1643–1658.
85. Lee B, Schjerling CK, Kirkby N, Hoffmann N, Borup R et al. Mucoicid *Pseudomonas aeruginosa* isolates maintain the biofilm formation capacity and the gene expression profiles during the chronic lung infection of CF patients. *APMIS* 2011;119:263–274.
86. Schuster M, Lostrich CP, Ogi T, Greenberg EP. Identification, timing, and signal specificity of *Pseudomonas aeruginosa* quorum-controlled genes: a transcriptome analysis. *J Bacteriol* 2003;185:2066–2079.
87. Wagner VE, Bushnell D, Passador L, Brooks AI, Iglewski BH. Microarray analysis of *Pseudomonas aeruginosa* quorum-sensing regulons: effects of growth phase and environment. *J Bacteriol* 2003;185:2080–2095.
88. Damron FH, Owings JP, Okkotsu Y, Varga JJ, Schurr JR et al. Analysis of the *Pseudomonas aeruginosa* regulon controlled by the sensor kinase KinB and sigma factor RpoN. *J Bacteriol* 2012;194:1317–1330.
89. Schultz A, Stick S. Early pulmonary inflammation and lung damage in children with cystic fibrosis: early inflammation and lung damage in CF. *Respirology* 2015;20:569–578.
90. Gifford AH, Willger SD, Dolben EL, Moulton LA, Dorman DB et al. Use of a multiplex transcript method for analysis of *Pseudomonas aeruginosa* gene expression profiles in the cystic fibrosis lung. *Infect Immun* 2016;84:2995–3006.
91. Rossi E, Falcone M, Molin S, Johansen HK. High-resolution in situ transcriptomics of *Pseudomonas aeruginosa* unveils genotype independent patho-phenotypes in cystic fibrosis lungs. *Nat Commun* 2018;9:3459.
92. Cornforth DM, Dees JL, Ibberson CB, Huse HK, Mathiesen IH et al. *Pseudomonas aeruginosa* transcriptome during human infection. *Proc Natl Acad Sci USA* 2018;115:E5125–E5134.
93. Kordes A, Preusse M, Willger SD, Braubach P, Jonigk D et al. Genetically diverse *Pseudomonas aeruginosa* populations display similar transcriptomic profiles in a cystic fibrosis explanted lung. *Nat Commun* 2019;10:3397.
94. Kumar SS, Tandberg JI, Penesyan A, Elbourne LDH, Suarez-Bosche N et al. Dual transcriptomics of host-pathogen interaction of cystic fibrosis isolate *Pseudomonas aeruginosa* PASS1 with zebrafish. *Front Cell Infect Microbiol* 2018;8:406.
95. Damron FH, Oglesby-Sherrouse AG, Wilks A, Barbier M. Dual-seq transcriptomics reveals the battle for iron during *Pseudomonas aeruginosa* acute murine pneumonia. *Sci Rep* 2016;16:39172.
96. Hare NJ, Cordwell SJ. Proteomics of bacterial pathogens: *Pseudomonas aeruginosa* infections in cystic fibrosis - a case study. *Proteomics Clin Appl* 2010;4:228–248.
97. Kamath KS, Kumar SS, Kaur J, Venkatakrishnan V, Paulsen IT et al. Proteomics of hosts and pathogens in cystic fibrosis. *Proteomics Clin Appl* 2015;9:134–146.
98. Penesyan A, Kumar SS, Kamath K, Shathili AM, Venkatakrishnan V et al. Genetically and phenotypically distinct *Pseudomonas aeruginosa* cystic fibrosis isolates share a core proteomic signature. *PLoS One* 2015;10:e0138527.
99. Kamath KS, Pascovici D, Penesyan A, Goel A, Venkatakrishnan V et al. *Pseudomonas aeruginosa* cell membrane protein expression from phenotypically diverse cystic fibrosis isolates demonstrates host-specific adaptations. *J Proteome Res* 2016;15:2152–2163.
100. Kamath KS, Krisp C, Chick J, Pascovici D, Gygi SP et al. *Pseudomonas aeruginosa* proteome under hypoxic stress conditions mimicking the cystic fibrosis lung. *J Proteome Res* 2017;16:3917–3928.
101. Wu X, Siehnell RJ, Garudathri J, Staudinger BJ, Hisert KB et al. In vivo proteome of *Pseudomonas aeruginosa* in airways of cystic fibrosis patients. *J Proteome Res* 2019;18:2601–2612.
102. Hare NJ, Solis N, Harmer C, Marzook NB, Rose B et al. Proteomic profiling of *Pseudomonas aeruginosa* AES-1R, PAO1 and PA14 reveals potential virulence determinants associated with a transmissible cystic fibrosis-associated strain. *BMC Microbiol* 2012;12:16.
103. Hare NJ, Soe CZ, Rose B, Harbour C, Codd R et al. Proteomics of *Pseudomonas aeruginosa* Australian epidemic strain 1 (AES-1) cultured under conditions mimicking the cystic fibrosis lung reveals increased iron acquisition via the siderophore pyochelin. *J Proteome Res* 2012;11:776–795.
104. Sousa AM, Pereira MO. *Pseudomonas aeruginosa* diversification during infection development in cystic fibrosis lungs - a review. *Pathogens* 2014;3:680–703.
105. Klockgether J, Miethke N, Kubesch P, Bohn Y-S, Brockhausen I et al. Intracolon diversity of the *Pseudomonas aeruginosa* cystic fibrosis airway isolates TBCF10839 and TBCF121838: distinct signatures of transcriptome, proteome, metabolome, adherence and pathogenicity despite an almost identical genome sequence. *Environ Microbiol* 2013;15:191–210.
106. Faure E, Kwong K, Nguyen D. *Pseudomonas aeruginosa* in chronic lung infections: how to adapt within the host? *Front Immunol* 2018;9:2416.
107. La Rosa R, Johansen HK, Molin S. Adapting to the airways: metabolic requirements of *Pseudomonas aeruginosa* during the infection of cystic fibrosis patients. *Metabolites* 2019;9:234.
108. Riquelme SA, Wong Fok Lung T, Prince A. Pulmonary pathogens adapt to immune signaling metabolites in the airway. *Front Immunol* 2020;11:385.
109. Schick A, Kassen R. Rapid diversification of *Pseudomonas aeruginosa* in cystic fibrosis lung-like conditions. *Proc Natl Acad Sci USA* 2018;115:10714–10719.
110. La Rosa R, Johansen HK, Molin S. Convergent metabolic specialization through distinct evolutionary paths in *Pseudomonas aeruginosa*. *mBio* 2018;9:e00269-18.
111. Palmer KL, Aye LM, Whiteley M. Nutritional cues control *Pseudomonas aeruginosa* multicellular behavior in cystic fibrosis sputum. *J Bacteriol* 2007;189:8079–8087.
112. Barth AL, Pitt TL. The high amino-acid content of sputum from cystic fibrosis patients promotes growth of auxotrophic *Pseudomonas aeruginosa*. *J Med Microbiol* 1996;45:110–119.
113. Kumar SS, Penesyan A, Elbourne LDH, Gillings MR, Paulsen IT. Catabolism of nucleic acids by a cystic fibrosis *Pseudomonas aeruginosa* isolate: an adaptive pathway to cystic fibrosis sputum environment. *Front Microbiol* 2019;10:1199.
114. Cramer N, Fischer S, Hedtfeld S, Dorda M, Tümmeler B. Intracolon competitive fitness of longitudinal cystic fibrosis *Pseudomonas aeruginosa* airway isolates in liquid cultures. *Environ Microbiol* 2020;22:2536–.

115. Evans TJ. Small colony variants of *Pseudomonas aeruginosa* in chronic bacterial infection of the lung in cystic fibrosis. *Future Microbiol* 2015;10:231–239.
116. Mangiaterra G, Amiri M, Di Cesare A, Pasquaroli S, Manso E et al. Detection of viable but non-culturable *Pseudomonas aeruginosa* in cystic fibrosis by qPCR: a validation study. *BMC Infect Dis* 2018;18:701.
117. Al Ahmar R, Kirby BD, Yu HD. Culture of small colony variant of *Pseudomonas aeruginosa* and quantitation of its alginate. *J Vis Exp* 2020;156:e60466.
118. López-Causapé C, Cabot G, Del Barrio-Tofiño E, Oliver A. The versatile mutational resistome of *Pseudomonas aeruginosa*. *Front Microbiol* 2018;9:685.
119. Suresh M, Nithya N, Jayasree PR, Vimal KP, Manish Kumar PR. Mutational analyses of regulatory genes, mexR, nalC, nalD and mexZ of mexAB-oprM and mexXY operons, in efflux pump hyper-expressing multidrug-resistant clinical isolates of *Pseudomonas aeruginosa*. *World J Microbiol Biotechnol* 2018;34:83.
120. Huszczyński SM, Lam JS, Khursigara CM. The role of *Pseudomonas aeruginosa* lipopolysaccharide in bacterial pathogenesis and physiology. *Pathogens* 2019;9:6.
121. Maldonado RF, Sá-Correia I, Valvano MA. Lipopolysaccharide modification in Gram-negative bacteria during chronic infection. *FEMS Microbiol Rev* 2016;40:480–493.
122. Bricio-Moreno L, Sheridan VH, Goodhead I, Armstrong S, Wong JKL et al. Evolutionary trade-offs associated with loss of PmrB function in host-adapted *Pseudomonas aeruginosa*. *Nat Commun* 2018;9:2635.
123. Poon KKH, Westman EL, Vinogradov E, Jin S, Lam JS. Functional characterization of MigA and WapR: putative rhamnosyltransferases involved in outer core oligosaccharide biosynthesis of *Pseudomonas aeruginosa*. *J Bacteriol* 2008;190:1857–1865.
124. Döbelmann B, Willmann M, Steglich M, Bunk B, Nübel U et al. Rapid and consistent evolution of colistin resistance in extensively drug-resistant *Pseudomonas aeruginosa* during morbidity-dostat culture. *Antimicrob Agents Chemother* 2017;61:e00043–17.
125. Cullen L, Weiser R, Olszak T, Maldonado RF, Moreira AS et al. Phenotypic characterization of an international *Pseudomonas aeruginosa* reference panel: strains of cystic fibrosis (CF) origin show less in vivo virulence than non-CF strains. *Microbiology* 2015;161:1961–1977.
126. Römling U, Fiedler B, Bosshammer J, Grothues D, Greipel J et al. Epidemiology of chronic *Pseudomonas aeruginosa* infections in cystic fibrosis. *J Infect Dis* 1994;170:1616–1621.
127. Ghoult M, West SA, Johansen HK, Molin S, Harrison OB et al. Bacteriocin-mediated competition in cystic fibrosis lung infections. *Proc Biol Sci* 2015;282:20150972.
128. Redero M, López-Causapé C, Aznar J, Oliver A, Blázquez J et al. Susceptibility to R-pyocins of *Pseudomonas aeruginosa* clinical isolates from cystic fibrosis patients. *J Antimicrob Chemother* 2018;73:2770–2776.
129. Franklin MJ, Nivens DE, Weadge JT, Howell PL. Biosynthesis of the *Pseudomonas aeruginosa* extracellular polysaccharides, alginate, Pel, and Psl. *Front Microbiol* 2011;2:167.
130. Colvin KM, Irie Y, Tart CS, Urbano R, Whitney JC et al. The Pel and Psl polysaccharides provide *Pseudomonas aeruginosa* structural redundancy within the biofilm matrix. *Environ Microbiol* 2012;14:1913–1928.
131. Colvin KM, Gordon VD, Murakami K, Borlee BR, Wozniak DJ et al. The Pel polysaccharide can serve a structural and protective role in the biofilm matrix of *Pseudomonas aeruginosa*. *PLoS Pathog* 2011;7:e1001264.
132. Billings N, Millan M, Caldara M, Rusconi R, Tarasova Y et al. The extracellular matrix component Psl provides fast-acting antibiotic defense in *Pseudomonas aeruginosa* biofilms. *PLoS Pathog* 2013;9:e1003526.
133. Harrison JJ, Almlad H, Irie Y, Wolter DJ, Eggleston HC et al. Elevated exopolysaccharide levels in *Pseudomonas aeruginosa* flagellar mutants have implications for biofilm growth and chronic infections. *PLoS Genet* 2020;16:e1008848.
134. Starkey M, Hickman JH, Ma L, Zhang N, De Long S et al. *Pseudomonas aeruginosa* rugose small-colony variants have adaptations that likely promote persistence in the cystic fibrosis lung. *J Bacteriol* 2009;191:3492–3503.
135. Henry RL, Mellis CM, Petrovic L. Mucoid *Pseudomonas aeruginosa* is a marker of poor survival in cystic fibrosis. *Pediatr Pulmonol* 1992;12:158–161.
136. Parad RB, Gerard CJ, Zurakowski D, Nichols DP, Pier GB. Pulmonary outcome in cystic fibrosis is influenced primarily by mucoid *Pseudomonas aeruginosa* infection and immune status and only modestly by genotype. *Infect Immun* 1999;67:4744–4750.
137. Hengzhuang W, Wu H, Ciofu O, Song Z, Høiby N. Pharmacokinetics/pharmacodynamics of colistin and imipenem on mucoid and nonmucoid *Pseudomonas aeruginosa* biofilms. *Antimicrob Agents Chemother* 2011;55:4469–4474.
138. Malhotra S, Hayes D, Wozniak DJ. Mucoid *Pseudomonas aeruginosa* and regional inflammation in the cystic fibrosis lung. *J Cyst Fibros* 2019;18:796–803.
139. Cornelis P, Dingemans J. *Pseudomonas aeruginosa* adapts its iron uptake strategies in function of the type of infections. *Front Cell Infect Microbiol* 2013;3:75.
140. Minandri F, Imperi F, Frangipani E, Bonchi C, Visaggio D et al. Role of iron uptake systems in *Pseudomonas aeruginosa* virulence and airway infection. *Infect Immun* 2016;84:2324–2335.
141. Marvig RL, Damkiær S, Khademi SMH, Markussen TM, Molin S et al. Within-host evolution of *Pseudomonas aeruginosa* reveals adaptation toward iron acquisition from hemoglobin. *mBio* 2014;5:e00966–14.
142. Ballarini A, Scalet G, Kos M, Cramer N, Wiehlmann L et al. Molecular typing and epidemiological investigation of clinical populations of *Pseudomonas aeruginosa* using an oligonucleotide-microarray. *BMC Microbiol* 2012;12:152.
143. Shaver CM, Hauser AR. Relative contributions of *Pseudomonas aeruginosa* ExoU, ExoS, and ExoT to virulence in the lung. *Infect Immun* 2004;72:6969–6977.
144. Sawa T, Shimizu M, Moriyama K, Wiener-Kronish JP. Association between *Pseudomonas aeruginosa* type III secretion, antibiotic resistance, and clinical outcome: a review. *Crit Care* 2014;18:668.
145. SargesEDSNF, Rodrigues YC, Furlaneto IP, de Melo MVH, Brabo GLDC et al. *Pseudomonas aeruginosa* type III secretion system virulotypes and their association with clinical features of cystic fibrosis patients. *Infect Drug Resist* 2020;13:3771–3781.
146. Tognon M, Köhler T, Gdaniec BG, Hao Y, Lam JS et al. Co-evolution with *Staphylococcus aureus* leads to lipopolysaccharide alterations in *Pseudomonas aeruginosa*. *ISME J* 2017;11:2233–2243.
147. Zhao K, Du L, Lin J, Yuan Y, Wang X et al. *Pseudomonas aeruginosa* quorum-sensing and type vi secretion system can direct interspecific coexistence during evolution. *Front Microbiol* 2018;9:2287.
148. Diggie SP, Griffin AS, Campbell GS, West SA. Cooperation and conflict in quorum-sensing bacterial populations. *Nature* 2007;450:411–414.
149. Sandoz KM, Mitzimberg SM, Schuster M. Social cheating in *Pseudomonas aeruginosa* quorum sensing. *Proc Natl Acad Sci USA* 2007;104:15876–15881.
150. Dandekar AA, Chugani S, Greenberg EP. Bacterial quorum sensing and metabolic incentives to cooperate. *Science* 2012;338:264–266.
151. Tashiro Y, Yawata Y, Toyofuku M, Uchiyama H, Nomura N. Interspecies interaction between *Pseudomonas aeruginosa* and other microorganisms. *Microbes Environ* 2013;28:13–24.
152. Sana TG, Berni B, Bleves S. The T6SSs of *Pseudomonas aeruginosa* strain PAO1 and their effectors: beyond bacterial-cell targeting. *Front Cell Infect Microbiol* 2016;6:61.

153. Nguyen AT, Oglesby-Sherrouse AG. Interactions between *Pseudomonas aeruginosa* and *Staphylococcus aureus* during co-cultivations and polymicrobial infections. *Appl Microbiol Biotechnol* 2016;100:6141–6148.
154. Hotterbeekx A, Kumar-Singh S, Goossens H, Malhotra-Kumar S. *In vivo* and *In vitro* interactions between *Pseudomonas aeruginosa* and *Staphylococcus* spp. *Front Cell Infect Microbiol* 2017;7:106.
155. Fourie R, Pohl CH. Beyond Antagonism: The Interaction Between *Candida* Species and *Pseudomonas aeruginosa*. *J Fungi* 2019;5:34.
156. Baldan R, Cigana C, Testa F, Bianconi I, De Simone M et al. Adaptation of *Pseudomonas aeruginosa* in cystic fibrosis airways influences virulence of *Staphylococcus aureus* in vitro and murine models of co-infection. *PLoS One* 2014;9:e89614.
157. Michelsen CF, Christensen A-MJ, Bojer MS, Høiby N, Ingmer H et al. *Staphylococcus aureus* alters growth activity, autolysis, and antibiotic tolerance in a human host-adapted *Pseudomonas aeruginosa* lineage. *J Bacteriol* 2014;196:3903–3911.
158. Frydenlund Michelsen C, Hossein Khademi SM, Krogh Johansen H, Ingmer H, Dorrestein PC et al. Evolution of metabolic divergence in *Pseudomonas aeruginosa* during long-term infection facilitates a proto-cooperative interspecies interaction. *ISME J* 2016;10:1323–1336.
159. Briaud P, Camus L, Bastien S, Doléans-Jordheim A, Vandenesch F et al. Coexistence with *Pseudomonas aeruginosa* alters *Staphylococcus aureus* transcriptome, antibiotic resistance and internalization into epithelial cells. *Sci Rep* 2019;9:16564.
160. Camus L, Briaud P, Bastien S, Elsen S, Doléans-Jordheim A et al. Trophic cooperation promotes bacterial survival of *Staphylococcus aureus* and *Pseudomonas aeruginosa*. *ISME J* 2020;14:3093–3105.
161. Flynn JM, Cameron LC, Wiggen TD, Dunitz JM, Harcombe WR et al. Disruption of cross-feeding inhibits pathogen growth in the sputa of patients with cystic fibrosis. *mSphere* 2020;5:e00343–20.
162. Scott JE, O'Toole GA. The yin and yang of *Streptococcus* lung infections in cystic fibrosis: a model for studying polymicrobial interactions. *J Bacteriol* 2019;201:e00115–19.
163. Cigana C, Bianconi I, Baldan R, De Simone M, Riva C et al. *Staphylococcus aureus* impacts *Pseudomonas aeruginosa* chronic respiratory disease in murine models. *J Infect Dis* 2018;217:933–942.
164. Granchelli AM, Adler FR, Keogh RH, Kartsonaki C, Cox DR. Microbial interactions in the cystic fibrosis airway. *J Clin Microbiol* 2018;56:e00354–18.

Five reasons to publish your next article with a Microbiology Society journal

1. The Microbiology Society is a not-for-profit organization.
2. We offer fast and rigorous peer review – average time to first decision is 4–6 weeks.
3. Our journals have a global readership with subscriptions held in research institutions around the world.
4. 80% of our authors rate our submission process as 'excellent' or 'very good'.
5. Your article will be published on an interactive journal platform with advanced metrics.

Find out more and submit your article at microbiologyresearch.org.

Table S1: *P. aeruginosa* intergenic regions under positive selection. Mutations in intergenic regions were identified as positively selected by Khademi et al. (80) and sorted in this table according to the index of interest (Column D). For each intergenic region, the index was calculated by multiplying the number of intergenic mutations (Column A) by the number of impacted lineages (Column B) and the number of independent studies identifying the region as mutated (Column C).

Name of up-stream gene	Name of down-stream gene	PAO1 locus	Product	No. of intergenic mutation	No. of lineages with mutated isolate	No. of independent studies identifying the region as mutated	Index of interest (Column A x Column B x Column C)	References
<i>phus</i>	<i>phuR</i>	PA4709 - PA4710	PhuS/Heme/Hemoglobin uptake outer membrane receptor PhuR precursor	40	4	4	640	7,9,17,80
		PA0428 - PA0429	probable ATP-dependent RNA helicase/hypothetical protein	34	10	1	340	80
		PA4786 - PA4787	probable short-chain dehydrogenase/probable transcriptional regulator	28	12	1	336	80
		PA4690.5 - PA4691	16S ribosomal RNA/hypothetical protein	54	6	1	324	80
		PA2535 - PA2536	probable oxidoreductase/probable phosphatidate cytidyltransferase	18	6	2	216	7,80
<i>motY</i>	<i>pyrC</i>	PA3526 - PA3527	probable outer membrane protein precursor/dihydroorotase	32	6	1	192	80
		PA3230 - PA3231	conserved hypothetical protein/downstream hypothetical protein	24	7	1	168	80
		PA3547 - PA3548	poly(beta-d-mannuronate) lyase precursor AlgU/alginate O-acetyltransferase AlgI	14	6	2	168	7,80
		PA0976.1 - PA0977	tRNA-Lys/hypothetical protein	26	6	1	156	80
<i>rpIU</i>	<i>ispB</i>	PA4568 - PA4569	50S ribosomal protein L21/octaprenyl-diphosphate synthase	22	7	1	154	80
<i>phzM</i>	<i>phzA1</i>	PA4209 - PA4210	probable phenazine-specific methyltransferase/probable phenazine biosynthesis protein	12	6	2	144	7,80
		PA3280 - PA3281	Pyrophosphate-specific outer membrane porin OprO precursor/hypothetical protein	10	5	2	100	7,80
		PA3418 - PA3419	leucine dehydrogenase/hypothetical protein	10	5	2	100	7,80
<i>ampR</i>	<i>ampC</i>	PA4109 - PA4110	transcriptional regulator AmpR/beta-lactamase precursor	12	4	2	96	9,80
	<i>mlb</i>	PA5160.1 - PA5161	tRNA-Trp/tTDP-D-glucose 4,6-dehydratase	16	6	1	96	80
		PA1334 - PA1335	probable oxidoreductase/probable two-component response regulator	28	3	1	84	80
		PA0979 - PA0980	conserved hypothetical protein/hypothetical protein	16	5	1	80	80
<i>ndvB</i>		PA1163 - PA1164	NdvB/conserved hypothetical protein	10	4	2	80	7,80
<i>norM</i>		PA1361 - PA1362	NorM/hypothetical protein	10	4	2	80	7,80
		PA3965 - PA3966	probable transcriptional regulator/hypothetical protein	16	5	1	80	80
		PA1941 - PA1942	hypothetical protein/hypothetical protein	12	6	1	72	80
<i>effB</i>		PA2952 - PA2953	electron transfer flavoprotein beta-subunit/electron transfer flavoprotein-ubiquinone oxidoreduc	14	5	1	70	80
	<i>aph</i>	PA4118 - PA4119	hypothetical protein/aminoglycoside 3'-phosphotransferase type Ib	14	5	1	70	80
		PA0595 - PA0596	LPS-assembly protein LptD/hypothetical protein	16	4	1	64	80
<i>pdxB</i>	<i>aceK</i>	PA1375 - PA1376	erythronate-4-phosphate dehydrogenase/isocitrate dehydrogenase kinase/phosphatase	12	5	1	60	80
		PA1841 - PA1842	hypothetical protein/hypothetical protein	12	5	1	60	80
<i>xthA</i>		PA2545 - PA2546	exodeoxyribonuclease III/probable ring-cleaving dioxygenase	20	3	1	60	80
<i>moaC</i>		PA3918 - PA3919	molybdopterin biosynthetic protein C/conserved hypothetical protein	12	5	1	60	80
		PA4960 - PA4961	probable phosphoserine phosphatase/hypothetical protein	12	5	1	60	80
<i>poxB</i>		PA5297 - PA5298	pyruvate dehydrogenase (cytochrome)/xanthine phosphoribosyltransferase	12	5	1	60	80
		PA0588 - PA0589	conserved hypothetical protein/conserved hypothetical protein	14	4	1	56	80
		PA0977 - PA0978	hypothetical protein/conserved hypothetical protein	14	4	1	56	80
		PA1191 - PA1192	hypothetical protein/conserved hypothetical protein	14	4	1	56	80
<i>ppc</i>		PA3687 - PA3688	phosphoenolpyruvate carboxylase/hypothetical protein	14	4	1	56	80

PA1348 - PA1349	hypothetical protein//conserved hypothetical protein	10	5	1	1	50	80
<i>bacA</i>	probable transporter/bacitracin resistance protein	16	3	1	1	48	80
PA1958 - PA1959	hypothetical protein//putative TRAP-type C4-dicarboxylate transport	12	4	1	1	48	80
PA3779 - PA3780	conserved hypothetical protein//hypothetical protein	8	3	2	2	48	7,80
PA3785 - PA3786	conserved hypothetical protein//hypothetical protein	16	3	1	1	48	80
PA4792 - PA4793	probable cytochrome//conserved hypothetical protein	8	3	2	2	42	80
PA5491 - PA5492	probable transcriptional regulator//hypothetical protein	14	3	1	1	42	80
PA0980 - PA0981	probable transcriptional regulator//hypothetical protein	14	3	1	1	42	80
PA3341 - PA3342	hypothetical protein//PhtD	10	4	1	1	40	80
PA0714 - PA0714.1	probable sensor/response regulator hybrid//hypothetical protein	10	4	1	1	40	80
PA1243 - PA1244	tyrosine porin OpdT//hypothetical protein	10	4	1	1	40	80
PA2505 - PA2506	probable short-chain dehydrogenase//hypothetical protein	10	4	1	1	40	80
PA4089 - PA4090	tRNA-Met//conserved hypothetical protein	12	3	1	1	36	80
PA0574.1 - PA0575	tyrosyl-tRNA synthetase 2//16S ribosomal RNA	18	2	1	1	36	80
<i>ccoP1</i>	probable ferredoxin/Cytochrome c oxidase, cbb3-type, CcoQ subunit	12	3	1	1	36	80
<i>hisF1</i>	hypothetical protein//imidazoleglycerol-phosphate synthase, cyclase subunit	12	3	1	1	36	80
PA3673 - PA3674	glycerol-3-phosphate acyltransferase//hypothetical protein	6	3	2	2	36	7,80
PA0845 - PA0846	CerN//probable sulfate uptake protein	10	3	1	1	30	80
PA2561 - PA2562	probable chemotaxis transducer//hypothetical protein	10	3	1	1	30	80
PA3768 - PA3769	probable metallo-oxidoreductase//GMP synthase	10	3	1	1	30	80
PA1142 - PA1143	probable transcriptional regulator//hypothetical protein	8	3	1	1	24	80
<i>nagZ</i>	beta-N-acetyl-D-glucosaminidase/transcriptional regulator PsrA	8	3	1	1	24	80
<i>gshB</i>	glutathione synthetase// twitching motility protein PilG	6	3	1	1	18	80
<i>plcR</i>	glycosyl transferase//phospholipase accessory protein PlcR precursor	6	3	1	1	18	80
<i>popD</i>	Translocator outer membrane protein PopD precursor/ExsC, exoenzyme S synthesis protein C	6	3	1	1	18	80
<i>hmgA</i>	homogenisate 1,2-dioxygenase//probable transcriptional regulator	6	3	1	1	18	80
PA2069 - PA2070	probable carbamoyl transferase//hypothetical protein	6	3	1	1	18	80
PA2418 - PA2419	hypothetical protein//probable hydrolase	6	3	1	1	18	80
PA4216 - PA4217	probable pyridoxamine 5'-phosphate oxidase//flavin-containing monooxygenase	6	3	1	1	18	80
PA4873 - PA4874	probable heat-shock protein//conserved hypothetical protein	6	3	1	1	18	80
<i>nasS</i>	NasS/acorniate hydratase 2	10	1	1	1	10	80
<i>treA</i>	hypothetical protein/periplasmic trehalase precursor	8	1	1	1	8	80
PA2415 - PA2416	ribosomal large subunit pseudouridine synthase C//ribonuclease E	8	1	1	1	8	80
<i>rluC</i>	hypothetical protein//hypothetical protein	6	1	1	1	6	80
PA0014 - PA0015	tRNA-Ser//probable glycosyl transferase	6	1	1	1	6	80
PA1013.1 - PA1014	hydrogen cyanide synthase HcnC//probable transcriptional regulator	6	1	1	1	6	80
PA2195 - PA2196	probable two-component sensor//hypothetical protein	6	1	1	1	6	80
PA2480 - PA2481	hypothetical protein//lyso-phospholipase A	6	1	1	1	6	80
PA2855 - PA2856	conserved hypothetical protein//orfotidine 5'-phosphate decarboxylase	6	1	1	1	6	80
<i>apeA</i>	regulatory RNA RsmZ//sigma factor RpoS	6	1	1	1	6	80
<i>pyrF</i>	hypothetical protein//hypothetical protein	6	1	1	1	6	80
<i>rpoS</i>	probable outer membrane protein precursor//hypothetical protein	6	1	1	1	6	80
PA4040 - PA4041	conserved hypothetical protein//DNA polymerase I	6	1	1	1	6	80
PA4837 - PA4838	conserved hypothetical protein//DNA polymerase I	6	1	1	1	6	80
<i>polA</i>	conserved hypothetical protein//DNA polymerase I	6	1	1	1	6	80

3 Etude de cas : les interactions entre *P. aeruginosa* et *S. aureus* chez les patients atteints de mucoviscidose

La forte prévalence de *S. aureus* et *P. aeruginosa* dans les poumons des patients atteints de mucoviscidose favorise les co-infections à ces deux pathogènes, qui touchent 25% (France) à 35% (Etats-Unis) des sujets selon les cohortes (133, 163, 164). L'impact de la co-infection par *S. aureus* et *P. aeruginosa* sur l'état de santé des patients atteints de mucoviscidose est de plus en plus investigué mais encore débattu. Si certaines études n'observent pas d'effet négatif de la co-infection sur le bilan clinique par rapport à une infection uniquement causée par *P. aeruginosa* (163, 165), d'autres décrivent une diminution des fonctions respiratoires ainsi qu'une augmentation de l'inflammation et de la fréquence des exacerbations chez les patients co-infectés (131, 132, 164). Ces résultats contradictoires proviennent probablement de la disparité des cohortes et des méthodes d'analyses statistiques utilisées dans ces différentes études, et devraient être éclaircis par de prochaines analyses.

Les études décrivant une co-infection plus sévère que la mono-infection à *P. aeruginosa* suggèrent que ce phénomène serait lié à des interactions microbiennes entre les deux pathogènes. Plusieurs éléments soutiennent cette hypothèse : d'une part, *S. aureus* et *P. aeruginosa* sont co-localisés dans les poumons et occupent donc les mêmes niches écologiques, indiquant une probable interaction *in vivo* (166). D'autre part, de plus en plus d'études mettent en évidence un impact de cette interaction sur les propriétés de colonisation, de résistance et de persistance de souches de ces deux pathogènes isolées de patients atteints de mucoviscidose (55, 58, 63, 167–169). L'activation de la virulence de *P. aeruginosa* par les composés membranaires de *S. aureus* pourrait par exemple expliquer pourquoi les co-infections affectent plus sévèrement l'état de santé de patients que les mono-infections à *P. aeruginosa* (37, 131, 132, 164). La compréhension des interactions microbiennes entre *P. aeruginosa* et *S. aureus* apparaît ainsi essentielle pour mieux appréhender leur pathogénicité et leur persistance dans le contexte des infections pulmonaires chez les patients atteints de mucoviscidose.

3.1. L'état de compétition

Les premiers éléments témoignant d'une relation négative entre *P. aeruginosa* et *S. aureus* ont été découverts dès 1956, engendrant alors de nombreuses études sur le phénomène (170). Les tenants et aboutissants de cette interaction négative sont aujourd'hui

bien décrits et indiquent que les souches de référence et environnementales de *P. aeruginosa* et *S. aureus* sont en compétition (37). Comme la plupart des compétitions, elle est médiée par les besoins nutritionnels proches des deux bactéries, et est ainsi favorisée dans les environnements nutritifs simples (37, 171–174) (Cf. Partie « Types d'interactions microbiennes »).

De façon intéressante, des mécanismes de compétition d'exploitation mais aussi d'interférence sont développés au cours de cette interaction. La compétition d'exploitation entre *P. aeruginosa* et *S. aureus* repose notamment sur l'acquisition du fer exogène, essentiel à leurs métabolismes respectifs. Les sidérophores de *S. aureus* et de *P. aeruginosa* rentrent ainsi en compétition dans le milieu extracellulaire pour la captation du fer, tout comme leurs systèmes d'import de l'hème (156, 174, 175). En revanche, les stratégies d'interférence semblent uniquement employées par *P. aeruginosa* et reposent sur la sécrétion de nombreux facteurs anti-staphylococciques. En plus des sidérophores, *P. aeruginosa* acquiert ainsi le fer de *S. aureus* en le lysant grâce à la protéase extracellulaire LasA (37, 174). La pyocyanine, les 2-heptyl-4-hydroxyquinoline N-oxide (HQNO) ainsi que le signal du QS N-3-oxo-dodecanoyl homoserine lactone (3OC12-HSL) induisent un métabolisme fermentaire chez *S. aureus* et inhibent sa croissance. Ce changement métabolique participe d'ailleurs au développement du phénotype SCV chez *S. aureus* (37, 176–178). Les rhamnolipides et l'acide cis-2-décénoïque produits par *P. aeruginosa* limitent également la formation de biofilm de *S. aureus* en favorisant sa dispersion ou limitant son attachement aux surfaces (37). Enfin, une compétition plus indirecte peut s'opérer entre les deux pathogènes, puisque *P. aeruginosa* peut favoriser l'élimination de *S. aureus* en agissant sur les systèmes d'immunité des cellules hôtes. Il a ainsi été démontré que l'injection de la toxine ExoS par le SST3 de *P. aeruginosa* au sein des cellules eucaryotes induisait la synthèse d'une phospholipase ayant une activité bactéricide envers *S. aureus* (179).

Si *S. aureus* n'arbore pas de telles stratégies et semble avoir un impact mineur sur *P. aeruginosa*, il est nécessaire de rappeler que la production de toutes ces molécules anti-staphylococciques est énergétiquement coûteuse pour *P. aeruginosa*. La capacité de *P. aeruginosa* à produire ces facteurs reste toutefois le principal déterminant de l'interaction compétitive s'opérant entre les deux pathogènes (55, 63). Le caractère compétiteur de *P. aeruginosa* a ainsi été mis en évidence chez une majorité de souches – dont les souches isolées des patients atteints de mucoviscidose – et est considéré comme le comportement basal de la bactérie face à *S. aureus* (37, 63, 168, 169, 167, 163, 55).

3.2. Evolution des interactions entre *P. aeruginosa* et *S. aureus*

Le comportement compétiteur de *P. aeruginosa* est suspecté d'être à l'origine de la cinétique d'infection particulière de *P. aeruginosa* et *S. aureus* (55, 63, 163). En effet, l'arrivée de *P. aeruginosa* dans les poumons semble associé à une décroissance de la prévalence de *S. aureus*, pouvant témoigner de l'état de compétition s'opérant entre les deux bactéries lors des infections intermittentes par *P. aeruginosa* (Fig. 9).

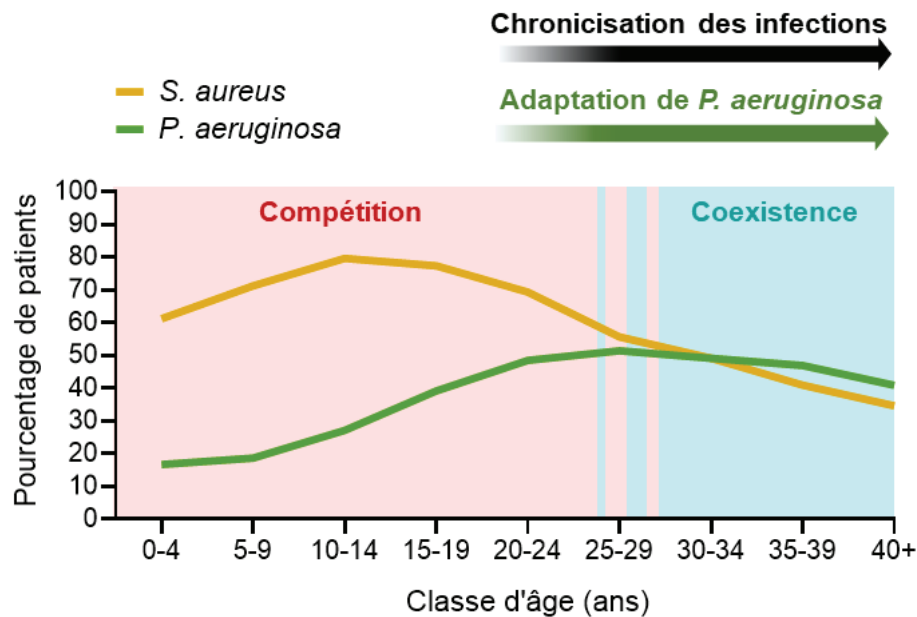


Figure 9 : Modélisation de la relation existant entre la cinétique d'infection par *S. aureus* et *P. aeruginosa*, leur état d'interaction et l'adaptation de *P. aeruginosa* au milieu pulmonaire. Les cinétiques de prévalence ont été adaptées du Registre Français de la Mucoviscidose 2017 (75).

Cependant, la prévalence de *S. aureus* semble ensuite se stabiliser et les co-infections avec *P. aeruginosa* deviennent fréquentes, suggérant une modification de la compétitivité de *P. aeruginosa*. Et effectivement, un nombre croissant d'études montrent que les souches de *P. aeruginosa* isolées de co-infections chroniques ne sont plus capables d'inhiber la croissance de *S. aureus*, permettant aux deux espèces de coexister durablement dans les poumons (55, 63, 167, 168). D'une part, cet état de coexistence reste encore mal compris mais pourrait favoriser les comportements coopératifs entre les deux pathogènes (55, 168). D'autre part, l'établissement de cette coexistence est concomitant avec la chronicisation des infections à *P. aeruginosa*, suggérant que cet état d'interaction résulterait de l'adaptation de la bactérie au milieu pulmonaire des patients atteints de mucoviscidose. L'évolution des interactions entre *P. aeruginosa* et *S. aureus* est développé dans la revue suivante (Front. Microbiol., 2021).



How Bacterial Adaptation to Cystic Fibrosis Environment Shapes Interactions Between *Pseudomonas aeruginosa* and *Staphylococcus aureus*

Laura Camus¹, Paul Briaud¹, François Vandenesch^{1,2,3} and Karen Moreau^{1*}

¹ CIRI-Centre International de Recherche en Infectiologie, Université de Lyon/Inserm U1111/Université Claude Bernard Lyon 1/CNRS UMR 5308/ENS de Lyon, Lyon, France, ² Centre National de Référence des Staphylocoques, Hospices Civils de Lyon, Lyon, France, ³ Institut des Agents Infectieux, Hospices Civils de Lyon, Lyon, France

OPEN ACCESS

Edited by:

Axel Cloeckaert,
Institut National de Recherche pour
l'Agriculture, l'Alimentation et
l'Environnement (INRAE), France

Reviewed by:

You-Hee Cho,
CHA University, South Korea
Mariana Carmen Chifiriuc,
University of Bucharest, Romania

*Correspondence:

Karen Moreau
karen.moreau@univ-lyon1.fr

Specialty section:

This article was submitted to
Infectious Diseases,
a section of the journal
Frontiers in Microbiology

Received: 15 October 2020

Accepted: 10 February 2021

Published: 03 March 2021

Citation:

Camus L, Briaud P, Vandenesch F
and Moreau K (2021) How Bacterial
Adaptation to Cystic Fibrosis
Environment Shapes Interactions
Between *Pseudomonas aeruginosa*
and *Staphylococcus aureus*.
Front. Microbiol. 12:617784.
doi: 10.3389/fmicb.2021.617784

Pseudomonas aeruginosa and *Staphylococcus aureus* are the two most prevalent bacteria species in the lungs of cystic fibrosis (CF) patients and are associated with poor clinical outcomes. Co-infection by the two species is a frequent situation that promotes their interaction. The ability of *P. aeruginosa* to outperform *S. aureus* has been widely described, and this competitive interaction was, for a long time, the only one considered. More recently, several studies have described that the two species are able to coexist. This change in relationship is linked to the evolution of bacterial strains in the lungs. This review attempts to decipher how bacterial adaptation to the CF environment can induce a change in the type of interaction and promote coexisting interaction between *P. aeruginosa* and *S. aureus*. The impact of coexistence on the establishment and maintenance of a chronic infection will also be presented, by considering the latest research on the subject.

Keywords: *P. aeruginosa*, *S. aureus*, interaction, evolution, cystic fibrosis

INTRODUCTION

Cystic fibrosis (CF) patients suffer from severe pulmonary infections. *Pseudomonas aeruginosa* is one of the most prevalent bacteria within CF lungs and is the main factor responsible for poor clinical outcomes due to the difficulty of eradicating it. Indeed, this bacterium has been shown to rapidly adapt to the CF lung environment and persist efficiently despite host immune responses and antibiotic treatments. This adaptation is mainly due to the accumulation of genetic mutations that alter the expression profiles and phenotypes of *P. aeruginosa* (Smith et al., 2006; Marvig et al., 2015a; Winstanley et al., 2016; La Rosa et al., 2019).

Another important feature of *P. aeruginosa* is its ability to interact with other CF microorganisms such as *Aspergillus fumigatus*, *Candida albicans*, and *Staphylococcus aureus*. *S. aureus* is also one of the most predominant pathogens in CF lungs and is detected simultaneously with *P. aeruginosa* in 20 to 50% of patients (Limoli et al., 2016; Briaud et al., 2020). *P. aeruginosa* can exhibit particularly aggressive behavior toward *S. aureus* (Michelsen et al., 2016). This antagonistic interaction was the only one observed between the two species for a long time. However,

P. aeruginosa strains with more tolerant behavior toward *S. aureus* have recently been isolated from chronic CF infections (Baldan et al., 2014; Michelsen et al., 2016; Briaud et al., 2019, 2020; Pallett et al., 2019; Camus et al., 2020). The establishment of such coexisting interaction between the two species seems to arise from their evolution in the lung ecosystem.

In this review, we aim to clarify the relationship between the adaptation of *P. aeruginosa* and *S. aureus* to the CF environment and the evolution of their interactions. We will present the genetic and phenotypic evolutions of the two partners and their impacts. The characterization of this coexisting interaction status and how it can contribute to the establishment and maintenance of a chronic infection will also be assessed.

ADAPTATION TO THE CF ENVIRONMENT REDUCES *P. aeruginosa*'s ANTI-STAPHYLOCOCCAL BEHAVIOR

P. aeruginosa Evolves During the Establishment of Chronic Infection

Lungs of CF patients constitute a stressful environment for colonizing microorganisms, especially due to toxic, osmotic, or oxidative stresses induced by the host immune system and recurring antibiotic treatments. Anoxia or micro-anaerobia, acidity and the nutritional characteristics of the CF environment can also hamper bacterial growth and persistence (Yang et al., 2011; La Rosa et al., 2019). Nevertheless, *P. aeruginosa* was shown to adapt in response to these different selective pressures. Numerous sequencing studies of longitudinal isolates of *P. aeruginosa* revealed that the bacterium accumulates a significant number of small mutations (SNP and small insertions and deletions) during its evolution in CF lungs. So, some genomic modifications were found to be positively selected due to their beneficial impacts on *P. aeruginosa* fitness in the stressful CF environment (Smith et al., 2006; Marvig et al., 2015b,c; Klockgether et al., 2018; Khademi et al., 2019). There were called pathoadaptive modifications as they promote the pathogen survival and persistence at the infectious site. As a result, CF-adapted isolates of *P. aeruginosa* present convergent expression profiles and phenotypes, conferring advantageous features (Folkesson et al., 2012; Winstanley et al., 2016; La Rosa et al., 2019). **Table 1** gathers the main pathoadaptive genomic regions of *P. aeruginosa*, as well as the associated phenotypes (**Table 1**).

Firstly, CF-adapted strains of *P. aeruginosa* adjust their energetic metabolism to the particular nutritional composition of the CF environment (Palmer et al., 2007; La Rosa et al., 2018, 2019). This is mainly reflected by a restriction of the catabolic repertoire and the slowed growth of clinical isolates in comparison to non-adapted strains (Marvig et al., 2015a; La Rosa et al., 2018, 2019). In response to iron sequestration by the host, *P. aeruginosa* also adapts its iron uptake mechanisms for the benefit of heme-based assimilation. Alteration of *pvd* genes in CF isolates was indeed shown to decrease the production of the pyoverdine siderophore and thus ferric iron acquisition.

In contrast, mutations in the *phuS*/*phuR* intergenic region increase the expression of the heme receptor PhuR and thus acquisition of host-sequestered iron (**Table 1**; Marvig et al., 2014; Minandri et al., 2016). Iron and nutrient acquisition nonetheless remains difficult in CF lung, hampering the costly production of many iron-dependent virulence factors. *P. aeruginosa* virulence is also reduced by genetic alterations and/or transcriptomic dysregulations of genomic regions involved in motility (*pilJ* and *chpA*), secretion (*phz* and *Hcp* genes) and regulation of virulence (*lasR*, *retS*, *exxA*, and *rpoN*) (Marvig et al., 2015a; Winstanley et al., 2016). Most of these factors being immunogenic, the down-regulation of their production allows a better escape of *P. aeruginosa* from the host immune system. Such escape and resistance to immune responses is also promoted by the increased biofilm production of CF-adapted *P. aeruginosa*. In particular, mutations in *mucA* and *alg* genes induce the overproduction of alginate, an exopolysaccharide composing the biofilm matrix and responsible for the frequent mucoid phenotype (Marvig et al., 2015b; Winstanley et al., 2016). Finally, adapted strains of *P. aeruginosa* exhibit increased antibiotic resistance related to genetic alterations of antibiotic targets (for instance the gyrases *gyrA*, *gyrB*), efflux pumps (*mex* genes), lactamases (*amp* genes), as well as lipopolysaccharide (LPS) and porin synthesis (*pagL*, *pmrB*, and *opr* genes) (**Table 1**; Folkesson et al., 2012; Marvig et al., 2015b; Winstanley et al., 2016). Altogether, these adaptations induce a weakly virulent but highly resistant state of *P. aeruginosa*, promoting its persistence within CF lungs.

Impact of *P. aeruginosa* Adaptation on Its Anti-staphylococcal Behavior

In addition to limiting the effectiveness of the immune response and antibiotic treatments, adaptations of *P. aeruginosa* can also modify its interactions with other microbial species, in particular with *S. aureus*. The anti-staphylococcal behavior of *P. aeruginosa* relies on mechanisms of bacterial lysis and growth suppression, as well as metabolic alterations, virulence and biofilm formation (**Figure 1A**; Hotterbeekx et al., 2017). However, several studies demonstrated that such behavior was not conserved in CF-adapted strains of *P. aeruginosa*, allowing the establishment of a coexisting interaction with *S. aureus* (Baldan et al., 2014; Michelsen et al., 2014, 2016; Limoli et al., 2017; Briaud et al., 2019). It thus appears that the relationship between *P. aeruginosa* and *S. aureus* evolves from competition to coexistence, a process resulting from the adaptation of *P. aeruginosa*.

Nutrient Competition and Virulence

One of the main factors involved in the competitive interaction between *P. aeruginosa* and *S. aureus* is that of resources, notably iron-availability in the environment. Indeed, it has been shown that *P. aeruginosa*'s aggressive behavior toward the Gram positive bacterium varies according to medium richness and is even promoted during iron depletion (Mashburn et al., 2005; Filkins et al., 2015; Nguyen et al., 2015; Miller et al., 2017). In these conditions, *P. aeruginosa* uses *S. aureus* as an iron source by lysing its cells thanks to the LasA protease, whose production is regulated by the quorum-sensing (QS) regulator LasR (Toder et al., 1991; Mashburn et al., 2005; Hotterbeekx et al., 2017).

TABLE 1 | Main genetic and phenotypic adaptations of *Pseudomonas aeruginosa* during its evolution in the CF lung environment.

Associated functions and phenotypes		Intragenic non-synonymous mutations	Intergenic mutations	Transcriptomic pattern
Metabolic adaptation	Adaptation of energetic metabolism Increase of heme acquisition Adaptation of resource transport/sensing Decrease of siderophore production	<i>atsA, xdhB, purL, spoT</i> <i>hasR</i> <i>cbrAB</i> <i>pvdL, pvdS</i>	<i>ldh//PA3419</i> <i>phus//phuR</i>	
Increase of biofilm formation	Increase of alginate EPS production Increase of pel EPS production Alteration of biofilm formation	<i>algU, mucA, algG</i> <i>pelA</i> <i>wspA</i>	<i>algU/algI</i>	
Virulence decrease	Loss of motility Decrease of secretion activity QS rewiring	<i>pilJ, chpA</i> <i>retS, exsA, clpA</i> <i>lasR</i>	<i>motY//pyrC</i> <i>phzM//phzA1</i>	↓ HSI-I, ↓ <i>phnA</i>
Increase of antibiotic resistance	Increase of antibiotic degradation Porins alteration Alteration of antibiotic targets LPS alteration Efflux increase	<i>ampC, ampD</i> <i>oprD</i> <i>gyrB, gyrA, ftsI, fusA1</i> <i>migA, wbpM, pagL, pmrB</i> <i>mexAB, mexY, mexZ,</i> <i>mexS, mexT, nfxB</i>	<i>ampR//ampC</i> <i>oprO//PA3281</i>	↑ <i>mexX</i>
Other	Alteration of DNA repair Alteration of transcription/translation Global regulatory dysregulations	<i>dnaX, recC</i> <i>rpoB, rpoC</i> <i>rpoN</i>		

Gray cells indicate adaptations that can impact microbial interactions of *P. aeruginosa*.

As *P. aeruginosa*'s adaptation to CF lungs is accompanied by *lasR* mutations and QS network rewiring, protease activity and especially LasA production are frequently reduced in chronic clinical isolates (Table 1, Figure 1B; Manos et al., 2013; Marvig et al., 2015a; Feltner et al., 2016; van Mansfeld et al., 2016; O'Brien et al., 2017). The ability of *P. aeruginosa* CF strains to lyse *S. aureus* cells was recently assessed on a limited set of three isolates. It was nonetheless depicted that the isolate lacking LasA production and protease activity was the only one unable to outcompete and lyse *S. aureus* (Pallett et al., 2019). Studies including larger sets of strains with different colonization times (as longitudinal ones) would be of great interest to evaluate the relationship between *P. aeruginosa*'s adaption to the CF lung environment and its ability to efficiently lyse *S. aureus*. In addition, *S. aureus* lysis leads to increased concentrations of N-acetyl glucosamine (GlcNac) which induces the production of virulence factors by *P. aeruginosa* (Hotterbeekx et al., 2017). Thus, the absence of *S. aureus* lysis may contribute to the decrease in virulence of *P. aeruginosa*.

As a strategy to limit nutritional competition, *P. aeruginosa* is also able to inhibit the growth of *S. aureus* by altering its metabolic activities. Indeed, the secondary metabolites HQNO (2-heptyl-4-hydroxyquinoline N-oxide) and pyocyanin secreted through the PQS (*Pseudomonas* Quinolone Signal) system induce a fermentative metabolism in the Gram positive bacterium (Hoffman et al., 2006; Proctor et al., 2014; Hotterbeekx et al., 2017; Noto et al., 2017). This metabolic switch is also responsible for the well-described small colony variant (SCV) phenotype of *S. aureus* (Proctor et al., 2014; Figure 1A). Genes involved in HQNO synthesis (*phn* genes) are under-expressed in adapted *P. aeruginosa* isolates, whereas pyocyanin production through *phz* genes can be impacted by intergenic mutations (Table 1). As a result, adapted strains of *P. aeruginosa* frequently present reduced HQNO and pyocyanin production in

comparison to early ones (Bianconi et al., 2015; Cullen et al., 2015; Michelsen et al., 2016; Limoli et al., 2017; O'Brien et al., 2017; Figure 1B). This is especially the case for isolates from the DK2 lineage, which is known for developing a proto-cooperative interaction with *S. aureus* (Michelsen et al., 2016). However, HQNO and pyocyanin production are not always reduced in CF-adapted *P. aeruginosa* since these molecules can still be detected at active concentrations within CF sputum of chronically infected patients (Wilson et al., 1988; Hoffman et al., 2006; Alatraktchi et al., 2020). In fact, O'Brien et al. (2017) observed considerable variances in pyocyanin production between strains from different patients, but also between lineages recovered from a single subject. These results suggest that the isolates evolve differently according to their niches within the lungs, leading to different metabolic activities and thus interactions with co-colonizing microorganisms. Therefore, growth inhibition of *S. aureus* would vary depending on the ability of the nearest *P. aeruginosa* bacterium to produce pyocyanin or HQNO.

In the same way, the QS signal N-3-oxo-dodecanoyl homoserine lactone (3OC12-HSL) was shown to inhibit *S. aureus* growth in a dose-dependent manner (Hotterbeekx et al., 2017; Figure 1A). Production of this long-chain acyl-homoserine lactone (AHL) is regulated by LasR and thus frequently reduced in *lasR*-mutated CF isolates of *P. aeruginosa*. Instead, these isolates generally maintain the production of the short-chain AHL butyryl-HSL (C4-HSL) whose production is regulated by the second QS system of *P. aeruginosa*, Rhl (Bjarnsholt et al., 2010; Feltner et al., 2016; Chen et al., 2019; Cruz et al., 2020). And interestingly, C4-HSL signals have not been shown to affect *S. aureus* (Figure 1B).

Mixed-Species Biofilm Formation

Another important feature of bacterial interaction is the formation of mix-biofilm. The relationship between the two

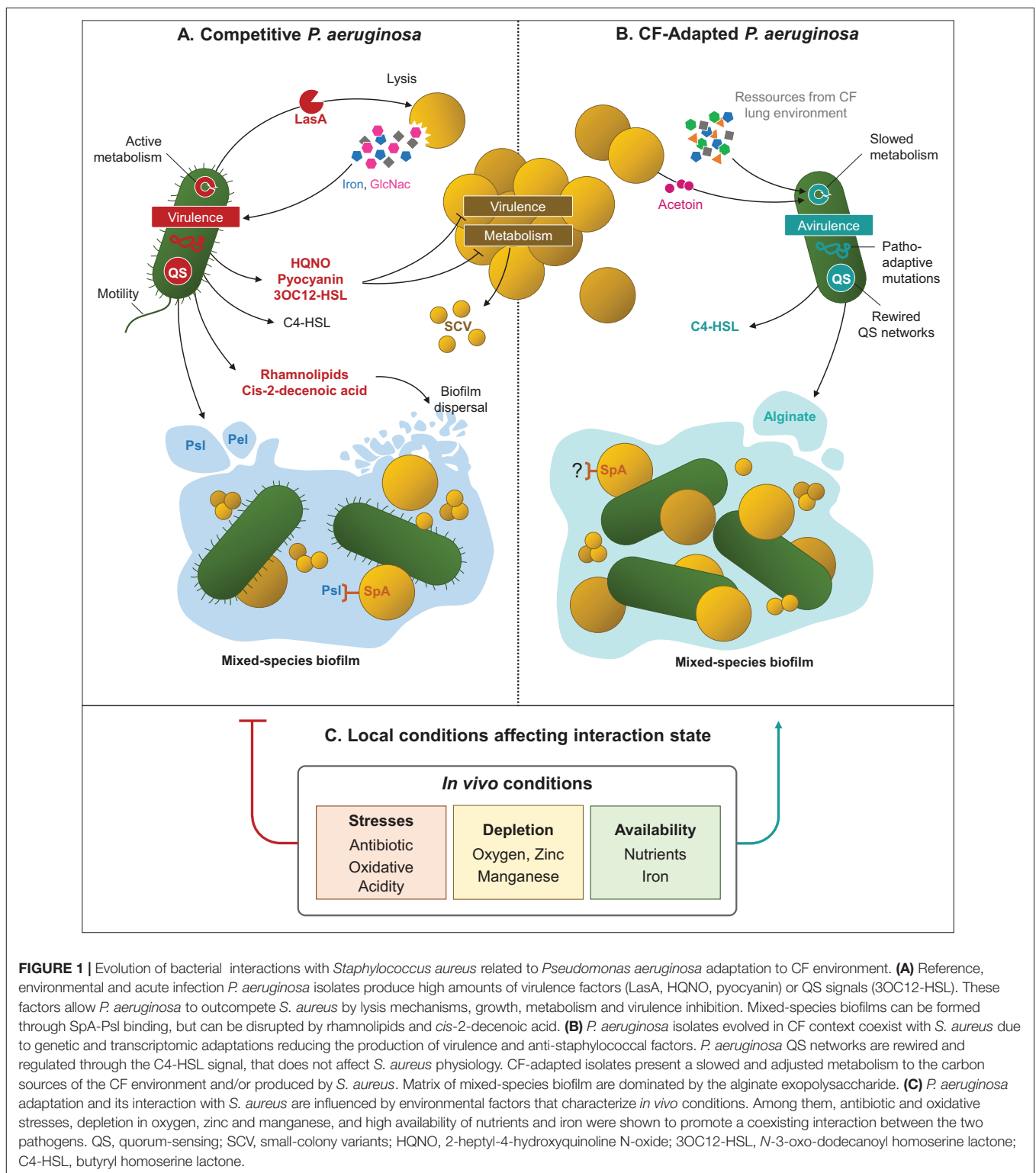


FIGURE 1 | Evolution of bacterial interactions with *Staphylococcus aureus* related to *Pseudomonas aeruginosa* adaptation to CF environment. **(A)** Reference, environmental and acute infection *P. aeruginosa* isolates produce high amounts of virulence factors (LasA, HQNO, pyocyanin) or QS signals (3OC12-HSL). These factors allow *P. aeruginosa* to outcompete *S. aureus* by lysis mechanisms, growth, metabolism and virulence inhibition. Mixed-species biofilms can be formed through SpA-Psl binding, but can be disrupted by rhamnolipids and *cis*-2-decenoic acid. **(B)** *P. aeruginosa* isolates evolved in CF context coexist with *S. aureus* due to genetic and transcriptomic adaptations reducing the production of virulence and anti-staphylococcal factors. *P. aeruginosa* QS networks are rewired and regulated through the C4-HSL signal, that does not affect *S. aureus* physiology. CF-adapted isolates present a slowed and adjusted metabolism to the carbon sources of the CF environment and/or produced by *S. aureus*. Matrix of mixed-species biofilm are dominated by the alginate exopolysaccharide. **(C)** *P. aeruginosa* adaptation and its interaction with *S. aureus* are influenced by environmental factors that characterize *in vivo* conditions. Among them, antibiotic and oxidative stresses, depletion in oxygen, zinc and manganese, and high availability of nutrients and iron were shown to promote a coexisting interaction between the two pathogens. QS, quorum-sensing; SCV, small-colony variants; HQNO, 2-heptyl-4-hydroxyquinoline N-oxide; 3OC12-HSL, *N*-3-oxo-dodecanoyl homoserine lactone; C4-HSL, butyryl homoserine lactone.

pathogens within biofilms appears to be a complex situation, highly dependent on isolates and culture conditions. A first study on 63 isolates demonstrated that *S. aureus* biofilm formation was enhanced by the secondary metabolites HQNO and Alkyl Quinolones (AQs) secreted by *P. aeruginosa*. However, although

the effect was clear on a specific *S. aureus* clinical strain used as control, it was less manifest on other clinical CF isolates (Fugère et al., 2014). Conversely, *S. aureus* supernatant can either stimulate or inhibit *P. aeruginosa* biofilm formation in a strain-dependent manner as well (Armbruster et al., 2016).

These effects involve the surface protein A (SpA) of *S. aureus*, an immunoglobulin-binding factor responsible for immune suppression (Kobayashi and DeLeo, 2013). Besides host proteins, SpA can bind two *P. aeruginosa* structures important for biofilm formation: (i) type IV pili, involved in twitching motility, and (ii) Psl, one of the three main exopolysaccharides (EPS), with alginate and Pel, that form the extracellular matrix of *P. aeruginosa* biofilm (Leid et al., 2005; Ryder et al., 2007; Colvin et al., 2011, 2012; Armbruster et al., 2016). Chew et al. (2018) observed that Psl enables wild-type *P. aeruginosa* to outcompete *S. aureus* in early biofilm development. On the contrary, Pel is required to reduce the effective crosslinking of the matrix in late-stage biofilm development, improving super-diffusivity in microcolony regions and dual-species biofilm growth (Chew et al., 2018).

Pseudomonas aeruginosa's adaptation to the CF environment affects both motility and exopolysaccharide production. As a result, chronic isolates frequently lack type IV pili and present a biofilm matrix dominated by alginate, especially in the mucoid phenotype (Høiby et al., 2017). Therefore, one might wonder if the modulation of mixed-species biofilm formation through Pel, Psl, and SpA occur in adapted CF isolates in the same way as for reference strains (**Figure 1B**).

Competitive *P. aeruginosa* are also able to disperse *S. aureus* biofilm or limit its establishment through the secretion of rhamnolipids and *cis*-2-decenoic acid (Hotterbeekx et al., 2017; **Figure 1A**). To our knowledge, the production of *cis*-2-decenoic acid was not assessed in CF-adapted clinical *P. aeruginosa*, but rhamnolipid synthesis has been studied more extensively. These molecules induce significant inflammatory host responses, promote *P. aeruginosa* motility, and their synthesis is favored during planktonic growth (Dézziel et al., 2003; Alhede et al., 2014; Hotterbeekx et al., 2017). As these phenotypes are frequently reduced in chronic *P. aeruginosa* isolates, it therefore seems likely that bacterial adaptation to the CF lung is accompanied by a decrease of rhamnolipid production. Indeed, chronic isolates studied by Bjarnsholt et al., and the CF-adapted lineage DK2 were shown to produce less rhamnolipids than intermittent and reference *P. aeruginosa* strains (Bjarnsholt et al., 2010; Michelsen et al., 2016). Low rhamnolipid synthesis was also recently associated with alginate overproduction and the common mucoid phenotype of *P. aeruginosa*. The presence of alginate, either produced by *mucaA*-mutated mucoid strains or exogenously added in the medium, induced transcriptomic and post-transcriptomic down-regulation of rhamnolipid synthesis (Limoli et al., 2017; Price et al., 2020). Alginate-producing *P. aeruginosa* also presented reduced ability to outcompete *S. aureus* (Limoli et al., 2017; Price et al., 2020). Altogether, this suggests that decreased rhamnolipid production and increased alginate synthesis in adapted *P. aeruginosa* isolates contribute to improve *S. aureus* survival during mixed-biofilm formation (**Figure 1B**). In connection with this, Baldan et al. (2014) showed that early and late CF *P. aeruginosa* isolates presented different behaviors when grown in biofilm with *S. aureus*. This latter exhibited better viability with the CF-adapted isolate of *P. aeruginosa* and was also able to alter its biofilm production (Baldan et al., 2014).

Impact of Environmental Factors on the Anti-staphylococcal Behavior of *P. aeruginosa*

Although bacterial features play an important role in shaping inter-species interaction, environmental factors can have an even more decisive impact on them. Environmental conditions such as antibiotic and oxidant stresses are known to shape the CF ecosystem and promote a biofilm-based lifestyle of microorganisms within lungs (Feraco et al., 2016; Riquelme et al., 2020). Biofilm conditions reducing the competitive relationship between *P. aeruginosa* and *S. aureus*, the CF environment may favor a coexistence interaction between the two pathogens independently of *P. aeruginosa's* genetic adaptation. Indeed, several environmental factors inherent to CF lungs were shown to decrease the anti-staphylococcal behavior of *P. aeruginosa*. Pallett et al. (2019) recently observed that oxygen limitation decreased the production of *P. aeruginosa* virulence factors such as proteases and pyocyanin. In these conditions, not only the reference strain PAO1 but also clinical isolates thus coexisted with *S. aureus* despite competitive behavior under normoxia (Pallett et al., 2019). Within mixed-species biofilm formed with the PA14 reference strain, *S. aureus* survival was improved thanks to bacterial stratification as a function of oxygen levels (Cendra et al., 2019). In addition to oxygen, nutrient availability can also modify interaction within biofilm (Mashburn et al., 2005; Filkins et al., 2015; Nguyen et al., 2015; Hotterbeekx et al., 2017; Miller et al., 2017; Cendra et al., 2019). Miller et al. (2017) observed that *S. aureus* was even able to strongly outcompete *P. aeruginosa* within mixed-species biofilm grown under rich conditions, but not in the same diluted and thus impoverished medium. Besides nutritive richness, limited alkalization of the co-culture medium was also shown to improve *S. aureus* survival during interaction with the PA14 reference strain (Cendra et al., 2019). Finally, the depletion of zinc and manganese, notably observed on the edge of the biofilm architecture, represses the expression of *P. aeruginosa's* virulence genes and thus *S. aureus* inhibition (Wakeman et al., 2016; **Figure 1C**).

Interestingly, all these conditions promoting coexistence interaction between the two pathogens seem to be combined in the CF environment. CF sputum is indeed considered a rich medium but it contains limited oxygen concentrations, favoring anaerobic and micro-anaerobic metabolisms (La Rosa et al., 2019). Sputa from CF patients were also shown to be relatively acidic (Bhagirath et al., 2016). Moreover, host-pathogen interfaces are known to be depleted in zinc and manganese, especially through sequestration by the host protein calprotectin (Kehl-Fie and Skaar, 2010; Hood et al., 2012; Wakeman et al., 2016). Altogether, this suggests that *in vivo* conditions, and especially the CF environment, may promote non-competitive interaction between *P. aeruginosa* and *S. aureus* (**Figure 1C**). This hypothesis is supported by several studies showing the improved survival of *S. aureus* during non-human *in vivo* co-infections with *P. aeruginosa*, in comparison to *in vitro* co-cultures. Yadav and colleagues demonstrated a higher proportion of *S. aureus* within an *in vivo* mixed-species biofilm in the presence of *P. aeruginosa* (Yadav et al., 2017; Millette et al., 2019).

In addition, *P. aeruginosa* strains such as PA14 were shown to promote *S. aureus* colonization and maintenance in a murine lung infection model (Yadav et al., 2017; Millette et al., 2019). Similar results were obtained in the context of chronic wound co-infections (Pastar et al., 2013; DeLeon et al., 2014). Since these co-infections were maintained for a limited duration (24 h to 1 week), it is unlikely that genetic adaptation drove the establishment of a coexistence interaction between *P. aeruginosa* and *S. aureus*. This phenomenon seems to be more related to non-fixed acclimatization reducing *P. aeruginosa* virulence, or spatial compartmentalization isolating the two species from each other *in vivo*. In all cases, it appears that besides promoting *P. aeruginosa* genetic adaptation and then reducing anti-staphylococcal behavior, *in vivo* conditions are themselves favorable to non-competitive interactions with *S. aureus* (Figure 1C).

S. aureus* ADAPTATION TO THE CF ENVIRONMENT CAN ALSO IMPACT ITS INTERACTION WITH *P. aeruginosa

The relationship between the two pathogens was shown to rely solely on *P. aeruginosa* anti-staphylococcal factors, whose production evolves during its adaptation and allows steady coexistence with *S. aureus*. However, although less studied, the adaptive mechanisms of *S. aureus* also promote its long-term persistence within CF lungs and may impact its interactions with co-colonizing *P. aeruginosa* strains.

***S. aureus* Adaptation to the CF Environment**

A 21-month longitudinal study performed on 183 CF patients depicted that the clonal diversity of *S. aureus* strains decreased as patient aged, pointing out that some isolates tended to adapt more efficiently and dominate the airway sphere during infection history (Westphal et al., 2020). Several studies indeed highlighted that *S. aureus* isolates evolve in the CF lung environment and acquire features leading to better-fitted isolates (Figure 2; Chatterjee et al., 2008; Treffon et al., 2018, 2020; Herzog et al., 2019; Lennartz et al., 2019; Tan et al., 2019; Westphal et al., 2020).

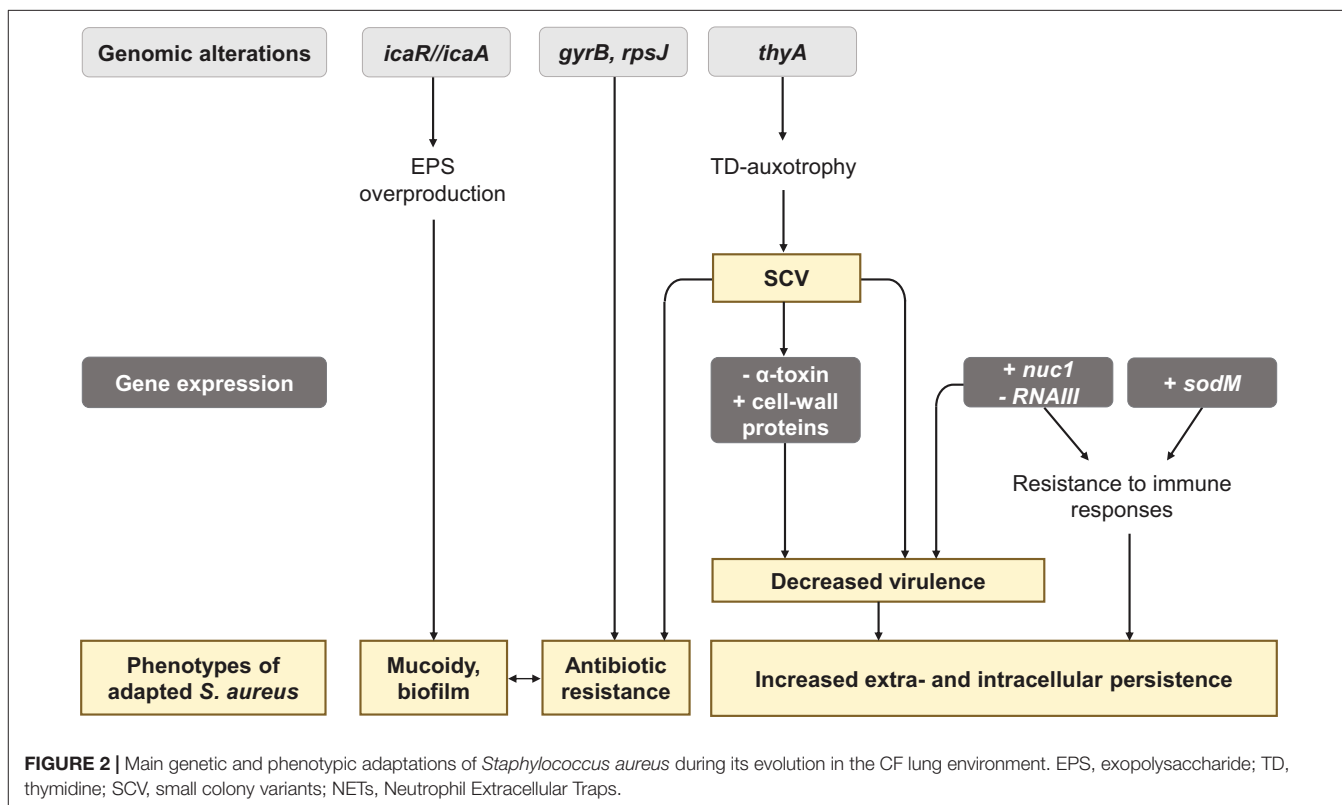
Genomic, transcriptomic, and proteomic comparisons between early and late strains of *S. aureus* highlighted adaptations in the transport and the metabolism of carbohydrates and amino acids (Treffon et al., 2018; Tan et al., 2019). Late isolates thus often presented auxotrophies toward thymidine (TD), menadione or hemin (Kahl et al., 1998). These auxotrophies promote the formation of SCV (Chatterjee et al., 2008; Tan et al., 2019), a frequent *S. aureus* phenotype isolated from 4 to 50% of CF patients depending on the studies (Kahl et al., 2016). *S. aureus* SCVs are associated with worse lung function and patient age, in relation with their increased antibiotic resistance and persistence (Besier et al., 2007). Indeed, mutations in the *thyA* gene hindering TD biosynthesis were shown to facilitate resistance to trimethoprim-sulfamethoxazole (SXT) and the presence of TD-auxotrophic SCV is associated with previous

antibiotic treatment with SXT (Kahl et al., 1998; Chatterjee et al., 2008; Yagci et al., 2013; Figure 2). Late isolates from antibiotic-treated patients showed other mutations in *gyrB* and *rpsJ*, that are not associated with the SCV phenotype but can explain antibiotic resistance to fluoroquinolones and cyclines (Kriegeskorte et al., 2015; Tan et al., 2019; Figure 2). Besides antibiotic resistance, SCVs are specialized for extracellular and intracellular persistence. This phenomenon is related to: (i) decreased expression of the α -toxin involved in lysis of eukaryotic cells by *S. aureus*, and (ii) increased expression of cell wall-associated genes which facilitate colonization to extracellular matrix proteins and internalization in eukaryotic cells (Figure 2). In line with this, *S. aureus* SCVs were shown to survive better intracellularly in eukaryotic cells than their isogenic parental strain (Kahl et al., 2016). CF-adapted *S. aureus* strains also tend to be better intracellular survivors than the corresponding early isolates (Treffon et al., 2020).

Another feature promoting the persistence of *S. aureus* CF isolates is the improvement of defense mechanisms against killing by polymorphonuclear leukocytes. Neutrophils usually eradicate invading pathogens by releasing reactive oxygen species (ROS) or forming Neutrophil Extracellular Trap (NETs). In comparison to their early counterparts, CF-adapted *S. aureus* presented an increased genic expression of the superoxide dismutase SodM involved in ROS detoxification (Treffon et al., 2018, 2020). Moreover, Herzog et al. (2019) showed that late isolates were more resistant to NETs mediated-killing through the over-expression of the *nuc1* gene encoding the nuclease protein. Given the high pro-inflammatory territory in patient lungs overwhelmed by the neutrophilic attacks, the over-production of SodM and Nuc1 could be a major step in the adaptation of *S. aureus* in CF lungs (Figure 2).

Interestingly, *S. aureus* isolates overexpressing the *nuc1* gene also presented a down-expression of the RNA regulator RNAPIII. RNAPIII is the major effector of the *agr* QS-system of *S. aureus* that positively controls the expression of many virulence factors. A decrease of RNAPIII expression thus reflects reduced production of virulence factors. *nuc1*-overexpressing *S. aureus* were also shown to overexpress protein A (SpA), permease, coagulase, and adhesins (Jenul and Horswill, 2018), involved in colonization. Similarly, transcriptional analysis revealed that *S. aureus* SCVs have a less virulent phenotype in comparison to normal isolates (Kahl et al., 2005; Moisan et al., 2006; Seggewiss et al., 2006). Altogether, these results suggest that adaptation to the CF environment could lead toward a low-virulence but highly invasive state of *S. aureus*.

Finally, biofilm production appears to be increased in late *S. aureus* isolates. In the study of Tan et al. (2019), two out of three CF-late isolates over-produced biofilm and the same pattern was observed within late isolates of non-CF lung infections, suggesting that this characteristic was independent of the CF-lung environment. Such increased biofilm production by late isolates can be related to the development of mucoidy in *S. aureus*. This phenotype arises from a 5 bp deletion within the intergenic region of *icaR/icaA* genes, inducing an overproduction of *S. aureus* exopolysaccharide poly-*N*-acetylglucosamine (Schwartbeck et al., 2016; Figure 2). Mucoid



S. aureus isolates are thus found in 2.5% of CF airways and tend to be more frequently isolated from older patients than non-mucoid isolates (Lennartz et al., 2019). These data suggest that mucoidy and strong biofilm production play a role in *S. aureus* adaptation to the CF environment.

Impact of *S. aureus* Adaptation on Its Interaction With *P. aeruginosa*

Some of the *S. aureus* adaptations to the CF environment can impact its relationship with *P. aeruginosa*. Among them, the SCV phenotype appears to be crucial for *S. aureus* survival during competitive interaction, as SCV present increased resistance to *P. aeruginosa* mediated-killing (Hotterbeekx et al., 2017). Once *P. aeruginosa* has evolved to a non-aggressive status toward *S. aureus*, the staphylococcus can then switch to a non-defective growth mode and coexist with its partner. The increased biofilm production of CF-adapted *S. aureus* isolates could also promote the formation of mixed-species biofilm with *P. aeruginosa*, although no direct correlation has yet been established. These hypotheses could explain (i) the high proportion of co-infected patients with *S. aureus* and *P. aeruginosa* in international cohorts (Hubert et al., 2013; Limoli et al., 2016; Briaud et al., 2020), and (ii) the high proportion of isolates presenting a non-competitive interaction (Briaud et al., 2020). Further investigations need to be conducted to confirm this model and fully understand the effects of *S. aureus* adaptation on its relationship with *P. aeruginosa*.

However, several studies suggested that *S. aureus* can influence the establishment of a coexisting interaction through alterations

of the adaptive process of *P. aeruginosa*. Using an *in vitro* evolution assay, the adaptation of *P. aeruginosa* was studied in the presence or absence of *S. aureus* over 150 generations (Tognon et al., 2017). Mutations in the LPS biosynthesis pathway occurred only in the presence of *S. aureus* and increased *P. aeruginosa*'s fitness and resistance toward β -lactams antibiotics (Tognon et al., 2017). Repeated *in vitro* co-cultures with *S. aureus* also induced a decrease of *P. aeruginosa* QS regulation and may provide a departure point for a coexisting interaction (Zhao et al., 2018). It is worth recalling that modifications of LPS production, increased antibiotic resistance and down-regulation of QS are also frequently depicted in CF-adapted *P. aeruginosa* isolates (Folkesson et al., 2012; Marvig et al., 2015b; Winstanley et al., 2016). These results indicate that the presence of *S. aureus* influences *P. aeruginosa*'s adaptation, and that a co-evolution phenomenon could even promote a non-competitive relationship between the two pathogens. Several results obtained from CF clinical strains support these hypotheses. First, Martha et al. (2010) observed that *P. aeruginosa* presented a higher probability to develop a mucoid phenotype in the absence of *S. aureus*. Secondly, coexisting strains of *S. aureus* and *P. aeruginosa* were shown to better produce and catabolize acetoin, respectively, in comparison to competitive strains. The authors concluded that strains co-evolved to promote trophic cooperation (Camus et al., 2020). Finally, the genetic alterations of LasR that reduce *P. aeruginosa* anti-staphylococcal behavior are frequently observed in longitudinal studies (Marvig et al., 2015b,c). One might wonder if the presence of *S. aureus* in CF lungs could contribute to the selection of *lasR* mutants

and thus non-competitive *P. aeruginosa*. Indeed, promoting a coexisting and even a cooperative behavior with other co-colonizing microorganisms can be a strategy to improve fitness in a stressful environment such as CF lungs. However, most of longitudinal studies focused on *P. aeruginosa* and no data are available concerning potential co-infections with *S. aureus*. It thus remains difficult to determine if *S. aureus* can effectively influence the fixation of *lasR* mutations in *P. aeruginosa* genome. It would be interesting to study the long-term evolution of both *S. aureus* and *P. aeruginosa* in several co-infected CF patients to reveal the bacterial adaptations leading to the establishment of coexistence.

COEXISTENCE PROMOTES COOPERATIVE BEHAVIORS BETWEEN *P. aeruginosa* AND *S. aureus*

Characterization of the Coexistence Interaction Status

Co-existence interaction leads to increased *S. aureus* survival in comparison to a common competitive interaction with *P. aeruginosa*. Bacterial enumerations performed during co-culture kinetics can thus easily reveal and quantify this phenomenon (Miller et al., 2017; Cendra et al., 2019; Pallett et al., 2019; **Figure 3A**). Less cumbersome procedures were nonetheless developed to assess interaction status between clinical CF isolates in large set of strains (**Figure 3B**; Baldan et al., 2014; Michelsen et al., 2014, 2016; Limoli et al., 2017; Briaud et al., 2019, 2020; Camus et al., 2020). Baldan and colleagues thus performed competition tests on plates during which a spot of *P. aeruginosa* culture is deposited on a lawn of *S. aureus*. Four categories of interaction status were established (no, weak, strong, and very strong inhibition) according to the size of the inhibition halo of *S. aureus* induced by the 24 *P. aeruginosa* strains tested (Baldan et al., 2014). In other studies, growth inhibition of *S. aureus* was observed through cross-streak assays and visual evaluation of each bacterium population after the streak intersection (Michelsen et al., 2014, 2016; Limoli et al., 2017; **Figure 3C**).

Despite the different methods and media employed, several studies highlighted that the interaction pattern with *S. aureus* was related to the adaptation of *P. aeruginosa* to the CF environment. Reduced anti-staphylococcal behavior was indeed observed for late isolates of *P. aeruginosa*, which were recovered several years after their clonal ancestor and presented common pathoadaptive traits. This evolution was thus shown in the DK2 lineage as well as in mucoid isolates (Michelsen et al., 2014, 2016; Limoli et al., 2017). However, it is noteworthy that the adaptation of *P. aeruginosa* in the CF lung is driven by adaptive radiation and spatial isolation mechanisms, inducing a high genotypic and phenotypic heterogeneity in the evolving population (Winstanley et al., 2016). It is therefore likely that clonally related isolates simultaneously recovered from the same patient can present different interaction statuses with *S. aureus* due to such

diversification processes. On the other hand, it is also conceivable that the interaction statuses of competition and coexistence are dynamic and transitional within a single *P. aeruginosa* population. Assessing the interaction status of numerous *P. aeruginosa* isolates, collected longitudinally or recovered from different pulmonary niches, would lead to better understanding of this phenomenon.

In all cases, coexistence could be defined as a neutral interaction during which both bacteria are not affected by each other. However, increasing evidence shows that cooperative behaviors can positively affect *P. aeruginosa* and *S. aureus* during coexistence (**Figure 4**).

Increased Resistance to Antimicrobial Compounds

Several *in vitro* studies focusing on CF isolates highlighted that coexistence between *P. aeruginosa* and *S. aureus* can improve the antibiotic resistance of both pathogens (**Figure 4A**). *S. aureus* was recently shown to overexpress genes coding efflux pumps from the Nor family during coexisting interaction with *P. aeruginosa*. As a result, clinical *S. aureus* isolates presented significantly increased resistance to tetracycline and ciprofloxacin in the presence of *P. aeruginosa*, in comparison to monocultures (Briaud et al., 2019). While direct contact between bacterial cells was presumed to mediate this effect, other studies identified *P. aeruginosa* secreted products affecting the resistance of *S. aureus* to antimicrobial compounds. In particular, secondary metabolites from the 4-hydroxy-2-alkylquinolines (HAQ) family such as HQNO increase the resistance of *S. aureus* to aminoglycosides notably through the induction of the SCV phenotype i (Hoffman et al., 2006; Mitchell et al., 2010; DeLeon et al., 2014; Orazi and O'Toole, 2017; Orazi et al., 2019, 2020). Interestingly, late *P. aeruginosa* isolates from CF infections often lack HQNO production but are still able to protect *S. aureus* from tobramycin. The implication of other molecules than HQNO was confirmed by an atypical HAQ profile developed during adaptation to the CF environment (Michelsen et al., 2016). It thus appears that both competitive (i.e., HQNO-producing) and coexisting *P. aeruginosa* can protect *S. aureus* from antibiotic effects but through different mechanisms. Alginate produced by CF-adapted *P. aeruginosa* may also protect *S. aureus* from antimicrobial compounds since this exopolysaccharide can impact HAQ synthesis and mixed-species biofilm formation (Limoli et al., 2017; Price et al., 2020).

Conversely, interaction with *S. aureus* can also trigger resistance mechanisms in *P. aeruginosa* (**Figure 4A**). Co-evolution with *S. aureus* was shown to promote the alteration of genes from the LPS biosynthesis pathway in PAO1, leading to greater resistance to β -lactam antibiotics (Tognon et al., 2017). Michelsen and colleagues demonstrated that *S. aureus* cells and their supernatant can also induce the SCV phenotype and antibiotic tolerance in CF-adapted strains of *P. aeruginosa* (Fugère et al., 2014; Michelsen et al., 2014). Similar results were obtained using persistent CF isolates of *P. aeruginosa* grown in biofilm, as they presented improved tobramycin resistance upon exposure to *S. aureus* supernatant. In this case, the phenomenon

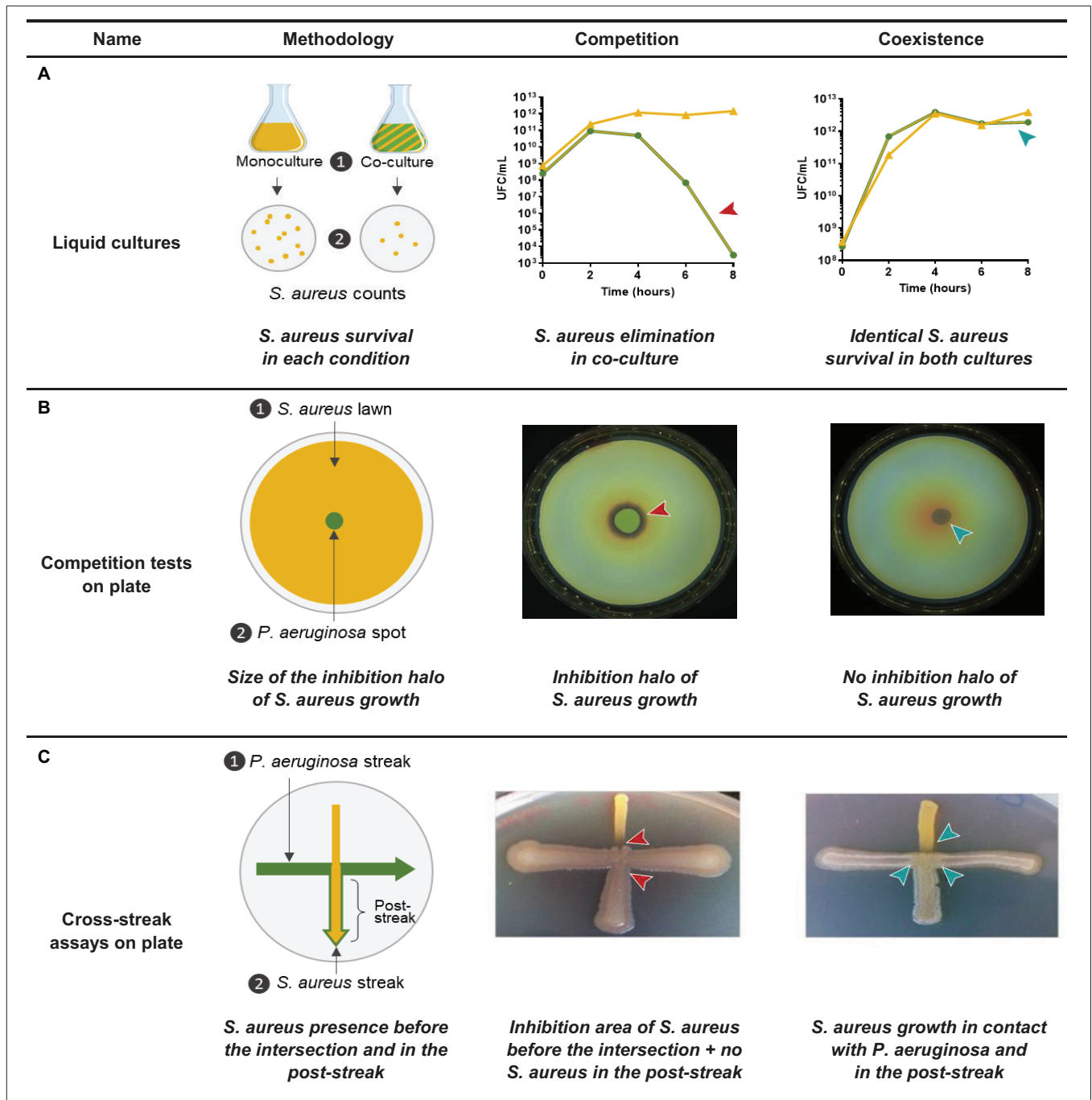


FIGURE 3 | Identification methods of the coexisting interaction between *Pseudomonas aeruginosa* and *Staphylococcus aureus*. **(A)** *P. aeruginosa* and *S. aureus* are cultivated in liquid mono- and co-culture in a rich medium during 8-h and *S. aureus* cells are counted in each condition. Competition is characterized by a rapid elimination of *S. aureus* in co-culture in comparison to the monoculture, whereas *S. aureus* growth is not affected during the whole kinetic in the case of a coexisting interaction (Briaud et al., 2019; Camus et al., 2020). **(B)** *P. aeruginosa* and *S. aureus* suspensions are prepared from overnight precultures in a rich medium and *S. aureus* lawn is uniformly plated on a rich agar medium. A *P. aeruginosa* spot is deposited in the center of the lawn and the plate is incubated 24 h. Competition is characterized by an inhibition halo of *S. aureus* growth in contact with the spot of *P. aeruginosa*, whereas *S. aureus* growth is not affected by *P. aeruginosa* during the coexisting interaction. Size of the inhibition halo can be measured (Baldan et al., 2014; Briaud et al., 2019, 2020; Camus et al., 2020). **(C)** *P. aeruginosa* streak is performed on a rich agar medium, after what a perpendicular *S. aureus* streak is added. The plate is incubated during 24 h. Competition is characterized by an inhibition of *S. aureus* growth in contact with the streak of *P. aeruginosa* and a low *S. aureus* proportion in the post-streak. Coexistence is characterized by a *S. aureus* growth in contact with the streak of *P. aeruginosa* and a high *S. aureus* proportion in the post-streak. Both of these parameters are visually determined (Michelsen et al., 2016; Minandri et al., 2016; Hotterbeek et al., 2017). Arrows indicate when or where the competitive (red arrow) or coexisting (blue arrow) interaction is observed.

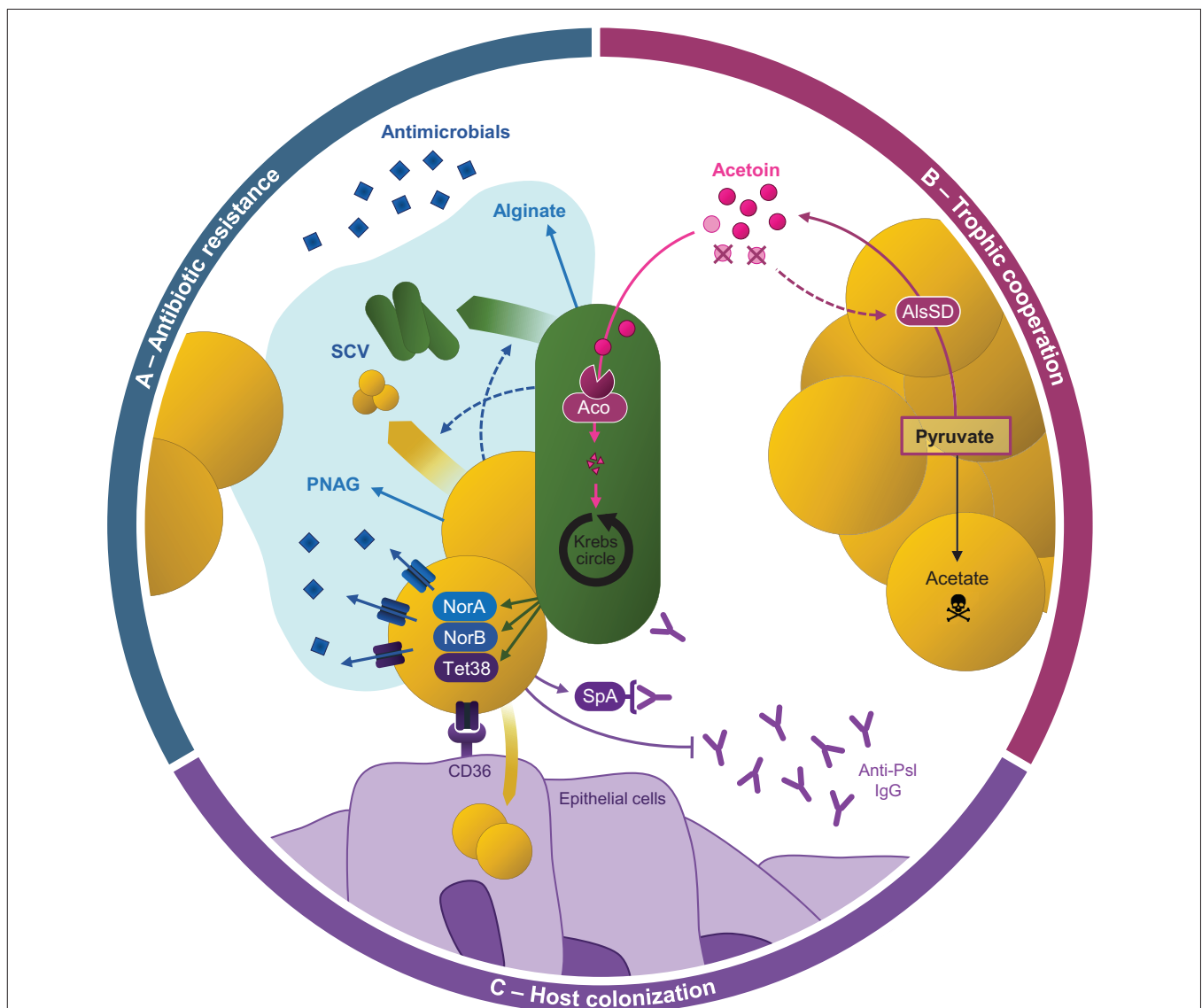


FIGURE 4 | Cooperative behaviors between *Pseudomonas aeruginosa* and *Staphylococcus aureus* during coexistence. **(A)** Antibiotic resistance of both pathogens can be increased by the formation of mixed-species biofilm, especially through the production of alginate and poly-*N*-acetylglucosamine (PNAG) by *P. aeruginosa* and *S. aureus*, respectively. *P. aeruginosa* and *S. aureus* formation of small-colony variants (SCV) is also promoted during their interaction. *P. aeruginosa* presence was also shown to induce the over-expression of efflux pumps from the Nor family in *S. aureus*, enhancing its antibiotic resistance. **(B)** *S. aureus* produces acetoin from pyruvate thanks to AlsSD. *P. aeruginosa* catabolizes the acetoin produced by *S. aureus* and uses it as an alternative carbon source thanks to the *aco* system to feed the Krebs cycle. It improves its growth during co-culture with *S. aureus*. This catabolism also increases *S. aureus* survival potentially through a feed-back on acetoin production: the medium depletion in acetoin would promote AlsSD activity, limiting acetate production from pyruvate and thus cell acidification. **(C)** Resistance to immune system. *P. aeruginosa*-induced overexpression of *tet38* improves *S. aureus* internalization in epithelial cells, allowing to hide from the immune system. *S. aureus* can limit *P. aeruginosa*-induced immune responses, notably through the binding of *S. aureus* protein A (SpA) to anti-*P. aeruginosa* antibodies (Anti-Psl IgG).

was attributed to the formation of *P. aeruginosa* aggregates within the biofilm architecture (Beaudoin et al., 2017).

Development of Trophic Cooperation

Recent transcriptomic studies suggested that trophic cooperation could establish between *S. aureus* and *P. aeruginosa* (Figure 4B). The four-carbon molecule acetoin, produced by *S. aureus*, was shown to induce the overexpression of the *aco* system in CF *P. aeruginosa* strains during coexistence interaction (Camus

et al., 2020). In line with this, *P. aeruginosa* presented an enhanced ability to catabolize acetoin produced by *S. aureus* as an alternative carbon source, resulting in increased survival during co-culture. Acetoin catabolism was also shown to benefit *S. aureus* and improve its survival in co-culture. Acetoin thus appears to be the keystone of trophic cooperation between *P. aeruginosa* and *S. aureus* during which both partners are beneficiaries. Interestingly, this cooperative behavior seems to be selected during bacterial evolution in the CF environment.

Acetoin production by *S. aureus* and catabolism by *P. aeruginosa* were indeed more efficient for coexisting isolates in comparison to competitive ones (Camus et al., 2020). As acetoin could be detected in CF sputa, these results go along with the trophic adaptation of *P. aeruginosa* strains to resources present in the CF environment (Španěl et al., 2016; La Rosa et al., 2018, 2019; Camus et al., 2020). Other studies suggest that lactate, also detected in CF sputa, may also play a role in metabolic interactions between *P. aeruginosa* and *S. aureus* (Filkins et al., 2015; Tognon et al., 2017; La Rosa et al., 2019). Co-culture with *P. aeruginosa* was shown to induce the overexpression of genes involved in glucose fermentation and lactate production in *S. aureus*, leading to lactate accumulation in the medium. In turn, *P. aeruginosa* overexpressed genes responsible for lactate utilization and was able to use the molecule as a carbon source (Filkins et al., 2015; Tognon et al., 2017). However, this phenomenon was observed during a competitive interaction (using PAO1 or PA14 strains) and the impacts of lactate catabolism on both pathogens remain unknown.

Modification of Host-Bacterium Interaction

Cooperative behaviors such as protection against antimicrobials and trophic cooperation probably contribute to the establishment and maintenance of *P. aeruginosa* and *S. aureus* co-infections. In addition, interactions between the two pathogens were shown to affect their abilities to colonize host and settle as chronic infections (Figure 4C). Adhesion to host components is an important feature for colonization, and *S. aureus* can attach more efficiently to abiotic surfaces during co-culture with *P. aeruginosa* (Kumar and Ting, 2015). In these conditions, *S. aureus* presented an up-regulation of several proteins involved in adhesion to platelets or to the extracellular matrixes of various hosts, such as serine rich glycoproteins and the Ehb protein. These results suggest that co-culture may increase *S. aureus*'s adhesion to host cells (Kumar and Ting, 2015). In line with this, co-culture with *P. aeruginosa* CF strains was shown to induce the overexpression of nine virulence factors of *S. aureus*. Among them, the Tet38 transporter promoted the internalization of *S. aureus* within epithelial pulmonary cells during coexistence with *P. aeruginosa* (Briard et al., 2019). Finally, HQNO-mediated induction of the SCV phenotype can increase the intracellular survival of *S. aureus* (Mitchell et al., 2010). Cell internalization and the SCV phenotype, both promoted by *P. aeruginosa*, could thus contribute to the success of *S. aureus* infection.

Limiting the induction and efficiency of immune responses is a strategy already developed by *P. aeruginosa* during its genetic adaptation to the CF environment. Interestingly, *P. aeruginosa*-*S. aureus* co-infection induces a specific host response different from mono-infections in a rat otitis model (Yadav et al., 2017). Using bacterial supernatants, Chekabab et al. (2015) observed that molecules secreted by *S. aureus* decreased the hosts' immune response induced by *P. aeruginosa* supernatant. Thus, the protein SpA produced by *S. aureus* was shown to bind either to *P. aeruginosa* Psl exopolysaccharide or to anti-Psl IgG antibodies, protecting *P. aeruginosa* from Psl

recognition by neutrophils and thus phagocytosis (Armbruster et al., 2016; Figure 4C). In addition, *S. aureus* presence induces transcriptomic down-regulation of several antigenic factors in *P. aeruginosa*, such as genes involved in secretion and flagellum synthesis (Miller et al., 2017).

Consequently, several studies suggest that *P. aeruginosa* and *S. aureus* co-infection favors chronic infections. Cigana et al. (2018) indeed observed that preliminary colonization by *S. aureus* increased the ability of PA14 and CF-adapted strains to establish a chronic infection in a murine model. Interestingly, such infection kinetics are frequent in CF patients as *S. aureus* is one of the first colonizers in the lungs of young children, whereas *P. aeruginosa* infection occurs upon adolescence (French Cystic Fibrosis Register, 2017). On another note, *S. aureus*-*P. aeruginosa* co-infections were shown to delay chronic wound healing and thus bacterial clearing (Pastar et al., 2013). Finally, Zhao et al. (2018) observed that mice presented an improved survival when their lungs were infected by a mix of *P. aeruginosa*, *S. aureus* and *Klebsiella pneumoniae*, in comparison to mice infected only with *P. aeruginosa*. Although this effect cannot be specifically attributed to the presence of *S. aureus* and/or *K. pneumoniae*, co-infection appears to reduce the host mortality of *P. aeruginosa* infections and thus promote longer infections. Altogether, these studies suggest that co-infection favors the establishment of chronicity, since the concomitant presence of pathogens will improve their persistence within the infection site (Limoli and Hoffman, 2019).

P. aeruginosa AND *S. aureus* ARE NOT ALONE

So far, the adaptive process and interactions of *P. aeruginosa* and *S. aureus* remain those most documented, as their infections are the most prevalent and severe in the context of CF (Machan et al., 1992; Mashburn et al., 2005; Hotterbeekx et al., 2017). However, numerous other microorganisms can colonize the CF environment and are thus susceptible to interact with *P. aeruginosa* (French Cystic Fibrosis Register, 2017). Among them, the fungus *Aspergillus fumigatus* is involved in a nutritional competition with *P. aeruginosa*. In this context, growth, biofilm formation and hyphal structure of the fungus are altered by *P. aeruginosa* secreted factors such as rhamnolipids, phenazines and the QS signals 3OC12-HSL and PQS (O'Brien and Fothergill, 2017; Briard et al., 2019; Sass et al., 2019; Chatterjee et al., 2020). As *P. aeruginosa*'s adaptation to the CF lung environment affects the secretion of these factors, it is likely that its relationship with *A. fumigatus* also evolves toward a coexistence-like interaction allowing the establishment of stable *P. aeruginosa*-*A. fumigatus* co-infections. Although no direct evidence has been established yet, this hypothesis is supported by the reduced antifungal activity shown for mucoid *P. aeruginosa* isolates (Briard et al., 2019; Chatterjee et al., 2020). Moreover, *P. aeruginosa* infection rather precedes *A. fumigatus* colonization and can even promote aspergillosis (O'Brien and Fothergill, 2017; Briard et al., 2019; Chatterjee et al., 2020). The aggressive behavior of *P. aeruginosa* is also observed toward the yeast *C. albicans* and the bacteria

from the *Burkholderia* spp (Fourie et al., 2016; O'Brien and Fothergill, 2017; Fourie and Pohl, 2019; Limoli et al., 2019). However, it appears that these microorganisms are not powerless in front of *P. aeruginosa* and can even take advantage of this interaction within mixed-species biofilm. Antimicrobial resistance and virulence of *C. albicans* and *P. aeruginosa* are thus enhanced during their interaction, particularly through an increased production of phenazines by *P. aeruginosa* and ethanol by *C. albicans* (Fourie et al., 2016; O'Brien and Fothergill, 2017; Fourie and Pohl, 2019; Alam et al., 2020; Bandara et al., 2020; Hůlková et al., 2020; Ibberson and Whiteley, 2020). In the same way, *P. aeruginosa* alginate can protect *B. cenocepacia* from the host immune system (O'Brien and Fothergill, 2017).

If microbial adaptation to the CF environment favors such win-win interactions is yet to be determined. In particular, one might wonder if the increased virulence within mixed-species biofilm with *C. albicans* is a conserved response in CF-adapted *P. aeruginosa*, as the bacterium preferentially evolves toward an avirulent lifestyle (Bianconi et al., 2015; Marvig et al., 2015; Riquelme et al., 2020). One another note, and as described earlier for *S. aureus*, *P. aeruginosa* is not alone in evolving. Notably, modifications in LPS and siderophore production, as well as a decrease of mucoidy, virulence and biofilm formation, were demonstrated during *B. cenocepacia*'s adaption to the CF environment (Cullen et al., 2015; Maldonado et al., 2016). These alterations are susceptible to affect its interactions with *P. aeruginosa*, and with other co-colonizing microorganisms.

CONCLUDING REMARKS AND PERSPECTIVES

In addition to the persistence features of microorganisms, their interactions play a key role in their survival within infectious sites. Although poorly described, this "social" aspect is particularly essential in CF lung infections as they gather significant microorganism richness and densities. *P. aeruginosa*'s adaptation to the CF environment appears to drastically impact its microbial interactions, allowing the development of neutralist and even cooperative behaviors with co-colonizing microorganisms such as *S. aureus* or *C. albicans*. This raises questions about the impacts of these microorganisms on *P. aeruginosa*'s adaptation to the CF lung environment: can their presence constitute a selective force and promote the establishment of cooperative interactions?

REFERENCES

- Alam, F., Catlow, D., Di Maio, A., Blair, J. M. A., and Hall, R. A. (2020). *Candida albicans* enhances meropenem tolerance of *Pseudomonas aeruginosa* in a dual-species biofilm. *J. Antimicrob. Chemother.* 75, 925–935. doi: 10.1093/jac/dkz514
- Alatraktchi, F. A., Dimaki, M., Støvring, N., Johansen, H. K., Molin, S., and Svendsen, W. E. (2020). Nanograss sensor for selective detection of *Pseudomonas aeruginosa* by pyocyanin identification in airway samples. *Anal. Biochem.* 593, 113586. doi: 10.1016/j.ab.2020.113586

Such cooperation is indeed an attractive strategy to promote microbial persistence within lungs: (i) it is less costly for both partners as the production of virulence or resistance factors is no longer required, and (ii) it can provide advantageous features to both partners of the interaction. CF-adapted strains of *P. aeruginosa* and *S. aureus* can thus benefit from reciprocal protection against antibiotics and metabolic cooperation, despite strong competition *in vitro* and/or between non-adapted strains.

Ultimately, these cooperative interactions could contribute to the establishment of "Climax communities," i.e., microbial communities with a steady structure within the CF ecosystem (Quinn et al., 2016). Interestingly, *S. aureus* and *P. aeruginosa* are part of one of these Climax communities *in vivo*, suggesting that their interaction may stabilize and maintain co-infection by these two pathogens. This phenomenon could explain the high proportion of *P. aeruginosa*-*S. aureus* co-infected patients within CF cohorts (Limoli et al., 2016; Briaud et al., 2020), and more broadly the positive or negative associations observed between different pathogens (Granchelli et al., 2018). Nevertheless, the impacts of *P. aeruginosa* and *S. aureus* co-infections on clinical outcomes remain unclear and poorly described (Limoli et al., 2016; Briaud et al., 2020). Taking into account the nature of their interaction might unveil new aspects of their pathogenesis and their ability to durably persist within CF lungs.

AUTHOR CONTRIBUTIONS

KM and LC were primarily responsible for preparing the review. FV and PB contributed to writing the review and editing the final version. All authors contributed to the article and approved the submitted version.

FUNDING

This work was supported by the Fondation pour la Recherche Médicale, grant number ECO20170637499 to LC, Finovi Foundation to KM, and associations "Vaincre la Mucoviscidose" and "Gregory Lemarchal" to KM.

ACKNOWLEDGMENTS

We thank Dr. Anne Doléans-Jordheim and Rachel Zapf for proofreading and advice.

- Alhede, M., Bjarnsholt, T., Givskov, M., and Alhede, M. (2014). *Pseudomonas aeruginosa* biofilms: mechanisms of immune evasion. *Adv. Appl. Microbiol.* 86, 1–40.
- Armbruster, C. R., Wolter, D. J., Mishra, M., Hayden, H. S., Radey, M. C., Merrihew, G., et al. (2016). *Staphylococcus aureus* protein A mediates interspecies interactions at the cell surface of *Pseudomonas aeruginosa*. *mBio* 7:e00538-16. doi: 10.1128/mBio.00538-16
- Baldan, R., Cigana, C., Testa, F., Bianconi, I., De Simone, M., Pellin, D., et al. (2014). Adaptation of *Pseudomonas aeruginosa* in cystic fibrosis airways influences virulence of *Staphylococcus aureus* in vitro and murine models of co-infection. *3. PLoS One* 9:e89614. doi: 10.1371/journal.pone.0089614

- Bandara, H. M. H. N., Wood, D. L. A., Vanwonderghem, I., Hugenholtz, P., Cheung, B. P. K., and Samaranyake, L. P. (2020). Fluconazole resistance in *Candida albicans* is induced by *Pseudomonas aeruginosa* quorum sensing. *Sci. Rep.* 10:7769. doi: 10.1038/s41598-020-64761-3
- Beaudoin, T., Yau, Y. C. W., Stapleton, P. J., Gong, Y., Wang, P. W., Guttman, D. S., et al. (2017). *Staphylococcus aureus* interaction with *Pseudomonas aeruginosa* biofilm enhances tobramycin resistance. *NPJ Biofilms Microbiomes* 3:25. doi: 10.1038/s41522-017-0035-0
- Besier, S., Ludwig, A., Ohlsen, K., Brade, V., and Wichelhaus, T. A. (2007). Molecular analysis of the thymidine-auxotrophic small colony variant phenotype of *Staphylococcus aureus*. *Int. J. Med. Microbiol.* 297, 217–225. doi: 10.1016/j.ijmm.2007.02.003
- Bhagirath, A. Y., Li, Y., Somayajula, D., Dadashi, M., Badr, S., and Duan, K. (2016). Cystic fibrosis lung environment and *Pseudomonas aeruginosa* infection. *BMC Pulm. Med.* 16:174. doi: 10.1186/s12890-016-0339-5
- Bianconi, I., Jeukens, J., Freschi, L., Alcalá-Franco, B., Facchini, M., Boyle, B., et al. (2015). Comparative genomics and biological characterization of sequential *Pseudomonas aeruginosa* isolates from persistent airways infection. *BMC Genom.* 16:1105. doi: 10.1186/s12864-015-2276-8
- Bjarnsholt, T., Jensen, P. Ø., Jakobsen, T. H., Phipps, R., Nielsen, A. K., Rybtke, M. T., et al. (2010). Quorum sensing and virulence of *Pseudomonas aeruginosa* during lung infection of cystic fibrosis patients. *PLoS One* 5:e10115. doi: 10.1371/journal.pone.0010115
- Briard, B., Mislin, G. L. A., Latgé, J.-P., and Beauvais, A. (2019). Interactions between *Aspergillus fumigatus* and pulmonary bacteria: current state of the field, new data, and future perspective. *J. Fungi (Basel)* 5:48. doi: 10.3390/jof5020048
- Briard, P., Bastien, S., Camus, L., Boyadjian, M., Reix, P., Mainguy, C., et al. (2020). Impact of coexistence phenotype between *Staphylococcus aureus* and *Pseudomonas aeruginosa* isolates on clinical outcomes among Cystic Fibrosis patients. *Front. Cell Infect. Microbiol.* 10:266. doi: 10.3389/fcimb.2020.00266
- Briard, P., Camus, L., Bastien, S., Doléans-Jordheim, A., Vandenesch, F., and Moreau, K. (2019). Coexistence with *Pseudomonas aeruginosa* alters *Staphylococcus aureus* transcriptome, antibiotic resistance and internalization into epithelial cells. *Sci. Rep.* 9:16564. doi: 10.1038/s41598-019-52975-z
- Camus, L., Briard, P., Bastien, S., Elsen, S., Doléans-Jordheim, A., Vandenesch, F., et al. (2020). Trophic cooperation promotes bacterial survival of *Staphylococcus aureus* and *Pseudomonas aeruginosa*. *ISME J.* 14, 3093–3105. doi: 10.1038/s41396-020-00741-9
- Cendra, M. D. M., Blanco-Cabra, N., Pedraz, L., and Torrents, E. (2019). Optimal environmental and culture conditions allow the in vitro coexistence of *Pseudomonas aeruginosa* and *Staphylococcus aureus* in stable biofilms. *Sci. Rep.* 9:16284. doi: 10.1038/s41598-019-52726-0
- Chatterjee, I., Kriegeskorte, A., Fischer, A., Deiwick, S., Theimann, N., Proctor, R. A., et al. (2008). In vivo mutations of thymidylate synthase (encoded by thyA) are responsible for thymidine dependency in clinical small-colony variants of *Staphylococcus aureus*. *J. Bacteriol.* 190, 834–842. doi: 10.1128/jb.00912-07
- Chatterjee, P., Sass, G., Swietnicki, W., and Stevens, D. A. (2020). Review of potential *pseudomonas* weaponry, relevant to the *pseudomonas*-*aspergillus* interplay, for the mycology community. *J. Fungi (Basel)* 6:81. doi: 10.3390/jof6020081
- Chekabab, S. M., Silverman, R. J., Lafayette, S. L., Luo, Y., Rousseau, S., and Nguyen, D. (2015). *Staphylococcus aureus* inhibits IL-8 responses induced by *Pseudomonas aeruginosa* in airway epithelial cells. *PLoS One* 10:e0137753. doi: 10.1371/journal.pone.0137753
- Chen, R., Déziel, E., Groleau, M.-C., Schaefer, A. L., and Greenberg, E. P. (2019). Social cheating in a *Pseudomonas aeruginosa* quorum-sensing variant. *Proc. Natl. Acad. Sci. U.S.A.* 116, 7021–7026. doi: 10.1073/pnas.1819801116
- Chew, S. C., Yam, J. K. H., Matysik, A., Seng, Z. J., Klebensberger, J., Givskov, M., et al. (2018). Matrix polysaccharides and SiaD diguanylate cyclase alter community structure and competitiveness of *pseudomonas aeruginosa* during dual-species biofilm development with *Staphylococcus aureus*. *mBio* 9:e00585-18. doi: 10.1128/mBio.00585-18
- Cigana, C., Bianconi, I., Baldan, R., De Simone, M., Riva, C., Sipione, B., et al. (2018). *Staphylococcus aureus* impacts *Pseudomonas aeruginosa* Chronic respiratory disease in murine models. *J. Infect. Dis.* 217, 933–942. doi: 10.1093/infdis/jix621
- Colvin, K. M., Gordon, V. D., Murakami, K., Borlee, B. R., Wozniak, D. J., Wong, G. C. L., et al. (2011). The pel polysaccharide can serve a structural and protective role in the biofilm matrix of *Pseudomonas aeruginosa*. *PLoS Pathog* 7:e1001264. doi: 10.1371/journal.ppat.1001264
- Colvin, K. M., Irie, Y., Tart, C. S., Urbano, R., Whitney, J. C., Ryder, C., et al. (2012). The Pel and Psl polysaccharides provide *Pseudomonas aeruginosa* structural redundancy within the biofilm matrix. *Environ. Microbiol.* 14, 1913–1928. doi: 10.1111/j.1462-2920.2011.02657.x
- Cruz, R. L., Asfahl, K. L., Bossche, SV den, Coenye, T., Crabbé, A., and Dandekar, A. A. (2020). RhlR-regulated Acyl-homoserine lactone quorum sensing in a cystic fibrosis isolate of *Pseudomonas aeruginosa*. *mBio* 11:e00532-20. doi: 10.1128/mBio.00532-20
- Cullen, L., Weiser, R., Olszak, T., Maldonado, R. F., Moreira, A. S., Slachmuylders, L., et al. (2015). Phenotypic characterization of an international *Pseudomonas aeruginosa* reference panel: strains of cystic fibrosis (CF) origin show less in vivo virulence than non-CF strains. *Microbiology (Reading Engl.)* 161, 1961–1977. doi: 10.1099/mic.0.000155
- DeLeon, S., Clinton, A., Fowler, H., Everett, J., Horswill, A. R., and Rumbaugh, K. P. (2014). Synergistic interactions of *Pseudomonas aeruginosa* and *Staphylococcus aureus* in an in vitro wound model. *Infect. Immun.* 82, 4718–4728. doi: 10.1128/IAI.02198-14
- Déziel, E., Lépine, F., Milot, S., and Villemur, R. (2003). rhlA is required for the production of a novel biosurfactant promoting swarming motility in *Pseudomonas aeruginosa*: 3-(3-hydroxyalkanoxy)alkanoic acids (HAAs), the precursors of rhamnolipids. *Microbiology (Reading Engl.)* 149, 2005–2013. doi: 10.1099/mic.0.26154-0
- Feltner, J. B., Wolter, D. J., Pope, C. E., Groleau, M.-C., Smalley, N. E., Greenberg, E. P., et al. (2016). LasR variant cystic fibrosis isolates reveal an adaptable quorum-sensing hierarchy in *Pseudomonas aeruginosa*. *mBio* 7:e01513-16. doi: 10.1128/mBio.01513-16
- Feraco, D., Blaha, M., Khan, S., Green, J. M., and Plotkin, B. J. (2016). Host environmental signals and effects on biofilm formation. *Microb. Pathog.* 99, 253–263. doi: 10.1016/j.micpath.2016.08.015
- Filkins, L. M., Graber, J. A., Olson, D. G., Dolben, E. L., Lynd, L. R., Bhujju, S., et al. (2015). Coculture of *Staphylococcus aureus* with *Pseudomonas aeruginosa* Drives *S. aureus* towards fermentative metabolism and reduced viability in a cystic fibrosis model. *J. Bacteriol.* 197, 2252–2264. doi: 10.1128/jb.00591-15
- Folkesson, A., Jelsbak, L., Yang, L., Johansen, H. K., Ciofu, O., Høiby, N., et al. (2012). Adaptation of *Pseudomonas aeruginosa* to the cystic fibrosis airway: an evolutionary perspective. *Nat. Rev. Microbiol.* 10, 841–851. doi: 10.1038/nrmicro2907
- Fourie, R., Ells, R., Swart, C. W., Sebolai, O. M., Albertyn, J., and Pohl, C. H. (2016). *Candida albicans* and *Pseudomonas aeruginosa* Interaction, with Focus on the Role of Eicosanoids. *Front. Physiol.* 7:64. doi: 10.3389/fphys.2016.00064
- Fourie, R., and Pohl, C. H. (2019). Beyond antagonism: the interaction between *candida* species and *Pseudomonas aeruginosa*. *J. Fungi (Basel)* 5:34. doi: 10.3390/jof5020034
- French Cystic Fibrosis Register (2017). Available online at: <https://www.vaincrelamuco.org/2019/05/17/statistiques-et-publications-204> (accessed February 18, 2021).
- Fugère, A., Lalonde Séguin, D., Mitchell, G., Déziel, E., Dekimpe, V., Cantin, A. M., et al. (2014). Interspecific small molecule interactions between clinical isolates of *Pseudomonas aeruginosa* and *Staphylococcus aureus* from adult cystic fibrosis patients. *PLoS One* 9:e86705. doi: 10.1371/journal.pone.0086705
- Granchelli, A. M., Adler, F. R., Keogh, R. H., Kartsonaki, C., Cox, D. R., and Liou, T. G. (2018). Microbial interactions in the cystic fibrosis airway. *J. Clin. Microbiol.* 56:e00354-18. doi: 10.1128/JCM.00354-18
- Herzog, S., Dach, F., de Buhr, N., Niemann, S., Schlagowski, J., Chaves-Moreno, D., et al. (2019). High nuclease activity of long persisting *Staphylococcus aureus* isolates within the airways of cystic fibrosis patients protects against NET-mediated killing. *Front. Immunol.* 10:2552. doi: 10.3389/fimmu.2019.02552
- Hoffman, L. R., Déziel, E., D'Argenio, D. A., Lépine, F., Emerson, J., McNamara, S., et al. (2006). Selection for *Staphylococcus aureus* small-colony variants due

- to growth in the presence of *Pseudomonas aeruginosa*. 52. *Proc. Natl. Acad. Sci. U.S.A.* 103, 19890–19895. doi: 10.1073/pnas.0606756104
- Hoiby, N., Bjarnsholt, T., Moser, C., Jensen, P. Ø, Kolpen, M., Qvist, T., et al. (2017). Diagnosis of biofilm infections in cystic fibrosis patients. *APMIS* 125, 339–343. doi: 10.1111/apm.12689
- Hood, M. I., Mortensen, B. L., Moore, J. L., Zhang, Y., Kehl-Fie, T. E., Sugitani, N., et al. (2012). Identification of an *Acinetobacter baumannii* zinc acquisition system that facilitates resistance to calprotectin-mediated zinc sequestration. *PLoS Pathog.* 8:e1003068. doi: 10.1371/journal.ppat.1003068
- Hotterbeekx, A., Kumar-Singh, S., Goossens, H., and Malhotra-Kumar, S. (2017). In vivo and In vitro interactions between *Pseudomonas aeruginosa* and *Staphylococcus* spp. *Front. Cell. Infect. Microbiol.* 7:106. doi: 10.3389/fcimb.2017.00106
- Hubert, D., Réglie-Poupet, H., Sermet-Gaudelus, I., Ferroni, A., Le Bourgeois, M., Burgel, P.-R., et al. (2013). Association between *Staphylococcus aureus* alone or combined with *Pseudomonas aeruginosa* and the clinical condition of patients with cystic fibrosis. *J. Cyst. Fibros.* 12, 497–503. doi: 10.1016/j.jcf.2012.12.003
- Hůlková, M., Soukupová, J., Carlson, R. P., and Maršálek, B. (2020). Interspecies interactions can enhance *Pseudomonas aeruginosa* tolerance to surfaces functionalized with silver nanoparticles. *Colloid. Surf. B Biointerfac.* 192:111027. doi: 10.1016/j.colsurfb.2020.111027
- Ibberson, C. B., and Whiteley, M. (2020). The social life of microbes in chronic infection. *Curr. Opin. Microbiol.* 53, 44–50. doi: 10.1016/j.mib.2020.02.003
- Jenul, C., and Horswill, A. R. (2018). Regulation of *Staphylococcus aureus* virulence. *Microbiol. Spectr.* 6:1128. doi: 10.1128/microbiolspec.GPP3-0031-2018
- Kahl, B., Herrmann, M., Everding, A. S., Koch, H. G., Becker, K., Harms, E., et al. (1998). Persistent infection with small colony variant strains of *Staphylococcus aureus* in patients with cystic fibrosis. *J. Infect. Dis.* 177, 1023–1029. doi: 10.1086/515238
- Kahl, B. C., Becker, K., and Löffler, B. (2016). Clinical significance and pathogenesis of staphylococcal small colony variants in persistent infections. *Clin. Microbiol. Rev.* 29, 401–427. doi: 10.1128/cmr.00069-15
- Kahl, B. C., Belling, G., Becker, P., Chatterjee, I., Wardecki, K., Hilgert, K., et al. (2005). Thymidine-dependent *Staphylococcus aureus* small-colony variants are associated with extensive alterations in regulator and virulence gene expression profiles. *Infect. Immun.* 73, 4119–4126. doi: 10.1128/iai.73.7.4119-4126.2005
- Kehl-Fie, T. E., and Skaar, E. P. (2010). Nutritional immunity beyond iron: a role for manganese and zinc. *Curr. Opin. Chem. Biol.* 14, 218–224. doi: 10.1016/j.cbpa.2009.11.008
- Khademi, S. M. H., Sazinas, P., and Jelsbak, L. (2019). Within-host adaptation mediated by intergenic evolution in *Pseudomonas aeruginosa*. *Genome Biol. Evol.* 11, 1385–1397. doi: 10.1093/gbe/evz083
- Klockgether, J., Cramer, N., Fischer, S., Wiehlmann, L., and Tümmler, B. (2018). Long-term microevolution of *Pseudomonas aeruginosa* differs between mildly and severely affected cystic fibrosis lungs. 2. *Am. J. Respir. Cell Mol. Biol.* 59, 246–256. doi: 10.1165/rcmb.2017-0356oc
- Kobayashi, S. D., and DeLeo, F. R. (2013). *Staphylococcus aureus* protein A promotes immune suppression. *mBio* 4:e00764-13. doi: 10.1128/mBio.00764-13
- Kriegeskorte, A., Lorè, N. I., Bragonzi, A., Riva, C., Kelkenberg, M., Becker, K., et al. (2015). Thymidine-dependent *Staphylococcus aureus* small-colony variants are induced by trimethoprim-sulfamethoxazole (SXT) and have increased fitness during SXT challenge. *Antimicrob. Agents Chemother.* 59, 7265–7272. doi: 10.1128/aac.00742-15
- Kumar, A., and Ting, Y. P. (2015). Presence of *Pseudomonas aeruginosa* influences biofilm formation and surface protein expression of *Staphylococcus aureus*. *Environ. Microbiol.* 17, 4459–4468. doi: 10.1111/1462-2920.12890
- La Rosa, R., Johansen, H. K., and Molin, S. (2018). Convergent Metabolic specialization through distinct evolutionary paths in *Pseudomonas aeruginosa*. *mBio* 9:e00269-18. doi: 10.1128/mBio.00269-18
- La Rosa, R., Johansen, H. K., and Molin, S. (2019). Adapting to the airways: metabolic requirements of *Pseudomonas aeruginosa* during the infection of cystic fibrosis patients. *Metabolites* 9:234. doi: 10.3390/metabo9100234
- Leid, J. G., Willson, C. J., Shirtliff, M. E., Hassett, D. J., Parsek, M. R., and Jeffers, A. K. (2005). The exopolysaccharide alginate protects *Pseudomonas aeruginosa* biofilm bacteria from IFN-gamma-mediated macrophage killing. *J. Immunol.* 175, 7512–7518. doi: 10.4049/jimmunol.175.11.7512
- Lennartz, F. E., Schwartbeck, B., Dübbers, A., Große-Onnebrink, J., Kessler, C., Küster, P., et al. (2019). The prevalence of *Staphylococcus aureus* with mucoid phenotype in the airways of patients with cystic fibrosis—A prospective study. *Int. J. Med. Microbiol.* 309, 283–287. doi: 10.1016/j.ijmm.2019.05.002
- Limoli, D. H., and Hoffman, L. R. (2019). Help, hinder, hide and harm: what can we learn from the interactions between *Pseudomonas aeruginosa* and *Staphylococcus aureus* during respiratory infections? 7. *Thorax* 74, 684–692. doi: 10.1136/thoraxjnl-2018-212616
- Limoli, D. H., Warren, E. A., Yarrington, K. D., Donegan, N. P., Cheung, A. L., and O'Toole, G. A. (2019). Interspecies interactions induce exploratory motility in *Pseudomonas aeruginosa*. *Elife* 8:e47365. doi: 10.7554/eLife.47365.sa2
- Limoli, D. H., Whitfield, G. B., Kitao, T., Ivey, M. L., Davis, M. R., Grahl, N., et al. (2017). *Pseudomonas aeruginosa* alginate overproduction promotes coexistence with *Staphylococcus aureus* in a model of cystic fibrosis respiratory infection. *mBio* 8:e00186-17. doi: 10.1128/mBio.00186-17
- Limoli, D. H., Yang, J., Khansaheb, M. K., Helfman, B., Peng, L., Stecenko, A. A., et al. (2016). *Staphylococcus aureus* and *Pseudomonas aeruginosa* co-infection is associated with cystic fibrosis-related diabetes and poor clinical outcomes. *Eur. J. Clin. Microbiol. Infect. Dis.* 35, 947–953. doi: 10.1007/s10096-016-2621-0
- Machan, Z. A., Taylor, G. W., Pitt, T. L., Cole, P. J., and Wilson, R. (1992). 2-Heptyl-4-hydroxyquinoline N-oxide, an antistaphylococcal agent produced by *Pseudomonas aeruginosa*. *J. Antimicrob. Chemother.* 30, 615–623. doi: 10.1093/jac/30.5.615
- Maldonado, R. F., Sá-Correia, I., and Valvano, M. A. (2016). Lipopolysaccharide modification in Gram-negative bacteria during chronic infection. *FEMS Microbiol. Rev.* 40, 480–493. doi: 10.1093/femsre/fuw007
- Manos, J., Hu, H., Rose, B. R., Wainwright, C. E., Zablotska, I. B., Cheney, J., et al. (2013). Virulence factor expression patterns in *Pseudomonas aeruginosa* strains from infants with cystic fibrosis. *Eur. J. Clin. Microbiol. Infect. Dis.* 32, 1583–1592. doi: 10.1007/s10096-013-1916-7
- Martha, B., Croisier, D., Fanton, A., Astruc, K., Piroth, L., Huet, F., et al. (2010). Factors associated with mucoid transition of *Pseudomonas aeruginosa* in cystic fibrosis patients. *Clin. Microbiol. Infect.* 16, 617–623. doi: 10.1111/j.1469-0691.2009.02786.x
- Marvig, R. L., Damkier, S., Khademi, S. M. H., Markussen, T. M., Molin, S., and Jelsbak, L. (2014). Within-host evolution of *Pseudomonas aeruginosa* reveals adaptation toward iron acquisition from hemoglobin. *mBio* 5:e00966-14. doi: 10.1128/mBio.00966-14
- Marvig, R. L., Dolce, D., Sommer, L. M., Petersen, B., Ciofu, O., Campana, S., et al. (2015a). Within-host microevolution of *Pseudomonas aeruginosa* in Italian cystic fibrosis patients. *BMC Microbiol.* 15:218. doi: 10.1186/s12866-015-0563-9
- Marvig, R. L., Sommer, L. M., Jelsbak, L., Molin, S., and Johansen, H. K. (2015b). Evolutionary insight from whole-genome sequencing of *Pseudomonas aeruginosa* from cystic fibrosis patients. 4. *Future Microbiol.* 10, 599–611. doi: 10.2217/fmb.15.3
- Marvig, R. L., Sommer, L. M., Molin, S., and Johansen, H. K. (2015c). Convergent evolution and adaptation of *Pseudomonas aeruginosa* within patients with cystic fibrosis. 1. *Nat. Genet.* 47, 57–64. doi: 10.1038/ng.3148
- Mashburn, L. M., Jett, A. M., Akins, D. R., and Whiteley, M. (2005). *Staphylococcus aureus* serves as an iron source for *Pseudomonas aeruginosa* during in vivo coculture. 2. *J. Bacteriol.* 187, 554–566. doi: 10.1128/jb.187.2.554-566.2005
- Michelsen, C. F., Christensen, A.-M. J., Bojer, M. S., Hoiby, N., Ingmer, H., and Jelsbak, L. (2014). *Staphylococcus aureus* alters growth activity, autolysis, and antibiotic tolerance in a human host-adapted *Pseudomonas aeruginosa* lineage. *J. Bacteriol.* 196, 3903–3911. doi: 10.1128/jb.02006-14
- Michelsen, C. F., Khademi, S. M. H., Johansen, H. K., Ingmer, H., Dorrestein, P. C., and Jelsbak, L. (2016). Evolution of metabolic divergence in *Pseudomonas aeruginosa* during long-term infection facilitates a proto-cooperative interspecies interaction. *ISME J.* 10, 1323–1336. doi: 10.1038/ismej.2015.220
- Miller, C. L., Van Laar, T. A., Chen, T., Karna, S. L. R., Chen, P., You, T., et al. (2017). Global transcriptome responses including small RNAs during mixed-species interactions with methicillin-resistant *Staphylococcus aureus*

- and *Pseudomonas aeruginosa*. *Microbiologyopen* 6:e00427. doi: 10.1002/mbo3.427
- Millette, G., Langlois, J.-P., Brouillette, E., Frost, E. H., Cantin, A. M., and Malouin, F. (2019). Despite antagonism in vitro, *Pseudomonas aeruginosa* enhances *Staphylococcus aureus* colonization in a murine lung infection model. *Front. Microbiol.* 10:2880. doi: 10.3389/fmicb.2019.02880
- Minandri, F., Imperi, F., Frangipani, E., Bonchi, C., Visaggio, D., Facchini, M., et al. (2016). Role of iron uptake systems in *Pseudomonas aeruginosa* virulence and airway infection. *Infect. Immun.* 84, 2324–2335. doi: 10.1128/iai.00098-16
- Mitchell, G., Séguin, D. L., Asselin, A.-E., Déziel, E., Cantin, A. M., Frost, E. H., et al. (2010). *Staphylococcus aureus* sigma B-dependent emergence of small-colony variants and biofilm production following exposure to *Pseudomonas aeruginosa* 4-hydroxy-2-heptylquinoline-N-oxide. *BMC Microbiol.* 10:33. doi: 10.1186/1471-2180-10-33
- Moisan, H., Brouillette, E., Jacob, C. L., Langlois-Bégin, P., Michaud, S., and Malouin, F. (2006). Transcription of virulence factors in *Staphylococcus aureus* small-colony variants isolated from cystic fibrosis patients is influenced by SigB. *J. Bacteriol.* 188, 64–76. doi: 10.1128/jb.188.1.64-76.2006
- Nguyen, A. T., Jones, J. W., Ruge, M. A., Kane, M. A., and Oglesby-Sherrouse, A. G. (2015). Iron depletion enhances production of antimicrobials by *Pseudomonas aeruginosa*. *J. Bacteriol.* 197, 2265–2275. doi: 10.1128/jb.00072-15
- Noto, M. J., Burns, W. J., Beavers, W. N., and Skaar, E. P. (2017). Mechanisms of pyocyanin toxicity and genetic determinants of resistance in *Staphylococcus aureus*. *J. Bacteriol.* 199:e00221-17. doi: 10.1128/JB.00221-17
- O'Brien, S., and Fothergill, J. L. (2017). The role of multispecies social interactions in shaping *Pseudomonas aeruginosa* pathogenicity in the cystic fibrosis lung. *FEMS Microbiol. Lett.* 364:fnx128.
- O'Brien, S., Williams, D., Fothergill, J. L., Paterson, S., Winstanley, C., and Brockhurst, M. A. (2017). High virulence sub-populations in *Pseudomonas aeruginosa* long-term cystic fibrosis airway infections. *BMC Microbiol.* 17:30. doi: 10.1186/s12866-017-0941-6
- Orazi, G., Jean-Pierre, F., and O'Toole, G. A. (2020). *Pseudomonas aeruginosa* PA14 enhances the efficacy of norfloxacin against *Staphylococcus aureus* Newman biofilms. *J. Bacteriol.* 202:e00159-20. doi: 10.1128/JB.00159-20
- Orazi, G., and O'Toole, G. A. (2017). *Pseudomonas aeruginosa* alters *Staphylococcus aureus* sensitivity to vancomycin in a biofilm model of cystic fibrosis infection. *mBio* 8:e00873-17. doi: 10.1128/mBio.00873-17
- Orazi, G., Ruoff, K. L., and O'Toole, G. A. (2019). *Pseudomonas aeruginosa* increases the sensitivity of biofilm-grown *Staphylococcus aureus* to membrane-targeting antiseptics and antibiotics. *mBio* 10:e01501-19. doi: 10.1128/mBio.01501-19
- Pallett, R., Leslie, L. J., Lambert, P. A., Milic, I., Devitt, A., and Marshall, L. J. (2019). Anaerobiosis influences virulence properties of *Pseudomonas aeruginosa* cystic fibrosis isolates and the interaction with *Staphylococcus aureus*. *Sci. Rep.* 9:6748. doi: 10.1038/s41598-019-42952-x
- Palmer, K. L., Aye, L. M., and Whiteley, M. (2007). Nutritional cues control *Pseudomonas aeruginosa* multicellular behavior in cystic fibrosis sputum. *J. Bacteriol.* 189, 8079–8087. doi: 10.1128/jb.01138-07
- Pastar, I., Nusbaum, A. G., Gil, J., Patel, S. B., Chen, J., Valdes, J., et al. (2013). Interactions of methicillin resistant *Staphylococcus aureus* USA300 and *Pseudomonas aeruginosa* in polymicrobial wound infection. *PLoS One* 8:e56846. doi: 10.1371/journal.pone.0056846
- Price, C. E., Brown, D. G., Limoli, D. H., Phelan, V. V., and O'Toole, G. A. (2020). Exogenous alginate protects *Staphylococcus aureus* from killing by *Pseudomonas aeruginosa*. *J. Bacteriol.* 202:e00559-19. doi: 10.1128/JB.00559-19
- Proctor, R. A., Kriegeskorte, A., Kahl, B. C., Becker, K., Löffler, B., and Peters, G. (2014). *Staphylococcus aureus* small colony variants (SCVs): a road map for the metabolic pathways involved in persistent infections. *Front. Cell Infect. Microbiol.* 4:99. doi: 10.3389/fcimb.2014.00099
- Quinn, R. A., Whiteson, K., Lim, Y. W., Zhao, J., Conrad, D., LiPuma, J. J., et al. (2016). Ecological networking of cystic fibrosis lung infections. *NPJ Biofilms Microb.* 2:4. doi: 10.1038/s41522-016-0002-1
- Riquelme, S. A., Wong Fok, Lung, T., and Prince, A. (2020). Pulmonary pathogens adapt to immune signaling metabolites in the airway. *Front. Immunol.* 11:385. doi: 10.3389/fimmu.2020.00385
- Ryder, C., Byrd, M., and Wozniak, D. J. (2007). Role of polysaccharides in *Pseudomonas aeruginosa* biofilm development. *Curr. Opin. Microbiol.* 10, 644–648. doi: 10.1016/j.mib.2007.09.010
- Sass, G., Nazik, H., Penner, J., Shah, H., Ansari, S. R., Clemons, K. V., et al. (2019). Aspergillus-*Pseudomonas* interaction, relevant to competition in airways. *Med. Mycol.* 57, S228–S232. doi: 10.1093/mmy/myy087
- Schwartzbeck, B., Birtel, J., Treffon, J., Langhanki, L., Mellmann, A., Kale, D., et al. (2016). Dynamic in vivo mutations within the ica operon during persistence of *Staphylococcus aureus* in the airways of cystic fibrosis patients. *PLoS Pathog.* 12:e1006024. doi: 10.1371/journal.ppat.1006024
- Seggewiss, J., Becker, K., Kotte, O., Eisenacher, M., Yazdi, M. R. K., Fischer, A., et al. (2006). Reporter metabolite analysis of transcriptional profiles of a *Staphylococcus aureus* strain with normal phenotype and its isogenic hemB mutant displaying the small-colony-variant phenotype. *J. Bacteriol.* 188, 7765–7777. doi: 10.1128/jb.00774-06
- Smith, E. E., Buckley, D. G., Wu, Z., Saenphimmachak, C., Hoffman, L. R., D'Argenio, D. A., et al. (2006). Genetic adaptation by *Pseudomonas aeruginosa* to the airways of cystic fibrosis patients. *Proc. Natl. Acad. Sci. U.S.A.* 103, 8487–8492. doi: 10.1073/pnas.0602138103
- Španěl, P., Sovová, K., Dryahina, K., Doušová, T., Dřevínek, P., and Smith, D. (2016). Do linear logistic model analyses of volatile biomarkers in exhaled breath of cystic fibrosis patients reliably indicate *Pseudomonas aeruginosa* infection? *J. Breath Res.* 10:036013. doi: 10.1088/1752-7155/10/3/036013
- Tan, X., Coureuil, M., Ramond, E., Euphrasie, D., Dupuis, M., Tros, F., et al. (2019). Chronic *Staphylococcus aureus* lung infection correlates with proteogenomic and metabolic adaptations leading to an increased intracellular persistence. *Clin. Infect. Dis.* 69, 1937–1945. doi: 10.1093/cid/ciz106
- Toder, D. S., Gambello, M. J., and Iglewski, B. H. (1991). *Pseudomonas aeruginosa* LasA: a second elastase under the transcriptional control of lasR. *Mol. Microbiol.* 5, 2003–2010. doi: 10.1111/j.1365-2958.1991.tb00822.x
- Tognon, M., Köhler, T., Gdaniec, B. G., Hao, Y., Lam, J. S., Beaume, M., et al. (2017). Co-evolution with *Staphylococcus aureus* leads to lipopolysaccharide alterations in *Pseudomonas aeruginosa*. *ISME J.* 11, 2233–2243. doi: 10.1038/ismej.2017.83
- Treffon, J., Block, D., Moche, M., Reiss, S., Fuchs, S., Engelmann, S., et al. (2018). Adaptation of *Staphylococcus aureus* to airway environments in patients with cystic fibrosis by upregulation of superoxide dismutase M and iron-scavenging proteins. *J. Infect. Dis.* 217, 1453–1461. doi: 10.1093/infdis/jiy012
- Treffon, J., Chaves-Moreno, D., Niemann, S., Pieper, D. H., Vogl, T., Roth, J., et al. (2020). Importance of superoxide dismutases A and M for protection of *Staphylococcus aureus* in the oxidative stressful environment of cystic fibrosis airways. *Cell Microbiol.* 22:e13158. doi: 10.1111/cmi.13158
- van Mansfeld, R., de Been, M., Paganelli, F., Yang, L., Bonten, M., and Willems, R. (2016). Within-host evolution of the dutch high-prevalent *Pseudomonas aeruginosa* clone ST406 during chronic colonization of a patient with cystic fibrosis. *PLoS One* 11:e0158106. doi: 10.1371/journal.pone.0158106
- Wakeman, C. A., Moore, J. L., Noto, M. J., Zhang, Y., Singleton, M. D., Prentice, B. M., et al. (2016). The innate immune protein calprotectin promotes *Pseudomonas aeruginosa* and *Staphylococcus aureus* interaction. *Nat. Commun.* 7:11951. doi: 10.1038/ncomms11951
- Westphal, C., Görlich, D., Kampmeier, S., Herzog, S., Braun, N., Hitschke, C., et al. (2020). Antibiotic treatment and age are associated with *Staphylococcus aureus* carriage profiles during persistence in the airways of cystic fibrosis patients. *Front. Microbiol.* 11:230. doi: 10.3389/fmicb.2020.00230
- Wilson, R., Sykes, D. A., Watson, D., Rutman, A., Taylor, G. W., and Cole, P. J. (1988). Measurement of *Pseudomonas aeruginosa* phenazine pigments in sputum and assessment of their contribution to sputum sol toxicity for respiratory epithelium. *Infect. Immun.* 56, 2515–2517. doi: 10.1128/iai.56.9.2515-2517.1988
- Winstanley, C., O'Brien, S., and Brockhurst, M. A. (2016). *Pseudomonas aeruginosa* evolutionary adaptation and diversification in cystic fibrosis chronic lung infections. *Trends Microbiol.* 24, 327–337. doi: 10.1016/j.tim.2016.01.008
- Yadav, M. K., Chae, S.-W., Go, Y. Y., Im, G. J., and Song, J.-J. (2017). In vitro Multi-species biofilms of methicillin-resistant

- Staphylococcus aureus* and *Pseudomonas aeruginosa* and Their host interaction during In vivo colonization of an otitis media rat model. *Front. Cell Infect. Microbiol.* 7:125. doi: 10.3389/fcimb.2017.00125
- Yagci, S., Hascelik, G., Dogru, D., Ozcelik, U., and Sener, B. (2013). Prevalence and genetic diversity of *Staphylococcus aureus* small-colony variants in cystic fibrosis patients. *Clin. Microbiol. Infect.* 19, 77–84. doi: 10.1111/j.1469-0691.2011.03742.x
- Yang, L., Jelsbak, L., and Molin, S. (2011). Microbial ecology and adaptation in cystic fibrosis airways. *Environ. Microbiol.* 13, 1682–1689. doi: 10.1111/j.1462-2920.2011.02459.x
- Zhao, K., Du, L., Lin, J., Yuan, Y., Wang, X., Yue, B., et al. (2018). *Pseudomonas aeruginosa* quorum-sensing and type VI secretion system can direct interspecific coexistence during evolution. *Front. Microbiol.* 9:2287. doi: 10.3389/fmicb.2018.02287
- Conflict of Interest:** The authors declare that the research was conducted in the absence of any commercial or financial relationships that could be construed as a potential conflict of interest.
- Copyright © 2021 Camus, Briaud, Vandenesch and Moreau. This is an open-access article distributed under the terms of the Creative Commons Attribution License (CC BY). The use, distribution or reproduction in other forums is permitted, provided the original author(s) and the copyright owner(s) are credited and that the original publication in this journal is cited, in accordance with accepted academic practice. No use, distribution or reproduction is permitted which does not comply with these terms.

4 Objectifs de la thèse

Les récentes recherches portant sur les interactions entre *P. aeruginosa* et *S. aureus* tendent à montrer que la coexistence bactérienne serait favorisée par l'évolution des souches bactériennes dans le milieu pulmonaire des patients atteints de mucoviscidose (63, 163). Cet état de coexistence permettrait la mise en place de comportements coopératifs entre les deux bactéries : Paul Briaud a ainsi pu démontrer au cours de son doctorat effectué au laboratoire que cette interaction protégeait *S. aureus* de l'action des antibiotiques (55, 168). Cependant, aucune étude n'a encore évalué l'impact de la coexistence sur la physiologie de *P. aeruginosa*. Par ailleurs, bien que cet état d'interaction semble découler de l'adaptation génétique de *P. aeruginosa* à l'environnement pulmonaire, les déterminants génétiques exacts de la coexistence demeurent inconnus. **Ce projet de doctorat a donc pour objectif d'examiner les causes et impacts de la coexistence entre *P. aeruginosa* et *S. aureus* afin d'améliorer la compréhension et la caractérisation de cet état d'interaction encore mal compris.**

Pour cela, une première approche transcriptomique a été employée pour étudier comment l'expression génique et le métabolisme de *P. aeruginosa* sont affectés par la coexistence avec *S. aureus*. Les résultats de ce premier axe de recherche ont été publiés en août 2020 dans le journal International Society for Microbial Ecology (ISME).

Les facteurs génétiques de *P. aeruginosa* impliqués dans l'établissement de la coexistence ont ensuite été étudiés par deux approches complémentaires : une approche de génomique comparative d'isolats cliniques compétiteurs ou coexistants, et une technique d'évolution expérimentale *in vitro*. Les résultats de ce deuxième axe de recherche font l'objet d'une publication scientifique en cours de préparation.

Enfin, la technique de Transposon-sequencing a été développée au laboratoire pour déterminer les facteurs d'une souche clinique de *P. aeruginosa* impliqués dans le maintien de l'état de coexistence. Une liste de gènes favorables et défavorables à la survie de *P. aeruginosa* durant l'interaction de coexistence avec *S. aureus* a ainsi pu être établie.

Ce projet vient donc compléter les recherches effectuées par Paul Briaud au cours de son doctorat, auxquelles j'ai pu participer en tant que deuxième et troisième auteur (Cf. Partie « *Autres travaux* »). L'ensemble de ces travaux ont ainsi permis une meilleure compréhension de la coexistence et de ses effets sur *S. aureus*, *P. aeruginosa* et la santé des patients.

TRAVAUX DE RECHERCHE

1 AXE 1 : Impact de la coexistence sur le transcriptome et le métabolisme de *P. aeruginosa*

1.1. Introduction

Bien que l'effet de *P. aeruginosa* sur la physiologie de *S. aureus* soit bien décrit, peu d'études ont évalué comment *P. aeruginosa* pouvait être affecté par la présence du staphylocoque. Nous avons donc cherché à étudier les dérégulations transcriptomiques et métaboliques chez *P. aeruginosa* induites par la coexistence avec *S. aureus*.

Nous avons pour cela mené une étude transcriptomique sur quatre couples de souches cliniques de *P. aeruginosa* et *S. aureus* isolés de patients atteints de mucoviscidose co-infectés. Dans une première approche sans a priori, un séquençage des ARN de *P. aeruginosa* cultivé en monoculture ou en co-culture avec *S. aureus* a été effectué, permettant l'établissement d'une liste de gènes dont l'expression est spécifiquement affectée lors de l'interaction de coexistence. Une sous-régulation de gènes impliqués dans le catabolisme du glucose, ainsi qu'une sur-régulation de gènes impliqués dans le catabolisme de sources de carbone alternative telles que l'acétoïne et les acides aminés, ont été observées.

Nous avons ensuite cherché à confirmer ces dérégulations chez davantage de paires de souches de *P. aeruginosa* et *S. aureus*, par une approche ciblée de RT-qPCR. En testant jusqu'à 21 couples, nous avons pu observer que la dérégulation de l'expression des gènes impliqués dans le catabolisme du glucose, des acides aminés et de l'acétoïne était très fréquente. En présence de *S. aureus*, environ 70% des souches de *P. aeruginosa* ont présenté une forte surexpression du système *aco*, responsable du catabolisme de l'acétoïne.

Nous avons pu mettre en évidence que la surexpression du système *aco* chez *P. aeruginosa* était induite par l'acétoïne de manière dose-dépendante, suggérant la présence de la molécule dans nos conditions de co-culture. Effectivement, des suivis de la concentration en acétoïne ont montré que la molécule était spécifiquement produite par *S. aureus* en mono- et en co-culture. En réponse à cela, la surexpression du système *aco* permet à *P. aeruginosa* de cataboliser l'acétoïne produite par *S. aureus*. De manière intéressante, ce catabolisme bénéficie aux deux partenaires de l'interaction : il fournit à *P. aeruginosa* une source de carbone alternative et améliore sa survie en milieu appauvri, mais il favorise également la survie de *S. aureus* lors de son interaction prolongée avec *P. aeruginosa*. En effet, l'accumulation d'acétoïne dans le milieu, en absence de catabolisme par *P. aeruginosa*,

apparaît toxique pour le staphylocoque. Le métabolisme de l'acétoïne entre ces deux pathogènes s'apparente donc à une coopération trophique.

Enfin, nous avons pu montrer que cette coopération trophique était favorisée par l'interaction de coexistence : en comparaison à des souches isolées de couples compétiteurs, les souches coexistantes de *S. aureus* et *P. aeruginosa* ont présenté une capacité augmentée à produire et cataboliser l'acétoïne, respectivement. Ces résultats suggèrent qu'une co-évolution des deux pathogènes *in vivo* pourrait favoriser l'établissement de coopérations trophiques, et plus généralement de la coexistence bactérienne. Cette étude a donc permis de montrer que le métabolisme énergétique de *P. aeruginosa* est largement affecté par la coexistence avec *S. aureus*, permettant la mise en place de stratégies coopératives favorisant la survie des deux pathogènes.

1.2. **Publication : Trophic cooperation promotes bacterial survival of *Staphylococcus aureus* and *Pseudomonas aeruginosa*** (ISME, 2020)

(Page suivante)



Trophic cooperation promotes bacterial survival of *Staphylococcus aureus* and *Pseudomonas aeruginosa*

Laura Camus¹ · Paul Briaud¹ · Sylvère Bastien¹ · Sylvie Elsen² · Anne Doléans-Jordheim^{3,4} · François Vandenesch^{1,3,5} · Karen Moreau¹

Received: 11 March 2020 / Revised: 30 July 2020 / Accepted: 6 August 2020
© The Author(s), under exclusive licence to International Society for Microbial Ecology 2020

Abstract

In the context of infection, *Pseudomonas aeruginosa* and *Staphylococcus aureus* are frequently co-isolated, particularly in cystic fibrosis (CF) patients. Within lungs, the two pathogens exhibit a range of competitive and coexisting interactions. In the present study, we explored the impact of *S. aureus* on the physiology of *P. aeruginosa* in the context of coexistence. Transcriptomic analyses showed that *S. aureus* significantly and specifically affects the expression of numerous genes involved in *P. aeruginosa* carbon and amino acid metabolism. In particular, 65% of the strains presented considerable overexpression of the genes involved in the acetoin catabolic (*aco*) pathway. We demonstrated that acetoin is (i) produced by clinical *S. aureus* strains, (ii) detected in sputa from CF patients and (iii) involved in *P. aeruginosa*'s *aco* system induction. Furthermore, acetoin is catabolized by *P. aeruginosa*, a metabolic process that improves the survival of both pathogens by providing a new carbon source for *P. aeruginosa* and avoiding the toxic accumulation of acetoin on *S. aureus*. Due to its beneficial effects on both bacteria, acetoin catabolism could testify to the establishment of trophic cooperation between *S. aureus* and *P. aeruginosa* in the CF lung environment, thus promoting their persistence.

Introduction

Infectious sites constitute rich microbial ecosystems shared by a large diversity of microorganisms, including the native microbiota and pathogens. Lungs of cystic fibrosis (CF)

patients are a well-known example of this microbial richness as they gather more than 60 genera of bacteria [1, 2]. This density of microorganisms promotes their interactions, through which they model their biological activities and their environment [3, 4]. However, microbial interactions are dynamic and range from antagonism to cooperation according to species and environmental conditions [5]. For instance, the opportunistic pathogen *Pseudomonas aeruginosa* is well known for its competitiveness in various ecosystems due to many quorum-sensing-mediated factors, such as phenazines, rhamnolipids and the type 6 secretion system [6]. *P. aeruginosa* thus can alter the growth, biofilm formation and respiration of yeasts, fungi and Gram-negative and Gram-positive bacteria [6]. Among them, *Staphylococcus aureus* is particularly sensitive to *P. aeruginosa* virulence factors as they can directly lyse staphylococci [7]. This competitive interaction between *P. aeruginosa* and *S. aureus* is observed for both environmental and clinical strains as both pathogens are frequently co-isolated from wounds and CF lung samples [7, 8]. Until recently, the anti-staphylococcal behaviour of *P. aeruginosa* was the only expression observed between the two species and was thus extensively described [7]. In the context of CF lung infections, this competitive interaction is highlighted

Supplementary information The online version of this article (<https://doi.org/10.1038/s41396-020-00741-9>) contains supplementary material, which is available to authorized users.

✉ Karen Moreau
karen.moreau@univ-lyon1.fr

- ¹ CIRI, Centre International de Recherche en Infectiologie, Université de Lyon, Inserm, U1111, Université Claude Bernard Lyon 1, CNRS, UMR5308, ENS de Lyon, Lyon, France
- ² Université Grenoble Alpes, CNRS ERL5261, CEA-IRIG-BCI, INSERM UMR1036, 38000 Grenoble, France
- ³ Institut des agents infectieux, Hospices Civils de Lyon, Lyon, France
- ⁴ Bactéries Pathogènes Opportunistes et Environnement, UMR CNRS 5557 Ecologie Microbienne, Université Lyon 1 and VetAgro Sup, Villeurbanne, France
- ⁵ Centre National de Référence des Staphylocoques, Hospices Civils de Lyon, Lyon, France

by the decreased prevalence of *S. aureus* as *P. aeruginosa* colonizes lungs during adolescence [9]. However, Baldan et al. [10] first noted that a non-competitive state between *P. aeruginosa* and *S. aureus* could establish during the development of CF chronic infections, calling into question the antagonistic model between the two pathogens.

The establishment of this particular non-competitive state between *P. aeruginosa* and *S. aureus* seems to be linked to the adaptation of *P. aeruginosa* to the pulmonary ecosystem. In fact, selective pressures present in the CF lung environment, such as the host immune system and antibiotic treatments, drive *P. aeruginosa* isolates towards a state of low virulence and high resistance [11–14]. Major virulence factors involved in quorum sensing and motility are often mutated in *P. aeruginosa* chronic infection isolates, inducing a decrease in the production of anti-staphylococcal factors followed by non-competitive interaction [15]. In addition, the rewiring of metabolism networks and the decrease of its catabolic repertoire also accompany *P. aeruginosa*'s adaptation to the CF environment. This trophic specialization commonly leads to the slower growth of chronic isolates and thus less competitive behaviour regarding shared resources [16]. Several independent studies observed this state of coexistence between *S. aureus* and *P. aeruginosa* isolated from chronic infections [10, 15, 17, 18]. Briaud et al. [18, 19] recently demonstrated that this interaction pattern appears to be more frequent than expected. Indeed, among the quarter of CF patients co-infected by both pathogens, 65% were infected by a coexisting *S. aureus*–*P. aeruginosa* pair. Recent studies have shown that coexistence between *P. aeruginosa* and *S. aureus* could promote their persistence throughout the establishment of cooperative interaction. In these conditions, coexisting bacteria demonstrated increased tolerance to antibiotics: to tobramycin and tetracycline for *S. aureus* and to gentamicin for *P. aeruginosa*. This appeared to be related to the induction of small colony variants [15, 17, 18, 20]. However, the effects of coexistence on general bacterial physiology, and not only virulence-associated traits, have not yet been explored. Therefore, despite its significance in infectious ecosystems, coexistence between *P. aeruginosa* and *S. aureus* remains poorly understood.

Using global and targeted transcriptomic approaches, we evaluated the impact of the presence of *S. aureus* on the gene expression of *P. aeruginosa* using a set of clinical pairs of strains isolated from CF co-infected patients. Coexistence with *S. aureus* induced the overexpression of many genes involved in the utilization of alternative carbon sources in *P. aeruginosa*, such as amino acids and acetoin. Acetoin was shown to be produced by clinical *S. aureus* isolates in vitro and in CF sputum, and catabolized by *P. aeruginosa*. The beneficial effects of acetoin catabolism

on both bacteria during their interaction highlighted trophic cooperation between *P. aeruginosa* and *S. aureus* in CF lung infections.

Materials and methods

Bacterial strains

The bacterial strains and plasmids used in this study are listed in Supplementary Tables S1 and S2. CF clinical strains were isolated by the Infectious Agents Institute from sputa of patients monitored in the two CF centres of Lyon (Hospices Civils de Lyon (HCL)). *S. aureus* and *P. aeruginosa* strains were isolated from patients co-infected by both bacteria. Each strain pair indicated in Supplementary Table S1 was recovered from a single sample, obtained from different patients in most cases, as indicated in Supplementary Table S1. All the methods were carried out in accordance with relevant French guidelines and regulations. This study was submitted to the Ethics Committee of the HCL and registered under CNIL No. 17-216. All the patients were informed of the study and consented to the use of their data.

As schematized in Supplementary Fig. S1A, interaction state was determined for each pair by growth inhibition tests on tryptic soy agar (TSA) and in liquid cultures [18]. As previously described, coexistence was characterized by: (i) the absence of inhibition halo on agar tests, and (ii) similar growth in monocultures and co-cultures for 8 h [18].

The knockout Δ *acoR* and Δ *aco* mutants were generated in the *P. aeruginosa* PA2600 strain via allelic exchange owing to suicide plasmids pEXG2 Δ *acoR* and pEXG2 Δ *aco* constructed as described previously [21, 22]. Gentamicin (Euromedex) was used at final concentrations of 50 μ g/ml. Detailed protocols are given in Supplementary Data.

Cultures conditions

Strains were grown in monoculture or co-culture in brain–heart infusion (BHI), as described by Briaud et al. [18]. Briefly, *S. aureus*, *P. aeruginosa*, *Burkholderia cenocepacia*, *Stenotrophomonas maltophilia* and *Bacillus subtilis* overnight pre-cultures were diluted to an OD₆₀₀ of 0.1 in BHI and grown for 2 h30 at 37 °C and 200 r.p.m. Cultures were then diluted to an OD₆₀₀ of 2 in fresh medium and 10 ml was mixed with 10 ml BHI for monocultures. Co-cultures were performed by mixing 10 ml of *P. aeruginosa* suspension with 10 ml of *S. aureus*, *B. cenocepacia*, *S. maltophilia* or *B. subtilis* suspension. For supernatant exposure, 10 ml of *S. aureus* supernatant from a 4-h culture was filtered on a 0.22- μ m filter and added to 10 ml of *P. aeruginosa* suspension. Cultures were grown for 8 h at

200 r.p.m. and at 37 °C for transcriptomic studies. Long-term survival assays were performed by extending the incubation time of *S. aureus* and *P. aeruginosa* monocultures and co-cultures up to 5 days. Plating at days 0, 3 and 5 was performed on mannitol salt agar (MSA, BBL™ Difco) and ceftrimide (Difco™) for *S. aureus* or *P. aeruginosa* counts, respectively. For growth monitoring in the presence of acetoin, minimal medium M63 (76 mM (NH₄)₂SO₄, 500 mM KH₂PO₄, 9 μM FeSO₄·7H₂O, 1 mM MgSO₄·7H₂O) was inoculated with *P. aeruginosa* to an OD₆₀₀ of 0.1 and incubated for 25 h at 37 °C and 200 r.p.m. Every 2 h during 10 h and at $t = 24$ h, acetoin was added to obtain a final concentration of 1.5 mM in the culture. Plating on TSA was performed at $t = 0$, 1 h after each acetoin addition and at $t = 24$ h.

Genome sequencing and annotation

Genome sequencing and annotation of PA2596 and PA2600 strains were performed as previously described [18]. In order to compare CDS from PA2596 and PA2600, PAO1 strain (NC_002745.2) was used as a reference. Protein sequences were compared and grouped using a similarity threshold of 95% through Roary (V3.8.2) [23]. Gene names and numbers were gathered from PAO1 and used as ID tags for common genes. For non-common genes, CDS from PA2596 and PA2600 were tagged with a specific name (gene number and name recovered from the UniProtKB database). Functional classification was performed using the KEGG (Kyoto Encyclopaedia of Genes and Genomes) database and by a manual literature check of each gene function. The complete genome sequences for the PA2596 and PA2600 strains were deposited in GenBank under the accession number GCA_009650455.1 and GCA_009650545.1.

Transcriptomic analysis

Supplementary Fig. S1 schematizes the global methodology used for the transcriptomic analysis. RNA-sequencing (RNAseq) analysis was performed on four pairs: the patient-specific pairs SA2597/PA2596 (competitive) and SA2599/PA2600 (coexisting), and the crossed pairs SA2599/PA2596 (competitive) and SA2597/PA2600 (coexisting). RNA extraction, cDNA library preparation and sequencing and read treatment were conducted as previously described [18]. Gene expression was considered as dysregulated when: (i) the fold change between co-culture and monoculture was at least 4-fold with an adjusted P value < 0.05 , (ii) dysregulation was observed in the two pairs of strains with the same interaction state and (iii) the dysregulation was specific to either coexistence or competition state. RNAseq data that support our findings are

available in the SRAdatabase under the BioprojectID: PRJNA562449, PRJNA562453, PRJNA554085, PRJNA552786, PRJNA554237 and PRJNA554233.

Confirmation of gene expression was achieved by quantitative reverse transcription PCR (RT-qPCR) as previously described on 14 or 21 coexisting pairs including the SA2599/PA2600 couple used in the RNAseq experiment (Supplementary Fig. S1) [18]. Housekeeping genes *gyrB* and *rpoD* were used as an endogenous control. Supplementary Table S3 lists the primers used and the target genes.

Acetoin and glucose dosages

Acetoin was quantified using a modified Voges–Proskauer test [24] optimized in 96-well microplates. Thirty-five microlitres of creatine (0.5% m/v, Sigma), 50 μl of α -naphthol (5% m/v, Sigma) and 50 μl of KOH (40% m/v, Sigma) were added sequentially to 50 μl of culture supernatant. The mix was incubated for 15 min at room temperature and optical density at 560 nm was read using spectrophotometry (Tecan Infinite Pro2000, Tecan-Switzerland). Glucose dosages were performed with a glucose (Trinder, GOPOD) assay kit (LIBIOS) in microplates. A measure of 185 μl of dosage reagent was added to 5 μl of culture supernatant and incubated at 37 °C for 5 min. Optical density at 540 nm was measured. Acetoin and glucose standards (Sigma) were performed in water, BHI or M63 according to the experiment.

Statistical analysis

Statistical analyses were performed using the Prism GraphPad 8.0 software (San Diego, CA). Differences in gene expression fold change and bacterial survival were studied using one-way analysis of variance (ANOVA) with Dunnett's or Tukey's post-test comparisons, as specified in the corresponding figures. Median acetoin and glucose concentrations were compared using Mann–Whitney tests or Kruskal–Wallis tests with Dunn's correction when appropriate. Differences were considered significant when P values were < 0.05 .

Results

The *P. aeruginosa* transcriptome is affected by the presence of *S. aureus*

We studied the genetic expression of *P. aeruginosa* in the absence or presence of *S. aureus* in two contexts: when *P. aeruginosa* and *S. aureus* were in competition or when they were in coexistence. We thus performed RNAseq

analyses using a competitive strain pair (SA2597/PA2596) and a coexisting one (SA2599/PA2600). Each pair was recovered from a single sample of a co-infected CF patient (Supplementary Table S1). As the nature of interaction was determined solely by *P. aeruginosa* [18], the pairs were crossed to study gene expression in additional competitive (SA2599/PA2596) and coexisting (SA2597/PA2600) pairs. The transcriptomic effect was therefore evaluated during co-cultures of two competitive and two coexisting strain pairs (Supplementary Fig. S1). *P. aeruginosa* gene expression was considered dysregulated when dysregulation was common to both co-cultures in comparison to monoculture. Each dysregulated gene was then associated with a functional class by carrying out a KEGG analysis (Fig. 1a and Supplementary Tables S4 and S5).

Sixty-eight *P. aeruginosa* genes were dysregulated in co-culture in the context of competition, with a majority of down-regulated genes (79.4%; Fig. 1a). Fifteen genes involved in nitrogen metabolism and 19 genes involved in iron metabolism were down-regulated, making these two functional classes the most affected in competition. Among these genes, the *nir* and *nos* systems involved in denitrification as well as genes implicated in iron uptake and transport (*isc* and *fec* genes) were down-regulated (Supplementary Table S4). Other functional classes were less affected, as only four genes linked to carbon and amino acid metabolism (*bauA*, *ddaR*, *gntK* and *arcD*) and three genes encoding membrane and virulence factors (*rfaD*, *PA2412* and *cdrA*) were dysregulated in the presence of *S. aureus*.

More genes were affected during coexistence interaction, as the dysregulation of 105 genes was observed in *P. aeruginosa* (Fig. 1a). In spite of a trend of up-regulation (56.4% of genes), we could observe the down-regulation of 11 genes involved in nitrogen metabolism. Among these, eight were also down-regulated in the context of competition, especially genes from the *nir* system. We can thus presume that the down-regulation of *nir* genes is not specific to coexistence or competition interaction states. Conversely, the dysregulations of iron metabolism-related genes appeared to be specific to competition strains, as only one gene (*flp*) of this functional class was down-regulated in coexistence. However, coexistence specifically affected numerous genes belonging to functional classes of carbon and amino acid metabolism (18 and 23 genes) and membrane and virulence factors (15 genes). Concerning the latter class, a trend towards lower expression was observed, probably due to the down-regulation of membrane-associated factors, such as the *flp-tad* system (*flp*, *tad* and *rcpC* genes encoding Flp pilus) and the *PA1874-1876* operon (encoding an efflux pump) (Supplementary Table S5).

The classes most affected in coexistence with *S. aureus* were related to *P. aeruginosa* energetic metabolism

(Supplementary Fig. S2). We observed a down-regulation of genes coding for major pentose phosphate pathway enzymes, like the gluconokinase *GntK*, its regulator *GntR* and the operon *zwf-edaA* (*PA3183-PA3181*), encoding a glucose-6-phosphate 1-dehydrogenase, a 6-phosphogluconolactonase and a 2-keto-3-deoxy-6-phosphogluconate aldolase [25]. We also noticed the down-regulation of five other genes clustered near this operon and involved in the same pathway (*edd* and *gapA* genes) and glucose transport (*gltB*, *gltF* and *gltK*) [25, 26].

In contrast, an up-regulation of numerous genes involved in the utilization of alternative carbon sources as butanoate and amino acids was observed. The *aco* system, comprising the operon *PA4148-PA4153* and the gene encoding its transcriptional regulator *acoR* (*PA4147*), was up-regulated in *P. aeruginosa* coexisting with *S. aureus*. This system has been described in *P. aeruginosa* PAO1 to be responsible for 2,3-butanediol and acetoin catabolism [27]. According to KEGG analysis, the up-regulated genes *acsA* (*PA0887*), *PA2555* (*acs* family) and *hdhA* (*PA4022*) are also involved in the butanoate pathway and energy production from 2,3-butanediol and acetoin, as their products catalyse the production of acetyl-coA from acetaldehyde and acetate (Supplementary Fig. S2). Finally, 23 genes implicated in amino acid metabolism were up-regulated in *P. aeruginosa* in the presence of *S. aureus*. Most of them were linked to the catabolism of several amino acids (Supplementary Fig. S2). In particular, we observed the *liu* operon (*PA2015-PA2012*), the *mmsAB* operon (*PA3569-PA3570*) and the *hut* gene system (*PA5097-PA5100*) involved in leucine, valine and histidine catabolism, respectively.

In order to confirm these transcriptomic effects, we co-cultivated a set of *P. aeruginosa*–*S. aureus* coexistence CF pairs and performed RT-qPCR to evaluate *P. aeruginosa* gene expression in the presence of *S. aureus* (Fig. 1b). Each pair was isolated from a single sputum. Twenty-six genes were tested, including 19 identified as dysregulated during RNAseq analysis and belonging to the most impacted categories, that is, carbon and amino acid metabolism, and membrane and virulence factors. Most of the genes were tested in a total of 14 *P. aeruginosa*–*S. aureus* pairs; the expression of four of these genes was assessed in seven additional pairs to confirm the dysregulations observed. The different *P. aeruginosa* strains presented very different transcriptomic patterns during co-cultivation with *S. aureus*, especially for membrane-associated and virulence factor genes. We noticed an overexpression of *rcpC*, *tadA*, *tadG* and *flp* from the *flp-tad* system from 52.4 to 35.7% of the *P. aeruginosa* strains. We also tested seven additional genes encoding virulence factors previously described as involved in *P. aeruginosa* interaction with *S. aureus* as *las*, *rhl*, *pch* and *pvd* genes [7]. Regarding the latter genes, no clear effect of *S. aureus* co-cultivation was observed.

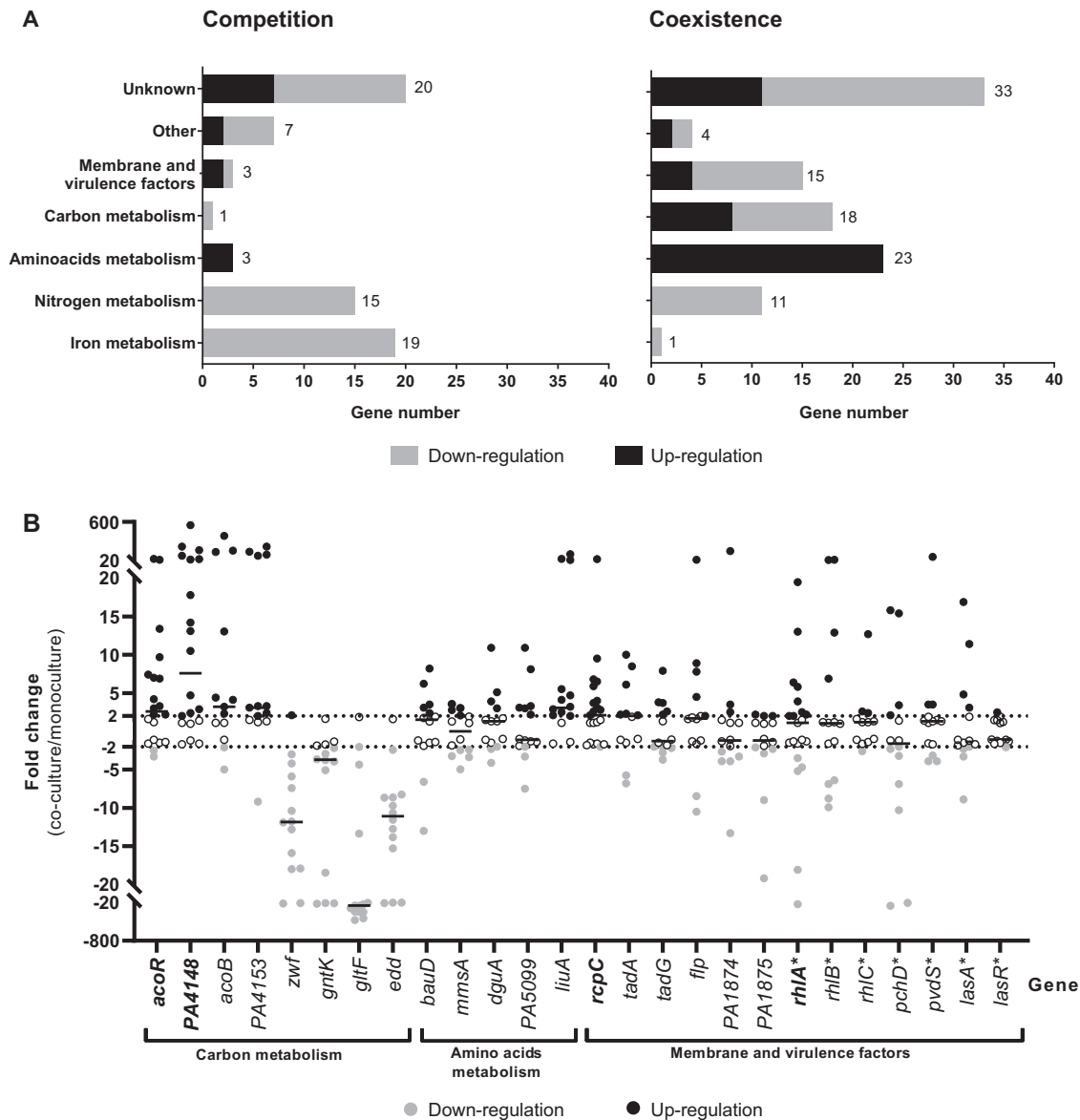


Fig. 1 Alteration of the *P. aeruginosa* transcriptome induced by co-culture with *S. aureus*. **a** Number of under-expressed (grey bars) and overexpressed (black bars) genes of *P. aeruginosa* during co-culture with *S. aureus* for competitive (left) or coexisting (right) pairs. PA2596 competition and PA2600 coexistence strains were cultivated in the absence or presence of SA2597 or SA2599, as described in Supplementary Fig. S1. RNAs were extracted after 4 h of culture and the RNAseq analysis was performed as described in the “Material and methods” section. A gene was considered as differentially expressed when the fold change was $>|2\log_2|$ with an adjusted *P* value <0.05 . Functional classification was performed using the KEGG database and the literature. **b** Fold change of 26 *P. aeruginosa* gene expression

induced by co-culture with *S. aureus* during coexistence interaction. Twenty-one coexisting *S. aureus*–*P. aeruginosa* pairs were isolated from separate CF sputa recovered from 20 different patients. Each *P. aeruginosa* strain was cultivated in the absence or presence of its co-isolated *S. aureus* strain. RNAs were extracted after 4 h of culture and gene expression was assayed by RT-qPCR. A gene was considered as differentially expressed when the fold change was $>|2|$, indicated by dotted lines. Black lines indicate the median. Genes were tested in 14 (regular character) or 21 (bold character) strains. The list of the strains used is shown in Supplementary Table S1. Genes annotated with (*) were not identified as dysregulated during the RNAseq experiment.

However, clearer transcriptomic patterns were observed for genes linked to carbon and amino acid metabolism, the two gene classes most impacted during the RNAseq experiment (Fig. 1b). We confirmed the up-regulation of *liuA* gene in 78.6% (11/14) of *P. aeruginosa* strains co-cultivated with *S. aureus*. We also confirmed the

down-regulation of glucose metabolism genes in a high proportion of strains, ranging from 92.9% (13/14) for *zwf*, *glfF* and *edd* genes to 71.4% (10/14) for *gntK* gene. Finally, the up-regulation of genes involved in butanoate metabolism was confirmed for *acoR* (57.2%, 12/21), *PA4148* (66.7%, 14/21), *acoB* (57.1%, 8/14) and *PA4153* (64.3%, 9/14),

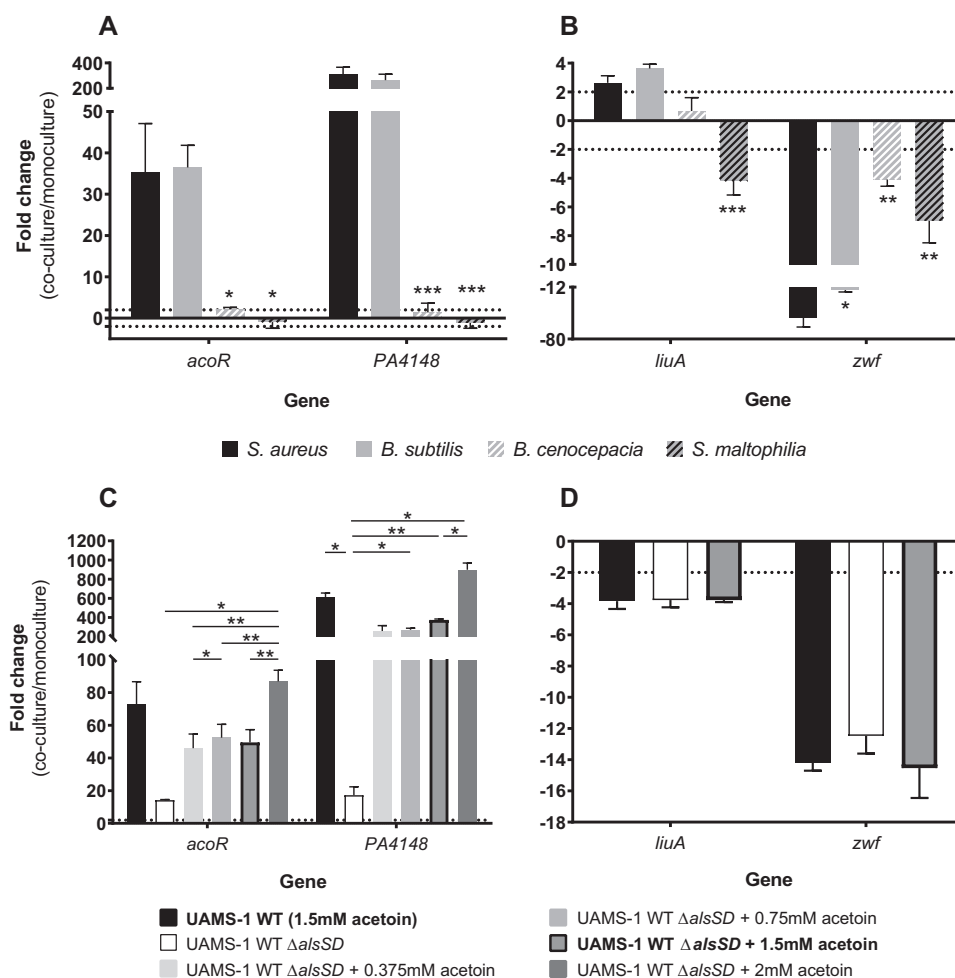


Fig. 2 Fold changes of *P. aeruginosa* *acoR*, *PA4148*, *liuA* and *zwf* induced by culture conditions. **a, b** Fold changes of *acoR* and *PA4148* (A) and *liuA* and *zwf* (b) induced by co-culture with *S. aureus* (black bars), *B. subtilis* (grey bars), *B. cenocepacia* (hatched white bars) or *S. maltophilia* (hatched black bars). *P. aeruginosa* PA2600 strain was cultivated in the absence or presence of *S. aureus* SA2599, *B. subtilis*, *B. cenocepacia* or *S. maltophilia*. RNAs were extracted after 4 h of culture and gene expression was assayed by RT-qPCR. Bars represent the mean fold change + SEM from three independent experiments. Dotted lines indicate a fold change = |2|. * $P_{\text{adj}} < 0.05$, ** $P_{\text{adj}} < 0.01$ and *** $P_{\text{adj}} < 0.001$ ANOVA with Dunnett's correction (*S. aureus* vs. condition). **c, d** Fold changes of *acoR* and

PA4148 (c) and *liuA* and *zwf* (d) induced by culture in supernatant of *S. aureus* UAMS-1 wild type (WT, black bars), Δ alsSD mutant (white bars) and Δ alsSD mutant complemented with increasing acetoin concentrations (grey bars). *P. aeruginosa* PA2600 strain was cultivated in the absence or presence of filtered supernatant from *S. aureus* UAMS-1 WT, Δ alsSD or Δ alsSD complemented with acetoin concentrations ranging from 0.375 to 2 mM. RNAs were extracted after 4 h of culture and gene expression was assayed by RT-qPCR. Bars represent the mean fold change + SEM from three independent experiments. The dotted line indicates a fold change = |2|. * $P_{\text{adj}} < 0.05$ and ** $P_{\text{adj}} < 0.01$ ANOVA with Tukey's correction.

suggesting an impact of co-culture on the whole *aco* system in *P. aeruginosa*. In view of these results, we focused our study on four genes: *liuA* and *zwf*, respectively involved in leucine and glucose catabolism, *PA4148*, the first gene of the *aco* operon and *acoR*, both responsible for acetoin catabolism.

The *P. aeruginosa* *aco* system is induced by *S. aureus* acetoin

In order to determine if the transcriptomic dysregulations of *acoR*, *PA4148*, *liuA* and *zwf* in *P. aeruginosa* PA2600 are

specific to interaction with *S. aureus*, we tested the effect of three other bacterial species: *B. cenocepacia* and *S. maltophilia*, as they are sometimes associated with *P. aeruginosa* in CF patients, and *B. subtilis*, as it produces a large amount of acetoin [28]. Dosages in *B. cenocepacia* and *S. maltophilia* monocultures confirmed that these bacteria do not produce acetoin (Supplementary Fig. S3) as previously described [29–31]. We observed a down-regulation of *P. aeruginosa* *zwf* gene expression in all co-cultures in comparison to monocultures, although the down-regulation induced by *S. aureus* was significantly greater ($P_{\text{adj}} < 0.02$) (Fig. 2b). Regarding *aco* system genes (*acoR* and *PA4148*) and *liuA*

gene, only *B. subtilis* induced levels of overexpression similar to *S. aureus* SA2599 (Fig. 2a, b). We thus hypothesized that acetoin, produced by these two species during our experiment (Supplementary Fig. S3), may be the inductor signal for these genes during co-culture with *S. aureus*.

In order to test this hypothesis, we first explored whether an inductor signal was present in the supernatant of *S. aureus* culture. We indeed observed an overexpression of *acoR* and *PA4148* when *P. aeruginosa* PA2600 was cultivated in *S. aureus* SA2599 culture supernatant, as well as the down-expression of *zwf*, but to a lesser extent in comparison to co-culture (Supplementary Fig. S4). On the contrary, we did not observe overexpression of the *liuA* gene, suggesting that this effect is not due to acetoin and requires the presence of *S. aureus* cells. Second, we cultivated *P. aeruginosa* PA2600 in the presence of *S. aureus* UAMS-1 wild-type (WT) supernatant or its Δ *alsSD* derivative defective in acetoin synthesis [32]. The supernatant of the WT UAMS-1 strain induced the same transcriptomic patterns on *P. aeruginosa* as those obtained with the CF SA2599 strain (Supplementary Fig. S4). In the presence of UAMS-1 Δ *alsSD* supernatant, the overexpression of *aco* genes was almost totally eliminated ($P = 0.0150$ for *PA4148*) (Fig. 2c). However, the addition of acetoin to this supernatant restored this overexpression in a dose-dependent manner ($P = 0.0020$ for 0 vs. 1.5 mM for *PA4148*), but with threshold effects between 0.375 and 1.5 mM of acetoin (Fig. 2c). This indicates that induction through acetoin is one of the mechanisms involved in *aco* system overexpression in *P. aeruginosa*. This experiment showed that *zwf* gene down-regulation did not seem to be mediated by acetoin (Fig. 2d).

Coexisting isolates of *S. aureus* and *P. aeruginosa* efficiently metabolize acetoin

As the *aco* system is involved in acetoin catabolism in *P. aeruginosa* [27] and *S. aureus* produces this molecule [27, 28], we hypothesized that *P. aeruginosa* could catabolize *S. aureus* acetoin. To explore this hypothesis, we monitored acetoin concentration during monocultures and co-cultures of three pairs of strains: SA2599/PA2600 (Fig. 3a), SA146/PA146 and SA153/PA153A (Supplementary Fig. S5A, B). *P. aeruginosa* strains did not produce acetoin, but acetoin accumulation up to 1.3 mM was observed in *S. aureus* monocultures. Interestingly, a reduction of acetoin accumulation of at least 30% was observed when *S. aureus* was co-cultivated with *P. aeruginosa*, in comparison to *S. aureus* monoculture ($P_{\text{adj}} = 0.0172$ for the pair SA2599/PA2600). The same trend could be observed in CF patient sputa, as a higher acetoin concentration was detected in sputa from *S. aureus* mono-infected patients ($n = 9$) in comparison to sputa from

S. aureus–*P. aeruginosa* co-infected patients ($n = 11$), although it was not significant (Supplementary Fig. S6). This effect could be due to a down-regulation of *S. aureus* acetoin biosynthesis, or acetoin catabolism in co-culture. Growth of *P. aeruginosa* PA2600 in *S. aureus* SA2599 supernatant containing acetoin actually led to a reduction of acetoin concentration ($P = 0.0247$), demonstrating the ability of *P. aeruginosa* to catabolize acetoin (Fig. 3c). This ability was confirmed for the two other strains PA146 and PA153A when grown in the supernatant of SA146 and SA153, respectively (Supplementary Fig. S5C, D). We also noted that acetoin catabolism started after glucose depletion in the supernatant and could be delayed by glucose addition (Fig. 3c). This suggests that *P. aeruginosa* uses acetoin as an alternative carbon source in the absence of easily available substrates such as glucose. The early glucose depletion observed during co-culture supports this hypothesis (Fig. 3a).

In order to test if this acetoin metabolism was specific to the interaction state between *S. aureus* and *P. aeruginosa*, we evaluated acetoin production and catabolism for 12 couples of competition and 12 couples of coexistence (Supplementary Table S1). Cultivated in *P. aeruginosa* supernatant, *S. aureus* strains from coexisting pairs were able to produce four times more acetoin (230 μ M) than strains from competitive pairs (60 μ M) ($P < 0.0001$) (Fig. 4a). This distinction was not observed during culture in rich medium (Supplementary Fig. S7). Regarding *P. aeruginosa*, we cultivated the sets of competitive and coexisting *P. aeruginosa* strains in SA2599 supernatant and monitored acetoin catabolism (Fig. 4b). Both competitive and coexisting strains catabolized acetoin since we observed a decrease in acetoin concentration for both groups ($P_{\text{adj}} = 0.0004$ for coexistence). However, coexisting strains showed increased catabolism efficiency. Indeed, this group catabolized 98.6% of acetoin after 4 h of culture, while competitive strains catabolized only 47% of acetoin ($P_{\text{adj}} = 0.0315$). This increased efficiency of acetoin production and catabolism for coexisting strains could not be explained by a difference in glucose utilization between competition and coexistence strains, as both groups catabolized glucose with the same efficiency (Supplementary Fig. S8). Acetoin production by *S. aureus* and catabolism by *P. aeruginosa* therefore seems to be more efficient in isolates from coexisting couples.

Acetoin catabolism by *P. aeruginosa* increases survival rates of both pathogens in co-culture

As *P. aeruginosa* catabolizes acetoin when medium is glucose-depleted, we tested the effect of acetoin on PA2600 growth in minimal medium M63 (containing no glucose or amino acids) supplemented with 1.5 mM acetoin every 2 h

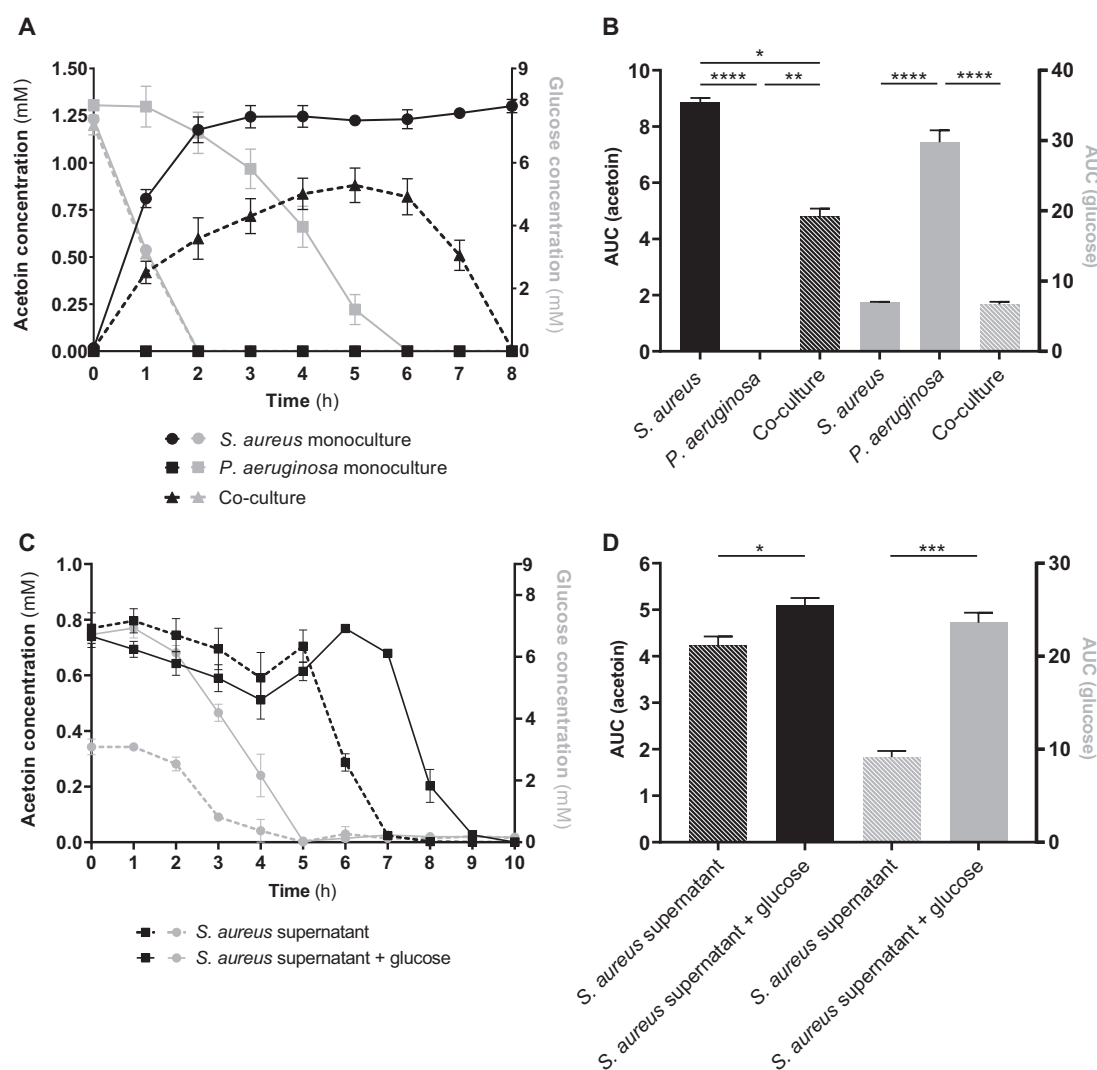


Fig. 3 Acetoin and glucose concentrations in *S. aureus* and *P. aeruginosa* cultures during coexisting interaction. **a, b** *S. aureus* SA2599 and *P. aeruginosa* PA2600 were cultivated in monoculture or co-culture. Acetoin (black) and glucose (grey) were quantified from the supernatant each hour. **A** Points represent the mean acetoin or glucose concentration \pm SEM from three independent experiments. **b** Bars represent the mean area under the curves presented in **a** + SEM. * $P_{\text{adj}} < 0.05$, ** $P_{\text{adj}} < 0.01$ and **** $P_{\text{adj}} < 0.0001$ ANOVA with Tukey's correction. Similar acetoin accumulation results are shown in Supplementary Fig. S5 for couples 146 and 153A. **c, d**

A filtered supernatant of *S. aureus* SA2599 was inoculated with *P. aeruginosa* PA2600 culture or sterile medium for controls. The supernatant was used unaltered (dotted lines) or complemented with glucose (solid lines). Acetoin (black) and glucose (grey) were quantified from the supernatant each hour. **c** Points represent the mean acetoin or glucose concentration \pm SEM from three independent experiments. **d** Bars represent the mean area under the curves presented in **c** + SEM. * $P < 0.05$ and *** $P < 0.001$ Student's *t* test. Similar results of acetoin catabolism are shown in Supplementary Fig. S5 for couples 146 and 153A.

(Fig. 5). *P. aeruginosa* was able to grow up to 1.6×10^9 colony-forming unit (CFU)/ml after 24 h of culture with acetoin as sole carbon source, while PA2600 ΔacoR and Δaco mutants grew significantly less, reaching a maximum cell concentration of 1.5×10^8 CFU/ml at 24 h (Fig. 5a). In parallel, we quantified acetoin concentration. We observed an accumulation of acetoin throughout the experiment in the presence of PA2600 ΔacoR and Δaco mutants. For the WT strain, the accumulation of acetoin reached its maximum at 5 h of culture and afterwards slowly decreased to reach undetectable values at 10 h of culture, demonstrating the

consumption of acetoin in such conditions (Fig. 5b). A delay of 3 h between the start of acetoin catabolism and the increased growth of the WT strain was noticed, possibly due to the adaptation of metabolism. Acetoin catabolism nonetheless promoted a 10-fold increase in growth of *P. aeruginosa* during extended culture in glucose-depleted medium.

In order to assess the impact of acetoin catabolism on the survival of both pathogens, we co-cultivated *P. aeruginosa* PA2600, ΔacoR and Δaco mutants with *S. aureus* SA2599. As *S. aureus* was not able to grow in M63-poor medium, and

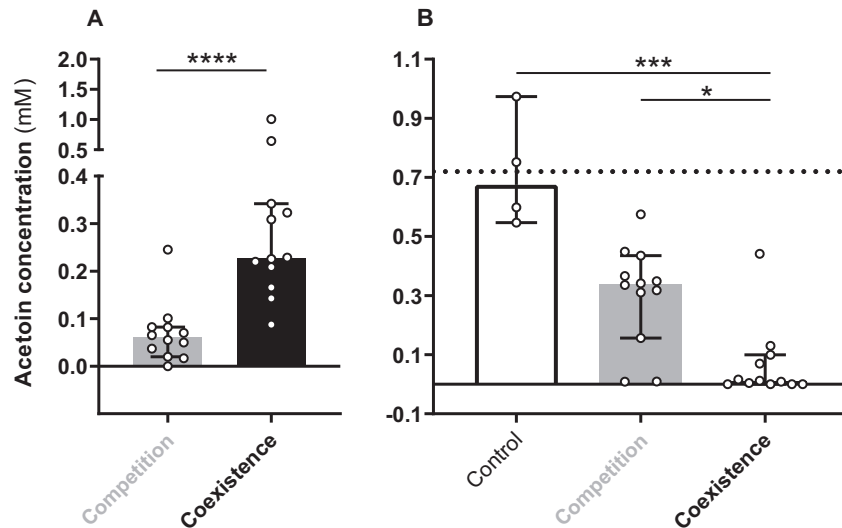


Fig. 4 Production and catabolism of acetoin by competitive and coexisting strains of *S. aureus* and *P. aeruginosa*. **a** Acetoin concentration in *P. aeruginosa* supernatant inoculated with *S. aureus* strains from competition and coexistence couples. Each *S. aureus* strain from competition ($n = 12$, grey bar) and coexistence ($n = 12$, black bar) couples was cultivated in *P. aeruginosa* PA2600 filtered supernatant and acetoin was quantified from the supernatant after 6 h of culture. Bars represent the median acetoin concentration \pm 95% CI. **** $P < 0.0001$ Mann–Whitney test. **b** Acetoin concentration in

S. aureus supernatant inoculated with *P. aeruginosa* strains from competition and coexistence couples. Each *P. aeruginosa* strain from competition ($n = 12$, grey bar) and coexistence ($n = 12$, black bar) couples was cultivated in *S. aureus* SA2599 filtered supernatant and acetoin was quantified from the supernatant after 4 h of culture. Sterile supernatant was used as control (white bar) for acetoin degradation. Bars represent the median acetoin concentration \pm 95% CI. The dotted line indicates the initial acetoin concentration. * $P_{\text{adj}} < 0.05$, **** $P_{\text{adj}} < 0.001$ Kruskal–Wallis test with Dunn’s correction.

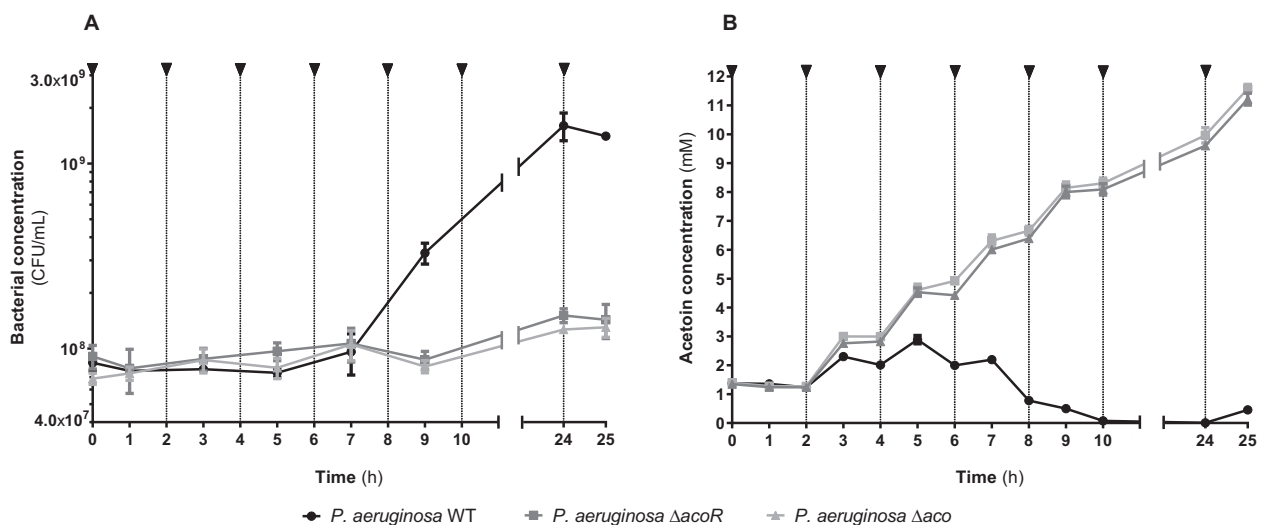


Fig. 5 *P. aeruginosa* growth and acetoin concentration in minimal medium supplemented with acetoin. *P. aeruginosa* PA2600 WT (black lines), ΔacoR (dark grey lines) and Δaco (light grey lines) strains were grown in M63 medium and 1.5 mM acetoin was added every 2 h, indicated by black arrows. **a** Cultures were plated on

TSA each 2 h to count bacteria. Points represent the mean bacterial concentration \pm SEM from three independent experiments. **b** Acetoin was quantified from the supernatant each hour. Points represent the mean acetoin concentration \pm SEM from three independent experiments.

since acetoin affects its long-term survival [33, 34], we performed a long-term culture (5 days) in BHI medium. We determined the survival rate of *S. aureus* co-cultivated with *P. aeruginosa* in comparison to monoculture (Fig. 6a). Co-culture with the WT strain of *P. aeruginosa* induced a

S. aureus survival rate of 4.7×10^{-1} after 3 days of culture and of 5.1×10^{-3} after 5 days. *S. aureus* survival thus appears to be highly affected by long-term co-culture with *P. aeruginosa*, even if the strains coexist stably during shorter spans of culture [18]. The state of interaction with *S. aureus* thus

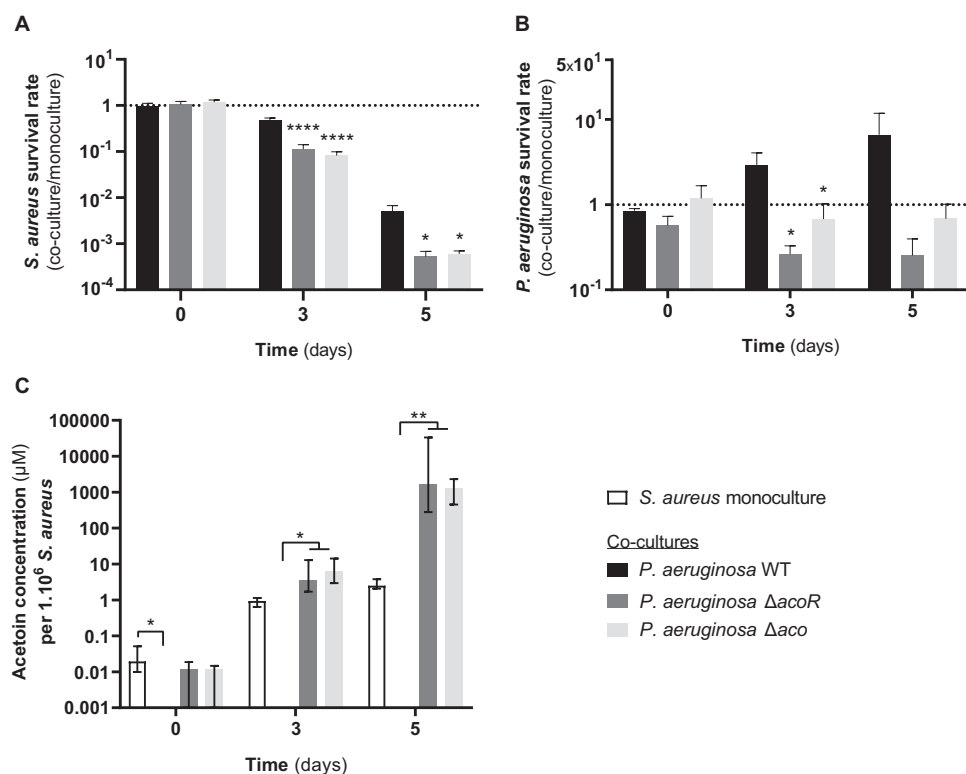


Fig. 6 *S. aureus* and *P. aeruginosa* survival and acetoin concentration during long-term co-culture. *S. aureus* SA2599 was cultivated in monoculture (white bars) or in the presence of *P. aeruginosa* PA2600 WT (black bars), Δ *acoR* (dark grey bars) and Δ *aco* (light grey bars) during 5 days. Cultures were plated at days 0, 3 and 5 on MSA and cetrimide to count *S. aureus* and *P. aeruginosa*, respectively, and acetoin was quantified from supernatant. **a**, **b** Survival rate was estimated by dividing the bacterial concentration in

co-culture by bacterial concentration in monoculture for each bacterium. Bars represent the mean survival rate + SEM from five independent experiments. $*P_{\text{adj}} < 0.05$, $****P_{\text{adj}} < 0.0001$ one-way ANOVA with Dunnett correction (WT vs. condition). **c** Acetoin concentration was normalized to *S. aureus* counts. Bars represent the median acetoin concentration per 10^6 *S. aureus* $\pm 95\%$ CI from five independent experiments. $*P_{\text{adj}} < 0.05$, $**P_{\text{adj}} < 0.01$, Kruskal–Wallis with Dunn’s correction.

seems to rely on nutritional conditions, a fact already observed elsewhere [35, 36]. However, the survival rate of *S. aureus* was even lower during co-culture with *P. aeruginosa* Δ *acoR* and Δ *aco* mutants, reaching only 9.7×10^{-2} at 3 days of culture and 5.6×10^{-4} at 5 days. *S. aureus* survival was thus four to ten times lower when *P. aeruginosa* was not able to catabolize acetoin, in comparison to co-culture with a strain that catabolize the molecule efficiently. These results suggest that the accumulation of acetoin may impact *S. aureus* survival during co-culture with *P. aeruginosa*.

In parallel, we determined the survival rate of *P. aeruginosa* (Fig. 6b). We noticed that in such conditions, the *P. aeruginosa* WT strain presented a growth advantage in co-culture, with a maximum 6.6-fold increase of the *P. aeruginosa* population after 5 days in the presence of *S. aureus* in comparison to monoculture (Fig. 6b). The opposite effect was observed for *aco* mutant strains, as their populations were reduced by 75% for Δ *acoR* and 32% for Δ *aco* after 3 days of co-culture in comparison to monoculture, confirming the role of acetoin catabolism in favouring *P. aeruginosa* growth and survival.

In order to figure out if acetoin accumulation was involved in the decreased survival rate of *S. aureus*, we monitored acetoin concentration in *S. aureus* monoculture and co-cultures (Fig. 6c). As expected, we did not detect acetoin in co-culture with the PA2600 WT strain over the 5 days, but we observed an significant accumulation of acetoin with PA2600 Δ *acoR* and Δ *aco* mutants ($P_{\text{adj}} < 0.002$). The proportion of acetoin in co-culture ($1300\text{--}1700 \mu\text{M}/10^6$ *S. aureus*) was >500 times higher than in monoculture ($2.5 \mu\text{M}/10^6$ *S. aureus*) (Fig. 6c). We thus cultivated *S. aureus* in different acetoin/cells proportions and observed that acetoin had an inhibitory dose-dependent effect on *S. aureus* growth from $20 \mu\text{M}/10^6$ *S. aureus* ($P_{\text{adj}} < 0.0001$) (Supplementary Fig. S9). We concluded that acetoin accumulation may be responsible for decreased *S. aureus* survival during co-culture with PA2600 Δ *acoR* and Δ *aco* mutants.

Taken together, these results demonstrated that acetoin catabolism improves *S. aureus* survival in co-culture, in comparison to co-culture with strains unable to catabolize acetoin, since high concentration of acetoin appears to impair *S. aureus* growth. In parallel, acetoin catabolism

promotes *P. aeruginosa* survival as a nutritional alternative carbon source.

Discussion

Co-infection with *S. aureus* and *P. aeruginosa* is a frequent situation, especially in the lungs of CF patients, where co-infection accounts for 25–50% of cases [17–19]. In this context of co-infection, two states of interaction between the two pathogens have been described: the well-known competitive interaction where *P. aeruginosa* is able to inhibit the growth of *S. aureus* and the coexistence state where the growth of both species is not affected by either individual species. The first state was studied extensively and the leading bacterial determinants of *S. aureus* growth inhibition were described [7]. On the contrary, little is known about the impact of the state of coexistence on bacterial physiology. In the present study, we explored the impact of *S. aureus* on *P. aeruginosa* gene expression and physiology.

Comparing competitive and coexistence states, we observed that the down-regulation of the genes involved in iron metabolism was specific to competition. Most of these, such as *fec* genes and *PA4467-PA4471* operon, are involved in ferrous iron uptake and down-regulated during iron-replete conditions [37–39]. These conditions are certainly generated by the lysis of *S. aureus* that provides an iron source to *P. aeruginosa* during competitive interaction [7, 36], a situation not observed in coexistence. This hypothesis is supported by the work of Tognon et al. [40] that also identified the down-regulation of iron metabolism genes during competitive interaction. Interestingly, they also noted typical responses of amino acid starvation, including the down-regulation of genes involved in branched-chain amino acid degradation in competitive *P. aeruginosa*. While we did not identify such dysregulation in competition, an overexpression of numerous genes involved in amino acid catabolism was noted during coexistence (Supplementary Table S5), emphasizing that these dysregulations depend on interaction.

More interestingly, we observed that both carbon and amino acid metabolism was specifically affected during coexisting interaction. Many genes involved in glucose catabolism were down-regulated in coexisting isolates during co-culture with *S. aureus*, especially when the medium was glucose-depleted (Fig. 3). It is noteworthy that the *zwf* gene, down-regulated in almost all the *P. aeruginosa* strains tested, encodes a glucose-6-phosphate dehydrogenase that converts glucose-6-phosphate to 6-phosphogluconate; the first enzyme in the Entner–Doudoroff pathway, which is central to carbon metabolism in *Pseudomonas* sp.

In this condition of glucose depletion, we demonstrated that *P. aeruginosa* was able to use an alternative carbon

source provided by *S. aureus*: acetoin. Acetoin is a four-carbon molecule produced by the decarboxylation of α -acetolactate. Owing to its neutral nature, the production and excretion of acetoin during exponential growth prevents over acidification of the cytoplasm and the surrounding medium. When other carbon sources are exhausted, it can constitute an external energy source for fermentive bacteria [28].

Acetoin produced by *S. aureus* was shown to be an inductor of the *aco* operon and *acoR* expression in *P. aeruginosa* (Fig. 2c) [27], allowing acetoin catabolism. This occurred in the absence of glucose and was potentially mediated by carbon catabolic repression (Fig. 3), a situation that was already described in other bacteria such as *B. subtilis* [28]. However, threshold effects in acetoin-mediated induction and variability in *aco* system overexpression in *P. aeruginosa* strains (Figs. 1b and 2c) suggest that other regulatory mechanisms may be involved. Our study may also support the relationship between acetoin and branched-chain amino acid pathways. Indeed, the biosynthesis pathways of acetoin and leucine are co-regulated and share the same precursor α -acetolactate in *S. aureus* [28]. In response to co-culture with *S. aureus*, *P. aeruginosa* clinical strains showed overexpression of acetoin and leucine catabolism genes (Figs. 1b and 2), suggesting the presence of both compounds in our co-culture conditions. All of our analyses were performed in vitro. However, using Voges–Proskauer dosage, we were able to confirm the presence of acetoin in CF patient sputa, and in lower concentrations for *P. aeruginosa*-positive samples (Supplementary Fig. S6). No direct correlation between the presence of *P. aeruginosa* presence and the quantity of acetoin can be established as other microorganisms present in sputa may also have an impact on acetoin concentration. Nevertheless, our data support the work of Španěl et al. [41] and suggest that *P. aeruginosa* may catabolize and use *S. aureus* acetoin in the lung environment.

More importantly, we observed that the catabolism of acetoin by *P. aeruginosa* and acetoin production by *S. aureus* were both more efficient for coexisting isolates, in comparison to competitive ones (Fig. 4). This underlines the adapted metabolic regulation in coexisting isolates in comparison to competitive ones. It is well known that the coexistence phenotype between *P. aeruginosa* and *S. aureus* is a consequence of an adaptation process. Indeed, *P. aeruginosa* strains isolated from early infection out-compete *S. aureus*, while strains isolated from chronic infection are less antagonistic and can be co-cultivated with *S. aureus* [7, 10, 17]. It has also been widely described how both pathogens evolve during colonization to evade the immune response and antibiotic treatment [42]. Here, for the first time, we suggest that an evolutionary process leads

to an adaptation of interspecies metabolic pathways between *P. aeruginosa* and *S. aureus*.

Therefore, we suggest that acetoin produced by *S. aureus* could contribute to sputum nutritional richness and be used by *P. aeruginosa* to survive in this nutritionally competitive environment during chronic infection. This hypothesis is supported by the beneficial effect of acetoin catabolism on *P. aeruginosa* growth and survival, especially during co-culture with *S. aureus* (Figs. 5 and 6b). *S. aureus* survival in the presence of *P. aeruginosa* was also shown to be highly affected by nutrient availability induced by co-culture conditions (Fig. 6a). While coexistence is characterized by an absence of *S. aureus* growth inhibition during 8-h co-culture [18], it appears that nutritional competition can still occur under unfavourable conditions and affect *S. aureus*'s survival. Therefore, coexistence between the two pathogens is promoted in nutritionally rich environments, in line with previous observations [35, 36]. Although its survival rate is affected under adverse nutritional conditions induced by long-term culture, acetoin catabolism benefits its producer, *S. aureus* (Fig. 6a). While this effect seems to be linked to acetoin accumulation in the medium, as demonstrated by *P. aeruginosa* Δ *acoR* and Δ *aco* mutants that do not catabolize acetoin anymore (Figs. 5b and 6c), the precise mechanism remains unclear. In *S. aureus*, cell death in the stationary phase may be induced by acetate production and ensuing intracellular acidification. Thomas et al. [34] showed that acetoin production counters cytoplasmic acidification by consuming protons and promotes *S. aureus*'s survival in the late-stationary phase. We hypothesize that acetoin accumulation in the medium may induce a negative control of acetoin synthesis, affecting *S. aureus*'s survival during co-culture conditions.

Previous studies demonstrated the potential benefits of *S. aureus* and *P. aeruginosa* during co-infection. For example, *S. aureus* facilitates the survival of *P. aeruginosa* *lasR* mutants commonly found in CF patients by detoxifying surrounding nitric oxide released by host immune cells [43]. On the other hand, 4-hydroxy-2-heptylquinoline-N-oxide produced by *P. aeruginosa* cells inhibits respiration in *S. aureus* and also protects *S. aureus* cells from aminoglycosides [44]. In addition, we recently demonstrated that *S. aureus* antibiotic resistance and internalization into epithelial cells were increased in the presence of coexisting *P. aeruginosa* [18]. Here, we show that carbon metabolism is largely affected and that *P. aeruginosa* uses the acetoin produced by *S. aureus* as an alternative carbon source. This metabolic dialogue between the two pathogens is selected during bacterial adaptation in CF lungs and promotes their survival. Thus, we highlight for the first time trophic cooperation between *S. aureus* and *P. aeruginosa* during cooperative interaction.

Acknowledgements This work was supported by the Fondation pour la Recherche Médicale, grant number ECO20170637499 to LC; the Finovi foundation to KM; the associations “Vaincre la mucoviscidose” and “Gregory Lemarchal” to KM. We thank Kenneth W Bayles from the University of Nebraska Medical Center (Omaha) for providing *S. aureus* UAMS-1 WT and mutant strains.

Compliance with ethical standards

Conflict of interest The authors declare that they have no conflict of interest.

Ethical statement All the strains used in this study were collected as part of the periodic monitoring of patients at the Hospices Civils de Lyon (HCL). This study was submitted to the Ethics Committee of the HCL and registered under CNIL No. 17-216. All the patients were informed of the study; however, as the study was non-interventional, no written informed consent was required under local regulations.

Publisher's note Springer Nature remains neutral with regard to jurisdictional claims in published maps and institutional affiliations.

References

- Sibley CD, Rabin H, Surette MG. Cystic fibrosis: a polymicrobial infectious disease. *Future Microbiol.* 2006;1:53–61.
- Guss AM, Roeselers G, Newton ILG, Young CR, Klepac-Ceraj V, Lory S, et al. Phylogenetic and metabolic diversity of bacteria associated with cystic fibrosis. *ISME J.* 2011;5:20–29.
- Peters BM, Jabra-Rizk MA, O'May GA, Costerton JW, Shirtliff ME. Polymicrobial interactions: impact on pathogenesis and human disease. *Clin Microbiol Rev.* 2012;25:193–213.
- Murray JL, Connell JL, Stacy A, Turner KH, Whiteley M. Mechanisms of synergy in polymicrobial infections. *J Microbiol Seoul Korea.* 2014;52:188–99.
- Abisado RG, Benomar S, Klaus JR, Dandekar AA, Chandler JR. Bacterial quorum sensing and microbial community interactions. *mBio.* 2018;9:e02331–17.
- Tashiro Y, Yawata Y, Toyofuku M, Uchiyama H, Nomura N. Interspecies interaction between *Pseudomonas aeruginosa* and other microorganisms. *Microbes Environ.* 2013;28:13–24.
- Hotterbeekx A, Kumar-Singh S, Goossens H, Malhotra-Kumar S. In vivo and in vitro interactions between *Pseudomonas aeruginosa* and *Staphylococcus spp.* *Front Cell Infect Microbiol.* 2017;7:106.
- Serra R, Grande R, Butrico L, Rossi A, Settimo UF, Caroleo B, et al. Chronic wound infections: the role of *Pseudomonas aeruginosa* and *Staphylococcus aureus*. *Expert Rev Anti Infect Ther.* 2015;13:605–13.
- O'Brien TJ, Welch M. Recapitulation of polymicrobial communities associated with cystic fibrosis airway infections: a perspective. *Future Microbiol.* 2019;14:1437–50.
- Baldan R, Cigana C, Testa F, Bianconi I, De Simone M, Pellin D, et al. Adaptation of *Pseudomonas aeruginosa* in cystic Fibrosis airways influences virulence of *Staphylococcus aureus* in vitro and murine models of co-infection. *PLoS ONE.* 2014;9:e89614.
- Smith EE, Buckley DG, Wu Z, Saenphimmachak C, Hoffman LR, D'Argenio DA, et al. Genetic adaptation by *Pseudomonas aeruginosa* to the airways of cystic fibrosis patients. *Proc Natl Acad Sci USA.* 2006;103:8487–92.
- Hoffman LR, Kulasekara HD, Emerson J, Houston LS, Burns JL, Ramsey BW, et al. *Pseudomonas aeruginosa lasR* mutants are associated with cystic fibrosis lung disease progression. *J Cyst Fibros J Eur Cyst Fibros Soc.* 2009;8:66–70.

13. Folkesson A, Jelsbak L, Yang L, Johansen HK, Ciofu O, Høiby N, et al. Adaptation of *Pseudomonas aeruginosa* to the cystic fibrosis airway: an evolutionary perspective. *Nat Rev Microbiol*. 2012;10:841–51.
14. Marvig RL, Sommer LM, Molin S, Johansen HK. Convergent evolution and adaptation of *Pseudomonas aeruginosa* within patients with cystic fibrosis. *Nat Genet*. 2015;47:57–64.
15. Limoli DH, Whitfield GB, Kitao T, Ivey ML, Davis MR, Grahl N, et al. *Pseudomonas aeruginosa* alginate overproduction promotes coexistence with *Staphylococcus aureus* in a model of cystic fibrosis respiratory infection. *mBio*. 2017;8:e00186–17.
16. La Rosa R, Johansen HK, Molin S. Adapting to the airways: metabolic requirements of *Pseudomonas aeruginosa* during the infection of cystic fibrosis patients. *Metabolites*. 2019;9:234.
17. Michelsen CF, Christensen A-MJ, Bojer MS, Høiby N, Ingmer H, Jelsbak L. *Staphylococcus aureus* alters growth activity, autolysis, and antibiotic tolerance in a human host-adapted *Pseudomonas aeruginosa* lineage. *J Bacteriol*. 2014;196:3903–11.
18. Briaud P, Camus L, Bastien S, Doléans-Jordheim A, Vandenesch F, Moreau K. Coexistence with *Pseudomonas aeruginosa* alters *Staphylococcus aureus* transcriptome, antibiotic resistance and internalization into epithelial cells. *Sci Rep*. 2019;9:16564.
19. Briaud P, Bastien S, Camus L, Boyadjian M, Reix P, Mainguy C, et al. Impact of coexistence phenotype between *Staphylococcus aureus* and *Pseudomonas aeruginosa* isolates on clinical outcomes among cystic fibrosis patients. *Front Cell Infect Microbiol*. 2020;10:266.
20. Frydenlund Michelsen C, Hossein Khademi SM, Krogh Johansen H, Ingmer H, Dorrestein PC, Jelsbak L. Evolution of metabolic divergence in *Pseudomonas aeruginosa* during long-term infection facilitates a proto-cooperative interspecies interaction. *ISME J*. 2016;10:1323–36.
21. Carriel D, Simon Garcia P, Castelli F, Lamourette P, Fenaille F, Brochier-Armanet C, et al. A novel subfamily of bacterial AAT-fold basic amino acid decarboxylases and functional characterization of its first representative: *Pseudomonas aeruginosa* LdcA. *Genome Biol Evol*. 2018;10:3058–75.
22. Rietsch A, Vallet-Gely I, Dove SL, Mekalanos JJ. ExsE, a secreted regulator of type III secretion genes in *Pseudomonas aeruginosa*. *Proc Natl Acad Sci USA*. 2005;102:8006–11.
23. Page AJ, Cummins CA, Hunt M, Wong VK, Reuter S, Holden MTG, et al. Roary: rapid large-scale prokaryote pan genome analysis. *Bioinforma Oxf Engl*. 2015;31:3691–3.
24. Nicholson WL. The *Bacillus subtilis* ydjL (bdhA) gene encodes acetoin reductase/2,3-butanediol dehydrogenase. *Appl Environ Microbiol*. 2008;74:6832–8.
25. Lessie TG, Phibbs PV. Alternative pathways of carbohydrate utilization in pseudomonads. *Annu Rev Microbiol*. 1984;38:359–88.
26. Chevalier S, Bouffartigues E, Bodilis J, Maillot O, Lesouhaitier O, Feuilloley MGJ, et al. Structure, function and regulation of *Pseudomonas aeruginosa* porins. *FEMS Microbiol Rev*. 2017;41:698–722.
27. Liu Q, Liu Y, Kang Z, Xiao D, Gao C, Xu P, et al. 2,3-Butanediol catabolism in *Pseudomonas aeruginosa* PAO1: 2,3-butanediol catabolism in *Pseudomonas aeruginosa*. *Environ Microbiol*. 2018;20:3927–40.
28. Xiao Z, Xu P. Acetoin metabolism in bacteria. *Crit Rev Microbiol*. 2007;33:127–40.
29. Gade N, Negi SS, Jindal A, Gaikwad U, Das P, Bhargava A. Dual lower respiratory tract infection by *Burkholderia cepacia* and *Acinetobacter baumannii* in a neonate: a case report. *J Clin Diagn Res*. 2016;10:DD01–DD03.
30. Amoli RI, Nowroozi J, Sabokbar A, Rajabniya R. Isolation of *Stenotrophomonas maltophilia* from clinical samples: an investigation of patterns motility and production of melanin pigment. *Asian Pac J Trop Biomed*. 2017;7:826–30.
31. Dryahina K, Sovová K, Nemeč A, Španěl P. Differentiation of pulmonary bacterial pathogens in cystic fibrosis by volatile metabolites emitted by their in vitro cultures: *Pseudomonas aeruginosa*, *Staphylococcus aureus*, *Stenotrophomonas maltophilia* and the *Burkholderia cepacia* complex. *J Breath Res*. 2016;10:037102.
32. Tsang LH, Cassat JE, Shaw LN, Beenken KE, Smeltzer MS. Factors contributing to the biofilm-deficient phenotype of *Staphylococcus aureus* sarA mutants. *PLoS ONE*. 2008;3:e3361.
33. Chaudhari SS, Thomas VC, Sadykov MR, Bose JL, Ahn DJ, Zimmerman MC, et al. The LysR-type transcriptional regulator, CidR, regulates stationary phase cell death in *Staphylococcus aureus*: metabolic control of cell death in *S. aureus*. *Mol Microbiol*. 2016;101:942–53.
34. Thomas VC, Sadykov MR, Chaudhari SS, Jones J, Endres JL, Widhelm TJ, et al. A central role for carbon-overflow pathways in the modulation of bacterial cell death. *PLoS Pathog*. 2014;10:e1004205.
35. Miller CL, Van Laar TA, Chen T, Karna SLR, Chen P, You T, et al. Global transcriptome responses including small RNAs during mixed-species interactions with methicillin-resistant *Staphylococcus aureus* and *Pseudomonas aeruginosa*. *MicrobiologyOpen*. 2017;6:e427.
36. Mashburn LM, Jett AM, Akins DR, Whiteley M. *Staphylococcus aureus* serves as an iron source for *Pseudomonas aeruginosa* during in vivo coculture. *J Bacteriol*. 2005;187:554–66.
37. Visca P, Imperi F. An essential transcriptional regulator: the case of *Pseudomonas aeruginosa* Fur. *Future Microbiol*. 2018;13:853–6.
38. Cornelis P, Matthijs S, Van Oeffelen L. Iron uptake regulation in *Pseudomonas aeruginosa*. *Biomaterials Int J Role Met Ions Biol Biochem Med*. 2009;22:15–22.
39. Ochsner UA, Wilderman PJ, Vasil AI, Vasil ML. GeneChip expression analysis of the iron starvation response in *Pseudomonas aeruginosa*: identification of novel pyoverdine biosynthesis genes. *Mol Microbiol*. 2002;45:1277–87.
40. Tognon M, Köhler T, Luscher A, van Delden C. Transcriptional profiling of *Pseudomonas aeruginosa* and *Staphylococcus aureus* during in vitro co-culture. *BMC Genomics*. 2019;20:30.
41. Španěl P, Sovová K, Dryahina K, Doušová T, Dřevínek P, Smith D. Do linear logistic model analyses of volatile biomarkers in exhaled breath of cystic fibrosis patients reliably indicate *Pseudomonas aeruginosa* infection? *J Breath Res*. 2016;10:036013.
42. Baishya J, Wakeman CA. Selective pressures during chronic infection drive microbial competition and cooperation. *NPJ Biofilms Microbiomes*. 2019;5:16.
43. Hoffman LR, Richardson AR, Houston LS, Kulasekara HD, Martens-Habbena W, Klausen M, et al. Nutrient availability as a mechanism for selection of antibiotic tolerant *Pseudomonas aeruginosa* within the CF airway. *PLoS Pathog*. 2010;6:e1000712.
44. Hoffman LR, Déziel E, D'Argenio DA, Lépine F, Emerson J, McNamara S, et al. Selection for *Staphylococcus aureus* small-colony variants due to growth in the presence of *Pseudomonas aeruginosa*. *Proc Natl Acad Sci USA*. 2006;103:19890–5.

Supplementary data

Materials and methods: Generation of PA2600 knock-out Δ acoR and Δ aco mutants.

Table S1: Clinical CF strains used in this study.

Table S2: Non-CF strains and plasmids used in this study.

Table S3: Primers used in this study.

Table S4: List of *P. aeruginosa* genes differentially expressed in presence of *S. aureus* in the context of a competitive interaction.

Table S5: List of *P. aeruginosa* genes differentially expressed in presence of *S. aureus* in the context of coexistence.

Figure S1: Schematic representation of the employed methodology.

Figure S2: *P. aeruginosa* metabolic pathways and associated genes up-regulated or down-regulated in coexistence with *S. aureus*.

Figure S3: Acetoin concentration in supernatant of *S. aureus*, *B. subtilis*, *B. cenocepacia* and *S. maltophilia* monocultures or co-cultures with *P. aeruginosa*.

Figure S4: Fold change of *P. aeruginosa* *acoR*, *PA4148*, *liuA* and *zwf* gene expression induced by culture with *S. aureus* or its supernatant.

Figure S5: Monitoring of acetoin concentration in *S. aureus* and *P. aeruginosa* monocultures or co-culture or in *S. aureus* supernatant inoculated with *P. aeruginosa* and corresponding AUC, for the pairs SA146/PA146 and SA153/PA153A.

Figure S6: Acetoin concentration in CF sputa from patients.

Figure S7: Acetoin concentration in cultures of *S. aureus* strains from competition and coexistence couples.

Figure S8: Glucose concentrations in cultures of *S. aureus* and *P. aeruginosa* strains from competition and coexistence pairs.

Figure S9: Growth kinetic of *S. aureus* cultivated in absence or presence of acetoin (A) and corresponding AUC analysis.

Materials and methods : Generation of PA2600 knock-out Δ acoR and Δ aco mutants: upstream and downstream flanking regions of *acoR* and *aco* operon (474 bp and 486 bp fragments for *acoR* ; 654 bp and 708 bp for *aco*) were PCR amplified (GoTaq polymerase, Promega) and cloned into pEXG2 by Sequence Ligation and Independent Cloning (SLIC) method (1,2). Resulting plasmids pEXG2-*acoR* and pEXG2-*aco* were then transferred into PA2600 by triparental mating. A first conjugation was performed between the two *E. coli* strains carrying either the pRK2013 helper plasmid or the constructed pEXG2 plasmid by spotting 30 μ L of pre-culture of each strain on LB plates. After two hours at 37°C, 30 μ L of PA2600 pre-culture were added on the dried spot and the plate was incubated five hours at 37°C. The spot was then re-suspended in LB medium and plated on Cetrimide plates supplemented with gentamycin. Resulting clones were then plated on LB containing 10% sucrose to select for plasmid excision by crossing-over. The resulting strains were checked for gentamicin sensitivity and gene deletion by PCR.

CF clinical strains	CF patient	Strain name	Interaction state	Experiments	Reference
<i>P. aeruginosa</i> (PA) and <i>S. aureus</i> (SA)	1	PA2596	Competition (SA2599, SA2597)	RNAseq	3
		SA2597		RNAseq	3
	2 (■)	PA2600	Coexistence (SA2599, SA2597)	RNAseq; qRT-PCR screening; <i>aco</i> induction qRT-PCR; Acetoin monitoring in co-culture; Acetoin catabolism in SA supernatant; Culture in minimal medium; 5-day co-cultures	3
		SA2599		RNA seq; qRT-PCR screening; <i>aco</i> induction qRT-PCR; Acetoin production screening; Acetoin monitoring in co-culture; Production of SA supernatant; 5 days co-cultures; Growth in presence of acetoin	3
	3	PA7A SA7	Coexistence	qRT-PCR screening qRT-PCR screening	This study This study
	4	PA13 SA13	Coexistence	qRT-PCR screening qRT-PCR screening	This study This study
	5 (●)	PA27 SA27	Coexistence	qRT-PCR screening qRT-PCR screening	3 3
	6	PA30 SA30	Coexistence	qRT-PCR screening qRT-PCR screening	3 3
	7	PA31 SA31	Coexistence	qRT-PCR screening qRT-PCR screening	3 3
	8	PA37 SA37	Coexistence	qRT-PCR screening qRT-PCR screening	This study This study
	9	PA42 SA42	Coexistence	qRT-PCR screening qRT-PCR screening	3 3
	10	PA48 SA48	Coexistence	qRT-PCR screening qRT-PCR screening	This study This study
	11	PA53 SA53	Coexistence	qRT-PCR screening qRT-PCR screening	This study This study
	12	PA54 SA54	Coexistence	qRT-PCR screening qRT-PCR screening	This study This study
	13	PA69 SA69	Coexistence	qRT-PCR screening qRT-PCR screening	3 3
	14 (▲)	PA80 SA80	Coexistence	qRT-PCR screening qRT-PCR screening	3 3
	15	PA82 SA82	Coexistence	qRT-PCR screening qRT-PCR screening	3 3
	16	PA146	Coexistence	qRT-PCR screening; Acetoin catabolism screening; Acetoin monitoring in co-culture; Acetoin catabolism in SA supernatant	3
		SA146		qRT-PCR screening; Acetoin production screening; Acetoin monitoring in co-culture; Production of SA supernatant	3
	14 (▲)	PA148B SA148	Coexistence	qRT-PCR screening; Acetoin catabolism screening qRT-PCR screening; Acetoin production screening	3 3
	17	PA152 SA152	Coexistence	qRT-PCR screening; Acetoin catabolism screening qRT-PCR screening; Acetoin production screening	3 3
	18	PA153A	Coexistence	qRT-PCR screening; Acetoin catabolism screening; Acetoin monitoring in co-culture; Acetoin catabolism in SA supernatant	3
		PA153B SA153		Transcriptomic (qRT-PCR) qRT-PCR screening; Acetoin production screening; Acetoin monitoring in co-culture; Production of SA supernatant	3 3

19	PA154A PA154B SA154	Coexistence	qRT-PCR screening; Acetoin catabolism screening qRT-PCR screening; Acetoin catabolism screening qRT-PCR screening; Acetoin production screening	3 3 3
20	PA156 SA156	Coexistence	qRT-PCR screening; Acetoin catabolism screening qRT-PCR screening; Acetoin production screening	3 3
21	PA166A SA166	Coexistence	qRT-PCR screening; Acetoin catabolism screening qRT-PCR screening; Acetoin production screening	3 3
22	PA167 SA167	Competition	Acetoin catabolism screening Acetoin production screening	3 3
2 (■)	PA171A SA171	Coexistence	Acetoin catabolism screening Acetoin production screening	3 3
23	PA172 SA172	Competition	Acetoin catabolism screening Acetoin production screening	This study This study
24	PA178 SA178	Coexistence	Acetoin catabolism screening Acetoin production screening	3 3
25	PA179 SA179	Competition	Acetoin catabolism screening Acetoin production screening	3 3
26	PA181 SA181	Competition	Acetoin catabolism screening Acetoin production screening	3 3
27 (♦)	PA186 SA186	Competition	Acetoin catabolism screening Acetoin production screening	3 3
28	PA187	Competition	Acetoin catabolism screening	This study
29	PA188A SA188	Competition	Acetoin catabolism screening Acetoin production screening	This study This study
30	PA193A SA193	Competition	Acetoin catabolism screening Acetoin production screening	This study This study
5 (●)	PA194A PA194B SA194	Coexistence	Acetoin catabolism screening Acetoin catabolism screening Acetoin production screening	This study This study This study
31	PA197 SA197	Competition	Acetoin catabolism screening Acetoin production screening	This study This study
32	SA198	Competition	Acetoin production screening	This study
33	PA199A PA199C	Competition	Acetoin catabolism screening Acetoin catabolism screening	This study This study
34	PA200 SA200	Competition	Acetoin catabolism screening Acetoin production screening	This study This study
35	SA205	Competition	Acetoin production screening	This study
36	SA207	Coexistence	Acetoin production screening	This study
27 (♦)	SA213	Competition	Acetoin production screening	This study
<i>B. cenocepacia</i>	LUG2886	Coexistence (PA2600)	qRT-PCR (<i>aco</i> induction)	This study
<i>S. maltophilia</i>	LUG2884	Coexistence (PA2600)	qRT-PCR (<i>aco</i> induction)	This study

Table S1: Clinical CF strains used in this study. Unless indicated, interaction state was tested between strains from the same clinical pair (*ie.* isolated from a single patient). Four strain pairs were recovered from a same patient but at different time points and are annotated with identical patient number and symbol (■, ●, ▲ or ♦).

Strains / plasmids	Name	Characteristics	Interaction state	Experiments	Reference
<i>P. aeruginosa</i>	PA2600 Δ <i>acoR</i>	<i>acoR</i> deletion mutant	Coexistence (SA2599)	Culture in minimal medium; 5-day co-cultures	This study
	PA2600 Δ <i>aco</i>	<i>aco</i> operon deletion mutant	Coexistence (SA2599)	Culture in minimal medium; 5-day co-cultures	This study
<i>S. aureus</i>	SA UAMS-1	WT strain	Coexistence (PA2600)	Production of SA supernatant (<i>aco</i> induction)	4
	SA UAMS-1 Δ <i>alsSD</i>	UAMS-1489, <i>alsSD</i> deletion mutant	Coexistence (PA2600)	Production of SA supernatant (<i>aco</i> induction)	4
<i>B. subtilis</i>	LUG2953	WT strain	Coexistence (PA2600)	qRT-PCR (<i>aco</i> induction)	This study
Plasmids	pEXG2	Gm ^R ; mobilizable, non-replicative vector in <i>P. aeruginosa</i>		<i>acoR</i> and <i>aco</i> deletions	2
	pEXG2- Δ <i>acoR</i>	pEXG2 carrying upstream and downstream sequences of <i>acoR</i> for gene deletion		<i>acoR</i> deletion	This study
	pEXG2- Δ <i>aco</i>	pEXG2 carrying upstream and downstream sequences of <i>aco</i> for operon deletion		<i>aco</i> deletion	This study
	pRK2013	Km ^R , helper plasmid with conjugative properties		<i>acoR</i> and <i>aco</i> deletions	5

Table S2: Non-CF strains and plasmids used in this study. *P. aeruginosa* Δ *acoR* and Δ *aco* mutants were constructed from the clinical CF isolate PA2600 (Table S1). Interaction state was tested with the strain indicated in brackets.

Use	Name	Sequence	Target	Amplicon Size
qPCR	PArpoD-F	GCGCAACAGCAATCTCGTCT	<i>rpoD</i>	177
	PArpoD-R	ATCCGGGGCTGTCTCGAATA		
	PAgyrB-F	ATCTCGGTGAAGGTACCGGA	<i>gyrB</i>	160
	PAgyrB-R	TGCCTTCGTTGGGATTCTCC		
	OLC8-F	GCGAGGATCTCTACTTCCGC	<i>acoR</i>	140
	OLC8-R	CTCACCGAGTTCGATGCGTA		
	OLC9-F	GCGGATCGTCAACCTGTCAT	<i>PA4148</i>	86
	OLC9-R	CGATCACGGCAAACCTTCGAG		
	OLC14-F	GTTCTTCAGGCTCCAGTCGG	<i>pvdS</i>	81
	OLC14-R	TTGCGGACGATCTGGAACAG		
	OLC16-F	CGCGACAAGAGCGAATACCT	<i>lasA</i>	71
	OLC16-R	AGGGTCAGCAACACTTTTCGG		
	OLC17-F	CTGGACTGAACCAGGCGATG	<i>rhlA</i>	113
	OLC17-R	CAGGTATTTGCCGACGGTCT		
	OLC22-F	CGACGGTATCCAGGTGATG	<i>PA1874</i>	70
	OLC22-R	GAACTTGACCGTGACCACCT		
	OLC23-F	CGGTGTTGCTCGGATACCTC	<i>rcpC</i>	120
	OLC23-R	GCTTGCGTTCGAGCTTTTCC		
	OLC25-F	ATCGCCTGCTTCCAGTTGTC	<i>pchD</i>	166
	OLC25-R	AGAGAGTGAAGTTGTGCGCC		
	OLC29-F	GAGCGACGAACTGACCTACC	<i>rhlB</i>	200
	OLC29-R	TACTTCTCGTGAGCGATGCG		
	OLC31-F	TGCTCACTTCGCTATGGACC	<i>acoB</i>	117
	OLC31-R	AGAAGATCACCGGGTCGTTG		
	OLC33-F	CCGACGTGATCGCCTTCATA	<i>PA4153</i>	83
	OLC33-R	GACGATTTCTTCCAGGCCGA		
	OLC35-F	GCCATCGAGTTCGGTATGT	<i>bauD</i>	151
	OLC35-R	GAGGCAGACGGTGAAGATCG		
	OLC39-F	GACGAAGACGGCATGAACCT	<i>tadA</i>	119
	OLC39-R	TCCAGTTCGTAGCGGGAGAT		
	OLC41-F	CCACCACGAACTGCAACTG	<i>tadG</i>	107
	OLC41-R	GCTTCTCCAACCGAAGTCCA		
	OLC54-F	TTGCCGTATTGAGTCCCACG	<i>flp</i>	77
	OLC54-R	GACTTTTTTCGCCGACTCCGT		
	OLC56-F	GGA CTGACGCTCAGGCAAT	<i>rhlC</i>	74
	OLC56-R	CCGGAGGAGATCAGGAACGA		
	OLC71-F	CAGCCGGACGAAGGTATCTC	<i>zwf</i>	113
	OLC71-R	GCGTGGTAGGTCTCGGAAAA		
	OLC72-F	GCTATACCCGCTCAAGGGC	<i>dguA</i>	92
	OLC72-R	TCTTGCGGTCGTAATCGGTG		
OLC73-F	CTTCGCCTACCTGTTAGCC	<i>PA5099</i>	163	
OLC73-R	CGGCAGGTAGCGTGAATAGT			
OLC74-F	GCAGTTCGGAGCACATCAAC	<i>PA1874</i>	130	
OLC74-R	TCGATGCTGACGAAATCGGT			
OLC75-F	TGGTATCCGGCGAACACATC	<i>liuA</i>	127	

	OLC75-R	CACATCTTGCTGCCGTTGAG		
	OLC92-F	CAGCCAGGACTACGAGAACG	<i>lasR</i>	153
	OLC92-R	TGGTAGATGGACGGTTCCCA		
	OLC93-F	GGCATTCCCCTCACCGAC	<i>gntK</i>	181
	OLC93-R	GGGTCAGTTCCAGGTAGACGA		
	OLC94-F	TGGAAGTGGCTGCTCAATCC	<i>gltF</i>	81
	OLC94-R	CCAGTCGAAGCGGAAACCTT		
	OLC95-F	CACCTGCACCTTCTATGGCA	<i>edd</i>	96
	OLC95-R	GTGTTCCGGGTTGACGAAGGA		
	OLC96-F	CAACGGCACCTCGATCTTCA	<i>mmsA</i>	94
	OLC96-R	AATCGGGATGTTGATGCCCA		
Cloning	OLC58-F	GGTCGACTCTAGAGGATCCCC AGGGCGATGCCCCGGCCGATG	<i>acoR</i> downstream	474
	OLC58-R	CACATGGTCCTTCGAGTGTGC		
	OLC59-F	GCACACTCGAAGGACCATGTG CGCCGGCATGGCATCCGCATG	<i>acoR</i> upstream	486
	OLC59-R	ACCGAATTCGAGCTCGAGCCC CTCGATCGCGCGGACGAACCA		
	OLC64-F	GGTCGACTCTAGAGGATCCCC TAGTCGGCATCGCGCACCCGT	<i>aco</i> operon downstream	654
	OLC64-R	GGAGAAATCGTCGGACGACGT		
	OLC65-F	ACGTCGTCCGACGATTTCTCCA GTTGGTGAACAACAAGGAGC	<i>aco</i> operon upstream	708
	OLC65-R	ACCGAATTCGAGCTCGAGCCC ACAGCCTGACCACTTTCGTGC		

Table S3: Primers used in this study.

Gene (clinical strains)	Gene (PAO1)		UniProt	Product	Function	SA2599/PA2596		SA2597/PA2596		LasR regulation	Ref.
						Log ₂ fold- change	Adjusted p- value	Log ₂ fold- change	Adjusted p- value		
fecI_2	NA	NA	P23484	Putative RNA polymerase sigma factor FecI	Iron metabolism	-2.67	4.02E-06	-2.51	1.85E-04		6
group_1318	NA	NA	P40883	Regulatory protein PchR	Iron metabolism	-3.57	3.88E-23	-3.13	6.04E-25		6
group_1539	NA	NA	NA	Hypothetical protein	Unknown	-2.96	3.51E-11	-3.58	3.20E-13		
bauA_1	PA0132	bauA	Q9I700	Beta-alanine-pyruvate aminotransferase	Aminoacids (ILV) catabolism, propanoate metabolism	3.15	1.00E-06	3.44	6.25E-39	Activation	7
nirS_1	PA0509	nirN	a Q9I609	Nitrite reductase	Nitrogen metabolism	-2.92	6.77E-10	-2.93	3.30E-09	Repression	8,9
cysG_2	PA0510	nirE	a G3XD80	Siroheme synthase NirE	Nitrogen, porphyrin and chlorophyll metabolism	-3.00	8.64E-09	-2.56	5.61E-06	Repression	8,9
group_5012	PA0512	nirH	a P95415	NirH	Nitrogen metabolism	-3.27	8.64E-09	-2.23	4.94E-04	Repression	8,9
group_3026	PA0513	nirG	a P95414	NirG	Nitrogen metabolism	-2.79	5.29E-06	-2.35	9.60E-04		8
group_4848	PA0514	nirL	a P95413	Heme d1 biosynthesis protein NirL	Nitrogen metabolism	-3.09	1.71E-08	-3.47	2.61E-08		8
group_3339	PA0515	nirD	a P95412	Probable transcriptional regulator	Nitrogen metabolism	-2.99	2.04E-07	-2.03	1.30E-03		8
group_5595	PA0516	nirF	a Q51480	Heme d1 biosynthesis protein NirF	Nitrogen metabolism	-3.34	1.03E-10	-3.47	6.65E-16		8
nirS_2	PA0519	nirS	a P24474	Nitrite reductase	Nitrogen metabolism	-3.29	3.53E-07	-5.39	6.48E-51		8
nirQ	PA0520	nirQ	b Q51481	Denitrification regulatory protein NirQ	Nitrogen metabolism	-4.27	3.41E-28	-4.51	3.08E-33		8
qoxC	PA0521	nirO	b G3XD44	Quinol oxidase subunit 3	Unknown	-4.65	2.60E-22	-4.60	4.38E-15		
group_6044	PA0522	nirP	b Q51483	Hypothetical protein	Unknown	-2.90	1.59E-05	-2.99	7.07E-05		
norB	PA0524	norB	Q59647	Nitric oxide reductase subunit B	Nitrogen metabolism	-5.53	1.99E-23	-8.08	1.91E-79		8
group_3360	PA0672	hemO	G3XCZ8	Heme oxygenase	Porphyrin and chlorophyll metabolism	-2.38	9.28E-05	-2.53	1.57E-17		
ppsC	PA1137	PA1137	Q9I4J8	Phthiocerol/phenolphthiocerol synthesis polyketide synthase	Unknown	-4.31	1.74E-21	-3.55	1.62E-19		
rocR	PA1196	ddaR	Q9I4E2	Arginine utilization regulatory protein RocR	Aminoacids (arginine) metabolism	2.51	3.23E-05	3.22	5.81E-21		10
fecI_5	PA1300	PA1300	c Q9I444	Putative RNA polymerase sigma factor FecI	Iron metabolism	-3.17	3.51E-11	-2.50	2.25E-11		6
fecR_1	PA1301	PA1301	c Q9I443	Protein FecR	Iron metabolism	-3.02	1.71E-08	-2.53	1.01E-13		6
ctpF	PA1429	PA1429	Q9I3R5	Putative cation-transporting ATPase F	Unknown	2.89	8.45E-09	3.63	7.15E-35		
group_3703	PA1673	PA1673	Q9I352	Bacteriohemerythrin	Unknown	2.16	1.57E-04	2.57	1.30E-14		
group_5526	PA1746	PA1746	Q9I2Z1	Hypothetical protein	Unknown	2.42	1.59E-06	2.42	1.38E-09		
group_2540	PA1747	PA1747	Q9I2Z0	Hypothetical protein	Unknown	2.57	8.64E-09	2.46	1.07E-08		
group_269	PA2033	PA2033	Q9I282	Hypothetical protein	Unknown	-2.24	1.65E-03	-2.84	7.11E-23		
ybdM	PA2126	cgrC	Q9I1Y9	CupA gene regulator C, CgrC	Unknown	2.60	3.18E-07	2.46	1.05E-06		
group_6509	PA2321	gntK	G3XD53	Gluconokinase	Carbon metabolism (pentose phosphate)	-2.73	4.03E-06	-2.41	2.68E-05	Repression	9
group_3203	PA2384	PA2384	Q9I195	Ferric uptake regulation protein	Iron metabolism	-2.44	1.09E-04	-2.56	8.25E-10		6
mbtH	PA2412	PA2412	Q9I169	Hypothetical protein	Monobactam biosynthesis	-2.12	1.66E-03	-2.27	6.19E-08		
group_3129	PA2468	foxI	Q9I114	Putative RNA polymerase sigma factor FecI	Iron metabolism	-2.32	1.63E-07	-2.03	1.07E-08		6
hmp	PA2664	fhp	Q9I0H4	Flavoheмоprotein	Iron metabolism, NO detoxification	-2.41	1.85E-05	-2.38	1.86E-03		11
group_3982	PA2691	PA2691	Q9I0F1	NADH dehydrogenase-like protein	Oxidative phosphorylation	-4.38	1.03E-18	-3.45	3.32E-07		
hldD	PA3337	rfaD	Q9HYQ8	ADP-L-glycero-D-mannoheptose-6-epimerase	Lipopolysaccharide biosynthesis	3.40	1.45E-12	4.26	1.62E-48		
yccM	PA3391	nosR	d Q9HYL3	Regulatory protein NosR	Nitrogen metabolism	-3.57	7.09E-14	-4.08	1.98E-30	Repression	8,9
nosZ	PA3392	nosZ	d Q9HYL2	Nitrous-oxide reductase	Nitrogen metabolism	-3.62	1.57E-10	-5.50	6.62E-51	Repression	8,9
nosD	PA3393	nosD	d Q9HYL1	Putative ABC transporter binding protein NosD	Nitrogen metabolism	-3.13	1.38E-10	-3.97	3.44E-20	Repression	8,9
nosY	PA3395	nosY	d Q9HYK9	Putative ABC transporter permease protein NosY	ABC transporters (nitrogen metabolism)	-3.14	1.69E-07	-2.91	1.48E-06	Repression	8,9

nosL	PA3396	<i>nosL</i>	d	Q9HYK8	Copper-binding lipoprotein NosL	Nitrogen metabolism	-2.60	3.86E-05	-2.46	5.00E-05	Repression	8,9
group_3537	PA3411	PA3411		Q9HYJ4	Hypothetical protein	Unknown	-2.59	3.63E-06	-2.05	1.41E-03		
bfd	PA3530	<i>bfd</i>		Q9HY80	Bacterioferritin-associated ferredoxin	Unknown	-2.24	3.28E-10	-2.04	1.81E-10		
ykgO	PA3600	<i>rpl36</i>	e	Q9HY26	50S ribosomal protein L36 2	Ribosome structure	-2.99	6.77E-10	-2.87	3.60E-08		
rpmE2	PA3601	<i>ykgM</i>	e	Q9HY25	50S ribosomal protein L31 type B	Ribosome structure	-2.92	2.37E-10	-3.21	2.69E-26		
fdx_1	PA3809	<i>fdx2</i>	f	Q51383	2Fe-2S ferredoxin	Iron-sulfur protein	-2.72	4.17E-12	-3.02	7.98E-16		
hscA	PA3810	<i>hscA</i>	f	Q51382	Chaperone protein HscA	Protein stabilization	-2.56	4.41E-11	-2.60	6.55E-16		12
hscB	PA3811	<i>hscB</i>	f	Q9HXJ1	Co-chaperone protein HscB	Protein stabilization	-2.04	1.40E-06	-2.28	1.35E-14		12
iscA	PA3812	<i>iscA</i>	f	Q9HXJ0	Iron-binding protein IscA	[Fe-S] cluster biogenesis	-2.51	2.80E-10	-3.37	7.39E-26		13
iscU	PA3813	<i>iscU</i>	f	Q9HXI9	Iron-sulfur cluster assembly scaffold protein IscU	[Fe-S] cluster biogenesis	-2.40	3.46E-06	-3.34	1.95E-27		13
iscS_1	PA3814	<i>iscS</i>	f	Q9HXI8	Cysteine desulfurase IscS	Sulfur relay system, thiamine metabolism, [Fe-S] cluster biogenesis	-2.24	5.79E-05	-3.44	3.85E-29		13
iscR	PA3815	<i>iscR</i>	f	Q9HXI7	HTH-type transcriptional regulator IscR	[Fe-S] cluster biogenesis regulation	-2.42	4.44E-06	-3.65	4.38E-31		13
copA_4	PA3920	<i>yvgX</i>		Q9HX93	Copper-exporting P-type ATPase	Unknown	-2.28	3.75E-07	-2.63	4.15E-14		
ntaA	PA4155	PA4155		Q9HWM6	Nitritotriacetate monoxygenase component A	Unknown	-3.09	5.86E-10	-2.23	6.24E-06		
fyuA_1	PA4156	<i>fvbA</i>		Q9HWM5	Pesticin receptor	Iron metabolism	-2.70	8.32E-12	-2.48	2.30E-09		14
fepC_1	PA4158	<i>fepC</i>		Q9HWM3	Ferric enterobactin transport ATP-binding protein FepC	ABC transporters (iron complex)	-2.30	6.59E-05	-2.21	3.50E-04		
fepB	PA4159	<i>fepB</i>		Q9HWM2	Ferrienterobactin-binding periplasmic protein	ABC transporters (iron complex)	-3.21	1.20E-10	-2.48	7.35E-06		
zupT	PA4467	PA4467	g	Q9HVV1	Zinc transporter ZupT	Unknown	-3.12	1.92E-08	-2.97	1.40E-15		
sodB_2	PA4468	<i>sodM</i>	g	P53652	Superoxide dismutase [Mn/Fe]	Oxydative and iron stress response	-3.17	1.19E-09	-3.09	4.37E-19		15
group_2514	PA4469	PA4469	g	Q9HVV0	Hypothetical protein	Unknown	-3.32	8.79E-09	-3.28	2.91E-23		
fumC_1	PA4470	<i>fumC1</i>	g	Q51404	Fumarate hydratase class II	Carbon metabolism (cytrate circle), iron stress response	-3.14	6.08E-08	-3.16	2.75E-18		15
group_4225	PA4471	<i>fagA</i>	g	G3XD99	Hypothetical protein	Unknown	-3.52	3.14E-17	-3.23	1.64E-25		
group_3398	PA4570	PA4570		Q9HVL4	Hypothetical protein	Unknown	-4.12	3.14E-17	-4.32	4.87E-31		
ccpA	PA4587	<i>ccpR</i>		P14532	Cytochrome c551 peroxidase	Oxydative stress response	3.16	3.49E-11	3.27	6.90E-16	Repression	7,16
group_1579	PA4625	<i>cdrA</i>		Q9HVG6	Cyclic diguanylate-regulated TPS partner A, CdrA	Adhesion and biofilm matrix structure	2.53	8.83E-05	2.06	6.78E-10		17
fecI_3	PA4896	PA4896		Q9HUR7	Putative RNA polymerase sigma factor FecI	Iron metabolism	-3.04	6.78E-10	-2.23	1.49E-08		6
group_4196	PA5027	PA5027		Q9HUE2	Hypothetical protein	Unknown	2.35	7.70E-05	2.82	2.70E-20	Activation	9
arcD	PA5170	<i>arcD</i>		P18275	Arginine/ornithine antiporter	Aminoacids (arginine) metabolism	2.36	4.52E-04	2.49	5.13E-04		10
NA	PA5369.3	PA5369.3	NA		tRNA-Ala	Aminoacyl-tRNA biosynthesis	2.12	7.09E-03	4.50	3.69E-21		
pka	PA5475	PA5475		Q9HT95	Protein lysine acetyltransferase Pka	Unknown	2.04	4.85E-04	2.30	1.81E-10		

Table S4: List of *P. aeruginosa* genes differentially expressed in presence of *S. aureus* in the context of a competitive interaction. PA2596 competition strain was cultivated in absence or presence of SA2599 or SA2597. RNAs were extracted after 4 hours of culture and RNAseq analysis was performed as described in material and methods. A gene was considered as differentially expressed when the Fold Change (FC) was $> |2\log_2|$ with an adjusted P -value < 0.05 in presence of both SA strains. Genes from the same operon are annotated with an identical letter. Grey cells indicate genes that were also dysregulated in the context of coexistence (Table S5). Functional classification was performed thanks to KEGG database and literature.

Gene (clinical strains)	Gene (PAO1)		UniProt	Product	Function	SA2599/PA2600		SA2597/PA2600		LasR regulation	Ref.
						Log ₂ fold-change	Adjusted p-value	Log ₂ fold-change	Adjusted p-value		
group_955	NA	NA	NA	Hypothetical protein	Unknown	-2,20	3,84E-09	-2,56	1,54E-05		
eamB_1	NA	NA	P38101	Cysteine/O-acetylserine efflux protein	Aminoacids transport	2,04	5,37E-04	2,31	2,69E-03		
group_511	NA	NA	NA	Hypothetical protein	Unknown	-2,04	2,34E-03	-2,77	5,28E-03		
▶ bauD	PA0129	bauD	Q91703	Putative GABA permease	Aminoacids (β-alanine) catabolism	2,90	1,53E-15	3,07	2,83E-14		18
bauB	PA0131	bauB	Q91701	Beta-alanine degradation protein BauB	Aminoacids (β-alanine) catabolism	2,27	2,30E-05	2,61	2,31E-04		18
cysG_2	PA0510	nirE	a G3XD80	Siroheme synthase NirE	Nitrogen, porphyrin and chlorophyll metabolism	-2,42	6,73E-05	-2,72	1,36E-03	Repression	8,9
group_3026	PA0513	nirG	a P95414	NirG	Nitrogen metabolism	-2,69	3,29E-05	-2,97	2,87E-03		8
group_3339	PA0515	nirD	a P95412	Probable transcriptional regulator	Nitrogen metabolism	-2,62	1,99E-03	-3,37	3,73E-04		8
group_5595	PA0516	nirF	a Q51480	Heme d1 biosynthesis protein NirF	Nitrogen metabolism	-3,53	1,60E-08	-3,88	1,44E-06		8
nirM	PA0518	nirM	a P00099	Cytochrome c-551	Nitrogen metabolism	-2,62	4,27E-03	-3,27	3,88E-03		8
nirS_2	PA0519	nirS	a P24474	Nitrite reductase	Nitrogen metabolism	-3,27	7,25E-06	-4,43	2,95E-08		8
nirQ	PA0520	nirQ	Q51481	Denitrification regulatory protein NirQ	Nitrogen metabolism	-3,25	7,06E-05	-4,12	2,10E-06		8
norC	PA0523	norC	h Q59646	Nitric oxide reductase subunit C	Nitrogen metabolism	-3,59	2,99E-05	-6,23	4,50E-14		8
norB	PA0524	norB	h Q59647	Nitric oxide reductase subunit B	Nitrogen metabolism	-5,82	3,20E-18	-5,77	2,52E-12		8
group_4191	PA0525	norD	h Q51484	Probable dinitrification protein NorD	Nitrogen metabolism	-3,86	1,68E-06	-4,82	1,23E-08		8
group_364	PA0526	PA0526	G3XDA0	Hypothetical protein	Unknown	-3,38	6,53E-05	-4,60	3,45E-06		
NA	PA0668.3	NA	NA	tRNA-Ala(tgc)	Aminoacyl-tRNA biosynthesis	3,45	5,66E-05	7,57	1,86E-22		
acrC_2	PA0746	PA0746	i Q91513	Acryloyl-CoA reductase (NADH)	Unknown	2,80	1,01E-12	3,12	2,02E-15		
mmsA_2	PA0747	PA0747	i Q91512	Methylmalonate-semialdehyde dehydrogenase	Aminoacids (isoleucine, leucine, valine) catabolism, propanoate and carbon metabolism	2,08	1,04E-05	2,31	1,44E-06		
acnM	PA0794	PA0794	Q915E4	Aconitate hydratase A	Propanoate metabolism	2,18	5,28E-10	2,90	1,80E-07		
aroP_2	PA0866	aroP2	Q91575	Aromatic amino acid transport protein AroP	Unknown	2,30	8,73E-06	2,74	1,02E-03		
acs_1	PA0887	acsA	Q91558	Acetyl-coenzyme A synthetase	Propanoate, carbon and pyruvate metabolism	3,08	5,58E-10	3,27	2,24E-07	Repression	7
yybH	PA1325	yybH	j Q91419	Putative protein YybH	Unknown	2,16	1,03E-03	2,73	1,94E-05		
ilvA_1	PA1326	ilvA	j Q91418	L-threonine dehydratase biosynthetic IlvA	Carbon metabolism, aminoacids (isoleucine, leucine, valine) biosynthesis	2,19	4,61E-05	2,46	6,93E-04		
▶ group_1804	PA1874	PA1874	k Q912M3	Hypothetical protein	Antibiotic resistance, quorum sensing	-2,54	5,92E-05	-2,68	2,83E-04	Activation	9,19
▶ group_4895	PA1875	PA1875	k Q912M2	Hypothetical protein	Antibiotic resistance	-2,94	1,72E-09	-2,80	1,14E-05	Activation	9,19
prsE_3	PA1877	PA1877	k Q912M0	Type I secretion system membrane fusion protein PrsE	Antibiotic resistance	-2,29	8,13E-03	-3,04	1,51E-07		19
group_6609	PA1878	PA1878	Q912L9	Hypothetical protein	Unknown	-2,03	2,47E-05	-2,38	1,01E-03		
group_2034	PA1914	hvn	Q912J0	Hypothetical protein	Unknown	-3,87	9,10E-16	-4,61	3,05E-20	Activation	7
degU_4	PA1978	erbR	P29369	Transcriptional regulatory protein DegU	Ethanol stress response	2,28	2,43E-05	3,06	1,45E-07	Repression	9,20
luxQ	PA1992	ercS	Q912B7	Autoinducer 2 sensor kinase/phosphatase LuxQ	Ethanol stress response	2,13	9,50E-08	2,11	2,65E-04		20
accA1_2	PA2012	liuD	l Q91299	Acetyl-/propionyl-coenzyme A carboxylase alpha chain	Aminoacids (leucine) and monoterpenes catabolism	2,30	7,81E-07	2,69	2,15E-06		21
menB	PA2013	liuC	l Q91298	1%2C4-dihydroxy-2-naphthoyl-CoA synthase	Aminoacids (leucine) and monoterpenes catabolism	3,02	1,20E-11	3,29	7,09E-12		21
group_2911	PA2014	liuB	l Q91297	Methylmalonyl-CoA carboxyltransferase 12S subunit	Aminoacids (leucine) and monoterpenes catabolism	2,61	1,20E-08	2,85	4,87E-10	Activation	9,21
▶ mmgC_7	PA2015	liuA	l Q91296	Acyl-CoA dehydrogenase	Aminoacids (leucine) and monoterpenes catabolism	2,62	3,07E-08	2,76	5,26E-09		21
cueR_2	PA2016	liuR	Q91295	HTH-type transcriptional regulator CueR	Aminoacids (leucine) and monoterpenes catabolism	2,61	4,02E-08	3,17	4,01E-06		21

group_13	PA2040	pauA4	Q9I275	Gamma-glutamylputrescine synthetase PuuA	Polyamines catabolism, aminoacids (glutamine) biosynthesis	2,36	2,02E-08	2,77	8,62E-09		22
kynU	PA2080	kynU	Q9I235	Kynureninase KynU	Aminoacids (tryptophan) catabolism	2,63	9,29E-10	2,67	7,28E-07	Activation	7
group_1851	PA2166	PA2166	Q9I1U9	Hypothetical protein	Unknown	-2,23	5,77E-05	-2,82	1,56E-04	Activation	7
gntR_3	PA2320	gntR	Q9I1F6	HTH-type transcriptional regulator GntR	Carbon metabolism (pentose phosphate)	-2,63	9,55E-11	-2,71	1,51E-05		
▶ group_6509	PA2321	gntK	G3XD53	Gluconokinase GntK	Carbon metabolism (pentose phosphate)	-3,67	1,18E-14	-3,42	5,37E-06	Repression	9,23
group_1686	PA2462	PA2462	Q9I120	Hypothetical protein	Unknown	2,36	1,33E-10	2,34	7,08E-11		
tsdA	PA2481	PA2481	m Q9I101	Thiosulfate dehydrogenase	Unknown	2,68	1,47E-07	2,09	1,59E-04		
group_3818	PA2482	PA2482	m Q9I100	Cytochrome c4	Unknown	2,73	8,24E-08	2,39	6,15E-04		
mmgC_5	PA2552	acdB	n Q9I0T2	Acyl-CoA dehydrogenase	Unknown	2,49	6,18E-12	2,82	2,35E-10	Activation	9
thlA_1	PA2553	PA2553	n Q9I0T1	Acetyl-CoA acetyltransferase	Carbon and fatty acids metabolism	2,46	7,14E-11	2,72	1,52E-08	Activation	9
group_5789	PA2554	PA2554	n Q9I0T0	Putative oxidoreductase	Unknown	2,78	1,75E-13	3,05	1,43E-09	Activation	9
acsA_1	PA2555	PA2555	n Q9I0S9	Acetyl-coenzyme A synthetase	Propanoate, carbon and pyruvate metabolism	2,83	1,51E-10	2,93	8,32E-07	Activation	9
fadD3	PA2557	PA2557	Q9I0S7	3-[(3aS%2C4S%2C7aS)-7a-methyl-1%2C5-dioxo-octahydro-1H-inden	Unknown	3,04	2,30E-14	3,16	2,62E-11		
lecA	PA2570	lecA	Q05097	PA-I galactophilic lectin LecA	Adhesion, biofilm formation	-3,40	1,59E-12	-2,61	1,13E-03	Activation	7,9,24
group_5847	PA2662	PA2662	o Q9I0H6	Hypothetical protein	Unknown	-3,18	1,66E-07	-3,57	3,71E-05		
group_3164	PA2663	ppyR	o Q9I0H5	Psl and pyoverdine operon regulator, PpyR	Iron metabolism, biofilm formation and virulence	-2,83	7,91E-04	-4,04	9,15E-07		25
hmp	PA2664	hmp	Q9I0H4	Flavoheomprotein	Iron metabolism, NO detoxification	-5,40	1,82E-18	-5,66	3,69E-14		11
lip_2	PA2862	lipA	P26876	Triacylglycerol lipase	Glycerolipid metabolism, virulence (lipase activity)	2,31	6,63E-05	2,47	4,68E-04		
group_2901	PA3038	opdQ	Q9HZH0	Porin-like protein NicP	Membrane transports (in response to stress)	2,75	8,42E-07	2,98	2,71E-06	Repression	7,26
ydfJ	PA3079	PA3079	p Q9HZC9	Membrane protein YdfJ	Unknown	2,43	2,32E-07	2,29	2,55E-06		
group_6150	PA3080	PA3080	p Q9HZC8	Ycf48-like protein	Unknown	2,33	5,77E-09	2,24	1,34E-04		
eda_2	PA3181	edaA	q O68283	2-dehydro-3-deoxy-phosphogluconate aldolase	Carbon metabolism (pentose phosphate)	-2,85	2,30E-14	-3,17	6,61E-11	Activation	7
pgl_1	PA3182	pgl	q Q9X2N2	6-phosphogluconolactonase	Carbon metabolism (pentose phosphate)	-3,10	1,45E-13	-3,13	1,21E-08	Activation	7
▶ zwf_2	PA3183	zwf	q O68282	Glucose-6-phosphate 1-dehydrogenase	Carbon metabolism (pentose phosphate)	-2,77	4,39E-08	-3,05	4,13E-11	Activation	7
ugpC	PA3187	gltK	r Q9HZ51	Sn-glycerol-3-phosphate import ATP-binding protein UgpC	ABC transporter (oligosaccharides, polyol, lipids and monosaccharides)	-3,88	1,55E-18	-3,03	4,95E-08		
▶ ugpA	PA3189	gltF	r Q9HZ49	Sn-glycerol-3-phosphate transport system permease	ABC transporter (glucose/mannose)	-2,66	7,46E-08	-2,25	4,99E-03	Activation	7
group_5842	PA3190	gltB	Q9HZ48	Putative sugar-binding periplasmic protein	Carbon metabolism (pentose phosphate)	-5,31	1,43E-59	-4,96	2,08E-23	Activation	7
▶ edd	PA3194	edd	P31961	Phosphogluconate dehydratase	Carbon metabolism (pentose phosphate)	-2,16	1,26E-04	-2,55	2,31E-10	Activation	7
epd_1	PA3195	gapA	P27726	D-erythrose-4-phosphate dehydrogenase	Carbon metabolism (pentose phosphate)	-2,27	1,15E-05	-2,42	1,87E-07	Activation	7
group_5870	PA3233	PA3233	Q9HZ07	Hypothetical protein	Unknown	2,04	1,84E-08	2,35	1,90E-05	Repression	7
actP_1	PA3234	yjcG	s Q9HZ06	Cation/acetate symporter ActP	Unknown	2,86	3,07E-07	2,89	5,65E-05	Repression	7
yjcH_1	PA3235	yjcH	s Q9HZ05	Inner membrane protein YjcH	Unknown	2,09	4,22E-04	2,31	6,97E-05	Repression	7
nosL	PA3396	nosL	Q9HYK8	Copper-binding lipoprotein NosL	Nitrogen metabolism	-2,63	2,89E-04	-3,00	7,77E-03	Repression	9
mmsB	PA3569	mmsB	t P28811	3-hydroxyisobutyrate dehydrogenase	Aminoacids (ILV) catabolism	2,30	2,60E-10	3,27	1,43E-09		
▶ mmsA_1	PA3570	mmsA	t P28810	Methylmalonate-semialdehyde dehydrogenase	Aminoacids (ILV) catabolism, propanoate and carbon metabolism	2,32	8,63E-09	3,32	3,75E-08		
iscR	PA3815	iscR	Q9HXI7	HTH-type transcriptional regulator IscR	isc operon regulation	-2,41	2,64E-06	-2,10	3,56E-03		13
dauA	PA3863	dauA	Q9HXE3	FAD-dependent catabolic D-arginine dehydrogenase DauA	Aminoacids (arginine, ornithine) catabolism	2,12	6,53E-05	2,10	3,23E-03		
argT_1	PA3865	PA3865	Q9HXE1	Lysine/arginine/ornithine-binding periplasmic protein	ABC transporter (arginine, ornithine)	2,47	2,45E-05	2,54	2,08E-04		

group_3022	PA3922	PA3922	u	Q9HX91	Hypothetical protein	Unknown	2,18	3,16E-07	2,13	8,05E-11		
group_4203	PA3923	PA3923	u	Q9HX90	Hypothetical protein	Unknown	2,39	2,29E-07	2,38	6,61E-11	Activation	9
group_2095	PA4022	hdhA		Q9HX05	Hypothetical protein	Pyruvate and carbon metabolism, hydrazine utilization	2,35	8,00E-12	2,50	4,71E-07		27
yhdG_3	PA4023	eutP		Q9HX04	Putative amino acid permease YhdG	Unknown	2,79	7,48E-07	3,33	4,81E-08		
▶ acoR_1	PA4147	acoR		Q9HWN4	Acetoin catabolism regulatory protein	Unknown	2,02	1,07E-05	2,26	1,51E-05		
▶ fabG_10	PA4148	PA4148	v	Q9HWN3	3-oxoacyl-[acyl-carrier-protein] reductase FabG	Butanoate metabolism	2,52	7,65E-03	4,20	2,95E-08		
acoA	PA4150	acoA	v	Q9HWN1	Acetoin:2%2C6-dichlorophenolindophenol oxidoreductase subunit a	Unknown	2,42	6,84E-03	3,89	5,15E-16		
▶ acoB	PA4151	acoB	v	Q9HWN0	Acetoin:2%2C6-dichlorophenolindophenol oxidoreductase subunit b	Unknown	2,95	8,68E-07	3,51	3,12E-15		
acoC	PA4152	acoC	v	Q9HWM9	Dihydrolypoyllysine-residue acetyltransferase component of acetoin cleaving system	Carbon and pyruvate metabolism	3,00	4,18E-04	4,89	3,22E-19		
▶ ydjJ_2	PA4153	PA4153	v	Q9HWM8	2,3-butanediol dehydrogenase	Butanoate metabolism	2,33	9,28E-03	3,94	1,07E-13		
pchA_2	PA4231	pchA		Q51508	Salicylate biosynthesis isochorismate synthase	Ubiquinone and non-ribosomal siderophore peptides synthesis	-2,72	3,55E-05	-2,18	5,58E-03		
cckA	PA4293	pprA	w	Q9HWA7	Sensor kinase CckA	Membrane permeability	-2,54	2,98E-06	-3,28	1,55E-08	Activation	9,28
group_719	PA4294	PA4294	w	Q9HWA6	Hypothetical protein	Unknown	-3,35	9,82E-14	-5,10	7,29E-14	Activation	9
group_2484	PA4300	tadC	x	Q9HWA0	TadC	Flp pilus assembly	-2,45	8,38E-06	-2,73	4,22E-05	Activation	7,9
group_6095	PA4301	tadB	x	Q9HW99	TadB	Flp pilus assembly	-2,47	1,84E-06	-2,73	1,06E-04		31
▶ group_4498	PA4302	tadA	x	Q9HW98	TadA ATPase	Flp pilus assembly	-2,07	3,10E-05	-2,99	4,73E-06	Activation	7,9,29
outD	PA4304	rcpA	x	Q9HW96	RcpA	Flp pilus assembly	-2,48	2,53E-07	-2,92	1,79E-08	Activation	7,9,29
▶ group_95	PA4306	flp		Q9HW94	Type IVb pilin, Flp	Flp pilus assembly	-2,94	1,73E-05	-2,67	1,65E-03	Activation	7,9,29
group_1582	PA4638	PA4638		Q9HVF3	Hypothetical protein	Unknown	-2,33	3,36E-08	-2,42	1,55E-04		
yabJ_1	PA5083	dguB	y	Q9HUA0	2-iminobutanoate/2-iminopropanoate deaminase	Aminoacids (glutamine) metabolism	2,70	1,04E-04	3,77	1,29E-09		30
▶ dadA1_1	PA5084	dguA	y	Q9HU99	D-amino acid dehydrogenase 1	Aminoacids (glutamine, phenylalanine) metabolism	2,70	7,78E-05	4,01	2,78E-08		30
group_5220	PA5096	PA5096		Q9HU87	Glycine betaine-binding periplasmic protein OusX	ABC transporter (glycine, betaine, proline)	2,51	2,24E-10	2,54	7,31E-06		
proY_1	PA5097	hutT	z	Q9HU86	Proline-specific permease ProY	Aminoacids (histidine) catabolism	2,46	1,71E-09	2,37	3,88E-07		31
hutH_1	PA5098	hutH	z	Q9HU85	Histidine ammonia-lyase	Aminoacids (histidine) catabolism	3,16	3,35E-16	2,95	2,39E-12		31
▶ pucI_1	PA5099	PA5099	z	Q9HU84	Putative allantoin permease	Aminoacids (histidine) catabolism	2,84	6,41E-08	2,07	1,95E-05		31
hutU	PA5100	hutU		Q9HU83	Urocanate hydratase	Aminoacids (histidine) catabolism	2,65	4,00E-06	2,19	2,65E-08		31
artJ	PA5153	PA5153		Q9HU31	ABC transporter arginine-binding protein 1	ABC transporter (arginine)	2,06	3,96E-05	2,23	8,34E-13		
NA	PA5160.1	PA5160.1	NA		tRNA-Thr(tgt)	Aminoacyl-tRNA biosynthesis	3,26	5,20E-08	6,82	3,05E-20		
group_4368	PA5383	yeiH		Q9HTI1	Hypothetical protein	Unknown	-2,93	3,32E-06	-3,25	1,16E-03		
group_3039	PA5460	PA5460		Q9HTB0	Hypothetical protein	Unknown	-2,24	7,66E-09	-2,23	4,96E-03		
group_5371	PA5469	PA5469		Q9HTA1	Hypothetical protein	Unknown	2,26	1,56E-03	3,02	4,99E-04		

Table S5: List of *P. aeruginosa* genes differentially expressed in presence of *S. aureus* in the context of coexistence. PA2600 coexistence strain was cultivated in the absence or presence of SA2599 or SA2597. RNAs were extracted after 4 hours of culture and a RNAseq analysis was performed as described in material and methods. A gene was considered as differentially expressed when the Fold Change (FC) was $> |2\log_2|$ with an adjusted P -value < 0.05 in presence of both SA strains. Genes from the same operon are annotated with an identical letter. Grey cells indicate genes that were also dysregulated in competition couples (Table S4). Symbol ▶ indicates genes tested in RT-qPCR (Fig. 1B). Functional classification was performed thanks to KEGG database and literature.

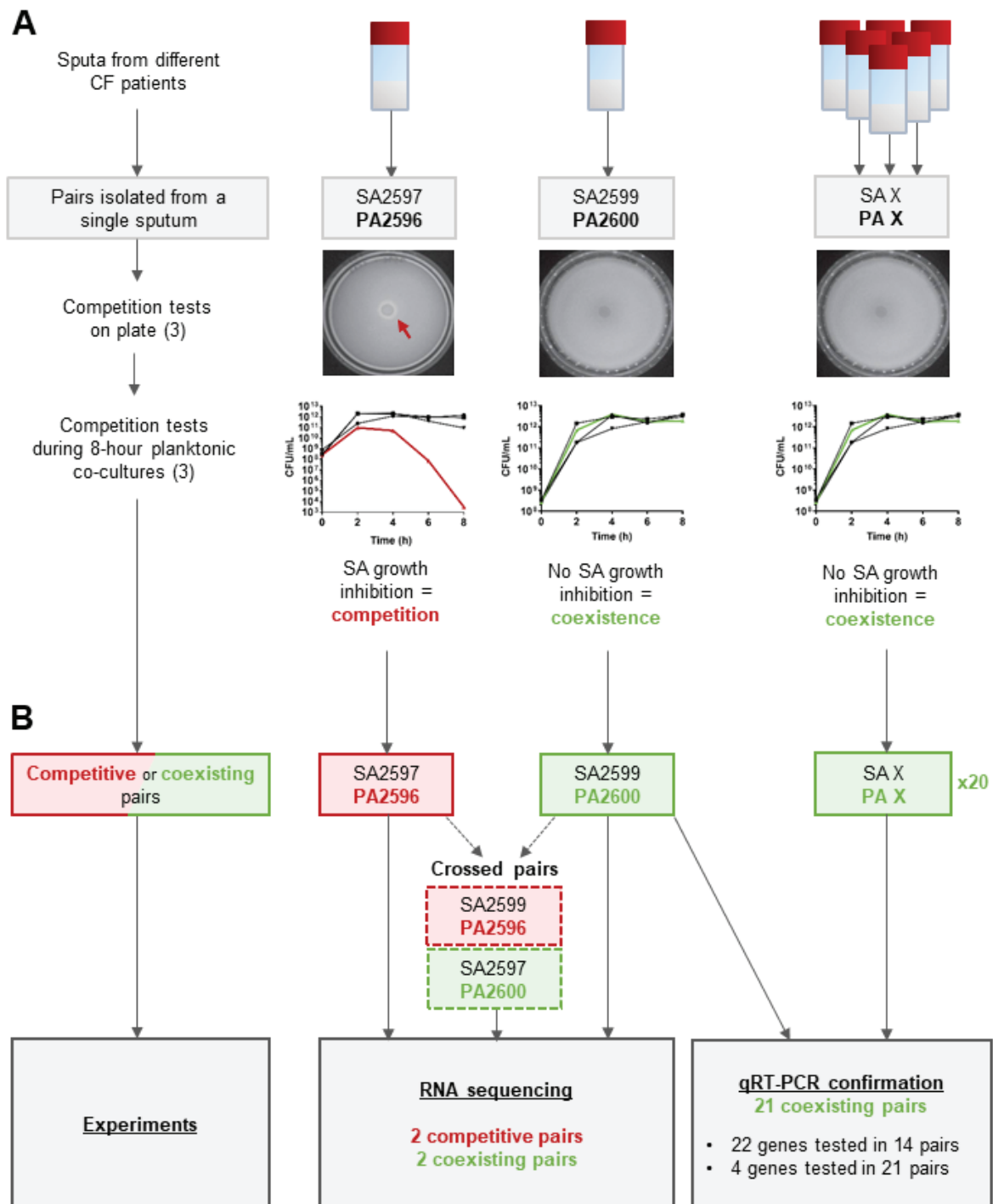


Figure S1: Schematic representation of the employed methodology.

A. Determination of interaction state within *S. aureus*-*P. aeruginosa* co-isolated pairs. Pairs of strains are co-isolated from a single sputum sample. Interaction state is tested during plate and liquid tests, as described in materials and methods and by Briaud *et al.* (3). Results of competition tests (pictures and kinetics) were obtained for a previous study (3).

B. Strain pairs used in transcriptomic analyses. Pairs SA2597/PA2596 and SA2599/PA2600 were isolated from two different patients. Interaction state of crossed pairs was determined as above and confirmed that it is solely led by *P. aeruginosa* (3). The 21 strain pairs used for qRT-PCR confirmation were both isolated from different patients, except in one case (Table S1).

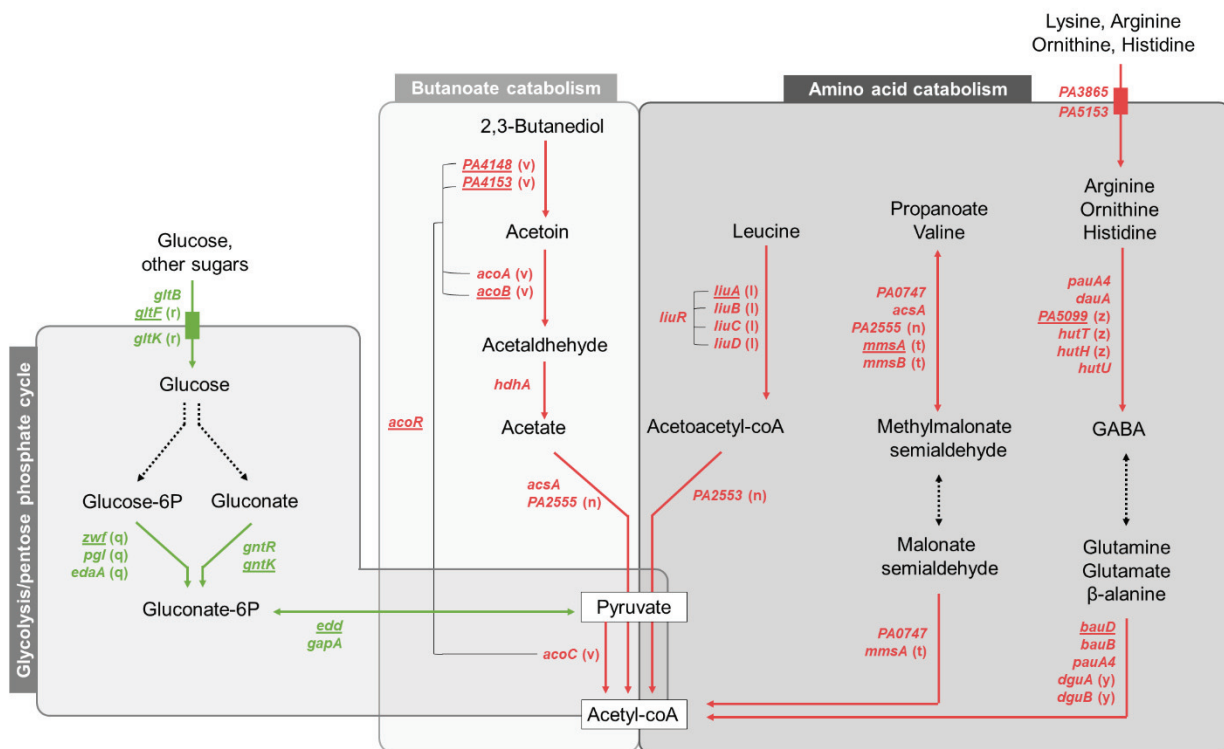


Figure S2: *P. aeruginosa* metabolic pathways and associated genes up-regulated (red) or down-regulated (green) in coexistence with *S. aureus*. PA2600 coexistence strain was cultivated in absence or presence of SA2599 or SA2597. RNAs were extracted after 4 hours of culture and RNAseq analysis was performed. A gene was considered as differentially expressed when the Fold Change (FC) was $> |2\log_2|$ with an adjusted P -value < 0.05 . Genes from the same operon are annotated with an identical letter. Genes tested in RT-qPCR and confirmed for PA2600 are underlined. Functional classification and pathway constructions were performed thanks to KEGG database and literature.

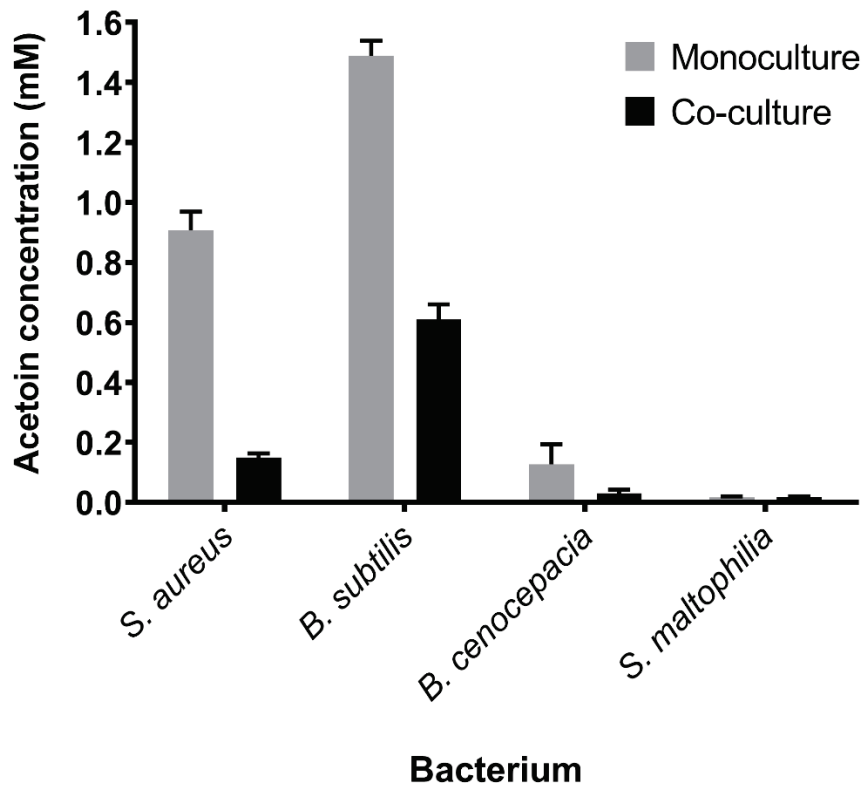


Figure S3: Acetoin concentration in supernatant of *S. aureus* SA2599, *B. subtilis*, *B. cenocepacia* and *S. maltophilia* monocultures (grey bars) or co-cultures with *P. aeruginosa* PA2600 (black bars). Acetoin was quantified from supernatant after 4h of culture. Bars represent the mean acetoin concentration + SEM from three independent experiments.

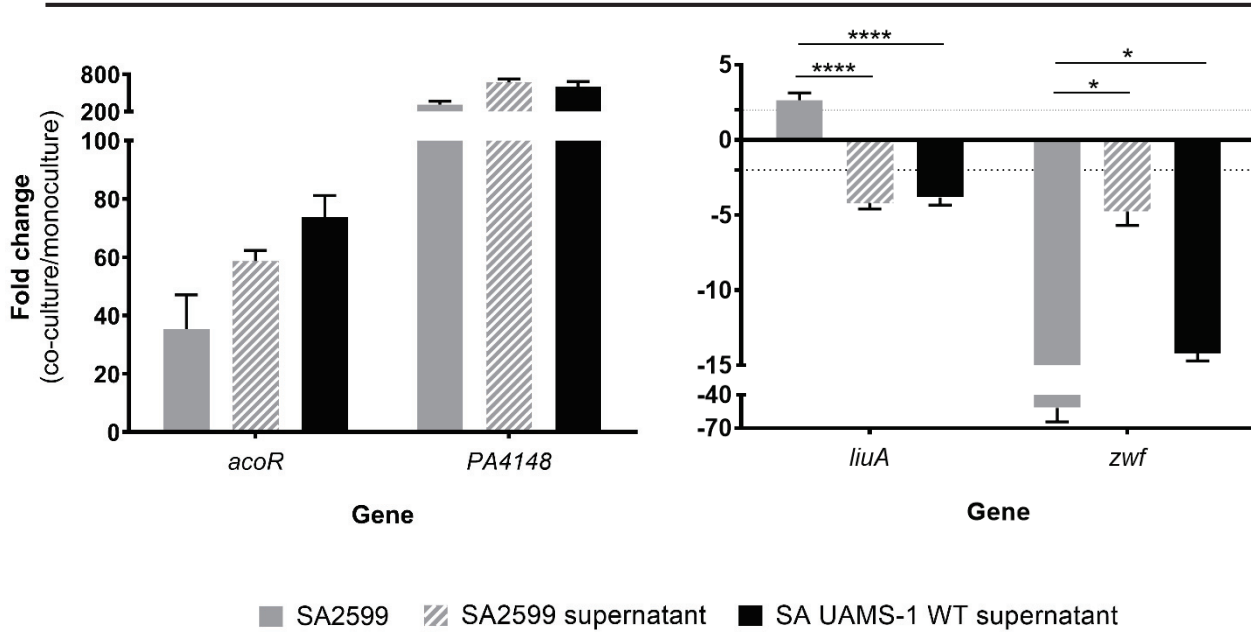
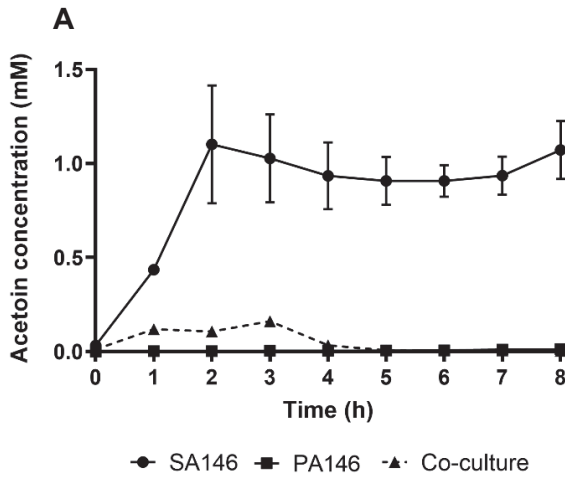


Figure S4: Fold change of *P. aeruginosa acoR*, *PA4148*, *liuA* and *zwf* gene expression induced by culture with *S. aureus* (grey bars) or its supernatant (hatched and black bars). *P. aeruginosa* PA2600 strain was cultivated in the absence or presence of *S. aureus* SA2599 or filtered supernatant of *S. aureus* SA2599 and UAMS-1 WT. RNAs were extracted after 4 hours of culture and gene expression was assayed by RT-qPCR. Bars represent the mean fold change + SEM from three independent experiments. Dot lines indicate a fold change = ± 2 . * $P_{adj} < 0.05$, ** $P_{adj} < 0.0001$ ANOVA with Tukey's correction.**

Pair SA146/PA146



Pair SA153/PA153A

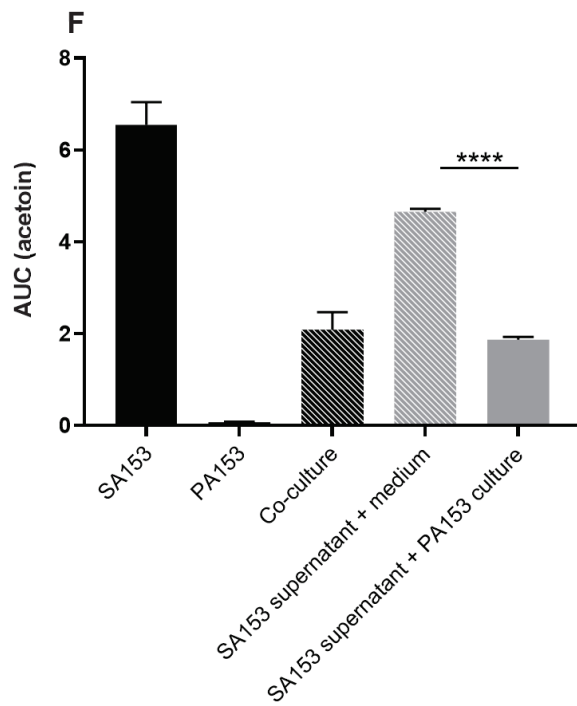
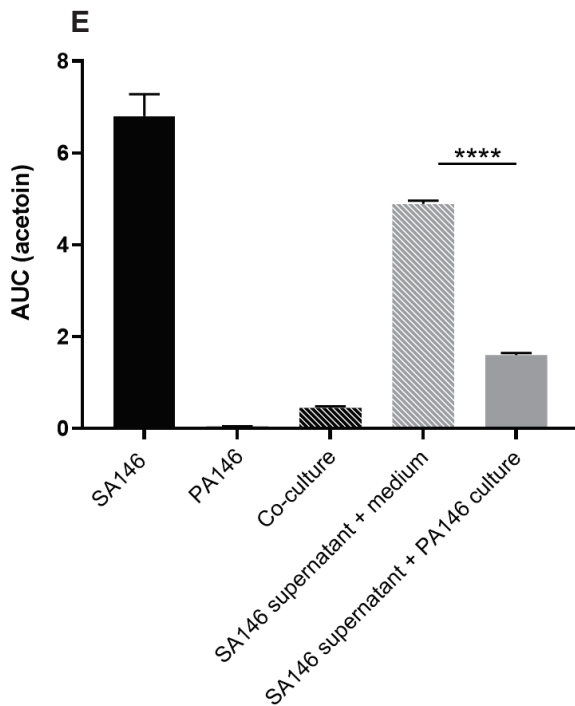
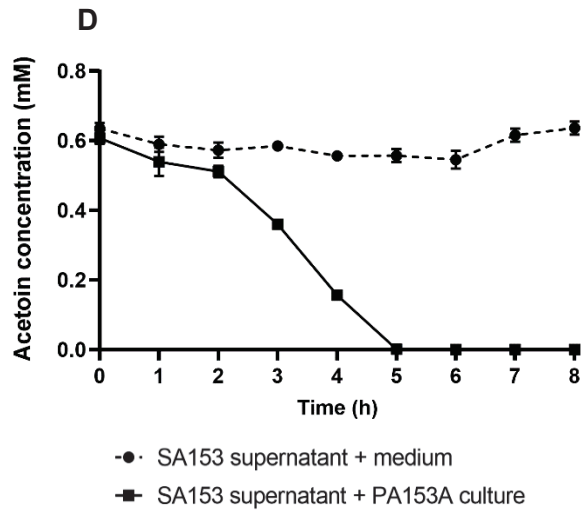
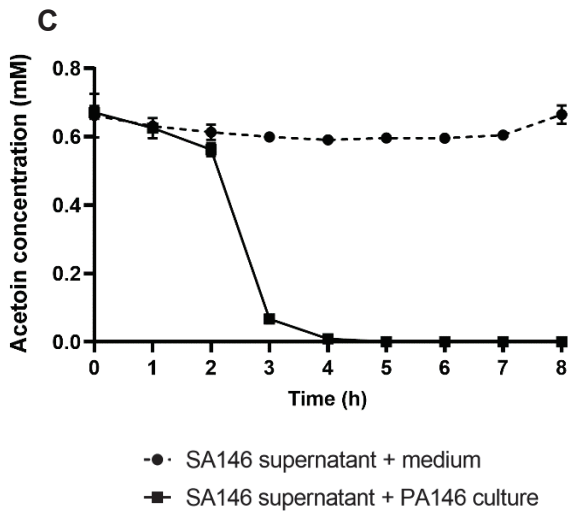
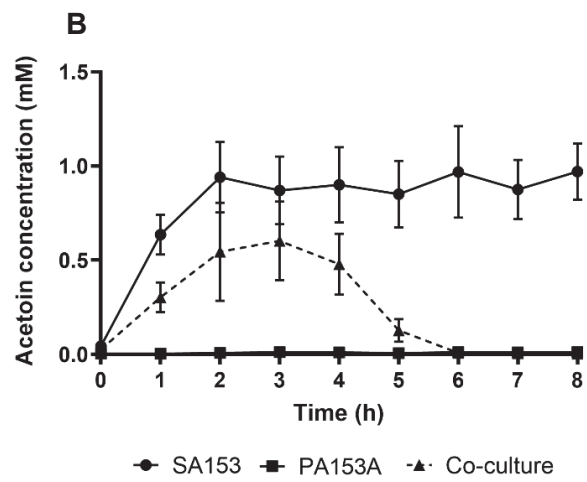


Figure S5: Monitoring of acetoin concentration in *S. aureus* and *P. aeruginosa* monocultures or co-culture (A,B) or in *S. aureus* supernatant inoculated with *P. aeruginosa* (C,D) and corresponding AUC (E,F) , for the pairs SA146/PA146 (A,C,E) and SA153/PA153A (B,D,F).

A,B. *S. aureus* and *P. aeruginosa* were cultivated in monoculture or co-culture. Acetoin was quantified from supernatant each hour. Points represent the mean acetoin concentration \pm SEM from two independent experiments per pair.

C,D. A 4-hour filtered supernatant of *S. aureus* was inoculated with *P. aeruginosa* culture or sterile medium for controls. Acetoin was quantified from supernatant each hour. Points represent the mean acetoin \pm SEM from three independent experiments per pair.

E. For the pair SA146/PA146, the bars represent the mean area under the curves presented in panels A and C \pm SEM. **** $P < 0.0001$ Student test.

F. For the pair SA153/PA153A, the bars represent the mean area under the curves presented in panels B and D \pm SEM. **** $P < 0.0001$ Student test.

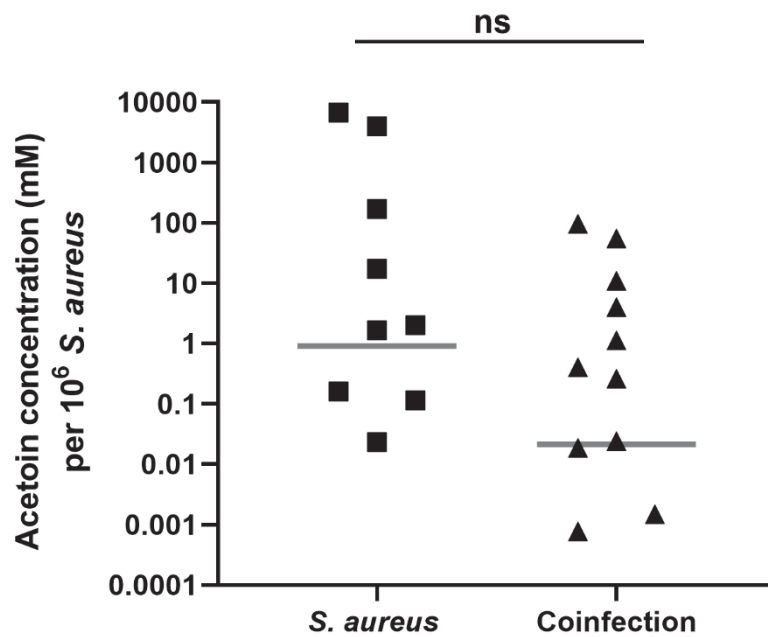


Figure S6: Acetoin concentration in CF sputa from patients. Sputa from *S. aureus* mono-infected patients (n=9) or *S. aureus* and *P. aeruginosa* co-infected patients (n=11) were gathered and acetoin concentration was quantified. Bars represent the median acetoin concentration normalized on *S. aureus* concentration in each sputum. ns $P > 0.05$ student test.

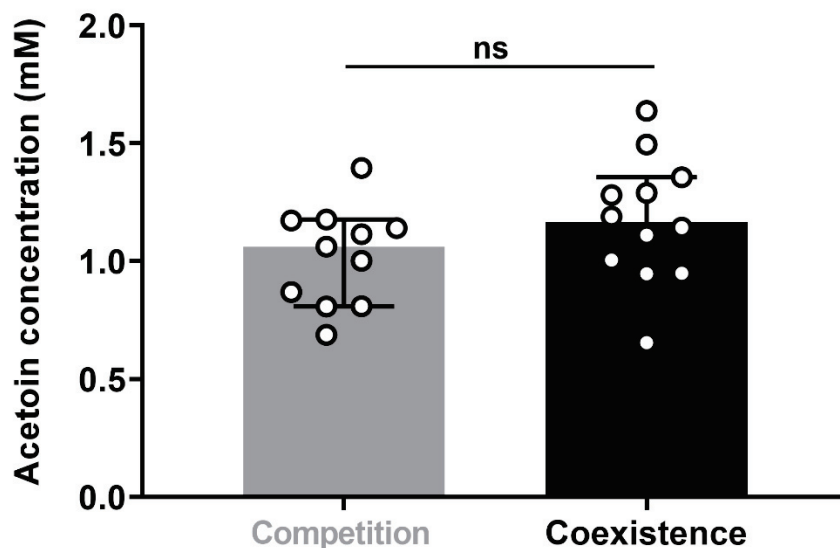


Figure S7: Acetoin concentration in cultures of *S. aureus* strains from competition and coexistence couples. Each *S. aureus* strain from competition (n=11) and coexistence (n=12) couples was cultivated for 6 hours in BHI and acetoin was dosed from supernatant. Bars represent the median acetoin concentration \pm 95% CI. ns $P > 0.05$ Mann-Whitney test.

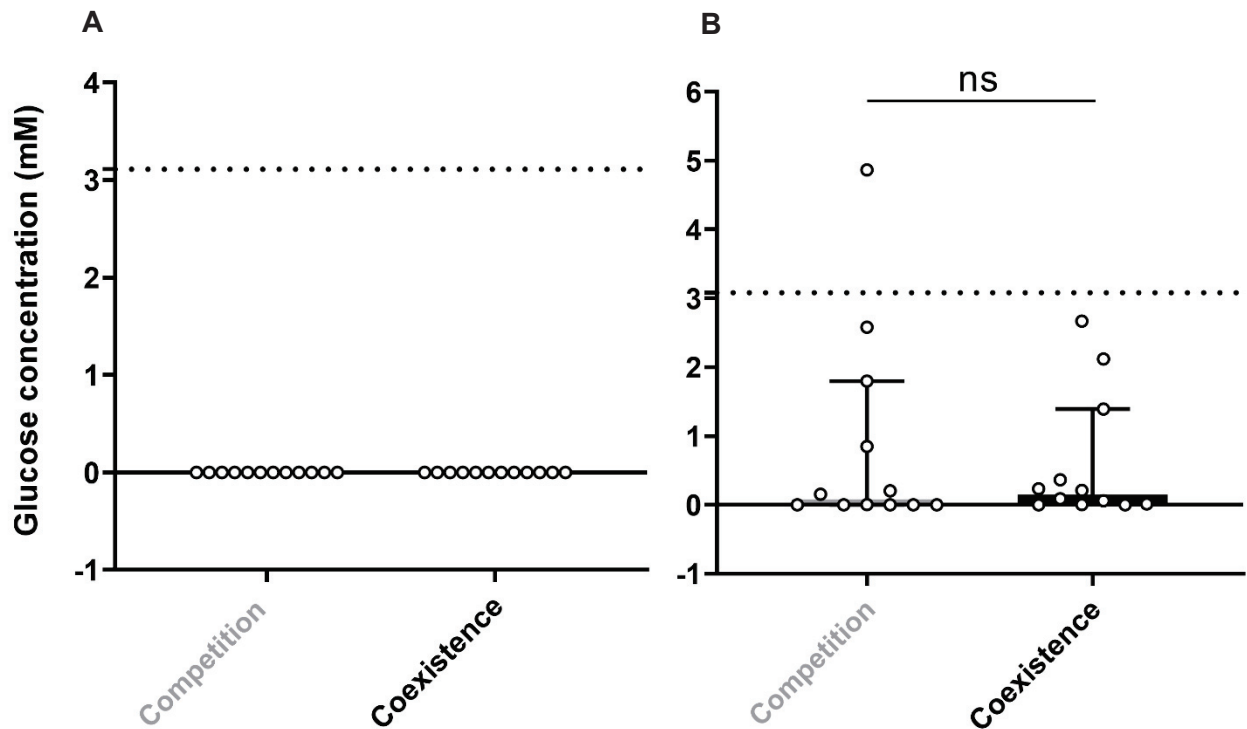


Figure S8: Glucose concentrations in cultures of *S. aureus* (A) and *P. aeruginosa* (B) strains from competition and coexistence pairs.

A. Each *S. aureus* strain from competition ($n=12$) and coexistence ($n=12$) couples was cultivated in *P. aeruginosa* PA2600 filtered supernatant for 6 hours and glucose was quantified from supernatant. No glucose was detected. Dotted line indicates the initial glucose concentration in *P. aeruginosa* supernatant.

B. Each *P. aeruginosa* strain from competition ($n=12$) and coexistence ($n=12$) couples was cultivated in *S. aureus* SA2599 filtered supernatant for 4 hours and glucose was quantified from supernatant. Bars represent the median glucose concentration \pm 95% CI. Dotted line indicates the initial glucose concentration in *S. aureus* supernatant. ns $P>0.05$ Mann-Whitney test.

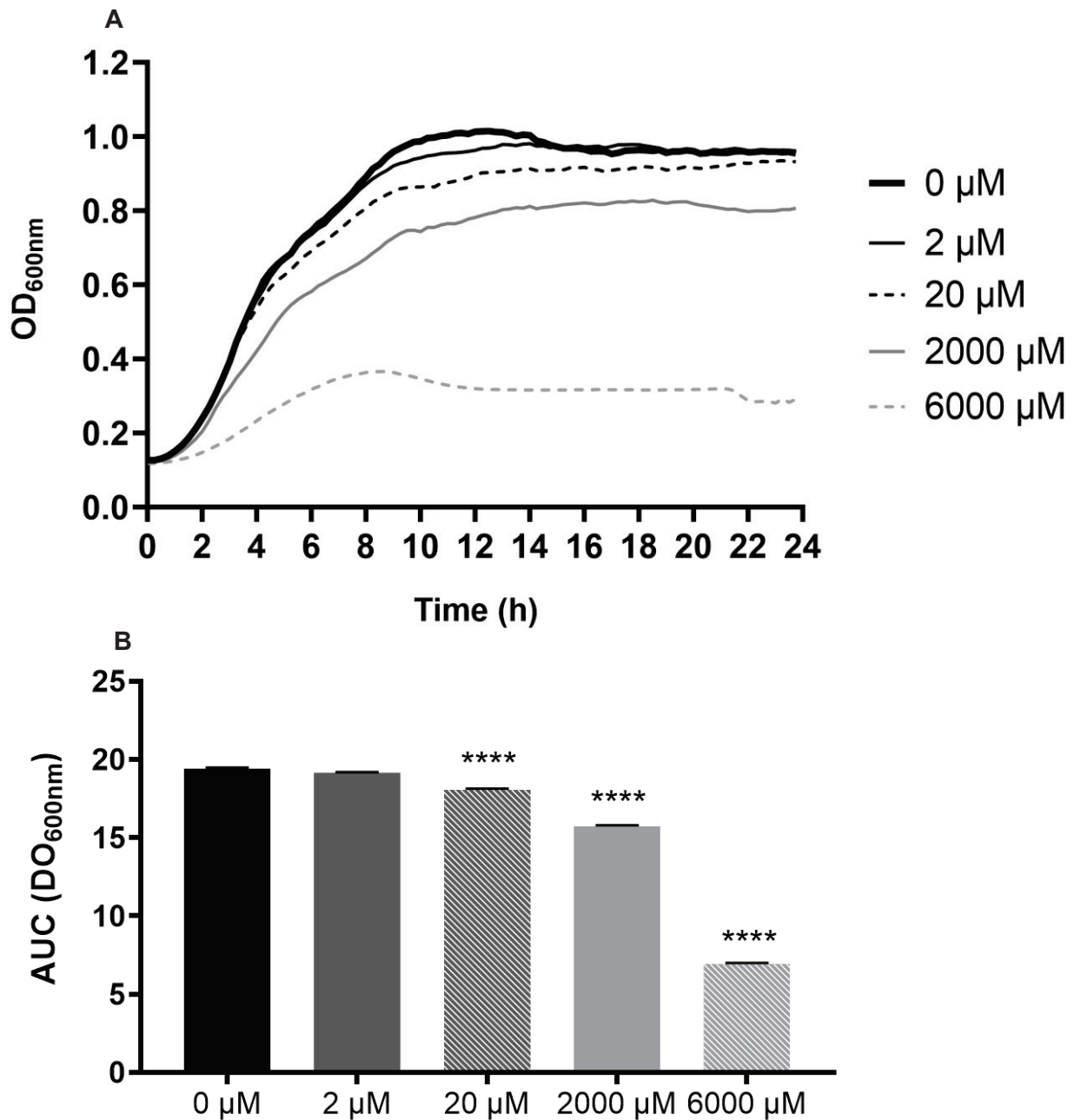


Figure S9: Growth kinetic of *S. aureus* cultivated in absence or presence of acetoin (A) and corresponding AUC analysis (B). SA2599 was cultivated during 24h in the absence of acetoin or in the presence of acetoin in different proportions ranging from 0.2 μM to 6000 μM per 10^6 *S. aureus*. **A.** Lines represent the mean optical density of three technical replicates. **B.** Bars represent the mean area under the curves presented in panel A \pm SEM. **** $P_{\text{adj}} < 0.0001$ one-way ANOVA with Dunnett correction (0 μM vs. condition).

Supplementary data references

1. Carriel D, Simon Garcia P, Castelli F, Lamourette P, Fenaille F, Brochier-Armanet C, Elsen S, Gutsche I. 2018. A Novel Subfamily of Bacterial AAT-Fold Basic Amino Acid Decarboxylases and Functional Characterization of Its First Representative: *Pseudomonas aeruginosa* LdcA. *Genome Biol Evol* 10:3058–3075.
2. Rietsch A, Vallet-Gely I, Dove SL, Mekalanos JJ. 2005. ExsE, a secreted regulator of type III secretion genes in *Pseudomonas aeruginosa*. *Proc Natl Acad Sci U S A* 102:8006–8011.
3. Briaud P, Camus L, Bastien S, Doléans-Jordheim A, Vandenesch F, Moreau K. 2019. Coexistence with *Pseudomonas aeruginosa* alters *Staphylococcus aureus* transcriptome, antibiotic resistance and internalization into epithelial cells. *Sci Rep* 9.
4. Tsang LH, Cassat JE, Shaw LN, Beenken KE, Smeltzer MS. 2008. Factors Contributing to the Biofilm-Deficient Phenotype of *Staphylococcus aureus* sarA Mutants. *PLoS ONE* 3:e3361.
5. Figurski DH, Helinski DR. 1979. Replication of an origin-containing derivative of plasmid RK2 dependent on a plasmid function provided in trans. *Proc Natl Acad Sci USA* 76:1648–1652.
6. Chevalier S, Bouffartigues E, Bodilis J, Maillot O, Lesouhaitier O, Feuilloley MGJ, Orange N, Dufour A, Cornelis P. 2017. Structure, function and regulation of *Pseudomonas aeruginosa* porins. *FEMS Microbiol Rev* 41:698–722.
7. Schuster M, Lostroh CP, Ogi T, Greenberg EP. 2003. Identification, timing, and signal specificity of *Pseudomonas aeruginosa* quorum-controlled genes: a transcriptome analysis. *J Bacteriol* 185:2066–2079.
8. Borrero-de Acuña JM, Rohde M, Wissing J, Jänsch L, Schobert M, Molinari G, Timmis KN, Jahn M, Jahn D. 2016. Protein Network of the *Pseudomonas aeruginosa* Denitrification Apparatus. *J Bacteriol* 198:1401–1413.
9. Wagner VE, Bushnell D, Passador L, Brooks AI, Iglewski BH. 2003. Microarray analysis of *Pseudomonas aeruginosa* quorum-sensing regulons: effects of growth phase and environment. *J Bacteriol* 185:2080–2095.
10. Lundgren BR, Sarwar Z, Pinto A, Ganley JG, Nomura CT. 2016. Ethanolamine Catabolism in *Pseudomonas aeruginosa* PAO1 Is Regulated by the Enhancer-Binding Protein EatR (PA4021) and the Alternative Sigma Factor RpoN. *J Bacteriol* 198:2318–2329.
11. Arai H, Hayashi M, Kuroi A, Ishii M, Igarashi Y. 2005. Transcriptional regulation of the flavohemoglobin gene for aerobic nitric oxide detoxification by the second nitric oxide-responsive regulator of *Pseudomonas aeruginosa*. *J Bacteriol* 187:3960–3968.
12. Campos-García J, G Ordóñez L, Soberón-Chávez G. 2000. The *Pseudomonas aeruginosa* hscA gene encodes Hsc66, a DnaK homologue. *Microbiology (Reading, Engl)* 146 (Pt 6):1429–1435.
13. Romsang A, Duang-Nkern J, Leesukon P, Saninjuk K, Vattanaviboon P, Mongkolsuk S. 2014. The iron-sulphur cluster biosynthesis regulator IscR contributes to iron homeostasis and resistance to oxidants in *Pseudomonas aeruginosa*. *PLoS ONE* 9:e86763.
14. Elias S, Degtyar E, Banin E. 2011. FvbA is required for vibriobactin utilization in *Pseudomonas aeruginosa*. *Microbiology (Reading, Engl)* 157:2172–2180.
15. Hassett DJ, Howell ML, Ochsner UA, Vasil ML, Johnson Z, Dean GE. 1997. An operon containing fumC and sodA encoding fumarase C and manganese superoxide dismutase is controlled by the ferric uptake regulator in *Pseudomonas aeruginosa*: fur mutants produce elevated alginate levels. *J Bacteriol* 179:1452–1459.
16. Eichner A, Günther N, Arnold M, Schobert M, Heesemann J, Hogardt M. 2014. Marker genes for the metabolic adaptation of *Pseudomonas aeruginosa* to the hypoxic cystic fibrosis lung environment. *Int J Med Microbiol* 304:1050–1061.
17. Borlee BR, Goldman AD, Murakami K, Samudrala R, Wozniak DJ, Parsek MR. 2010. *Pseudomonas aeruginosa* uses a cyclic-di-GMP-regulated adhesin to reinforce the biofilm extracellular matrix. *Mol Microbiol* 75:827–842.

18. Yao X, He W, Lu C-D. 2011. Functional characterization of seven γ -Glutamylpolyamine synthetase genes and the bauRABCD locus for polyamine and β -Alanine utilization in *Pseudomonas aeruginosa* PAO1. *J Bacteriol* 193:3923–3930.
19. Zhang L, Mah T-F. 2008. Involvement of a novel efflux system in biofilm-specific resistance to antibiotics. *J Bacteriol* 190:4447–4452.
20. Mern DS, Ha S-W, Khodaverdi V, Gliese N, Görisch H. 2010. A complex regulatory network controls aerobic ethanol oxidation in *Pseudomonas aeruginosa*: indication of four levels of sensor kinases and response regulators. *Microbiology (Reading, Engl)* 156:1505–1516.
21. Aguilar JA, Zavala AN, Díaz-Pérez C, Cervantes C, Díaz-Pérez AL, Campos-García J. 2006. The atu and liu clusters are involved in the catabolic pathways for acyclic monoterpenes and leucine in *Pseudomonas aeruginosa*. *Appl Environ Microbiol* 72:2070–2079.
22. Chou HT, Li J-Y, Peng Y-C, Lu C-D. 2013. Molecular characterization of PauR and its role in control of putrescine and cadaverine catabolism through the γ -glutamylation pathway in *Pseudomonas aeruginosa* PAO1. *J Bacteriol* 195:3906–3913.
23. Daddaoua A, Corral-Lugo A, Ramos J-L, Krell T. 2017. Identification of GntR as regulator of the glucose metabolism in *Pseudomonas aeruginosa*. *Environ Microbiol* 19:3721–3733.
24. Worstell NC, Singla A, Saenkham P, Galbadage T, Sule P, Lee D, Mohr A, Kwon JS-I, Cirillo JD, Wu H-J. 2018. Hetero-Multivalency of *Pseudomonas aeruginosa* Lectin LecA Binding to Model Membranes. *Sci Rep* 8:8419.
25. Attila C, Ueda A, Wood TK. 2008. PA2663 (PpyR) increases biofilm formation in *Pseudomonas aeruginosa* PAO1 through the psl operon and stimulates virulence and quorum-sensing phenotypes. *Appl Microbiol Biotechnol* 78:293–307.
26. Fowler RC, Hanson ND. 2015. The OpdQ porin of *Pseudomonas aeruginosa* is regulated by environmental signals associated with cystic fibrosis including nitrate-induced regulation involving the NarXL two-component system. *Microbiologyopen* 4:967–982.
27. Taniyama K, Itoh H, Takuwa A, Sasaki Y, Yajima S, Toyofuku M, Nomura N, Takaya N. 2012. Group X aldehyde dehydrogenases of *Pseudomonas aeruginosa* PAO1 degrade hydrazones. *J Bacteriol* 194:1447–1456.
28. Wang Y, Ha U, Zeng L, Jin S. 2003. Regulation of membrane permeability by a two-component regulatory system in *Pseudomonas aeruginosa*. *Antimicrob Agents Chemother* 47:95–101.
29. Bernard CS, Bordi C, Termine E, Filloux A, de Bentzmann S. 2009. Organization and PprB-dependent control of the *Pseudomonas aeruginosa* tad Locus, involved in Flp pilus biology. *J Bacteriol* 191:1961–1973.
30. He W, Li G, Yang C-K, Lu C-D. 2014. Functional characterization of the dguRABC locus for D-Glu and d-Gln utilization in *Pseudomonas aeruginosa* PAO1. *Microbiology (Reading, Engl)* 160:2331–2340.
31. Gerth ML, Ferla MP, Rainey PB. 2012. The origin and ecological significance of multiple branches for histidine utilization in *Pseudomonas aeruginosa* PAO1. *Environ Microbiol* 14:1929–1940.

1.3. Résultats complémentaires et perspectives

1.3.1. Facteurs influençant le métabolisme de l'acétoïne

a. Induction du système *aco* par l'acétoïne

Lors de l'interaction de coexistence avec *S. aureus*, *P. aeruginosa* présente un profil transcriptomique adapté et surexprime les gènes du système *aco*. Cette surexpression est induite par l'acétoïne de façon dose-dépendante mais non linéaire, suggérant l'existence de seuils d'induction et/ou d'autres régulateurs. Plusieurs observations effectuées au laboratoire soutiennent ces hypothèses. Tout d'abord, une surexpression du système *aco* a été observée en co-culture avec *E. coli* malgré une absence de production d'acétoïne. L'expression de *acoR* induite par *E. coli* est ainsi similaire à celle obtenue avec les deux producteurs d'acétoïne *S. aureus* et *B. subtilis* ; une induction moindre mais importante est observée pour le gène *PA4148* (Fig. I-1). Ces données confirment que d'autres signaux, notamment produits par *E. coli*, régulent l'expression du système *aco*. De plus, l'opéron *aco* et son activateur transcriptionnel *acoR* ne semblent pas répondre aux mêmes signaux : *acoR* est pleinement induit en absence d'acétoïne en présence de *E. coli*, tandis que l'expression de *PA4148* n'est pas complète en l'absence de la molécule. Si la surexpression restante de *PA4148* résulte de son activation par *acoR* ou par un autre signal reste à déterminer.

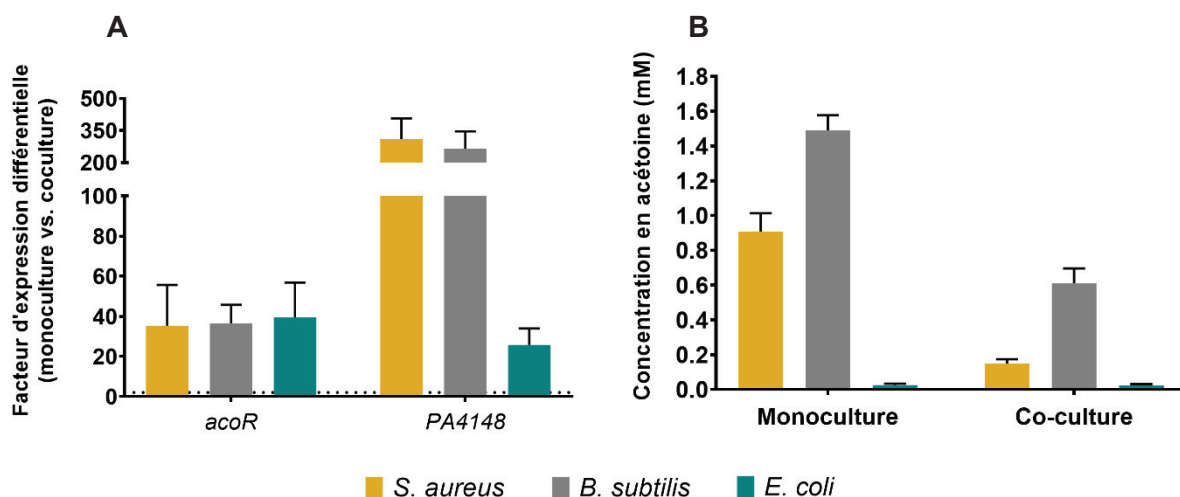


Figure I-1 : Facteurs d'expression différentielle des gènes *acoR* et *PA4148* chez *P. aeruginosa* en co-culture avec *S. aureus*, par rapport à la monoculture (A) et dosages de l'acétoïne en monoculture et co-cultures de *S. aureus*, *B. subtilis* et *E. coli* (B). Les souches ont été cultivées en BHI pendant 4h. **A.** Les ARN ont été extraits et quantifiés par RT-qPCR. Les expressions sont normalisées grâce au gène de ménage *rpoD*. Les barres représentent le facteur moyen + SEM, issu de trois expériences indépendantes. **B.** L'acétoïne a été dosée dans le surnageant de culture. Les barres représentent la concentration moyenne en acétoïne + SEM, issue de trois expériences indépendantes.

Afin de mieux comprendre les mécanismes d'induction du système *aco* chez *P. aeruginosa* en co-culture avec *S. aureus*, nous avons déterminé l'expression des gènes *acoR* et *PA4148* en présence de souches cliniques ou de référence de *S. aureus*. Parallèlement à cela, nous avons dosé l'acétoïne produite par ces souches de staphylocoque afin d'établir une potentielle relation avec les résultats transcriptomiques. Comme présenté en Figure I-2, aucune corrélation entre la production d'acétoïne par *S. aureus* et l'induction des gènes du système *aco* chez *P. aeruginosa* n'a pu être établie, corroborant l'existence d'autres signaux inducteurs dans nos conditions (Fig. I-2).

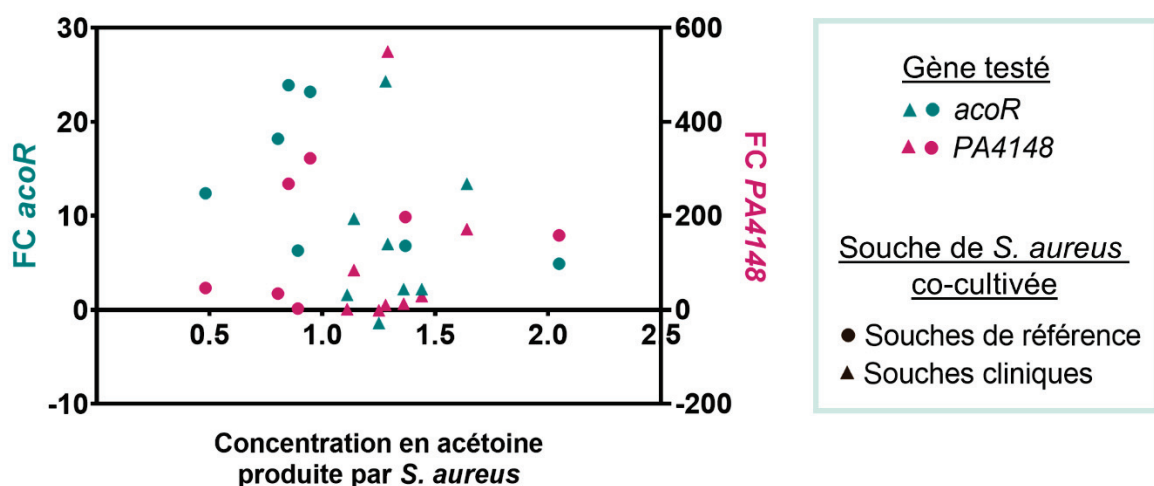


Figure I-2 : Facteurs d'expression différentielle (FC) des gènes *acoR* et *PA4148* chez *P. aeruginosa* en co-culture avec *S. aureus*, en fonction de la concentration en acétoïne produite par *S. aureus*. Les souches ont été cultivées en BHI pendant 4h. Les ARN ont été extraits et quantifiés par RT-qPCR. Les expressions sont normalisées grâce au gène de ménage *rpoD*. L'acétoïne a été dosée dans le surnageant de culture. Les souches cliniques sont indiquées par des triangles, et les souches de référence (COL, MU50, MW2, N315, Newman, RN6911 et SH1000) par des ronds.

b. Autres régulateurs du système *aco*

Bien que les mécanismes exacts de régulation ne soient pas élucidés, plusieurs régulateurs du système *aco* ont été décrits chez *P. aeruginosa* et *B. subtilis* (180, 181). Si l'acétoïne et son précurseur le 2,3-butanediol activent effectivement l'expression de l'opéron *aco* chez *P. aeruginosa*, il a récemment été démontré que cette induction était indirecte et faisait en fait intervenir l'acétaldéhyde. Cette molécule peut être obtenue après clivage de l'acétoïne par l'action de AcoABC, mais peut aussi résulter d'autres voies métaboliques bactériennes telles que la fermentation de l'éthanol (180). Il est donc possible que l'induction de l'opéron *aco* dans nos expériences soit liée à la présence d'acétaldéhyde, potentiellement produit par *E. coli* ou *S. aureus* indépendamment de l'acétoïne. L'ajout d'acétaldéhyde dans le milieu de culture et le suivi de l'expression du système *aco* permettrait de valider cette hypothèse. Evaluer la proportion d'acétaldéhyde, de 2,3-butanediol et d'acétoïne dans nos

conditions serait également intéressant pour mieux comprendre l'induction de l'opéron *aco* chez les souches cliniques de *P. aeruginosa*. Nous avons d'ailleurs tenté de mettre au point une quantification précise des concentrations en ces molécules par chromatographie en phase gazeuse couplée à la spectrométrie de masse (GC-MS), en collaboration avec le Centre d'Etude des Substances Naturelles (CESN) de Lyon. Cette quantification a cependant été limitée par la complexité du milieu riche utilisé, ainsi que par la petite taille et la structure des molécules d'intérêt.

Chez *B. subtilis*, l'induction de l'opéron *aco* nécessite une activation transcriptionnelle *via* les régulateurs AcoR et SigL (σ^{54}). La délétion de *acoR* abolit totalement le catabolisme de l'acétoïne chez *P. aeruginosa*, confirmant l'essentialité de cet activateur dans l'expression de l'opéron *aco* (56, 180). Le facteur σ^{54} de *P. aeruginosa*, RpoN, présente quant à lui une forte homologie de séquence protéique avec SigL de *B. subtilis* (36% d'identité pour 77% de couverture). Deux éléments soutiennent l'importance de RpoN dans la régulation du système *aco* chez *P. aeruginosa* : (i) *acoR* présente un domaine ATPase caractéristique des activateurs de promoteurs transcrits *via* le complexe ARN polymérase-RpoN (182) et (ii) les gènes *PA4148* et *acoAB* présentent des sites de fixation de RpoN (183). Deux études ont toutefois observé l'absence des gènes de l'opéron *aco* dans le régulon de RpoN (184–186). Il est cependant nécessaire de noter que ces régulons ont été déterminés en phase exponentielle de croissance dans du milieu riche. Il serait donc intéressant d'étudier le rôle de RpoN dans la régulation du système *aco* dans des conditions favorisant le catabolisme de l'acétoïne, c'est-à-dire dans un milieu appauvri et en fin de phase exponentielle de croissance. Notre dispositif expérimental de co-culture réunit ces deux conditions (55, 56).

Le rôle des conditions nutritives apparaît d'autant plus important que l'expression de *acoR* et *sigL* est sous contrôle de la répression catabolique chez *B. subtilis*. En présence de glucose, la protéine CcpA (*Catabolite control protein A*) se fixe au site *cre* (*catabolite responsive element*) présent dans les régions promotrices de *acoR* et *sigL* pour empêcher leur transcription. *acoR*, *sigL* et ainsi l'opéron *aco* sont alors exprimés uniquement en absence de glucose dans le milieu (181). Chez *P. aeruginosa*, la répression catabolique a lieu au niveau post-transcriptionnel et fait intervenir la chaperonne Hfq, la protéine de répression cataboliques Crc et l'ARN régulateur CrcZ (187–189) (Fig. I-3A). En présence d'une source de carbone primaire, la traduction des protéines impliquées dans l'utilisation de sources de carbone alternatives est inhibée par la liaison du complexe Crc-Hfq au site de fixation du ribosome (RBS) de l'ARNm. A l'inverse, l'absence de source de carbone primaire est détectée par le senseur CbrA et active le régulateur CbrB par transfert de phosphate. Ce dernier permet la production de l'ARN CrcZ, qui séquestre alors le complexe Crc-Hfq, libérant par la même occasion le RBS des ARNm cibles et autorisant leur traduction (Fig. I-3B) (187–189).

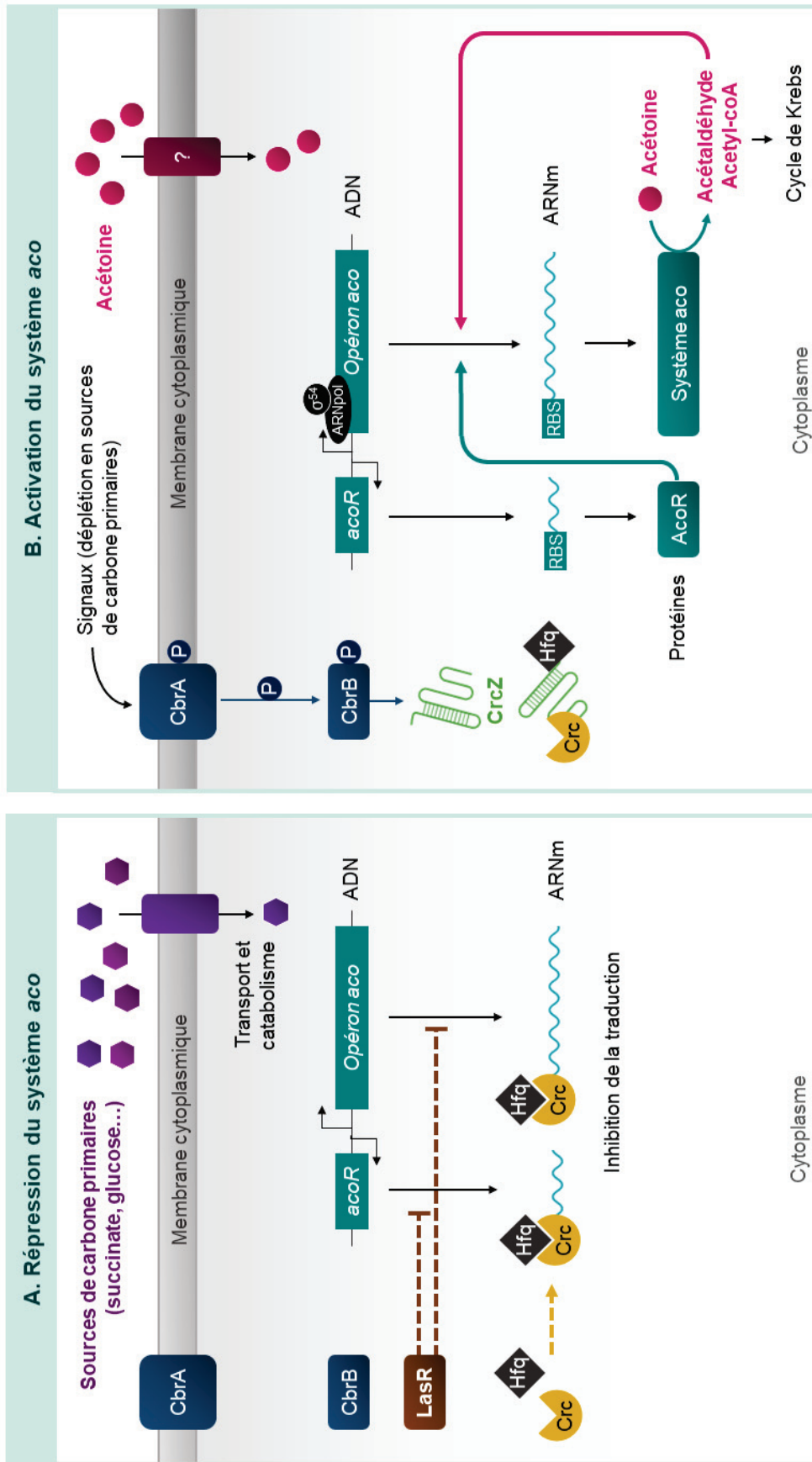


Figure I-3 : Mécanismes hypothétiques de répression (A) et d'activation (B) du système aco chez *P. aeruginosa*.

A. En présence de sources de carbone primaires, les protéines Crc et Hfq s'associent et se lient au site de fixation du ribosome (RBS) pour empêcher la traduction des ARNm du système aco. Une répression transcriptionnelle par LasR est également possible. B. Le senseur CbrA détecte l'absence de sources de carbone primaires et active CbrB par transfert de phosphate (P) afin d'induire la production de l'ARN régulateur CrcZ. Celui-ci capture Crc et Hfq et empêche leur fixation au RBS. La traduction du système aco est permise. AcoR et l'acétylaldéhyde, entre autre produit par clivage de l'acétoïne, activent la transcription de l'opéron aco.

Le rôle de la répression catabolique et du complexe Crc-Hfq dans la régulation du système *aco* n'est pas encore décrit chez *P. aeruginosa*. Cependant, Sonnleitner *et al.* ont observé que la quantité d'ARNm de la totalité des gènes du système *aco* est augmentée en l'absence de Hfq et/ou de Crc lorsque PAO1 est cultivée en milieu riche (**Tableau 1**) (189). Ces données suggèrent donc qu'une répression catabolique médiée par Hfq et Crc pourrait effectivement s'opérer sur les gènes du système *aco* en présence de sources de carbone primaires (**Fig. 3A**). Dans nos conditions, le glucose est épuisé du milieu rapidement et préalablement à l'acétoïne, suggérant que le glucose est la source de carbone préférée en co-culture (56). L'acétoïne est par la suite métabolisée grâce au système *aco*, dont le fonctionnement est induit par la présence d'acétoïne dans le milieu et potentiellement par la levée de répression médiée par Crc-Hfq selon le modèle que nous proposons (**Fig. 3B**).

Gène du système <i>aco</i>		Abondance des transcrits par rapport à PAO1 WT	
Locus PAO1	Nom	Mutant Hfq	Mutant Crc
PA4147	<i>acoR</i>	9,7	5,9
PA4148	<i>PA4148</i>	26,3	ND
PA4149	<i>acoX</i>	29,7	ND
PA4150	<i>acoA</i>	20,3	ND
PA4151	<i>acoB</i>	59,6	ND
PA4152	<i>acoC</i>	24,9	ND
PA4153	<i>PA4153</i>	13,7	ND

Tableau I-1 : Abondance des transcrits des gènes du système *aco* chez un mutant Hfq et un mutant Crc, en comparaison à la souche PAO1 sauvage (WT). Les souches ont été cultivées dans du milieu BSM (*Bifidus Selective Medium*) complexe (supplémenté en succinate, acétate, glucose, mannitol, acétamide, histidine, tryptophane, phénylalanine, leucine, isoleucine, glutamate, arginine, valine and lysine, anthranilate et glycerol) jusqu'à une DO de 1,5. Les ARN ont été extraits et séquencés. Toutes les abondances exposées présentent une *P*-valeur significative ($P < 0,05$). Adapté de Sonnleitner *et al.* (189).

Le rôle de la répression catabolique *via* Crc-Hfq dans la régulation du système *aco* pourrait être confirmé en étudiant la capacité de *P. aeruginosa* à cataboliser l'acétoïne en l'absence de Hfq et Crc, et également dans un milieu contenant d'autres sources de carbone primaires telles que le succinate (187). En lien avec cela, il serait pertinent de doser les différentes sources de carbone présentes dans nos conditions de culture. Les expectorations des patients atteints de mucoviscidose contiennent quant à elles plusieurs sources de carbone primaires pour *P. aeruginosa*, telles que les acides aminés, le lactate, ou le glucose (1, 190). L'acétoïne présente dans les poumons est ainsi probablement utilisée dans un second temps par *P. aeruginosa* (56, 191). Il est toutefois possible que le catabolisme de l'acétoïne soit favorisé dans le milieu pulmonaire par l'épuisement des sources de carbone primaires par les autres microorganismes co-colonisateurs.

Enfin, il est également probable que l'expression du système *aco* soit sous contrôle des systèmes de QS de *P. aeruginosa*. Nous avons en effet observé une augmentation de l'expression des gènes *acoR* et *PA4148* chez une souche de PA14 Δ *lasR* en comparaison à la souche sauvage correspondante (Fig. I-4A et B). De manière intéressante, cet effet n'est pas observé pour *PA4148* lorsque *P. aeruginosa* est cultivée en absence d'acétoïne (Fig. I-4B), soulignant l'importance de la molécule pour l'induction de *PA4148*. En lien avec cela, la souche de PA14 Δ *lasR* est capable de cataboliser l'acétoïne plus efficacement que la souche sauvage (Fig. I-4C). Bien que ces résultats doivent être répétés, ils suggèrent que LasR serait un inhibiteur de l'expression du système *aco* chez *P. aeruginosa*.

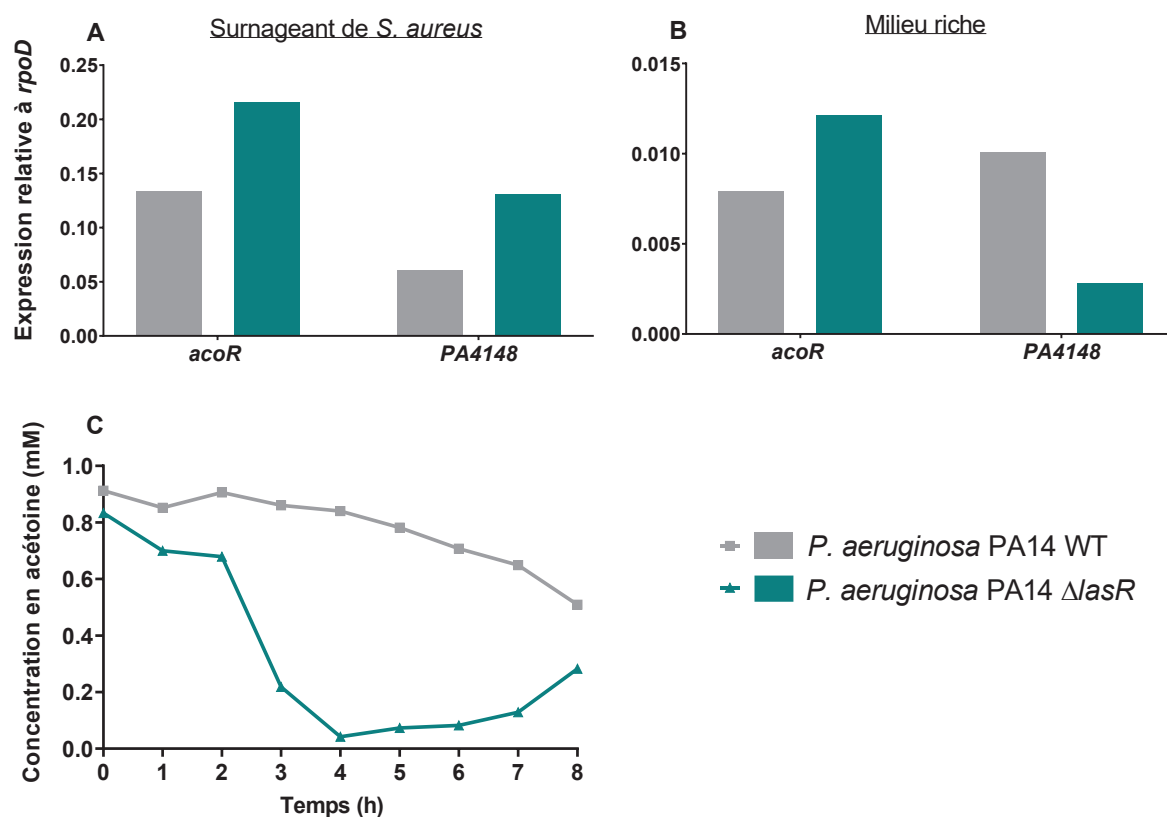


Figure I-4 : Expression du système *aco* (A,B) et catabolisme de l'acétoïne (C) chez *P. aeruginosa* PA14 sauvage (WT) et Δ *lasR* cultivées dans du surnageant de *S. aureus* (A,C) ou dans du milieu riche (B). Les souches ont été cultivées dans du surnageant filtré de *S. aureus* SA2599 ou dans du milieu riche BHI. **A, B.** Les ARN ont été extraits après 4h de culture et quantifiés par RT-qPCR. Les barres représentent l'expression relative des gènes *acoR* et *PA4148* par rapport à *rpoD*. **C.** L'acétoïne a été dosée dans le surnageant de culture toutes les heures.

Le fait que LasR soit un inhibiteur de l'expression du système *aco* pourrait expliquer pourquoi les souches de coexistence de *P. aeruginosa* catabolisent plus efficacement l'acétoïne que les souches de compétition (56). En effet, les isolats cliniques semblent évoluer d'un phénotype compétiteur vers un phénotype coexistant par le biais de mutations dans le

gène *lasR* (Cf. Introduction partie 2.3.2. et Axe 2), qui est également un gène pathoadaptatif de *P. aeruginosa* dans les poumons des patients atteints de mucoviscidose (192). Nous supposons donc que le milieu pulmonaire favorise une altération des fonctions de LasR, induisant le phénotype de coexistence et levant par la même occasion la répression du système *aco*. Cette hypothèse pourrait être étudiée en séquençant le gène *lasR* d'isolats avec différentes capacités de catabolisme de l'acétoïne. Nous pourrions également introduire une mutation *lasR* dans le génome de souches cliniques et évaluer ses conséquences sur le catabolisme de l'acétoïne.

c. Rôle des conditions acido-basiques

Chez le staphylocoque, le pyruvate résultant de la glycolyse est préférentiellement transformé en acétate. Cependant, l'accumulation de cet acide faible à de hautes concentrations induit une acidification du milieu et accélère la mort de *S. aureus*. Afin d'éviter cela, le staphylocoque est capable de rediriger le flux de carbone afin de convertir le pyruvate en acétoïne plutôt qu'en acétate *via* le système AlsSD. L'acétoïne étant une molécule neutre, sa production et son accumulation n'altèrent pas l'homéostasie acido-basique de la bactérie. La biosynthèse d'acétoïne est ainsi favorisée par l'excès de glucose et l'acidification (Fig. I-5) (193–195). Le glucose étant rapidement épuisé dans nos conditions (56), nous avons cherché à savoir si une potentielle acidification du milieu pouvait favoriser la synthèse d'acétoïne par le staphylocoque en co-culture. La concentration en acétoïne et le pH ont donc été évalués dans des mono- et co-cultures de *S. aureus* et de deux souches incapables de cataboliser l'acétoïne : *P. aeruginosa* Δ *aco* et *E. coli*. Nous avons également modifié artificiellement le pH de monocultures de *S. aureus* par l'ajout d'acides (acide chlorhydrique HCl, acide acétique CH₃COOH) ou de base (hydroxyde de sodium NaOH).

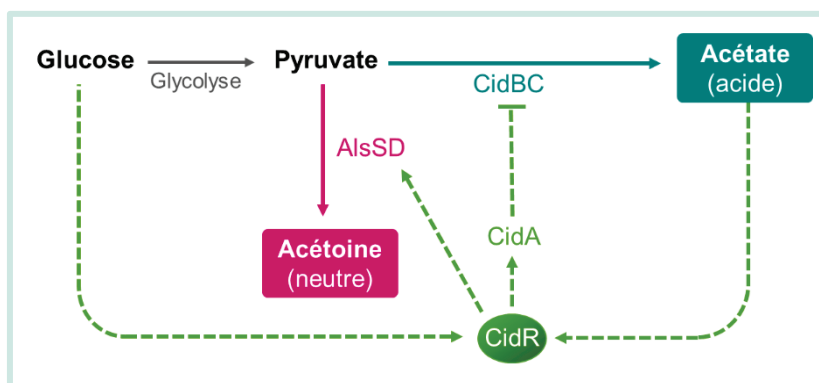


Figure I-5 : Régulation simplifiée de la synthèse d'acétate et d'acétoïne chez *S. aureus*. L'excès de glucose et l'accumulation d'acétate peuvent activer la voie de régulation de CidR (vert) afin de réguler les productions d'acétate et d'acétoïne. Adapté de Chaudhari et al. (194).

Contrairement à notre hypothèse, la co-culture avec *P. aeruginosa* induit une alcalinisation du milieu et une réduction de 70% de la production d'acétoïne par *S. aureus*. Des tendances similaires ont été obtenues en co-culture avec *E. coli* ainsi qu'en alcalinisant artificiellement une culture de *S. aureus* avec du NaOH (Fig. I-6). A l'inverse, la production d'acétoïne par *S. aureus* est favorisée en conditions acidifiées, confirmant les précédentes observations (193). Ainsi, ces résultats suggèrent que la réduction de l'accumulation d'acétoïne observée en co-culture par rapport à la monoculture de *S. aureus* provient à la fois (i) d'un catabolisme par *P. aeruginosa*, favorisé par la déplétion en glucose (56) et (ii) d'une production par le staphylocoque diminuée par l'alcalinisation du milieu.

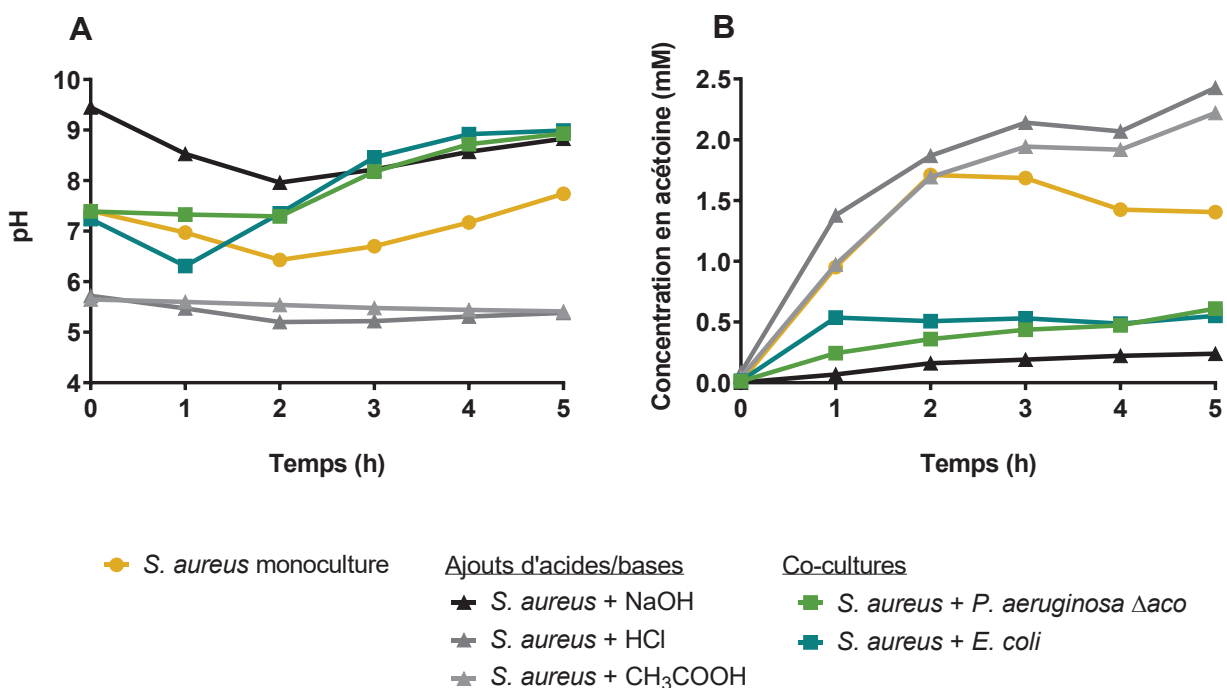


Figure I-6 : Suivi du pH (A) et de la concentration en acétoïne (B) dans la culture de *S. aureus* en absence ou en présence d'acide (HCl, CH₃COOH), de base (NaOH), de *P. aeruginosa* Δ_{aco} ou de *E. coli*. Les souches ont été cultivées dans du milieu riche BHI. La concentration en acétoïne et le pH ont été dosés dans le surnageant de culture toutes les heures. Les points représentent le pH (A) ou la concentration en acétoïne (B) d'une seule expérience.

L'alcalinisation du milieu de culture par *P. aeruginosa* a été confirmée lors des expériences de co-cultures prolongées pendant cinq jours. De manière intéressante, les mutants Δ_{acoR} et Δ_{aco} induisent une alcalinisation du milieu similaire ou très légèrement inférieure à celle provoquée par la souche sauvage (Fig. I-7). D'une part, ces résultats confirment que l'accumulation d'acétoïne ne modifie pas drastiquement les propriétés acido-basiques du milieu de culture. D'autre part, nous avons supposé que cette accumulation d'acétoïne déséquilibre la réaction effectuée par AlsSD chez le staphylocoque (Fig. I-5), induisant une production d'acétate et une acidification délétère pour *S. aureus* en co-culture

avec les souches *P. aeruginosa* Δ *acoR* et Δ *aco*. Bien qu'une légère acidification soit observée en co-culture avec le mutant Δ *aco*, il reste difficile de conclure concernant les causes exactes de la diminution de survie de *S. aureus* dans ces conditions. Il est également possible que l'acétoïne accumulée ait d'autres impacts délétères sur la physiologie du staphylocoque, directement ou par le biais d'une dérégulation du fonctionnement de AlsSD. Cette protéine est en effet importante pour d'autres phénotypes de *S. aureus*, comme par exemple la formation de biofilm (193, 194).

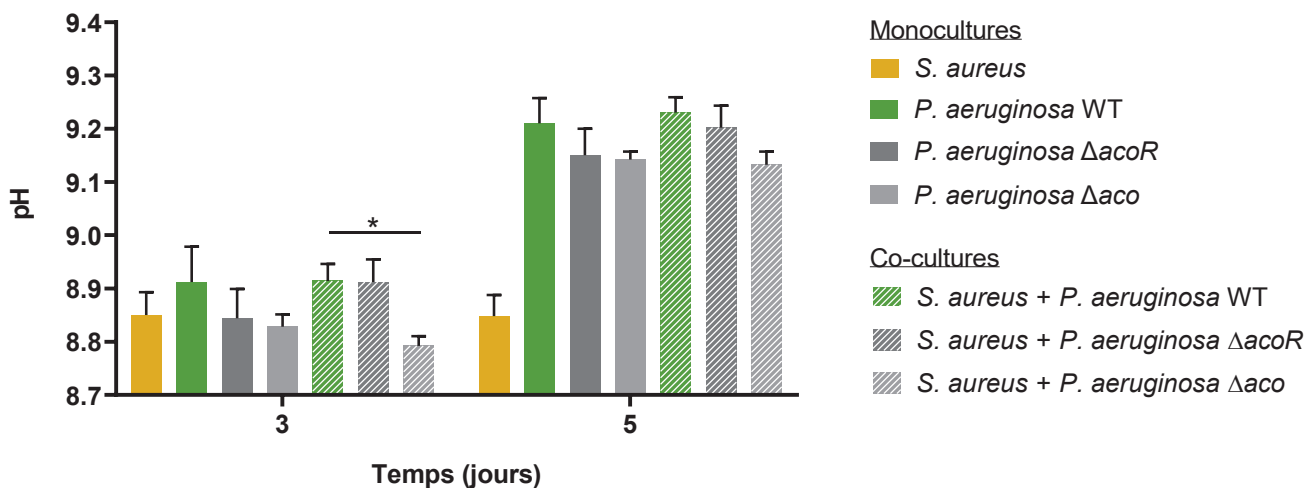


Figure I-7 : Suivi du pH dans des monocultures et co-cultures de *S. aureus*, *P. aeruginosa* sauvage (WT), Δ *acoR* et Δ *aco* pendant 5 jours. Les souches ont été cultivées dans du milieu riche BHI pendant cinq jours et le pH a été déterminé dans le surnageant de culture. Les barres représentent le pH moyen + SEM de 5 expériences indépendantes.

1.3.2. Restauration chromosomique du système *aco* chez PA2600

Les expériences de croissance en milieu pauvre et en co-culture prolongées sur cinq jours ont indiqué que le catabolisme de l'acétoïne favorisait la survie de *P. aeruginosa* et *S. aureus*. Cet effet a pu être mis en évidence par l'utilisation des souches mutantes de *P. aeruginosa* PA2600 Δ *acoR* et Δ *aco* incapables de dégrader l'acétoïne. Nous avons souhaité confirmer ces résultats en effectuant des complémentations chromosomiques (ou restaurations) de *acoR* et *aco*. Ces restaurations reposent sur le clonage des séquences de *acoR* et de l'opéron *aco* dans le vecteur intégratif miniCTX, ensuite transféré par conjugaison dans les mutants correspondants (196). Malgré l'utilisation de plusieurs jeux d'amorces, de polymérases et de protocoles d'amplification, nous n'avons cependant pas réussi à amplifier la séquence du gène *acoR*. Des difficultés dans l'expression et la purification de AcoR ont été rencontrées dans des études antérieures (180).

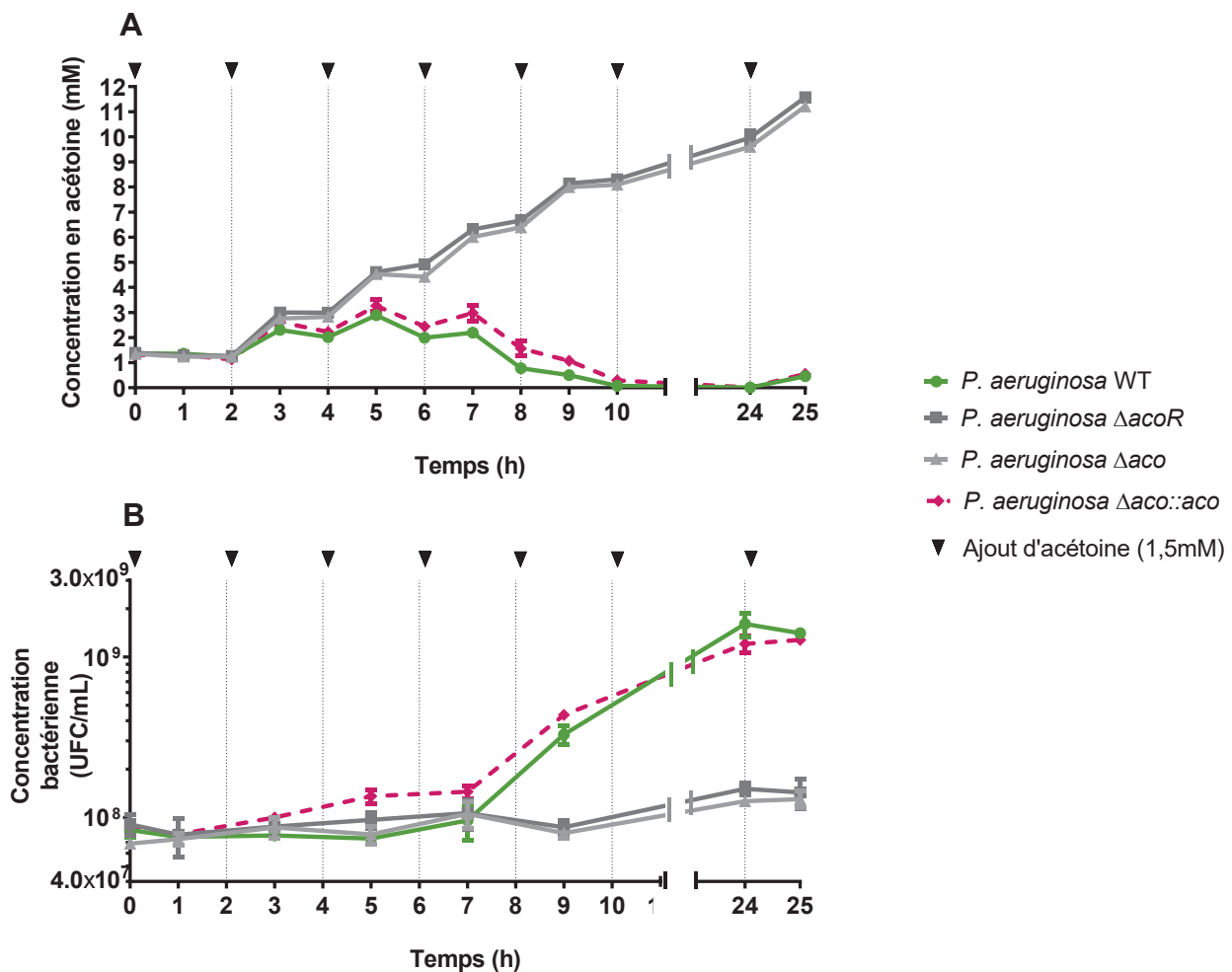


Figure I-8 : Cinétiques de la concentration en acétoïne (A) et de la croissance de *P. aeruginosa* (B) dans du milieu minimum supplémenté en acétoïne. Les souches PA2600 sauvage (WT), ΔacoR , Δaco et $\Delta\text{aco}::\text{aco}$ ont été cultivées en milieu M63 et 1,5mM d'acétoïne a été ajouté toutes les 2 heures. **A.** L'acétoïne a été dosée dans le surnageant de culture toutes les heures. Les points représentent la concentration moyenne en acétoïne \pm SEM de 3 expériences indépendantes. **B.** Les bactéries ont été étalées sur TSA et dénombrées toutes les 2 heures. Les points représentent la concentration bactérienne moyenne \pm SEM de 3 expériences indépendantes.

La restauration du système *aco* a quant à elle pu être achevée afin d'obtenir la souche de *P. aeruginosa* PA2600 $\Delta\text{aco}::\text{aco}$. Cette dernière a présenté une restauration totale du catabolisme de l'acétoïne et des phénotypes de survie en monoculture et en milieu pauvre par rapport à la souche sauvage (Fig. I-8). *P. aeruginosa* PA2600 $\Delta\text{aco}::\text{aco}$ n'a cependant présenté qu'une restauration partielle de ces phénotypes lors des co-cultures prolongées pendant 5 jours (Fig. I-9). Le gain de survie en co-culture observé pour la souche sauvage n'a pas été reproduit pour la souche restaurée (Fig. I-9B), potentiellement en lien avec la restauration partielle du catabolisme de l'acétoïne dans ces conditions. En effet, l'acétoïne était encore présente dans la co-culture de PA2600 $\Delta\text{aco}::\text{aco}$ après 5 jours alors qu'elle est normalement totalement catabolisée par la souche sauvage (Fig. I-9C).

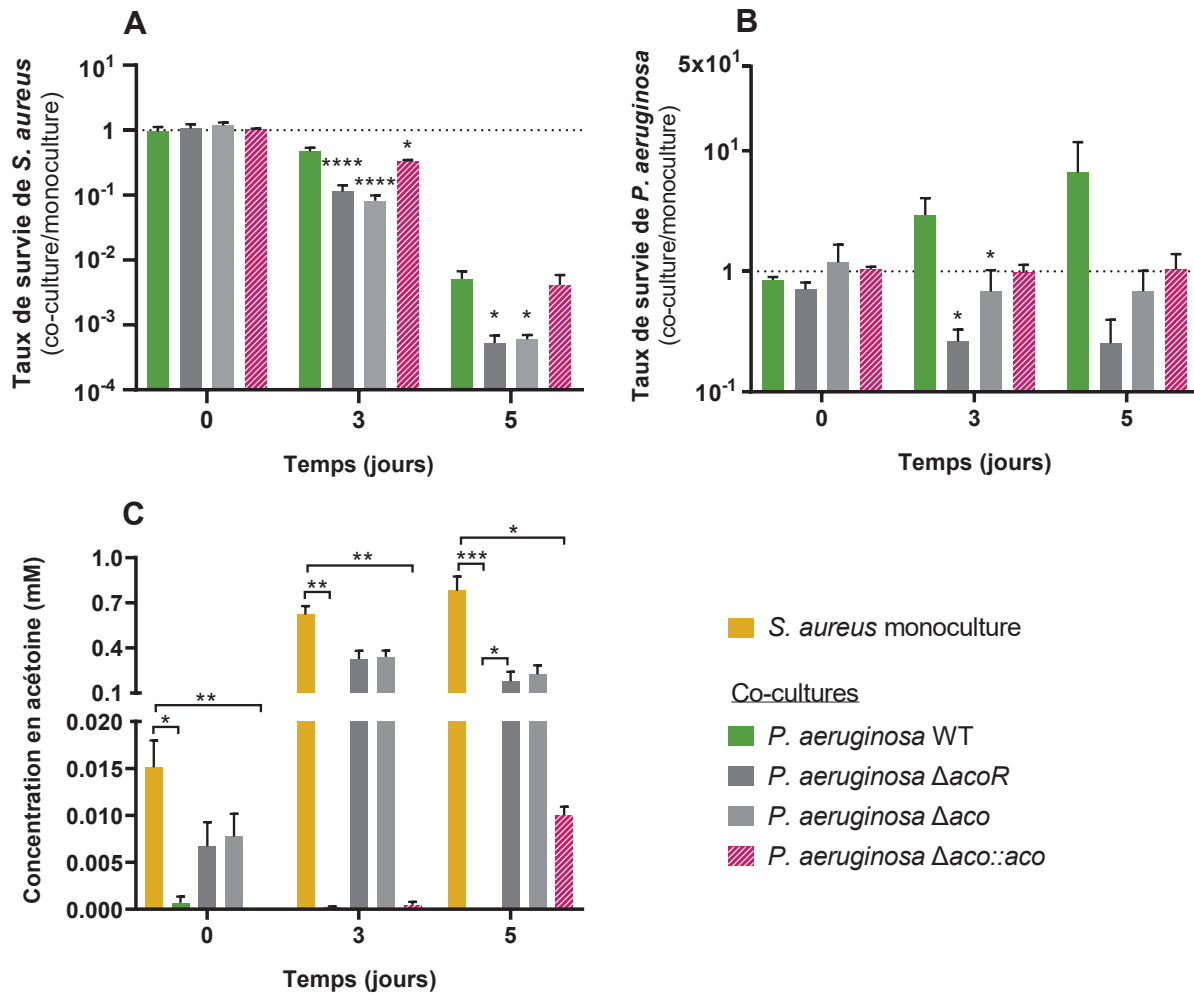


Figure I-9 : Cinétiques de survie de *S. aureus* (A), *P. aeruginosa* (B) et de la concentration en acétoïne (C) durant les co-cultures prolongées. *S. aureus* SA2599 a été cultivée en présence de *P. aeruginosa* PA2600 sauvage (WT), Δ acoR, Δ aco et Δ aco::aco pendant 5 jours. Les cultures ont été étalées à J0, J3 et J5 sur MSA et cétrimide afin de dénombrer *S. aureus* et *P. aeruginosa*, respectivement, et l'acétoïne a été dosée dans le surnageant de culture. **A, B.** Le taux de survie a été estimé en divisant la concentration bactérienne en co-culture par la concentration bactérienne en monoculture pour chaque bactérie. Les barres représentent le taux de survie moyen + SEM de 5 expériences indépendantes. * $P_{adj} < 0.05$, **** $P_{adj} < 0.0001$ one-way ANOVA avec la correction de Dunnett (WT vs. condition). **C.** Les barres représentent la concentration moyenne en acétoïne + SEM de 5 expériences indépendantes. * $P_{adj} < 0.05$, ** $P_{adj} < 0.01$, *** $P_{adj} < 0.001$ one-way ANOVA avec la correction de Tukey.

Un comportement atypique de la souche PA2600 Δ aco::aco a été observé en étudiant les comptages bactériens bruts après 5 jours : en co-culture, la souche restaurée présente bien une croissance similaire à la souche sauvage et augmentée par rapport aux souches mutées, témoignant de l'efficacité de la restauration. En monoculture, elle présente cependant une croissance supérieure à celle de PA2600 sauvage, à l'image de celle observée pour les mutants Δ acoR et Δ aco (Fig. I-10). D'une part, ces dénombrements expliquent pourquoi le taux de survie (obtenu par division de la concentration bactérienne en co-culture par celle en

monoculture) n'est pas restauré chez la souche PA2600 $\Delta\text{aco}::\text{aco}$. D'autre part, il apparaît que toutes les souches mutées (ΔacoR , Δaco et $\Delta\text{aco}::\text{aco}$) présentent une croissance augmentée en monoculture par rapport à la souche d'origine sauvage. Ce phénomène n'a été observé que dans ces conditions de culture prolongées sur 5 jours, les souches mutées et sauvage présentant des cinétiques de croissance similaires sur 24h dans différents milieux (BHI, LB, M63) (résultats non montrés).

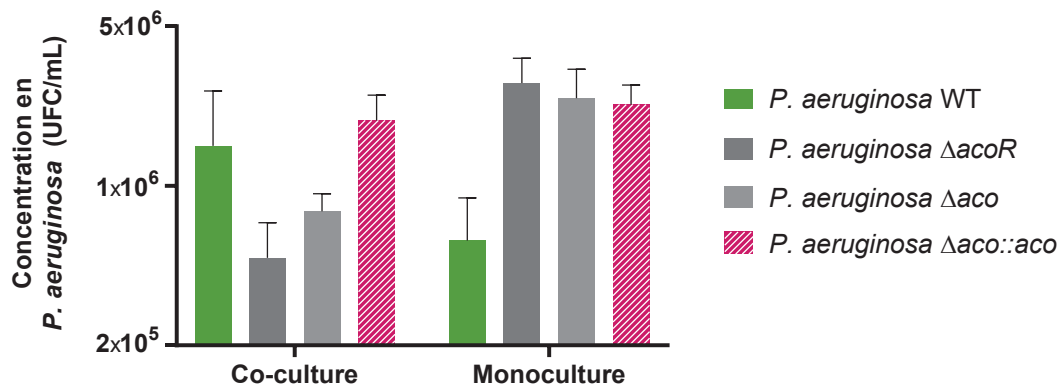


Figure I-10 : Dénombrements bactériens de *P. aeruginosa* après 5 jours de monoculture ou de co-culture avec *S. aureus*. *P. aeruginosa* PA2600 sauvage (WT), ΔacoR , Δaco et $\Delta\text{aco}::\text{aco}$ ont été cultivées en absence ou en présence de *S. aureus* SA2599 pendant 5 jours. Les cultures ont été étalées à J5 sur cétrimide afin de dénombrer *P. aeruginosa*. Ces dénombrements ont été utilisés pour calculer le taux de survie présenté en Figure I-9B.

Les causes exactes de cette différence de croissance demeurent inconnues, mais il est probable qu'elles soient liées au protocole de mutagenèse dirigée employé. Ce dernier repose sur des conjugaisons bactériennes dont les produits sont étalés sur milieu supplémenté en antibiotique. Les mutants sont ensuite sélectionnés à partir d'une colonie isolée sur ce milieu. Les souches de *P. aeruginosa* évoluant très rapidement lors des repiquages successifs, ces étalements sur milieu sélectif peuvent avoir légèrement modifié le comportement de nos isolats, notamment *via* l'acquisition de mutations génétiques ponctuelles.

2 AXE 2 : Facteurs génétiques de *P. aeruginosa* impliqués dans l'établissement de l'état de coexistence

2.1. Introduction

P. aeruginosa est capable de persister durablement dans les poumons des patients atteints de mucoviscidose en s'adaptant génétiquement et phénotypiquement à cet environnement. Plusieurs données suggèrent que cette adaptation favoriserait l'établissement d'une coexistence avec *S. aureus*, notamment par le biais de l'altération génétique de nombreux facteurs de virulence chez *P. aeruginosa* (Cf. Introduction partie 2.3.2.). De plus, l'état de coexistence est observé chez une forte proportion d'isolats cliniques et impacte positivement la survie de *S. aureus* et *P. aeruginosa*, suggérant une sélection de ce phénotype au cours de l'adaptation au milieu pulmonaire (55, 56, 63, 163, 164, 168, 169). Nous avons donc cherché à déterminer les mutations et facteurs génétiques de *P. aeruginosa* impliqués dans la mise en place de la coexistence bactérienne avec *S. aureus* dans ce contexte de co-infection pulmonaire.

Nous avons pour cela étudié les souches de 11 patients co-infectés par *S. aureus* et au moins deux isolats de *P. aeruginosa* présentant des états d'interaction différents : un isolat en compétition et un isolat en coexistence avec la souche de staphylocoque co-isolée (Fig. II-1). Les génomes de ces paires d'isolats de *P. aeruginosa* ont été séquencés afin de comparer, pour chaque patient, les caractéristiques génétiques de l'isolat de coexistence par rapport à l'isolat de compétition. Les résultats indiquent que les deux isolats co-isolés appartiennent au même clone, suggérant l'existence de transitions *in vivo* entre les phénotypes coexistant et compétiteur de *P. aeruginosa*. Cette évolution semble faire intervenir l'opéron *yecS-fliY* et le gène *lasR*, qui ont présenté des mutations non-synonymes chez respectivement 66% et 50% des isolats de coexistence en comparaison aux isolats de compétition. Si le rôle de LasR dans le comportement compétiteur de *P. aeruginosa* est déjà connu (37), l'implication de YecS-FliY dans ce phénotype n'a jamais été décrite jusqu'alors.

Afin de déterminer si ces facteurs étaient spécifiquement altérés *in vivo* et/ou par la présence de *S. aureus*, un protocole d'évolution expérimentale *in vitro* en monoculture et en co-culture avec le staphylocoque a été développé chez deux souches cliniques de *P. aeruginosa* compétitrice et coexistante (Fig. II-1). La coexistence est demeurée stable toute la durée de l'évolution, mais les isolats initialement compétiteurs ont développé un état de coexistence dans 55% des cas. Le séquençage de ces souches évoluées a mis en évidence l'acquisition de mutations non-synonymes dans LasR dans la quasi-totalité de cas, confirmant

le rôle de ce régulateur dans la transition compétition-coexistence. Le comportement coexistant de *P. aeruginosa* apparaît donc favorisé à la fois *in vivo* et *in vitro*, mais *via* des voies mutationnelles diverses probablement induites par des forces sélectives différentes. Ces recherches ont ainsi permis de mieux comprendre la forte fréquence de la coexistence chez les isolats cliniques de *P. aeruginosa* et de caractériser de nouveaux déterminants de cette interaction. Bien que le rôle de LasR dans l'interaction avec *S. aureus* soit bien étudié (37), l'opéron *yecS-fliY* apparaît comme un potentiel facteur de l'établissement de la coexistence *in vivo*, jusqu'alors jamais mis en évidence.

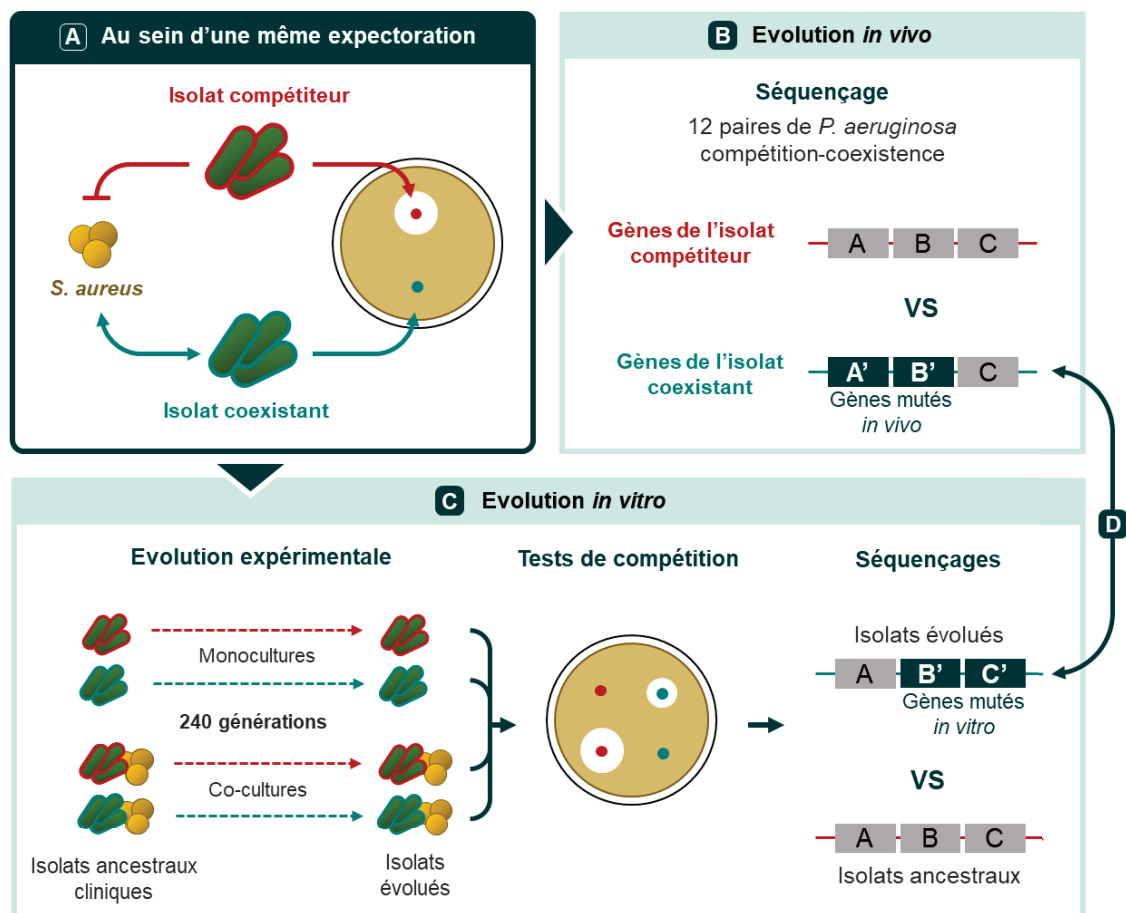


Figure II-1 : Schéma de la méthodologie employée. **A.** Pour 11 patients, une souche de *S. aureus* et au moins deux isolats de *P. aeruginosa* présentant une interaction différente (compétition ou coexistence) avec la souche de *S. aureus* co-isolée ont été isolés d'une même expectoration. **B.** Pour chaque patient, les génomes des isolats de *P. aeruginosa* ont été séquencés et comparés afin de déterminer les gènes mutés dans l'isolat de coexistence. **C.** Une paire d'isolats compétiteur et coexistant de *P. aeruginosa* a été évoluée expérimentalement en monoculture et en co-culture avec *S. aureus*. L'état d'interaction des isolats a été suivi par des tests de compétition sur gélose au cours de l'évolution. A l'issue de l'expérience, les génomes des isolats évolués ont été séquencés et comparés au génome des isolats ancestraux afin de déterminer les mutations impliquées dans la modification de l'état d'interaction. **D.** Les gènes identifiés par les deux approches ont été comparés.

2.1. Publication (en préparation)

Pseudomonas aeruginosa* genetic factors involved in establishment of coexistence interaction state with *Staphylococcus aureus

Laura Camus^{1,*} and Sylvère Bastien^{1,*}, Paul Briaud¹, Anne Doléans-Jordheim^{2,3}, François Vandenesch^{1,2,4} and Karen Moreau^{1#}.

¹ CIRI, Centre International de Recherche en Infectiologie, Université de Lyon, Inserm, U1111, Université Claude Bernard Lyon 1, CNRS, UMR5308, ENS de Lyon, Lyon, France.

² Institut des agents infectieux, Hospices Civils de Lyon, Lyon, France.

³ Bactéries Pathogènes Opportunistes et Environnement, UMR CNRS 5557 Ecologie Microbienne, Université Lyon 1 & VetAgro Sup, Villeurbanne, France.

⁴ Centre National de Référence des Staphylocoques, Hospices Civils de Lyon, Lyon, France

* Both authors contributed equally to this work.

Address correspondence to Karen Moreau, karen.moreau@univ-lyon1.fr – Université Claude Bernard Lyon1 – CIRI – Pathogénie des staphylocoques – 7 rue Guillaume Paradin – 69 008 Lyon - France – tel. : +33 (0)4 78 77 86 57

Supplementary tables are available upon request at karen.moreau@univ-lyon1.fr or loo.camus@gmail.com

ABSTRACT

The genetic adaptation and diversification of *Pseudomonas aeruginosa* in the lungs of Cystic Fibrosis (CF) patients seems to affect its interactions with co-infecting microorganisms such as the highly prevalent *Staphylococcus aureus*. Acute infection strains of *P. aeruginosa* are thus in competition with *S. aureus*, whereas chronic infection strains are able to coexist. However, the genetic factors involved in the establishment of coexistence remain unknown. For 11 CF patients, a pair of *P. aeruginosa* strains isolated from the same sample but presenting the two interaction states with *S. aureus* was sequenced. In parallel, one pair of strains was experimentally evolved *in vitro* in presence or in absence of *S. aureus*.

The two *P. aeruginosa* co-infecting strains were shown to belong to the same clone, indicating that competitive isolates can evolve towards coexistence *in vivo*. This transition was confirmed *in vitro* and was shown to involve several evolutionary paths: mutations in genes related to alginate production (*mucA*, *algG*) and amino acid transport (*yecS*-*fliY*) were specifically identified in clinical coexisting isolates of *P. aeruginosa*, whereas the genetic alteration of quorum-sensing systems (*lasR*) was observed in both clinical and experimentally evolved isolates. These results confirm that the establishment of coexistence with *S. aureus* is linked to the pathoadaptation of *P. aeruginosa* to the CF environment and highlight several of its factors.

INTRODUCTION

Pseudomonas aeruginosa can colonize various ecosystems thanks to the versatility of its genome and its high adaptability. These features are particularly important in Cystic Fibrosis (CF) pulmonary infections during which the bacterium has to cope with antibiotic, oxidative and nutritive stresses (1,2). Despite the hostility of this environment, *P. aeruginosa* is able to persist durably within lungs, making its infections chronic and hardly treatable.

The adaptation of *P. aeruginosa* to the CF lung environment occurs through a rapid accumulation of genetic mutations during the first years of colonization (1,3–7). Small non-synonymous mutations such as single nucleotide polymorphisms (SNPs) and small insertions and deletions (indels) are the most frequent, demonstrating the positive selection mechanisms taking place on the bacterium genome (8–10). However, synonymous and intergenic mutations as well as larger events of deletion/recombination are also documented and can contribute to *P. aeruginosa* adaptive process (8,11–13). The numerous longitudinal studies performed on CF isolates actually depicted a wide variety of mutations in CF-adapted *P. aeruginosa* as a result of the intense diversification promoted by the lung ecosystem (3–6,12,13,8,14–16,9–11). Indeed, the heterogeneity of this environment favors diverse adaptive mechanisms and the emergence of numerous *P. aeruginosa* sub-populations specialized to a particular ecological niche (2,6,7,17).

Despite this diversification, several genes and intergenic regions of *P. aeruginosa* are frequently mutated and considered as pathoadaptive: the genes encoding antibiotic targets and efflux pumps (*gyrAB*, *mex* genes), regulators of biofilm formation (*algU*, *mucA*) and resources acquisition (*cbrAB*), as well as major virulence factors (*pvdS*, *lasR*, *rpoN*, *exsA*) (2,7). As a result, this genic adaptation leads *P. aeruginosa* towards high-persistence phenotypes such as increased antibiotic resistance and biofilm formation, slowed metabolism and decreased virulence compared to reference and non-adapted strains (2,18). Besides improving its resistance to

antimicrobials and the host immune system, this adaptation appears to affect its intra- and interspecies microbial interactions. Indeed, the low-virulence state of *P. aeruginosa* is related to a rewiring of its quorum sensing (QS) systems and a decreased secretion of antimicrobial factors such as the protease LasA, phenazines and HQNO molecules (15,16,19,20). This non-competitive behavior seems to benefit the Gram-positive *Staphylococcus aureus*, another CF pathogen. Indeed, *S. aureus* survival is particularly affected by reference and acute strains of *P. aeruginosa* (21,22). However, several studies described that CF-adapted *P. aeruginosa* isolates with a reduced antagonistic behavior were unable to lyse and inhibit *S. aureus*' growth (22–29). This so-called coexistence interaction state was even shown to promote the survival of both pathogens by increasing their antibiotic resistance and allowing trophic cooperation (24,26,29). In that respect, coexistence between *P. aeruginosa* and *S. aureus* could explain the difficulty to eradicate their infections and thus explain the high proportion of co-infected CF patients (20–50% according to studies) (27,30).

Although coexistence seems to arise from the decreased virulence of *P. aeruginosa* induced by its adaptation in CF lungs, the precise genetic factors involved in the establishment of this interaction state remain unknown. Using genomic sequencing of competitive and coexisting *P. aeruginosa* strains isolated from CF lungs or experimentally evolved, we identified the genetic alterations responsible for the establishment of coexistence. Different mutational pathways leading to coexistence were identified, including non-synonymous mutations in the sequences of the amino acid transporter YecS-FliY and the QS regulator LasR of *P. aeruginosa*.

MATERIAL AND METHODS

Bacterial strains

Bacterial strains used in this study and their morphological features (mucoidy, pigmentation, metallic sheen) are listed in Table S1. *S. aureus* and *P. aeruginosa* CF clinical strains were isolated by the Infectious Agents

Institute (IAI) from sputa of patients monitored in the two CF centres of Lyon (Hospices Civils de Lyon (HCL)). For 11 different patients, one *S. aureus* strain and 2 or 3 *P. aeruginosa* strains were isolated from the same sputum sample. These patients were co-infected by *P. aeruginosa* and *S. aureus* for 24 to 66 months (Table S1). All the methods were carried out in accordance with relevant French guidelines and regulations. This study was approved by the Ethics Committee of the HCL and registered under CNIL No 17-216. All the patients were informed of the study and consented to the use of their data.

Interaction state was determined for each *S. aureus*-*P. aeruginosa* pair by growth inhibition tests on Tryptic Soy Agar (TSA) and in liquid co-cultures in Brain-Heart Infusion (BHI) as described previously (26,29). Coexistence was characterized by: (i) the absence of inhibition halo on agar tests, and (ii) similar growth in mono and co-cultures for 8 hours (26,29).

Experimental evolution

The experimental evolution of *P. aeruginosa* strains PA190A (competitive: Cp) and PA190B (coexisting: Cx) was conducted through cross-streak assays TSA during approximately 240 generations. The number of generations was determined by suspending the streak before and after the step of 24h incubation in sterile medium and plating on TSA. As schematized in Figure S1, *P. aeruginosa* was cultivated in monoculture in a vertical streak, or in co-culture by crossing the *P. aeruginosa* streak by a streak of *S. aureus* SA190 (Fig. S1A). The resulting plate was incubated 24h à 37°C. Each day during 30 days, subcultures were performed as following: (i) a fresh streak of the ancestral *S. aureus* SA190 strain was spread on a new TSA plate and (ii) the *P. aeruginosa* streaks were subcultured from the monoculture streak or the center of the co-culture cross-streak (Fig. S1B). Every five days, the evolving *P. aeruginosa* were isolated from the monoculture streak and the center of the co-culture cross-streak by plating on Cetrimide agar. The interaction state of the evolving *P. aeruginosa* was then tested with the ancestral *S. aureus* SA190 strain by

growth inhibition tests on plates as described previously (26,29) (Fig. S1C). At the end of the experiment, the evolved *P. aeruginosa* strains were isolated and conserved at -80°C for phenotypic characterization and sequencings. The experiment was performed in 10 replicates in order to obtain 40 evolved *P. aeruginosa* strains: 10 evolved in monoculture (M1-M10) and 10 evolved in co-culture (C1-C10) from both of the ancestral strains PA190A (Cp) and PA190B (Cx).

Sequencing and bioinformatics

The genomic DNA of the 23 *P. aeruginosa* clinical CF strains (Table S1) and the 20 strains evolved from the ancestral PA190A strain (Table S2) were sequenced using Illumina Hiseq, Miseq or Nanopore as indicated in Table S2. For Hiseq sequencing, genomic DNA was extracted using the DNA Isolation Kit (MO BIO). Library preparation was performed with the Nextera XT DNA sample preparation kit (Illumina) and index kit (Illumina). Library validation was conducted on a 2100 Bioanalyzer (Agilent Technologies) to control the distribution of fragmented DNA. WGS was performed with an Illumina HiSeq (Illumina) to generate 150-bp paired end reads. Genomes were sequenced with an average coverage of 130x. For Miseq sequencing, genomic DNA was extracted using the NucleoSpin Microbial DNA Mini kit (Macherey-Nagel) and treated with RNase A (Qiagen) following the manufacturers' recommendations. Whole genome sequencing was then performed by Genewiz to generate 250pb paired end reads. For Nanopore sequencing of PA190A, genomic DNA was extracted using the DNA Isolation Kit (MO BIO), prepared using the kits SQK-RBK004 (barcoding) and EXP-FLP001 (priming) and sequenced using the flowcell FLO-MIN106 following the manufacturers' recommendations.

Adapters and other illumina-specific sequences have been cut from the reads for each raw data. An additional trimming step was performed using Trimmomatic v0.36 (31) and a sliding window with a 20 average quality threshold. Data quality was checked through FastQC v0.11.9 (S. Andrews, 2010. FastQC: a quality control tool for high throughput sequence data. Available online at:

<http://www.bioinformatics.babraham.ac.uk/projects/fastqc>) and a global report was generated by MultiQC v1.8. Assemblies have been performed with SPAdes v3.13.0 (32) and assembly quality control has been performed using Quast v4.6.1 (33). Total genome length was determined by adding the length of all contigs. Genome annotation has been processed through Prokka v1.14.5 (34), using PAO1 genbank file (Refseq NC_02516.2; metadata version DB19.1) as first protein database in complement with Refseq database.

For the 23 *P. aeruginosa* clinical CF isolates (Table S2A), each trimmed data set was firstly mapped on PAO1 genome. A phylogenetic analysis was achieved using a maximum likelihood approximation based on the SNPs identified through the conserved core genome of the 23 *P. aeruginosa* strains. For analysis of gene presence/absence, proteins from all samples were clustered with a threshold of 95% of similarity in order to set one label for each protein's group using ROARY(35). If gene correspond to a PAO1 gene, the PAO1 annotation was used; otherwise a group number was attributed. Then, each coexistence trimmed data set was mapped on the assembled genome of the competition strain. Variant calling analyses were processed by Snippy v4.4.5 (Seemann T, (2015). Available online at: <https://github.com/tseemann/snippy>) and results were separated in synonymous, non-synonymous and intergenic regions. Each mutation was associated either with the

impacted gene or with the two genes surrounding the impacted intergenic region. A final matrix was manually constructed which sums up the presence of at least one mutation in each gene/intergenic region.

For strains experimentally evolved from PA190A, each trimmed data set was mapped on PA190A complete genome (Table S2B). For this purpose, PA190A's genome was circularized with a specific assembly step using both Illumina and Nanopore reads using Unicycler v0.4.8 (36). Annotation and variant calling analyses were performed as previously described.

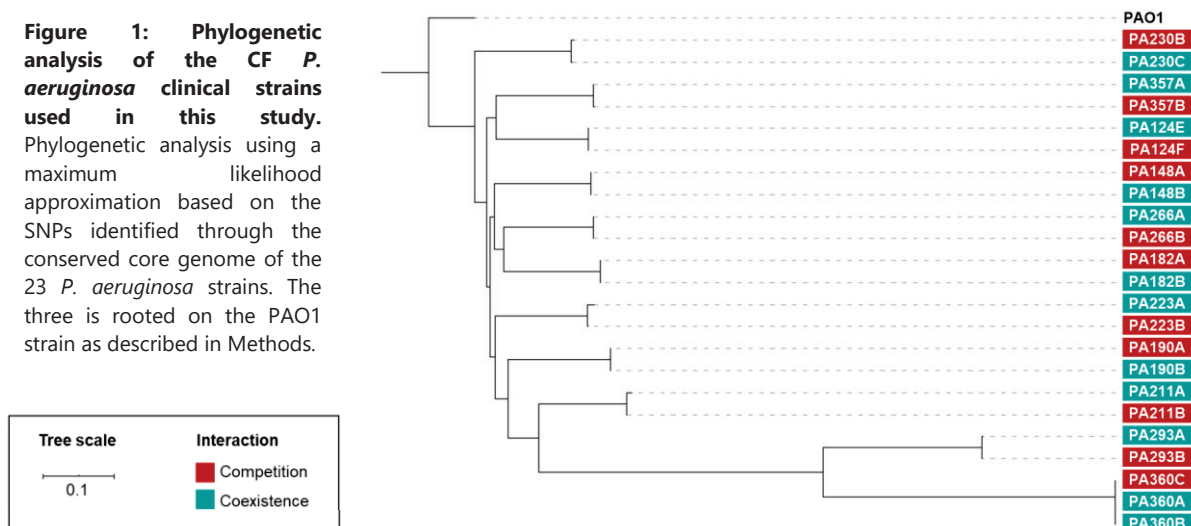
RESULTS

In vivo, coexistence is associated with frequent mutations in *lasR*, *algG* and *yecS-fltY* genes

In order to study the genomic features related to the coexistence interaction state, we studied eleven sets of *S. aureus* and *P. aeruginosa* strains isolated from eleven CF patients co-infected since at least 24 months. Each set was comprised of one *S. aureus* strain and at least two *P. aeruginosa* isolates presenting a different interaction state with the co-isolated *Staphylococcus*, as determined by competition tests (Table S1). The twelve coexisting and eleven competitive isolates of *P. aeruginosa* were sequenced and their genomes

Figure 1: Phylogenetic analysis of the CF *P. aeruginosa* clinical strains used in this study.

Phylogenetic analysis using a maximum likelihood approximation based on the SNPs identified through the conserved core genome of the 23 *P. aeruginosa* strains. The tree is rooted on the PAO1 strain as described in Methods.



were compared to the PAO1 reference genome (Table S2A). The competitive and coexisting *P. aeruginosa* isolates recovered from a same patient appeared to be clonally related as they clustered together and shared a specific common ancestor (Fig. 1).

We hypothesized that the competitive isolate was the ancestor of the coexisting isolate as previously suggested (21,22). In accordance with that, we used the competitive isolates as a reference to determine the genomic specificities of each coexisting isolate. In comparison to their related competitive isolate, all coexisting *P. aeruginosa* presented a reduced genome size (Table S2A). Four coexisting isolates (PA190B, PA293A, PA360A and PA360B) presented large deletion events of 57kb to 191kb (Fig. 2). The other eight

coexisting isolates presented smaller deletions of less than 15kb. We cannot exclude that these short deletions can correspond to regions that have not been sequenced. However, in a first approach, we sought to determine the genomic specificities of coexisting isolates using a presence/absence gene analysis within each *P. aeruginosa* pair. Depending on pairs, 19 to 484 genes were specific to the competitive isolate, and 6 to 415 were only detected in the coexisting isolate (Fig. S2) (Table S3). For most pairs (9/12), more genes were specific to the competitive *P. aeruginosa* than for the related coexisting isolate, supporting the hypothesis of deletions events throughout *P. aeruginosa* evolution and the establishment of coexistence. As a result, the greatest number of competition-specific genes was identified in the PA190,

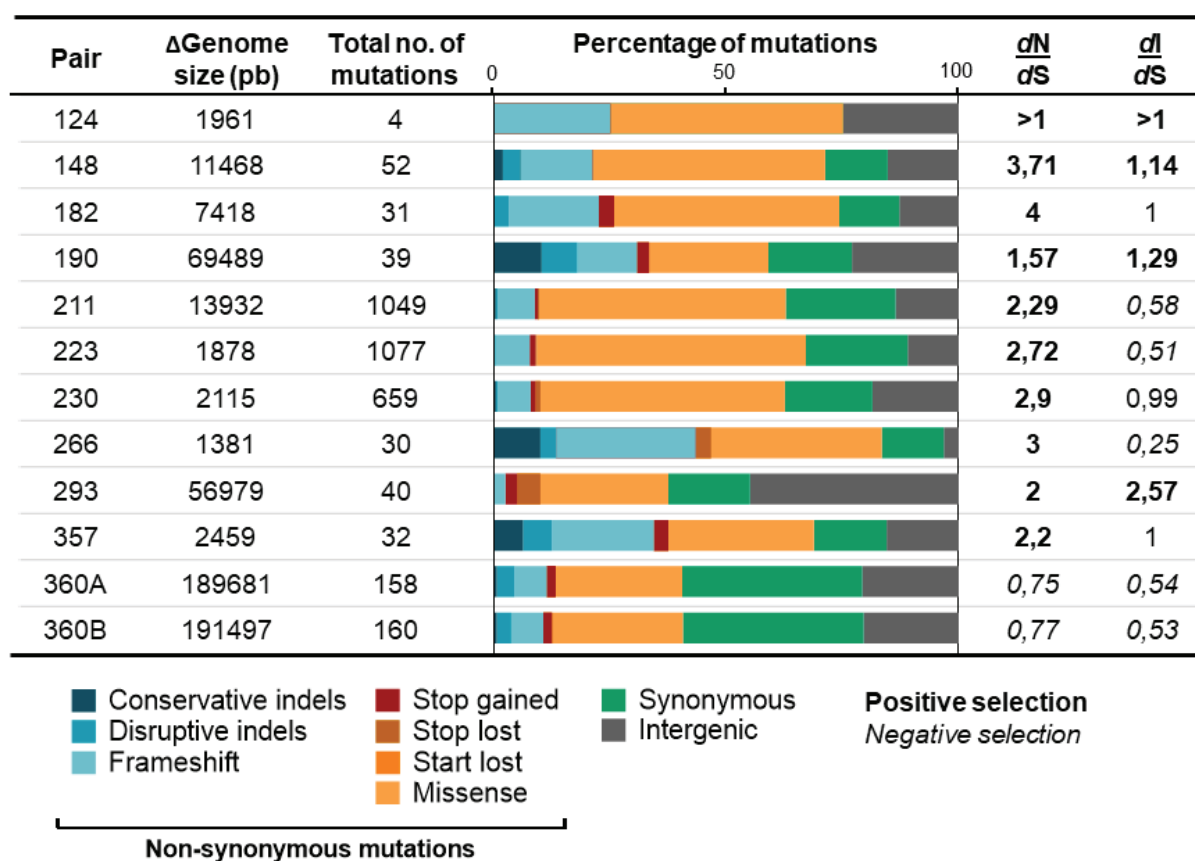


Figure 2: Number and types of mutations identified in clinical *P. aeruginosa* coexisting isolates in comparison to competitive ones. For each pair or trio co-isolated strains from CF patients (Table S1), the difference in genome size was calculated by deducting the genome size of the coexisting isolate from the genome of the competitive isolate. The genome of the coexisting isolate was then mapped on the genome of the competitive isolate to determine the genetic alterations: insertions and deletions (indels) and frameshifts (blue shades), non-synonymous SNPs (orange shades), synonymous SNPs (green) and intergenic mutations (grey). The dN/dS ratio was calculated by dividing the number of non-synonymous SNPs by the number of synonymous SNPs. The dI/dS ratio was calculated by dividing the number of intergenic mutations by the number of synonymous SNPs. Sequencing data information are detailed in Table S2. The complete lists of mutations are shown in tables S3 to S5.

PA293, PA360A and PA360B pairs, corresponding to the coexisting strains exhibiting the greatest genome size reduction. (Fig. S2). Five genes were found to be deleted only in coexisting isolates: *exaC*, *group_133*, *group_1972*, *group_3055* and *group_881*. However, these deletions events concerned only 4 out of 12 pairs. In the same way, the gene *narK1* appeared to be coexistence-specific in 4 pairs (Fig. S2). These results could suggest that these genes are specific of an interaction state. However, it concerns only a few strains and no marked profile characterizing either interaction state could be highlighted. Of note, the virulence-associated genes *phzD1* and *phzC1* (phenazine biosynthesis) were absent in 4 and 3 coexisting isolates respectively, as well as *lasR* (QS regulator) was not detected in 2 coexisting *P. aeruginosa*. (Fig. S2).

We then aimed to identify smaller mutational events (ie. SNPs, insertions and deletions) in coexisting isolates in comparison to competitive ones. The number of such events was highly variable, ranging from 4 to 1077 mutations for PA124E and PA223A, respectively (Fig. 2). The coexisting strains were mostly affected by missense mutations, but they also all presented frameshifts and intergenic mutations with respect to their competitive counterpart. The distribution of mutations was nonetheless heterogeneous and some coexisting strains presented a higher proportion of frameshifts (PA266A) or intergenic mutations (PA293A), whereas others were not affected by synonymous mutations (PA124E). Interestingly, synonymous mutations were less frequent than non-synonymous mutations in 10 out of the 12 coexisting isolates, allowing the calculation of a dN/dS ratio over one (Fig. 2). This suggests that positive selection mechanisms occurred within coding regions of coexisting isolates in comparison to their competitive ancestor. The selective mechanisms operating on intergenic regions were assessed by calculating the dI/dS ratio, but no clear profile could be highlighted as negative and positive selections were observed for 6 and 4 strains respectively (Fig. 2). Altogether, these results suggest that coexisting isolates evolved from a competitive ancestor by positive selection within coding regions.

We thus determined the genes that were non-synonymously mutated in each coexisting *P. aeruginosa* with respect to its relative competitive isolate (Fig. 3). We identified 1530 genes impacted by non-synonymous mutations in the twelve coexisting strains (Table S4); 1269 of these genes were mutated in only one strain (Fig. S3A). Interestingly, numerous genes of *P. aeruginosa* described as pathoadaptive in the CF environment were mutated in several coexisting isolates in comparison to competitive ones, such as the *mex* genes, *lasR*, *mucA*, *pvdS*, *gyrAB*, *pmrAB*, *pagL*, *rpoN*, or *nfxB* (Fig. 3).

Few genes appear to be frequently mutated in coexisting isolates: the genes encoding the alginate-c5-mannuronan-epimerase AlgG involved in alginate biosynthesis (mutated in 5/12 isolates) and the QS regulator LasR (6/12). The *lasR* gene was also totally absent in two other coexisting isolates (PA360A, PA360B), making this gene altered by non-synonymous mutations or deletion in seven coexisting *P. aeruginosa*. Finally, the L-cysteine transporter YecS (7/12) was the most non-synonymously mutated gene in coexisting strains. Interestingly, the gene *fliY*, co-transcribed with *yecS*, also appeared mutated in 2 coexisting strains (Fig. 3). As one of them was already mutated in *yecS*, it implies that the *yecS-fliY* operon was non-synonymously mutated in 8/12 cases (66,7%). In these 8 strains, a total of 11 mutations was identified in *yecS-fliY*, making this operon the most mutated coding region in coexisting strains in comparison to competitive *P. aeruginosa*. It is also noteworthy that 9 out of the 11 mutations identified had a unique position, excluding the hypothesis of a precise mutational hotspot within this operon.

Using a similar approach, we investigated the genomic regions of coexisting strains impacted by synonymous mutations and intergenic mutations. Less alterations were identified with a total of 564 genes impacted by synonymous SNPs in coexisting *P. aeruginosa* (Table S5). These genes were synonymously mutated in only one to three isolates; the genes *group_1026*, *hscA* and *magD* were thus identified as synonymously mutated in three coexisting isolates (Fig. S3B). Four-hundred

Non-synonymously mutated genes			Mutated coexisting strains											
Gene names or PAO1 locci	No. of genes	No. of strains	PA124E	PA148B	PA182B	PA190B	PA211A	PA223A	PA230C	PA266A	PA293A	PA357A	PA360A	PA360B
<i>yecS</i>	1	7												
<i>lasR</i>	1	6							Cx	Cx			Cp	Cp
<i>algG</i>	1	5												
<i>mucA</i>	1	4										Cp		
PA0429	1	4												
<i>mexB_1</i>	1	4				Cx			Cx					
<i>gyrA</i>	1	4												
<i>mexY</i>	1	4												
PA4398	1	3												
<i>cyaB</i>	1	3	Cp					Cx						
<i>pvdS</i>	1	3												
<i>gyrB</i>	1	3												
PA4586, <i>nfxB</i> , <i>narX</i> , PA1623	4	3												
<i>pilR</i>	1	3												
<i>pchA</i>	1	3												
<i>pmrB</i>	1	3												
<i>pslC</i> , PA0670, <i>rpoC</i> , <i>rpoN</i>	4	3												
<i>fusA1</i>	1	3												
<i>gidA</i>	1	3												
<i>pelA</i> , PA5234	2	3												
PA2418, <i>pqqF</i>	2	3												
<i>cafA</i>	1	3												
<i>pml</i> , <i>pagL</i>	2	3												
<i>kdpD</i>	1	3												
List in table S4	14	3												
<i>fljY</i>	1	2												
PA5438	1	2					Cp	Cx						
<i>accD</i> , <i>pmrA</i>	2	2												
List in table S4	27	2												
<i>rpoA</i>	1	2												
<i>ptsP</i>	1	2												
<i>dnaX</i>	1	2												
<i>birA</i> , <i>mexB</i> , <i>opgH</i>	3	2												
<i>gltA</i> , <i>pheT</i>	2	2												
<i>aceA</i> , <i>waaA</i>	2	2												
<i>accC</i> , PA3110, <i>gcl</i> , PA2049, <i>yerD</i>	5	2												
PA0484, PA4163	2	2												
<i>lcp</i>	1	2												
PA0151, <i>ylcC</i> , PA1765, <i>mexS</i>	4	2												
List in table S4	54	2												
<i>mucD</i> , PA2078	2	2												
<i>yrbD</i>	1	2												
<i>fadD1</i> , <i>gltB</i> , <i>bifA</i> , group_2257, <i>pslE</i>	5	2												
PA0383, <i>lhr</i>	2	2												
List in table S4	40	2												
List in table S4	57	2												
Total number of non-synonymous mutations in comparison to the corresponding competitive strain			3	36	22	23	592	638	391	24	14	22	43	44

Figure 3: Genes impacted by non-synonymous mutations in coexisting *P. aeruginosa* isolates in comparison to competitive ones. The genomes of 11 pairs or trio of coexisting and competitive *P. aeruginosa* strains were sequenced. For each pair or trio, the genome of the coexisting isolate was mapped on the genome of the competitive isolate to determine the non-synonymous mutations. Black dots indicate mutation in the coexisting isolate. Non-synonymous mutations identified in only one strain are shown in Figure S3. The complete list of non-synonymous mutations is shown in Table S4. Light grey cases indicate genes that were identified only in competitive (Cp) or coexisting (Cx) strains within a pair by the gene presence/absence analysis, as detailed in Figure S2.

and fifty-five intergenic regions were identified as mutated in coexisting *P. aeruginosa* in comparison to competitive ones (Table S6A). The genes surrounding 91 of these intergenic regions could not be annotated due to a lack of coverage on the sequencing contig extremities (Table S6B). Seventeen non-coding regions were mutated in a maximum of two coexisting

P. aeruginosa, including the *pilI*~*pilH* and the *algQ*~*dsbH* intergenic regions (Fig. S3C). Thus, analyses of synonymous and intergenic mutations did not reveal any evidence of convergent mutational patterns within coexisting strains of *P. aeruginosa*. These results, along with the high number of non-synonymous mutations, suggest that

coexistence is less likely to establish through synonymous and intergenic mutations. Moreover, the genes identified as frequently non-synonymously mutated were not impacted by synonymous mutations, confirming the positive selection mechanisms occurring within these genes.

The coexisting interaction is promoted by *in vitro* evolution of *P. aeruginosa*

We then employed an approach of experimental evolution to address if transitions between competitive and coexisting interaction statuses can occur spontaneously in *P. aeruginosa* and if *S. aureus* presence can affect these transitions. The competitive strain PA190A and its related coexisting clone PA190B, both co-isolated from a *P. aeruginosa*-*S. aureus* co-infected CF patient, were thus evolved in absence or in presence of *S. aureus* SA190 for 30 days (approximately 240 generations) using cross-streak assay on plates (Fig. S1). Each five days, the evolving *P. aeruginosa* were isolated and their interaction status with SA190 was determined (Fig. 4A). The evolution process did not importantly affect the interaction state of the isolates derived from

the coexisting ancestor PA190B, as 95% (19/20) of them conserved a coexisting behavior with SA190 at the end of the experiment. Nonetheless, several isolates transiently harbored a mild competitive behavior (inhibition disc of 1-3mm) throughout the evolution, lowering the proportion of coexisting isolates to 80% (16/20) after 5, 10 and 25 days (Fig. 4A) (Table S7A). We hypothesized that this non-fixed competitive behavior may be related to a heterogeneity of the evolving *P. aeruginosa* population, containing both competitive and coexisting variants whose proportions varied during our experiment. *S. aureus* presence did not seem to affect this phenomenon, as it was observed for *P. aeruginosa* evolving in both monoculture and co-culture (Table S7A).

Interestingly, several isolates evolving from the competitive PA190A developed a forthright coexisting interaction with *S. aureus* (no inhibition halo) from the tenth day of the experiment (3/20 evolving isolates). Coexistence was then observed in an increasing number of isolates, reaching 55% of the isolates (11/20) at the end of the experiment. Here again, no clear effect of *S. aureus* presence could be highlighted, as *P.*

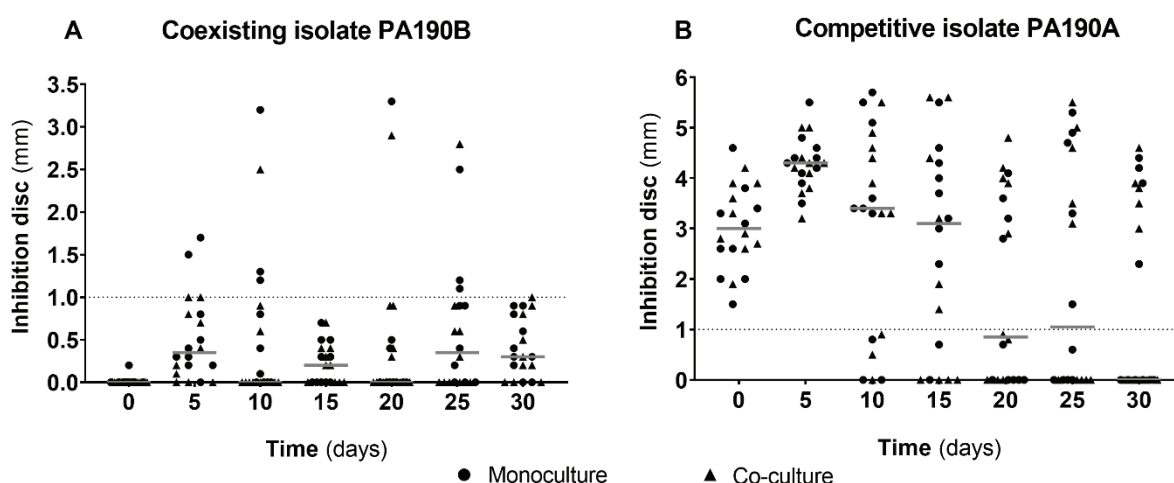


Figure 4: *S. aureus* growth inhibition during the experimental evolution of *P. aeruginosa*. The ancestral strains PA190B (coexisting, **A**) and PA190A (competitive, **B**) were experimentally evolved in monoculture (circles) or in co-culture with *S. aureus* SA190 (triangles) for 30 days (Fig. S1). Every five days, the evolving *P. aeruginosa* strains were isolated and their interaction state with *S. aureus* SA190 was determined by competition tests on plates. Points represent the size of the inhibition halo of *S. aureus* for evolved isolates from PA190B (**A**) or from PA190A (**B**). Grey bars represent the median disc size. The dotted line of 1mm disc size defines the threshold between coexistence and competition. The numeric values are given in Table S7.

aeruginosa developed a coexisting behavior during evolution in both monoculture (6/11) and co-culture (5/11) conditions (Fig. 4B) (Table S7B). However, it is noteworthy that once established, this coexisting interaction remained stable during all the evolution process. The nine other evolving isolates retained a competitive behavior similar to their competitive ancestor PA190A (inhibition disc of 3-4mm) (Fig. 4B) (Table S7B).

In order to determine the genetic factors involved in the establishment of coexistence, we sequenced the genomes of the twenty *P. aeruginosa* derived from the competitive PA190A. Regarding the size of the genomes (Table S2), we observed that all evolved strains presented a genome that was slightly longer than the original one. In comparison to the original isolate, the evolved isolates presented a total of 33 unique mutations affecting 16 different genes and one intergenic region. The intragenic mutations were all non-synonymous and included conservative and disruptive indels, frameshifts, and stop- or missense-inducing SNPs (Fig. 5A). While all these types of non-synonymous mutations could be identified in the isolates evolved in monoculture, the isolates evolved in co-culture with *S. aureus* were only impacted by frameshifts and missense mutations (Fig. 5A). These results suggest that *S. aureus* presence might influence the type of mutations fixed in *P. aeruginosa* genome, although co-culture did not have any effect of the establishment of coexistence during our experiment (Fig. 4B). Concerning the number of mutations, the genomes of isolates that developed a coexisting interaction were more mutated (2.72 mutations per isolate) than those which remained in competition (1.77 mutations per isolate) (Fig. 5A), indicating that the development of coexistence was favored by an accumulation of genetic alterations in *P. aeruginosa* genome.

The most frequently mutated gene in evolved isolates was *dnpA*, a gene coding a de-N-acetylase and belonging to the *wap* gene cluster involved in lipopolysaccharide (LPS) biosynthesis (Fig. 5B) (37,38). Thirteen evolved isolates (65%) were thus impacted by frameshifts in *dnpA*; twelve of these strains

presented an identical 21bp deletion at the gene position 703/1419, suggesting that this position constitutes a mutational hotspot in *P. aeruginosa* (Fig. 5B) (Table S8). Interestingly, other genes belonging to the *wap* cluster (*wapR*, *ssg* and *wapH*) were also non-synonymously mutated in the remaining isolates, making this cluster mutated in a total of 17 isolates out of the 20 sequenced. It thus appears that the alteration of the Wap LPS biosynthesis pathway is promoted during *in vitro* evolution of *P. aeruginosa*. As both evolved competitive and coexisting isolates were impacted, this alteration was probably not responsible for the establishment of coexistence with *S. aureus* (Fig. 5B).

The second most mutated gene was the QS regulator *lasR*, which presented single but different missense SNPs in 81.8% (9/11) of the evolved coexisting isolates (Fig. 5B) (Table S8). A particular green pigmentation and sheen coverage characteristic of *lasR* loss-of-function mutations were observed for these isolates (Table S1B) (39). None of the evolved competitive *P. aeruginosa* presented such mutation, indicating that the genetic alteration of *lasR* was most likely responsible for the establishment of coexistence *in vitro*. It nonetheless doesn't exclude that other mutational pathways have similar consequences. Indeed, two isolates that have evolved towards coexistence did not present any *lasR* alteration but mutations in *ptsP*, *pqsR* and *clpA* (isolate M1) or *aat*, *yfhD* and *mifS~poxA* (isolate M4) (Fig. 5B). Although the role of *pqsR* and the *Pseudomonas* Quinolone Signal (PQS) system in the anti-staphylococcal behavior of *P. aeruginosa* is well-described (21), the contribution of these other genes and intergenic regions in the establishment of coexistence is yet to be assessed.

We finally studied the relationship between the mutational profiles induced by evolution of *P. aeruginosa* *in vivo* or *in vitro*. To this end, we compared the mutations in (i) the CF coexisting isolate PA190B and (ii) the *P. aeruginosa* isolates that experimentally evolved from competition to coexistence, in both cases identified with respect to the competitive CF strain PA190A. None of the 39 mutated genes in PA190B appeared to be mutated in *P.*

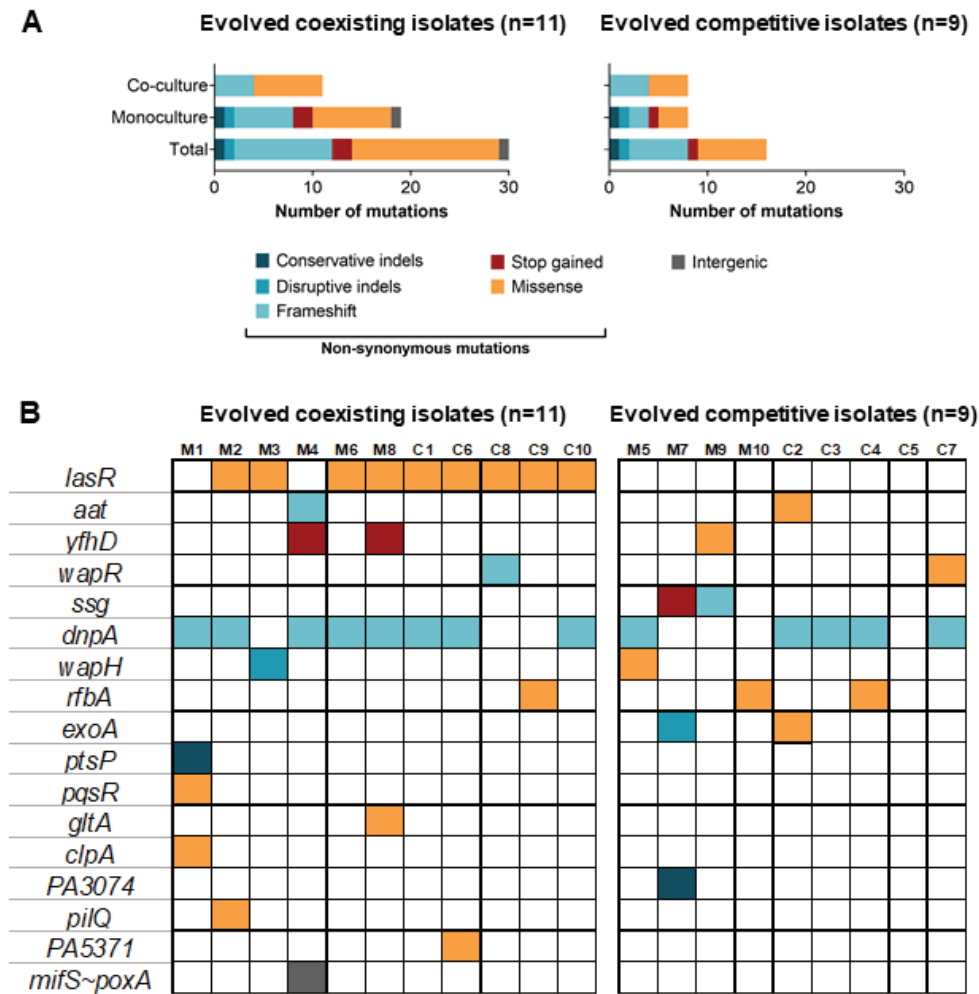


Figure 5: Number and types of mutations identified in the evolved isolates arising from PA190A competitive strain.

The ancestral strain PA190A (competitive) was experimentally evolved in monoculture or in co-culture with *S. aureus* SA190 for 30 days (Fig. S1). At the end of the experiment, the 20 evolved *P. aeruginosa* were isolated and their interaction state with *S. aureus* SA190 was determined by competition tests on plates. Eleven presented a coexistence phenotype while nine conserved a competitive phenotype. **A.** Their genomes were sequenced and compared to the ancestral PA190A strain to determine the genetic alterations: number and repartition of insertions and deletions (indels) and frameshifts (blue shades), non-synonymous SNPs (orange shades) and intergenic mutations (grey) are presented for coexisting (left) and competitive (right) evolved isolates. **B.** Squares represent the different mutations identified for each isolate evolved in monoculture (M), in co-culture (C) for coexisting (left) and competitive (right) evolved isolates. Supplementary information on genes and mutations is detailed in Table S8.

aeruginosa isolates evolved *in vitro* (Table S8). This indicates that the selective forces induced by *in vivo* and *in vitro* conditions are different, not surprisingly, and drive *P. aeruginosa* towards divergent mutational pathways. However, these different evolutionary trajectories both converged to a coexisting behavior with *S. aureus*, confirming the existence of several genes involved in its establishment of coexistence in this strain.

DISCUSSION AND PERSPECTIVES

The aim of this study was to identify the genetic factors of *P. aeruginosa* involved in the establishment of the coexistence state with *S. aureus*. Several studies suggest that coexisting strains arise from the evolution of competitive strains. Indeed, *P. aeruginosa* strains isolated from early infection outcompete *S. aureus*, whereas strains isolated from chronic infection

appear less aggressive and can be co-cultivated with *S. aureus* (22,23). However, there is no direct evidence of this transition.

Several elements of our study tend to confirm that coexisting strains of *P. aeruginosa* are derived from competitive strains. First, in our experimental evolution protocol, the coexistence phenotype appears relatively stable since the phenotype of the PA190B coexistence isolate did not drastically change during the experiment (Fig. 5A). In contrast, the competitive PA190A isolate spontaneously evolved towards a coexistence phenotype in more than half of the cases. This phenotype remained stable once established (Fig. 5B). The genomic comparison of competitive and coexisting strains from CF patients brought out two other important features: (i) positive selection mechanism occurs within genomes of coexisting isolates since they accumulate non-synonymous mutations in comparison to competitive ones and (ii) numerous of these non-synonymous mutations affect so-called "pathoadaptive" genes in the coexisting strains (Fig. 3). Indeed, the genetic alteration of the genes from the *mex* family, *lasR*, *mucA*, *algG*, *pvdS*, *gyrAB*, *pmrAB*, *pagL*, *rpoN*, or *nfxB* have been described as resulting from the adaptation of *P. aeruginosa* to the pulmonary environment (2,7).

Several of these mutations may contribute to the change in interaction with *S. aureus*, and more specifically those affecting genes involved in alginate production and QS activity of *P. aeruginosa*. The anti-sigma factor MucA acts as a repressor of alginate production since it sequesters the σ^{22} factor, activator of the *alg* operon involved in alginate biosynthesis. Inactivation of MucA through mutations thus unleashes the expression of *alg* genes, resulting in an over-production of the exopolysaccharide alginate and induction of the mucoid phenotype of *P. aeruginosa*. Interestingly, alginate was shown to decrease the production of several anti-staphylococcal factors such as the siderophores pyoverdine and pyocheline, rhamnolipids and HQNO (25,40). As a result, *mucA*-deficient and thus mucoid isolates of *P. aeruginosa* appear less competitive towards *S. aureus* (25). Seventy-five percent of coexisting strains isolated from

CF patients were impacted by either mutation or deletion in *mucA* and/or *algG* in our study (Fig. 3) and might thus be able to coexist with *S. aureus* through an overproduction of alginate. However, the consequences of the identified mutations on the functions of *mucA* and *algG* and more broadly on alginate production remain unclear, since the affected strains did not present a particular mucoid phenotype (Table S1A). A more precise quantification and comparison of alginate production of our different strains is thus necessary to address this question. Whether the deletion of *algG* alters the competitive behavior of *P. aeruginosa* in co-culture with *S. aureus* in the same manner than the *mucA* alteration is also yet to be determined (25).

Besides alginate production, the impairment of QS activities through *lasR* alteration is probably involved in the establishment of coexistence between *P. aeruginosa* and *S. aureus*. Indeed, mutations in the coding sequence of LasR, the major regulator of the QS system and virulence of *P. aeruginosa*, causes a decrease in the production of major anti-staphylococcal factors such as the protease LasA, phenazines and HQNO (21). In connection with this, seven of the 12 coexisting strains isolated from CF patients presented an alteration of the *lasR* gene, by either non-synonymous mutation or deletion (Fig. 3) (Fig. S2). Similarly, in our approach of *in vitro* experimental evolution, the transition to the coexistence state could be explained for almost all strains by an alteration of genes from the QS system. Out of the 11 isolates that developed a coexisting interaction with *S. aureus*, only one isolate did not present mutations in any QS-related genes; the origin of the transition to coexistence for this isolate remains to be determined (Fig. 5B). Among the 10 remaining, nine harbored a missense mutation in the *lasR* gene, and the last one isolate was non-synonymously mutated in the coding sequence of PqsR, the regulator of the PQS system (21) (Fig. 5B). However, our analyzes do not provide any direct evidence that these LasR and PqsR alterations are responsible for the establishment of coexistence through a down-production of *P. aeruginosa* anti-staphylococcal factors. This hypothesis could be tested by quantifying and

comparing the expression of these factors in the competitive and coexistence strains, by a proteomic approach for example. Furthermore, it would be necessary to generate isogenic mutants with the observed *lasR* mutations to verify their impact on the competitive behavior of *P. aeruginosa* towards *S. aureus*.

Although the results of both of our approaches support a relationship between QS and coexistence, it is noteworthy that the coexisting strains from CF patients did not present the same profile as the strains evolved *in vitro* (Table S8). We were not able to experimentally reproduce the same mutations as it seems to take place in CF patients. Indeed, our *in vitro* experimental conditions are obviously simplistic and do not reflect the environmental conditions of the CF lung such as the nutrient access, oxygenation or inflammatory response (1,2). The heterogeneity of the lung ecosystem is also a condition that is hardly reproducible *in vitro*, but this parameter importantly impacts bacterial adaptation by generating specialized subpopulation of *P. aeruginosa* with different genotypes and phenotypes (2,6,17). Such diversification is certainly at the origin of the co-isolation of both competitive and coexisting *P. aeruginosa* isolates from a same sputum sample but hampers the identification of convergent mutational patterns. Hence, it is possible that the genetic alterations of alginate production and QS activities constitute divergent evolutionary paths leading to a similar phenotype, coexistence. In contrast, our controlled and homogeneous *in vitro* conditions generated only one major road to coexistence involving the alteration of LasR. Probably because of these *in vitro* conditions, many potential coexistence factors have only been revealed by genomic comparisons of clinical strains of *P. aeruginosa* (Fig. 3). It is thus important to develop an experimental procedure that mimics as much as possible the *in vivo* conditions in order to study these evolutionary events more precisely.

Among the genes specifically impacted in clinical isolates of coexistence features the *yecS-fliY* operon, mutated in 66.7% of cases (Fig. 3). Little is known about the function of

these two genes apart from their genomic annotation as L-cysteine transporters of ABC system. The construction of *yecS-fliY* mutants and their cultivation in co-culture thus appears essential to decipher the role of this operon in the interaction between *P. aeruginosa* and *S. aureus*. Interestingly, the transport and the metabolism of amino acids are particularly affected during both coexistence with *S. aureus* (29) and *P. aeruginosa* adaptation within lungs (18). Moreover, the *yecS* gene has been identified as non-synonymously mutated in two longitudinal genomic studies of *P. aeruginosa* CF isolates (8,14). Like *lasR*, *algG* or *mucaA*, alteration of *yecS* might thus contribute to *P. aeruginosa* pathoadaptation within the CF lung environment and interaction with *S. aureus*.

Altogether, our results indicate that the state of coexistence seems to arise mainly from the pathoadaptive mutations induced by the evolution of *P. aeruginosa* within the pulmonary environment. One might thus wonder whether this state of coexistence is a side effect of *P. aeruginosa* adaptation, or actually positively selected within CF lungs. Up until now, the main selective forces considered to drive *P. aeruginosa* adaptation were the presence of the host-immune system or abiotic forces such as antibiotic treatments, oxidative or nutritive stresses (1,2,4). However, the presence of other microorganisms and in particular *S. aureus* could influence this adaptation, by either influencing the local conditions or directly interacting with *P. aeruginosa*. In a previous study, we demonstrated that the two bacterial species set up a trophic cooperation via the acetoin (29). In this context, acetoin production by *S. aureus* and catabolism by *P. aeruginosa* were both more efficient for coexisting isolates in comparison to competitive ones. This phenomenon underscores a co-evolution process towards adjusted interspecies metabolic pathways, suggesting that co-infection might affect the metabolic adaptation of both *P. aeruginosa* and *S. aureus*.

The influence of *S. aureus* on the evolution of *P. aeruginosa* thus remains an open question. Two recent researches investigated this issue using different approaches: the experimental evolution of reference strains indicated that *P. aeruginosa*

evolves differently in co-culture than in monoculture (41), and *P. aeruginosa* strains isolated from co-infected CF patients are less competitive with *S. aureus* than those from mono-infected patients (25). Hence, both of these results support an impact of *S. aureus* presence on *P. aeruginosa* adaptation. However, the *in vitro* experimental evolution approach conducted in our study did not demonstrate any impact of *S. aureus* on the development of coexistence in *P. aeruginosa*. Indeed, coexistence established at the same rate in the presence (6/10 replicates) or the absence (5/10) of *S. aureus* (Fig. 4B). We nonetheless noticed that *S. aureus* presence seemed to select for particular types of mutations in *P. aeruginosa*, since a less diverse mutational profile was observed in co-culture in comparison to monoculture (Fig. 5A). It is thus possible that *S. aureus* might have affected the evolution of *P. aeruginosa* in our conditions although no phenotypical signature could be highlighted. It would be interesting to replicate these results in other *P. aeruginosa* isolates, and as suggested before in a more complex *in vitro* study model. Regarding these last results, this model should not only mimic the *in vivo* conditions but also include the other partners of the ecosystem such as the native microbiota, pathogens or host cells.

Acknowledgments

This work was supported by the Fondation pour la Recherche Médicale, grant number ECO20170637499 to LC; the Finovi foundation to KM; the associations “Vaincre la mucoviscidose” and “Gregory Lemarchal” to KM.

Conflict of interest

All the authors declare no competing interests.

Ethical statement

All the strains used in this study were collected as part of the periodic monitoring of patients at the Hospices Civils de Lyon. This study was submitted to the Ethics Committee of the Hospices Civils de Lyon (HCL) and registered under CNIL No 17-216. All the patients were informed of the study; however, as the study was non-interventional no written informed consent was required under local regulations.

References

1. Folkesson A, Jelsbak L, Yang L, Johansen HK, Ciofu O, Høiby N, et al. Adaptation of *Pseudomonas aeruginosa* to the cystic fibrosis airway: an evolutionary perspective. *Nat Rev Microbiol.* 2012 Dec;10(12):841–51.
2. Winstanley C, O'Brien S, Brockhurst MA. *Pseudomonas aeruginosa* Evolutionary Adaptation and Diversification in Cystic Fibrosis Chronic Lung Infections. *Trends Microbiol.* 2016 May;24(5):327–37.
3. Cramer N, Klockgether J, Wrasman K, Schmidt M, Davenport CF, Tümmler B. Microevolution of the major common *Pseudomonas aeruginosa* clones C and PA14 in cystic fibrosis lungs. *Environ Microbiol.* 2011 Jul;13(7):1690–704.
4. Yang L, Jelsbak L, Marvig RL, Damkjaer S, Workman CT, Rau MH, et al. Evolutionary dynamics of bacteria in a human host environment. *Proc Natl Acad Sci USA.* 2011 May 3;108(18):7481–6.
5. Bianconi I, D'Arcangelo S, Esposito A, Benedet M, Piffer E, Dinnella G, et al. Persistence and Microevolution of *Pseudomonas aeruginosa* in the Cystic Fibrosis Lung: A Single-Patient Longitudinal Genomic Study. *Front Microbiol.* 2018;9:3242.
6. Markussen T, Marvig RL, Gómez-Lozano M, Aanæs K, Burleigh AE, Høiby N, et al. Environmental heterogeneity drives within-host diversification and evolution of *Pseudomonas aeruginosa*. *mBio.* 2014 Sep 16;5(5):e01592-01514.
7. Marvig RL, Sommer LM, Jelsbak L, Molin S, Johansen HK. Evolutionary insight from whole-genome sequencing of *Pseudomonas aeruginosa* from cystic fibrosis patients. *Future Microbiol.* 2015;10(4):599–611.
8. Smith EE, Buckley DG, Wu Z, Saenphimmachak C, Hoffman LR, D'Argenio DA, et al. Genetic adaptation by *Pseudomonas aeruginosa* to the airways of cystic fibrosis patients. *Proc Natl Acad Sci USA.* 2006 May 30;103(22):8487–92.
9. van Mansfeld R, de Been M, Paganelli F, Yang L, Bonten M, Willems R. Within-Host Evolution of the Dutch High-Prevalent *Pseudomonas aeruginosa* Clone ST406 during Chronic Colonization of a Patient with Cystic Fibrosis. *PLoS ONE.* 2016;11(6):e0158106.
10. Klockgether J, Cramer N, Fischer S, Wiehlmann L, Tümmler B. Long-Term Microevolution of *Pseudomonas aeruginosa* Differs between Mildly and Severely Affected Cystic Fibrosis Lungs. *Am J Respir Cell Mol Biol.* 2018;59(2):246–56.
11. Khademi SMH, Sazinas P, Jelsbak L. Within-Host Adaptation Mediated by Intergenic Evolution in *Pseudomonas aeruginosa*. *Genome Biol Evol.* 2019 01;11(5):1385–97.
12. Feliziani S, Marvig RL, Luján AM, Moyano AJ, Di Rienzo JA, Krogh Johansen H, et al. Coexistence and within-host evolution of diversified lineages of hypermutable

- Pseudomonas aeruginosa* in long-term cystic fibrosis infections. *PLoS Genet.* 2014 Oct;10(10):e1004651.
13. Marvig RL, Johansen HK, Molin S, Jelsbak L. Genome analysis of a transmissible lineage of *Pseudomonas aeruginosa* reveals pathoadaptive mutations and distinct evolutionary paths of hypermutators. *PLoS Genet.* 2013;9(9):e1003741.
 14. Marvig RL, Sommer LM, Molin S, Johansen HK. Convergent evolution and adaptation of *Pseudomonas aeruginosa* within patients with cystic fibrosis. *Nat Genet.* 2015 Jan;47(1):57–64.
 15. Marvig RL, Dolce D, Sommer LM, Petersen B, Ciofu O, Campana S, et al. Within-host microevolution of *Pseudomonas aeruginosa* in Italian cystic fibrosis patients. *BMC Microbiol.* 2015 Oct 19;15:218.
 16. Bianconi I, Jeukens J, Freschi L, Alcalá-Franco B, Facchini M, Boyle B, et al. Comparative genomics and biological characterization of sequential *Pseudomonas aeruginosa* isolates from persistent airways infection. *BMC Genomics.* 2015 Dec 29;16:1105.
 17. Jorth P, Staudinger BJ, Wu X, Hisert KB, Hayden H, Garudathri J, et al. Regional Isolation Drives Bacterial Diversification within Cystic Fibrosis Lungs. *Cell Host Microbe.* 2015 Sep 9;18(3):307–19.
 18. La Rosa R, Johansen HK, Molin S. Adapting to the Airways: Metabolic Requirements of *Pseudomonas aeruginosa* during the Infection of Cystic Fibrosis Patients. *Metabolites.* 2019 Oct 16;9(10).
 19. Feltner JB, Wolter DJ, Pope CE, Groleau M-C, Smalley NE, Greenberg EP, et al. LasR Variant Cystic Fibrosis Isolates Reveal an Adaptable Quorum-Sensing Hierarchy in *Pseudomonas aeruginosa*. *mBio.* 2016 04;7(5).
 20. Chen R, Déziel E, Groleau M-C, Schaefer AL, Greenberg EP. Social cheating in a *Pseudomonas aeruginosa* quorum-sensing variant. *Proc Natl Acad Sci USA.* 2019 02;116(14):7021–6.
 21. Hotterbeekx A, Kumar-Singh S, Goossens H, Malhotra-Kumar S. In vivo and In vitro Interactions between *Pseudomonas aeruginosa* and *Staphylococcus* spp. *Front Cell Infect Microbiol* [Internet]. 2017 Apr 3 [cited 2019 Aug 26];7. Available from: <http://journal.frontiersin.org/article/10.3389/fcimb.2017.00106/full>
 22. Baldan R, Cigana C, Testa F, Bianconi I, De Simone M, Pellin D, et al. Adaptation of *Pseudomonas aeruginosa* in Cystic Fibrosis airways influences virulence of *Staphylococcus aureus* in vitro and murine models of co-infection. *PLoS ONE.* 2014;9(3):e89614.
 23. Michelsen CF, Christensen A-MJ, Bojer MS, Høiby N, Ingmer H, Jelsbak L. *Staphylococcus aureus* alters growth activity, autolysis, and antibiotic tolerance in a human host-adapted *Pseudomonas aeruginosa* lineage. *J Bacteriol.* 2014 Nov;196(22):3903–11.
 24. Frydenlund Michelsen C, Hossein Khademi SM, Krogh Johansen H, Ingmer H, Dorrestein PC, Jelsbak L. Evolution of metabolic divergence in *Pseudomonas aeruginosa* during long-term infection facilitates a proto-cooperative interspecies interaction. *ISME J.* 2016 Jun;10(6):1323–36.
 25. Limoli DH, Whitfield GB, Kitao T, Ivey ML, Davis MR, Grahl N, et al. *Pseudomonas aeruginosa* Alginate Overproduction Promotes Coexistence with *Staphylococcus aureus* in a Model of Cystic Fibrosis Respiratory Infection. *mBio.* 2017 21;8(2).
 26. Briaud P, Camus L, Bastien S, Doléans-Jordheim A, Vandenesch F, Moreau K. Coexistence with *Pseudomonas aeruginosa* alters *Staphylococcus aureus* transcriptome, antibiotic resistance and internalization into epithelial cells. *Sci Rep* [Internet]. 2019 Nov 12 [cited 2019 Nov 25];9. Available from: <https://www.ncbi.nlm.nih.gov/pmc/articles/PMC6851120/>
 27. Briaud P, Bastien S, Camus L, Boyadjian M, Reix P, Mainguy C, et al. Impact of coexistence phenotype between *Staphylococcus aureus* and *Pseudomonas aeruginosa* isolates on clinical outcomes among Cystic Fibrosis patients. *Front Cell Infect Microbiol* [Internet]. 2020 [cited 2020 May 29];10. Available from: <https://www.frontiersin.org/articles/10.3389/fcimb.2020.00266/full#supplementary-material>
 28. Pallett R, Leslie LJ, Lambert PA, Milic I, Devitt A, Marshall LJ. Anaerobiosis influences virulence properties of *Pseudomonas aeruginosa* cystic fibrosis isolates and the interaction with *Staphylococcus aureus*. *Sci Rep.* 2019 01;9(1):6748.
 29. Camus L, Briaud P, Bastien S, Elsen S, Doléans-Jordheim A, Vandenesch F, et al. Trophic cooperation promotes bacterial survival of *Staphylococcus aureus* and *Pseudomonas aeruginosa*. *ISME J.* 2020 Aug 19;
 30. Limoli DH, Yang J, Khansaheb MK, Helfman B, Peng L, Stecenko AA, et al. *Staphylococcus aureus* and *Pseudomonas aeruginosa* co-infection is associated with cystic fibrosis-related diabetes and poor clinical outcomes. *Eur J Clin Microbiol Infect Dis.* 2016 Jun;35(6):947–53.
 31. Bolger AM, Lohse M, Usadel B. Trimmomatic: a flexible trimmer for Illumina sequence data. *Bioinformatics.* 2014 Aug 1;30(15):2114–20.
 32. Bankevich A, Nurk S, Antipov D, Gurevich AA, Dvorkin M, Kulikov AS, et al. SPAdes: a new genome assembly algorithm and its applications to single-cell sequencing. *J Comput Biol.* 2012 May;19(5):455–77.
 33. Gurevich A, Saveliev V, Vyahhi N, Tesler G. QUAST: quality assessment tool for genome assemblies. *Bioinformatics.* 2013 Apr 15;29(8):1072–5.
 34. Seemann T. Prokka: rapid prokaryotic genome annotation. *Bioinformatics.* 2014 Jul 15;30(14):2068–9.
 35. Page AJ, Cummins CA, Hunt M, Wong VK, Reuter S, Holden MTG, et al. Roary: rapid

- large-scale prokaryote pan genome analysis. *Bioinformatics*. 2015 Nov 15;31(22):3691–3.
36. Wick RR, Judd LM, Gorrie CL, Holt KE. Unicycler: Resolving bacterial genome assemblies from short and long sequencing reads. *PLOS Computational Biology*. 2017 Jun 8;13(6):e1005595.
 37. Khandekar S, Liebens V, Fauvart M, Tulkens PM, Michiels J, Van Bambeke F. The Putative De-N-acetylase DnpA Contributes to Intracellular and Biofilm-Associated Persistence of *Pseudomonas aeruginosa* Exposed to Fluoroquinolones. *Front Microbiol* [Internet]. 2018 Jul 10 [cited 2020 Aug 31];9. Available from: <https://www.ncbi.nlm.nih.gov/pmc/articles/PM6048251/>
 38. King JD, Kocíncová D, Westman EL, Lam JS. Review: Lipopolysaccharide biosynthesis in *Pseudomonas aeruginosa*. *Innate Immun*. 2009 Oct;15(5):261–312.
 39. D’Argenio DA, Wu M, Hoffman LR, Kulasekara HD, Déziel E, Smith EE, et al. Growth phenotypes of *Pseudomonas aeruginosa* lasR mutants adapted to the airways of cystic fibrosis patients. *Molecular Microbiology*. 2007 Apr;64(2):512–33.
 40. Price CE, Brown DG, Limoli DH, Phelan VV, O’Toole GA. Exogenous Alginate Protects *Staphylococcus aureus* from Killing by *Pseudomonas aeruginosa*. *J Bacteriol*. 2020 Mar 26;202(8).
 41. Tognon M, Köhler T, Gdaniec BG, Hao Y, Lam JS, Beaume M, et al. Co-evolution with *Staphylococcus aureus* leads to lipopolysaccharide alterations in *Pseudomonas aeruginosa*. *ISME J*. 2017 Oct;11(10):2233–43.

SUPPLEMENTARY DATA

Supplementary figures

Figure S1: Schematic representation of the employed methodology for the experimental evolution of *P. aeruginosa* PA190A and PA190B.

Figure S2: Competitive- and coexisting-specific genes within the 12 *P. aeruginosa* pairs/trio.

Figure S3: Mutated genes and intergenic regions identified in coexisting *P. aeruginosa* isolates in comparison to the corresponding competitive isolate.

Supplementary tables (available upon request at karen.moreau@univ-lyon1.fr or loo.camus@gmail.com)

Table S1: Clinical CF strains used in this study.

Table S2: Sequencing data.

Table S3: Competitive- and coexisting-specific genes identified in the 12 *P. aeruginosa* pairs/trio by the gene presence/absence analysis.

Table S4: Non-synonymous mutations identified in *P. aeruginosa* coexisting isolates in comparison to competitive ones.

Table S5: Synonymous mutations identified in *P. aeruginosa* coexisting isolates in comparison to competitive ones.

Table S6A and B: Intergenic mutations identified in *P. aeruginosa* coexisting isolates in comparison to competitive ones.

Table S7: Size of inhibition halo and pigmentation of *P. aeruginosa* evolved isolates from ancestral competitive PA190A and coexisting PA190B isolates.

Table S8: Mutations identified in evolved *P. aeruginosa* isolates in comparison to the ancestral PA190A isolate.

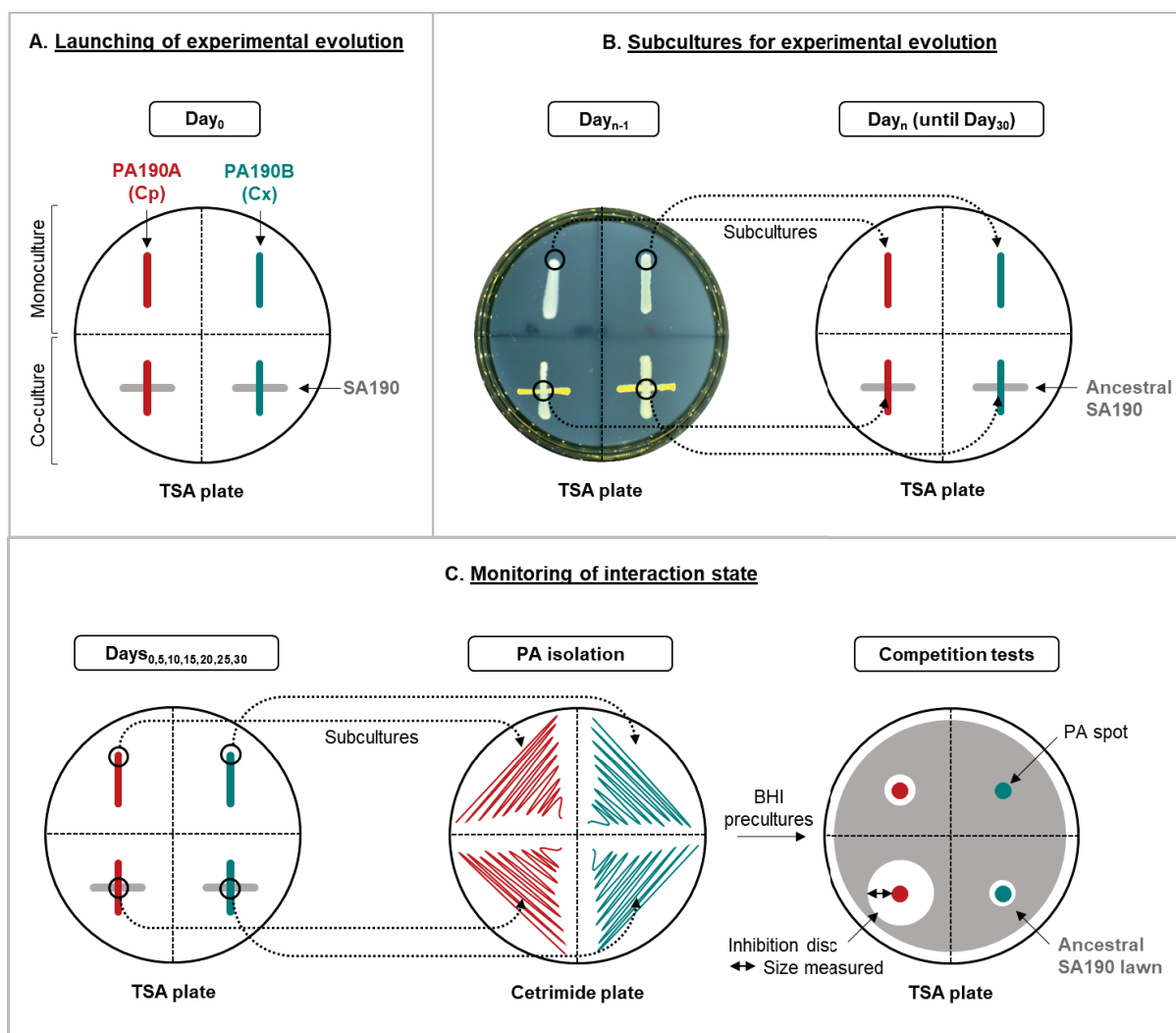


Figure S1: Schematic representation of the employed methodology for the experimental evolution of *P. aeruginosa* PA190A and PA190B.

A. *P. aeruginosa* PA190A (competitive, Cp, red) and PA190B (coexisting, Cx, blue) were streaked in monoculture (single vertical streak) or in co-culture (crossed with a horizontal streak of *S. aureus* SA190) on a TSA plate and grown 24h at 37°C.

B. Each day for 30 days, on a fresh TSA plate were subcultured the *P. aeruginosa* streaks from the monoculture streak and from the intersection of the co-culture cross-streak. The *S. aureus* streak was performed from a fresh culture of the ancestral strain.

C. Every 5 days during the experimental evolution, the evolving *P. aeruginosa* were isolated on Cetrimide, after what they were precultured in BHI to perform competition tests with the ancestral *S. aureus* SA190 strain (3, 4).

Gene names or PAO1 locci	No. of strains	Cp. Specific	Cx. Specific	Strain pair												
				PA124	PA148	PA182	PA190	PA211	PA223	PA230	PA266	PA293	PA357	PA360A	PA360B	
<i>cdrA</i>	6	3	3	Cp		Cx	Cp	Cx	Cx				Cp			
<i>phzD1</i>	5	4	1	Cp	Cx	Cp		Cp	Cp							
<i>group_190</i>	5	4	1				Cp		Cx					Cp	Cp	Cp
<i>PA1874</i>	5	2	3		Cx			Cx	Cp	Cp	Cx					
<i>exaC</i>	4	4	0				Cp	Cp							Cp	Cp
<i>hdhA</i>	4	2	2			Cp	Cp	Cx	Cp							
<i>cspD</i>	4	1	3	Cp		Cx				Cx		Cx				
<i>group_133</i>	4	4	0					Cp			Cp				Cp	Cp
<i>group_136</i>	4	2	2			Cp		Cx		Cp		Cx				
<i>group_179</i>	4	1	3	Cp							Cx				Cx	Cx
<i>group_1821</i>	4	1	3			Cx	Cx	Cp		Cx						
<i>group_192</i>	4	2	2				Cp		Cp						Cx	Cx
<i>group_1972</i>	4	4	0		Cp			Cp	Cp				Cp			
<i>group_2</i>	4	1	3	Cx		Cp	Cx					Cx				
<i>lasR</i>	4	2	2								Cx	Cx			Cp	Cp
<i>group_3055</i>	4	4	0		Cp		Cp								Cp	Cp
<i>group_37</i>	4	2	2		Cp				Cx	Cx	Cp					
<i>group_449</i>	4	1	3				Cx		Cx	Cx					Cp	
<i>phzC1</i>	4	3	1	Cp	Cx	Cp			Cp							
<i>group_881</i>	4	4	0		Cp				Cp						Cp	Cp
<i>lasA</i>	4	1	3		Cx				Cp	Cx	Cx					
<i>narK1</i>	4	0	4		Cx			Cx	Cx			Cx				
<i>phzD2</i>	4	1	3	Cx	Cp			Cx	Cx							
<i>phzG2</i>	4	1	3			Cp			Cx						Cx	Cx
Total number of genes exclusive to the competitive isolate (Cp)				17	35	52	484	50	85	41	29	120	19	200	203	

Figure S2: Competitive- and coexisting-specific genes within the 12 *P. aeruginosa* pairs/trio. A gene presence/absence analysis was performed for each pair or trio of *P. aeruginosa* to determine the genes present only in the competitive isolate (dark grey cells, Cp) or in the coexisting isolate (light grey cells, Cx). Gene impacted in at least four isolates are presented. The complete list of competitive- and coexisting-specific genes is presented in Table S3.

A Non-synonymously mutated genes

Gene names or PAO1 loci	No. of genes	No. of strains	Mutated coexisting strains																	
			PA124E	PA148B	PA182B	PA190B	PA211A	PA223A	PA230C	PA266A	PA293A	PA357A	PA360A	PA360B						
<i>mvfR</i>	1	1	■																	
<i>anr, fleR, group_3179, PA2581, kinB, PA0267, pvdE</i>	7	1																		
<i>emrA, flil, group_1156, group_2304, group_294, PA1766, infC, wspR</i>	8	1			■															
List in table S4	14	1																		
<i>fpvH, PA3211, cpxS, PA1218, PA0372, PA1790, metC, mexR, shaB, yeiG</i>	10	1				■														
List in table S4	11	1																		
List in table S4	19	1		■																
<i>bioH, creC, algW, pgK</i>	4	1																		
<i>PA3315, PA2571</i>	2	1																		
List in table S4	264	1																		
List in table S4	433	1																		
List in table S4	496	1																		

No. of non-synonymous mutations in comparison to the corresponding competitive strain

3	36	22	23	592	638	391	24	14	22	43	44
---	----	----	----	-----	-----	-----	----	----	----	----	----

B Synonymously mutated genes

Gene name or PAO1 locus	No. of genes	No. of strains	Mutated coexisting strains																	
			PA124E	PA148B	PA182B	PA190B	PA211A	PA223A	PA230C	PA266A	PA293A	PA357A	PA360A	PA360B						
<i>group_1026</i>	1	3																		
<i>hscA</i>	1	3																		
<i>magD</i>	1	3																		
<i>coxA</i>	7	2																		
<i>wbpM</i>	1	2																		
<i>alaS, argG, dnaE, PA4923, PA4677, PA0747</i>	6	2																		
<i>PA4899</i>	1	2																		
<i>ambE, dnaN, bglX, PA4011, PA1022, leuA, fhpR, PA1402</i>	8	2																		
List in Table S5	12	2																		
<i>hsbA, algF, PA4437, PA5146</i>	4	1																		
<i>group_225, pdtA, PA1736, phzD2</i>	4	1																		
<i>PA1313, yfbS</i>	2	1																		
<i>aer2, gshB, PA1938, yfjB, narK1, PA5402</i>	6	1																		
<i>alpR, flgF, kynB, tadA, carB, PA0476, PA1833</i>	7	1																		
<i>PA1626, PA2464, PA3329, mucP, recB</i>	5	1																		
<i>PA2393</i>	1	1																		
List in Table S5	109	1																		
List in Table S5	179	1																		
List in Table S5	209	1																		

No. of synonymous mutations in comparison to the corresponding competitive strain

0	7	4	6	108	231	124	4	7	5	10	9
---	---	---	---	-----	-----	-----	---	---	---	----	---

2.3. Résultats complémentaires et perspectives

2.3.1. *Diversification au sein de la population bactérienne*

Une des principales conclusions de notre étude est que l'état de coexistence peut s'établir chez *P. aeruginosa* par le biais de différentes voies mutationnelles. Ces voies semblent reposer sur une altération de la synthèse d'alginate (*algG*), du fonctionnement du QS (*lasR*) ou du transport des acides aminés (*yecS-fliY*). L'existence de plusieurs voies évolutives convergeant vers des phénotypes similaires est un phénomène connu lors de l'adaptation de *P. aeruginosa* dans les poumons (147, 197). Cette diversification conduit à la coexistence de nombreuses sous-populations bactériennes adaptées et spécialisées à une niche écologique de l'écosystème pulmonaire, et est observable à différentes échelles : (i) entre lignées divergentes (149, 150), comme lors de notre étude de génomique comparative de souches de différents patients, et (ii) au sein d'une même lignée clonale (198), comme lors de notre approche d'évolution expérimentale d'une souche clinique de *P. aeruginosa*.

Cette diversification intra-clonale est probablement à l'origine du comportement compétitif sporadiquement observé lors de l'évolution de la souche PA190B, présentant un état de coexistence durant la quasi-totalité de l'expérience. Nous avons pu tester cette hypothèse lors d'une expérience préliminaire d'évolution de PA190B. Au 25^{ème} repiquage, la souche PA190B²⁵ avait développé un comportement légèrement compétitif avec présence d'un fin halo d'inhibition de la croissance de *S. aureus* lors des tests de compétition sur gélose. Afin de vérifier cela, nous avons isolé 12 colonies de PA190B²⁵ et testé leur interaction avec *S. aureus*. Parmi ces 12 colonies, 6 ont conduit à l'observation d'un comportement compétitif, 2 un comportement coexistant, et 4 un comportement ambigu (**Tableau II-1**). Si ces différences d'interaction sont liées à des mutations génétiques ou des dérégulations non-fixées reste à déterminer.

Ces résultats démontrent toutefois la coexistence d'individus compétiteurs et coexistants au sein d'une même population de *P. aeruginosa*, dont la proportion peut probablement varier selon certains paramètres. Nous supposons ainsi que dans certaines cultures, et pour une raison inconnue, les individus compétiteurs se sont mieux développés que les individus coexistants, conduisant à une population globale majoritairement compétitrice comme identifié par les tests de compétition sur gélose. Cette tendance se serait ensuite inversée lors des cultures suivantes, menant à une population majoritairement constituée d'individus en coexistence (**Fig. II-2A**).

Colonie	Halo	Interaction	Colonie	Halo	Interaction
Colonie 1		Compétition	Colonie 7		Coexistence
Colonie 2		Compétition	Colonie 8		Coexistence
Colonie 3		Compétition	Colonie 9		Ambigu
Colonie 4		Compétition	Colonie 10		Ambigu
Colonie 5		Compétition	Colonie 11		Ambigu
Colonie 6		Compétition	Colonie 12		Ambigu

Tableau II-1 : Résultats des tests de compétition réalisés pour 12 colonies de la souche PA190B²⁵. La souche de coexistence PA190B a été repiquée pendant 25 jours sur TSA, puis l'état d'interaction de douze de ses colonies a été testé par des tests de compétition sur gélose avec la souche SA190.

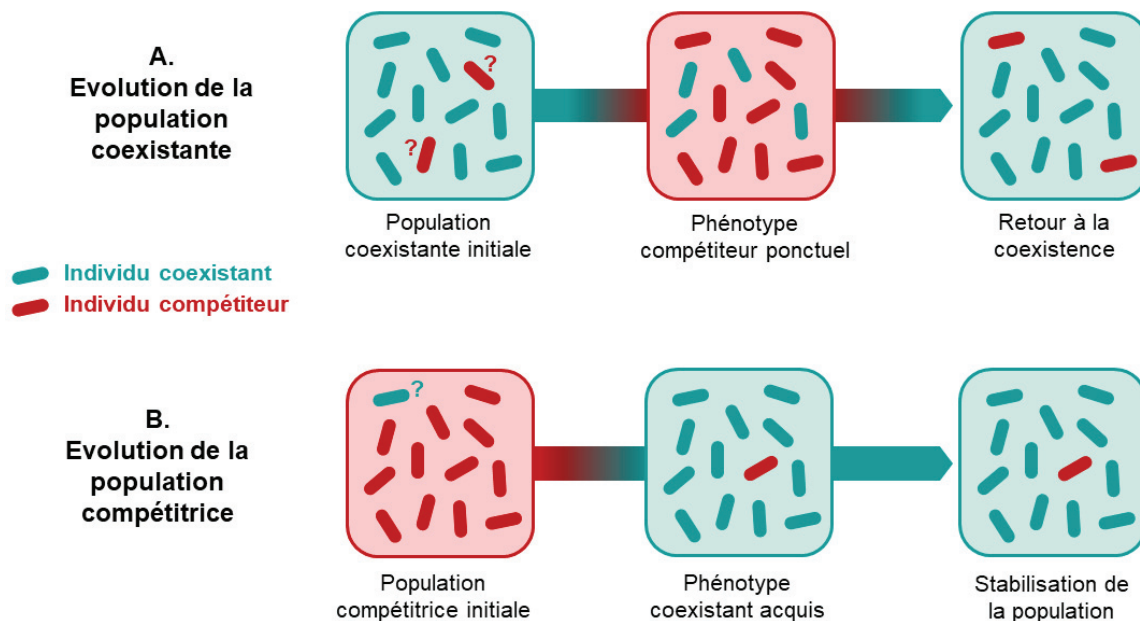


Figure II-2 : Evolution hypothétique des populations de *P. aeruginosa* initialement coexistante (A) ou compétitrice (B). Un changement de proportion d'individus compétiteurs et coexistants au sein de la population peut influencer les résultats des tests de compétition. Ce changement de proportion semble non-fixé pour la souche de coexistence (A), ou stabilisé pour la souche de compétition (B). La présence d'individus compétiteurs ou coexistants dans les populations initiales est supposée.

De façon intéressante, ce phénomène n'a pas été observé lors de l'évolution de la souche compétitrice. En effet, une fois établie, la coexistence est demeurée stable jusqu'à la fin de l'expérience, renforçant l'idée que la coexistence est l'état d'interaction privilégié dans ce contexte malgré la diversification de *P. aeruginosa* (Fig. II-2B). Ces résultats soulèvent cependant de nombreuses questions et perspectives d'études sur l'hétérogénéité des populations de *P. aeruginosa*, qui semble affecter ses interactions microbiennes. Les mécanismes génétiques de cette hétérogénéité pourraient être explorés en séquençant plusieurs colonies indépendantes au sein d'une population. Cette approche est d'ailleurs de plus en plus utilisée pour la caractérisation des souches de *P. aeruginosa* isolées des patients atteints de mucoviscidose, qui présentent notamment des profils de résistance aux antibiotiques très hétérogènes (149, 150, 199, 200). Cette diversification intra-population peut cependant aussi résulter de mécanismes non-fixés comme des dérégulations transcriptomiques, protéomiques ou épigénétiques. Il serait donc intéressant de vérifier si un état de coexistence transitoire peut être induit par de telles dérégulations et donc par des conditions environnementales particulières.

2.3.2. Pigmentation et coexistence

A l'issue de l'évolution expérimentale conduite dans cette étude, 8 des 11 isolats ayant développé un phénotype de coexistence ont présenté un aspect dit « métallique » sur boîte : des colonies irisées et peu bombées. Cet aspect est caractéristique d'un dysfonctionnement de LasR (201). Et effectivement, 6 de ces 8 isolats ont présenté une mutation non-synonyme dans le gène *lasR* (Tableau II-2), suggérant que cette altération génétique est bien à l'origine de l'aspect métallique observé dans notre expérience. Des exceptions ont toutefois été notées : deux isolats n'ont pas présenté ce phénotype malgré des mutations dans *lasR* (M6 et C6, tous deux coexistants), et deux autres ont présenté un aspect métallique malgré l'absence d'altération de *lasR* (M4, coexistant, et C5, compétiteur) (Tableau II-2). Ces résultats suggèrent donc que ce phénotype : (i) n'est pas induit par toutes les mutations dans *lasR*, (ii) peut résulter de l'altération d'autres gènes et (iii) n'est pas exclusivement associé à l'état de coexistence.





Par ailleurs, les isolats ayant développé un état de coexistence ont présenté une pigmentation verte dans 9 cas sur 11. A l'exception d'un isolat (C9), ce phénotype est associé à l'aspect métallique décrit précédemment, suggérant que ce gain de pigmentation pourrait également être induit par une altération de *lasR* (Tableau II-2). En temps normal, l'expression de LasR active les systèmes de QS sous-jacents RhIRI et PQS, conduisant à la production des principaux facteurs de virulence de la bactérie (161). Parmi ces facteurs figurent les sidérophores et les phénazines, les deux familles de molécules responsables de la

pigmentation de *P. aeruginosa*. Chez PAO1, la délétion de *lasR* conduit ainsi à une sous-production du sidérophore pyoverdine et de la phénazine pyocyanine (202, 203). Ceci n'est cependant pas toujours vrai chez les souches cliniques de *P. aeruginosa*, puisque aucune corrélation n'a pu être établie entre l'inactivation de LasR et la synthèse de pyocyanine ou d'autres phénotypes QS-dépendants (203). Certains isolats peuvent ainsi présenter une surproduction de pyocyanine malgré une activité nulle de LasR induite par des mutations non-synonymes (203). Le rôle de LasR dans le gain de pigmentation observé chez nos souches évoluées expérimentalement reste donc à élucider. La construction et la caractérisation de mutants de *P. aeruginosa* présentant les mutations non-synonymes identifiées dans notre expérience apparaît essentielle pour comprendre leur impact sur les caractères morphologiques de la bactérie.

Isolat évolué	Interaction avec <i>S. aureus</i>	Pigment vert	Métallique	<i>lasR</i> muté NS
M1	Coexistence			
C1	Coexistence			
M2	Coexistence			
M3	Coexistence			
M4	Coexistence			
M6	Coexistence			
C6	Coexistence			
M8	Coexistence			
C8	Coexistence			
C9	Coexistence			
C10	Coexistence			
C2	Compétition			
C3	Compétition			
C4	Compétition			
M5	Compétition			
C5	Compétition			
M7	Compétition			
C7	Compétition			
M9	Compétition			
M10	Compétition			

Tableau II-2 : Tableau récapitulatif des caractéristiques des isolats évolués expérimentalement.

La souche PA190A (compétitrice) a évolué expérimentalement pendant 30 jours en monoculture (M) ou en coculture (C), en 10 réplicats (1 à 10). A l'issue de l'évolution, l'état d'interaction avec *S. aureus* a été déterminé par des tests de compétition sur gélose ; les caractéristiques morphologiques ont été étudiées après croissance sur LB ; l'intégrité du gène *lasR* a été évaluée par séquençage haut-débit. NS = non synonyme.

	Oui
	Non
	Ambigu
	Pigment marron

La compréhension de l'origine de cette pigmentation apparaît importante dans notre contexte. D'une part, la production de sidérophores et/ou de phénazines est généralement associée à un état virulence et un comportement anti-staphylococcique chez *P. aeruginosa* (37, 161). Il est donc étonnant que la majorité des isolats ayant développé un état de coexistence avec *S. aureus* présentent une telle pigmentation. D'autre part, cette pigmentation s'est développée de manière concomitante à l'établissement de la coexistence dans la plupart des cas, soulignant une relation entre ces deux phénotypes (Fig. II-3).

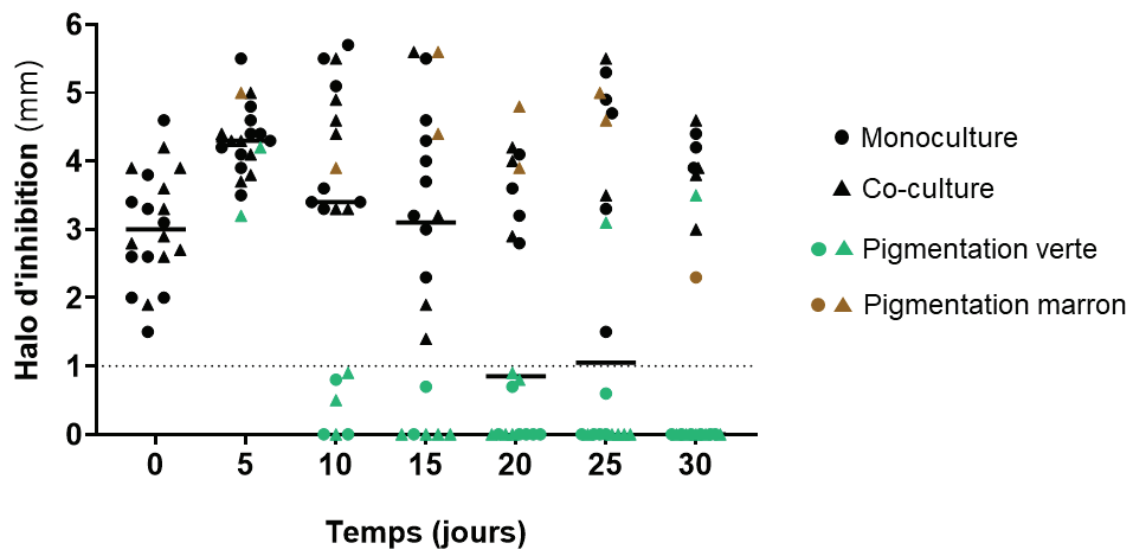


Figure II-3 : Suivi de l'état d'interaction de *P. aeruginosa* au cours du protocole d'évolution expérimentale. La souche PA190A (compétitrice) a évolué expérimentalement pendant 30 jours en monoculture ou en co-culture et en 10 réplicats. Tous les 5 jours, l'état d'interaction avec *S. aureus* a été déterminé par des tests de compétition sur gélose TSA et mesure du diamètre du halo d'inhibition. La pigmentation a été observée lors de ces mêmes tests sur TSA et est indiquée par la coloration des points. Les barres noires représentent la médiane de la taille du halo d'inhibition.

Nous avons donc cherché à caractériser ce pigment et les conditions favorisant sa production. La pyoverdine est le principal sidérophore à pigmentation verte produit par *P. aeruginosa* et est caractérisé par deux éléments : sa fluorescence, et sa production favorisée en l'absence de fer (204). La pigmentation de nos souches évoluées de *P. aeruginosa* a ainsi été étudiée sous lumière blanche et sous UV, en présence de fer et en conditions de privation induite par ajout d'un chélateur du fer au milieu de culture. De façon intéressante, le pigment vert produit ne s'est pas avéré fluorescent, et sa production n'a pas été augmentée en conditions de privation en fer (Fig. II-4) (isolats M2, M3, M4). Ces résultats suggèrent donc que le gain de pigmentation observé chez nos isolats évolués en coexistence ne résulte pas d'une production augmentée de pyoverdine.

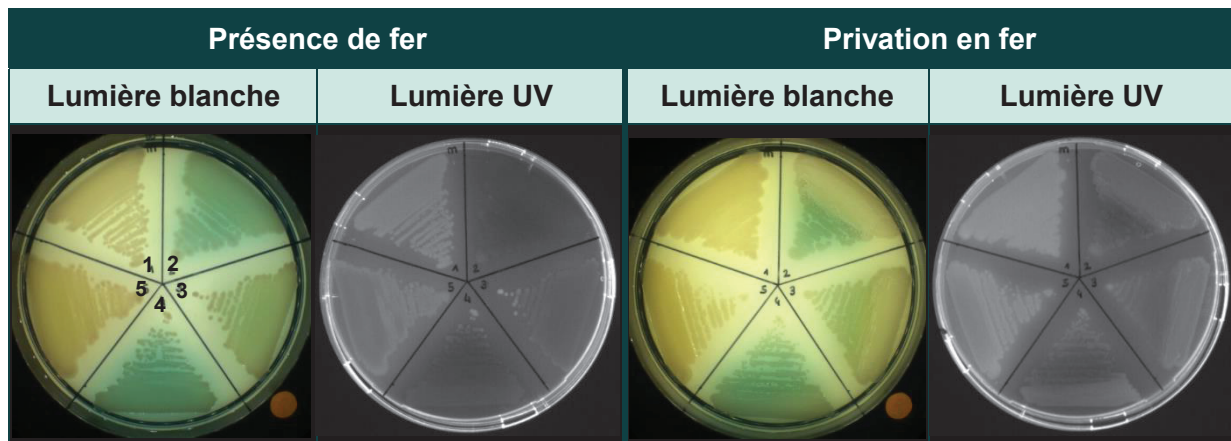


Figure II-4 : Pigmentation et fluorescence des isolats évolués M1 à M5 en présence ou en conditions de privation en fer. Les isolats évolués ont été cultivés en présence de fer (TSA) ou en privation de fer (TSA + éthylènediamine-N, N'-bis (EDDHA)) pendant 24h, puis photographiés sous lumière blanche ou UV. Les deux boîtes présentées sont organisées de façon similaire et sont représentatives des résultats obtenus pour les autres isolats évolués. Les vignettes orange permettent un contrôle colorimétrique de l'image.

Cependant, ce phénotype peut également être associé aux phénazines, dont la production confère différentes pigmentations à *P. aeruginosa* : jaune (PCA, MPCAB), rouge (aeruginosines A et B), bleue (pyocyanine) ou verte (PCN, 1-OH-PHZ) (Fig. II-5) (205, 206). Il est ainsi possible que la pigmentation verte observée chez nos isolats évolués résulte d'une altération de la régulation des voies de biosynthèses des phénazines, par exemple au profit de la production des pigments verts PCN et 1-OH-PHZ. Une quantification précise des phénazines apparaît essentielle pour identifier le pigment produit par nos isolats, et ainsi comprendre son rôle dans l'établissement de la coexistence.

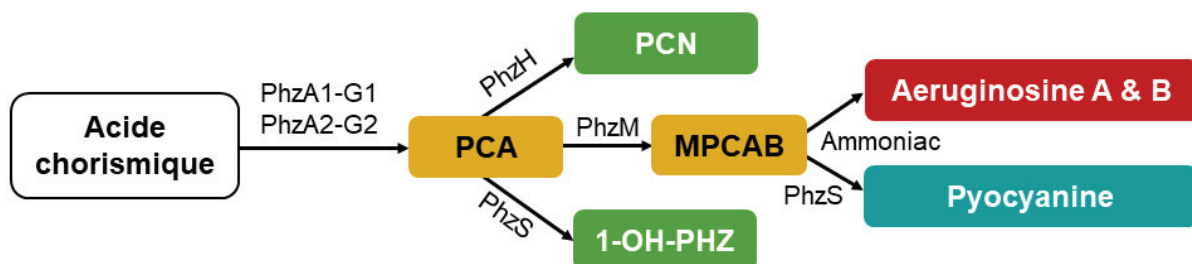


Figure II-5 : Voie de synthèse des principales phénazines chez *P. aeruginosa*. PCA = phénazine-2-carboxylique ; PCN = phénazine-1-carboxamide ; 1-OH-PHZ = 1-hydroxyphénazine ; MPCAB = 5-méthylphénazine-1-carboxylique acide bétaine ; Aeruginosine A = 5-méthyl-7-amino-1-carboxyméthylphénazinium bétaine ; Aeruginosine B = 5-méthyl-7-amino-1-carboxy-3-sulfophénazinium bétaine ; Pyocyanine = 5-Nméthyl-1-hydroxyphénazine. La couleur des cases indique la coloration du pigment. Adapté de Dietrich *et al.* et Mavrodi *et al.* (205, 206).

3 AXE 3 : Facteurs génétiques de *P. aeruginosa* favorables à son maintien lors de l'interaction de coexistence

3.3. Introduction

Une fois l'état de coexistence établi entre *P. aeruginosa* et *S. aureus*, les deux partenaires bactériens doivent parvenir à se maintenir lors de cette interaction. Chez *S. aureus*, plusieurs gènes ont été identifiés comme favorables à son maintien en présence de *P. aeruginosa*, tels que les régulateurs globaux *agr*, *sigB* ou *sarR in vitro* (207) ou *rot in vivo* (208). A l'instar de ces deux études, nous avons employé la méthode de Transposon-sequencing (Tn-seq) pour déterminer les gènes de *P. aeruginosa* impliqués dans son maintien en coexistence avec *S. aureus*. Cette méthode a pu être développée au laboratoire en collaboration avec Erwan Guéguen (Laboratoire de Microbiologie, Adaptation et Pathogénie, Lyon) et Sylvère Bastien (CIRI, Lyon), bio-informaticien de l'équipe.

La technique de Tn-seq repose sur la construction et l'utilisation d'une banque de mutants par transposition chez *P. aeruginosa* (209). Le transposon et sa transposase sont apportés par une souche donneuse de *E. coli* et transférés chez *P. aeruginosa* par conjugaison bactérienne. Le transposon s'insère alors de façon unique et aléatoire au niveau des sites TA du génome de *P. aeruginosa*, permettant de générer une population dans laquelle chaque individu ne présente qu'une seule insertion (**Fig. III-1**). Une banque d'au moins 500 000 mutants permet d'assurer que statistiquement, le transposon s'insérera au moins une fois par gène de *P. aeruginosa*. La banque produite est ensuite cultivée en présence d'une pression sélective, éliminant les mutants les moins aptes à survivre dans ces conditions. A l'issue de cette étape de culture, l'ADNg de l'ensemble des mutants encore présents est extrait et digéré par l'enzyme Mmel, libérant un fragment contenant 16 nucléotides d'ADNg en amont du transposon (**Fig. III-3**). Ces fragments sont ensuite amplifiés puis séquencés en Illumina et alignés sur le génome de *P. aeruginosa* afin de déterminer : (i) la position de l'insertion de chaque transposon, permettant d'identifier les gènes mutés, et (ii) le nombre d'insertions détectées du transposon pour un gène muté, quantifiant le nombre de mutants de ce gène. Le nombre d'insertions détectées est ensuite comparé dans les conditions non-sélective et sélective pour déterminer les gènes favorables ou défavorables. Sous une pression de sélection donnée, un gène apparaît ainsi :

- Favorable (ou essentiel dans la littérature) si le nombre d'insertions est inférieur à celui observé en absence de pression sélective, signifiant que les mutants de ce gène ont été éliminés (Fig. III-1, Gène A).
- Défavorable (ou délétère) si le nombre d'insertions est supérieur à celui observé en absence de pression sélective, signifiant que les mutants de ce gène sont favorisés (Fig. III-1, Gène B).

En parallèle, la banque pure (c'est-à-dire avant toute étape de culture) est également séquencée afin d'en évaluer le nombre de sites TA et de gènes impactés, témoignant de la qualité de la banque produite. Cela permet également de déterminer les gènes de *P. aeruginosa* essentiels à sa croissance dans nos conditions expérimentales, qui correspondent aux gènes présentant une densité d'insertion diminuée après toute étape de culture (Fig. III-1, Gène C). Il est important de noter que les gènes essentiels identifiés ici sont indispensables à la croissance dans nos conditions expérimentales, à l'inverse des gènes dits « favorables » (Gène A) dont l'expression n'est pas requise mais améliore la survie de la bactérie dans ces mêmes conditions.

Nous avons dans un premier temps construit une banque de 680 000 mutants chez la souche clinique PA235A de *P. aeruginosa*. Cette banque a ensuite été cultivée en monoculture ou en co-culture avec la souche clinique de co-infection *S. aureus* SA235. Ces cultures ont été maintenues en phase exponentielle de croissance pendant 18h afin d'évaluer au mieux la pression de sélection induite par le staphylocoque sur *P. aeruginosa*, puis les librairies de séquençage ont été préparées et séquencées. L'analyse bio-informatique des résultats a ainsi permis d'identifier 37 gènes de *P. aeruginosa* importants pour son maintien en coexistence avec *S. aureus*. Les voies de biosynthèse des acides aminés et de thiamine apparaissent favorables, alors que les voies d'utilisation du glucose et du pyruvate ont un impact négatif sur la survie de *P. aeruginosa* en présence de *S. aureus*.

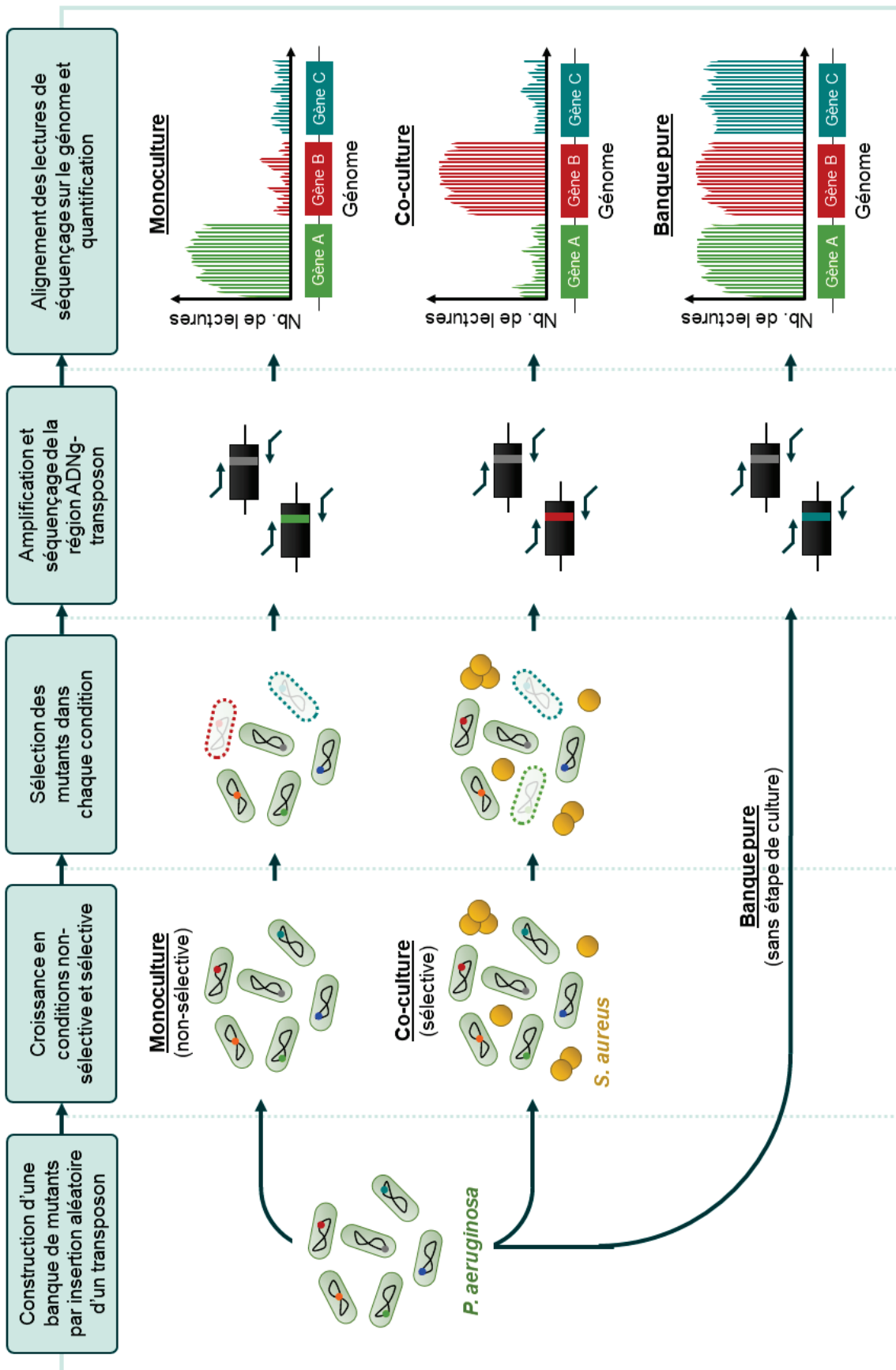


Figure III-1 : Principe du Transposon-sequencing. La banque de mutants de *P. aeruginosa* est soumise à différentes conditions de culture : nulle (banque pure), non-sélective (monoculture) ou sélective (co-culture avec *S. aureus*). Les régions ADN-transposon sont amplifiées puis séquencées. Les lectures de séquençage sont alignées sur le génome de *P. aeruginosa* afin de comparer les fréquences de mutants sous chaque condition et déterminer les gènes favorables (gène A) ou défavorables (gène B) en co-culture avec *S. aureus*, ainsi que les gènes essentiels pour la croissance nos conditions de culture (gène C).

3.4. Matériels et méthodes

3.4.1. Souches bactériennes et plasmides

Les souches bactériennes et plasmides utilisés dans cet axe sont listés dans le **Tableau III-1**. Les souches ont été cultivées en milieu LB (BD®) ou BHI (BD®) à 37°C ou 30°C sous agitation à 200rpm. L'antibiotique gentamycine (Euromedex®) a été utilisé à une concentration finale de 50µg/mL. L'acide diaminopimélique (DAP, Sigma®) a été utilisé à une concentration finale de 0,3mM pour les cultures de *E. coli* EGE207, auxotrophe à cette molécule.

Les souches cliniques de sujets mucoviscidosiques ont été isolées par l'Institut des Agents Infectieux (IAI) depuis les expectorations de patients suivis dans les deux centres CF des Hospices Civils de Lyon (HCL). La paire de souches *P. aeruginosa* PA235A-*S. aureus* SA235 a été isolée d'un même patient co-infecté. Toutes les souches cliniques de *P. aeruginosa* utilisées dans cette étude sont dans un état de coexistence avec *S. aureus*, comme déterminé précédemment (55, 56). Toutes les expériences ont été conduites suivant les recommandations françaises en vigueur, et cette étude a été soumise au comité d'éthique des HCL et enregistrée CNIL No 17-216. Tous les patients ont été informés de cette étude et ont consenti à l'utilisation de leurs données.

Souches	Nom	Caractéristiques	Références
<i>E. coli</i>	EGE207	Auxotrophe au DAP - Gm ^R pSAM_DGm	E. Gueguen
<i>Pseudomonas putida</i>	PP1	KT2440 - Gm ^S	E. Gueguen
<i>P. aeruginosa</i>	PAO1	Gm ^S	E. Gueguen
	PA153B	Souche clinique - Gm ^S	Cette étude
	PA190B	Souche clinique - Gm ^S	Cette étude
	PA230C	Souche clinique - Gm ^S	Cette étude
	PA243B	Souche clinique - Gm ^S	Cette étude
	PA293A	Souche clinique - Gm ^S	Cette étude
	PA124A	Souche clinique - Gm ^S	Cette étude
	PA135E	Souche clinique - Gm ^S	Cette étude
	PA235A	Souche clinique - Gm ^S	Cette étude
PA2600	Souche clinique - Gm ^S	Cette étude	
<i>S. aureus</i>	SA235	Souche clinique	Cette étude
Plasmides	pSAM_DGm	<i>oriT</i> _{R6K} , transposase Mariner C9, Gm ^R , <i>bla</i>	Skurnik <i>et al.</i> (210)

Tableau III-1 : Souches bactériennes et plasmides utilisés dans cette étude.

Le témoin positif *Pseudomonas putida* 1 (PP1), ainsi que la souche de *E. coli* EGE207 portant le plasmide pSAM_DGm, ont été fournies par E. Guéguen (MAP, Lyon). Le plasmide suicide pSAM_DGm (210) est schématisé en **Figure III-2** et porte :

1. L'origine de réplication $oriT_{R6K}$, fonctionnelle en présence du gène *pir* présent dans le chromosome de *E. coli* EGE207 (211).
2. Le gène codant pour la transposase Mariner C9.
3. Le transposon de type Mariner, contenant une cassette de résistance à la gentamycine.
4. Le gène codant pour la β -lactamase Bla.

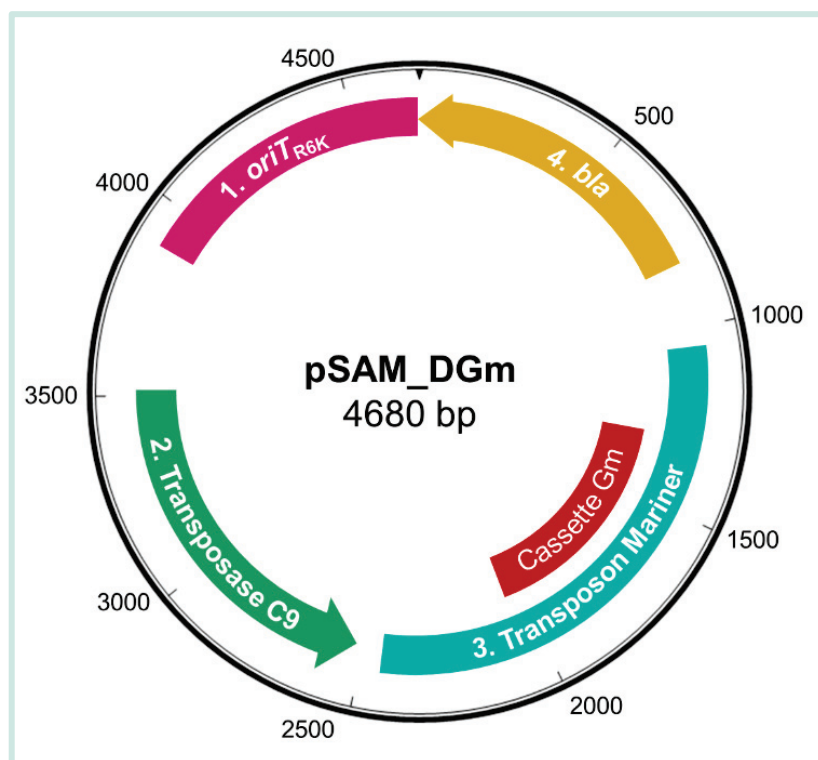


Figure III-2 : Carte du plasmide pSAM_DGm. Adapté de Skurnik *et al.* (210).
La structure du transposon est détaillée en Figure III-3.

3.4.2. Conjugaison et mutation de *P. aeruginosa* par transposition

a. Détermination de l'efficacité de la conjugaison

Le transposon utilisé dans cette étude contenant un gène de résistance à la gentamycine, la sensibilité à cet antibiotique des souches de *P. aeruginosa* receveuses a été évaluée par étalements sur LB Gm³⁰ (**Tableau III-1**).

Les volumes équivalents à $2,5DO_{600nm}$ de la souche donneuse *E. coli* EGE207 et de chaque souche receveuse de *P. aeruginosa* ont été prélevés de précultures de nuit en bouillon LB et mélangés dans un tube stérile. Après homogénéisation et centrifugation 10min à 4000g, le surnageant a été éliminé et le culot repris dans 100 μ L de LB supplémenté en DAP à 0,3mM. Le mélange a été déposé, sous forme de goutte, sur une gélose LB dont la dureté a été augmentée en doublant la concentration en agar (15g/L) et préalablement séchée. Les gouttes ont été laissées sous PSM pendant 30 minutes puis incubées à 37°C pendant 2h. Chaque goutte a été remise en suspension dans 1mL de milieu LB. Des dilutions au dixième en cascade ont ensuite été réalisées jusqu'à 10^{-4} et étalées aux billes sur LB Gm³⁰. Les boîtes ont été incubées 12 à 36h à 37°C.

Après dénombrement des boîtes de conjugaison, les souches ayant permis d'obtenir au moins 10 000 clones/conjugaison ont été sélectionnées. L'expérience de conjugaison a été répétée en triplicat pour ces souches (2600, 235A, 124A et 135E) ainsi que le témoin positif PP1. Des clones pris au hasard sur les boîtes de conjugaison ont été repiqués sur LB Gm³⁰ afin de vérifier l'acquisition de la résistance à l'antibiotique.

b. Construction de la banque de mutants chez PA235A

Pour la production de la banque de mutants par transposition chez PA235A, 18 gouttes de conjugaison ont été réalisées comme précédemment et étalées sur un total de 71 géloses de diamètre 145mm et 32 géloses de diamètre 90mm, à la dilution 10^{-2} .

Après incubation à 37°C pendant 30h, les mutants ont été récoltés au râteau et transférés dans du LB. La DO a été mesurée et ajustée à 30DO/mL avec du milieu LB. Du glycérol 100% a été rajouté au mélange à un ration 1:1 afin d'obtenir une DO finale de 15DO/mL. Cinq-cents microlitres de la suspension à 15DO/mL ont été prélevés et dilués avec du LB à une DO de 1 puis dilué en cascade jusqu'à 10^{-10} . Ces dilutions ont été étalées aux billes sur gélose LB puis incubées 37°C pendant 24h pour vérifier la pureté et la densité de la banque. Le reste de la banque à 15DO/mL a été conservée dans 160 tubes de congélation à -80°C.

Ces mêmes étalements ont par la suite été réalisés sur LB supplémenté ou non en gentamicine 30ug/mL à partir d'un tube de banque préalablement décongelé dans la glace afin de déterminer la concentration exacte de mutants en UFC/mL dans chaque tube après décongélation.

3.4.3. Culture de la banque

Une pré-culture de la nuit en milieu BHI de SA235 a été transférée dans des tubes de 50mL et centrifugées à 4000 rpm pendant 10 minutes. Le culot a été repris en milieu BHI afin d'ajuster la DO à 0,2. Pour *P. aeruginosa*, une suspension à DO 0,2 en BHI a été préparée à partir d'un tube de banque à 15DO/mL de PA235A décongelé. Les monocultures et la co-culture ont été préparées en erlenmeyer, en mélangeant 10ml de chaque suspension à 10ml de BHI (monocultures) ou en mélangeant les suspensions de *S. aureus* et *P. aeruginosa* à un ratio 1:1 (co-culture). Les cultures ont été étalées sur Cétrimide et/ou Chapman afin de dénombrer les inoculum initiaux, puis incubées à 37°C à 200 rpm. Au bout de 6h, les cultures ont été étalées et parallèlement diluées dans du BHI stérile à une DO de 0,1 pour les monocultures et 0,2 pour les co-cultures, puis incubées à nouveau pendant 6h. Les cultures ont ainsi été étalées et repiquées pendant 18h. A t=18h, le volume équivalent à 3DO a été prélevé des mono- et co-cultures et centrifugé 5min à 13,000rpm. Le surnageant a été retiré pour conserver les culots à -80°C. L'expérience a été réalisée en triplicats, et deux tubes de banque pure (sans étape culture) ont été isolés, permettant l'obtention des 8 échantillons listés en [Tableau III-2](#).

Adaptateurs simple brin			
T1	TTCCCTACACGACGCTCTTCCGATCTXXXXXNN		
T2	XXXXXAGATCGGAAGAGCGTCGTGTAGGGAA		

Adaptateurs double-brin		Echantillons	
N°	Code-barres	N°	Correspondance
EG1	GGTAT	1	Banque pure réplikat A
EG2	CTAGA	2	Banque pure réplikat B
EG3	GCTGC	3	Monoculture réplikat A
EG4	CTCGG	4	Monoculture réplikat B
EG5	ATCTT	5	Monoculture réplikat C
EG6	TACTA	6	Co-culture réplikat A
EG7	AGTTC	7	Co-culture réplikat B
EG8	CATTG	8	Co-culture réplikat C

Tableau III-2 : Adaptateurs, codes-barres et échantillons correspondants utilisés dans cette étude. **A.** Séquences 5'-3' des adaptateurs simple brin T1 et T2 permettant la synthèse des adaptateurs double-brin EG1 à EG8. Les X représentent le code-barres associé. L'extrémité 3'-NN permet l'hybridation à l'ADN adjacent au transposon. **B.** Séquences des codes-barres associés aux adaptateurs double-brin EG1 à EG8 et échantillons correspondants.

3.4.4. Préparation des librairies de séquençage

a. Extraction des ADNg

L'ADNg a été extrait des culots conservés à -80°C à l'aide du kit Wizard® Genomic DNA Purification Kit (Promega). Le culot a été repris dans 600µL de solution de lyse (Nucleic Lysis Solution) et incubé 5min à 80°C. Après refroidissement à température ambiante, ont été ajoutés 3µL de solution RNase A à 4mg/mL au mélange ; le tube a été homogénéisé par retournement et incubé 60min à 37°C. Après refroidissement à température ambiante, 200µL de solution de précipitation des protéines (Protein Precipitation Solution) ont été ajoutés, puis le mélange a été vortexé pendant 20s et incubé 5min sur glace. Le mélange a été centrifugé 10min à 13,000g à 4°C afin d'en isoler le surnageant ; cette étape a été répétée jusqu'à obtention d'un surnageant limpide. A ce surnageant ont ensuite été ajoutés 600µL d'isopropanol et l'homogénéisation a été effectuée par retournements du tube jusqu'à visibilité des fils d'ADNg. La suspension a été centrifugée 2min à 13,000g afin d'en éliminer le surnageant. Six-cents microlitres d'éthanol 70% ont été ajoutés au culot et le mélange a été homogénéisé par retournement, puis centrifugé une nouvelle fois 2min à 13,000g. Le surnageant a été totalement éliminé par pipetage, absorption au papier puis séchage pendant 15min. Les ADN ont été repris en ajoutant cent microlitres de la solution de réhydratation (DNA Rehydration Solution), en homogénéisant doucement le tube et en l'incubant 60min à 65°C. Après incubation à 4°C sur la nuit, la quantité d'ADNg extraite a été évaluée par dosages spectrophotométriques (Nanodrop et Qubit). La qualité des ADNg a également été vérifiée par électrophorèse.

b. Digestion de l'ADNg par Mmel et purifications

A 50µg d'ADNg ont été ajoutés 120µL de CutSmart Buffer 10X (NEB), 1,875µL de S-Adenosylméthionine (SAM) 32mM, 25µL d'enzyme Mmel à 2000U/mL (NEB) et de l'eau pour compléter à 1200µL. Après incubation 1h30 à 37°C, l'efficacité de la digestion a été vérifiée par électrophorèse sur 10µL de réaction (**Fig. III-3**).

Chaque digestion de 1200µL a été séparée en 6 afin d'effectuer les purifications sur colonnes sur des aliquots de 200µL (6 purifications par digestion). Les purifications ont été menées à l'aide du kit QIAquick® PCR Purification (QIAGEN) selon les recommandations du fournisseur. Pour chaque digestion, les 6 produits de purification ont été rassemblés et concentrés au Speed-Vac jusqu'à obtention d'un volume final de 25µL.

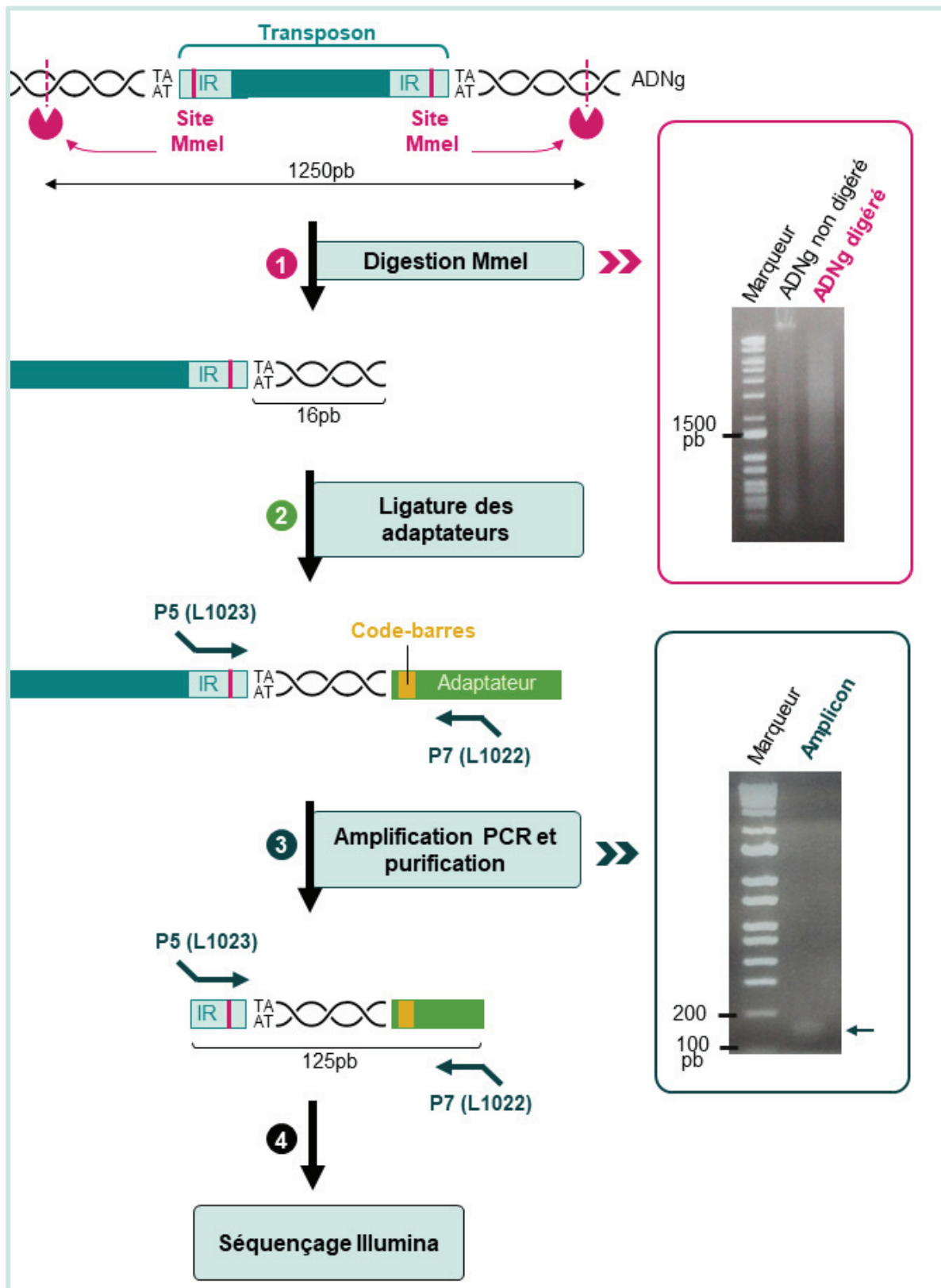


Figure III-3 : Préparation des bibliothèques de séquençage de la région ADN-transposon. L'ADNg extrait est digéré par l'enzyme de restriction MmeI qui effectue une coupure 16 paires de base (pb) en amont et aval du transposon. La région correspondant au transposon et ces 16pb est purifiée sur gel et ligaturée aux adaptateurs. Ces adaptateurs contiennent les code-barres et les séquences nécessaires à l'hybridation des amorces de séquençage. Ces amorces permettent l'amplification finale de la jonction ADN-transposon, qui est purifiée puis séquencée. IR = séquence répétée inversée.

Les digestions purifiées ont ensuite été déposées sur gel d'agarose supplémenté en Gel Green. Après migration, une bande comprise entre 1000 et 1500pb a été découpée afin d'isoler le produit de digestion de 1250pb environ (**Fig. III-3**). L'ADN contenu dans la bande a été purifié à l'aide du kit QIAquick® Gel Extraction (QIAGEN) selon les recommandations du fournisseur. Les ADN digéré et purifiés ont été dosés par spectrophotométrie (Nanodrop).

c. Création des adaptateurs double-brin

Pour la construction de chaque adaptateur double-brin (EG1 à EG8), 10µL de chaque adaptateur simple-brin T1 et T2 (**Tableau III-2A**) ont été mélangés à 10µL de tampon d'hybridation 10X (500mM NaCl, 100mM Tris-HCl pH 8, 500mM EDTA), dans un volume final de 1mL. Les mélanges ont été incubés dans de l'eau bouillante pendant 30sec puis laissés refroidir à température ambiante. L'hybridation des adaptateurs simple-brin a été vérifiée par migration sur gel acrylamide/bisacrylamide 10% 19:1 et révélation au bain de BET (Bromure d'éthydiuim).

d. Ligature des échantillons aux adaptateurs double-brin

Pour chaque échantillon (1 à 8) et chaque adaptateur double-brin (EG1 à EG8) (**Tableau III-2**), 1µg d'ADN digéré et purifié obtenu en étape b. ont été mélangés à 4,4µL d'adaptateur double-brin à 5µM, 5µL de tampon de T4 DNA ligase 10X (NEB) et 5µL de T4 DNA ligase (NEB), dans un volume final de 50µL. Le mélange a été incubé sur la nuit à 16°C.

e. Amplification et purification des produits de ligature

Pour chaque échantillon, 5 réactions d'amplifications ont été préparées en mélangeant 5µL du produit de ligature obtenu en étape d., 2µL de chaque amorce L1022 et L1023 à 10µM (**Tableau III-3**), 10µL de tampon Q5 5X (NEB), 1µL de dNTP à 10mM et 0,5µL de polymérase Q5 à 2000U/mL, dans un volume final de 50µL. L'amplification a été effectuée sur 18 cycles de la manière suivante : dénaturation initiale de 30sec à 98°C, dénaturation de 10sec à 98°C, hybridation-élongation de 6sec à 72°C, élongation finale de 10sec à 72°C. Les 5 produits d'amplification réalisés par échantillon ont ensuite été rassemblés et concentrés au Speed-Vac jusqu'à obtention d'un volume final de 25µL.

Les produits d'amplification ont ensuite été déposés sur gel d'agarose et purifiés à l'aide du kit QIAquick® Gel Extraction (QIAGEN), en suivant les recommandations du fournisseur (**Fig. III-3**). Enfin, les échantillons purifiés ont été dialysés sur membrane de nitrocellulose 0,025µM pendant 4h, puis dosés par spectrophotométrie (Nanodrop et Qubit). La qualité des échantillons a également été vérifiée par électrophorèse.

Nom	Séquence 5'-3'	Taille d'amplicon attendue
L1022	CAAGCAGAAGACGGCATAACGAGATAGACCGGGGACTTAT CATCCAACCTGT	125pb
L1023	ATGATACGGCGACCACCGAGATCTACACTCTTTCCCTAC ACGACGCTCTTCCGATCT	

Tableau III-3 : Amorces utilisées lors de la construction des bibliothèques de séquençage.

3.4.5. Séquençage et analyse bio-informatique

a. Séquençage et annotations

Deux technologies ont été utilisées pour générer le génome de référence PA235A. D'une part, un séquençage Illumina® en lecture pairée de 150 nucléotides et d'autre part, un séquençage en lecture longue utilisant la technologie Nanopore®. Les lectures longues ont été démultiplexées et nettoyées grâce à Guppy avec un score minimum de l'alignement de la séquence du code-barres fixé à 30 et un score de qualité de base fixé à 7. Les lectures Illumina® ont été nettoyées avec Trimmomatic v0.36 (212). Ce nettoyage a été exécuté en se basant sur un seuil minimum de qualité de bases fixé à 20 et une longueur minimum de 30 nucléotides. FastQC v0.11.9 (213) a été utilisé pour vérifier la qualité de ces lectures. Le génome de PA235A a été circularisé grâce à l'utilisation des deux types de technologies au travers d'Unicycler v0.4.8 (214).

L'annotation de ce génome fermé a été rendu possible par l'intermédiaire de Prokka v1.14.5 (215) en utilisant le génome de référence PAO1 comme première base de données (Refseq : NC_002516.2). Les annotations de PA235A et de PAO1 ont été comparées via Roary v3.13.0 (216) afin de créer les liens entre les gènes communs partagés par ces deux souches. Un ajout manuel de certains ARN non-codants additionnels et non détectés par Prokka issus du génome de PA14 (217) ont été ajoutés. Cela a été possible via Blast v2.6.0-1 (218) en paramétrant le pourcentage d'identité et de couverture à 100.

Le séquençage des ADN issus de la banque de mutants a été effectué à l'aide d'un MiSeq (Illumina®) dans une seule direction correspondant à une longueur de 150 nucléotides. Les adaptateurs universels de séquençage Illumina® P5 ont été ensuite retirés. Les lectures ont été démultiplexées suivant les code-barres utilisés pour identifier chaque condition (**Tableau III-2**). FastQC v0.11.9 (213) a été utilisé pour vérifier la qualité des lectures obtenues.

Les six premiers nucléotides ont été également enlevés ainsi que les adaptateurs universels de séquençages P7 situés en fin de lecture à l'aide de Cutadapt v2.8 (219). Seules les lectures d'une taille comprise entre 15 et 17 nucléotides ont été gardées. Les lectures nettoyées de 15 à 17 nucléotides ont été soumises au logiciel BWA v0.7.17 (220). Cette étape permet d'aligner les lectures sur le génome PA235A et de compter le nombre d'insertions du transposon au niveau des sites individuels di-nucléotidiques TA.

b. Détermination des gènes essentiels, favorables et défavorables

Les calculs statistiques pour déterminer l'essentialité des gènes ont été effectués à l'aide du logiciel Transit v3.1.0 (221). L'essentialité des gènes dans la banque pure a été déterminée par les méthodes Gumbel (222) et HMM (Hidden Markov Model) (223). L'essentialité des gènes dans une condition par rapport à une autre a ensuite été étudiée par les méthodes Resampling et Zinb (224).

La méthode de Resampling permet de calculer, pour chaque gène, la différence de lectures de séquençage entre deux conditions. Cette différence est ensuite comparée à une distribution générée aléatoirement de l'insertion du transposon sur 100 000 sites TA de l'ensemble du génome. La significativité de cette comparaison est évaluée par un test statistique de Mann-Whitney. Un gène a été considéré favorable ou défavorable si la différence de comptage de lectures et donc du nombre d'insertions (FC pour Fold-Change) entre deux conditions est supérieure ou inférieure à 2 avec une *P*-valeur ajustée inférieure à 0,05.

La méthode Zinb permet quant à elle de comparer la différence de moyenne de comptages de lectures de séquençage d'une condition par rapport à la somme des moyennes des comptages de toutes les conditions. La significativité de cette comparaison est évaluée par un test statistique de ratio de vraisemblance. Cette méthode a été appliquée pour effectuer pour comparer les conditions deux à deux ou les trois conditions (banque pure, mono et co-culture) conjointement.

3.5. Résultats

3.5.1. Choix des souches

Au sein de la banque de souches isolées de patients mucoviscidosiques de la cohorte lyonnaise co-infectés par *P. aeruginosa* et *S. aureus*, dix souches de *P. aeruginosa* ont été sélectionnées pour cette étude du fait de : (i) leur interaction de coexistence avec la souche de *S. aureus* co-isolée et (ii) leur sensibilité à la gentamycine, essentielle à la mutagénèse par transposition avec le plasmide pSAM_DGm (Tableau III-1). Le transfert de ce plasmide repose cependant sur le mécanisme de conjugaison bactérienne dont l'efficacité varie selon les souches bactériennes. Une efficacité de conjugaison élevée est nécessaire pour la construction d'une banque de mutants suffisamment dense.

L'efficacité du protocole de conjugaison a donc été évaluée chez les dix souches de *P. aeruginosa* cliniques présélectionnées, ainsi que chez les contrôles positifs de conjugaison *P. aeruginosa* PAO1 et *P. putida* PP1. Ces contrôles permettent en moyenne l'obtention de $5,8 \cdot 10^4$ et $7,4 \cdot 10^4$ clones de conjugaison, respectivement (Fig. III-4). Les souches cliniques ont quant à elles présenté des efficacités de conjugaison très variables, variant de $1 \cdot 10^2$ clones (PA153B) à $2,8 \cdot 10^5$ clones (PA235A). Quatre ont permis l'obtention d'un nombre de clones de conjugaison important et supérieur à 10^4 : PA2600, PA235A, PA124A et PA135E (Fig. III-4). Une variabilité importante du nombre de clones obtenus par conjugaison a cependant été observée pour les souches PA124A et PA135E, les excluant de la suite des expériences. Les souches PA235A et PA2600 ont donc été retenues du fait de leur capacité à produire un nombre important et répétable de clones par conjugaison.

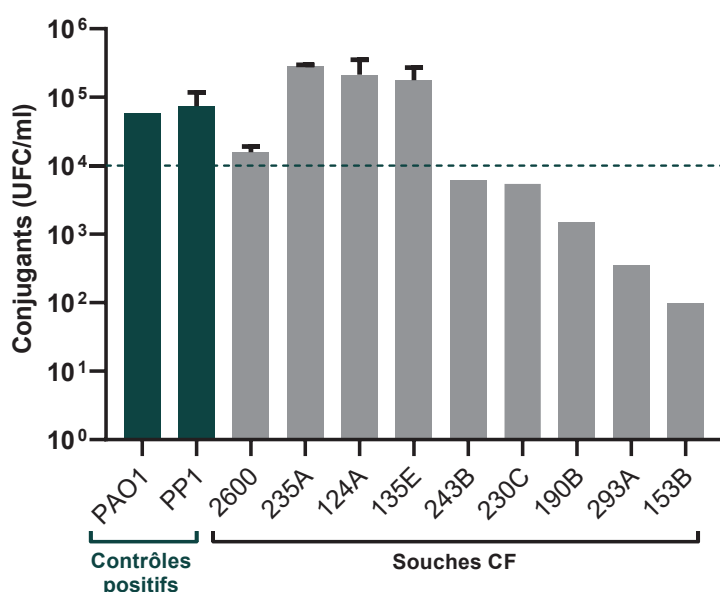


Figure III-4 : Nombre de clones obtenus par expérience de conjugaison chez deux souches contrôles et dix souches cliniques de *P. aeruginosa*. Les barres représentent le nombre de moyens de clones obtenus \pm SEM, issus d'une ou de trois (PP1, PA2600, PA235A, PA124A, PA135E) expériences indépendantes.

3.5.2. Production de la banque de mutants chez PA235A

Le protocole de transfert du plasmide pSAM_DGm a pu être optimisé chez PA235A en multipliant le nombre de gouttes de conjugaison et de boîtes étalées, avec pour objectif la production d'au moins 500 000 mutants. Nous avons ainsi réussi à produire une banque d'environ 680 000 mutants par transposition chez cette souche de *P. aeruginosa* (Fig. III-5).



Les dénombrements effectués avant et après congélation ont permis d'estimer (i) un taux de mortalité de 1% lié au cycle de congélation/décongélation, (ii) une concentration de $2,16 \cdot 10^8$ mutants/mL de banque et (iii) un taux de résistance à la gentamycine de 96%.

Figure III-5 : Gélises étalées pour la construction de la banque chez PA235A. Le plasmide pSAM_DGm a été transféré chez PA235A par conjugaison et les clones ayant intégré le plasmide ont été sélectionnés sur milieu supplémenté en gentamycine.

Le séquençage de la banque pure a permis d'obtenir un nombre de lectures totales de 9,3 à 10,8 millions, et un nombre de lectures alignées sur le génome de PA235A de 7,9 à 9,1 millions. Le transposon s'est inséré dans 86 840 à 86 827 sites TA sur 103 745. Ceci représente une densité d'insertion d'au moins 83,7% permettant d'impacter 97% des 6 343 gènes de PA235A.

Echantillon	Nb. de lectures uniques alignées	Nombre total de sites TA	Nombre de sites TA impactés	Densité
Banque pure A	9 077 582	103 745	86 927	83,8 %
Banque pure B	7 935 921	103 745	86 840	83,7 %
Monoculture A	9 158 900	103 745	82 947	80 %
Monoculture B	7 990 207	103 745	82 974	80 %
Monoculture C	11 951 385	103 745	84 829	81,8 %
Co-culture A	11 810 697	103 745	84 260	81,2 %
Co-culture B	10 805 865	103 745	83 590	80,6 %
Co-culture C	8 633 614	103 745	83 495	80,5 %

Tableau III-4 : Nombre de lectures de séquençage et densité d'insertion du transposon dans la banque pure de PA235A, la monoculture et la co-culture de la banque. Les lettres A, B, C désignent les répliquats. La densité évalue la proportion de sites TA impactés par rapport au nombre total de sites TA présents dans le génome bactérien.

Une première analyse par les méthodes Gumbel et HMM (TRANSIT) a été effectuée sur les données de séquençage de la banque pure. Ces méthodes comparent le nombre d'insertions au niveau des sites TA effectif par rapport à un nombre d'insertions théorique. Ceci permet d'identifier les sites pour lesquels peu ou pas d'insertions sont détectées (sites essentiels), et les sites pour lesquels l'insertion est fréquemment détectée (sites non essentiels). La proportion de sites essentiels et non essentiels est ensuite évaluée pour chaque gène, permettant de déterminer les gènes essentiels de *P. aeruginosa* dans la banque pure. Les méthodes Gumbel et HMM ont permis l'identification de 212 et 296 gènes essentiels respectivement (Fig. III-6A). Les 151 gènes identifiés par ces deux méthodes sont particulièrement impliqués dans la traduction, la biogénèse de la membrane et le transport et métabolisme des co-enzymes, en accord avec de précédentes observations (225, 226) (Fig. III-6B). La liste des gènes essentiels identifiés est accessible sur demande auprès de karen.moreau@univ-lyon1.fr ou loo.camus@gmail.com.

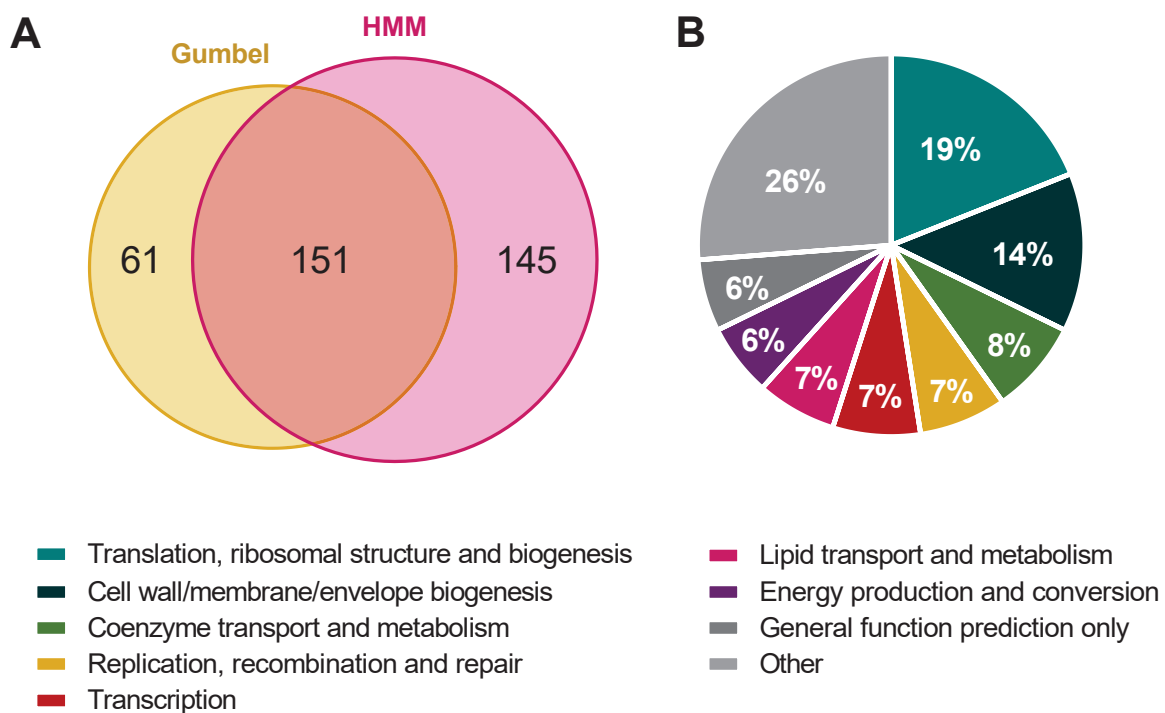


Figure III-6 : Gènes essentiels de *P. aeruginosa* PA235A identifiés par séquençage de la banque pure. **A.** Nombre de gènes essentiels identifiés par les méthodes de Gumbel et HMM. **B.** Catégories fonctionnelles COG (*Clusters of Orthologous Groups*) des 151 gènes essentiels identifiés dans la banque pure par les deux méthodes d'analyse Gumbel et HMM.

3.5.3. Identification des gènes favorables et défavorables à la coexistence

Afin d'identifier les gènes importants pour la coexistence, la banque de mutants de PA235A a été soumise à la pression de sélection que constitue une co-culture avec *S. aureus* SA235. Il est important de noter que ces deux souches ont été co-isolées du même échantillon d'expectoration d'un patient atteint de mucoviscidose. La banque de mutants de PA235A a donc été cultivée en monoculture ou en co-culture avec SA235 pendant 18 heures, avec un repiquage toutes les 6h afin de maintenir les bactéries en phase exponentielle de croissance. La concentration bactérienne est restée supérieure à 10^8 bactéries/mL durant toute la cinétique, bien que *P. aeruginosa* ait présenté une croissance supérieure en co-culture par rapport à la monoculture ($2,7 \cdot 10^8$ vs. $3,9 \cdot 10^9$ à 18h) (Fig. III-7).

P. aeruginosa a ainsi croît pendant 19 générations bactériennes en monoculture, contre 21 générations en présence de *S. aureus*. La concentration de *S. aureus* est quant à elle restée équivalente en mono- et co-culture durant les 18 heures de croissance. Ces conditions ont donc permis de maintenir une pression de sélection suffisamment longue et importante sur la banque de *P. aeruginosa* en co-culture.

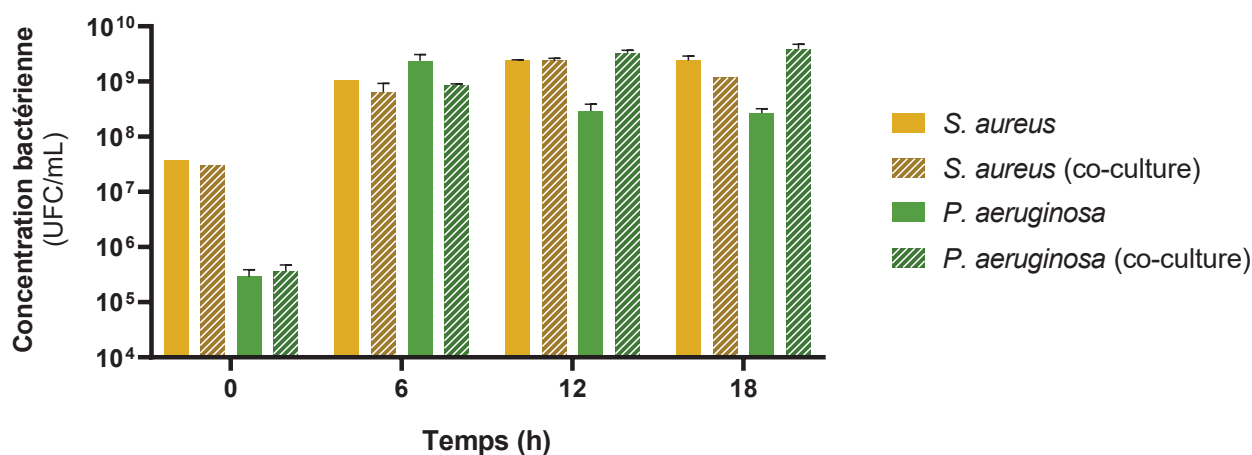


Figure III-7 : Cinétique de croissance bactérienne de la banque de mutants de *P. aeruginosa* PA235A et de *S. aureus* SA235 en monoculture et co-culture. La banque de mutants de *P. aeruginosa* PA235A (barres vertes) et la souche de co-infection SA235 (barres jaunes) ont été inoculées en monoculture (barres pleines) ou en co-culture (barres hachurées) à DO équivalente et cultivées en BHI à 37°C sous agitation. Toutes les 6h pendant 18h, les cultures ont été étalées sur milieu sélectif puis repiquées.

Le séquençage réalisé à l'issue de l'étape de culture a permis d'obtenir 11 et 11,8 millions de lectures en moyenne pour les monocultures et co-cultures, respectivement. Dans ces deux conditions, environ 88% des lectures ont pu être alignées sur le génome de la souche PA235A, permettant de déterminer une insertion effective du transposon au niveau de 80,6% des sites TA de *P. aeruginosa*. Une densité d'insertion légèrement plus élevée (83,7%) avait été observée pour la banque pure (**Tableau III-4**).

Les méthodes de Resampling et Zinb (TRANSIT) (*Cf. Méthodes*) ont ensuite été appliquées pour comparer les nombres d'insertions par gène obtenus dans la monoculture et dans la co-culture, afin de mettre en évidence les gènes de *P. aeruginosa* favorables et défavorables en co-culture. Ces deux analyses ont permis d'identifier au total 37 gènes de *P. aeruginosa* importants pour son maintien lors de l'interaction de coexistence avec *S. aureus*. Parmi ces gènes, 20 ont été mis en évidence par les deux analyses, renforçant leur importance pour *P. aeruginosa* dans ces conditions. Six et 11 gènes ont été identifiés uniquement par les méthodes Resampling et Zinb, respectivement (**Fig. III-8A**).

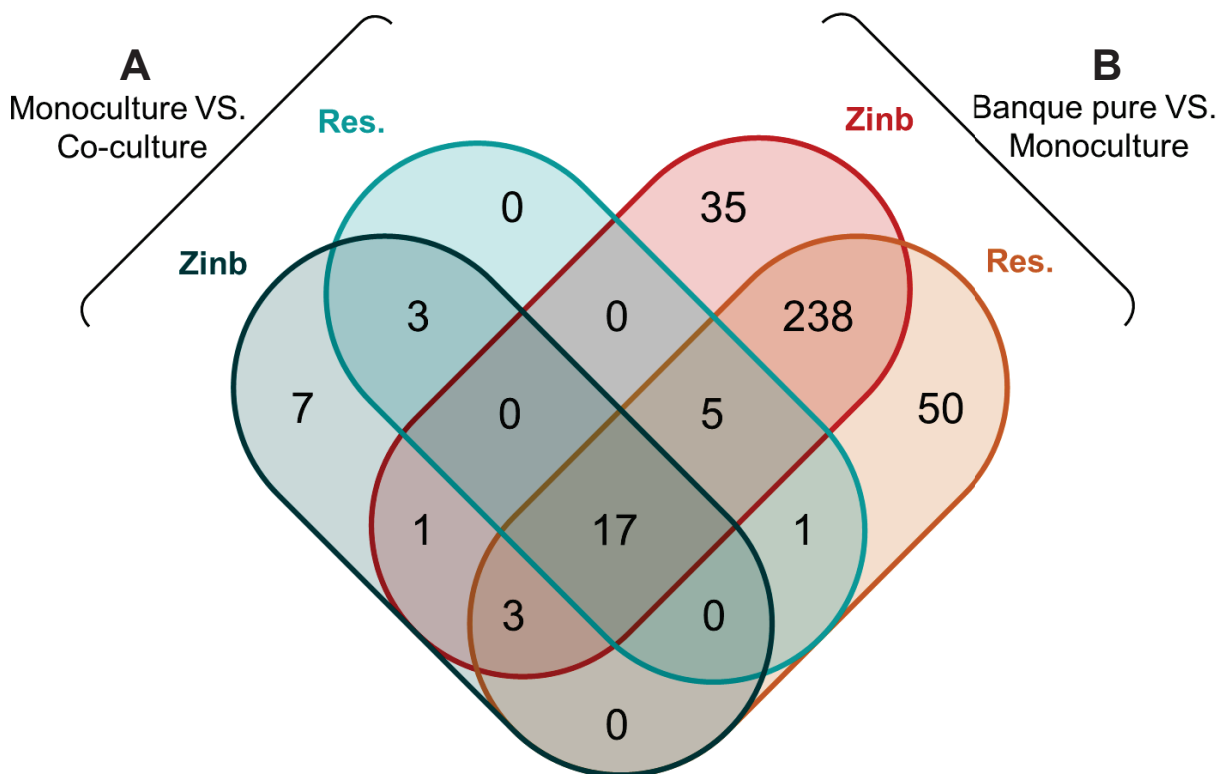


Figure III-8 : Nombre de gènes favorables et défavorables de *P. aeruginosa* PA235A identifiés en co-culture par rapport à la monoculture (A) et en monoculture par rapport à la banque pure (B). Les méthodes de Resampling (Res.) et Zinb ont été utilisées pour comparer les conditions deux à deux.

Parmi les 37 gènes identifiés, 13 ont été prédits comme favorables avec un nombre d'insertions 1,08 à 34,1 fois moins élevé en co-culture par rapport à la monoculture (**Tableau III-5A**). Ces gènes sont impliqués dans le métabolisme de différentes molécules, comme les pyrimidines et purines (*PA3480*, *purF*), le soufre (*tusA*) ou le nicotinate (*sth*). Deux voies métaboliques semblent particulièrement favorables dans ce contexte : la biosynthèse des acides aminés thréonine (*thrC*, *hom*), sérine (*serA*), tyrosine (*aspC*) et histidine (*hisC2*), ainsi que le métabolisme de la thiamine (*thiG*, *thiD*), présentant les plus bas facteurs de nombre d'insertions en co-culture par rapport à la monoculture. De manière intéressante, le gène *mutT*, impliqué dans la réparation de l'ADN et favorable dans nos conditions, partage une forte homologie de séquence avec *thiE* et est suspecté d'intervenir également dans la synthèse de thiamine (227) (**Fig. III-9**).

	Locus PAO1	Nom	Produit	Fonction	FC Res.	FC Zinb
A. Gènes favorables	PA0381	<i>thiG</i>	Thiazole synthase	Métabolisme de la thiamine	-34,1 ****	NS
	PA4400	<i>mutT</i>	Probable pyrophosphohydrolase	Réparation de l'ADN (227)	-22,5 ****	-4,89 ****
	PA3975	<i>thiD</i>	Hydroxyméthylpyrimidine /phosphométhylpyrimidine kinase	Métabolisme de la thiamine	-9,71 *	NS
	PA3736	<i>hom</i> ^a	Homosérine déshydrogénase	Biosynthèse des acides aminés, métabolisme de la glycine, sérine, thréonine, cystéine et méthionine	-11,7 ****	-7,54 ****
	PA3735	<i>thrC</i> ^a	Thréonine synthase	Biosynthèse des acides aminés, métabolisme de la glycine, sérine, thréonine et vitamine B6	-9,58 ****	-4,05 ****
	PA1006	<i>tusA</i>	Protéine porteuse de soufre	Transport du soufre	-10,4 *	-3,45 **
	PA3139	<i>aspC</i>	Aminotransférase d'acides aminés aromatiques	Biosynthèse des acides aminés, métabolisme de la cystéine, méthionine et tyrosine	-3,39 **	-3,15 ***
	PA3480	<i>PA3480</i>	dCTP désaminase	Métabolisme des pyrimidines	-5,17 ****	-2,02 ****
	PA0316	<i>serA</i>	D-3-phosphoglycerate déshydrogénase	Biosynthèse des acides aminés, métabolisme du carbone, glycine, sérine, thréonine, cystéine, méthionine et méthane	-2,66 *	-1,57 *
	PA2991	<i>sth</i>	Pyridine nucléotide transhydrogénase soluble	Métabolisme du nicotinate et nicotinamide	-2,53 ****	-1,37 ***
	PA3165	<i>hisC2</i>	Histidinol-phosphate aminotransférase	Biosynthèse des acides aminés, de la phénylalanine, tyrosine, histidine et tryptophane	NS	-1,47 *
	PA3108	<i>purF</i>	Amidophosphoribosyltransférase	Métabolisme des purines	NS	-1,34 ***
	PA4015	<i>PA4015</i>	Protéine hypothétique	ND	NS	-1,08 *

Tableau III-5A : Gènes favorables au maintien de *P. aeruginosa* PA235A en coexistence avec *S. aureus* SA235. Pour chaque gène, les Fold Change (FC) comparant le nombre d'insertion en co-culture par rapport à la monoculture ont été déterminés par les méthodes de Resampling (Res.) et Zinb et sont indiqués en valeurs linéaires. * $P_{adj} < 0,05$, ** $P_{adj} < 0,01$, *** $P_{adj} < 0,001$, **** $P_{adj} < 0,0001$. Les gènes appartenant à un même opéron sont annotés d'une même lettre. Les fonctions associées ont été déterminées à l'aide de la base de données KEGG (*Kyoto Encyclopedia of Genes and Genomes*) Pathway et la littérature. ND = non déterminé ; NS = non significatif.

Vingt-quatre gènes ont été identifiés comme défavorables pour la survie de *P. aeruginosa* en présence de *S. aureus*, avec un nombre d'insertions 1,08 à 9,78 fois plus élevé en co-culture par rapport à la monoculture (**Tableau III-5B**). Les fonctions de ces gènes sont cette fois-ci plus diverses et impliquent le sensing (*cbrA*), le transport (*oprM*), la synthèse et réparation de l'ADN (*polA*, *rep*), ainsi que la production d'exopolysaccharides Psl pour la formation de biofilm (*psII*, *psIF*) et la synthèse de biotine (*bioA*, *bioC*, *bioF*) et de pyochéline (*pchl*). Le métabolisme carboné, et particulièrement l'alimentation du cycle du citrate à partir du glucose et du pyruvate (*aceE*, *ptsP*, *glpD*, *zwf*, *edaA*, *edd*), apparaît également défavorable dans ces conditions (**Fig. III-9**).

	Locus PAO1	Nom	Produit	Fonction	FC Res.	FC Zinb
B. Gènes défavorables	PA4717	PA4717	Protéine hypothétique	ND	NS	1,08 *
	PA0857	<i>bolA</i>	Protéine morphogène	ND	NS	1,09 ****
	PA0140	<i>ahpF</i>	Alkyl hydroperoxyde réductase	ND	NS	1,10 ****
	PA3133	<i>sawR</i>	Régulateur transcriptionnel	Synthèse des ARNt-aminoacyl et de la pyomélanine (228)	NS	1,10 **
	PA0952	PA0952	Protéine hypothétique	ND	NS	1,12 ***
	ND	ND	tmRNA	ND	NS	1,28 **
	PA4222	<i>pchl</i>	Composant probable de transporteur ABC	Production de pyochéline (229)	NS	1,67 *
	PA3584	<i>glpD</i>	Glycerol-3-phosphate déshydrogénase aérobie	Métabolisme des glycerophospholipides	2,27 **	1,72 *
	PA1767	PA1767	Protéine hypothétique	ND	2,35 *	1,67 *
	PA5296	<i>rep</i>	Hélicase ADN ATP-dépendante	Réplication (230)	2,46 ****	1,59 ****

B. Gènes défavorables (suite)	PA4717	<i>cbrA</i>	Senseur à deux composants	Réponse à la disponibilité en nutriments (231)	2,11 **	2,09 **
	PA0337	<i>ptsP</i>	Système phosphotransférase phosphoenolpyruvate-dépendant	Système phosphotransférase	2,58 ****	1,91 ****
	PA2239	<i>psII</i> ^a	Glycosyltransférase	Formation de biofilm (synthèse des Psl)	2,58 *	NS
	PA0501	<i>bioF</i>	8-amino-7-oxononanoate synthase	Métabolisme de la biotine	NS	2,65 **
	PA3194	<i>edd</i>	Phosphogluconate déshydratase	Voie des pentose phosphates, métabolisme carboné	3,61 **	2,11 *
	PA0371	<i>PA0371</i>	Protéine hypothétique	ND	3,66 ****	2,09 **
	PA5015	<i>aceE</i>	Pyruvate déshydrogénase composant E1	Glycolyse, gluconéogénèse, cycle des citrates, métabolisme carboné	3,32 ****	2,40 ****
	PA2236	<i>psIF</i> ^a	D-inositol-3-phosphate glycosyltransférase	Formation de biofilm (synthèse des Psl)	2,85 *	NS
	PA0420	<i>bioA</i>	Adenosylmethionine-8-amino-7-oxononanoate aminotransférase	Métabolisme de la biotine	4,06 ****	2,08 ***
	PA0503	<i>bioC</i>	Malonyl-[acyl-carrier protein] O-méthyltransférase	Métabolisme de la biotine	3,97 *	NS
	PA3181	<i>edaA</i> ^b	2-dehydro-3-deoxy-phosphogluconate aldolase	Voie des pentose phosphates, métabolisme carboné, du glyoxylate et dicarboxylate	4,69 *	NS
	PA0427	<i>oprM</i>	Protéine de la membrane externe	Résistance aux β-lactames, QS	7,46 ****	3,59 ****
	PA5493	<i>polA</i>	DNA polymérase I	Réparation de l'excision de bases, réplication de l'ADN, recombinaison homologue	6,96 ****	4,61 ****
PA3183	<i>zwf</i> ^b	Glucose-6-phosphate 1-déshydrogénase	Voie des pentose phosphates, métabolisme carboné et du glutathione	9,78 ****	6,58 ****	

Tableau III-5B : Gènes défavorables au maintien de *P. aeruginosa* PA235A en coexistence avec *S. aureus* SA235. Pour chaque gène, les Fold Change (FC) comparant le nombre d'insertion en co-culture par rapport à la monoculture ont été déterminés par les méthodes de Resampling (Res.) et Zinb et sont indiqués en valeurs linéaires. * $P_{adj} < 0,05$, ** $P_{adj} < 0,01$, *** $P_{adj} < 0,001$, **** $P_{adj} < 0,0001$. Les gènes appartenant à un même opéron sont annotés d'une même lettre. Les fonctions associées ont été déterminées à l'aide de la base de données KEGG Pathway et la littérature. ND = non déterminé ; NS = non significatif.

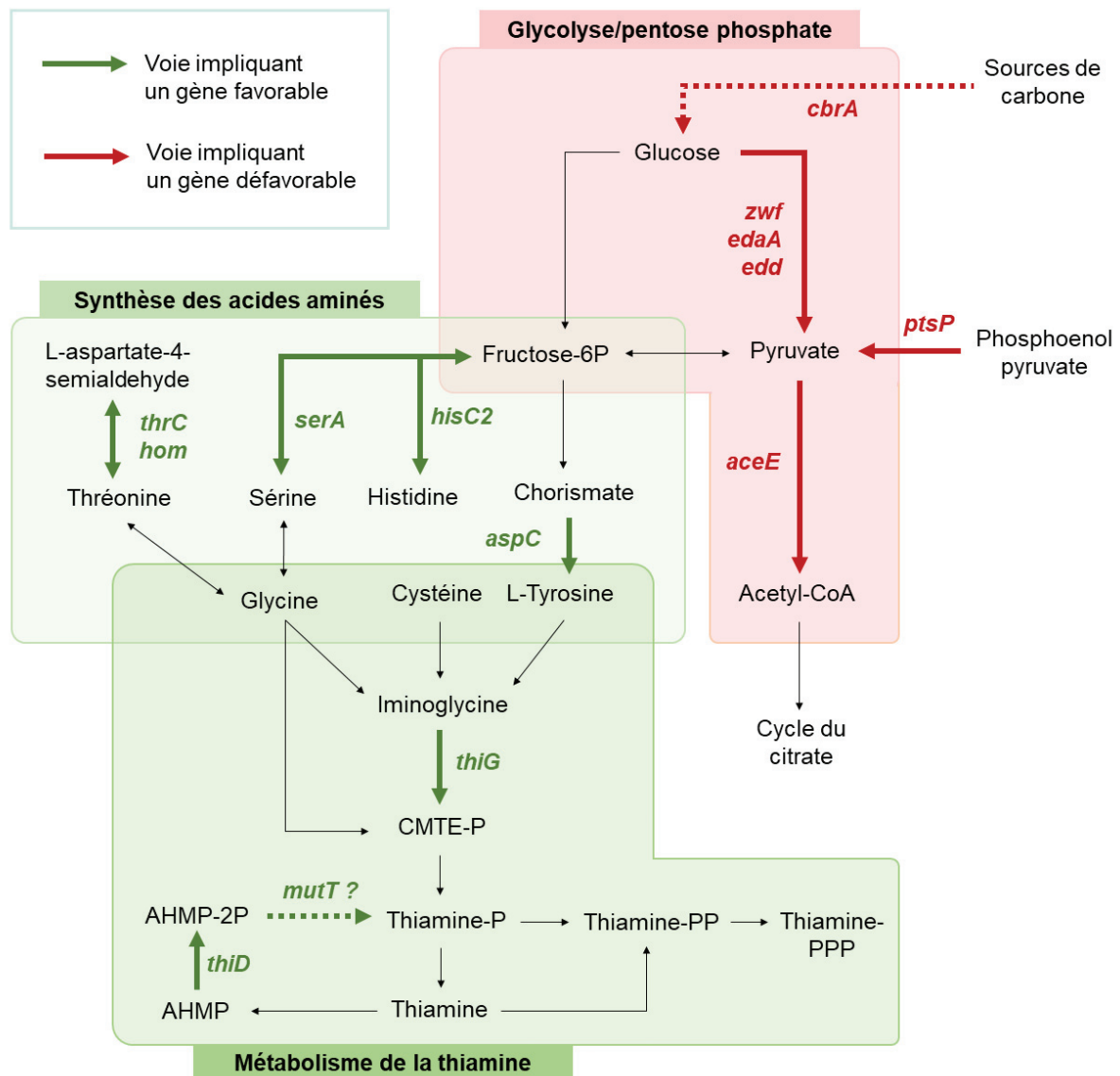


Figure III-9 : Voies métaboliques favorables (vert) ou défavorables (rouge) au maintien de *P. aeruginosa* PA235A en coexistence avec *S. aureus* SA235. Les voies métaboliques ont été construites à partir de la base de données KEGG Pathway et la littérature. La liste complète des gènes essentiels et délétères est fournie en Tableau 4. AHMP : 4-amino-5-hydroxyméthyl-2-méthylpyrimidine ; CMTE : 2-(2-carboxy-4-méthyl-thiazol-5-yl) éthyl phosphate ; P = phosphate.

Enfin, nous avons voulu déterminer si ces gènes favorables et défavorables identifiés en comparant le co-culture à la monoculture étaient également importants dans la survie de *P. aeruginosa*. Pour cela nous avons comparé la monoculture à la banque pure initiale en utilisant de nouveau les méthodes de Resampling et Zinb. Un total de 350 gènes a ainsi été mis en évidence, dont 263 ont été identifiés conjointement par les deux méthodes d'analyse (Fig. III-8B). De façon intéressante, parmi ces 350 gènes figurent 27 des 37 gènes identifiés

comme favorables et défavorables en co-culture par rapport à la monoculture (**Fig. III-8**). Cela signifie que les étapes de monoculture et de co-culture réalisées ont toutes deux induit une sélection des mutants par rapport à la banque pure. Afin d'étudier de manière plus approfondie ce phénomène, une dernière analyse *via* la méthode Zinb a été employée pour comparer les nombres d'insertions détectés dans la banque pure, la monoculture et la co-culture. Contrairement à la méthode de Resampling qui ne permet de comparer qu'une condition à une autre, Zinb permet d'analyser les trois conditions conjointement : pour chaque gène, elle compare le nombre d'insertions dans chaque condition au nombre d'insertion moyen déterminé dans les trois conditions (**Fig. III-10**). Deux éléments sont mis en évidence par cette analyse :

- (1) En comparaison à la banque pure, la quasi-totalité des gènes identifiés précédemment présente un nombre d'insertion plus élevé dans la banque pure que dans les conditions monoculture et co-culture.
- (2) Ces gènes présentent une différence significative du nombre d'insertions détectées en monoculture et en co-culture, confirmant leur rôle dans la survie de *P. aeruginosa* en présence de *S. aureus*.

Il apparaît donc que les mutants de ces gènes sont contre-sélectionnés par les conditions de croissance générées durant notre expérience, mais que cette contre-sélection est soit potentialisée (gènes favorables), soit atténuée (gènes défavorables) par la présence de *S. aureus* dans la culture (**Fig. III-10**).

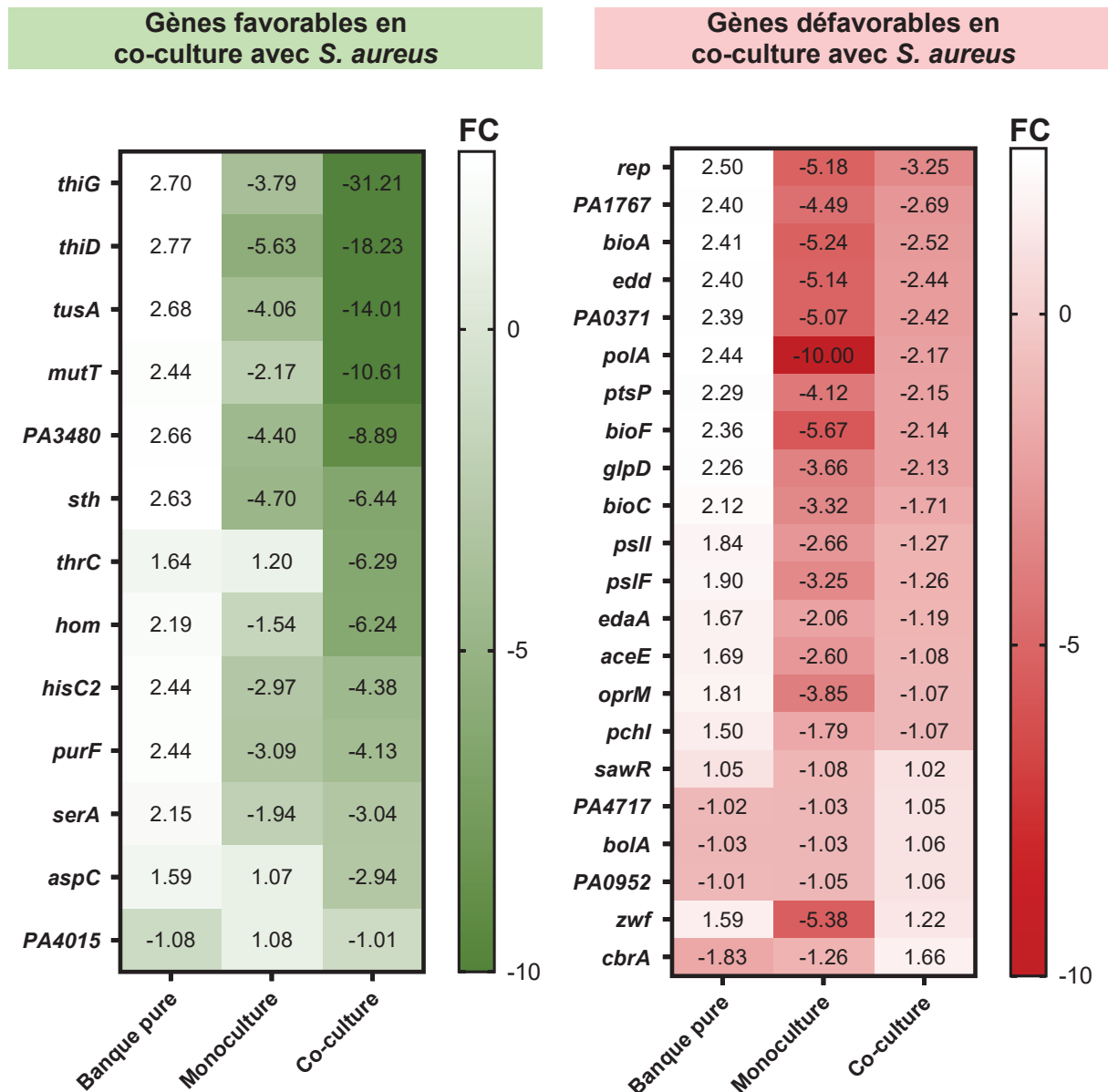


Figure III-10 : Comparaison des nombres d'insertions obtenus pour la banque de PA235A pure, cultivée en monoculture ou en co-culture, pour les gènes favorables et défavorables identifiés en Tableau III-5. Les Fold-Change (FC) comparent le nombre d'insertions pour chaque condition au nombre d'insertion moyen des trois conditions. Les FC ont été déterminés en utilisant la méthode Sinb et sont indiqués en valeurs linéaires. Toutes les valeurs présentées sont significatives ($P_{adj} < 0,05$). Pour une condition et un gène donné, un FC faible (case colorée) indique un nombre d'insertions détectées faible, c'est-à-dire une identification peu fréquente du mutant de ce gène et donc sa contre-sélection dans la condition d'intérêt.

3.6. Discussion et perspectives

3.6.1. *Production de la banque*

La technique de Tn-seq a permis d'étudier l'importance des gènes de *P. aeruginosa* dans un contexte de coexistence avec *S. aureus*, chez des souches responsables de co-infections pulmonaires. La première étape de cette méthode consistait en la production d'une banque de mutants par conjugaison/transposition. Cette banque doit être la plus dense possible afin de muter et ainsi évaluer l'importance d'un maximum de gènes. La technique de Tn-seq n'a été que rarement employée chez des souches cliniques de *P. aeruginosa* (226), les études se concentrant principalement sur des souches de référence. Plusieurs banques ont ainsi été construites chez PA14 (150 000 à 300 000 mutants) (210, 232–234) ou PAO1 (100 000 mutants) (232, 235, 236). Lee et ses collègues étaient parvenus à produire une banque de 1 000 000 de mutants chez PAO1 en sélectionnant les clones de conjugaison sur différents milieux (225). En effet, l'étalement des clones obtenus lors du protocole de mutagenèse constitue une première étape de sélection, puisque la croissance de certains mutants peut être limitée par la composition du milieu utilisé. Bien que nous n'ayons employé qu'un seul milieu, la banque de 680 000 mutants produite dans cette étude a permis de saturer plus de 80% des sites TA de la bactérie et impacter 97% des gènes de *P. aeruginosa*. Ces résultats sont très satisfaisants pour une utilisation optimale de la technique de Tn-seq.

Trente-sept gènes ont ainsi pu être identifiés comme favorables ou défavorables à la coexistence de *P. aeruginosa* avec *S. aureus*. Cette liste de gènes demeure assez restreinte en comparaison à d'autres études centrées sur la survie de *P. aeruginosa* sous pression antibiotique ou lors de la colonisation *in vivo*, qui ont identifié entre 100 et 700 gènes favorables au cours d'une même expérience (210, 233, 235, 236). Ces divergences de résultats sont potentiellement liées à des forces de pression de sélection différentes : en effet, il est probable que la présence d'antibiotique ou le contact avec l'hôte induisent une pression sélective plus importante sur *P. aeruginosa* que la co-culture *in vitro* avec *S. aureus*. La pression de sélection générée par la déplétion en source de carbone *in vitro* a permis d'identifier 24 gènes favorables chez *P. aeruginosa*, et se rapproche donc davantage de notre expérience (234). Le nombre de gènes, et bien sûr les gènes en eux-mêmes identifiés, dépendent donc très fortement des conditions de culture de la banque. Les gènes favorables à *P. aeruginosa* en co-culture avec *S. aureus* peuvent ainsi apparaître aussi favorables sous pression antibiotique, mais défavorables dans des conditions d'infection *in vivo*, comme c'est le cas pour *thrC*. Le gène *sth* apparaît quant à lui favorable en coexistence avec *P. aeruginosa*, en présence de tobramycine mais aussi en conditions d'infection *in vivo* (Fig. III-11).

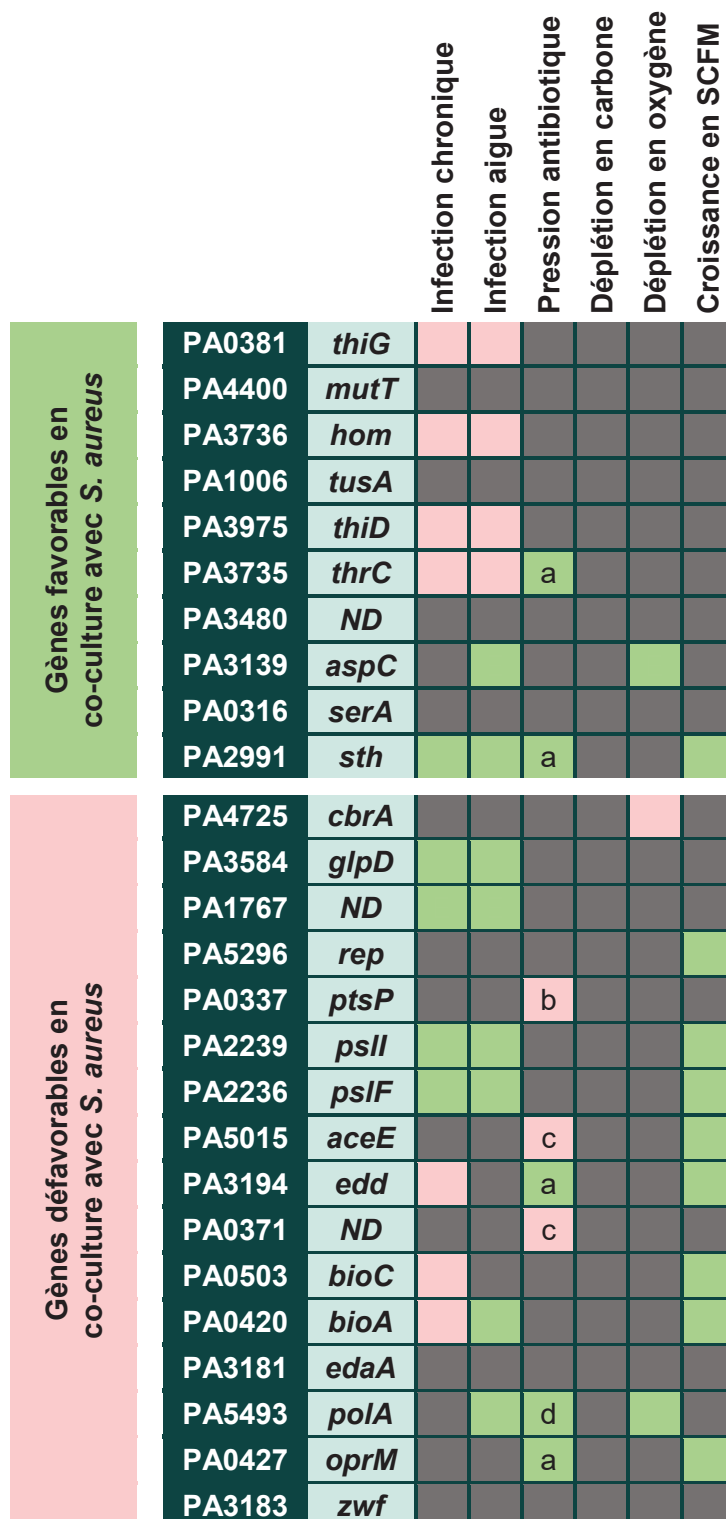
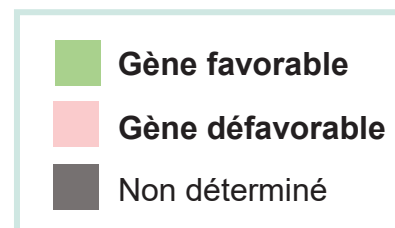


Figure III-11 : Comparaison des gènes favorables (vert) et défavorables (rouge) identifiés dans les études de Tn-seq chez *P. aeruginosa*. La couleur de la case indique si le gène a été identifié comme favorable (vert) ou défavorable (rouge) dans les conditions données : infection in vivo chronique (plaies) ou aigue (brûlures) (236), culture en présence d’antibiotiques (233, 235), déplétion en source de carbone et d’oxygène (234), culture en milieu SCFM (232). Les gènes listés sont ceux identifiés dans notre étude par la méthode de Resampling.

Les lettres indiquent les antibiotiques :

- (a) Tobramycine
- (b) Gentamycine
- (c) Céfopérazone
- Tobramycine, gentamycine, H₂O₂



Les caractéristiques intrinsèques de la souche utilisée peuvent également affecter les gènes identifiés (226, 232). Afin de limiter ce problème, notre projet reposait initialement sur la production et l’utilisation de banques de mutants de deux souches cliniques de *P. aeruginosa*. Si seule la banque chez PA235A a pu être construite au cours de ce doctorat, la souche PA2600 demeure une bonne candidate pour confirmer les résultats obtenus chez une souche clinique supplémentaire (Fig. III-4).

3.6.2. Gènes favorables

Les 13 gènes identifiés comme favorables au maintien de la souche *P. aeruginosa* PA235A en coexistence avec *S. aureus* sont impliqués dans le métabolisme bactérien. Le métabolisme des acides aminés apparaît important dans ce contexte, et particulièrement la synthèse de la thréonine, de l'histidine, de la sérine et de la tyrosine (Fig. III-9). Ces quatre acides aminés sont présents dans le milieu riche employé lors de cette expérience. Par ailleurs, il a été montré que *S. aureus* utilisait ces molécules en tant que source de carbone en absence de glucose (237), une condition rapidement induite par notre protocole de culture (56) (Fig. III-12). Il apparaît donc probable que *S. aureus* catabolise ces acides aminés durant notre expérience, les rendant indisponibles pour *P. aeruginosa* en co-culture. Nous supposons ainsi que l'altération des voies de biosynthèse de ces acides aminés induit chez *P. aeruginosa* une auxotrophie, qui apparaît délétère uniquement en co-culture du fait de l'épuisement de ces composés dans le milieu par *S. aureus*.

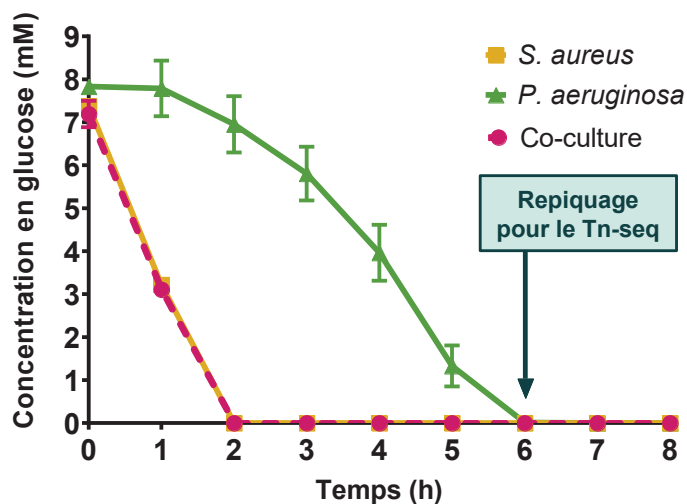


Figure III-12 : Cinétique de dosage du glucose en monoculture de *S. aureus* (jaune), *P. aeruginosa* (vert) ou en co-culture (rose). Adapté de Camus *et al.* (56). Les souches SA2599 et PA2600 ont été cultivées en BHI. Lors du protocole de Tn-seq, les souches ont été repiquées dans du milieu frais toutes les 6h, comme indiqué par la flèche.

Un mécanisme analogue pourrait expliquer l'importance des gènes *thiG*, *thiD* et *mutT*. En effet, la thiamine, et plus particulièrement sa forme active pyrophosphate (TPP), est nécessaire au fonctionnement d'enzymes clés du métabolisme carboné comme les pyruvate déshydrogénases (238). Une souche de *P. aeruginosa* ne produisant pas de TPP est ainsi incapable de croître en absence d'apport exogène de la molécule (238). Ainsi, nous supposons que l'altération des gènes *thiG*, *thiD* et *mutT* affecte la production de thiamine et de TPP chez *P. aeruginosa* et diminue sa croissance en l'absence de ces composés. Cet effet n'est observé qu'en co-culture, suggérant que *S. aureus* affecterait également la composition en thiamine du milieu. Le catabolisme de la thiamine n'est pas décrit chez *S. aureus*, mais cette molécule est aussi essentielle à son métabolisme. De plus, les souches de *S. aureus* peuvent être

auxotrophes à la thiamine (239, 240). Il est donc possible que *S. aureus* acquiert et épuise la thiamine du milieu de culture en co-culture, affectant alors le développement des mutants de *P. aeruginosa* incapables de synthétiser la molécule.

Des dosages de thréonine, histidine, sérine, tyrosine et thiamine en mono- et co-culture permettraient de mieux appréhender leur rôle exact dans l'interaction de *P. aeruginosa* avec *S. aureus in vitro*. Dans le contexte pulmonaire de la mucoviscidose, de hautes concentrations en acides aminés sont généralement dosées dans les expectorations de patients (1, 190, 241) (Fig. III-13). De ce fait, les isolats de *P. aeruginosa* s'adaptant au milieu pulmonaire développent fréquemment des auxotrophies, et ce particulièrement aux acides aminés méthionine, leucine et arginine. En revanche, les auxotrophies à la thréonine, l'histidine, la sérine et la tyrosine ne sont que très rarement observées malgré des quantités élevées dans les expectorations de patients (Fig. III-13) (1, 190, 242, 243, 241). L'auxotrophie à la thiamine est également peu documentée chez les souches cliniques de *P. aeruginosa* (243). La biosynthèse de ces composés apparaît donc conservée lors de l'adaptation de *P. aeruginosa* au milieu pulmonaire. D'une part, et comme le suggèrent nos résultats, la contre-sélection des isolats de *P. aeruginosa* incapables de synthétiser ces composés pourrait être induite par la présence de *S. aureus* dans les poumons. D'autre part, ceci suggère une importance de la production de la thréonine, de l'histidine, de la sérine, de la tyrosine et de la thiamine dans l'établissement et le maintien de *P. aeruginosa* dans le milieu pulmonaire. Un rôle de la synthèse de thiamine dans la virulence de *P. aeruginosa in vivo* a récemment été observé et soutient cette hypothèse (238).

Le gène *tusA*, identifié comme favorable dans nos conditions, aurait également un impact sur la virulence de *P. aeruginosa*. En effet, *tusA* code pour un transporteur du soufre dont l'activité régule positivement l'expression de nombreux facteurs QS-dépendants, la formation de biofilm ainsi que la virulence de la bactérie dans un contexte d'infection pulmonaire chez le rat (244). Ce transporteur est également important pour les activités de dénitrification de *P. aeruginosa* en condition d'anaérobiose et en présence de nitrate (244, 245). Ce processus ne semble cependant pas essentiel à *P. aeruginosa* lors de son interaction avec *S. aureus*, puisque nous avons précédemment observé une sous-expression de nombreux gènes de la dénitrification (*nor*, *nir* et *nos*) en co-culture (56). L'importance de *tusA* en co-culture semblerait ainsi davantage liée à son rôle dans la régulation de la virulence de *P. aeruginosa*. Ces résultats suggèrent que le maintien de *P. aeruginosa* en présence de *S. aureus* impliquerait certains facteurs de virulence, dépendants notamment de l'acquisition du soufre et de la synthèse de thiamine.

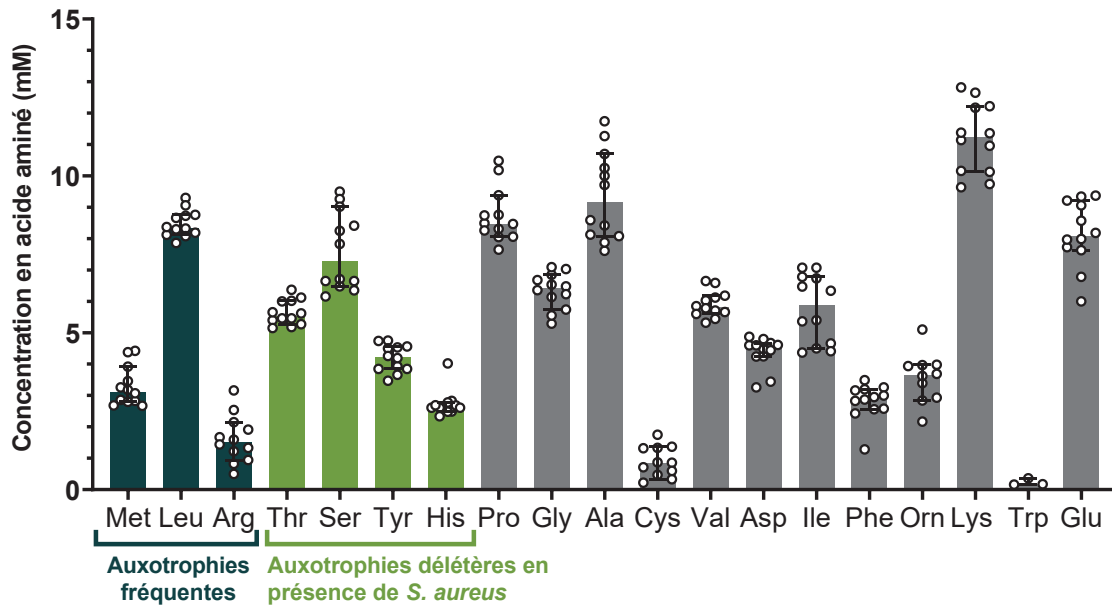


Figure III-13 : Concentrations médianes en acides aminés dosés dans les expectorations de 12 patients atteints de mucoviscidose. Adapté de Palmer *et al.* (1).

3.6.3. Gènes défavorables

Comme suggéré par les facteurs favorables identifiés, la coexistence avec *S. aureus* affecte fortement le métabolisme de *P. aeruginosa*. L'utilisation des sources de carbone est particulièrement touchée et implique CbrA, le senseur du système à deux composantes CbrAB qui régule la répression catabolique (246). Le gène *cbrA* est ainsi identifié comme défavorable pour *P. aeruginosa* dans nos conditions, suggérant que l'ajustement de l'utilisation des sources de carbone est un facteur important pour sa survie en présence de *S. aureus*. En accord avec cela, cinq gènes impliqués dans le métabolisme du glucose et du pyruvate (*edd*, *zwf*, *edaA*, *aceE* et *ptsP*) sont également identifiés comme défavorables en co-culture avec *S. aureus*. Le glucose étant précocement épuisé de la co-culture (Fig. III-12) (56), il est probable que ces voies métaboliques ne soient en effet plus utiles à la bactérie dans ces conditions. Cette hypothèse est soutenue par la sous-expression de gènes impliqués dans le métabolisme du glucose (dont *edd*, *zwf* et *edaA*) précédemment observée en présence de *S. aureus* (56). Nous supposons que les mutants de ces gènes sont sélectionnés du fait du coût énergétique économisé par *P. aeruginosa* en ne maintenant pas ces voies métaboliques devenues inutiles.

Au-delà de ce coût énergétique réduit, l'altération de ces gènes affecte probablement d'autres aspects de la physiologie de *P. aeruginosa*. Les gènes *zwf*, *psII* et *psIF*, défavorables dans nos conditions, sont en effet impliqués dans la production des exopolysaccharides

alginate et Psl, respectivement (247). Le gène *ptsP* régule quant à lui positivement la formation de biofilm chez *P. aeruginosa* (248). La production d'exopolysaccharides et de biofilm semble donc avoir un impact négatif sur la survie de *P. aeruginosa* en coexistence avec *S. aureus* dans nos conditions. De manière intéressante, la production d'alginate affecte positivement la survie *S. aureus* en co-culture avec *P. aeruginosa* (58, 167). Le rôle de l'alginate dans leur interaction apparaît donc complexe, suggérant que la survie optimale des deux pathogènes repose sur une production ajustée et équilibrée de la molécule. Il serait intéressant de confirmer le rôle des gènes *zwf*, *psII*, *psIF* et *ptsP* sur l'interaction *P. aeruginosa*-*S. aureus* dans des conditions expérimentales favorisant davantage la formation de biofilm et la production d'exopolysaccharides, contrairement à notre dispositif de culture liquide sous agitation.

Plusieurs gènes identifiés comme défavorables à la survie de *P. aeruginosa* en présence de *S. aureus* ont des fonctions dans la virulence de la bactérie. Les gènes *bioA*, *bioC* et *bioF* responsables de la synthèse de biotine, ainsi que le senseur *cbrA*, sont importants pour la colonisation *in vivo* (249, 250). De plus, le gène *pchl* intervient dans la production de pyochéline, un sidérophore impliqué dans la virulence de *P. aeruginosa* (156). La survie des mutants *bioA*, *bioC*, *bioF*, *cbrA* et *pchl* étant améliorée en présence de *S. aureus*, il est possible qu'un phénotype de virulence réduite soit ainsi favorisé chez *P. aeruginosa* en co-culture. Enfin, il est intéressant de noter que *aceE* et *cbrA* sont des gènes fréquemment mutés lors de l'adaptation de *P. aeruginosa* au milieu pulmonaire. De la même manière, les voies de d'entretien et de réparation de l'ADN ainsi que la biosynthèse des exopolysaccharides Psl, ici représentées par les gènes *polA* et *psIIF* respectivement, sont altérées lors de cette adaptation (192, 197). Il apparaît donc que les mutants de ces gènes sont sélectionnés à la fois par le milieu pulmonaire et par la coexistence avec *S. aureus* dans notre expérience. Ceci suggère que la présence de *S. aureus* dans les poumons pourrait favoriser la sélection des mutants de ces gènes, soutenant l'hypothèse d'un rôle de *S. aureus* dans la pathoadaptation de *P. aeruginosa*.

En plus d'une virulence diminuée, les mutants *cbrA* présentent une résistance accrue à une variété d'antibiotiques (249). Cependant, le gène codant la porine OprM, essentielle à l'efflux antibiotique *via* les systèmes MexAB-OprM et MexXY-OprM (251), est également identifié comme défavorable dans nos conditions. Le rôle de la résistance antibiotique de *P. aeruginosa* pour son maintien en présence de *S. aureus* demeure donc difficile à évaluer selon ces résultats contradictoires, d'autant plus que les gènes *mexAB* et *mexXY* n'ont pas été mis en évidence par nos analyses et que les étapes de cultures ont été effectuées en l'absence d'antibiotiques (Fig. III-14).

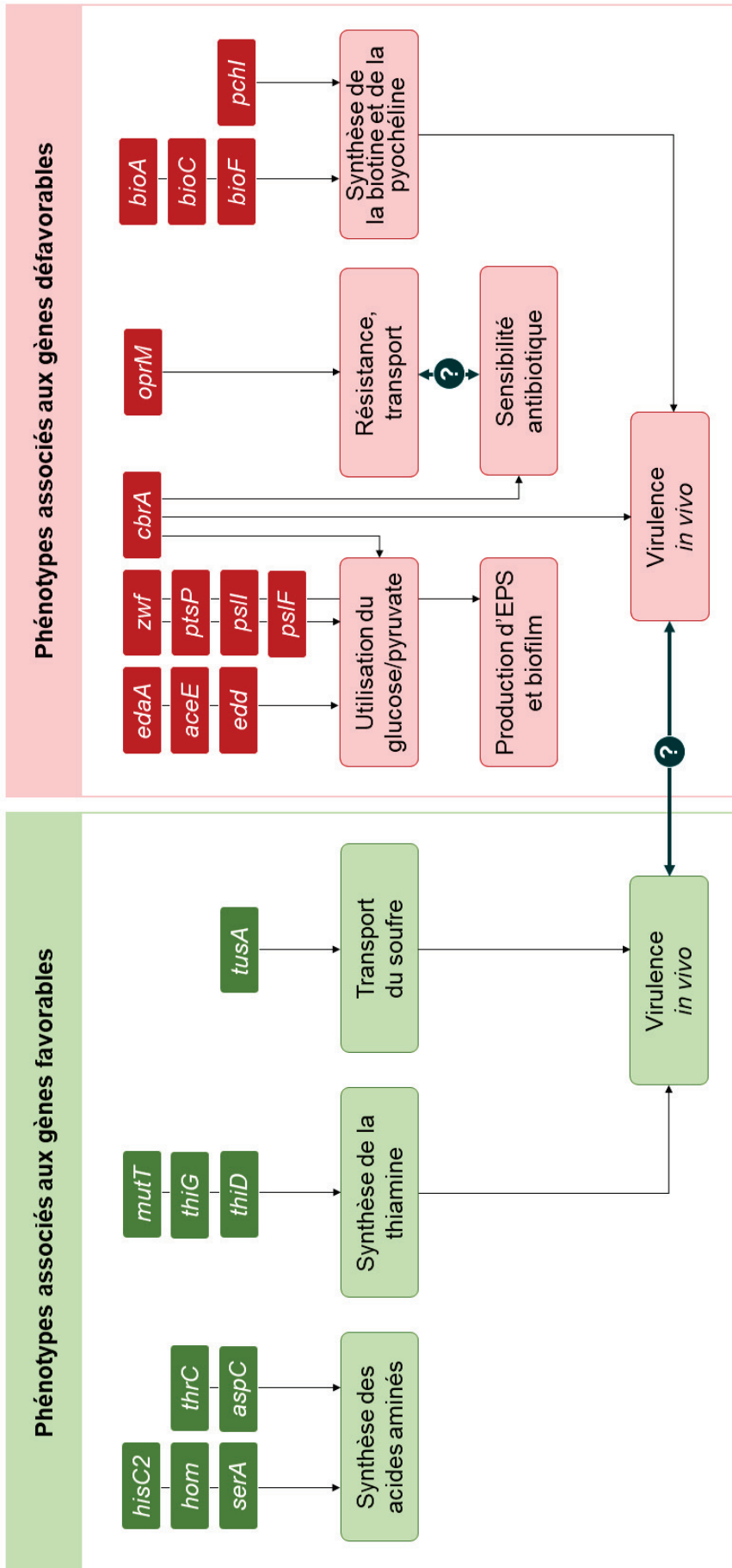


Figure III-14 : Phénotypes associés aux gènes favorables (vert) ou défavorables (rouge) au maintien de *P. aeruginosa* PA235A en coexistence avec *S. aureus* SA235. EPS : exopolysaccharides. Les flèches bleues indiquent les phénotypes dont le rôle reste incertain du fait de résultats contradictoires selon les gènes identifiés.

3.6.4. Perspectives et conclusions

Les résultats obtenus dans cet axe de recherche ouvrent de nombreuses questions et perspectives, notamment sur le rôle de *S. aureus* dans les processus adaptatifs de *P. aeruginosa*. Afin de mieux comprendre ce phénomène, il apparaît crucial de caractériser les phénotypes induits par les gènes favorables ou défavorables identifiés. Pour ces facteurs, des mutants devront donc être construits et étudiés phénotypiquement ; les phénotypes observés pourraient alors être comparés avec les phénotypes fréquemment développés lors de l'adaptation de *P. aeruginosa* au milieu pulmonaire. Ces mutants devront également être co-cultivés avec *S. aureus* pour confirmer ou infirmer leur rôle dans le maintien de *P. aeruginosa* en co-culture. Plusieurs fonds génétiques de *P. aeruginosa* pourraient être employés afin de limiter les effets isolat-dépendants liés à la diversification des isolats cliniques (252, 253).

L'utilisation de la technique de Tn-seq chez la souche clinique PA235A a cependant permis une première identification des facteurs de *P. aeruginosa* impliqués dans son maintien en coexistence avec *S. aureus*. La synthèse des acides aminés et de la thiamine apparaissent favorables, alors que l'utilisation du glucose et du pyruvate semblent non-essentiels et/ou défavorables à la survie de *P. aeruginosa*. En association avec l'approche transcriptomique présentée précédemment, ces résultats confirment que la coexistence avec le staphylocoque implique largement le métabolisme des acides aminés et du glucose chez *P. aeruginosa*. Ces modifications métaboliques sont primordiales pour la survie bactérienne dans les conditions nutritives induites par le milieu pulmonaire des patients atteints de mucoviscidose (190, 242). D'autres facteurs impliqués dans le maintien de *P. aeruginosa* en coexistence avec *S. aureus* pourraient également affecter sa colonisation et sa virulence *in vivo* (gènes *thiDG*, *tusA*, *cbrA*, *bioACF*) et donc sa persistance dans les poumons des patients atteints de mucoviscidose (Fig. III-14).

4 Autres travaux

Paul Briaud a également effectué sa thèse au sein du laboratoire et a travaillé sur l'interaction de coexistence entre *P. aeruginosa* et *S. aureus* (207). Nous avons mené nos projets de doctorat en étroite collaboration ; j'ai ainsi eu l'opportunité de participer à l'élaboration de deux publications scientifiques dont Paul est premier auteur.

4.1. Impact de la coexistence sur le transcriptome et la résistance antibiotique de *S. aureus*

L'approche transcriptomique décrite dans le premier axe du projet a également été développée pour étudier l'impact de *P. aeruginosa* sur *S. aureus* durant l'interaction de coexistence. En utilisant des paires de souches isolées de patients atteints de mucoviscidose co-infectés et présentant cet état de coexistence, nous avons observé que le transcriptome de *S. aureus* est largement affecté par la présence de *P. aeruginosa*. Des expériences de séquençage des ARN sur 2 couples, et de confirmation par RT-qPCR sur 12 couples de souches, ont ainsi mis en évidence la surexpression de nombreux gènes codant des transporteurs chez le staphylocoque en co-culture. Parmi ces transporteurs figurent Tet38, NorA et NorC, qui sont impliqués dans la résistance antibiotique de *S. aureus*. La surexpression des gènes codant ces pompes à efflux n'est induite que par un contact rapproché entre *S. aureus* et *P. aeruginosa*, et fait intervenir le régulateur majeur MgrA. La co-culture avec *P. aeruginosa* affecte ainsi la physiologie du staphylocoque : (i) sa survie est augmentée en présence d'antibiotiques tels que la tétracycline et la ciprofloxacine grâce à la surexpression de Tet38, et (ii) la bactérie présente une capacité d'internalisation augmentée dans les cellules épithéliales pulmonaires A549.

Les résultats de cette étude montrent que la coexistence avec *P. aeruginosa* affecte spécifiquement la physiologie de *S. aureus*. Le staphylocoque bénéficie de cette interaction via l'augmentation de phénotypes de persistance tels que l'antibio-résistance et l'internalisation dans les cellules de l'hôte. Ces résultats confirment que la coexistence entre *P. aeruginosa* et *S. aureus* n'est pas neutraliste et affecte positivement leur physiologie (56). Cette interaction pourrait favoriser la persistance des deux pathogènes au sein des poumons, et donc affecter l'état de santé des patients atteints de mucoviscidose.

OPEN

Coexistence with *Pseudomonas aeruginosa* alters *Staphylococcus aureus* transcriptome, antibiotic resistance and internalization into epithelial cells

Paul Briaud¹, Laura Camus¹, Sylvère Bastien¹, Anne Doléans-Jordheim^{3,4}, François Vandenesch^{1,2,3} & Karen Moreau^{1*}

Cystic fibrosis (CF) is the most common life-threatening genetic disease among Caucasians. CF patients suffer from chronic lung infections due to the presence of thick mucus, caused by *cftr* gene dysfunction. The two most commonly found bacteria in the mucus of CF patients are *Staphylococcus aureus* and *Pseudomonas aeruginosa*. It is well known that early-infecting *P. aeruginosa* strains produce anti-staphylococcal compounds and inhibit *S. aureus* growth. More recently, it has been shown that late-infecting *P. aeruginosa* strains develop commensal-like/coexistence interaction with *S. aureus*. The aim of this study was to decipher the impact of *P. aeruginosa* strains on *S. aureus*. RNA sequencing analysis showed 77 genes were specifically dysregulated in the context of competition and 140 genes in the context of coexistence in the presence of *P. aeruginosa*. In coexistence, genes encoding virulence factors and proteins involved in carbohydrates, lipids, nucleotides and amino acids metabolism were downregulated. On the contrary, several transporter family encoding genes were upregulated. In particular, several antibiotic pumps belonging to the Nor family were upregulated: *tet38*, *norA* and *norC*, leading to an increase in antibiotic resistance of *S. aureus* when exposed to tetracycline and ciprofloxacin and an enhanced internalization rate within epithelial pulmonary cells. This study shows that coexistence with *P. aeruginosa* affects the *S. aureus* transcriptome and virulence.

Most microorganisms are frequently embedded within communities of mixed species where different microbial interactions can occur between individual species. In the case of infection, these interactions between species can influence pathogenic behavior such as virulence, biofilm formation and antibiotic tolerance^{1–4}.

One of the most well-known examples of pathologies in which many bacterial interactions are described are lung diseases occurring during Cystic Fibrosis (CF). The airways of CF patients are colonized by multiple microorganisms whose prevalence varies with the age of the patients. Among them, *Staphylococcus aureus* and *Pseudomonas aeruginosa* are the most prevalent pathogens and are acquired in subsequent order. The typical pattern of chronic infection establishment begins with the early acquisition of *S. aureus*, (60% prevalence among children aged <2 years and the highest prevalence in children of 11–17 years (80%)), while prevalence slowly declines in adults (50%)⁵. In contrast, infections by *P. aeruginosa* occur later with the highest prevalence in adults (70% among 35–44 year-old patients). Although these bacteria seem to succeed one another, they are not mutually exclusive since patients are frequently diagnosed as being co-infected by *S. aureus* and *P. aeruginosa* (from 35% to 50%)^{6,7}.

While *P. aeruginosa* is recognized as the leading cause of lung function decline, the significance of *S. aureus* in the course of CF disease is still being debated. It has been shown that one of the risk factors for initial *P. aeruginosa*

¹CIRI, Centre International de Recherche en Infectiologie, Inserm U1111, Université Lyon1, Ecole Normale Supérieure de Lyon, CNRS UMR5308, Lyon, France. ²Centre National de Référence des Staphylocoques, Hospices Civils de Lyon, Lyon, France. ³Institut des agents infectieux, Hospices Civils de Lyon, Lyon, France. ⁴Bactéries Pathogènes Opportunistes et Environnement, UMR CNRS 5557 Ecologie Microbienne, Université Lyon 1 & VetAgro Sup, Villeurbanne, France. *email: karen.moreau@univ-lyon1.fr

airway infection includes *S. aureus* pre-colonization^{8–10}. However, the impact of coinfection by the two pathogens on the evolution of the disease remains unclear^{11–13}.

S. aureus and *P. aeruginosa* have been identified in the same lobe of CF lungs^{14,15}, suggesting that both pathogens are present in the same niche and can in fact interact *in vivo*. Interactions have been widely studied and it is commonly admitted that *P. aeruginosa* outcompetes *S. aureus*. Different mechanisms have been described¹⁶; for example, *P. aeruginosa* secreted products can inhibit the growth or lyse *S. aureus* as well as induce epithelial cells to kill *S. aureus* and other Gram-positive bacteria^{8,17,18}.

However, these interactions can evolve during chronic colonization. Indeed, *P. aeruginosa* strains isolated from early infection outcompete *S. aureus*, as previously described, while strains isolated from chronic infection are less aggressive and can be co-cultivated with *S. aureus*^{19,20}. Furthermore, *P. aeruginosa* isolates from mono-infected patients are more competitive towards *S. aureus* than isolates from coinfecting patients²¹.

In contrast to antagonistic interactions, nothing is known about the effects of *P. aeruginosa* and *S. aureus* interactions in this context of coexisting bacteria within the same infectious niche. Using a transcriptomic approach, we analyzed how co-cultivation with non-competitive *P. aeruginosa* altered *S. aureus* gene expression, especially genes encoding Nor family efflux pumps. In the presence of *P. aeruginosa*, over-expression of these genes increased *S. aureus* antibiotic tolerance and the rate of internalization into epithelial cells, two key determinants of chronic infection.

Results

Coexistence interaction involves more than half of the *S. aureus* and *P. aeruginosa* isolates from co-infected CF patients.

Two types of interactions between *S. aureus* and *P. aeruginosa* could be observed with CF patient isolates: the well-described competitive phenotype, where *P. aeruginosa* inhibits *S. aureus* growth¹⁶, and the newly described phenotype of coexistence, where *P. aeruginosa* is unable to outcompete *S. aureus*^{19–21}. In order to quantify the importance of this last phenotype, we collected 50 pairs of *S. aureus* and *P. aeruginosa* from 36 co-infected CF patients. The interaction between the two pathogens was analyzed by a competitive test on trypticase soy agar (TSA) plates (Table 1 - Fig. 1A). We observed that 61% of strain pairs presented a coexistence phenotype whereas 39% were in competitive interaction. To determine whether the pairs of coexisting strains and competitive strains were phenotypically different, we measured colony size, analyzed the hemolytic properties of each strain, and searched for pigmentation and mucoid phenotype for all *P. aeruginosa* strains. No significant differences were observed between coexisting and competitive strains with respect to pigment production, mucoid phenotype and hemolysis (Fig. S1). We observed a significant difference in the size of *S. aureus* colonies in which those of coexisting strains were larger than those of competition strains after 24 h of TSA plate culture. The significance of such a difference and its impact on interaction with *P. aeruginosa* remain to be explored. As others have already described that early infectious strains of *P. aeruginosa* are more aggressive for *S. aureus* than the late infectious strains^{19,20}, we wondered if the type of interaction could be related to the duration of colonization. To answer this question, we determined the duration of co-colonization of *S. aureus* and *P. aeruginosa* for each patient. The average duration of colonization for coexisting strains was 744.8 ± 97.64 days and for competing strains 941.2 ± 137 days. The difference was statistically non-significant (Fig. S1).

Planktonic cultures were conducted on two pairs of strains: one competitive pair (SA2597/PA2596) and one coexisting pair (SA2599/PA2600). In both cases, we observed that *P. aeruginosa* growth was not altered by *S. aureus*. On the other hand, in the case of the competitive pair, *P. aeruginosa* had a negative effect on *S. aureus* growth after 4 hours of coculture (Fig. 1B).

Agar plate competition assays mixing respectively PA2600 (from coexisting pair) and PA2596 (from competitive pair) with both SA2597 and SA2599 were performed (Fig. 1A). PA2596 outcompeted both SA strains whereas PA2600 was unable to inhibit any of the *S. aureus* strains, suggesting that the interaction phenotype is dependent on the *P. aeruginosa* strains. These results were confirmed with other combinations of strains (Fig. S2).

P. aeruginosa differentially dysregulates *S. aureus* transcriptome according to coexistence/competition.

To obtain an overview of the impact of *P. aeruginosa* on the expression of *S. aureus* genes, a comparative transcriptomic study was conducted between SA2597 and SA2599 in monocultures, and the same strains in coculture with a competition PA strain (PA2596) and a coexisting PA strain (PA2600). Thus, for each interaction state, we tested two pairs of strains, namely SA2597/PA2596 and SA2599/PA2596 for the competition and the SA2597/PA2600 and SA2599/PA2600 pairs for coexistence. Gene expression was considered dysregulated when dysregulation was common to both pairs of strains. Therefore, seventy-seven *S. aureus* genes were specifically dysregulated in the context of competition and 140 genes in the context of coexistence while only 16 genes were dysregulated both in competition and in co-existence (Table S4).

KEGG analyses were performed on dysregulated genes to associate each gene with a functional class (Fig. 2). In competition state, the main dysregulated class of genes belongs to genetic information and processing, with an increase of tRNA and ribosomal RNA (Fig. 2A). We also observed the dysregulation of genes involved in major metabolism pathways of carbohydrates and amino acids. The down-regulation of the Acetyl-coenzyme A synthetase encoding gene (*acsA*) was noted. Other genes involved in energetic metabolism were up-regulated in the presence of *P. aeruginosa*, especially dehydrogenase enzymes such as the lactate dehydrogenase (*ldhA*), the alanine dehydrogenase (*ald1*), the glutamate dehydrogenase (*gluD*), the 1-pyrroline-5-carboxylate dehydrogenase (*rocA*), the 2-oxoglutarate dehydrogenase (*odhA*) and the aldehyde-alcohol dehydrogenase (*adhE*). The upregulation of the *ldh* gene is consistent with the up regulation of the L-lactate permease (*lctP*) encoding gene. All these factors, as well as acetyl-coA, are involved in energetic metabolism and redox reactions conducted to feed the Krebs cycle and ensure the production of ATP.

In the context of coexistence, although *P. aeruginosa* does not appear to impact major metabolic pathways of *S. aureus* as it does not alter growth, the expression of 140 *S. aureus* genes was affected by the presence of *P.*

Patients	<i>S. aureus</i>					<i>P. aeruginosa</i>					co-colonisation length (days)	type of interaction
	strain number	hemolyse type	Colony size (mm)	pigmentation	MLST	strain number	hemolyse type	Colony size (mm)	pigmentation	mucoidy		
1	SA2597	γ	1	none		PA2596	β	4	Yellow	yes	1544	competition
2	SA2599	β	3	none	CC188	PA2600	γ	5	Yellow	yes	1902	coexistence
3	SA27	β	2	none	CC398	PA27	γ	3	none	no	295	coexistence
4	SA30	β	2	none	CC188	PA30	γ	1,2	none	no	133	coexistence
5	SA31	β	3	none	CC15	PA31	γ	1,1	none	yes	921	coexistence
6	SA42	γ	2	none	CC30	PA42	γ	20	Yellow	yes	?	coexistence
7	SA69	β	3	none	CC25	PA69	β	2,1	none	yes	92	coexistence
8	SA80	β	2	none	CC15	PA80A	α	2,2	Green	yes	623	coexistence
				none		PA80B	α	6	none	yes	623	coexistence
9	SA82	β	4	none	CC45	PA82	γ	4	none	yes	?	coexistence
10	SA146	γ	2	none	CC88	PA146	γ	4,5	Green	yes	928	coexistence
11	SA147	β	2	none		PA147A	γ	2	Green	no	?	competition
				none		PA147B	γ	1,4	none	no		competition
12	SA148	γ	1 à 2	none		PA148A	β	7	none	yes	839	competition
				none		PA148B	β	14	Green	yes		coexistence
13	SA150	β	2	none		PA150	γ	1	none	no	380	coexistence
14	SA151	β	2	none		PA151A	α	4,5	Brown	yes	538	coexistence
				none		PA151B	β	4	Yellow	yes		coexistence
15	SA152	β	3	none	CC8	PA152	γ	13	none	yes	991	coexistence
16	SA153	β	3	none	CC398	PA153A	β	3	none	no	967	coexistence
						PA153B	β	2,5	Green	yes		coexistence
17	SA154	γ	2	none		PA154A	γ	35	none	yes	595	coexistence
				none		PA154B	γ	5	Green	yes		coexistence
18	SA155	β	2	none		PA155	α	11	Green	yes	1256	competition
19	SA156	β	2	none	CC398	PA156	α	2,1	none	yes	49	coexistence
20	SA157	β	2	none		PA157	β	5	Green	yes	?	competition
21	SA158	γ	1 à 2	none		PA158	β	6	Green	yes	?	competition
22	SA159	β	<1 SCV (1,5)*	none		PA159A	β	5	none	yes	1353	competition
				none		PA159B	β	18	Green	yes		competition
23	SA160	γ	<1 SCV (1,1)*	none		PA160A	β	5	Green	yes	1332	competition
				none		PA160B	β	10	Yellow	yes		competition
24	SA161	β	2	none		PA161	α	2	none	no	1043	coexistence
25	SA165	β	3	none		PA165A	β	3,9	none	yes	343	coexistence
				none		PA165B	β	4,1	none	yes		coexistence
26	SA166	γ	2	none		PA166A	α	4	Green	yes	1355	coexistence
				none		PA166B	α	4,5	Green	yes		coexistence
27	SA167	β	3	none		PA167	α	13	Green	yes	938	competition
28	SA168A	β	2	none		PA168	γ	4	none	yes	294	competition
	SA168B	β	2	none								competition
29	SA169	β	4	none		PA169	γ	3,5	none	no	904	coexistence
30	SA171	β	1 à 2	none		PA171	β	1,1	none	yes	601	coexistence
31	SA177	β	3	none		PA177	γ	2	none	yes	1380	coexistence
32	SA178	β	3	none		PA178	β	2,5	none	yes	519	coexistence
33	SA179	β	1 à 2	none		PA179	β	3	none	yes	91	competition
34	SA181	β	4	none		PA181	β	6	none	yes	1096	competition
35	SA182	γ	2	none		PA182A	β	5	Yellow	yes	987	competition
				none		PA182B	α	7	none	yes		competition
				none		PA182C	β	4,2	none	yes		coexistence
36	SA186	β	2	none		PA186	β	3	none	yes	623	competition

Table 1. *S. aureus* and *P. aeruginosa* clinical strains used in this study. 50 couples of *S. aureus* and *P. aeruginosa* were collected from 36 patient sputum samples. Some patients presented several *P. aeruginosa* isolates, and one patient presented two *S. aureus* isolates. Colony size, pigmentation and mucoid phenotype were determined on TSA. Hemolysis type was determined on COS. Interaction type was determined by agar plate competition assay as described in the materials and methods section. The isolates in bold correspond to those used for the RNAseq and RT-qPCR analyses. MLST type were determined only for these isolates. *Colony size after 48 h incubation - ? colonization time before sampling could not be determined for these patients.

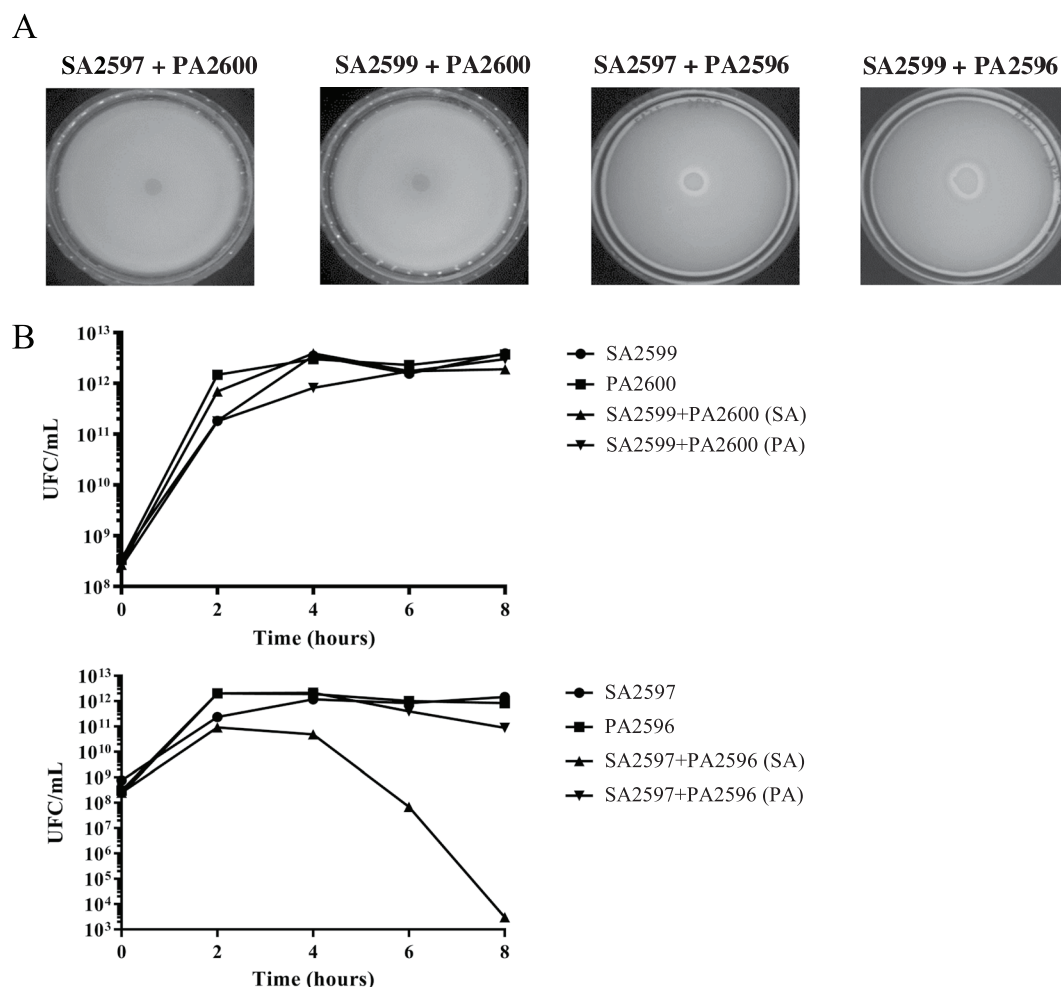


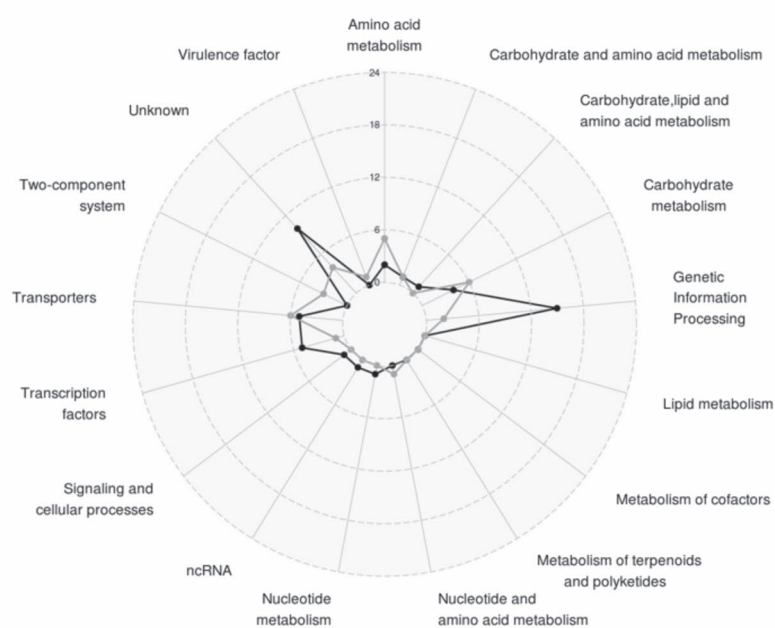
Figure 1. Competition assay between *S. aureus* and *P. aeruginosa*. **(A)** Competition test on agar plate. *S. aureus* and *P. aeruginosa* were grown on BHI for 8 hours at 37 °C. A layer of *S. aureus* was added on a TSA. After drying, a drop of *P. aeruginosa* was spotted. The inhibition halo indicates a competition state (SA2597 + PA2596 and SA2599 + PA2596). **(B)** Competition assay in planktonic culture. *S. aureus* and *P. aeruginosa* were mono-cultivated and co-cultivated for 8 hours. Every two hours, bacteria were plated on mannitol salt agar (MSA) and cetrимide to count *S. aureus* and *P. aeruginosa*, respectively. The results show one representative experiment from a triplicate. Upper panels, pairs in coexistence. Lower panels, pairs in competition.

aeruginosa (Fig. 2B). Nine known and predicted virulence factor encoding genes were upregulated, including alpha-hemolysin (*hla*), staphylokinase (*sak*), aureolysin (*aur*), the immunoglobulin-binding protein (*sbi*) and staphylococcal complement inhibitor (*scn*) genes. We also observed the overexpression of *saeRS* genes, coding a two component system that has been described as playing a major role in controlling the production of virulence factors such as those mentioned above²².

Other genes whose expression was affected by the presence of *P. aeruginosa* in a coexistence situation are involved in carbohydrates, lipids, nucleotides and amino acids metabolism. Most of them were down-regulated as several genes (*pgi*, *fbp*, *fda*) involved in glycolysis and the pentose phosphate pathway. Moreover, two operons (*nrdE*, *nrdI*, *nrdF* and *nrdG*, *nrdD*) belonging to ribonucleotide reductase (RNR) systems and converting nucleoside phosphate into deoxynucleotide phosphate, were both down-regulated (Table S4). RNRs are involved in the *de novo* production of deoxyribonucleotide di- or triphosphates, an essential process for the biosynthesis of DNA and its repair. They catalyze the limiting step of the synthesis of deoxyribonucleotide phosphates and thus control cell concentration²³.

Finally, several genes belonging to a transporter family were also over-expressed (polyamines, methionine, iron uptake and antibiotic resistance) in the coexistence state. Notably, all genes from the polyamine operon were over-expressed (*potABCD*) including *potR*, the regulator of polyamine genes. Polyamines control the physiology of *S. aureus* by acting as regulators of several genes involved in metabolism, transport and virulence^{24,25}. In addition, the same pattern was observed for the *metQPN* operon involved in methionine transport and *sirA/B* and *sstA/BC* genes for iron uptake, which may also reflect nutrient competition in coculture. Finally, transporter *norb_3* predicted as belonging to the *nor* family was over-expressed. Pumps from this family export a

A - Competition



B - Coexistence

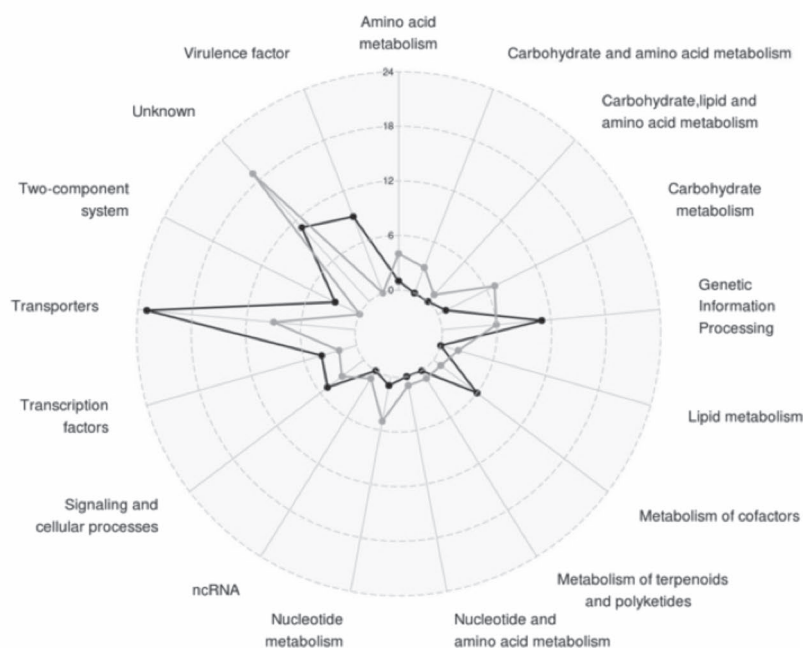


Figure 2. Number and functions of differentially expressed staphylococcal genes in the presence of *P. aeruginosa* when both species are: (A) in competition (SA2596 and SA2599 were co-cultivated with PA2597) or (B) in coexistence (SA2596 and SA2599 were co-cultivated with PA2600). RNAs were extracted at 4 hours and a RNAseq was performed in triplicates. KEGG mapper analysis was conducted on common significantly over-expressed (black) and under-expressed genes (grey) to address a functional classification. A gene was considered as differentially expressed when the fold change was strictly higher than 4 with $P_{adj} < 0.05$.

wide range of antibiotics such as erythromycin, tetracycline and quinolones. Indeed, *norB_3* corresponds to the well-described *tet38* gene involved in tetracycline resistance and internalization in pulmonary epithelial cells^{26,27}.

To confirm these results, we performed co-cultivations with 12 different co-existence *P. aeruginosa*-*S. aureus* strain pairs from CF patients. The 12 strain pairs came from 12 different patients and presented phenotypic diversity. *S. aureus* isolates belong to 8 different multilocus sequence typing (MLST) types (Table 1). Ten isolates of

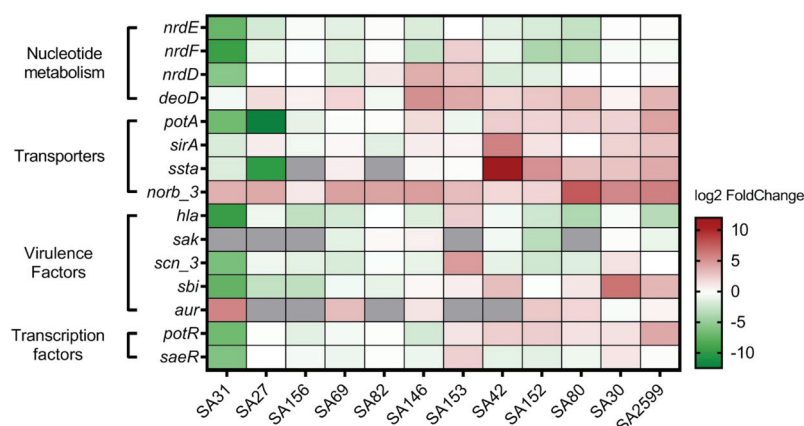


Figure 3. Confirmation of *S. aureus* gene expression dysregulation by *P. aeruginosa*. Twelve clinical SA-PA strain pairs were co-cultivated for 4 hours. RNAs were extracted and RT-qPCR were performed on 15 genes. The results are represented as fold change of expression (gene relative expression in coculture/gene relative expression in monoculture) on a heatmap. Under-expressed genes are indicated in green whereas over-expressed genes are indicated in red. No RNA detection is shown in grey. Pairs were hierarchically clustered by the Euclidean method.

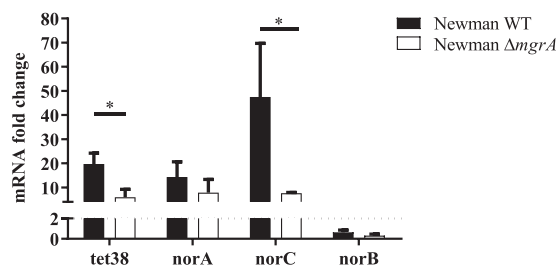


Figure 4. The *S. aureus* MgrA regulator is important for *nor* gene over-expression. Cocultures of *S. aureus* Newman wild type (WT) and $\Delta mgrA$ mutant with PA30 were performed. RNAs were extracted at 8 hours and *nor* gene expression was monitored by RT-qPCR. The results are shown as the mean + standard deviation of three independent experiments. Dotted lines indicate fold change = 2. Statistical analysis was performed by unpaired t-test (* $P < 0.05$).

P. aeruginosa were mucoid and four secreted pigmentation, which was representative of the collection of all the isolates. Gene expression was assessed by RT-qPCR for the two categories most impacted: virulence factors and transporters (Fig. 3). Regarding virulence factors, we confirmed the over-expression of the aureolysin encoding gene in 6 of the 7 strains that expressed the gene. For *sbi*, 5 out of 12 strains presented over-expression and 5 out of 12 presented decreased expression, meaning that there was no clear profile of *P. aeruginosa*'s impact on this gene expression. For the other virulence genes tested, we observed reduced expression in the majority of the strains (10/12 for *hla*, 5/7 for *sak*, 7/12 for *saeRS* and 8/12 for *scn*) (Fig. 3).

For transporter encoding genes, we confirmed the over-expression of *pot* genes and the *sstA* gene in 6/12 and 7/10 strains, respectively. Noticeably, we confirmed the up-regulation of *tet38* genes in 11/12 strains with a fold change ranging from 3 to 200. In addition, *deoD* gene upregulation was also confirmed in 9/12 strains, consistent with its operon structure with *tet38* gene²⁶.

The over-expression of the *tet38* gene is the most predominant transcriptomic alteration in our study and may be of great importance as it can affect the antibiotic susceptibility of *S. aureus*, an important element in the context of CF disease. Therefore, we aimed to better characterize this transcriptomic alteration.

Over-expression of the *tet38* gene is due to the dysregulation of the MgrA regulatory pathway that impacts other *nor* family genes. To decipher the molecular pathway involved in the over-expression of the *tet38* gene, we analyzed the expression of known regulators in the presence or absence of *P. aeruginosa*. Three transcriptional negative regulators of *tet38* have already been described: TetR21²⁶, SarZ²⁸ and MgrA²⁷. The expression of these regulators was quantified by RT-qPCR in coculture and compared to expression in monoculture. None of the *tetR21*, *sarZ* and *mgrA* RNA levels was affected by the presence of *P. aeruginosa* (Fig. S3).

However, it has been described that regulation by MgrA is dependent on its phosphorylation state²⁹ and that the deletion of *mgrA* induces increased expression of *tet38*²⁷. Therefore, we analyzed the impact of *P. aeruginosa* on *tet38* expression using a Newman $\Delta mgrA$ mutant (Fig. 4). The wild type Newman strain presented a 20-fold change over-expression of the *tet38* gene in the presence of *P. aeruginosa*, as we previously observed in clinical

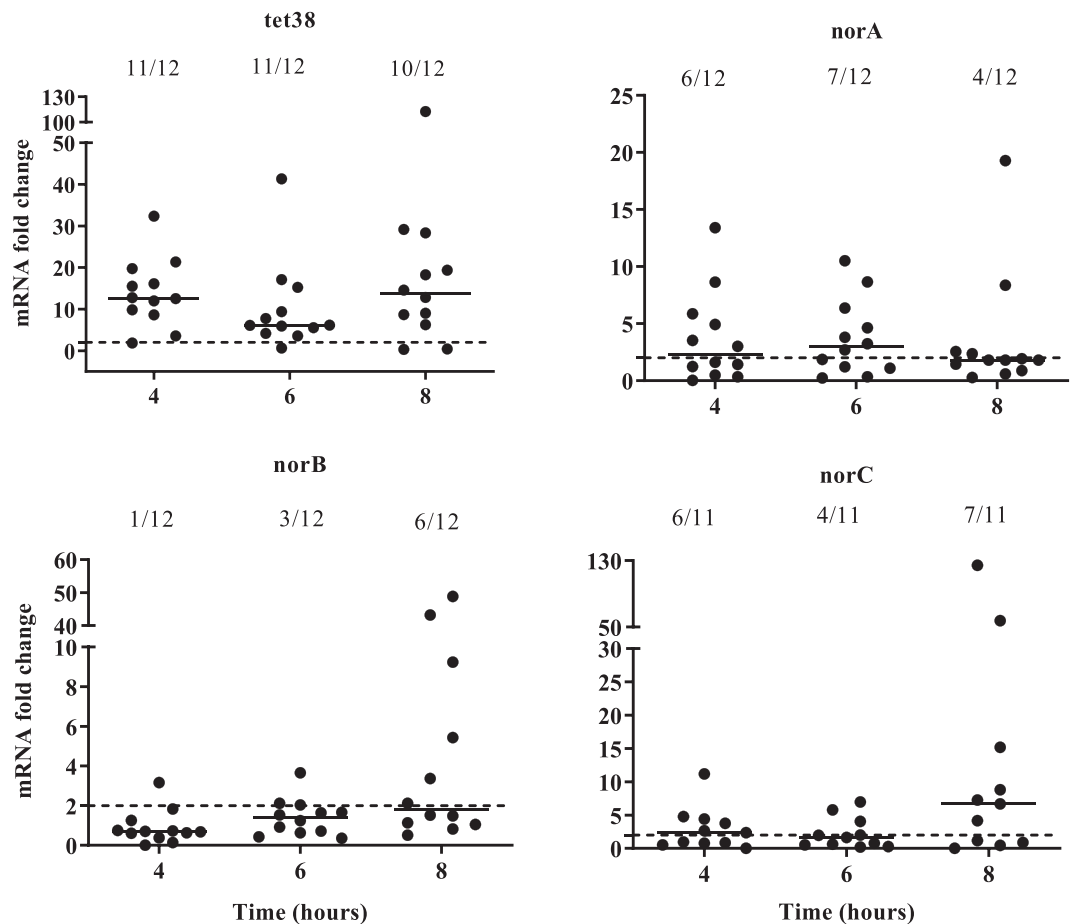


Figure 5. The over-expression of *S. aureus* *nor* family genes induced by *P. aeruginosa*. Mono- and cocultures with twelve clinical strain pairs were performed. RNAs were extracted and gene expression was monitored by RT-qPCR at 4, 6 and 8 hours. The results are represented as fold change expression. Dotted lines indicate fold change = 2. Numbers above each hour indicate the number of pairs with a fold change strictly higher than 2.

strains. This fold change was reduced to 6 for the $\Delta mgrA$ mutant. Therefore, it appears that the over-expression of the *tet38* gene is induced by an alteration of the MgrA regulatory pathway. These results were confirmed in *S. aureus* Lac isogenic strains (Fig. S4).

MgrA is also a transcriptional regulator of other *nor* family protein genes such as *norA*, *norB* and *norC*^{27,29,30}. Hence, the expression of *nor* genes in *S. aureus* was monitored throughout cocultures of the 12 *S. aureus* strains with *P. aeruginosa* (Fig. 5). The *tet38* gene was significantly overexpressed in the presence of *P. aeruginosa* throughout the 8 hours of the culture. The *norA* gene was over-expressed in at least 50% of cocultures (6/12 and 7/12) after 4 and 6 hours of culture and *norC* expression was increased at 4 and 8 hours in 6/11 and 7/11 strains, respectively (Fig. 5). *norB* was overexpressed only at 8 hours of culture in 50% of the strains tested.

From the analysis of expression in the $\Delta mgrA$ mutant in the *S. aureus* Newman strain, we concluded that over-expression of *norC* was dependent on MgrA integrity (Fig. 4). A milder effect was observed on *norA* over-expression. No overexpression of *norB* gene was observed with the *S. aureus* Newman strain. In the *S. aureus* Lac strain, we observed a diminution of *norA* and *norC* overexpression in the $\Delta mgrA$ mutant but the effect was less significant than on *tet38* gene expression (Fig. S4). Therefore, we concluded that the overexpression of *norA* and *norC* genes in the presence of *P. aeruginosa* was partially due to *mgrA* dysregulation.

The presence of *P. aeruginosa* induces over-expression of *nor* genes by specific and direct interaction.

To determine if a secreted product of *P. aeruginosa* induced the over-expression of *nor* genes, a transwell experiment was conducted in which cultures of *P. aeruginosa* and *S. aureus* were separated by a 0.4 μm filter. In these conditions, *nor* genes were not overexpressed (Fig. 6). The same results were obtained when *S. aureus* culture was exposed to supernatant of *P. aeruginosa* (Fig. S5), suggesting that at least a close interaction between the two species was necessary. Finally, to determine if the over-expression was specific to the interaction with *P. aeruginosa*, cocultures were conducted with other bacteria frequently associated with *S. aureus* in CF patients, such as *Burkholderia cenocepacia* and *Stenotrophomonas maltophilia* (Fig. 7). No over-expression was observed, suggesting that the effect was specific to the presence of *P. aeruginosa*. These results were confirmed with other clinical *S. aureus* strains (Fig. S6).

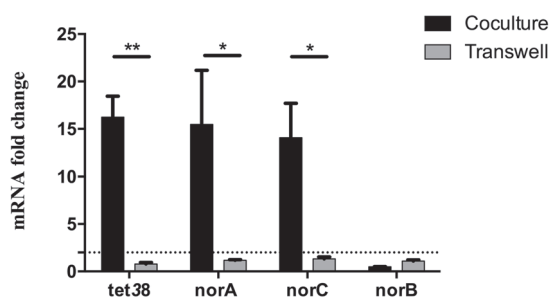


Figure 6. *S. aureus* *nor* gene over-expression requires close contact with *P. aeruginosa*. *S. aureus* was deposited onto the bottom of wells. *P. aeruginosa* was added either with *S. aureus* (black) or into the insert of transwells (gray). RNAs were extracted and *nor* gene expression was monitored by RT-qPCR. Dotted lines represent fold change = 2. The results are shown as the mean + standard deviation of three independent experiments on SA30-PA30 pair. Statistical analysis was performed by unpaired t-test (* $P < 0.05$, ** $P < 0.01$).

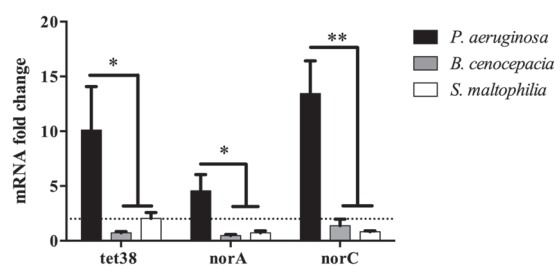


Figure 7. The overexpression of *S. aureus* *nor* genes is specifically induced by *P. aeruginosa*. *S. aureus* was mono- and cocultivated with *P. aeruginosa*, *B. cenocepacia* or *S. maltophilia*. RNAs were extracted and gene expression was monitored by RT-qPCR. Dotted lines indicate fold change = 2. The results represent the mean + standard deviation of three independent experiments on SA30-PA30 pair. Statistical analysis was performed by One-way Anova with Dunnett's multiple test correction (* $P_{adj} < 0.05$, ** $P_{adj} < 0.01$).

Over-expression of *nor* genes induces an increase of antibiotic resistance and internalization of *S. aureus* into epithelial cells. As Tet38 is involved in tetracycline resistance²⁷ and NorA and NorC are also implicated in quinolones (such as ciprofloxacin) uptake^{30,31}, the impact of coculture with *P. aeruginosa* on *S. aureus* antibiotic susceptibility was tested. Firstly, the MIC was determined for each of the 12 *S. aureus* strains used (Table S3). Monocultures and cocultures were then exposed to tetracycline and ciprofloxacin at MIC or 2xMIC. After plating on selective agar and numeration, the survival rate was determined by dividing the number of *S. aureus* after antibiotic treatment by the number of *S. aureus* without antibiotic treatment. A 3-fold increase in survival rate was observed at MIC and 2xMIC in the presence of *P. aeruginosa* (Fig. 8A,B).

In order to demonstrate that the over-expression of the *tet38* gene was responsible for tetracycline resistance, the impact of *P. aeruginosa* was tested on the RN6390 wild type strain and its isogenic $\Delta tet38$ mutant upon exposure to tetracycline. As expected, *P. aeruginosa* induced a higher survival rate of the RN6390 wild type strain after tetracycline exposure. On the contrary, it had no impact on the bacterial survival of the $\Delta tet38$ mutant after tetracycline exposure (Fig. 8C), confirming the role of the *tet38* gene in the enhancement of tetracycline resistance in the presence of *P. aeruginosa*.

Tet38 has also been described as being involved in pulmonary epithelial cell internalization²⁶, so the impact of the presence of *P. aeruginosa* on *S. aureus* cell internalization was tested using the Gentamicin protection assay. When A549 epithelial cells were infected with a monoculture of *S. aureus*, five percent of adherent bacteria were internalized into cells. When *S. aureus* was co-cultivated with *P. aeruginosa* before cell infection, 15% of *S. aureus* were internalized, meaning a 3-fold increase of the *S. aureus* internalization rate in the presence of *P. aeruginosa* (Fig. 9). No difference was observed in terms of bacterial adhesion onto A549 cells. To ensure that the effect we observed was not due to an alteration of the A549 cell layer by *P. aeruginosa* that could have facilitated *S. aureus* internalization, we performed an LDH measurement on the cell supernatant as an indicator of A549 cell viability (Fig. S7B). Although the LDH level was slightly higher for cells infected only with *P. aeruginosa*, we found no significant difference between the *S. aureus* infected and *S. aureus* plus *P. aeruginosa* co-infected cells. Indeed, the A549 co-infected cells had the lowest level of LDH. Moreover, microscopic observation of the cells revealed no difference between the mono- and co-infected cells (Fig. S7A). Therefore, it appeared that the presence of *P. aeruginosa* did not alter the A549 cells and the highest rate of *S. aureus* internalization was due to its direct impact on *S. aureus*. However, we could not be sure that the increase in the internalization rate was directly related to *tet38* overexpression. It could be the result of a modification of different factors involved in the internalization process, although we did not identify such factors in our transcriptomic analysis apart from the *tet38* gene.

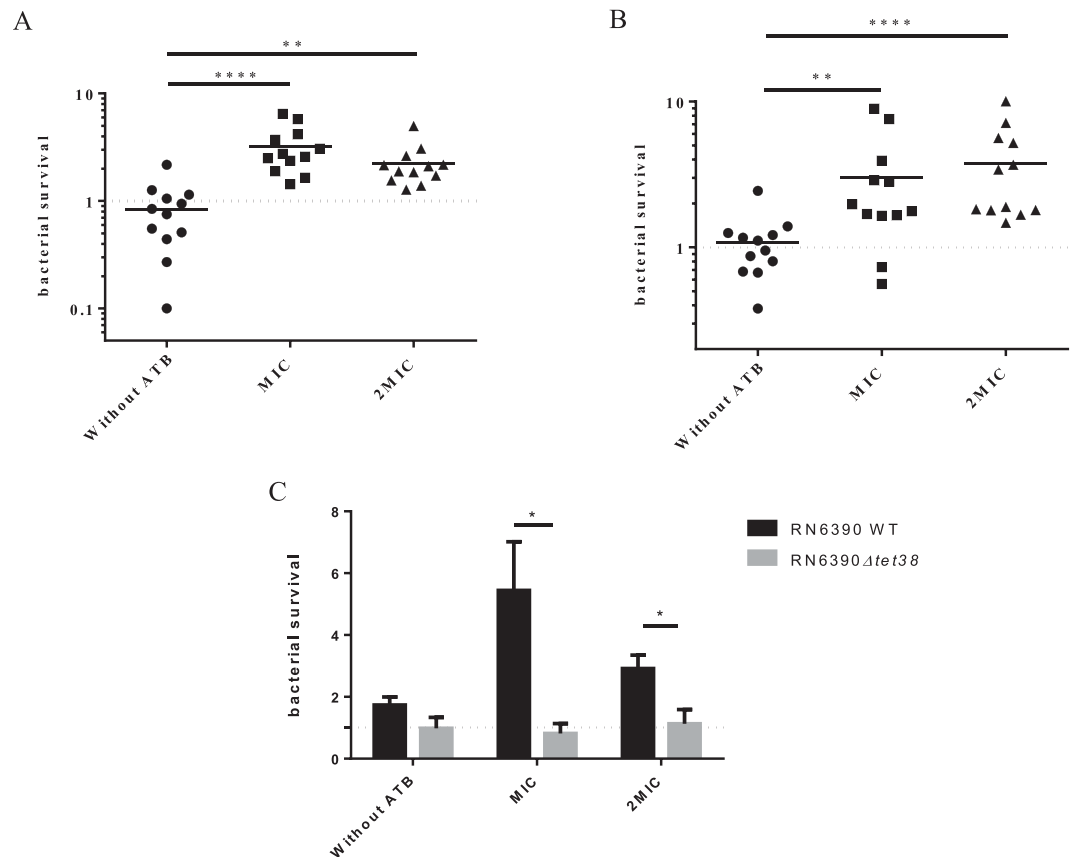


Figure 8. *S. aureus* antibiotic resistance increases when co-cultivated with *P. aeruginosa*. Twelve clinical *S. aureus* strains were mono- and cocultivated with coexisting *P. aeruginosa* strains and exposed to tetracycline (A) and ciprofloxacin (B) at MIC and 2xMIC. After 5 hours, cultures were plated on MSA to count remaining *S. aureus*. Bars represent the median and dotted lines bacterial survival equal to 1. Statistical significance was determined by One-way Anova with Dunnett's multiple test correction (** $P_{adj} < 0.01$, and **** $P_{adj} < 0.0001$). (C) *Tet38* is responsible for the increase of tetracycline resistance induced by *P. aeruginosa*. RN6390 and isogenic $\Delta tet38$ derivative were cultivated with and without *P. aeruginosa* and susceptibility to tetracycline was monitored. Statistical significance was determined by unpaired t-test (* $P < 0.05$) from three independent experiments. All the results are expressed as the number of surviving bacteria in monoculture.

Discussion

The goal of this study was to investigate the impact of the interaction of coexisting *S. aureus* and *P. aeruginosa* on *S. aureus* at the transcriptional and phenotypical levels.

Firstly, we collected isolates from co-colonized CF patients and demonstrated that in 61% of cases, *S. aureus* was able to coexist with *P. aeruginosa* with no alteration of its growth. So far, it appears that coexistence of the two pathogens may be a frequent situation in the context of CF patients' lung infection. Previous studies described that early infectious strains of *P. aeruginosa* are more aggressive for *S. aureus* than the late infectious strains^{19,20}. In the present study, we did not find any correlation between the interaction type and the duration of *S. aureus* and *P. aeruginosa* co-colonization. In the first studies, limited numbers of patients were studied (1 in Michelsen *et al.*, 2014 and 8 in Baldan *et al.*, 2014). Even in our present study, only 11 patients had competitive strain pairs, which might be not be enough to reach a conclusion. Up to now, it has been difficult to conclude whether the interaction type between the two species is linked to the evolution of the *P. aeruginosa* strain over the time of co-colonization. A larger cohort of patients would be needed to answer this question. Also, longitudinal clinical studies would be appropriate to analyze the kinetics of interaction evolution over time and determine how it could affect patients' health. Furthermore, the conditions and environmental factors leading to co-existence instead of competition require clarification, particularly through studies such one conducted recently that demonstrated the positive impact of hypoxia found in static mucus within CF airways on a coexisting interaction³².

The type of interaction may have an impact on the physiology of the two pathogens involved. In order to answer this question, we conducted a transcriptional study of the impact of *P. aeruginosa* on *S. aureus*.

In the context where *P. aeruginosa* inhibits *S. aureus* growth, transcriptomic modifications affect major metabolism pathways such as translation, Krebs cycle and genes involved in oxidative stress. The increase in the amount of tRNAs and ribosomal RNAs observed could be attributed to a decrease in translation efficiency. Regarding energetic metabolic pathways, we observed a down-expression of Acetyl-coA synthetase, a key factor metabolized

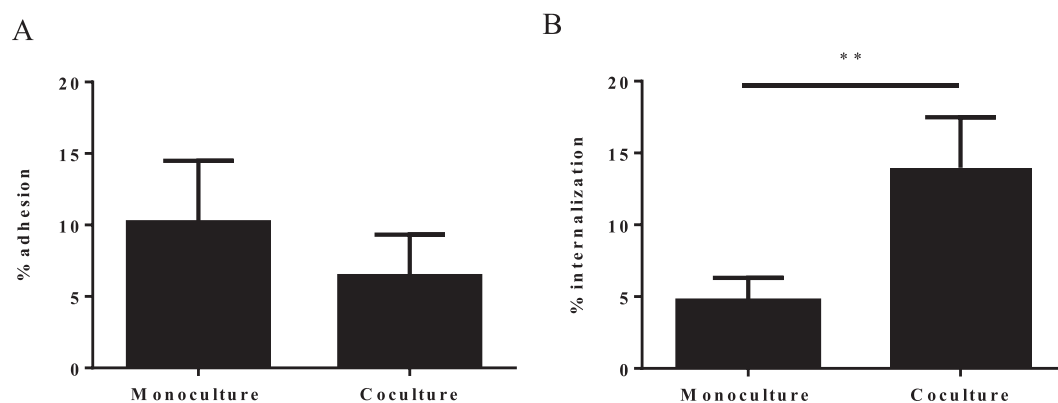


Figure 9. *S. aureus* internalization is increased within A549 epithelial pulmonary cells in the presence of *P. aeruginosa*. **(A)** Adhesion of *S. aureus* onto epithelial cells. A549 cells were infected at MOI 10:1 for *S. aureus* monoculture and 20:1 for *S. aureus*/*P. aeruginosa* coculture. After 2 hours of contact, cells were washed with phosphate buffer saline (PBS) to remove unattached bacteria and lysed with sterile water. Supernatants were plated on MSA to count *S. aureus*. The results are represented as the percentage of inoculum that adhered. **(B)** Internalization of *S. aureus* within epithelial cells. After 2 hours of contact, cells were treated with antibiotics and lysostaphine for one hour, lysed with sterile water and bacteria plated on MSA. The results are represented as the percentage of adhered cells that have internalized. All values represent the mean + standard deviation from three independent experiments with three strain pairs (SA27-PA27, SA31-PA31 and SA69-PA69). Statistical significance was determined by unpaired t-test (** $P < 0.01$).

into pyruvate to feed the Krebs cycle and produce energy. The down-regulation of expression observed may certainly lead to a defect in ATP production. Conversely, we observed the increased expression of several dehydrogenase enzymes, suggesting a shift from aerobic respiration to lactic acid fermentation to feed the Krebs cycle, as shown previously in laboratory strains^{33,34}. Some dehydrogenases, such as *adhE* and *gluD* genes, are also implicated in oxidative stress responses³⁵. All these major dysregulations observed are consistent with the lethal effect of *P. aeruginosa* on *S. aureus* in competitive interaction.

More genes were dysregulated when *S. aureus* and *P. aeruginosa* were coexisting. We observed a drastic modification in the nucleotide synthesis pathway with a down-regulation of genes involved in the *de novo* pathway (*nrd* operon) and upregulation of the *deoD* gene encoding a purine nucleoside phosphorylase involved in an alternative metabolic pathway for nucleotides when the *de novo* pathway is altered. We also observed a down-expression of genes involved in the classical energetic metabolism pathways: glycolysis and pentose phosphate pathways (*pgi*, *fbp*, *fda*). These results suggest nutritional competition between the two pathogens and indicate that in our conditions, *S. aureus* preferentially produced energy and nucleotides from sources other than glucose.

Finally, we observed the increased expression of several transporters, especially *tet38*, *norA* and *norC* genes. Curiously, the *tet38* gene belongs to the same transcription unit as the *deoD* gene. It is tempting to speculate that the overexpression of *tet38-deoD* operon may be linked to the down regulation of the *nrd* genes to compensate for the alteration of the *de novo* nucleotide synthesis pathway.

These genes are members of the Nor family and encode efflux pumps involved in antibiotic resistance. *Tet38* was the most impacted gene with 11 pairs of 12 for which we observed an increased expression throughout the coculture kinetic, whereas the over-expression of other *norA* and *norC* genes appeared on 7 pairs of 12 and 11 of 12 at 6 and 8 hours, respectively. Given that the pair 2599/2600 used for the RNA sequencing (RNAseq) was unable to upregulate *norA* and *norC* at 4 hours of coculture, it was expected that *norA* and *norC* genes would not appear in the RNAseq results. The over-expression of *tet38*, *norA* and *norC* genes appeared to be at least due to a dysregulation of the MgrA pathway. Indeed, the $\Delta mgrA$ mutant provoked a strong effect on *tet38* over-expression but only a slight effect on *norA* and *norC*. Thus, *mgrA* seems to be essential for *tet38* over-expression and other regulators must be implicated for the *norA* and *norC* genes. In addition, we were unable to observe clear *norB* up-regulation in the presence of *P. aeruginosa*. Indeed, MgrA acts as a repressor of *tet38*, *norA* and *norC* and an activator of *norB* in an *rsbU* positive background strain^{36,37}. This discrepancy may explain our results. Despite its role in *tet38* induction during coculture, *mgrA* expression was not affected by the presence of *P. aeruginosa*. However, it has been shown that the phosphorylation state of MgrA, regulated by RsbU and PknB factors, was a key mechanism for regulation of *nor* family gene expression²⁹. Thus, *P. aeruginosa* may induce a variation of MgrA phosphorylation leading to a modification of *nor* gene expression.

Nor proteins are responsible for antibiotic efflux (tetracycline and fluoroquinolone), and we demonstrated that *P. aeruginosa* increased the survival rate of *S. aureus* after exposure to tetracycline and ciprofloxacin. For tetracycline, the effect appears to be mainly due to *tet38*, as antibiotic resistance in presence of *P. aeruginosa* was eliminated in a *tet38* mutant. The same analysis could not be performed for *nor* genes due to the functional redundancy of the *norA*, *norB* and *norC* genes and the difficulty in obtaining triple mutants. *Tet38* is also able to interact with the CD36 receptor on pulmonary epithelial cells to favor *S. aureus* internalization³⁸. Indeed, in the presence of *P. aeruginosa*, we observed a higher rate of *S. aureus* internalization into epithelial cells. Internalized bacteria are more resistant to antibiotics and less detectable by the immune system³⁹. Our results suggest that by coexisting with *P. aeruginosa*, *S. aureus* could hide from the host immune system and be more resistant to antibiotics.

We did not identify the *P. aeruginosa* specific signal responsible for *S. aureus* gene expression dysregulation. However, we demonstrated that it seems to be specific to *P. aeruginosa* (no other species tested had the same effect) and requires very close proximity between *S. aureus* and *P. aeruginosa* to be effective. Transcriptomic analysis revealed that the *S. aureus* *potRABCD* operon for polyamine uptake and regulation exhibited significant fold change expression upon exposure to *P. aeruginosa*. The same effects were observed by Yoa and Lu²⁵ when exposing *S. aureus* to polyamines. Moreover, the exposure of *S. aureus* to spermine induces transcriptional modifications including over-expression of antibiotic efflux pumps such as *norA* and *tetM* genes and the decreased expression of many genes involved in carbohydrate metabolism and transport²⁴. These results are consistent with the reduced expression of genes involved in glycolysis and the pentose phosphate cycle described previously^{24,25}. Indeed, we observed the same profile after exposure to *P. aeruginosa* as other authors observed after exposure to spermine. Finally, *P. aeruginosa* presents polyamines at the outer surface of its membrane, more precisely putrescine and spermidine⁴⁰. Therefore, we suggest that the *P. aeruginosa* polyamines present at the outer surface may be a signal for *S. aureus* transcriptional modifications. Further investigation will be necessary to confirm this hypothesis.

To the best of our knowledge, this study is the first to characterize the transcriptomic profile of coexisting *S. aureus* and *P. aeruginosa* pairs in a clinical context. We demonstrate that this commensal-like interaction induces phenotypical changes in *S. aureus* such as increased antibiotic resistance and host cell internalization. These phenotypes may favor the persistence of *S. aureus* in the context of chronic infection. Since this state of coexistence is apparently solely attributable to *P. aeruginosa*, the selective advantage for *P. aeruginosa* leads to questions. Indeed, previous studies showed that cocultivation with *S. aureus* induces LPS mutation in *P. aeruginosa* associated with fitness gain and antibiotic resistance⁴¹, and that *S. aureus* exoproducts restore and enhance *P. aeruginosa* motility³². The state of coexistence could thus represent a trade-off allowing both pathogens to benefit mutually and maintain equilibrium. However, the impact of *S. aureus* on *P. aeruginosa* in this state of coexistence warrants further investigation.

Materials and Methods

Bacterial strains and culture growth. The bacterial strains and plasmids used in this study are listed in Tables 1 and S1. The clinical strains were originally isolated by the Institute for Infectious Agents from sputum samples of patients followed-up in the two CF Centers of Lyon (Hospices civils de Lyon, France). The strains were collected between May 2016 and June 2017 from 36 different patients. The size of the colonies, pigmentation and mucoid phenotype were determined after 24 h of culture on TSA. Hemolysis type was determined after 24 h of culture on Columbia agar (COS). MLST clonal complex assignment was inferred from microarray analysis⁴².

The $\Delta tet38$ mutant of *S. aureus* RN6390 strain was obtained using the pMAD vector⁴³. The two DNA fragments corresponding to the chromosomal regions upstream and downstream of the *tet38* coding sequence were amplified by PCR using primers listed in Table S2. They were subsequently cloned into the pMAD vector using the In-Fusion[®] HD Cloning Kit (Clontech). The resulting plasmid was electroporated into the RN4220 recipient strain and then transferred to RN6390. Growth at non-permissive temperature (44 °C) was followed by several subcultures at 30 °C and 37 °C to promote double crossing over as previously described⁴⁴.

All the strains were grown in Brain Heart Infusion (BHI, BBL[™] Difco) with shaking at 200 rpm at 37 °C overnight. Cultures were diluted to 0.1 OD_{600nm} and incubated for 2.5 hours (37 °C, 200 rpm). Bacteria were spun down at 4000 rpm for 10 min and re-suspended in fresh BHI medium to 2 OD_{600nm}. Ten ml of *S. aureus*, *P. aeruginosa*, *B. cenocepacia* and *S. maltophilia* suspension were added to 10 ml of BHI for monocultures. Ten ml of *S. aureus* suspension were mixed with respectively 10 ml of *P. aeruginosa*, *B. cenocepacia* or *S. maltophilia* for cocultures. Cultures were grown for 8 h. Every two hours, cultures were plated on mannitol salt agar (MSA, BBL[™] Difco) and cetrимide (Difco[™]) for *S. aureus* or *P. aeruginosa* counts, respectively.

For supernatant exposure, 10 mL of *S. aureus* culture were added to 10 ml of supernatant from 8 hours culture of *P. aeruginosa*.

Transwell[®] (Corning) preliminary experiment demonstrated that bacteria were not able to cross the 0.4 μm filter of the insert. *S. aureus* and *P. aeruginosa* suspensions from 2.5 h culture were pelleted and re-suspended to OD_{600nm} = 1 for *P. aeruginosa* and OD_{600nm} = 0.33–0.5 for *S. aureus*. The Transwell[®] experiment was carried out as previously described^{45,46} with a few modifications. For wells without insert, 400 μL of *S. aureus* OD_{600nm} = 0.5 suspension and 200 μL of either BHI or *P. aeruginosa* were added. For wells with insert, 600 μL of *S. aureus* 0.33 OD_{600nm} were deposited into the wells while 200 μL of either BHI or *P. aeruginosa* were placed onto the insert. The Transwell[®] system was incubated at 37 °C for 8 hours.

Staphylococcus aureus growth inhibition on TSA. From overnight cultures, *S. aureus* and *P. aeruginosa* suspensions were diluted to OD₆₀₀ = 0.5 and 100 μl of *S. aureus* suspension were spread uniformly onto TSA plates. Then, 5 μl of *P. aeruginosa* were added at the center of the plates. The plates were incubated at 37 °C. The competitive phenotype was characterized by an inhibition halo of *S. aureus* growth, which was measured. The strains were considered as coexisting in the absence of inhibition halo.

Genome sequencing and annotation. Sequencing libraries were prepared from 1 ng of SA2597 and SA2599 DNA extracted using the DNA Isolation Kit (MO BIO). Library preparation was performed with the Nextera XT DNA sample preparation kit (Illumina) and index kit (Illumina). Library validation was performed on a 2100 Bioanalyzer (Agilent Technologies) to control the distribution of fragmented DNA. WGS was performed with an Illumina HiSeq (Illumina) to generate 150-bp paired end reads. Genomes were sequenced with an average coverage of 130x. Adapters and other illumina-specific sequences were cut from the reads for each set of raw data. Furthermore, Trimmomatic v0.36⁴⁷ was used to perform an additional trimming step using a sliding window with an average quality threshold of 20. Data were checked for quality by FastQC v0.11.6 (S. Andrews,

2010. FastQC: a quality control tool for high throughput sequence data; available online at: <http://www.bioinformatics.babraham.ac.uk/projects/fastqc>). Assemblies were performed using SPAdes v3.11.1⁴⁸. Contigs smaller than 200 bp or with a coverage threshold smaller than 2 were removed manually. Assembly quality control was performed using Quast v4.6.1⁴⁹. Genome annotation was processed through Prokka v1.13 including ncRNA prediction⁵⁰.

To compare CDS and ncRNA from SA2597 and SA2599, the N315 strain (NC_002745.2) was used as a reference. Refseq numbers were gathered from N315 and used as ID tags for common genes. For non-common genes, CDS and ncRNA from SA2597 and SA2599 were blasted with each other with a coverage and identity of 90%. Finally, refseq numbers were also used to gather KEGG numbers and perform functional classification with the Kyoto database. The complete genome sequences for the SA2597 and SA2599 strains were deposited in GenBank under the accession numbers GCA_005280135.1 and GCA_005280145.1.

Transcriptomic analysis. Cultures and transcriptome sequencing were performed in duplicates or triplicates. The OD₆₀₀ of each culture was normalized to 1.0 at a time of 4 hours for the mono and cocultures. One mL was centrifuged for 5 minutes at 13,000 rpm. Bacteria were treated with lysostaphin (2.5 mg/mL) and lysozyme (50 mg/mL) prior to RNA extraction using the RNeasy Plus Mini Kit (Qiagen). RNAs were treated with TURBO DNA-free™ (Invitrogen). rRNAs were depleted using the Ribo-Zero rRNA Removal Kit (Illumina). The cDNA libraries were compiled using the TruSeq Stranded Total RNA Library Preparation Kit (Illumina). The quantification and quality of the DNA libraries was evaluated by Bioanalyzer. The libraries were sequenced using Illumina Hi-Seq 2500 with High-Output (HO) mode, using a V4 chemistry sequencing kit (Illumina). Reads were then processed to remove adapter sequences. Poor quality reads were excluded by Trimmomatic⁴⁷, using a sliding window with an average quality threshold of 20. Each RNAseq read sample was mapped against its own genome through Bowtie2 v2.3.0 with a sensitive local alignment method⁵¹. Output files were sorted by read names and converted into BAM format using Samtools v1.3.1. Reads were counted on all feature types (CDS, nc/tm/rRNA) using a union mode on Htseq-count v0.6.1 software⁵². To estimate the enrichment values for the differential expression analysis, statistical analysis was done using R v3.3.3 and DESeq2 v1.14.1⁵³. Gene expression was considered as dysregulated when: (i) the fold change between co-culture and monoculture was at least 4-fold, (ii) the dysregulation was observed in the two pairs of strains, (iii) the dysregulation was specific to coexistence or competition state. The RNAseq data that support our findings are available in the SRAdatabase under the BioprojectID PRJNA552713, PRJNA552715, PRJNA552786, PRJNA554237, PRJNA554233, PRJNA554237.

RT-qPCR. RNA extractions were performed using the RNeasy Plus Mini Kit (Qiagen). A DNase treatment was performed on 10 µg of RNAs using TURBO DNA-free™ (Invitrogen). The absence of contaminating gDNA was controlled by PCR. cDNA was synthesized from 1 µg RNA using the Reverse Transcription system kit (Promega). The qPCR reactions were performed with PowerUp™ SYBR™ Green Master Mix (ThermoFisher) following the manufacturer's instructions. The target genes and primers used are listed in Table S2. The house-keeping genes *gyrB* and *hu* were used as endogenous control. Gene expression analyses were performed using the ΔCt method.

Antibiotic resistance assay. MICs of tetracycline and ciprofloxacin (Sigma) were determined by BHI micro-dilution (Table S3). For the antibiotic resistance assay, 4 hour mono-cultures of *S. aureus* and cocultures of *S. aureus/P. aeruginosa* were diluted to OD_{600nm} = 0.002 or 0.004, respectively, and exposed to antibiotics at MIC and 2xMIC for 5 hours at 37 °C at 200 rpm in 1 mL of BHI. Cultures were plated on MSA agar plates for *S. aureus* counts. The percentage of bacterial survival after antibiotic treatment was determined by dividing the number of *S. aureus* after antibiotic treatment by the number of *S. aureus* without antibiotic treatment.

Internalization within A549 cells. *S. aureus* monocultures and *S. aureus/P. aeruginosa* cocultures were performed for 4 hours as previously described⁵⁴. A549 cells were grown in DMEM GlutaMAX™ medium (Gibco) supplemented with 10% of Fetal Bovine Serum (37 °C, 5% CO₂). 24-well tissue culture plates were seeded at 80 000 cells per well. After 24 hours, the cells were washed twice with 1 ml of Phosphate Buffered Saline (PBS, Gibco) and infected at a multiplicity of infection (MOI) of 10:1 for mono-culture and 20:1 for coculture. Cells were incubated for 2 hours, then washed once in PBS to remove non-adherent bacteria and incubated for 1 hour in DMEM GlutaMAX™ supplemented with 400 µg/mL gentamicin (Sigma), 100 µg/mL polymyxin B (Sigma) and 10 µg/mL lysostaphin to kill extra-cellular bacteria. Cells were washed again with PBS once and lysed with deionized water. Cell lysates were plated on MSA to quantify the intracellular bacteria.

Ethical statement. All the methods were carried out in accordance with relevant guidelines and regulations.

Data availability

The datasets generated during and/or analyzed during the current study are available from the corresponding author on reasonable request.

The complete genome sequences for the SA2597 and SA2599 strains have been deposited in GenBank under the accession number GCA_005280135.1 and GCA_005280145.1.

The RNAseq data that support our findings are available in the SRAdatabase under the BioprojectID PRJNA552713, PRJNA552715, PRJNA552786, PRJNA554237, PRJNA554233, PRJNA554237.

Received: 25 June 2019; Accepted: 26 October 2019;

Published online: 12 November 2019

References

- Armbruster, C. E. *et al.* Indirect Pathogenicity of *Haemophilus influenzae* and *Moraxella catarrhalis* in Polymicrobial Otitis Media Occurs via Interspecies Quorum Signaling. *mBio* **1**, e00102-10–e00102-19 (2010).
- Korgaonkar, A., Trivedi, U., Rumbaugh, K. P. & Whiteley, M. Community surveillance enhances *Pseudomonas aeruginosa* virulence during polymicrobial infection. *Proc. Natl. Acad. Sci.* **110**, 1059–1064 (2013).
- Sibley, C. D. *et al.* Discerning the Complexity of Community Interactions Using a *Drosophila* Model of Polymicrobial Infections. *PLoS Pathog.* **4**, e1000184 (2008).
- Vega, N. M., Allison, K. R., Samuels, A. N., Klempner, M. S. & Collins, J. J. *Salmonella typhimurium* intercepts *Escherichia coli* signaling to enhance antibiotic tolerance. *Proc. Natl. Acad. Sci.* **110**, 14420–14425 (2013).
- Zolin, Orenti, Naehrlich & van Rens. ECFS Patient Registry Annual Data Report 2017. (2019).
- Hubert, D. *et al.* Association between *Staphylococcus aureus* alone or combined with *Pseudomonas aeruginosa* and the clinical condition of patients with cystic fibrosis. *J. Cyst. Fibros.* **12**, 497–503 (2013).
- Wolter, D. J. *et al.* *Staphylococcus aureus* small-colony variants are independently associated with worse lung disease in children with cystic fibrosis. *Clin. Infect. Dis. Off. Publ. Infect. Dis. Soc. Am.* **57**, 384–391 (2013).
- Hoffman, L. R. *et al.* Selection for *Staphylococcus aureus* small-colony variants due to growth in the presence of *Pseudomonas aeruginosa*. *Proc. Natl. Acad. Sci.* **103**, 19890–19895 (2006).
- Maselli, J. H. *et al.* Risk factors for initial acquisition of *Pseudomonas aeruginosa* in children with cystic fibrosis identified by newborn screening. *Pediatr. Pulmonol.* **35**, 257–262 (2003).
- Junge, S. *et al.* Factors Associated with Worse Lung Function in Cystic Fibrosis Patients with Persistent *Staphylococcus aureus*. *PLoS ONE* **11**, e0166220 (2016).
- Raidt, L. *et al.* Increased Prevalence and Resistance of Important Pathogens Recovered from Respiratory Specimens of Cystic Fibrosis Patients During a Decade. *Pediatr. Infect. Dis. J.* **34**, 700–705 (2015).
- Hudson, V. L., Wielinski, C. L. & Regelmann, W. E. Prognostic implications of initial oropharyngeal bacterial flora in patients with cystic fibrosis diagnosed before the age of two years. *J. Pediatr.* **122**, 854–860 (1993).
- Sagel, S. D. *et al.* Impact of *Pseudomonas* and *Staphylococcus* Infection on Inflammation and Clinical Status in Young Children with Cystic Fibrosis. *J. Pediatr.* **154**, 183–188.e3 (2009).
- Wakeman, C. A. *et al.* The innate immune protein calprotectin promotes *Pseudomonas aeruginosa* and *Staphylococcus aureus* interaction. *Nat. Commun.* **7** (2016).
- Hogan, D. A. *et al.* Analysis of Lung Microbiota in Bronchoalveolar Lavage, Protected Brush and Sputum Samples from Subjects with Mild-To-Moderate Cystic Fibrosis Lung Disease. *PLOS ONE* **11**, e0149998 (2016).
- Hotterbeekx, A., Kumar-Singh, S., Goossens, H. & Malhotra-Kumar, S. *In vivo* and *In vitro* Interactions between *Pseudomonas aeruginosa* and *Staphylococcus* spp. *Front. Cell. Infect. Microbiol.* **7** (2017).
- Mashburn, L. M., Jett, A. M., Akins, D. R. & Whiteley, M. *Staphylococcus aureus* Serves as an Iron Source for *Pseudomonas aeruginosa* during *In Vivo* Coculture. *J. Bacteriol.* **187**, 554–566 (2005).
- Pernet, E. *et al.* *Pseudomonas aeruginosa* eradicates *Staphylococcus aureus* by manipulating the host immunity. *Nat. Commun.* **5**, 5105 (2014).
- Michelsen, C. F. *et al.* *Staphylococcus aureus* Alters Growth Activity, Autolysis, and Antibiotic Tolerance in a Human Host-Adapted *Pseudomonas aeruginosa* Lineage. *J. Bacteriol.* **196**, 3903–3911 (2014).
- Baldan, R. *et al.* Adaptation of *Pseudomonas aeruginosa* in Cystic Fibrosis Airways Influences Virulence of *Staphylococcus aureus* *In Vitro* and Murine Models of Co-Infection. *PLoS ONE* **9**, e89614 (2014).
- Limoli, D. H. *et al.* *Pseudomonas aeruginosa* Alginate Overproduction Promotes Coexistence with *Staphylococcus aureus* in a Model of Cystic Fibrosis Respiratory Infection. *mBio* **8**, e00186–17 (2017).
- Liu, Q., Yeo, W.-S. & Bae, T. The SaeRS Two-Component System of *Staphylococcus aureus*. *Genes* **7** (2016).
- Nordlund, P. & Reichard, P. Ribonucleotide Reductases. **29** (2006).
- Yao, X. & Lu, C.-D. Characterization of *Staphylococcus aureus* Responses to Spermine Stress. *Curr. Microbiol.* **69**, 394–403 (2014).
- Yao, X. & Lu, C.-D. Functional Characterization of the potRABCD Operon for Spermine and Spermidine Uptake and Regulation in *Staphylococcus aureus*. *Curr. Microbiol.* **69**, 75–81 (2014).
- Truong-Bolduc, Q. C. *et al.* Role of the Tet38 Efflux Pump in *Staphylococcus aureus* Internalization and Survival in Epithelial Cells. *Infect. Immun.* **83**, 4362–4372 (2015).
- Truong-Bolduc, Q. C., Dunman, P. M., Strahilevitz, J., Projan, S. J. & Hooper, D. C. MgrA Is a Multiple Regulator of Two New Efflux Pumps in *Staphylococcus aureus*. *J. Bacteriol.* **187**, 2395–2405 (2005).
- Chen, P. R. *et al.* A new oxidative sensing and regulation pathway mediated by the MgrA homologue SarZ in *Staphylococcus aureus*. *Mol. Microbiol.* **71**, 198–211 (2009).
- Truong-Bolduc, Q. C. & Hooper, D. C. Phosphorylation of MgrA and its effect on expression of the NorA and NorB efflux pumps of *Staphylococcus aureus*. *J. Bacteriol.* **192**, 2525–2534 (2010).
- Truong-Bolduc, Q. C., Strahilevitz, J. & Hooper, D. C. NorC, a New Efflux Pump Regulated by MgrA of *Staphylococcus aureus*. *Antimicrob. Agents Chemother.* **50**, 1104–1107 (2006).
- Fournier, B., Aras, R. & Hooper, D. C. Expression of the Multidrug Resistance Transporter NorA from *Staphylococcus aureus* Is Modified by a Two-Component Regulatory System. *J. Bacteriol.* **182**, 664–671 (2000).
- Pallett, R. *et al.* Anaerobiosis influences virulence properties of *Pseudomonas aeruginosa* cystic fibrosis isolates and the interaction with *Staphylococcus aureus*. *Sci. Rep.* **9**, 6748 (2019).
- Filkins, L. M. *et al.* Coculture of *Staphylococcus aureus* with *Pseudomonas aeruginosa* Drives *S. aureus* towards Fermentative Metabolism and Reduced Viability in a Cystic Fibrosis Model. *J. Bacteriol.* **197**, 2252–2264 (2015).
- Tognon, M., Köhler, T., Luscher, A. & van Delden, C. Transcriptional profiling of *Pseudomonas aeruginosa* and *Staphylococcus aureus* during *in vitro* co-culture. *BMC Genomics* **20** (2019).
- Korem, M., Gov, Y. & Rosenberg, M. Global gene expression in *Staphylococcus aureus* following exposure to alcohol. *Microb. Pathog.* **48**, 74–84 (2010).
- Truong-Bolduc, Q. C., Ding, Y. & Hooper, D. C. Posttranslational Modification Influences the Effects of MgrA on norA Expression in *Staphylococcus aureus*. *J. Bacteriol.* **190**, 7375–7381 (2008).
- Luong, T. T., Dunman, P. M., Murphy, E., Projan, S. J. & Lee, C. Y. Transcription Profiling of the mgrA Regulon in *Staphylococcus aureus*. *J. Bacteriol.* **188**, 1899–1910 (2006).
- Truong-Bolduc, Q. C., Khan, N. S., Vyas, J. M. & Hooper, D. C. Tet38 Efflux Pump Affects *Staphylococcus aureus* Internalization by Epithelial Cells through Interaction with CD36 and Contributes to Bacterial Escape from Acidic and Nonacidic Phagolysosomes. *Infect. Immun.* **85**, e00862–16 (2017).
- Löffler, B., Tuchscher, L., Niemann, S. & Peters, G. *Staphylococcus aureus* persistence in non-professional phagocytes. *Int. J. Med. Microbiol.* **304**, 170–176 (2014).
- Johnson, L., Mulcahy, H., Kanevets, U., Shi, Y. & Lewenza, S. Surface-Localized Spermidine Protects the *Pseudomonas aeruginosa* Outer Membrane from Antibiotic Treatment and Oxidative Stress. *J. Bacteriol.* **194**, 813–826 (2012).
- Tognon, M. *et al.* Co-evolution with *Staphylococcus aureus* leads to lipopolysaccharide alterations in *Pseudomonas aeruginosa*. *ISME J.*, <https://doi.org/10.1038/ismej.2017.83> (2017).

42. Tristan, A. *et al.* Rise of CC398 lineage of *Staphylococcus aureus* among Infective endocarditis isolates revealed by two consecutive population-based studies in France. *PLoS One* **7**, e51172 (2012).
43. Arnaud, M., Chastanet, A. & Debarbouille, M. New Vector for Efficient Allelic Replacement in Naturally Nontransformable, Low-GC-Content, Gram-Positive Bacteria. *Appl. Environ. Microbiol.* **70**, 6887–6891 (2004).
44. Boisset, S. *et al.* *Staphylococcus aureus* RNAIII coordinately represses the synthesis of virulence factors and the transcription regulator Rot by an antisense mechanism. *Genes Dev.* **21**, 1353–1366 (2007).
45. Nguyen, A. T. *et al.* Cystic Fibrosis Isolates of *Pseudomonas aeruginosa* Retain Iron-Regulated Antimicrobial Activity against *Staphylococcus aureus* through the Action of Multiple Alkylquinolones. *Front. Microbiol.* **7** (2016).
46. Nguyen, A. T., Jones, J. W., Ruge, M. A., Kane, M. A. & Oglesby-Sherrouse, A. G. Iron Depletion Enhances Production of Antimicrobials by *Pseudomonas aeruginosa*. *J. Bacteriol.* **197**, 2265–2275 (2015).
47. Bolger, A. M., Lohse, M. & Usadel, B. Trimmomatic: a flexible trimmer for Illumina sequence data. *Bioinforma. Oxf. Engl.* **30**, 2114–2120 (2014).
48. Bankevich, A. *et al.* SPAdes: a new genome assembly algorithm and its applications to single-cell sequencing. *J. Comput. Biol. J. Comput. Mol. Cell Biol.* **19**, 455–477 (2012).
49. Gurevich, A., Saveliev, V., Vyahhi, N. & Tesler, G. QUAST: quality assessment tool for genome assemblies. *Bioinforma. Oxf. Engl.* **29**, 1072–1075 (2013).
50. Seemann, T. Prokka: rapid prokaryotic genome annotation. *Bioinforma. Oxf. Engl.* **30**, 2068–2069 (2014).
51. Langmead, B., Trapnell, C., Pop, M. & Salzberg, S. L. Ultrafast and memory-efficient alignment of short DNA sequences to the human genome. *Genome Biol.* **10**, R25 (2009).
52. Anders, S., Pyl, P. T. & Huber, W. HTSeq—a Python framework to work with high-throughput sequencing data. *Bioinforma. Oxf. Engl.* **31**, 166–169 (2015).
53. Varet, H., Brillet-Guéguen, L., Coppée, J.-Y. & Dillies, M.-A. SARTools: A DESeq2- and EdgeR-Based R Pipeline for Comprehensive Differential Analysis of RNA-Seq Data. *PLoS One* **11**, e0157022 (2016).
54. Trouillet, S. *et al.* A novel flow cytometry-based assay for the quantification of *Staphylococcus aureus* adhesion to and invasion of eukaryotic cells. *J. Microbiol. Methods* **86**, 145–149 (2011).

Acknowledgements

This work was supported by the Fondation pour la Recherche Médicale, grant number ECO20170637499 to LC; Finovi foundation to KM and FV. We thank Xavier Charpentier of CIRI, Lyon-France, for discussing the work and providing valuable advice.

Author contributions

P.B., L.C., S.B., F.V. and K.M. designed and analyzed the experiments. P.B. conducted the experiments. S.B. conducted and analyzed all bioinformatics works. A.D.J. collected the clinical samples from C.F. patients. K.M. and F.V. coordinated the project. P.B. and K.M. collected the data and wrote the first draft of the manuscript. All the authors contributed to manuscript revision and read and approved the submitted version.

Competing interests

The authors declare no competing interests.

Additional information

Supplementary information is available for this paper at <https://doi.org/10.1038/s41598-019-52975-z>.

Correspondence and requests for materials should be addressed to K.M.

Reprints and permissions information is available at www.nature.com/reprints.

Publisher's note Springer Nature remains neutral with regard to jurisdictional claims in published maps and institutional affiliations.



Open Access This article is licensed under a Creative Commons Attribution 4.0 International License, which permits use, sharing, adaptation, distribution and reproduction in any medium or format, as long as you give appropriate credit to the original author(s) and the source, provide a link to the Creative Commons license, and indicate if changes were made. The images or other third party material in this article are included in the article's Creative Commons license, unless indicated otherwise in a credit line to the material. If material is not included in the article's Creative Commons license and your intended use is not permitted by statutory regulation or exceeds the permitted use, you will need to obtain permission directly from the copyright holder. To view a copy of this license, visit <http://creativecommons.org/licenses/by/4.0/>.

© The Author(s) 2019

4.2. Impact de la coexistence sur l'état de santé des patients co-infectés par *P. aeruginosa* et *S. aureus*

Dans le cadre de la mucoviscidose, il est reconnu que les infections pulmonaires causées par *P. aeruginosa* sont associées à une diminution des fonctions respiratoires et donc vitales de l'individu. Ces infections sont cependant polymicrobiennes, et la co-infection *P. aeruginosa*-*S. aureus* est fréquemment retrouvée. L'impact de cette co-infection sur l'état de santé des patients reste mal compris : selon les cohortes et les souches bactériennes étudiées, les patients co-infectés par *P. aeruginosa* et *S. aureus* présentent un état clinique similaire (130, 165), plus sévère (131–133, 164, 254) ou amélioré (133) par rapport aux patients mono-infectés par *P. aeruginosa*. Afin de mieux comprendre l'impact de la co-infection *P. aeruginosa*-*S. aureus* sur le bilan clinique des patients atteints de mucoviscidose, nous avons décidé de prendre en compte un nouveau paramètre : l'état d'interaction entre les deux bactéries. Les études transcriptomiques réalisées sur *P. aeruginosa* et *S. aureus* indiquent en effet que l'interaction de coexistence, contrairement à la compétition, pourrait promouvoir leur persistance dans les poumons des patients atteints de mucoviscidose et ainsi affecter leur état de santé (55, 56).

Pour 212 patients de la cohorte Lyonnaise, les données cliniques (sexe, génotype *cftr*, CFRD, malnutrition, IMC, âge, nombre d'exacerbations, nombre de jours et durée d'hospitalisation, FEV1 et nombre de traitements) et bactériologiques (mono-infection à *S. aureus*, à *P. aeruginosa* ou co-infection) ont été étudiées. L'état d'interaction entre les souches de *P. aeruginosa* et *S. aureus* isolées des patients co-infectés a également été déterminé. Une analyse par FAMD (*Factor Analysis of Mixed Data*) a été effectuée pour détecter les similarités et l'hétérogénéité entre les patients en utilisant les données cliniques. Des analyses statistiques en utilisant des tests de Kruskal Wallis/Mann-Whitney ou exacts de Fisher ont ensuite été réalisées.

Les résultats montrent que les infections à *P. aeruginosa* sont les plus sévères, confirmant les données bibliographiques. De plus, la sévérité de ces infections n'est pas augmentée par la présence du staphylocoque. Dans ce contexte de co-infection, l'état de coexistence bactérienne entre les souches co-isolées est très fréquemment observé (65,3% des cas), mais ne semble pas affecter l'état clinique du patient par rapport à la compétition. Toutefois, en comparaison aux patients mono-infectés par *S. aureus*, les patients co-infectés par des souches en coexistence présentent davantage d'hospitalisations et d'exacerbations.



OPEN ACCESS

Edited by:

Matthew C. Wolfgang,
The University of North Carolina at
Chapel Hill, United States

Reviewed by:

Sarah Rowe-Conlon,
The University of North Carolina at
Chapel Hill, United States
Dominique Limoli,
The University of Iowa, United States

***Correspondence:**

Karen Moreau
karen.moreau@univ-lyon1.fr

†ORCID:

Paul Briaud
orcid.org/0000-0001-7530-6803
Sylvère Bastien
orcid.org/0000-0002-3687-8646
Laura Camus
orcid.org/0000-0003-1335-8901
Philippe Reix
orcid.org/0000-0002-9192-8335
François Vandenesch
orcid.org/0000-0001-9412-7106
Anne Doléans-Jordheim
orcid.org/0000-0003-4985-3955
Karen Moreau
orcid.org/0000-0001-6297-3543

†These authors have contributed
equally to this work. Author order was
determined on the basis of lab position

Specialty section:

This article was submitted to
Clinical Microbiology,
a section of the journal
Frontiers in Cellular and Infection
Microbiology

Received: 23 January 2020

Accepted: 05 May 2020

Published: 03 June 2020

Citation:

Briaud P, Bastien S, Camus L,
Boyadjian M, Reix P, Mainguy C,
Vandenesch F, Doléans-Jordheim A
and Moreau K (2020) Impact of
Coexistence Phenotype Between
Staphylococcus aureus and
Pseudomonas aeruginosa Isolates on
Clinical Outcomes Among Cystic
Fibrosis Patients.
Front. Cell. Infect. Microbiol. 10:266.
doi: 10.3389/fcimb.2020.00266

Impact of Coexistence Phenotype Between *Staphylococcus aureus* and *Pseudomonas aeruginosa* Isolates on Clinical Outcomes Among Cystic Fibrosis Patients

Paul Briaud^{1†}, Sylvère Bastien^{1†}, Laura Camus^{1†}, Marie Boyadjian², Philippe Reix^{2†},
Catherine Mainguy², François Vandenesch^{1,3†}, Anne Doléans-Jordheim^{4†} and
Karen Moreau^{1*†}

¹ CIRI, Centre International de Recherche en Infectiologie, Univ Lyon, Inserm, U1111, Université Claude Bernard Lyon 1, CNRS, UMR5308, ENS de Lyon, Lyon, France, ² Pediatric Pulmonology Department, Hôpital Femme-Mère-Enfant, Hospices civils de Lyon, UMR5558, Lyon, France, ³ Institut des agents infectieux, Hospices Civils de Lyon, Lyon, France, ⁴ Equipe Bactéries Pathogènes Opportunistes et Environnement, Univ Lyon, Université Claude Bernard Lyon 1, CNRS, INRAE, VetAgro Sup, UMR Ecologie Microbienne, Lyon, France

Staphylococcus aureus (SA) is the major colonizer of the lungs of cystic fibrosis (CF) patients during childhood and adolescence. As patients age, the prevalence of SA decreases and *Pseudomonas aeruginosa* (PA) becomes the major pathogen infecting adult lungs. Nonetheless, SA remains significant and patients harboring both SA and PA are frequently found in the worldwide cohort. The overall impact of co-infection remains controversial. Furthermore, co-infecting isolates may compete or coexist. The aim of this study was to analyse if co-infection and the coexistence of SA and PA could lead to worse clinical outcomes. The clinical and bacteriological data of 212 Lyon CF patients were collected retrospectively, and patients were ranked into three groups, SA only ($n = 112$), PA only ($n = 48$) or SA plus PA ($n = 52$). In addition, SA and PA isolates from co-infected patients were tested *in vitro* to define their interaction profile. Sixty five percent ($n = 34$) of SA/PA pairs coexist. Using univariate and multivariate analysis, we confirm that SA patients have a less severe clinical condition than others, and PA induces a poor outcome independently of the presence of SA. Regarding co-infection, no significant difference in clinical outcomes was observed between patients with coexisting pairs and patients with competitive pairs. However, when compared to SA mono-infected patients, patients with coexisting pair presented higher frequency and length of hospitalizations and more exacerbations. We suggest that coexistence between SA and PA may be an important step in the natural history of lung bacterial colonization within CF patients.

Keywords: cystic fibrosis, infection, *Staphylococcus aureus*, *Pseudomonas aeruginosa*, clinical outcome

INTRODUCTION

Cystic fibrosis (CF) is the most common genetic disease among the Caucasian population that affects multiple organs and causes various complications associated with patient death, such as cystic fibrosis liver disease (Debray et al., 2017) (CFLD) and cystic fibrosis related diabetes (Brennan and Beynon, 2015) (CFRD).

However, the first cause of morbidity and mortality in CF remains the progressive decrease in pulmonary function, leading to an obstructive syndrome (Davis, 2006). This decline is generally due to the continuous inflammation provoked by polymicrobial infections (Davis, 2006). The main clinically significant bacteria are *Staphylococcus aureus* (SA) and *Pseudomonas aeruginosa* (PA). SA infection occurs early in children and affects up to 80% of patients aged 5–19 years (Zolin et al., 2019). SA infection is responsible for increasing inflammatory markers in early childhood (Sagel et al., 2009; Gangell et al., 2011), and adolescence patients with high SA density in throat swabs present deteriorated lung function (Junge et al., 2016). However, despite the implication of SA in a worse clinical status, PA, which becomes the dominant pathogen of the respiratory tract in adulthood (Zolin et al., 2019) (up to 60% of patients > 18 years), traditionally remains the most feared pathogen due to its strong association with most severe clinical outcomes, such as more aggravated inflammation, an increase in the number of exacerbations and a decrease in forced expiratory volume in one second (FEV1) (Kerem et al., 1990; Nixon et al., 2001; Hubert et al., 2013; Ahlgren et al., 2015).

Although SA colonization decreases as patients age, SA infection concerns more than 30% of CF adults (Zolin et al., 2019). Among these cases, co-infection by PA and SA remains significant (Hubert et al., 2013). However, it is difficult to determine whether this co-infection is a transitional stage between SA alone and PA alone or whether permanent co-infections with these two bacteria exist. Several *in vitro* studies deciphered the relationships between SA and PA in a context of pulmonary co-infection (Baldan et al., 2014; Michelsen et al., 2014; Limoli et al., 2016; Hotterbeekx et al., 2017). According to recent studies, an evolution occurs regarding interaction between SA and PA clinical isolates. PA early-colonizing isolates show strong antagonism toward SA strains (Baldan et al., 2014; Michelsen et al., 2014), especially by producing anti-staphylococcal compounds, leading to a competition state (Hotterbeekx et al., 2017). However, PA isolated from chronic lung infection lacks this competitiveness and SA succeeds in coexisting durably with PA (Limoli et al., 2016; Michelsen et al., 2016; Tognon et al., 2017). We previously demonstrated that the two bacteria may cooperate to persist more easily in lungs in this context of coexistence without antagonism (Briaud et al., 2019).

Few studies have investigated the impact of SA-PA co-infection and clinical outcomes. In addition, none of them considered the interaction state (competition vs. coexistence) between SA-PA. So far, available data have shown conflicting results on the link between SA-PA co-colonization and clinical outcomes. Ahlgren et al. did not find a significant clinical difference in adult patients co-colonized with SA and PA compared to patients colonized solely by PA (Ahlgren et al., 2015). Two studies highlighted a higher respiratory decline and rate of hospital admission for patients infected by PA alone in comparison with patients co-infected by SA-PA or by SA alone (Hubert et al., 2013; Cios et al., 2019). Finally, other studies reported that SA-PA co-infection is associated with a worse clinical outcome (Hudson et al., 1993; Sagel et al., 2009; Gangell et al., 2011; Limoli et al., 2016).

The aim of this study was to better characterize (i) co-infected patients with demographic data (age, BMI, gender), and (ii) the interaction state (competition or coexistence) between the two bacterial species. We also examined the consequence of SA-PA co-infection and SA-PA interaction state (competition vs. coexistence) on pulmonary functions (FEV1%) and clinical outcomes (e.g., number of exacerbations, number of hospitalizations). By computing demographic and clinical data with pulmonary infectious status, we gain more information on the impact of SA and PA infections and interactions on CF patients' health.

MATERIALS AND METHODS

Patients

The clinical and bacteriological data of CF patients supervised at the two CF Centers in Lyon, France (CRCM: Center de Ressources et de Compétences de la Mucoviscidose) were collected from February 2017 to August 2018.

The inclusion criterion was a stable microbiological status for SA and /or PA colonization, defined by the following criteria: (i) at least three respiratory samples collected for each patient throughout the period considered; (ii) at least 2 months between two successive samples; (iii) all the samples collected during the study for a patient had the same status with respect to the presence of SA and / or PA. The patients who did not match the criteria, or who were not co-colonized by SA or PA were excluded.

This study was submitted to the Ethics Committee of the Hospice Civil de Lyon (HCL) and registered under CNIL No 17-216. All the patients were informed of the study and did not oppose the use of their data.

Clinical Data Collection

Clinical data were extracted from computerized medical files (Easily[®]). The data collected were: gender, age at the time of the last sampling, CFTR genotype classified between severe and moderate genotype regardless of clinical severity (5, 19), pancreatic insufficiency defined by fecal elastase < 200 $\mu\text{g/g}$, CF-related diabetes (CFRD) or a carbohydrate intolerance, cirrhosis, need for long term oral or enteral supplementation and/or undernourishment (defined as a body mass index (BMI) (weight/height^2) lower than 17 kg/m^2 in an adult and -2 standard deviations (SD) in a child according to gender and age). The pulmonary function was defined by the FEV1 expressed as a percentage of the predicted value (%pred). We also collected the number of hospitalizations, the length of hospital stays and the number of exacerbations during the 9 months preceding the last sample.

Microbiology

The microbiological composition of each respiratory sample was determined by the Institute for Infectious Agents, HCL. The interaction state (coexistence or competition) of SA-PA pairs was defined by agar competition assay as previously described (Briaud et al., 2019). Briefly, SA and PA isolates recovered from co-infected patients' expectorations were cultured in 10 ml of

BHI, at 37°C, 200 rpm. From overnight cultures, SA and PA suspensions were diluted to $OD_{600nm} = 0.5$. Then, 100 μ L of SA suspension was spread uniformly onto trypticase soy agar (TSA) plates. After drying, 5 μ L of PA suspension were spotted at the center of the plates. The plates were incubated at 37°C for 24 h. The competitive phenotype was characterized by an inhibition halo of SA growth. In the absence of inhibition halo, isolates were defined in coexistence.

Based on these microbiological analyses, the patients were categorized into four groups: (i) SA alone, (ii) PA alone, (iii) SA-PA in competition, and (iv) SA-PA in coexistence.

Statistical Analysis

Two different analyses were performed using the same process: (i) SA vs. PA vs. SA+PA, and (ii) SA vs. PA vs. SA+PA in coexistence vs SA+PA in competition.

Factor Analysis of Mixed Data (FAMD) was used for initial data screening. Then, univariate analysis was performed to determine significant differences between groups. For continuous variables (age, BMI, FEV1, number of hospitalizations, length of hospitalization, and number of exacerbations), Kruskal-Wallis tests were used to identify whether one population was different from the others. Afterwards, to individually test each pair of populations with significant Kruskal-Wallis tests, a Mann-Whitney Wilcoxon tests was used. Fisher's exact tests were performed to compare categorical variables (CFTR genotype, gender, denutrition, pancreatic insufficiency, CFRD, liver cirrhosis, enteral nutrition, and oral food supply). For multiple comparisons, tests were corrected by a Bonferroni method and statistical significance was set with a q-value threshold at 0.05. Finally, a multinomial log-linear model [nnet package (William, 2016)] was used to determine significant associations between infectious status groups and variables selected using the Akaike information criterion (AIC) (Akaike, 1979). The AIC analysis was performed to identify the smallest and fittest set of variables describing our data. An adjusted odds-ratio with a 95% confidence interval was reported for each final variable. All the analyses were performed using R v3.5.3 (R Core Team, 2018).

RESULTS

Clinical Characteristics of Patients

Of the 655 CF patients monitored in Lyon hospitals, we selected patients with at least three respiratory specimens with SA and/or PA during the study period. Two seventy six patients were excluded because of the absence of the three samples required. Sixty-five patients had neither SA nor PA infection. Finally, 48 and 54 patients were excluded because of unstable SA-PA co-colonization during the period or the inability to assess their pulmonary function (age <4 years). For co-infected patients, we excluded five patients because they presented several PA isolates with both competitive and coexisting interaction phenotypes with SA. Finally, 212 patients with CF were included in this study.

The cohort consisted of 124 adults and 88 children with a mean age of 21.70 years (range 4–69). The male–female ratio was homogeneous with ~51.42% ($n = 109$) of men. About 80.66%

($n = 171$) had a severe CFTR genotype and 41 patients had a moderate one. During this period, 39.62% ($n = 84$) were subject to exacerbation and 25.94% ($n = 55$) of the patients were hospitalized (Table S1).

The 212 patients were classified following their chronic bronchial colonization into 3 different groups: SA alone, PA alone and SA+PA. Co-infected patients were split into 2 subclasses (competition and coexistence) regarding the SA-PA interaction state determined by agar competition assay (Table 1). Among the 212 patients, 52.83% ($n = 112$) had chronic bronchial colonization with SA, 22.64% ($n = 48$) with PA and 24.53% ($n = 52$) with SA+PA. Within the 52 co-infected patients, 65.38% ($n = 34$) of SA and PA isolates presented a coexistence interaction and 34.62% ($n = 18$) presented a competition phenotype. Patients colonized solely with PA were older (average of 32.02y) than co-infected patients (average of 23.38y) and the latter were older than patients colonized by SA (average of 16.49y) (Table 1). This is consistent with the natural history of infections and international values (4).

We proceeded to an FAMD analysis to decipher the similarity and heterogeneity between patient groups using both continuous and categorical variables. The first two axes retained accounted for 39.47% of the total variance of the data (Figure S1). Four variables contributed to the first axis: number of exacerbations, number and days of hospitalization and FEV1. Age, BMI and not having pancreatic insufficiency contributed to the second axis. The distribution of the 212 patients based on the two first dimensions overlapped between the 4 groups (Figure S1). Patients infected by SA were the most represented group and appeared to have more homogeneous clinical variable values than other patients. On the contrary, patients co-infected in a coexistence state seemed to have values with greater heterogeneity (Figure S1).

Impact of Co-infection on CF Patient Clinical Outcome

To define whether co-infection was associated with poorer clinical outcome, we compared three groups: patients infected with SA, patients infected with PA and patients co-infected with SA-PA (Figure 1). Continuous variable analysis differentiated the 3 patient groups (Table 2). SA patients seemed to be younger than co-infected patients, the latter being younger than PA patients ($p < 0.0001$). The SA group stood out from the others due to lower BMI values (PA vs. SA: $p < 0.0001$, SA+PA vs. SA: $p = 0.0074$), a smaller number of hospitalizations (PA vs. SA: $p = 0.0017$, SA+PA vs. SA: $p = 0.0013$), a reduced length of hospitalizations (PA vs. SA: $p = 0.0011$, SA+PA vs. SA: $p = 0.0010$), a lower number of exacerbations ($p < 0.0001$) and a higher FEV1 ($p < 0.0001$). Co-infected and PA groups were not statistically different for the number of hospitalizations or length of hospitalizations, the number of exacerbations or FEV1. Only age ($p = 0.0012$) and BMI ($p = 0.029$) values were significantly different. For the analysis of categorical variables, CFRD was only statistically significant between the PA vs. SA mono-infected groups ($p = 0.0031$) and co-infected patients vs. SA ($p = 0.0169$) (Table S2).

TABLE 1 | Clinical characteristics of CF patients according to their bacteriological status.

	SA alone (%)	PA alone (%)	SA and PA			p_value*
			Competition	Coexistence	Merge	
Number	112/212 (52.83)	48/212 (22.64)	18/52 (34.61)	34/52 (65.38)	52/212 (24.53)	
Age (years)	16.49 ± 8.77	32.02 ± 13.82	23.67 ± 8.98	23.24 ± 10.52	23.38 ± 9.93	<0.0001 ^a
≥18 years	45/112 (40.18)	42/48 (87.50)	14/18 (77.78)	23/34 (64.65)	37/52 (71.15)	
Sex, male	63/112 (56.25)	23/48 (47.92)	10/18 (55.6)	13/34 (38.24)	23/52 (44.23)	ns
Genotype						
Moderate	26/112 (23.21)	9/48 (18.75)	3/18 (16.67)	3/34 (8.82)	6/52 (11.54)	ns
Severe	86/112 (76.79)	39/48 (81.25)	15/18 (83.33)	31/34 (91.18)	46/52 (88.46)	
BMI (kg/m ²)	18.06 ± 2.68	20.74 ± 2.42	19.25 ± 2.56	19.71 ± 3.56	19.55 ± 3.23	<0.0001 ^a
Undernourishment	11/112 (9.82)	1/48 (2.08)	1/18 (5.56)	3/34 (8.82)	4/52 (7.69)	ns
Oral food supplementation	23/112 (20.54)	13/48 (27.08)	3/18 (16.67)	15/34 (44.12)	18/52 (34.62)	ns
Enteral nutrition	4/112 (3.57)	0/48 (0)	0/18 (0)	4/34 (11.76)	4/52 (7.69)	ns
Pancreatic insufficiency	101/112 (90.18)	45/48 (93.75)	17/18 (94.44)	33/34 (97.06)	50/52 (96.15)	ns
CF-related diabetes	9/112 (8.04)	14/48 (29.17)	3/18 (16.67)	10/34 (29.41)	13/52 (25.00)	0.0007 ^b
Cirrhosis	6/112 (5.36)	2/48 (4.17)	0/18 (0)	1/34 (2.94)	1/52 (1.92)	ns
Hospitalizations						
Number	17/112 (15.18)	18/48 (37.50)	6/18 (33.33)	14/34 (41.18)	20/52 (38.46)	0.0003 ^a
Length	8.00 ± 6.10	17.39 ± 14.39	7.33 ± 6.12	29.14 ± 27.39	22.60 ± 25.06	0.0002 ^a
Number of exacerbations	0.25 ± 0.69	1.44 ± 1.37	1.28 ± 1.60	1.35 ± 1.50	1.33 ± 1.52	<0.0001 ^a
FEV1 (% predicted)	85.87 ± 22.39	55.09 ± 18.64	59.72 ± 18.73	64.59 ± 21.79	62.90 ± 20.73	<0.0001 ^a

BMI, Body Mass Index; FEV1, Forced Expiratory Volume in one second.

*P values from comparison between three groups: SA vs. PA vs. SA+PA (merge).

^aP values from Kruskal-Wallis non-parametric test for comparison of the three groups (continuous variables).

^bP values from Fisher's exact test for comparison of the three groups (categorical variables).

Since the PA group appears to have the worst clinical outcome but also corresponds to the oldest group of patients, it is questionable whether the deterioration of the clinical condition of the patients is linked to the age or presence of PA. To answer this question, we classified the patients into three age groups (4–14, 15–25, and 26–69) and analyzed the impact of PA infection within these different groups on continuous variables (Figure 2). We showed that PA patients had significantly lower FEV1 and a higher number of exacerbations for all three age groups. We also observed a higher number and length of hospitalization for two of the age classes. Therefore, we concluded that the poor clinical outcome can be independently attributed to PA colonization and not to the age of the patients.

To further investigate these results and consider the potential association between variables, multinomial analysis with infection type as outcome was performed using age, BMI, FEV1, number of exacerbations, number of hospitalizations, length of hospitalizations and CFRD (Table 3). The aim of the multivariate analysis was to obtain only one set of variables which fit the entire dataset between groups. This was performed in order to compare odds ratio inside each comparison. Two kinds of variables were eliminated using AIC criteria: variables which could clearly not explain the outcome and variables which were correlated to each other.

In this context, variables about hospitalizations were not kept in the final model due to their correlation with the number

of exacerbations [Cor (95% CI): 0.6648 (0.5822, 0.7338) ($p < 0.0001$)], the number of hospitalizations and [Cor (95% CI): 0.5843 (0.4879, 0.6666) ($p < 0.0001$)] and the length of hospitalizations.

The final model demonstrated that patients infected with PA were more likely to have a high BMI [OR (95% CI): 1.2662 (1.0313, 1.5545)], a higher number of exacerbations; [OR (95% CI): 2.0282 (1.2559, 3.2755)], and lower FEV1 [OR (95% CI): 0.9612 (0.9355, 0.9877)] compared to patients infected with SA (Table 3). The results were similar when the co-infected group was compared to SA only [OR (95% CI): BMI: 1.2022 (1.0015, 1.4432); exacerbations: 2.1660 (1.3514, 3.4078); FEV1: 0.9701 (0.9478, 0.9930)]. When comparing the SA-PA group to the PA group, only age criteria was significant as co-infected patients were more likely to be younger than PA mono-infected patients [OR (95% CI): 0.9477 (0.9017, 0.9961)].

Impact of Bacterial Coexistence and Competition Within Co-infected CF Patients

The second objective of this study was to determine whether the interaction profile between SA and PA could affect patient clinical outcome. Thus, we compared the mono-infected groups (SA only and PA only) with two co-infected groups: SA plus PA in coexistence and SA plus PA in competition.

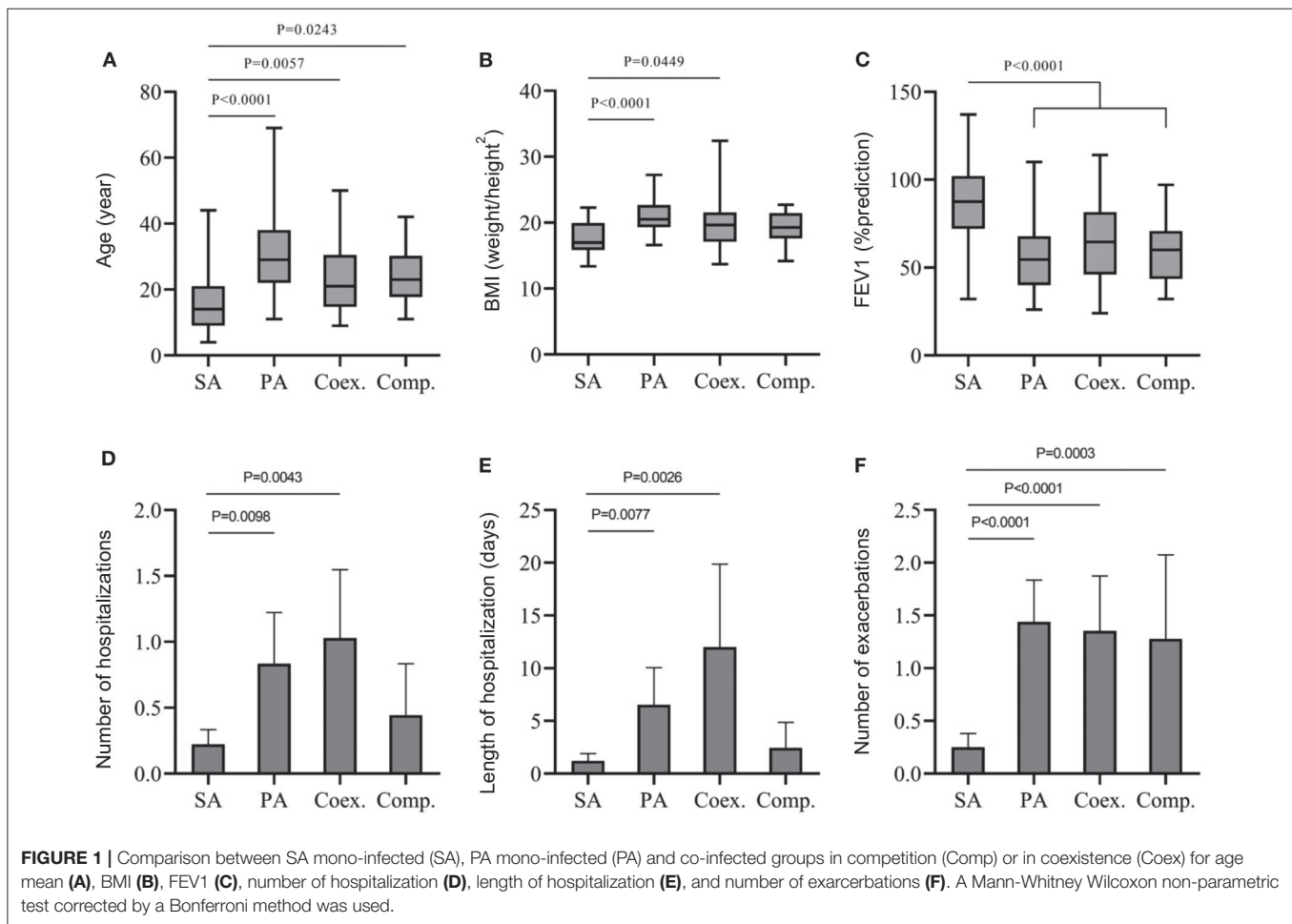


TABLE 2 | P-values for continuous variable comparisons between SA mono-infected (SA), PA mono-infected (PA) and co-infected groups (SA+PA).

	PA vs. SA	SA+ PA vs. SA	SA+PA vs. PA
Age	<0.0001	<0.0001	0.0012
BMI	<0.0001	0.0074	0.029
Number of hospitalizations	0.0017	0.0013	ns
Length of hospitalization	0.0011	0.0010	ns
Number of exacerbations	<0.0001	<0.0001	ns
FEV1	<0.0001	<0.0001	ns

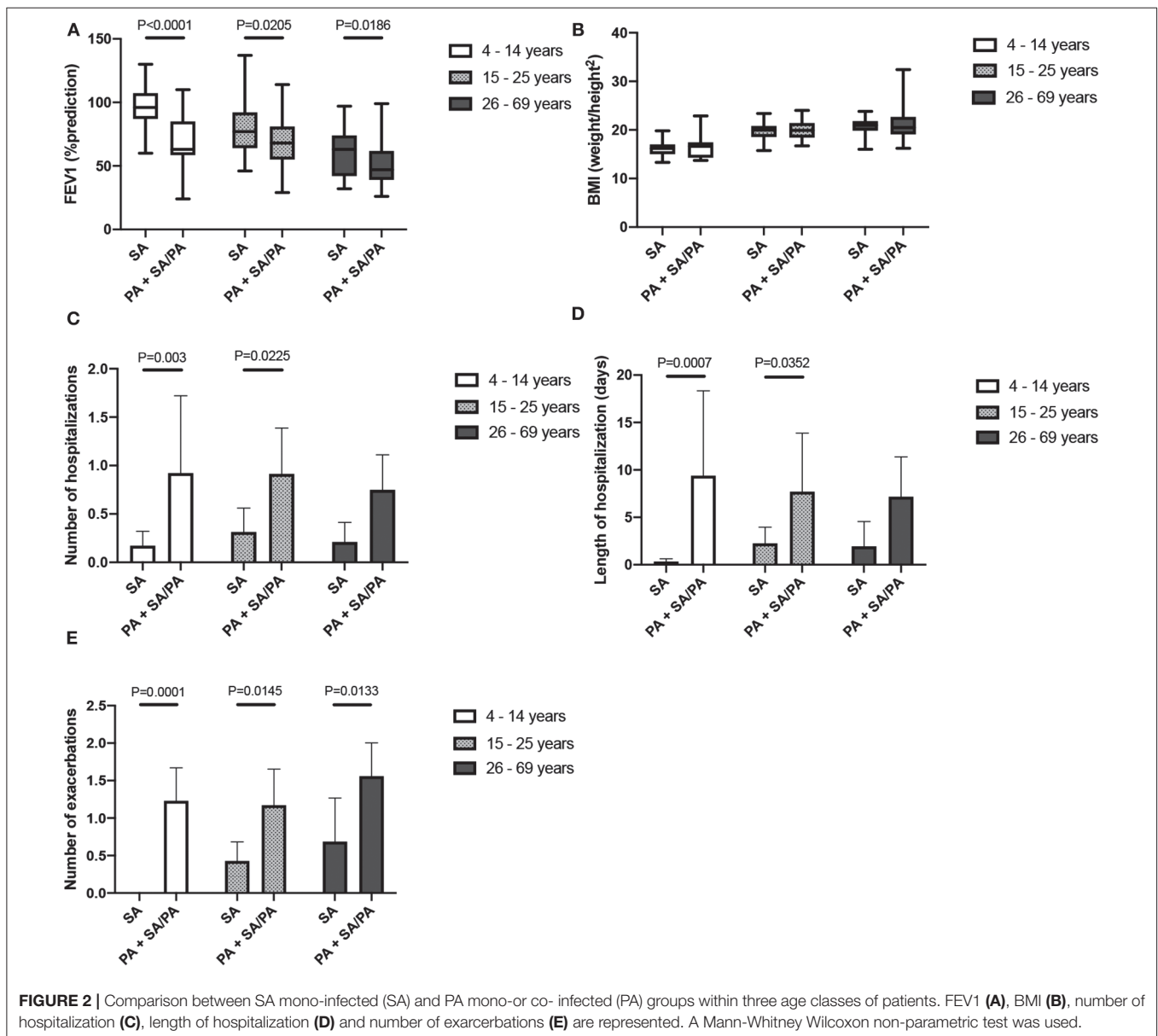
A Mann-Whitney Wilcoxon non-parametric test corrected by a Bonferroni method was used.

Using continuous variables, the comparison between coexistence and competition groups showed no significant difference (Figure 1). Furthermore, no statistical differences were found between PA mono-infected or SA plus PA in coexistence or in competition. Compared to SA groups, both SA plus PA interaction groups seemed to infect older patients (Coex. Vs. SA.: $p = 0.0057$; Comp. vs. SA.: $p = 0.0243$) with a higher number of exacerbations (Coex. Vs. SA.: $p < 0.0001$; Comp. vs. SA.: $p = 0.0003$) and lower values of FEV1 (Coex.

Vs. SA.: $p < 0.0001$; Comp. vs. SA.: $p = 0.0001$). However, it is noteworthy that, for BMI, number of hospitalizations and length of hospitalization criteria, only the coexistence group differs significantly from the SA groups (Figure 1). Thus, the coexistence group presented higher BMI values ($p = 0.0449$), a higher number of hospitalizations ($p = 0.0043$) and longer hospitalization stays ($p = 0.0026$) compared to the SA groups.

Considering categorical variables, no characteristics were statistically significant between the two types of interaction (Table S3). However, when comparing the SA group, there was a higher number of CFRD patients in the coexistence group ($p = 0.0164$); these criteria were not significant when the SA group was compared to the competition group.

Finally, multinomial analysis was performed using all the significant characteristics from the univariate tests. The final predictors retained after analyses of deviance through AIC criteria were BMI, need for oral food supplementation, number of exacerbations and FEV1. A significant difference was found between the two types of interaction in co-infected patients. The coexistence state group was more likely to need oral food supplementation than the competition group [OR (95% CI): 0.2262 (0.0536, 0.9541)] (Table 4). As with the univariate results,



the multivariate analyses confirmed that patients co-infected by either a coexisting SA-PA pair or a competition pair had higher odds of having more exacerbations than those infected only by SA [OR (95% CI): 2.2896 (1.3982, 3.7494): 1.9090 (1.0956, 3.3262), respectively]. Compared to the SA group, the competition state group seemed to have lower values of FEV1 [OR (95% CI): 0.9589 (0.9300, 0.9887)] whereas the coexistence state group was more likely to have higher BMI [OR (95% CI): 1.2047 (1.0210, 1.4213)].

Diabetes Outcome and Infectious Status Are Not Associated

Additional multivariate analyses were performed on CFRD patients due to a statistically significant difference between groups when performing univariate analyses (Tables S2, S3). First of all, a multinomial analysis was conducted with all

the variables (including infection status) and taking CFRD as outcome. On the basis of the analyses of deviance conducted with AIC criteria, the following variables were excluded from the multinomial analysis: sex, BMI, undernourishment, enteral nutrition, cirrhosis, length of hospitalization, number of exacerbations, FEV1, and type of infection. Thus, none of these variables were associated with CFRD and CFRD patients were not more likely to be infected by SA or PA, or co-infected by SA plus PA. Five characteristics were conserved in the final model in which odds ratios and associated adjusted *p*-values were reported (Table 5). CF-related diabetes patients were more likely to be older [OR (95% CI): 1.1013 (1.0543, 1.1504)], to need more oral food supplementation [OR (95% CI): 3.0259 (1.2297, 7.4459)] and were more hospitalized [OR (95% CI): 2.1662 (1.5254, 3.0763)].

TABLE 3 | Adjusted odds ratios of cystic fibrosis patients' infection status.

	PA vs. SA		SA+ PA vs. SA		SA+PA vs. PA	
	OR (95 % CI)	p_value	OR (95 % CI)	p_value	OR (95 % CI)	p_value
Age	–	0.1354	–	0.6767	0.9477 (0.9017, 0.9961)	0.0345
BMI	1.2662 (1.0313, 1.5545)	0.0242	1.2022 (1.0015, 1.4432)	0.0481	–	0.5913
Number of exacerbations	2.0282 (1.2559, 3.2755)	0.0038	2.1460 (1.3514, 3.4078)	0.0012	–	0.7298
FEV1	0.9612 (0.9355, 0.9877)	0.0043	0.9701 (0.9478, 0.9930)	0.0108	–	0.4947

Multinomial regression analyses were performed to study associations between the type of infection [SA mono-infected (SA), PA mono-infected (PA) and co-infected groups (SA+PA)] and clinical outcomes. Adjusted odds ratios with 95% confidence intervals (CI) are mentioned.

TABLE 4 | Adjusted odds ratios of cystic fibrosis patients' infection status.

	Coex vs. SA		Comp vs. SA		Comp vs. Coex	
	OR (95 % CI)	p_value	OR (95 % CI)	p_value	OR (95 % CI)	p_value
BMI	1.2047 (1.0210, 1.4213)	0.0273	–	0.3199	–	0.4872
Oral food supplementation	–	0.0801	–	0.3609	0.2262 (0.0536, 0.9541)	0.0430
Number of exacerbations	2.2896 (1.3982, 3.7494)	0.0010	1.9090 (1.0956, 3.3262)	0.0228	–	0.4472
FEV1	–	0.0861	0.9589 (0.9300, 0.9887)	0.0072	–	0.1885

Multinomial regression analyses were performed to study associations between the type of infection [SA mono-infected (SA), PA mono-infected (PA) and co-infected groups in coexistence state (Coex.), or in competition state (Comp.)] and clinical outcomes. Adjusted odds ratios with 95% confidence intervals (CI) are mentioned.

TABLE 5 | Adjusted odds ratios of cystic fibrosis-related diabetes (CFRD) patients' infection status.

	OR (95 % CI)	p_value
Age	1.1013 (1.0543, 1.1504)	<0.0001
Genotype	–	0.1022
Oral food supplementation	3.0259 (1.2297, 7.4459)	0.0160
Pancreatic insufficiency	–	0.8192
Number of hospitalizations	2.1662 (1.5254, 3.0763)	<0.0001

Multinomial regression analyses were performed to study associations between cystic fibrosis-related diabetes (CFRD) and other clinical outcomes including infection type. Adjusted odds ratios with 95% confidence intervals (CI) are mentioned.

DISCUSSION

The lungs of CF patients are colonized by multiple bacteria and several studies were conducted to decipher the impact of these colonisations on clinical outcomes. We focused our study on the two major pathogens responsible for chronic colonization: *Staphylococcus aureus* and *Pseudomonas aeruginosa*. There is no gold standard to define chronic colonization, especially for SA. For PA infection, Leeds criteria (Lee et al., 2003) are sometimes used and define "chronic" as being when more than 50% of the preceding 12 months were PA culture positive. This definition requires frequent expectoration sampling. Furthermore, these criteria may lack sensitivity and are not always considered by clinicians (Hoo et al., 2018). Alternatively, PA serology appears to be a sensitive criterion for classifying PA infection, especially in non-expectorating children, but is not always available (Taccetti

et al., 2019). In order to clearly study the impact of SA and/or PA infection, we focused on stabilized infections. Therefore, we considered chronic colonization when at least 3 samples over a 9-month period had the same colonization pattern. These criteria are close to the definition of European Consensus Criteria for PA colonization. However, this stringent method led to the exclusion of 33% of our cohort; 10% of patients were also excluded due to a change in colonization status during the period studied. Finally, in our study, 52.83% of the remaining patients had chronic SA colonization, 22.64% chronic PA colonization and 24.53% had chronic co-colonization with both bacteria. These data are consistent with those of previous studies (Hubert et al., 2013; Cios et al., 2019).

The first point of our study was to compare the impact of chronic colonization by SA alone, PA alone and SA plus PA on the clinical outcome of CF patients. Indeed, being able to evaluate (or even predict) the risks that a patient incurs depending on the type of bacterium and/or on bacterial associations (in particular between PA and another pathogen) that colonize the lungs, remains one of the major challenges in the management of patients. Thus, identifying patients with harmful bacterial associations would be of clinical interest as they have increased risks of a worse clinical outcome. These bacterial associations could become a therapeutic priority and be eradicated by targeting, for example, one of the pathogens. Conversely, we could speculate that co-infection between PA and another bacterium represents a milder step in disease evolution, probably an intermediate stage between SA alone and PA alone.

Our results showed that SA chronic colonization led to a higher FEV1 (85.87 ± 22.39), fewer exacerbations (0.25 ± 0.69), a smaller number of hospitalizations (15.18% of SA patients)

and shorter stays (8.00 ± 6.10) than SA plus PA co-infection or PA alone. We did not observe any differences regarding clinical status between patients co-infected by PA and SA and those infected by PA alone. This suggests that the SA plus PA combination does not lead to over or under morbidity compared to the presence of PA alone in the lungs, and that there is no synergism in term of pathogenicity. As soon as PA colonizes the CF patients' lungs, the clinical condition of the patients appears to deteriorate, whether SA is present or not. These results are in accordance with previous results from Ahlgren et al. that demonstrate by univariate analysis that there is no difference between PA mono-infected and PA plus SA co-infected patients (Ahlgren et al., 2015). However, they are in contradiction with others. Indeed, Hudson et al. (1993) and Sagel et al. (2009) conducted similar analyses on pediatric cohort patients and showed that SA plus PA co-infections led to the worst spirometry (measured by the forced expiratory flow or FEF) (Hudson et al., 1993), a 10 years survival of 57% lower (Hudson et al., 1993) and have the highest measurement of inflammation (Sagel et al., 2009) compared to the PA group. Gangell et al. (2011) also depicted that the inflammatory response to co-infection was greater but not significantly different from mono-infection. Similarly, studies conducted by Limoli et al. (2016) and Cios et al. (2019) on mixed patient cohorts (pediatric and adults) pointed out that (i) SA plus PA co-infections were responsible for more frequent exacerbations and lower FEV1 compared to the PA group (Limoli et al., 2016) and (ii) patients mono-infected by PA were more transplanted with a higher mortality rate, the highest rates of hospitalization, annual readmission and length of stay and the shortest time to subsequent hospitalization (Cios et al., 2019). These discrepancies within studies may reflect variabilities among cohorts (size, age...), and statistical analysis and models used. However, under our conditions, where we are studying stabilized mono or co-infections, it appears that there are no differences between PA mono-infected and PA plus SA co-infected patients.

Other studies analyzed the impact of co-infection based on the presence of methicillin-susceptible *Staphylococcus aureus* (MSSA) or methicillin-resistant *Staphylococcus aureus* (MRSA). Patients co-infected by MSSA plus PA presented better outcome than infected by PA only (higher FEV1, higher forced vital capacity (FVC) and lower number of intravenous antibiotics per year than those) (Hubert et al., 2013). Their univariate analysis showed that no difference could be established between the co-infection group and the PA mono-infection group. On the contrary, co-infection by MRSA plus PA were as severe as the PA infection (Hubert et al., 2013). Furthermore, linear regression models adjusted for gender, age at baseline, age at diagnostic, genotype, and pancreatic sufficiency in this same study showed that the MRSA/PA patients had the largest yearly decline in FEV1. This last result was confirmed by Maliniak et al. (2016). In our cohort, only 15 MRSA cases were reported. This low number of cases (9%—5/164) is slightly higher than the MRSA rate in France, which is 6.3% according to the French cystic fibrosis register, 2017. However, it was not enough to perform analyses and conclude on the impact of methicillin-resistance status on clinical outcomes. Further studies are required to

figure out why MRSA—*per se* or as a surrogate marker of other genetic determinants—negatively impacts the clinical outcome of CF patients.

CFRD is a severe complication of CF and its association with bacterial infection could be used as a predictive marker of severity. CFRD seemed to be overrepresented in mono-infected PA (29.17%) and co-infected (25%) patients and under-represented in mono-infected SA patients (8.04%). CFRD represented 16.98% of our total patients and was slightly higher than the CFRD rate in the European population (Kerem et al., 2014). Limoli et al. (2016) showed that CFRD status was marginally associated with co-infection by both SA and PA [OR (95% CI): 1.90 (0.99, 3.6)] in comparison to SA or PA mono-infection. We did not confirm this result. Indeed, our multivariate analysis demonstrated that CFRD was associated with the age of the patients [OR (95% CI): 1.1013 (1.0543, 1.1504)]. As co-infected and PA infected patients are older than SA patients, CFRD could be more represented in the first two groups. However, we cannot exclude that the difference between the two studies can be explained by a lower number of patients in our study.

The second objective of the present study was to evaluate the impact of the type of interaction between SA and PA (competition or coexistence) on clinical outcomes. Among the 52 patients co-colonized with SA and PA, 65.38% of strain pairs were in coexistent interaction and 34.61% in competition. These competitive and coexistence statuses have already been described (Baldan et al., 2014; Michelsen et al., 2014; Cigana et al., 2017; Limoli et al., 2017; Tognon et al., 2017; Briaud et al., 2019). However, this is the first time that this type of interaction was evaluated in a large number of clinical isolates and we described that coexistence is the predominant interaction type in chronically co-colonized patients.

It has long been recognized that PA could suppress SA growth by several mechanisms (Hotterbeekx et al., 2017). These data led to the theory that PA colonization causes SA elimination in patients' lungs. Indeed, in our cohort, 24% of patients were co-colonized, which is consistent with other studies (Hubert et al., 2013; Cios et al., 2019). Moreover, SA-PA pairs from co-infected patients were mostly coexisting. Thus, our study shows that in 34 patients, chronic co-colonization may be due, at least in part, to the inability of PA to suppress SA. It has been well-described that in CF lungs, PA strains evolve and adapt from virulent early-infecting strains to less-virulent late-infecting strains (Michelsen et al., 2016; Limoli et al., 2017). Stresses induced by the pulmonary environment (oxidative and osmotic), antibiotic treatments, the immune system and other bacteria species, constitute selective pressure forces for the selection of adaptive mutations (Baldan et al., 2014; Michelsen et al., 2014; Wakeman et al., 2016). Virulence changes could also reduce the antagonistic action of the PA isolates on SA (Baldan et al., 2014; Michelsen et al., 2014). However, of all the factors affecting the evolution of PA in the pulmonary environment, the role of SA in PA evolution remains to be explored.

Nonetheless, in the present study, we did not observe a difference in age between patients colonized with coexisting isolates (23.24 ± 10.52) and patients colonized with competitive

pairs (23.67 ± 8.98). This suggests that there may be no link between adapted late-infecting strains and coexistence. In order to clarify this point, longitudinal studies will be necessary to evaluate the link between bacteria interaction status and the evolution of isolates.

How PA tolerance toward SA may contribute to worse clinical outcomes is a point that has not been explored before. The analyses showed no significant difference in clinical outcomes between patients with coexisting pairs and patients with competitive pairs, except for the need of oral food supplementation observed with multinomial analysis.

Nevertheless, we highlighted several disparities between coexistence and competition groups when compared to SA mono-infected patients. The univariate analysis indicated that both groups were more likely to have a lower FEV1 and higher number of exacerbations. The multinomial analysis confirmed that patients with a competitive pair had a higher number of exacerbations and a lower FEV1, in comparison to SA group. However, we noticed that multinomial analysis did not confirm the lower FEV1 for the coexistence group in comparison to SA. Indeed, the number of exacerbations was correlated with FEV1. The correlation for the coexistence group [Cor (95% CI): -0.6159 (-0.7896 , -0.3508) ($p = 0.0001$)] was stronger than that for the competition group [Cor (95% CI): -0.5462 (-0.8072 , -0.1065) ($p = 0.0190$)]. The differences in correlation's strength could explain why multinomial results showed a significant lower FEV1 value for SA plus PA in competition state compared to SA mono-infected patients, unlike the analysis between SA plus PA in coexistence state compared to SA mono-infected patients.

More importantly, univariate analysis demonstrated that only patients with a coexisting pair were more likely to have higher BMI, number and length of hospitalizations than SA mono-infected group. This increased BMI was confirmed by multinomial analysis and might be the results of the long term oral food supply, which was more frequent in coexistence group. Multinomial analysis also indicated that coexistence group presented more exacerbations than the SA group, consistent with previous results about hospitalizations.

Overall, these results suggest that patients with coexisting pair required food supply more frequently than patients with competitive pair. Moreover, when compared to SA mono-infection, co-infection with coexisting PA appears to be more severe than co-infection with competitive PA (higher number and length of hospitalizations and more exacerbations).

Several quorum-sensing dependent virulence factors are produced by competitive PA strains such as rhamnolipids and phenazines (Hotterbeekx et al., 2017), that can trigger a higher inflammatory response leading to a lower FEV1. On the contrary, coexisting PA strains lack the production of virulence factors and should be less harmful for the lung environment (Yang et al., 2011; Michelsen et al., 2014). The clinical outcome is therefore mainly due to other genotype/phenotype traits of PA. PA adaptation, is related to many environmental factors,

including the surrounding bacteria (Yang et al., 2011; Winstanley et al., 2016; O'Brien and Fothergill, 2017). Thus, in the context of coexistence, current analysis of the impact of SA on the PA transcriptome and growth phenotype suggests that SA could favor PA persistence (Camus et al., in revision). Moreover, we previously demonstrated that PA can enhance SA antibiotic resistance (Briaud et al., 2019). Therefore, we suggest that cooperation between the two species in the coexistence state may be slightly more deleterious for the host than in the competition state. A larger patient cohort would be necessary to evaluate the real impact of the coexistence state on clinical outcomes. Coexistence between SA and PA may be an important step in lung bacterial colonization in CF patients, and preventing this phenomenon could participate in the adapted or even personalized management of CF patients.

DATA AVAILABILITY STATEMENT

All datasets generated for this study are included in the article/Supplementary Material.

ETHICS STATEMENT

All the strains and clinical information used in this study were collected as part of the periodic monitoring of patients at the Hospices Civils de Lyon. As the study is retrospective and non-interventional neither ethics committee approval nor written informed consent were required under local regulations.

AUTHOR CONTRIBUTIONS

PB, AD-J, and KM contributed to the conception and design of the study. PR, CM, and FV contributed to design of the study. PB and LC conducted the experiments. SB conducted and analyzed all the statistics. MB and AD-J collected the data. All the authors contributed to the manuscript and approved the submitted version.

ACKNOWLEDGMENTS

This work was funded by the associations Vaincre la mucoviscidose and Gregory Lemarchal. PB was funded by the French Ministry of Education and Research and L Camus by the Fondation pour la Recherche Médicale (grant number ECO20170637499). We thank Marie Verneret for her technical support.

SUPPLEMENTARY MATERIAL

The Supplementary Material for this article can be found online at: <https://www.frontiersin.org/articles/10.3389/fcimb.2020.00266/full#supplementary-material>

REFERENCES

- Ahlgren, H. G., Benedetti, A., Landry, J. S., Bernier, J., Matouk, E., Radzioch, D., et al. (2015). Clinical outcomes associated with *Staphylococcus aureus* and *Pseudomonas aeruginosa* airway infections in adult cystic fibrosis patients. *BMC Pulm. Med.* 15:67. doi: 10.1186/s12890-015-0062-7
- Akaike, H. (1979). A Bayesian extension of the minimum AIC procedure of autoregressive model fitting. *Biometrika* 66, 237–242. doi: 10.1093/biomet/66.2.237
- Baldan, R., Cigana, C., Testa, F., Bianconi, I., De Simone, M., Pellin, D., et al. (2014). Adaptation of *Pseudomonas aeruginosa* in cystic fibrosis airways influences virulence of *Staphylococcus aureus* in vitro and murine models of co-infection. *PLoS ONE* 9:e89614. doi: 10.1371/journal.pone.0089614
- Brennan, A. L., and Beynon, J. (2015). Clinical updates in cystic fibrosis-related diabetes. *Semin. Respir. Crit. Care Med.* 36, 236–250. doi: 10.1055/s-0035-1547319
- Briaud, P., Camus, L., Bastien, S., Doléans-Jordheim, A., Vandenesch, F., and Moreau, K. (2019). Coexistence with *Pseudomonas aeruginosa* alters *Staphylococcus aureus* transcriptome, antibiotic resistance and internalization into epithelial cells. *Sci. Rep.* 9:16564. doi: 10.1038/s41598-019-52975-z
- Camus, L., Briaud, P., Bastien, S., Elsen, S., Doléans-Jordheim, A., Vandenesch, F., et al. (in revision). Trophic cooperation promotes bacterial survival of *Staphylococcus aureus* and *Pseudomonas aeruginosa*. *ISME*.
- Cigana, C., Bianconi, I., Baldan, R., De Simone, M., Riva, C., Sipione, B., et al. (2017). *Staphylococcus aureus* impacts *Pseudomonas aeruginosa* chronic respiratory disease in murine models. *J. Infect. Dis.* 217, 933–942. doi: 10.1093/infdis/jix621
- Cios, K., Cohen, B., Quittell, L. M., Liu, J., and Larson, E. L. (2019). Impact of colonizing organism in the respiratory tract on the incidence, duration, and time between subsequent hospitalizations among patients with cystic fibrosis. *Am. J. Infect. Control* 47, 750–754. doi: 10.1016/j.ajic.2018.12.021
- Davis, P. B. (2006). Cystic fibrosis since 1938. *Am. J. Respir. Crit. Care Med.* 173, 475–482. doi: 10.1164/rccm.200505-8400E
- Debray, D., Narkewicz, M., Bodewes, F., Colombo, C., Housset, C., Jonge, H., et al. (2017). Cystic fibrosis-related liver disease: research challenges and future perspectives. *J. Pediatr. Gastroenterol. Nutr.* 65, 443–448. doi: 10.1097/MPG.0000000000001676
- Gangell, C., Gard, S., Douglas, T., Park, J., de Klerk, N., Keil, T., et al. (2011). Inflammatory responses to individual microorganisms in the lungs of children with cystic fibrosis. *Clin. Infect. Dis.* 53, 425–432. doi: 10.1093/cid/cir399
- Hoo, Z. H., Edenborough, F. P., Curley, R., Prtak, L., Dewar, J., Allenby, M. I., et al. (2018). Understanding pseudomonas status among adults with cystic fibrosis: a real-world comparison of the Leeds criteria against clinicians' decision. *Eur. J. Clin. Microbiol. Infect. Dis.* 37, 735–743. doi: 10.1007/s10096-017-3168-4
- Hotterbeekx, A., Kumar-Singh, S., Goossens, H., and Malhotra-Kumar, S. (2017). *In vivo* and *in vitro* interactions between *Pseudomonas aeruginosa* and *Staphylococcus* spp. *Front. Cell. Infect. Microbiol.* 7:106. doi: 10.3389/fcimb.2017.00106
- Hubert, D., Réglie-Poupet, H., Sermet-Gaudelus, I., Ferroni, A., Le Bourgeois, M., Burgel, P.-R., et al. (2013). Association between *Staphylococcus aureus* alone or combined with *Pseudomonas aeruginosa* and the clinical condition of patients with cystic fibrosis. *J. Cyst. Fibros.* 12, 497–503. doi: 10.1016/j.jcf.2012.12.003
- Hudson, V. L., Wielinski, C. L., and Regelman, W. E. (1993). Prognostic implications of initial oropharyngeal bacterial flora in patients with cystic fibrosis diagnosed before the age of two years. *J. Pediatr.* 122, 854–860. doi: 10.1016/S0022-3476(09)90007-5
- Junge, S., Görlich, D., den Reijer, M., Wiedemann, B., Tümmeler, B., Ellemunter, H., et al. (2016). Factors associated with worse lung function in cystic fibrosis patients with persistent *Staphylococcus aureus*. *PLoS ONE* 11:e0166220. doi: 10.1371/journal.pone.0166220
- Kerem, E., Corey, M., Gold, R., and Levison, H. (1990). Pulmonary function and clinical course in patients with cystic fibrosis after pulmonary colonization with *Pseudomonas aeruginosa*. *J. Pediatr.* 116, 714–719. doi: 10.1016/S0022-3476(05)82653-8
- Kerem, E., Viviani, L., Zolin, A., MacNeill, S., Hatziaorou, E., Ellemunter, H., et al. (2014). Factors associated with FEV1 decline in cystic fibrosis: analysis of the ECFS patient registry. *Eur. Respir. J.* 43, 125–133. doi: 10.1183/09031936.00166412
- Lee, T. W. R., Brownlee, K. G., Conway, S. P., Denton, M., and Littlewood, J. M. (2003). Evaluation of a new definition for chronic *Pseudomonas aeruginosa* infection in cystic fibrosis patients. *J. Cyst. Fibros.* 2, 29–34. doi: 10.1016/S1569-1993(02)00141-8
- Limoli, D. H., Whitfield, G. B., Kitao, T., Ivey, M. L., Davis, M. R., Grahl, N., et al. (2017). *Pseudomonas aeruginosa* alginate overproduction promotes coexistence with *Staphylococcus aureus* in a model of cystic fibrosis respiratory infection. *mBio* 8:e00186–e00117. doi: 10.1128/mBio.00186-17
- Limoli, D. H., Yang, J., Khansaheb, M. K., Helfman, B., Peng, L., Stecenko, A. A., et al. (2016). *Staphylococcus aureus* and *Pseudomonas aeruginosa* co-infection is associated with cystic fibrosis-related diabetes and poor clinical outcomes. *Eur. J. Clin. Microbiol. Infect. Dis.* 35, 947–953. doi: 10.1007/s10096-016-2621-0
- Maliniak, M. L., Stecenko, A. A., and McCarty, N. A. (2016). A longitudinal analysis of chronic MRSA and *Pseudomonas aeruginosa* co-infection in cystic fibrosis: a single-center study. *J. Cyst. Fibros.* 15, 350–356. doi: 10.1016/j.jcf.2015.10.014
- Michelsen, C. F., Christensen, A.-M. J., Bojer, M. S., Hoiby, N., Ingmer, H., and Jelsbak, L. (2014). *Staphylococcus aureus* alters growth activity, autolysis, and antibiotic tolerance in a human host-adapted *Pseudomonas aeruginosa* lineage. *J. Bacteriol.* 196, 3903–3911. doi: 10.1128/JB.02006-14
- Michelsen, C. F., Khademi, S. M. H., Johansen, H. K., Ingmer, H., Dorrestein, P. C., and Jelsbak, L. (2016). Evolution of metabolic divergence in *Pseudomonas aeruginosa* during long-term infection facilitates a proto-cooperative interspecies interaction. *ISME J.* 10, 1323–1336. doi: 10.1038/ismej.2015.220
- Nixon, G. M., Armstrong, D. S., Carzino, R., Carlin, J. B., Olinsky, A., Robertson, C. F., et al. (2001). Clinical outcome after early *Pseudomonas aeruginosa* infection in cystic fibrosis. *J. Pediatr.* 138, 699–704. doi: 10.1067/mpd.2001.112897
- O'Brien, S., and Fothergill, J. L. (2017). The role of multispecies social interactions in shaping *Pseudomonas aeruginosa* pathogenicity in the cystic fibrosis lung. *FEMS Microbiol. Lett.* 364:fnx128. doi: 10.1093/femsle/fnx128
- R Core Team (2018). *R: A Language and Environment for Statistical Computing*. Vienna, Austria: R Foundation for Statistical Computing. Available online at: <https://www.R-project.org/>.
- Sagel, S. D., Gibson, R. L., Emerson, J., McNamara, S., Burns, J. L., Wagener, J. S., et al. (2009). Impact of pseudomonas and staphylococcus infection on inflammation and clinical status in young children with cystic fibrosis. *J. Pediatr.* 154, 183–8.e3. doi: 10.1016/j.jpeds.2008.08.001
- Taccetti, G., Denton, M., Hayes, K., Drevinek, P., Sermet-Gaudelus, I., Bilton, D., et al. (2019). A critical review of definitions used to describe *Pseudomonas aeruginosa* microbiological status in patients with cystic fibrosis for application in clinical trials. *J. Cyst. Fibros.* 19, 52–67. doi: 10.1016/j.jcf.2019.08.014
- Tognon, M., Köhler, T., Gdaniec, B. G., Hao, Y., Lam, J. S., Beaume, M., et al. (2017). Co-evolution with *Staphylococcus aureus* leads to lipopolysaccharide alterations in *Pseudomonas aeruginosa*. *ISME J.* 11, 2233–2243. doi: 10.1038/ismej.2017.83
- Wakeman, C. A., Moore, J. L., Noto, M. J., Zhang, Y., Singleton, M. D., Prentice, B. M., et al. (2016). The innate immune protein calprotectin promotes *Pseudomonas aeruginosa* and *Staphylococcus aureus* interaction. *Nat. Commun.* 7:11951. doi: 10.1038/ncomms11951
- William, V. (2016). *nnet: Feed-Forward Neural Networks and Multinomial Log-Linear Models*. Available online at: <https://CRAN.R-project.org/package=nnet>.
- Winstanley, C., O'Brien, S., and Brockhurst, M. A. (2016). *Pseudomonas aeruginosa* evolutionary adaptation and diversification in cystic fibrosis chronic lung infections. *Trends Microbiol.* 24, 327–337. doi: 10.1016/j.tim.2016.01.008
- Yang, L., Jelsbak, L., Marvig, R. L., Damkjaer, S., Workman, C. T., Rau, M. H., et al. (2011). Evolutionary dynamics of bacteria in a human host environment. *Proc. Natl. Acad. Sci. U.S.A.* 108, 7481–7486. doi: 10.1073/pnas.1018249108
- Zolin, O., Naehrlich, L., and van Rens, J. (2019). *ECFS Patient Registry Annual Data Report 2017*.

Conflict of Interest: The authors declare that the research was conducted in the absence of any commercial or financial relationships that could be construed as a potential conflict of interest.

Copyright © 2020 Briaud, Bastien, Camus, Boyadjian, Reix, Mainguy, Vandenesch, Doléans-Jordheim and Moreau. This is an open-access article distributed under the terms of the Creative Commons Attribution License (CC BY). The use, distribution or reproduction in other forums is permitted, provided the original author(s) and the copyright owner(s) are credited and that the original publication in this journal is cited, in accordance with accepted academic practice. No use, distribution or reproduction is permitted which does not comply with these terms.

CONCLUSION GENERALE

Du fait de leur fréquence, leur sévérité et leur persistance, les infections pulmonaires à *P. aeruginosa* demeurent la principale cause de morbi-mortalité chez les patients atteints de mucoviscidose. Face à la difficulté de les traiter efficacement par les antibiothérapies habituelles, la compréhension des facteurs favorisant la survie de *P. aeruginosa* dans les poumons est essentielle. *P. aeruginosa* n'évolue cependant pas seul au sein de l'écosystème pulmonaire, et l'impact des interactions entre microorganismes sur la physiologie et la pathogénie microbienne est de plus en plus considéré. L'étude des interactions entre *P. aeruginosa* et les autres microorganismes pulmonaires apparaît donc prometteuse pour mieux comprendre les facteurs de sa persistance. Cette approche est particulièrement intéressante dans le cas des co-infections à *P. aeruginosa* et *S. aureus*, du fait de leur prévalence et de leur impact potentiel sur la santé du patient. Et effectivement, un nombre croissant d'études décrit que les deux pathogènes développent une interaction atypique au sein des poumons des patients atteints de mucoviscidose : l'état de coexistence (55, 56, 63, 163, 168). Cet état est suspecté de favoriser les comportements coopératifs entre *P. aeruginosa* et *S. aureus* et les co-infections à ces deux bactéries. La coexistence n'étant que peu décrite, nous avons étudié ses causes et impacts sur la physiologie de *P. aeruginosa* par plusieurs approches.

L'approche transcriptomique a ainsi mis en évidence que le métabolisme du glucose et des acides aminés de *P. aeruginosa* était fortement affecté par la coexistence avec *S. aureus*. Pour la première fois, **une coopération trophique impliquant l'acétoïne a été observée entre les deux pathogènes et suggère une co-évolution de *P. aeruginosa* et *S. aureus* au sein de l'écosystème pulmonaire**. Ces résultats confirment ainsi que l'état de coexistence favorise les comportements mutualistes entre les deux pathogènes, et donc potentiellement leur persistance dans les poumons. Si certains éléments de l'étude clinique rétrospective réalisée au cours de ce projet tendent à confirmer cette hypothèse (163), l'impact de la coexistence sur la persistance des co-infections à *P. aeruginosa* et *S. aureus* doit être plus largement investigué. La potentielle co-évolution observée entre les deux pathogènes soulève également de nombreuses questions. Si l'évolution de *P. aeruginosa* dans les poumons est bien décrite, celle de *S. aureus* l'est beaucoup moins. Dans quelles mesures *S. aureus* est-il capable d'adapter son métabolisme à la présence de *P. aeruginosa* ? Peut-il influencer les processus adaptatifs de *P. aeruginosa* pour favoriser les comportements coopératifs ?

Nous avons tenté de répondre à cette dernière question par une approche de génomique comparative de souches cliniques et évoluées expérimentalement. Nous n'avons pas observé d'effet de la présence de *S. aureus* sur l'évolution génétique de *P. aeruginosa in vitro*, mais nous avons pu identifier plusieurs facteurs génétiques de *P. aeruginosa*

potentiellement impliqués dans l'établissement de la coexistence. L'altération des voies du QS, de la synthèse d'alginate et du transport de la cystéine chez *P. aeruginosa* est ainsi suspectée d'induire la coexistence avec *S. aureus*. **A l'image de l'adaptation de *P. aeruginosa* dans les poumons, l'établissement de la coexistence reposerait donc sur plusieurs voies mutationnelles distinctes.** Finalement, l'approche de Transposon-sequencing a permis d'identifier plusieurs voies importantes pour le maintien de *P. aeruginosa* lors de cette interaction de coexistence : si la synthèse des acides aminés et de la thiamine paraît favorable à la survie de *P. aeruginosa* en coexistence avec *S. aureus*, les voies d'utilisation du glucose et de synthèse de biotine semblent défavorables.

De façon intéressante, les trois approches de ce projet soulignent l'importance du métabolisme et du transport des acides aminés de *P. aeruginosa* lors de la coexistence avec *S. aureus*, et indiquent également un impact négatif du métabolisme du glucose. Ces voies étant modifiées par l'adaptation de la bactérie au milieu pulmonaire, il serait intéressant d'évaluer leur rôle dans les capacités de colonisation et de persistance de *P. aeruginosa* (190). Pour cela, nous envisageons d'étudier le comportement métabolique (utilisation du glucose, de l'acétoïne et des acides aminés) de *P. aeruginosa* lors d'infections de cellules épithéliales pulmonaires en présence et en absence de *S. aureus*. De la même manière, plusieurs résultats de ce projet soutiennent une relation entre l'adaptation de *P. aeruginosa* au milieu pulmonaire et le développement de la coexistence avec *S. aureus* : les altérations génétiques impliquées dans l'établissement et le maintien de la coexistence sont en effet fréquemment identifiées chez les souches chroniques et donc adaptées de *P. aeruginosa* (147, 192, 197). Dans ce contexte, une étude longitudinale de souches de *P. aeruginosa* isolées de patients mono- et co-infectés avec *S. aureus* permettrait de mieux comprendre ce phénomène et l'impact de la présence de *S. aureus* sur cette évolution. **Le développement d'une coexistence avec *S. aureus* pourrait ainsi constituer une patho-adaptation de *P. aeruginosa* au milieu pulmonaire.** Si cette adaptation favorise les comportements coopératifs avec d'autres espèces du microbiote pulmonaire reste une nouvelle hypothèse intéressante à explorer.

En conclusion, la coexistence entre *P. aeruginosa* et *S. aureus* favorise les comportements coopératifs et leur persistance, et résulte probablement de l'adaptation bactérienne au milieu pulmonaire. Ces résultats soulignent donc l'importance des interactions entre bactéries sur leur physiopathologie, et ouvrent de nombreuses perspectives pour la compréhension de leurs mécanismes de persistance dans les poumons des patients atteints de mucoviscidose.

COMMUNICATIONS

1 Communication scientifique

1.1. Présentations orales

- Avril 2020**
Paris (annulé) **European Congress of Clinical Microbiology and Infectious Diseases (ECCMID)**
Trophic cooperation promotes bacterial survival of *Staphylococcus aureus* and *Pseudomonas aeruginosa*
- Février 2020**
Paris **European Young Investigators Meeting (EYIM)**
Trophic cooperation promotes bacterial survival of *Staphylococcus aureus* and *Pseudomonas aeruginosa*
- Février 2020**
Paris **Colloque français des Jeunes Chercheurs de la VLM (CFJC) et rencontre avec les patients atteints de mucoviscidose**
La coopération nutritionnelle favorise la survie de *Pseudomonas aeruginosa* et *Staphylococcus aureus* chez les patients atteints de mucoviscidose
Prix de la meilleure présentation orale
- Janvier 2020**
Lyon **Séminaire interne du CIRI**
Interactions between *Staphylococcus aureus* and *Pseudomonas aeruginosa* in a pulmonary co-infection context
- Octobre 2019**
Paris **15^{ème} congrès national de la Société Française de Microbiologie (SFM)**
Metabolic modifications in *Pseudomonas aeruginosa* during coexistence with *Staphylococcus aureus*
- Mars 2019**
Lyon **Workshop Ecofect : Evolution of infectious diseases**
Pseudomonas aeruginosa evolution during chronic lung infection in Cystic Fibrosis patients and interaction with *Staphylococcus aureus*
- Sept. 2018**
Lyon **Cérémonie des lauréats de la Fondation pour la Recherche Médicale**
Discours de remise de bourse doctorale
- Avril 2018**
Lyon **DECRYPThèse, séminaire de l'école doctorale E2M2**
Interactions entre *Pseudomonas aeruginosa* et *Staphylococcus aureus* chez les patients atteints de mucoviscidose

1.2. Présentations affichées

- Juin 2020**
Lyon
(annulé)
- 43rd European Cystic Fibrosis Conference (ECFS)**
- *Pseudomonas aeruginosa* evolution in cystic fibrosis patients promotes coexistence interaction with *Staphylococcus aureus*
 - Trophic cooperation promotes *Pseudomonas aeruginosa* and *Staphylococcus aureus* survival in cystic fibrosis patients
- Octobre 2019**
Paris
- 15ème congrès national de la Société Française de Microbiologie (SFM)**
Modifications métaboliques chez *Pseudomonas aeruginosa* en coexistence avec *Staphylococcus aureus* **Poster 1**
- Avril 2019**
Lyon
- DECRYPThèse, séminaire de l'école doctorale E2M2**
Interactions entre *Pseudomonas aeruginosa* et *Staphylococcus aureus* chez les patients atteints de mucoviscidose – **Prix du meilleur poster** **Poster 2**
- Octobre 2018**
Paris
- 14ème congrès national de la Société Française de Microbiologie (SFM)**
Modifications métaboliques chez *Pseudomonas aeruginosa* en coexistence avec *Staphylococcus aureus* **Poster 1**
- Avril 2018**
Vogüé
- Retraite du CIRI, séminaire interne du CIRI**
Interactions between *Staphylococcus aureus* and *Pseudomonas aeruginosa* in a pulmonary co-infection context **Poster 3**



Présentation de poster à la Retraite du CIRI 2018, avec le célèbre Dr. Paul Briaud



Remise des prix au Colloque français des Jeunes Chercheurs 2020

Modifications métaboliques chez *Pseudomonas aeruginosa* en coexistence avec *Staphylococcus aureus*

Laura Camus¹, Paul Briaud¹, Sylvère Bastien¹, Anne Doléans-Jordheim², François Vandenesch^{1,2} and Karen Moreau¹. ¹CIRI - Pathogénie des staphylocoques. ²IAI - HCL Lyon.

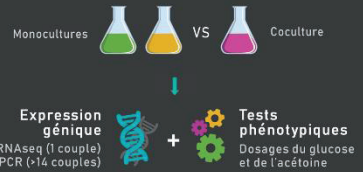


Introduction

Pseudomonas aeruginosa (PA) est un pathogène opportuniste pouvant causer de nombreuses infections, notamment grâce à ses capacités d'adaptation et sa compétitivité. Dans le cas des infections pulmonaires survenant chez les patients atteints de mucoviscidose, PA parvient à persister durablement dans les poumons malgré la présence de nombreux autres microorganismes co-colonisateurs. Parmi ceux-ci, la bactérie *Staphylococcus aureus* (SA) est la plus souvent retrouvée; jusqu'à 50% des patients présentent ainsi une co-infection par PA et SA. PA adapte son mode d'interaction avec SA au cours de l'infection: dans un premier temps, les souches de PA inhibent la croissance du staphylocoque selon des mécanismes bien décrits. Puis, après quelques mois de co-infection, une coexistence durable s'installe entre les deux bactéries.

Comment PA s'adapte à la coexistence avec SA ?
Quel est l'impact de cet état sur sa physiologie ?

Couples de souches PA/SA en coexistence
isolés des expectorations de patients atteints de mucoviscidose (HCL, Lyon)

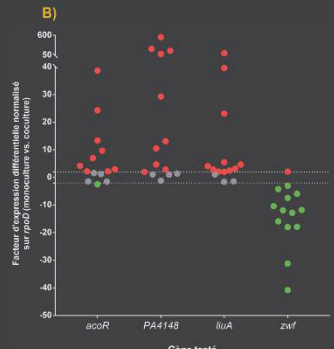
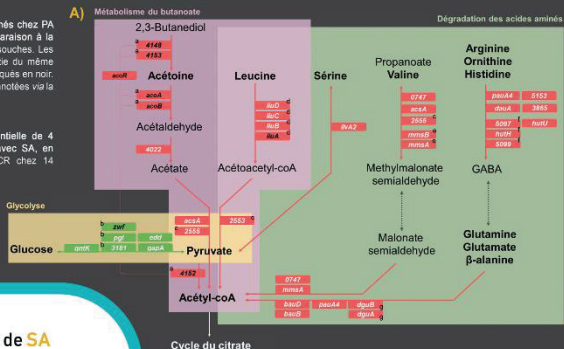


Méthodes

Figure A : Gènes différemment exprimés chez PA après 4h de coculture avec SA, en comparaison à la monoculture. RNAseq chez un couple de souches. Les gènes annotés d'une même lettre font partie du même opéron. Les gènes testés en qPCR sont indiqués en noir. Les voies métaboliques impactées ont été annotées via la base de données Kegg.

Figure B : Facteurs d'expression différentielle de 4 gènes chez PA après 4h de coculture avec SA, en comparaison à la monoculture. RT-qPCR chez 14 couples de souches.

Légendes
Facteurs supérieurs à 4 (Fig A) ou 2 (Fig B)
Facteurs inférieurs à -4 (Fig A) ou -2 (Fig B)
Facteurs non significatifs



La coculture avec SA affecte la régulation de nombreux gènes du métabolisme énergétique chez PA (Figure A), dont :

Le système *aco* (*acoR*-*PA4148*-*PA4153*), surexprimé chez 70% des souches, impliqué dans le catabolisme de l'acétoïne

L'opéron *liu* (*liuA*-*liuD*), surexprimé chez 78% des souches, impliqué dans le catabolisme de la leucine

Le gène *zwf*, sous-exprimé chez 93% des souches, impliqué dans la glycolyse (Figure B)

La présence de SA induit la surexpression du système *aco* chez PA...

... dont le signal inducteur est l'acétoïne, molécule notamment produite par SA

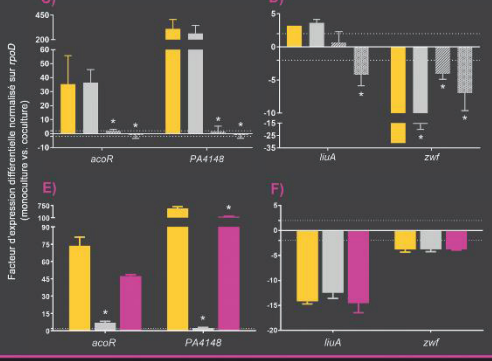
Grâce au système *aco*, PA utilise l'acétoïne comme source de carbone alternative

Figures C, D : Facteurs d'expression différentielle de 4 gènes chez PA après 4h de coculture avec SA, *Bacillus subtilis*, *Burkholderia cenocepacia* ou *Stenotrophomonas maltophilia*, en comparaison à la monoculture. RT-qPCR chez une souche PA, triplicats. * p<0.05 t-test apparié (SA vs. condition).

Légendes : souches utilisées
(a) Souches produisant de l'acétoïne
(b) Souches isolées d'expectorations de patients atteints de mucoviscidose

Figures E, F : Facteur d'expression différentielle de 4 gènes chez PA après 4h de culture en présence d'un surravageant de culture filtré de SA UAMS-1 WT, SA UAMS-1 Δ*alsSD* ou SA UAMS-1 Δ*alsSD* complétement en acétoïne. RT-qPCR chez une souche PA, triplicats. * p<0.05 t-test apparié (SA WT vs. condition).

Légendes : SA WT, SA Δ*alsSD*, SA Δ*alsSD* + acétoïne



Le système *aco* est surexprimé lorsque PA est cultivé en présence de bactéries produisant de l'acétoïne, telles que SA et *B. subtilis* (Figure C).

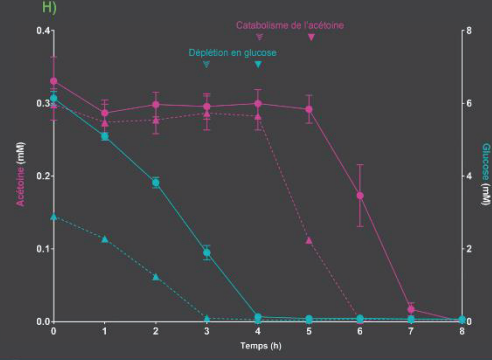
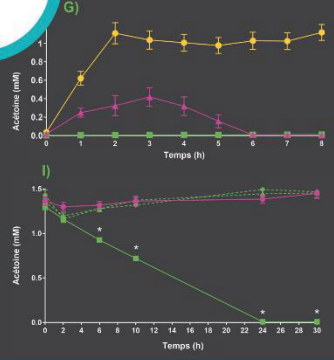
Ces bactéries produisent de l'acétoïne en grande quantité grâce à l'opéron *alsSD* afin de réguler leur acidification cellulaire au cours de la croissance (Xiao et al., 2006).

La surexpression du système *aco* est :
• abolie si SA ne produit pas d'acétoïne
• restaurée par l'ajout d'acétoïne au milieu (Figure E).

Figure G : Suivi de la concentration en acétoïne dans des monocultures ou coculture de PA et SA. Dosage colorimétrique chez 3 couples de souches, duplicats.

Figure H : Suivi de la concentration en acétoïne et en glucose dans un surravageant de culture de SA auquel a été ajouté une culture de PA. Dosage colorimétrique chez un couple de souches, triplicats. Le surravageant a été utilisé tel quel ou complétement en glucose.

Figure I : Suivi de la concentration en acétoïne dans du milieu supplémenté en acétoïne auquel a été ajouté du milieu stérile, une culture de PA14 WT, PA14 *acoR*, ou PA14 Δ*PA4153*. Dosage colorimétrique, triplicats. * p<0.05 t-test apparié (milieu vs. condition).



L'acétoïne est produite en grande quantité par les souches cliniques de SA et s'accumule dans leur surravageant de culture (Figure G).

Cultivé en présence de ce surravageant, PA catabolise l'acétoïne dès que le milieu ne contient plus de glucose. La complémentation du surravageant en glucose retarde le catabolisme de l'acétoïne (Figure H).

La fonction du système *aco* dans le catabolisme de l'acétoïne a été confirmée chez PA14 (Figure I) et chez PA01 (Liu et al., 2018).

Conclusions

Cette étude montre que l'état de coexistence avec *Staphylococcus aureus* affecte l'expression génique et le métabolisme de *Pseudomonas aeruginosa*, favorisant l'utilisation de sources de carbone alternatives au glucose. L'une d'elles, l'acétoïne, est produite par le staphylocoque afin de réguler son acidification cellulaire et affecte sa survie (Chaudhari et al., 2016), suggérant la mise en place de coopérations trophiques entre les deux bactéries.

- Confirmer ces résultats sur un modèle de co-infection d'épithélium pulmonaire reconstitué
- Mettre en évidence l'importance de l'utilisation de sources de carbone alternatives pour la virulence et la persistance de PA

Perspectives



Centre International de Recherche en Infectiologie

Interactions entre *Pseudomonas aeruginosa* et *Staphylococcus aureus* chez les patients atteints de mucoviscidose

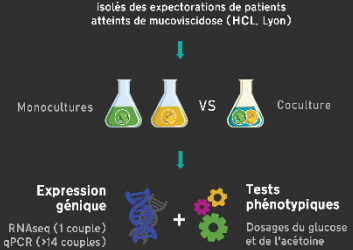
Laura Camus¹, Paul Briaud¹, Sylvère Bastien¹, Anne Doléans-Jordheim², François Vandenesch^{1,2} and Karen Moreau¹. ¹CIRI - Staphylococcal Pathogenesis. ²IAI - HCL Lyon

Introduction

Pseudomonas aeruginosa (PA) est une bactérie pathogène pouvant causer de nombreuses infections, notamment grâce à ses capacités d'adaptation et sa compétitivité. Dans le cas des infections pulmonaires survenant chez les patients atteints de mucoviscidose, PA parvient à persister durablement dans les poumons malgré la présence de nombreux autres microorganismes co-colonisateurs. Parmi ceux-ci, la bactérie *Staphylococcus aureus* (SA) est la plus souvent retrouvée : jusqu'à 50% des patients présentent ainsi une co-infection par PA et SA. PA adapte son mode d'interaction avec SA au cours de l'infection : dans un premier temps, les souches de PA inhibent la croissance du staphylocoque selon des mécanismes bien décrits. Puis, après quelques mois de co-infection, une coexistence durable s'installe entre les deux bactéries.

Nous cherchons à comprendre comment la coexistence avec SA affecte la physiologie de PA, tant sur son expression génique que son métabolisme.

Couples de souches PA/SA en coexistence



Méthodes

Comment la coexistence avec SA affecte-t-elle l'expression génique de PA ?

La coculture avec SA affecte l'expression de nombreux gènes du métabolisme chez PA (Figure A), dont le système *aco*. Ce système est surexprimé chez 70% des PA cultivés en présence de SA (n=22), et est impliqué dans l'utilisation de l'acétoïne.

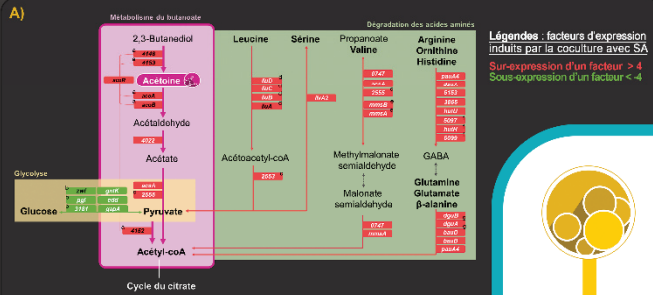


Figure A : Gènes différemment exprimés chez PA après 4h de coculture avec SA, en comparaison à la monoculture. Séquençage des ARN (méthode globale) chez 2 couples PA/SA en coexistence. Les gènes annotés d'une même lettre font partie du même opéron. Les gènes testés en qPCR (méthode ciblée) chez 12 couples PA/SA en coexistence et validés chez au moins 8 couples sont indiqués en noir. Les voies métaboliques affectées ont été déterminées à l'aide de la base de données Kegg.

PA catabolise-t-il l'acétoïne produit par SA ?

PA catabolise l'acétoïne présent dans le surnageant de culture de SA, dès que le glucose est épuisé. L'ajout de glucose retarde l'utilisation de l'acétoïne (Figure C). Les souches de PA en coexistence avec SA catabolisent plus efficacement l'acétoïne que les souches en compétition (Figure D).

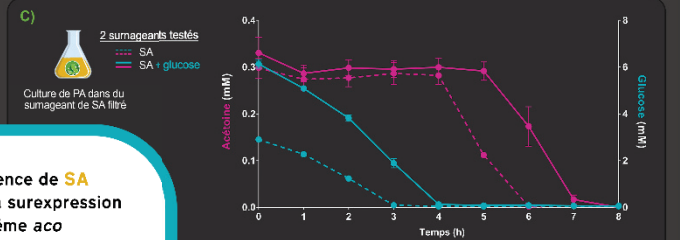


Figure C : Suivi de la concentration en acétoïne (rose) et en glucose (bleu) dans un surnageant de culture de SA auquel a été ajouté une culture de PA. Dosages colorimétriques chez un couple de souches. Indicateurs. Le surnageant a été utilisé tel quel (trait pointillé) ou complétement en glucose (trait plein).

La présence de SA induit la surexpression du système *aco* chez PA...

... dont le signal inducteur est l'acétoïne, molécule notamment produite par SA

Grâce au système *aco*, PA utilise l'acétoïne comme source de carbone alternative

Quels sont les signaux induisant la surexpression du système *aco* chez PA ?

L'acétoïne, molécule catabolisée par le système *aco* chez PA, est produite et sécrétée par SA et s'accumule dans son surnageant de culture.

La surexpression du système *aco* chez PA est :

- induite par la culture dans un surnageant de SA
- abolie si le surnageant de SA ne contient pas d'acétoïne (mutant de SA ne produisant plus d'acétoïne)
- restaurée par l'ajout d'acétoïne dans ce surnageant.

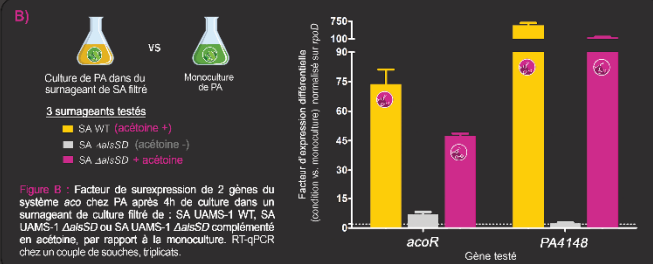


Figure B : Facteur de surexpression de 2 gènes du système *aco* chez PA après 4h de culture dans un surnageant de culture filtré de SA UAMS-1 WT, SA UAMS-1 ΔacoSD ou SA UAMS-1 ΔacoSD complétement en acétoïne, par rapport à la monoculture. RT-qPCR chez un couple de souches, triplicats.

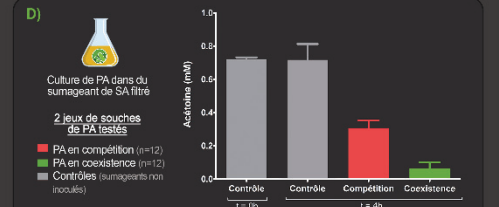


Figure D : Concentration en acétoïne après 4h de culture de souches de PA en coexistence ou compétition dans un surnageant filtré de SA. Dosage colorimétrique chez 12 souches de PA en coexistence, 12 souches de PA en compétition avec SA, ou du surnageant de SA non inoculée (contrôles).

Quel est l'impact du catabolisme de l'acétoïne chez PA ?

Cultivées dans un milieu sans glucose mais contenant de l'acétoïne, les souches de PA capables de cataboliser l'acétoïne présentent un avantage de croissance (Figure E).

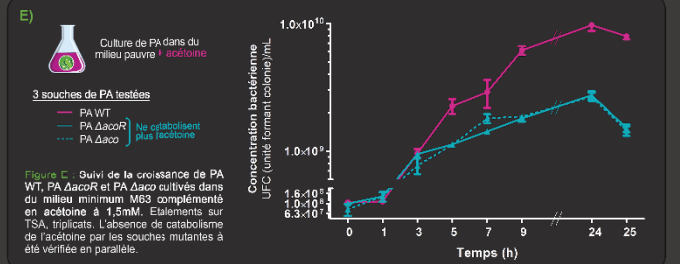


Figure E : Suivi de la croissance de PA WT, PA ΔacoR et PA ΔacoR complétement en acétoïne à 1.5mM. Éléments sur TSA, triplicats. L'absence de catabolisme de l'acétoïne par les souches mutantes a été vérifiée en parallèle.

Conclusions

Cette étude montre que l'état de coexistence avec *Staphylococcus aureus* affecte l'expression génique et le métabolisme de *Pseudomonas aeruginosa*, favorisant l'utilisation de sources de carbone alternatives au glucose. L'une d'elles, l'acétoïne, est produite par le staphylocoque afin de réguler son acidification cellulaire et affecte sa survie (Chaudhari et al., 2016), suggérant la mise en place de coopérations trophiques entre les deux bactéries.

- Confirmer ces résultats sur un modèle de co-infection d'épithélium pulmonaire reconstitué
- Mettre en évidence l'importance de l'utilisation de sources de carbone alternatives pour la virulence et la persistance de PA

Perspectives





Centre International de Recherche en Infectiologie

Interactions between *Staphylococcus aureus* and *Pseudomonas aeruginosa* in a pulmonary co-infection context

Laura Camus^{*1}, Paul Briaud^{*1}, Antoine Corbin², Sylvère Bastien¹, Anne Doléans- Jordheim³, François Vandenesch^{1,3} and Karén Moreau¹

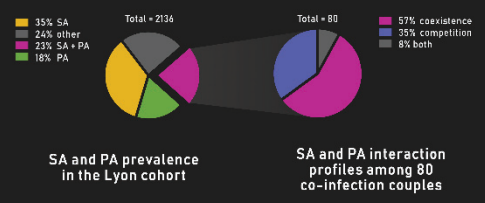
^{*} LC and PB contributed equally to this work. ¹ CIRI – Staphylococcal Pathogenesis. ² CIRI – BIBS. ³ IAI – HCL Lyon

Cystic fibrosis (CF) is a genetic disease that mainly affects ions and water transport in the lungs epithelium. The resulting thickened pulmonary mucus alters the mucociliary clearance and promotes lungs infection by various microorganisms. Among those, the Gram positive bacterium *Staphylococcus aureus* (SA) and the Gram negative *Pseudomonas aeruginosa* (PA) are the most prevalent and co-infection by these two agents is frequently observed (up to 50% of CF patients depending on age class). Interestingly, interactions between these pathogens evolve during infection. Early infection strains show a competition state, as PA inhibits SA growth by secretion of anti-staphylococci factors. However, strains of chronic infection are able to coexist.

Co-infection and coexistence among clinical strains

A retrospective study is performed on the Lyon cohort of CF patients. We observed that SA is the most prevalent bacterium among the 2136 samples of the cohort (600 patients, february 2017-january 2018). 23% of the patients are co-infected by SA and PA.

The interaction profile of co-infection strains is monitored thanks to competition experiments. At this time and on 80 tested couples, 57% of couples show a coexistence state. Interestingly, some patients are infected by several PA strains which can interact differently with the SA strain.



Objectives

- Understand the coexistence state between SA and PA strains
- Describe its impact on their gene expression and physiology

SA and PA coexistence couples from CF lungs (HCL)



Gene expression RNAseq (1 couple) qRT-PCR (>12 couples)

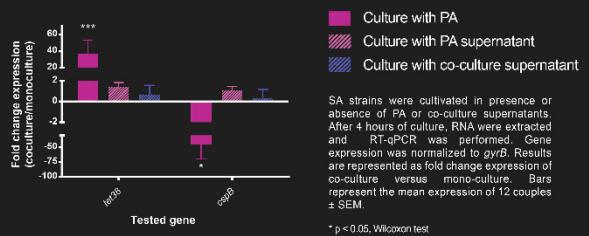
Phenotypic tests Antibiotic resistance Acetoin dosages



Increased tetracycline resistance for SA

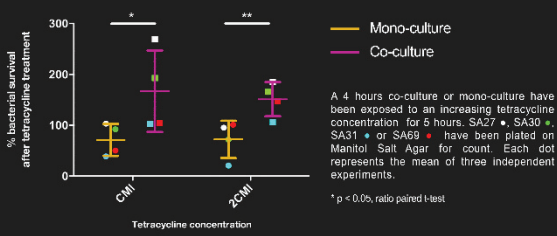
RNA-seq data from one SA coexistence strain pointed out 46 genes differentially expressed in presence of PA. Confirmation by qPCR reveals that *tet38* and *cspB* genes are respectively overexpressed and underexpressed among almost all the couples tested (12).

tet38 and *cspB* expressions are modified by direct contact with PA



Both genes are involved in antibiotic resistance. A *cspB* null mutant displayed increased resistance to aminoglycosides, trimethoprim-sulfamethoxazole (Duval *et al.*, 2010). Tet38 is an efflux pumps taking tetracycline, erythromycin and chloramphenicol out the cell (Truong-Bolduc *et al.*, 2015).

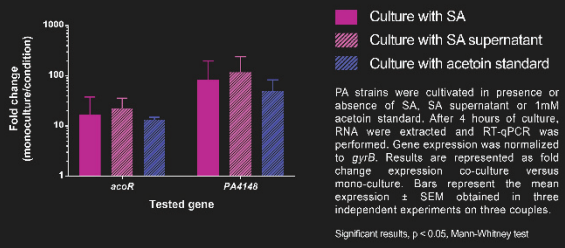
SA tetracycline resistance sharply goes up in presence of PA



A new carbon source for PA

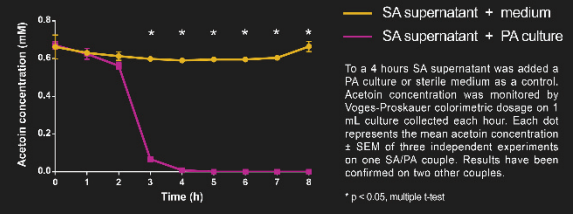
RNAseq analysis (1 couple) and qRT-PCR (22 couples) indicate that 70% of PA strains overexpress the *aco* operon (*PA4148-PA4153*) and its transcriptional activator *acoR* in presence of SA. These genes are implied in acetoin catabolism, a neutral molecule produced by bacteria to limit cell acidification during growth.

Acetoin produced by SA induces the expression of PA *aco* system



SA supernatant - containing large amount of acetoin - and acetoin standard also induce the *aco* system overexpression. The acetoin produced by SA seems to be the inductor signal of the *aco* system overexpression in PA.

PA catabolizes the acetoin produced by SA



In connection with transcriptomic results, PA catabolizes the acetoin produced by SA. This could provide a new carbon source for PA and affect SA regulation of cell acidification.

Conclusions The goal of these studies is to understand the poly-microbial interactions occurring in CF patients. Surprisingly, the majority of SA and PA strains from co-infection are in a coexistence state. For *Staphylococcus aureus*, this interaction leads to deregulation of *tet38* and *cspB* gene expression. Both genes are involved in antibiotic resistance. *tet38* overexpression may be responsible for the increasing tetracycline resistance observed in co-culture with PA. In *Pseudomonas aeruginosa*, the presence of SA drives the overexpression of the *aco* system, encoding genes implicated in acetoin catabolism. Produced by SA, acetoin is consumed by PA and may promote its fitness.

Fundings This work was supported by the Fondation pour la Recherche Médicale (FRM grant number ECO20170637499 to [LC]), and Finovi.



2 Médiation et vulgarisation scientifique

- Nov. 2020** **Conférence de l'Université Inter-Ages Drôme-Ardèche**
Guilherand-G. La sociabilité des bactéries : de la compétition à la coopération – Grand public
- 2018-2019** **Rencontre doctorants-lycéens et collégiens**
Lyon Dialogues Entre Chercheurs et Lycéens pour les Intéresser à la Construction des Savoirs (DECLICs) et rencontres organisées par Isabelle Bonardi (UDL)
Lycée du Parc (6^{ème}), Lycée Frédéric Fays (Villeurbanne), Festival Pop'Science
- 2018** **Organisation et participation à la Fête de la Science**
Lyon IUT de Génie Biologique (La Doua)
- Avril 2018** **FameLab France, concours de communication scientifique**
Lyon Microbes malicieux, voisinage harmonieux – *Finaliste national*



REFERENCES

1. Palmer KL, Aye LM, Whiteley M. 2007. Nutritional cues control *Pseudomonas aeruginosa* multicellular behavior in cystic fibrosis sputum. *J Bacteriol* 189:8079–8087.
2. Artegiani B, Clevers H. 2018. Use and application of 3D-organoid technology. *Hum Mol Genet* 27:R99–R107.
3. Russo DA, Couto N, Beckerman AP, Pandhal J. 2019. Metaproteomics of Freshwater Microbial Communities. *Methods Mol Biol* 1977:145–155.
4. Jansson JK, Hofmockel KS. 2018. The soil microbiome—from metagenomics to metaphenomics. *Curr Opin Microbiol* 43:162–168.
5. Lepage P, Leclerc MC, Joossens M, Mondot S, Blottière HM, Raes J, Ehrlich D, Doré J. 2013. A metagenomic insight into our gut's microbiome. *Gut* 62:146–158.
6. Konopka A. 2009. What is microbial community ecology? *ISME J* 3:1223–1230.
7. Huang YJ, LiPuma JJ. 2016. The Microbiome in Cystic Fibrosis. *Clin Chest Med* 37:59–67.
8. Freerksen E. 1982. [Tuberculosis etiology—its development and consequences (Robert Koch)]. *Prax Klin Pneumol* 36:122–134.
9. Murray JL, Connell JL, Stacy A, Turner KH, Whiteley M. 2014. Mechanisms of synergy in polymicrobial infections. 3. *J Microbiol* 52:188–199.
10. Brogden KA, Guthmiller JM, Taylor CE. 2005. Human polymicrobial infections. *The Lancet* 365:253–255.
11. Ibberson CB, Whiteley M. 2020. The social life of microbes in chronic infection. *Curr Opin Microbiol* 53:44–50.
12. Abisado RG, Benomar S, Klaus JR, Dandekar AA, Chandler JR. 2018. Bacterial Quorum Sensing and Microbial Community Interactions. 3. *mBio* 9.
13. Hassani MA, Durán P, Hacquard S. 2018. Microbial interactions within the plant holobiont. *Microbiome* 6.
14. Coulthurst S. 2019. The Type VI secretion system: a versatile bacterial weapon. *Microbiology (Reading)* 165:503–515.
15. Faust K, Raes J. 2012. Microbial interactions: from networks to models. 8. *Nature Reviews Microbiology* 10:538–550.
16. Lidicker WZ. 1979. A Clarification of Interactions in Ecological Systems. *BioScience* 29:475–477.
17. Hillesland KL. 2018. Evolution on the bright side of life: microorganisms and the evolution of mutualism. *Annals of the New York Academy of Sciences* 1422:88–103.
18. Cremer J, Melbinger A, Wienand K, Henriquez T, Jung H, Frey E. 2019. Cooperation in Microbial Populations: Theory and Experimental Model Systems. *Journal of Molecular Biology* 431:4599–4644.

19. Loarca D, Díaz D, Quezada H, Guzmán-Ortiz AL, Rebollar-Ruiz A, Presas AMF, Ramírez-Peris J, Franco-Cendejas R, Maeda T, Wood TK, García-Contreras R. 2019. Seeding Public Goods Is Essential for Maintaining Cooperation in *Pseudomonas aeruginosa*. *Front Microbiol* 10.
20. Yurtsev EA, Conwill A, Gore J. 2016. Oscillatory dynamics in a bacterial cross-protection mutualism. *Proc Natl Acad Sci U S A* 113:6236–6241.
21. Graber JR, Breznak JA. 2005. Folate cross-feeding supports symbiotic homoacetogenic spirochetes. *Appl Environ Microbiol* 71:1883–1889.
22. Laverde Gomez JA, Mukhopadhyaya I, Duncan SH, Louis P, Shaw S, Collie-Duguid E, Crost E, Juge N, Flint HJ. 2019. Formate cross-feeding and cooperative metabolic interactions revealed by transcriptomics in co-cultures of acetogenic and amyolytic human colonic bacteria. *Environ Microbiol* 21:259–271.
23. Seth EC, Taga ME. 2014. Nutrient cross-feeding in the microbial world. *Frontiers in Microbiology* 5.
24. Morris BEL, Henneberger R, Huber H, Moissl-Eichinger C. 2013. Microbial syntrophy: interaction for the common good. *FEMS Microbiol Rev* 37:384–406.
25. Pagnussat LA, Salcedo F, Maroniche G, Keel C, Valverde C, Creus CM. 2016. Interspecific cooperation: enhanced growth, attachment and strain-specific distribution in biofilms through *Azospirillum brasilense*-*Pseudomonas protegens* co-cultivation. *FEMS Microbiol Lett* 363.
26. Pompilio A, Crocetta V, De Nicola S, Verginelli F, Fiscarelli E, Di Bonaventura G. 2015. Cooperative pathogenicity in cystic fibrosis: *Stenotrophomonas maltophilia* modulates *Pseudomonas aeruginosa* virulence in mixed biofilm. *Front Microbiol* 6:951.
27. Elias S, Banin E. 2012. Multi-species biofilms: living with friendly neighbors. *FEMS Microbiol Rev* 36:990–1004.
28. Bondy-Denomy J, Davidson AR. 2014. When a virus is not a parasite: the beneficial effects of prophages on bacterial fitness. *J Microbiol* 52:235–242.
29. Mp S, NI B. 1966. Parasitic interaction of *Bdellovibrio bacteriovorus* with other bacteria. *Journal of bacteriology*.
30. Caulton SG, Lovering AL. 2020. Bacterial invasion and killing by predatory *Bdellovibrio* primed by predator prey cell recognition and self protection. *Current Opinion in Microbiology* 56:74–80.
31. García C, Rendueles M, Díaz M. 2017. Microbial amensalism in *Lactobacillus casei* and *Pseudomonas taetrolens* mixed culture. *Bioprocess Biosyst Eng* 40:1111–1122.
32. Ghouli M, Mitri S. 2016. The Ecology and Evolution of Microbial Competition. *Trends Microbiol* 24:833–845.
33. García-Bayona L, Comstock LE. 2018. Bacterial antagonism in host-associated microbial communities. *Science* 361.
34. Er S, İstanbullu Tosun A, Arık G, Kivanç M. 2019. Anticandidal activities of lactic acid bacteria isolated from the vagina. *Turk J Med Sci* 49:375–383.

35. Kovachev S. 2018. Defence factors of vaginal lactobacilli. *Crit Rev Microbiol* 44:31–39.
36. Egert M, Simmering R, Riedel CU. 2017. The Association of the Skin Microbiota With Health, Immunity, and Disease. *Clin Pharmacol Ther* 102:62–69.
37. Hotterbeekx A, Kumar-Singh S, Goossens H, Malhotra-Kumar S. 2017. In vivo and In vitro Interactions between *Pseudomonas aeruginosa* and *Staphylococcus* spp. *Front Cell Infect Microbiol* 7.
38. Fourie R, Ells R, Swart CW, Sebolai OM, Albertyn J, Pohl CH. 2016. *Candida albicans* and *Pseudomonas aeruginosa* Interaction, with Focus on the Role of Eicosanoids. *Front Physiol* 7:64.
39. Sass G, Nazik H, Penner J, Shah H, Ansari SR, Clemons KV, Groleau M-C, Dietl A-M, Visca P, Haas H, Déziel E, Stevens DA. 2019. *Aspergillus-Pseudomonas* interaction, relevant to competition in airways. *Med Mycol* 57:S228–S232.
40. Vogt SL, Finlay BB. 2017. Gut microbiota-mediated protection against diarrheal infections. *J Travel Med* 24:S39–S43.
41. Scoffield JA, Wu H. 2015. Oral Streptococci and Nitrite-Mediated Interference of *Pseudomonas aeruginosa*. *Infect Immun* 83:101–107.
42. Filkins LM, Hampton TH, Gifford AH, Gross MJ, Hogan DA, Sogin ML, Morrison HG, Paster BJ, O'Toole GA. 2012. Prevalence of streptococci and increased polymicrobial diversity associated with cystic fibrosis patient stability. *J Bacteriol* 194:4709–4717.
43. Sanches-Vaz M, Temporão A, Luis R, Nunes-Cabaço H, Mendes AM, Goellner S, Carvalho T, Figueiredo LM, Prudêncio M. 2019. *Trypanosoma brucei* infection protects mice against malaria. *PLoS Pathog* 15:e1008145.
44. Gonzalez AJ, Ijezie EC, Balemba OB, Miura TA. 2018. Attenuation of Influenza A Virus Disease Severity by Viral Coinfection in a Mouse Model. *J Virol* 92.
45. McArdle AJ, Turkova A, Cunnington AJ. 2018. When do co-infections matter? *Curr Opin Infect Dis* 31:209–215.
46. Learman BS, Brauer AL, Eaton KA, Armbruster CE. 2019. A Rare Opportunist, *Morganella morganii*, Decreases Severity of Polymicrobial Catheter-Associated Urinary Tract Infection. *Infect Immun* 88.
47. Kiedrowski MR, Bomberger JM. 2018. Viral-Bacterial Co-infections in the Cystic Fibrosis Respiratory Tract. *Front Immunol* 9.
48. Mazel-Sanchez B, Yildiz S, Schmolke M. 2019. Ménage à trois: Virus, Host, and Microbiota in Experimental Infection Models. *Trends in Microbiology* 27:440–452.
49. Scott JE, O'Toole GA. 2019. The Yin and Yang of *Streptococcus* Lung Infections in Cystic Fibrosis: a Model for Studying Polymicrobial Interactions. *J Bacteriol* 201.
50. Duan K, Dammel C, Stein J, Rabin H, Surette MG. 2003. Modulation of *Pseudomonas aeruginosa* gene expression by host microflora through interspecies communication. *Molecular Microbiology* 50:1477–1491.
51. Nair N, Biswas R, Götz F, Biswas L. 2014. Impact of *Staphylococcus aureus* on pathogenesis in polymicrobial infections. *Infect Immun* 82:2162–2169.

52. Partida-Martinez LP, Hertweck C. 2005. Pathogenic fungus harbours endosymbiotic bacteria for toxin production. *Nature* 437:884–888.
53. Grosskopf T, Soyer OS. 2014. Synthetic microbial communities. *Curr Opin Microbiol* 18:72–77.
54. Zuñiga C, Li T, Guarnieri MT, Jenkins JP, Li C-T, Bingol K, Kim Y-M, Betenbaugh MJ, Zengler K. 2020. Synthetic microbial communities of heterotrophs and phototrophs facilitate sustainable growth. *Nat Commun* 11:3803.
55. Briaud P, Camus L, Bastien S, Doléans-Jordheim A, Vandenesch F, Moreau K. 2019. Coexistence with *Pseudomonas aeruginosa* alters *Staphylococcus aureus* transcriptome, antibiotic resistance and internalization into epithelial cells. *Sci Rep* 9.
56. Camus L, Briaud P, Bastien S, Elsen S, Doléans-Jordheim A, Vandenesch F, Moreau K. 2020. Trophic cooperation promotes bacterial survival of *Staphylococcus aureus* and *Pseudomonas aeruginosa*. *ISME J* <https://doi.org/10.1038/s41396-020-00741-9>.
57. Tognon M, Köhler T, Gdaniec BG, Hao Y, Lam JS, Beaume M, Luscher A, Buckling A, van Delden C. 2017. Co-evolution with *Staphylococcus aureus* leads to lipopolysaccharide alterations in *Pseudomonas aeruginosa*. *ISME J* 11:2233–2243.
58. Price CE, Brown DG, Limoli DH, Phelan VV, O’Toole GA. 2020. Exogenous Alginate Protects *Staphylococcus aureus* from Killing by *Pseudomonas aeruginosa*. *J Bacteriol* 202.
59. Zhao K, Du L, Lin J, Yuan Y, Wang X, Yue B, Wang X, Guo Y, Chu Y, Zhou Y. 2018. *Pseudomonas aeruginosa* Quorum-Sensing and Type VI Secretion System Can Direct Interspecific Coexistence During Evolution. *Front Microbiol* 9:2287.
60. Venturelli OS, Carr AC, Fisher G, Hsu RH, Lau R, Bowen BP, Hromada S, Northen T, Arkin AP. 2018. Deciphering microbial interactions in synthetic human gut microbiome communities. *Mol Syst Biol* 14.
61. Gabriliska RA, Rumbaugh KP. 2015. Biofilm models of polymicrobial infection. *Future Microbiol* 10:1997–2015.
62. Cendra MDM, Blanco-Cabra N, Pedraz L, Torrents E. 2019. Optimal environmental and culture conditions allow the in vitro coexistence of *Pseudomonas aeruginosa* and *Staphylococcus aureus* in stable biofilms. *Sci Rep* 9:16284.
63. Baldan R, Cigana C, Testa F, Bianconi I, De Simone M, Pellin D, Di Serio C, Bragonzi A, Cirillo DM. 2014. Adaptation of *Pseudomonas aeruginosa* in Cystic Fibrosis airways influences virulence of *Staphylococcus aureus* in vitro and murine models of co-infection. *PLoS ONE* 9:e89614.
64. Hůlková M, Soukupová J, Carlson RP, Maršálek B. 2020. Interspecies interactions can enhance *Pseudomonas aeruginosa* tolerance to surfaces functionalized with silver nanoparticles. *Colloids Surf B Biointerfaces* 192:111027.
65. Lee Y-J, Jang H-J, Chung I-Y, Cho Y-H. 2018. *Drosophila melanogaster* as a polymicrobial infection model for *Pseudomonas aeruginosa* and *Staphylococcus aureus*. *J Microbiol* 56:534–541.
66. Bakaletz LO. 2004. Developing animal models for polymicrobial diseases. *Nat Rev Microbiol* 2:552–568.

67. Zhang C, Straight PD. 2019. Antibiotic discovery through microbial interactions. *Curr Opin Microbiol* 51:64–71.
68. Blanchard AC, Waters VJ. 2019. Microbiology of Cystic Fibrosis Airway Disease. *Semin Respir Crit Care Med* 40:727–736.
69. Françoise A, Héry-Arnaud G. 2020. The Microbiome in Cystic Fibrosis Pulmonary Disease. *Genes (Basel)* 11.
70. Andersen DH. 1938. CYSTIC FIBROSIS OF THE PANCREAS AND ITS RELATION TO CELIAC DISEASE: A CLINICAL AND PATHOLOGIC STUDY. *Am J Dis Child* 56:344–399.
71. Stephenson AL, Stanojevic S, Sykes J, Burgel P-R. 2017. The changing epidemiology and demography of cystic fibrosis. *Presse Med* 46:e87–e95.
72. Bruce Marshall, Albert Faro, Aliza Fink, Deena Loeffler, Alexander Elbert, Thomas O’Neil, Tucker Rush, Samar Rizvi. 2018. Cystic Fibrosis Foundation Patient Registry 2017 Annual Data Report.
73. Farrell PM. 2008. The prevalence of cystic fibrosis in the European Union. *J Cyst Fibros* 7:450–453.
74. Zolin A, Orenti A, Naehrlich L, van Rens J et al. 2019. ECFSPR Annual Report 2017.
75. French Cystic Fibrosis Register, 2017.pdf. https://www.vaincrelamuco.org/sites/default/files/rapport_du_registre_-_donnees_2017.pdf.
76. Scotet V, Gillet D, Duguépérroux I, Audrézet M-P, Bellis G, Garnier B, Roussey M, Rault G, Parent P, De Braekeleer M, Férec C, Réseau Mucoviscidose Bretagne et Pays de Loire. 2002. Spatial and temporal distribution of cystic fibrosis and of its mutations in Brittany, France: a retrospective study from 1960. *Hum Genet* 111:247–254.
77. Corriveau S, Sykes J, Stephenson AL. 2018. Cystic fibrosis survival: the changing epidemiology. *Curr Opin Pulm Med* 24:574–578.
78. Dodge JA, Lewis PA, Stanton M, Wilsher J. 2007. Cystic fibrosis mortality and survival in the UK: 1947-2003. *Eur Respir J* 29:522–526.
79. MacKenzie T, Gifford AH, Sabadosa KA, Quinton HB, Knapp EA, Goss CH, Marshall BC. 2014. Longevity of patients with cystic fibrosis in 2000 to 2010 and beyond: survival analysis of the Cystic Fibrosis Foundation patient registry. *Ann Intern Med* 161:233–241.
80. De Boeck K, Vermeulen F, Dupont L. 2017. The diagnosis of cystic fibrosis. *Presse Med* 46:e97–e108.
81. Kerem B, Rommens JM, Buchanan JA, Markiewicz D, Cox TK, Chakravarti A, Buchwald M, Tsui LC. 1989. Identification of the cystic fibrosis gene: genetic analysis. *Science* 245:1073–1080.
82. Fajac I, De Boeck K. 2017. New horizons for cystic fibrosis treatment. *Pharmacol Ther* 170:205–211.

83. Bobadilla JL, Macek M, Fine JP, Farrell PM. 2002. Cystic fibrosis: a worldwide analysis of CFTR mutations--correlation with incidence data and application to screening. *Hum Mutat* 19:575–606.
84. Bombieri C, Seia M, Castellani C. 2015. Genotypes and phenotypes in cystic fibrosis and cystic fibrosis transmembrane regulator-related disorders. *Semin Respir Crit Care Med* 36:180–193.
85. Castellani C, Cuppens H, Macek M, Cassiman JJ, Kerem E, Durie P, Tullis E, Assael BM, Bombieri C, Brown A, Casals T, Claustres M, Cutting GR, Dequeker E, Dodge J, Doull I, Farrell P, Ferec C, Girodon E, Johannesson M, Kerem B, Knowles M, Munck A, Pignatti PF, Radojkovic D, Rizzotti P, Schwarz M, Stuhmann M, Tzetis M, Zielenski J, Elborn JS. 2008. Consensus on the use and interpretation of cystic fibrosis mutation analysis in clinical practice. *J Cyst Fibros* 7:179–196.
86. Marson FAL, Bertuzzo CS, Ribeiro JD. 2016. Classification of CFTR mutation classes. *Lancet Respir Med* 4:e37–e38.
87. Sharma S, Hanukoglu A, Hanukoglu I. 2018. Localization of epithelial sodium channel (ENaC) and CFTR in the germinal epithelium of the testis, Sertoli cells, and spermatozoa. *J Mol Histol* 49:195–208.
88. Sharma S, Hanukoglu I. 2019. Mapping the sites of localization of epithelial sodium channel (ENaC) and CFTR in segments of the mammalian epididymis. *J Mol Histol* 50:141–154.
89. Childers M, Eckel G, Himmel A, Caldwell J. 2007. A new model of cystic fibrosis pathology: lack of transport of glutathione and its thiocyanate conjugates. *Med Hypotheses* 68:101–112.
90. Chen MH, Chen H, Zhou Z, Ruan YC, Wong HY, Lu YC, Guo JH, Chung YW, Huang PB, Huang HF, Zhou WL, Chan HC. 2010. Involvement of CFTR in oviductal HCO₃⁻ secretion and its effect on soluble adenylate cyclase-dependent early embryo development. *Hum Reprod* 25:1744–1754.
91. Ando-Akatsuka Y, Abdullaev IF, Lee EL, Okada Y, Sabirov RZ. 2002. Down-regulation of volume-sensitive Cl⁻ channels by CFTR is mediated by the second nucleotide-binding domain. *Pflugers Arch* 445:177–186.
92. Carrageta DF, Bernardino RL, Alves MG, Oliveira PF. 2020. CFTR regulation of aquaporin-mediated water transport. *Vitam Horm* 112:163–177.
93. Saint-Criq V, Gray MA. 2017. Role of CFTR in epithelial physiology. *Cell Mol Life Sci* 74:93–115.
94. Chandler JD, Min E, Huang J, McElroy CS, Dickerhof N, Mocatta T, Fletcher AA, Evans CM, Liang L, Patel M, Kettle AJ, Nichols DP, Day BJ. 2015. Antiinflammatory and Antimicrobial Effects of Thiocyanate in a Cystic Fibrosis Mouse Model. *Am J Respir Cell Mol Biol* 53:193–205.
95. Pezzulo AA, Tang XX, Hoegger MJ, Abou Alaiwa MH, Ramachandran S, Moninger TO, Karp PH, Wohlford-Lenane CL, Haagsman HP, van Eijk M, Bánfi B, Horswill AR, Stoltz DA, McCray PB, Welsh MJ, Zabner J. 2012. Reduced airway surface pH impairs bacterial killing in the porcine cystic fibrosis lung. *Nature* 487:109–113.

96. Egan ME. 2016. Genetics of Cystic Fibrosis: Clinical Implications. *Clin Chest Med* 37:9–16.
97. Hauser AR, Jain M, Bar-Meir M, McColley SA. 2011. Clinical significance of microbial infection and adaptation in cystic fibrosis. *Clin Microbiol Rev* 24:29–70.
98. de Souza D a. S, Faucz FR, Pereira-Ferrari L, Sotomaio VS, Raskin S. 2018. Congenital bilateral absence of the vas deferens as an atypical form of cystic fibrosis: reproductive implications and genetic counseling. *Andrology* 6:127–135.
99. Jacquot J, Delion M, Gangloff S, Braux J, Velard F. 2016. Bone disease in cystic fibrosis: new pathogenic insights opening novel therapies. *Osteoporos Int* 27:1401–1412.
100. Turcios NL. 2020. Cystic Fibrosis Lung Disease: An Overview. *Respir Care* 65:233–251.
101. Moffatt MF, Cookson WO. 2017. The lung microbiome in health and disease. *Clin Med (Lond)* 17:525–529.
102. Surette MG. 2014. The cystic fibrosis lung microbiome. *Ann Am Thorac Soc* 11 Suppl 1:S61-65.
103. Mahboubi MA, Carmody LA, Foster BK, Kalikin LM, VanDevanter DR, LiPuma JJ. 2016. Culture-Based and Culture-Independent Bacteriologic Analysis of Cystic Fibrosis Respiratory Specimens. *J Clin Microbiol* 54:613–619.
104. Permall DL, Pasha AB, Chen X-Q, Lu H-Y. 2019. The lung microbiome in neonates. *Turk J Pediatr* 61:821–830.
105. Dominguez-Bello MG, Costello EK, Contreras M, Magris M, Hidalgo G, Fierer N, Knight R. 2010. Delivery mode shapes the acquisition and structure of the initial microbiota across multiple body habitats in newborns. *Proc Natl Acad Sci U S A* 107:11971–11975.
106. Moran Losada P, Chouvarine P, Dorda M, Hedtfeld S, Mielke S, Schulz A, Wiehlmann L, Tümmler B. 2016. The cystic fibrosis lower airways microbial metagenome. *ERJ Open Res* 2.
107. Whelan FJ, Heirali AA, Rossi L, Rabin HR, Parkins MD, Surette MG. 2017. Longitudinal sampling of the lung microbiota in individuals with cystic fibrosis. *PLoS One* 12:e0172811.
108. da Costa Ferreira Leite C, Folescu TW, de Cássia Firmida M, Cohen RWF, Leão RS, de Freitas FAD, Albano RM, da Costa CH, Marques EA. 2017. Monitoring clinical and microbiological evolution of a cystic fibrosis patient over 26 years: experience of a Brazilian CF Centre. *BMC Pulm Med* 17:100.
109. Lamoureux C, Guilloux C-A, Beauruelle C, Jolivet-Gougeon A, Héry-Arnaud G. 2019. Anaerobes in cystic fibrosis patients' airways. *Crit Rev Microbiol* 45:103–117.
110. Hahn A, Whiteson K, Davis TJ, Phan J, Sami I, Koumbourlis AC, Freishtat RJ, Crandall KA, Bean HD. 2020. Longitudinal Associations of the Cystic Fibrosis Airway Microbiome and Volatile Metabolites: A Case Study. *Front Cell Infect Microbiol* 10:174.
111. Hampton TH, Green DM, Cutting GR, Morrison HG, Sogin ML, Gifford AH, Stanton BA, O'Toole GA. 2014. The microbiome in pediatric cystic fibrosis patients: the role of shared environment suggests a window of intervention. *Microbiome* 2:14.

112. Zemanick ET, Wagner BD, Robertson CE, Ahrens RC, Chmiel JF, Clancy JP, Gibson RL, Harris WT, Kurland G, Laguna TA, McColley SA, McCoy K, Retsch-Bogart G, Sobush KT, Zeitlin PL, Stevens MJ, Accurso FJ, Sagel SD, Harris JK. 2017. Airway microbiota across age and disease spectrum in cystic fibrosis. *Eur Respir J* 50.
113. Cox MJ, Allgaier M, Taylor B, Baek MS, Huang YJ, Daly RA, Karaoz U, Andersen GL, Brown R, Fujimura KE, Wu B, Tran D, Koff J, Kleinhenz ME, Nielson D, Brodie EL, Lynch SV. 2010. Airway microbiota and pathogen abundance in age-stratified cystic fibrosis patients. *PLoS One* 5:e11044.
114. Cuthbertson L, Walker AW, Oliver AE, Rogers GB, Rivett DW, Hampton TH, Ashare A, Elborn JS, De Soyza A, Carroll MP, Hoffman LR, Lanyon C, Moskowitz SM, O'Toole GA, Parkhill J, Planet PJ, Teneback CC, Tunney MM, Zuckerman JB, Bruce KD, van der Gast CJ. 2020. Lung function and microbiota diversity in cystic fibrosis. *Microbiome* 8:45.
115. Zhao J, Schloss PD, Kalikin LM, Carmody LA, Foster BK, Petrosino JF, Cavalcoli JD, VanDevanter DR, Murray S, Li JZ, Young VB, LiPuma JJ. 2012. Decade-long bacterial community dynamics in cystic fibrosis airways. *Proc Natl Acad Sci U S A* 109:5809–5814.
116. Quinn RA, Whiteson K, Lim YW, Zhao J, Conrad D, LiPuma JJ, Rohwer F, Widder S. 2016. Ecological networking of cystic fibrosis lung infections. *NPJ Biofilms Microbiomes* 2:4.
117. Quinn RA, Whiteson K, Lim Y-W, Salamon P, Bailey B, Mienardi S, Sanchez SE, Blake D, Conrad D, Rohwer F. 2015. A Winogradsky-based culture system shows an association between microbial fermentation and cystic fibrosis exacerbation. *ISME J* 9:1024–1038.
118. Carmody LA, Zhao J, Kalikin LM, LeBar W, Simon RH, Venkataraman A, Schmidt TM, Abdo Z, Schloss PD, LiPuma JJ. 2015. The daily dynamics of cystic fibrosis airway microbiota during clinical stability and at exacerbation. *Microbiome* 3:12.
119. Twomey KB, Alston M, An S-Q, O'Connell OJ, McCarthy Y, Swarbreck D, Febrer M, Dow JM, Plant BJ, Ryan RP. 2013. Microbiota and metabolite profiling reveal specific alterations in bacterial community structure and environment in the cystic fibrosis airway during exacerbation. *PLoS One* 8:e82432.
120. Caverly LJ, LiPuma JJ. 2018. Cystic fibrosis respiratory microbiota: unraveling complexity to inform clinical practice. *Expert Rev Respir Med* 12:857–865.
121. Cardines R, Giufrè M, Pompilio A, Fiscarelli E, Ricciotti G, Di Bonaventura G, Cerquetti M. 2012. *Haemophilus influenzae* in children with cystic fibrosis: antimicrobial susceptibility, molecular epidemiology, distribution of adhesins and biofilm formation. *Int J Med Microbiol* 302:45–52.
122. Trifonova A, Strateva T. 2019. *Stenotrophomonas maltophilia* - a low-grade pathogen with numerous virulence factors. *Infect Dis (Lond)* 51:168–178.
123. Isler B, Kidd TJ, Stewart AG, Harris P, Paterson DL. 2020. *Achromobacter* Infections and Treatment Options. *Antimicrob Agents Chemother* 64.
124. Degiacomi G, Sammartino JC, Chiarelli LR, Riabova O, Makarov V, Pasca MR. 2019. *Mycobacterium abscessus*, an Emerging and Worrisome Pathogen among Cystic Fibrosis Patients. *Int J Mol Sci* 20.

125. Cuthbertson L, Felton I, James P, Cox MJ, Bilton D, Schelenz S, Loebinger MR, Cookson WOC, Simmonds NJ, Moffatt MF. 2020. The fungal airway microbiome in cystic fibrosis and non-cystic fibrosis bronchiectasis. *J Cyst Fibros* <https://doi.org/10.1016/j.jcf.2020.05.013>.
126. Ziesing S, Suerbaum S, Sedlacek L. 2016. Fungal epidemiology and diversity in cystic fibrosis patients over a 5-year period in a national reference center. *Med Mycol* 54:781–786.
127. Breuer O, Schultz A, Garratt LW, Turkovic L, Rosenow T, Murray CP, Karpievitch YV, Akesson L, Dalton S, Sly PD, Ranganathan S, Stick SM, Caudri D. 2020. Aspergillus Infections and Progression of Structural Lung Disease in Children with Cystic Fibrosis. *Am J Respir Crit Care Med* 201:688–696.
128. Schwarz C, Hartl D, Eickmeier O, Hector A, Benden C, Durieu I, Sole A, Gartner S, Milla CE, Barry PJ. 2018. Progress in Definition, Prevention and Treatment of Fungal Infections in Cystic Fibrosis. *Mycopathologia* 183:21–32.
129. Hurley MN, Smyth AR. 2018. Staphylococcus aureus in cystic fibrosis: pivotal role or bit part actor? *Curr Opin Pulm Med* 24:586–591.
130. Gangell C, Cf on behalf of A, Gard S, Cf on behalf of A, Douglas T, Cf on behalf of A, Park J, Cf on behalf of A, de Klerk N, Cf on behalf of A, Keil T, Cf on behalf of A, Brennan S, Cf on behalf of A, Ranganathan S, Cf on behalf of A, Robins-Browne R, Cf on behalf of A, Sly PD, Cf on behalf of A. 2011. Inflammatory Responses to Individual Microorganisms in the Lungs of Children With Cystic Fibrosis. *Clin Infect Dis* 53:425–432.
131. Sagel SD, Gibson RL, Emerson J, McNamara S, Burns JL, Wagener JS, Ramsey BW. 2009. Impact of Pseudomonas and Staphylococcus Infection on Inflammation and Clinical Status in Young Children with Cystic Fibrosis. *The Journal of Pediatrics* 154:183-188.e3.
132. Hudson VL, Wielinski CL, Regelmann WE. 1993. Prognostic implications of initial oropharyngeal bacterial flora in patients with cystic fibrosis diagnosed before the age of two years. *The Journal of Pediatrics* 122:854–860.
133. Hubert D, Réglier-Poupet H, Sermet-Gaudelus I, Ferroni A, Le Bourgeois M, Burgel P-R, Serreau R, Dusser D, Poyart C, Coste J. 2013. Association between Staphylococcus aureus alone or combined with Pseudomonas aeruginosa and the clinical condition of patients with cystic fibrosis. 5. *Journal of Cystic Fibrosis* 12:497–503.
134. Dasenbrook EC. 2011. Update on methicillin-resistant Staphylococcus aureus in cystic fibrosis. *Curr Opin Pulm Med* 17:437–441.
135. Cohen RWF, Folescu TW, Daltro P, Boechat MCB, Lima DF, Marques EA, Leão RS. 2017. Methicillin-resistant Staphylococcus aureus in cystic fibrosis patients: do we need to care? A cohort study. *Sao Paulo Med J* 135:420–427.
136. Akil N, Muhlebach MS. 2018. Biology and management of methicillin resistant Staphylococcus aureus in cystic fibrosis. *Pediatr Pulmonol* 53:S64–S74.
137. Besier S, Ludwig A, Ohlsen K, Brade V, Wichelhaus TA. 2007. Molecular analysis of the thymidine-auxotrophic small colony variant phenotype of Staphylococcus aureus. *Int J Med Microbiol* 297:217–225.

138. Yagci S, Hascelik G, Dogru D, Ozcelik U, Sener B. 2013. Prevalence and genetic diversity of *Staphylococcus aureus* small-colony variants in cystic fibrosis patients. *Clin Microbiol Infect* 19:77–84.
139. Wolter DJ, Emerson JC, McNamara S, Buccat AM, Qin X, Cochrane E, Houston LS, Rogers GB, Marsh P, Prehar K, Pope CE, Blackledge M, Déziel E, Bruce KD, Ramsey BW, Gibson RL, Burns JL, Hoffman LR. 2013. *Staphylococcus aureus* Small-Colony Variants Are Independently Associated With Worse Lung Disease in Children With Cystic Fibrosis. 3. *Clin Infect Dis* 57:384–391.
140. Kahl BC, Becker K, Löffler B. 2016. Clinical Significance and Pathogenesis of *Staphylococcal* Small Colony Variants in Persistent Infections. *Clin Microbiol Rev* 29:401–427.
141. Konstan MW, Wagener JS, Vandevanter DR, Pasta DJ, Yegin A, Rasouliyan L, Morgan WJ. 2012. Risk factors for rate of decline in FEV1 in adults with cystic fibrosis. *J Cyst Fibros* 11:405–411.
142. Pittman JE, Calloway EH, Kiser M, Yeatts J, Davis SD, Drumm ML, Schechter MS, Leigh MW, Emond M, Van Rie A, Knowles MR. 2011. Age of *Pseudomonas aeruginosa* acquisition and subsequent severity of cystic fibrosis lung disease. *Pediatr Pulmonol* 46:497–504.
143. Milczewska J, Wołkowicz T, Zacharczuk K, Mierzejewska E, Kwiatkowska M, Walicka-Serzysko K, Sands D. 2020. Clinical outcomes for cystic fibrosis patients with *Pseudomonas aeruginosa* cross-infections. *Pediatr Pulmonol* 55:161–168.
144. Emerson J, Rosenfeld M, McNamara S, Ramsey B, Gibson RL. 2002. *Pseudomonas aeruginosa* and other predictors of mortality and morbidity in young children with cystic fibrosis. *Pediatr Pulmonol* 34:91–100.
145. Zemanick ET, Bell SC. 2019. Prevention of chronic infection with *Pseudomonas aeruginosa* infection in cystic fibrosis. *Curr Opin Pulm Med* 25:636–645.
146. Yum H-K, Park I-N, Shin B-M, Choi S-J. 2014. Recurrent *Pseudomonas aeruginosa* Infection in Chronic Lung Diseases: Relapse or Reinfection? *Tuberc Respir Dis (Seoul)* 77:172–177.
147. Folkesson A, Jelsbak L, Yang L, Johansen HK, Ciofu O, Høiby N, Molin S. 2012. Adaptation of *Pseudomonas aeruginosa* to the cystic fibrosis airway: an evolutionary perspective. *Nat Rev Microbiol* 10:841–851.
148. Kidd TJ, Ramsay KA, Vidmar S, Carlin JB, Bell SC, Wainwright CE, Grimwood K, Wainwright CE, Grimwood K, Francis PW, Dakin C, Cheney J, George N, Carlin JB, Robertson CF, Vidmar S, Moodie M, Carzino R, Carter R, Armstrong DS, Cooper PJ, McKay K, (James) Martin A, Whitehead B, Hunter J, Byrnes CA, Tiddens HA, Graniel K, Gerbrands K, Mott L. 2015. *Pseudomonas aeruginosa* genotypes acquired by children with cystic fibrosis by age 5-years. *Journal of Cystic Fibrosis* 14:361–369.
149. Williams D, Evans B, Haldenby S, Walshaw MJ, Brockhurst MA, Winstanley C, Paterson S. 2015. Divergent, coexisting *Pseudomonas aeruginosa* lineages in chronic cystic fibrosis lung infections. *American Journal of Respiratory and Critical Care Medicine* 191:775–785.

150. Williams D, Fothergill JL, Evans B, Caples J, Haldenby S, Walshaw MJ, Brockhurst MA, Winstanley C, Paterson S. 2018. Transmission and lineage displacement drive rapid population genomic flux in cystic fibrosis airway infections of a *Pseudomonas aeruginosa* epidemic strain. *Microbial Genomics* 4.
151. Bleves S, Viarre V, Salacha R, Michel GPF, Filloux A, Voulhoux R. 2010. Protein secretion systems in *Pseudomonas aeruginosa*: A wealth of pathogenic weapons. *Int J Med Microbiol* 300:534–543.
152. Jyot J, Balloy V, Jouvion G, Verma A, Touqui L, Huerre M, Chignard M, Ramphal R. 2011. Type II secretion system of *Pseudomonas aeruginosa*: in vivo evidence of a significant role in death due to lung infection. *J Infect Dis* 203:1369–1377.
153. Hauser AR. 2009. The type III secretion system of *Pseudomonas aeruginosa*: infection by injection. *Nat Rev Microbiol* 7:654–665.
154. Chen L, Zou Y, She P, Wu Y. 2015. Composition, function, and regulation of T6SS in *Pseudomonas aeruginosa*. *Microbiol Res* 172:19–25.
155. Winstanley C, Fothergill JL. 2009. The role of quorum sensing in chronic cystic fibrosis *Pseudomonas aeruginosa* infections. *FEMS Microbiol Lett* 290:1–9.
156. Cornelis P, Dingemans J. 2013. *Pseudomonas aeruginosa* adapts its iron uptake strategies in function of the type of infections. *Front Cell Infect Microbiol* 3:75.
157. Limoli DH, Warren EA, Yarrington KD, Donegan NP, Cheung AL, O'Toole GA. 2019. Interspecies interactions induce exploratory motility in *Pseudomonas aeruginosa*. *Elife* 8.
158. Leighton TL, Buensuceso RNC, Howell PL, Burrows LL. 2015. Biogenesis of *Pseudomonas aeruginosa* type IV pili and regulation of their function. *Environmental Microbiology* 17:4148–4163.
159. López-Causapé C, Cabot G, Del Barrio-Tofiño E, Oliver A. 2018. The Versatile Mutational Resistome of *Pseudomonas aeruginosa*. *Front Microbiol* 9:685.
160. Lechtzin N, John M, Irizarry R, Merlo C, Diette GB, Boyle MP. 2006. Outcomes of adults with cystic fibrosis infected with antibiotic-resistant *Pseudomonas aeruginosa*. *Respiration* 73:27–33.
161. Lee J, Zhang L. 2015. The hierarchy quorum sensing network in *Pseudomonas aeruginosa*. *Protein Cell* 6:26–41.
162. O'Brien S, Fothergill JL. 2017. The role of multispecies social interactions in shaping *Pseudomonas aeruginosa* pathogenicity in the cystic fibrosis lung. *FEMS Microbiol Lett* 364.
163. Briaud P, Bastien S, Camus L, Boyadijian M, Reix P, Mainguy C, Vandenesch F, Doléans-Jordheim A, Moreau K. 2020. Impact of coexistence phenotype between *Staphylococcus aureus* and *Pseudomonas aeruginosa* isolates on clinical outcomes among Cystic Fibrosis patients. *Front Cell Infect Microbiol* 10.
164. Limoli DH, Yang J, Khansaheb MK, Helfman B, Peng L, Stecenko AA, Goldberg JB. 2016. *Staphylococcus aureus* and *Pseudomonas aeruginosa* co-infection is associated with cystic fibrosis-related diabetes and poor clinical outcomes. *Eur J Clin Microbiol Infect Dis* 35:947–953.

165. Ahlgren HG, Benedetti A, Landry JS, Bernier J, Matouk E, Radzioch D, Lands LC, Rousseau S, Nguyen D. 2015. Clinical outcomes associated with *Staphylococcus aureus* and *Pseudomonas aeruginosa* airway infections in adult cystic fibrosis patients. *BMC Pulmonary Medicine* 15:67.
166. Wakeman CA, Moore JL, Noto MJ, Zhang Y, Singleton MD, Prentice BM, Gilston BA, Doster RS, Gaddy JA, Chazin WJ, Caprioli RM, Skaar EP. 2016. The innate immune protein calprotectin promotes *Pseudomonas aeruginosa* and *Staphylococcus aureus* interaction. *Nat Commun* 7:11951.
167. Limoli DH, Whitfield GB, Kitao T, Ivey ML, Davis MR, Grahl N, Hogan DA, Rahme LG, Howell PL, O'Toole GA, Goldberg JB. 2017. *Pseudomonas aeruginosa* Alginate Overproduction Promotes Coexistence with *Staphylococcus aureus* in a Model of Cystic Fibrosis Respiratory Infection. 2. *mBio* 8.
168. Frydenlund Michelsen C, Hossein Khademi SM, Krogh Johansen H, Ingmer H, Dorrestein PC, Jelsbak L. 2016. Evolution of metabolic divergence in *Pseudomonas aeruginosa* during long-term infection facilitates a proto-cooperative interspecies interaction. 6. *ISME J* 10:1323–1336.
169. Michelsen CF, Christensen A-MJ, Bojer MS, Høiby N, Ingmer H, Jelsbak L. 2014. *Staphylococcus aureus* alters growth activity, autolysis, and antibiotic tolerance in a human host-adapted *Pseudomonas aeruginosa* lineage. 22. *J Bacteriol* 196:3903–3911.
170. Lightbown JW, Jackson FL. 1956. Inhibition of cytochrome systems of heart muscle and certain bacteria by the antagonists of dihydrostreptomycin: 2-alkyl-4-hydroxyquinoline N-oxides. *Biochem J* 63:130–137.
171. Miller CL, Van Laar TA, Chen T, Karna SLR, Chen P, You T, Leung KP. 2017. Global transcriptome responses including small RNAs during mixed-species interactions with methicillin-resistant *Staphylococcus aureus* and *Pseudomonas aeruginosa*. 3. *Microbiologyopen* 6.
172. Nguyen AT, Jones JW, Ruge MA, Kane MA, Oglesby-Sherrouse AG. 2015. Iron Depletion Enhances Production of Antimicrobials by *Pseudomonas aeruginosa*. 14. *J Bacteriol* 197:2265–2275.
173. Filkins LM, Graber JA, Olson DG, Dolben EL, Lynd LR, Bhujji S, O'Toole GA. 2015. Coculture of *Staphylococcus aureus* with *Pseudomonas aeruginosa* Drives *S. aureus* towards Fermentative Metabolism and Reduced Viability in a Cystic Fibrosis Model. *J Bacteriol* 197:2252–2264.
174. Mashburn LM, Jett AM, Akins DR, Whiteley M. 2005. *Staphylococcus aureus* serves as an iron source for *Pseudomonas aeruginosa* during in vivo coculture. 2. *J Bacteriol* 187:554–566.
175. Conroy BS, Grigg JC, Kolesnikov M, Morales LD, Murphy MEP. 2019. *Staphylococcus aureus* heme and siderophore-iron acquisition pathways. *Biometals* 32:409–424.
176. Proctor RA, Kriegeskorte A, Kahl BC, Becker K, Löffler B, Peters G. 2014. *Staphylococcus aureus* Small Colony Variants (SCVs): a road map for the metabolic pathways involved in persistent infections. *Front Cell Infect Microbiol* 4:99.
177. Hoffman LR, Déziel E, D'Argenio DA, Lépine F, Emerson J, McNamara S, Gibson RL, Ramsey BW, Miller SI. 2006. Selection for *Staphylococcus aureus* small-colony variants

- due to growth in the presence of *Pseudomonas aeruginosa*. 52. *Proc Natl Acad Sci USA* 103:19890–19895.
178. Noto MJ, Burns WJ, Beavers WN, Skaar EP. 2017. Mechanisms of Pyocyanin Toxicity and Genetic Determinants of Resistance in *Staphylococcus aureus*. *J Bacteriol* 199.
179. Pernet E, Guillemot L, Burgel P-R, Martin C, Lambeau G, Sermet-Gaudelus I, Sands D, Leduc D, Morand PC, Jeamment L, Chignard M, Wu Y, Touqui L. 2014. *Pseudomonas aeruginosa* eradicates *Staphylococcus aureus* by manipulating the host immunity. *Nat Commun* 5:5105.
180. Liu Q, Liu Y, Kang Z, Xiao D, Gao C, Xu P, Ma C. 2018. 2,3-Butanediol catabolism in *Pseudomonas aeruginosa* PAO1: 2,3-Butanediol catabolism in *Pseudomonas aeruginosa*. 11. *Environ Microbiol* 20:3927–3940.
181. Xiao Z, Xu P. 2007. Acetoin Metabolism in Bacteria. 2. *Critical Reviews in Microbiology* 33:127–140.
182. Joly N, Zhang N, Buck M, Zhang X. 2012. Coupling AAA protein function to regulated gene expression. *Biochimica et Biophysica Acta (BBA) - Molecular Cell Research* 1823:108–116.
183. Shao X, Zhang X, Zhang Y, Zhu M, Yang P, Yuan J, Xie Y, Zhou T, Wang W, Chen S, Liang H, Deng X. 2018. RpoN-Dependent Direct Regulation of Quorum Sensing and the Type VI Secretion System in *Pseudomonas aeruginosa* PAO1. *J Bacteriol* 200.
184. Damron FH, Owings JP, Okkotsu Y, Varga JJ, Schurr JR, Goldberg JB, Schurr MJ, Yu HD. 2012. Analysis of the *Pseudomonas aeruginosa* regulon controlled by the sensor kinase KinB and sigma factor RpoN. *J Bacteriol* 194:1317–1330.
185. Schulz S, Eckweiler D, Bielecka A, Nicolai T, Franke R, Dötsch A, Hornischer K, Bruchmann S, Düvel J, Häussler S. 2015. Elucidation of sigma factor-associated networks in *Pseudomonas aeruginosa* reveals a modular architecture with limited and function-specific crosstalk. *PLoS Pathog* 11:e1004744.
186. Potvin E, Sanschagrin F, Levesque RC. 2008. Sigma factors in *Pseudomonas aeruginosa*. *FEMS Microbiol Rev* 32:38–55.
187. Linares JF, Moreno R, Fajardo A, Martínez-Solano L, Escalante R, Rojo F, Martínez JL. 2010. The global regulator Crc modulates metabolism, susceptibility to antibiotics and virulence in *Pseudomonas aeruginosa*. *Environ Microbiol* 12:3196–3212.
188. Flécharde M, Duchesne R, Tahrioui A, Bouffartigues E, Depayras S, Hardouin J, Lagy C, Maillot O, Tortuel D, Azuama CO, Clamens T, Duclairoir-Poc C, Catel-Ferreira M, Gicquel G, Feuilloley MGJ, Lesouhaitier O, Heipieper HJ, Groleau M-C, Déziel É, Cornelis P, Chevalier S. 2018. The absence of SigX results in impaired carbon metabolism and membrane fluidity in *Pseudomonas aeruginosa*. *Sci Rep* 8:17212.
189. Sonnleitner E, Wulf A, Campagne S, Pei X-Y, Wolfinger MT, Forlani G, Prindl K, Abdou L, Resch A, Allain FH-T, Luisi BF, Urlaub H, Bläsi U. 2018. Interplay between the catabolite repression control protein Crc, Hfq and RNA in Hfq-dependent translational regulation in *Pseudomonas aeruginosa*. *Nucleic Acids Res* 46:1470–1485.
190. La Rosa R, Johansen HK, Molin S. 2019. Adapting to the Airways: Metabolic Requirements of *Pseudomonas aeruginosa* during the Infection of Cystic Fibrosis Patients. 10. *Metabolites* 9.

191. Španěl P, Sovová K, Dryahina K, Doušová T, Dřevínek P, Smith D. 2016. Do linear logistic model analyses of volatile biomarkers in exhaled breath of cystic fibrosis patients reliably indicate *Pseudomonas aeruginosa* infection? 3. *J Breath Res* 10:036013.
192. Marvig RL, Sommer LM, Jelsbak L, Molin S, Johansen HK. 2015. Evolutionary insight from whole-genome sequencing of *Pseudomonas aeruginosa* from cystic fibrosis patients. 4. *Future Microbiol* 10:599–611.
193. Thomas VC, Sadykov MR, Chaudhari SS, Jones J, Endres JL, Widhelm TJ, Ahn J-S, Jawa RS, Zimmerman MC, Bayles KW. 2014. A Central Role for Carbon-Overflow Pathways in the Modulation of Bacterial Cell Death. 6. *PLoS Pathog* 10:e1004205.
194. Chaudhari SS, Thomas VC, Sadykov MR, Bose JL, Ahn DJ, Zimmerman MC, Bayles KW. 2016. The LysR-type transcriptional regulator, CidR, regulates stationary phase cell death in *Staphylococcus aureus*: Metabolic control of cell death in *S. aureus*. 6. *Molecular Microbiology* 101:942–953.
195. Yang S-J, Dunman PM, Projan SJ, Bayles KW. 2006. Characterization of the *Staphylococcus aureus* CidR regulon: elucidation of a novel role for acetoin metabolism in cell death and lysis. 2. *Mol Microbiol* 60:458–468.
196. Hoang TT, Karkhoff-Schweizer RR, Kutchma AJ, Schweizer HP. 1998. A broad-host-range Flp-FRT recombination system for site-specific excision of chromosomally-located DNA sequences: application for isolation of unmarked *Pseudomonas aeruginosa* mutants. 1. *Gene* 212:77–86.
197. Winstanley C, O'Brien S, Brockhurst MA. 2016. *Pseudomonas aeruginosa* Evolutionary Adaptation and Diversification in Cystic Fibrosis Chronic Lung Infections. 5. *Trends Microbiol* 24:327–337.
198. Marvig RL, Sommer LM, Molin S, Johansen HK. 2015. Convergent evolution and adaptation of *Pseudomonas aeruginosa* within patients with cystic fibrosis. *Nat Genet* 47:57–64.
199. Sherrard LJ, Tai AS, Wee BA, Ramsay KA, Kidd TJ, Ben Zakour NL, Whiley DM, Beatson SA, Bell SC. 2017. Within-host whole genome analysis of an antibiotic resistant *Pseudomonas aeruginosa* strain sub-type in cystic fibrosis. *PLoS One* 12:e0172179.
200. Qin X, Zhou C, Zerr DM, Adler A, Addetia A, Yuan S, Greninger AL. 2018. Heterogeneous Antimicrobial Susceptibility Characteristics in *Pseudomonas aeruginosa* Isolates from Cystic Fibrosis Patients. *mSphere* 3.
201. D'Argenio DA, Wu M, Hoffman LR, Kulasekara HD, Déziel E, Smith EE, Nguyen H, Ernst RK, Larson Freeman TJ, Spencer DH, Brittnacher M, Hayden HS, Selgrade S, Klausen M, Goodlett DR, Burns JL, Ramsey BW, Miller SI. 2007. Growth phenotypes of *Pseudomonas aeruginosa* lasR mutants adapted to the airways of cystic fibrosis patients. *Molecular Microbiology* 64:512–533.
202. Stintzi A, Evans K, Meyer JM, Poole K. 1998. Quorum-sensing and siderophore biosynthesis in *Pseudomonas aeruginosa*: lasR/lasI mutants exhibit reduced pyoverdine biosynthesis. *FEMS microbiology letters* 166:341–345.
203. Feltner JB, Wolter DJ, Pope CE, Groleau M-C, Smalley NE, Greenberg EP, Mayer-Hamblett N, Burns J, Déziel E, Hoffman LR, Dandekar AA. 2016. LasR Variant Cystic

- Fibrosis Isolates Reveal an Adaptable Quorum-Sensing Hierarchy in *Pseudomonas aeruginosa*. *mBio* 7.
204. Ringel MT, Brüser T. 2018. The biosynthesis of pyoverdines. *Microb Cell* 5:424–437.
205. Mavrodi DV, Parejko JA, Mavrodi OV, Kwak Y-S, Weller DM, Blankenfeldt W, Thomashow LS. 2013. Recent insights into the diversity, frequency and ecological roles of phenazines in fluorescent *Pseudomonas* spp. *Environmental Microbiology* 15:675–686.
206. Dietrich LEP, Price-Whelan A, Petersen A, Whiteley M, Newman DK. 2006. The phenazine pyocyanin is a terminal signalling factor in the quorum sensing network of *Pseudomonas aeruginosa*. *Mol Microbiol* 61:1308–1321.
207. Briaud P. 2019. Impact de *Pseudomonas aeruginosa* sur *Staphylococcus aureus* dans un contexte de coexistence bactérienne chez les patients atteints de mucoviscidose. Manuscrit de thèse, Université Claude Bernard Lyon 1.
208. Ibberson CB, Stacy A, Fleming D, Dees JL, Rumbaugh K, Gilmore MS, Whiteley M. 2017. Co-infecting microorganisms dramatically alter pathogen gene essentiality during polymicrobial infection. *Nat Microbiol* 2:17079.
209. van Opijnen T, Bodi KL, Camilli A. 2009. Tn-seq: high-throughput parallel sequencing for fitness and genetic interaction studies in microorganisms. 10. *Nat Methods* 6:767–772.
210. Skurnik D, Roux D, Aschard H, Cattoir V, Yoder-Himes D, Lory S, Pier GB. 2013. A comprehensive analysis of in vitro and in vivo genetic fitness of *Pseudomonas aeruginosa* using high-throughput sequencing of transposon libraries. *PLoS Pathog* 9:e1003582.
211. Metcalf WW, Jiang W, Daniels LL, Kim SK, Haldimann A, Wanner BL. 1996. Conditionally replicative and conjugative plasmids carrying lacZ alpha for cloning, mutagenesis, and allele replacement in bacteria. *Plasmid* 35:1–13.
212. Bolger AM, Lohse M, Usadel B. 2014. Trimmomatic: a flexible trimmer for Illumina sequence data. *Bioinformatics* 30:2114–2120.
213. FastQC: a quality control tool for high throughput sequence data – ScienceOpen.
214. Wick RR, Judd LM, Gorrie CL, Holt KE. 2017. Unicycler: Resolving bacterial genome assemblies from short and long sequencing reads. *PLOS Computational Biology* 13:e1005595.
215. Seemann T. 2014. Prokka: rapid prokaryotic genome annotation. *Bioinformatics* 30:2068–2069.
216. Page AJ, Cummins CA, Hunt M, Wong VK, Reuter S, Holden MTG, Fookes M, Falush D, Keane JA, Parkhill J. 2015. Roary: rapid large-scale prokaryote pan genome analysis. 22. *Bioinformatics* 31:3691–3693.
217. Wurtzel O, Yoder-Himes DR, Han K, Dandekar AA, Edelheit S, Greenberg EP, Sorek R, Lory S. 2012. The single-nucleotide resolution transcriptome of *Pseudomonas aeruginosa* grown in body temperature. *PLoS Pathog* 8:e1002945.
218. Altschul SF, Gish W, Miller W, Myers EW, Lipman DJ. 1990. Basic local alignment search tool. *J Mol Biol* 215:403–410.

219. Martin M. 2011. Cutadapt removes adapter sequences from high-throughput sequencing reads. 1. *EMBnet.journal* 17:10–12.
220. Li H, Durbin R. 2009. Fast and accurate short read alignment with Burrows-Wheeler transform. *Bioinformatics* 25:1754–1760.
221. DeJesus MA, Ambadipudi C, Baker R, Sassetti C, Ioerger TR. 2015. TRANSIT--A Software Tool for Himar1 TnSeq Analysis. *PLoS Comput Biol* 11:e1004401.
222. DeJesus MA, Zhang YJ, Sassetti CM, Rubin EJ, Sacchettini JC, Ioerger TR. 2013. Bayesian analysis of gene essentiality based on sequencing of transposon insertion libraries. *Bioinformatics* 29:695–703.
223. DeJesus MA, Ioerger TR. 2013. A Hidden Markov Model for identifying essential and growth-defect regions in bacterial genomes from transposon insertion sequencing data. *BMC Bioinformatics* 14:303.
224. Subramaniam S, DeJesus MA, Zaveri A, Smith CM, Baker RE, Ehrt S, Schnappinger D, Sassetti CM, Ioerger TR. 2019. Statistical analysis of variability in TnSeq data across conditions using zero-inflated negative binomial regression. *BMC Bioinformatics* 20:603.
225. Lee SA, Gallagher LA, Thongdee M, Staudinger BJ, Lippman S, Singh PK, Manoil C. 2015. General and condition-specific essential functions of *Pseudomonas aeruginosa*. *Proc Natl Acad Sci USA* 112:5189–5194.
226. Poulsen BE, Yang R, Clatworthy AE, White T, Osmulski SJ, Li L, Penaranda C, Lander ES, Shores N, Hung DT. 2019. Defining the core essential genome of *Pseudomonas aeruginosa*. *Proc Natl Acad Sci USA* 116:10072–10080.
227. Oliver A, Sánchez JM, Blázquez J. 2002. Characterization of the GO system of *Pseudomonas aeruginosa*. *FEMS Microbiol Lett* 217:31–35.
228. Ben-David Y, Zlotnik E, Zander I, Yerushalmi G, Shoshani S, Banin E. 2018. SawR a new regulator controlling pyomelanin synthesis in *Pseudomonas aeruginosa*. *Microbiol Res* 206:91–98.
229. Feinbaum RL, Urbach JM, Liberati NT, Djonovic S, Adonizio A, Carvunis A-R, Ausubel FM. 2012. Genome-wide identification of *Pseudomonas aeruginosa* virulence-related genes using a *Caenorhabditis elegans* infection model. *PLoS Pathog* 8:e1002813.
230. Martínez E, Campos-Gómez J. 2016. Pf Filamentous Phage Requires UvrD for Replication in *Pseudomonas aeruginosa*. *mSphere* 1.
231. Valentini M, García-Mauriño SM, Pérez-Martínez I, Santero E, Canosa I, Lapouge K. 2014. Hierarchical management of carbon sources is regulated similarly by the CbrA/B systems in *Pseudomonas aeruginosa* and *Pseudomonas putida*. *Microbiology (Reading)* 160:2243–2252.
232. Turner KH, Wessel AK, Palmer GC, Murray JL, Whiteley M. 2015. Essential genome of *Pseudomonas aeruginosa* in cystic fibrosis sputum. *Proc Natl Acad Sci USA* 112:4110–4115.
233. Murray JL, Kwon T, Marcotte EM, Whiteley M. 2015. Intrinsic Antimicrobial Resistance Determinants in the Superbug *Pseudomonas aeruginosa*. *mBio* 6.

234. Basta DW, Bergkessel M, Newman DK. 2017. Identification of Fitness Determinants during Energy-Limited Growth Arrest in *Pseudomonas aeruginosa*. *mBio* 8.
235. Gallagher LA, Shendure J, Manoil C. 2011. Genome-scale identification of resistance functions in *Pseudomonas aeruginosa* using Tn-seq. *mBio* 2:e00315-00310.
236. Turner KH, Everett J, Trivedi U, Rumbaugh KP, Whiteley M. 2014. Requirements for *Pseudomonas aeruginosa* Acute Burn and Chronic Surgical Wound Infection. *PLOS Genetics* 10:e1004518.
237. Halsey CR, Lei S, Wax JK, Lehman MK, Nuxoll AS, Steinke L, Sadykov M, Powers R, Fey PD. 2017. Amino Acid Catabolism in *Staphylococcus aureus* and the Function of Carbon Catabolite Repression. *mBio* 8.
238. Hj K, H L, Y L, I C, Y K, S L, S J. 2020. The ThiL enzyme is a valid antibacterial target essential for both thiamine biosynthesis and salvage pathways in *Pseudomonas aeruginosa*. *The Journal of biological chemistry*. *J Biol Chem*.
239. Knight BC. 1937. The nutrition of *Staphylococcus aureus*; nicotinic acid and vitamin B(1). *Biochem J* 31:731–737.
240. Bosi E, Monk JM, Aziz RK, Fondi M, Nizet V, Palsson BØ. 2016. Comparative genome-scale modelling of *Staphylococcus aureus* strains identifies strain-specific metabolic capabilities linked to pathogenicity. *PNAS* 113:E3801–E3809.
241. Barth AL, Pitt TL. 1996. The high amino-acid content of sputum from cystic fibrosis patients promotes growth of auxotrophic *Pseudomonas aeruginosa*. *J Med Microbiol* 45:110–119.
242. La Rosa R, Johansen HK, Molin S. 2018. Convergent Metabolic Specialization through Distinct Evolutionary Paths in *Pseudomonas aeruginosa*. *mBio* 9.
243. Taylor RF, Hodson ME, Pitt TL. 1992. Auxotrophy of *Pseudomonas aeruginosa* in cystic fibrosis. *FEMS Microbiol Lett* 71:243–246.
244. Filiatrault MJ, Tomblin G, Wagner VE, Alst NV, Rumbaugh K, Sokol P, Schwingel J, Iglewski BH. 2013. *Pseudomonas aeruginosa* PA1006, Which Plays a Role in Molybdenum Homeostasis, Is Required for Nitrate Utilization, Biofilm Formation, and Virulence. *PLoS ONE* 8.
245. Tata M, Wolfinger MT, Amman F, Roschanski N, Dötsch A, Sonnleitner E, Häussler S, Bläsi U. 2016. RNASeq Based Transcriptional Profiling of *Pseudomonas aeruginosa* PA14 after Short- and Long-Term Anoxic Cultivation in Synthetic Cystic Fibrosis Sputum Medium. *PLOS ONE* 11:e0147811.
246. Nishijyo T, Haas D, Itoh Y. 2001. The CbrA–CbrB two-component regulatory system controls the utilization of multiple carbon and nitrogen sources in *Pseudomonas aeruginosa*. *Molecular Microbiology* 40:917–931.
247. Silo-Suh L, Suh S-J, Phibbs PV, Ohman DE. 2005. Adaptations of *Pseudomonas aeruginosa* to the Cystic Fibrosis Lung Environment Can Include Dereglulation of *zwf*, Encoding Glucose-6-Phosphate Dehydrogenase. *Journal of Bacteriology* 187:7561–7568.

248. Cabeen MT, Leiman SA, Losick R. 2016. Colony-morphology screening uncovers a role for the *Pseudomonas aeruginosa* nitrogen-related phosphotransferase system in biofilm formation. *Molecular Microbiology* 99:557–570.
249. Yeung ATY, Janot L, Pena OM, Neidig A, Kukavica-Ibrulj I, Hilchie A, Levesque RC, Overhage J, Hancock REW. 2014. Requirement of the *Pseudomonas aeruginosa* CbrA Sensor Kinase for Full Virulence in a Murine Acute Lung Infection Model. *Infection and Immunity* 82:1256–1267.
250. Carfrae LA, MacNair CR, Brown CM, Tsai CN, Weber BS, Zlitni S, Rao VN, Chun J, Junop MS, Coombes BK, Brown ED. 2020. Mimicking the human environment in mice reveals that inhibiting biotin biosynthesis is effective against antibiotic-resistant pathogens. 1. *Nature Microbiology* 5:93–101.
251. Puzari M, Chetia P. 2017. RND efflux pump mediated antibiotic resistance in Gram-negative bacteria *Escherichia coli* and *Pseudomonas aeruginosa*: a major issue worldwide. *World J Microbiol Biotechnol* 33:24.
252. Klockgether J, Cramer N, Fischer S, Wiehlmann L, Tümmler B. 2018. Long-Term Microevolution of *Pseudomonas aeruginosa* Differs between Mildly and Severely Affected Cystic Fibrosis Lungs. 2. *Am J Respir Cell Mol Biol* 59:246–256.
253. Klockgether J, Miethke N, Kubesch P, Bohn Y-S, Brockhausen I, Cramer N, Eberl L, Greipel J, Herrmann C, Herrmann S, Horatzek S, Lingner M, Luciano L, Salunkhe P, Schomburg D, Wehsling M, Wiehlmann L, Davenport CF, Tümmler B. 2013. Intracolon diversity of the *Pseudomonas aeruginosa* cystic fibrosis airway isolates TBCF10839 and TBCF121838: distinct signatures of transcriptome, proteome, metabolome, adherence and pathogenicity despite an almost identical genome sequence. *Environ Microbiol* 15:191–210.
254. Cios K, Cohen B, Quittell LM, Liu J, Larson EL. 2019. Impact of colonizing organism in the respiratory tract on the incidence, duration, and time between subsequent hospitalizations among patients with cystic fibrosis. *American Journal of Infection Control* 47:750–754.